

# Everything I did for spin 2<sup>+</sup> model on X17

## Contents

<b>1 Abstract</b>	<b>4</b>
<b>2 Summary of this dissertation</b>	<b>5</b>
<b>3 Notation</b>	<b>7</b>
3.1 Pauli notation . . . . .	7
3.2 Gamma matrices . . . . .	8
3.3 Sum over fermion polarizations . . . . .	9
3.4 Feynman rules in Pauli notation . . . . .	10
3.5 From Pauli to Bjorken-Drell notation . . . . .	11
<b>4 Effective coupling with Standard Model</b>	<b>13</b>
4.1 Representation of a spin 2 massive particle . . . . .	13
4.2 Spin 2 Lagrangian . . . . .	14
4.2.1 Fierz-Pauli Lagrangian . . . . .	14
4.2.2 Non-Universal Couplings Model . . . . .	16
4.2.3 General interaction with matter . . . . .	19
4.3 Feynman rules . . . . .	20
4.4 Energy of EFT breaking . . . . .	22
<b>5 Bounds from ATOMKI and JINR</b>	<b>25</b>
5.1 Decay rate for electron-positron channel . . . . .	25
5.2 Decay rate for photon-electron-positron channel . . . . .	26
5.3 Decay rate for photon-photon channel . . . . .	29
5.4 Lower bound estimation for spin 2 couplings . . . . .	30
5.4.1 From ATOMKI collaboration only . . . . .	30
5.4.2 Adding JINR collaboration . . . . .	32
<b>6 Correction to Bhabha scattering</b>	<b>35</b>
6.1 Simplifying Bhabha result . . . . .	38
6.2 Testing spin 2 for Bhabha . . . . .	44
6.2.1 Behavior of Bhabha cross section . . . . .	44
6.2.2 Bhabha experimental results . . . . .	45
<b>7 Correction to Møller scattering</b>	<b>47</b>
7.1 Testing spin 2 for Møller . . . . .	50
7.1.1 Behavior of Møller cross section . . . . .	50
7.1.2 Møller experimental results . . . . .	51
<b>8 Digression on a spin 1 toy model</b>	<b>52</b>
8.1 Spin 1 coupling with fermions . . . . .	52
8.2 Spin 1 decay rate for electron-positron channel . . . . .	53
8.3 Spin 1 correction to Bhabha scattering . . . . .	54
8.3.1 Testing spin 1 for Bhabha . . . . .	59
<b>9 Correction to Compton scattering</b>	<b>62</b>
9.1 Polarized cross section . . . . .	66
9.2 Unpolarized cross section . . . . .	68
9.3 Testing spin 2 for Compton scattering . . . . .	71
9.3.1 Behavior of Compton cross section . . . . .	71
9.3.2 Compton experimental results . . . . .	72

<b>10 Correction to <math>e^+e^-</math> annihilation into two photons</b>	<b>74</b>
10.1 Correction to positronium decay . . . . .	78
10.1.1 Positronium . . . . .	78
10.1.2 Tree level decay rate . . . . .	80
10.1.3 Correction to parapositronium decay . . . . .	82
10.2 Simplifying annihilation result . . . . .	84
10.3 Testing spin 2 for annihilation . . . . .	85
10.3.1 Behavior of annihilation cross section . . . . .	85
10.3.2 Annihilation experimental results . . . . .	86
<b>11 Correction to two-photon scattering</b>	<b>88</b>
11.1 Simplifying two-photon result . . . . .	90
11.2 Testing spin 2 for two-photon . . . . .	96
11.2.1 Behavior of two-photon cross section . . . . .	96
11.2.2 Two-photon experiments . . . . .	98
<b>12 Other relevant phenomena</b>	<b>100</b>
12.1 Scattering process $e^+e^- \rightarrow X\gamma$ . . . . .	100
12.1.1 Differential cross section of $e^+e^- \rightarrow X\gamma$ . . . . .	102
12.1.2 Amplitude result . . . . .	103
12.2 $g - 2$ of the electron . . . . .	105
12.3 Perturbativity constraint . . . . .	106
12.4 Unitarity constraint . . . . .	108
12.4.1 Derivation . . . . .	109
12.4.2 Application to lepton scattering . . . . .	112
12.4.3 Application to photon scattering . . . . .	112
12.5 Constraints we did not consider . . . . .	113
<b>13 Constraints on one coupling spin 2 model</b>	<b>115</b>
<b>14 Constraints on two couplings spin 2 model</b>	<b>117</b>
<b>15 Conclusions</b>	<b>124</b>
<b>A Bhabha scattering at tree level</b>	<b>125</b>
A.1 Bhabha amplitude . . . . .	125
A.2 Bhabha amplitude from Wick contractions . . . . .	126
A.3 Bhabha kinematics . . . . .	129
A.4 Bhabha cross section . . . . .	130
<b>B Møller scattering at tree level</b>	<b>134</b>
B.1 Møller amplitude . . . . .	134
B.2 Møller Wick contractions . . . . .	134
B.3 Crossing symmetry argument . . . . .	135
<b>C Compton scattering at tree level</b>	<b>138</b>
C.1 Compton Wick contractions . . . . .	138
C.2 Compton amplitude . . . . .	139
C.3 Compton kinematics . . . . .	141
C.4 Compton cross section . . . . .	142
C.5 Compton squared modulus spin 2 correction . . . . .	144
C.5.1 Polarized cross section squared modulus . . . . .	145
C.5.2 Unpolarized cross section squared modulus . . . . .	147
<b>D <math>e^+e^- \rightarrow \gamma\gamma</math> at tree level</b>	<b>150</b>
D.1 Annihilation Wick contractions . . . . .	150
D.2 Annihilation amplitude . . . . .	150
D.3 Annihilation kinematics . . . . .	152
D.4 Annihilation cross section . . . . .	153
D.5 Annihilation squared modulus spin 2 correction . . . . .	155

<b>E Two-photon elastic scattering at one loop</b>	<b>158</b>
E.1 Two-photon Wick contractions . . . . .	158
E.2 Two-photon amplitude . . . . .	159
E.3 Two-photon kinematics . . . . .	162
E.4 Two-photon cross section . . . . .	164
<b>F More calculations</b>	<b>168</b>
F.1 Landau-Yang theorem . . . . .	168
F.2 Generic 2-body phase space . . . . .	169
F.3 Massless 3-body phase space . . . . .	170
F.4 Complex conjugates in Pauli notation . . . . .	171
F.5 Evaluation of decay rate using only 4-vertex interaction . . . . .	172
F.6 On helicity flip . . . . .	175
F.7 Useful photon polarization sums in Compton scattering . . . . .	177
F.8 Positronium in quantum mechanics . . . . .	178
<b>G Tools for calculations and graphs</b>	<b>181</b>
G.1 FORM codes . . . . .	181
G.2 Google Colab for graphs . . . . .	182

## 1 Abstract

The newly found  $X$  resonance at  $m_X = 17\text{ MeV}$ , in the electron positron channel, by the Hungarian collaboration ATOMKI, has sparked new interest in the scientific community about low energy research. While attempts for independent experiments have been inconclusive so far, on the theoretical side a new possible resonance at energies much lower than QCD energy scale has opened a new realm of scenarios. Theorists identified the best candidate that accommodates the nuclear transitions exhibiting the  $X$  peak to be a  $1^+$  axial vector state. However, recent studies in the two photons channel by the Russian collaboration JINR highlighted the same  $X_{17}$  peak. If these results are to be trusted, they would strongly negate any boson vector origin, as per Landau-Yang theorem.

In this thesis, we explore the spin 2 scenario for the  $X_{17}$  peak, first by constructing a massive spin 2 low energy effective theory, then by constraining the effective coefficients by computing corrections to well-known QED processes, and finally by linking our massive spin 2 model to more general theories and hypotheses on UV completions.

We will couple our spin 2 massive boson to both electrons and photons. This is crucial to be able to compute corrections to standard electrodynamics processes, whose measurements are among the most precise in physics, directly at tree level, with new  $X$  interfering diagrams. In particular, we will be doing this for Bhabha scattering, for Møller scattering, for Compton scattering, for electron - positron annihilation into two photons (with a digression on positronium decay) and for photon-photon elastic scattering (hereafter called two-photon scattering). We will be looking for independent upper and lower bounds to our couplings, and combine them all together to identify the acceptable range of parameters for our model.

## 2 Summary of this dissertation

The newly found  $X$  resonance at 17 MeV, in the electron positron channel, by the Hungarian collaboration ATOMKI, has sparked new interest in the scientific community in low energy search and prompted several phenomenological approaches to explain it. Theorists identified the best candidate that accommodates the nuclear transitions exhibiting the  $X$  peak to be a  $1^+$  axial vector particle. However, recent studies in the two photons channel by the Russian collaboration JINR highlighted the same  $X_{17}$  peak. If these results are to be trusted, they would strongly negate any boson vector origin, as per Landau-Yang theorem.

In this thesis, we explore the spin 2 scenario for the  $X_{17}$  peak, first by constructing a massive spin 2 low energy effective theory, then by constraining the effective coefficients by computing corrections to well-known QED processes, and finally by linking our massive spin 2 model to more general theories and hypotheses on UV completions.

We will couple our spin 2 massive boson to both electrons and photons. This is crucial to be able to compute corrections to standard electrodynamics processes, whose measurements are among the most precise in the field, directly at tree level, with new  $X$  interfering diagrams. In particular, we will be doing this for Bhabha scattering, for Møller scattering, for Compton scattering, for electron - positron annihilation into two photons (with a digression on positronium decay) and for photon-photon elastic scattering (hereafter called two-photon scattering). We will be looking for independent upper and lower bounds to our couplings  $g_e/\Lambda$  and  $g_\gamma/\Lambda$ , and compare them to the bounds set through decay processes, to check for consistency.

Let us outline the general layout of this dissertation:

- Firstly, a brief discussion on how to construct a coherent description of a massive spin 2 field, and how to let a spin 2 particle interact with the Standard Model, found in [section 4](#). We will be employing a model with two couplings:  $g_e/\Lambda$ , and  $g_\gamma/\Lambda$ . A derivation of Feynman rules between  $X$  and fermions, and  $X$  and photons will follow.
- Then, in [subsection 5.1](#), [subsection 5.2](#) and in [subsection 5.3](#), we will analytically evaluate decay rates at tree level for the processes  $X \rightarrow e^+e^-$ ,  $X \rightarrow e^+e^-\gamma$  and  $X \rightarrow \gamma\gamma$ , respectively.
- Lower bounds on the newly introduced couplings will be calculated ([subsection 5.4](#)), on the simple assumption that, had these couplings been smaller, no experiment would have been able to detect the resonance.
- It is important to stress (as done in [subsection 4.4](#)) that our effective model will have a cutoff energy  $\Lambda_c \approx \mathcal{O}(100 \text{ MeV})$ , so that high energy experimental results for colliders are out of bounds for our search for constraints.
- We will then start calculating our QED corrections due to this spin 2 model using only one new coupling,  $g_e$  (setting  $g_\gamma = 0$ ). This is the coupling that was experimentally verified by the ATOMKI collaboration ([[1](#)], [[2](#)], [[3](#)], [[4](#)], [[5](#)]). Processes only involving couplings with  $e^+e^-$ , only "unlocked" by the nuclear transition experiments performed in Hungary, are Bhabha ([section 6](#)) and Møller scattering ([section 7](#)).
- In [section 8](#), we will briefly repeat the same approach for a spin 1 model, but with a spin 1 model (not yet excluded if  $g_\gamma = 0$ ) and we will see why it yields very small corrections.
- Then, we will add a new coupling to photons  $g_\gamma \neq 0$ . This is the coupling we need to include to account for recent experimental result ([\[8\]](#)) by the JINR collaboration<sup>1</sup>, and will allow us tree level corrections for Compton scattering ([section 9](#)),  $e^+e^-$  annihilation into two photons ([section 10](#)), and two-photon scattering ([section 11](#)).
- In [subsection 10.1](#), we will discuss a brief application of the  $e^+e^- \rightarrow \gamma\gamma$  process to compute corrections to parapositronium decay rate.
- In [section 11](#), we will calculate the spin 2 correction for the two-photon elastic scattering process, to complete our review of QED. We will see that, although spin 2 corrections are relatively larger due to this process starting at one loop in QED, absence of significant experimental data will unfortunately limit our constraint (best result is [[69](#)]).
- Finally, we will be reporting other remarks and constraints in [section 12](#). Namely,  $g - 2$  of the electron, which is one of the most precise measurements in the field, will significantly constrain our model. We will also calculate the process  $e^+e^- \rightarrow X\gamma$  analytically, to compare with results in [[13](#)] and [[9](#)]. Finally, we will insert constraints due to perturbativity and unitarity of the spin 2 model.

---

<sup>1</sup>Apparently, the scientific community welcomed this result with skepticism.

- At the end of all QED corrections, we will be summing up all constraints for this model of massive spin 2 boson. In [section 13](#) we will be studying the case  $g_\gamma = 0$ . In [section 14](#), we will switch  $g_\gamma$  on, and focus on the complete model, using every constraint available. **Give anticipation on the result of the model.**

To perform all amplitude calculations, we rely on an algebraic tensor manipulation tool called **FORM**. All the codes used throughout this dissertation can be found in [subsection G.1](#), together with the link to a [Git Hub repository](#). Instead, for graphs, we used the following [Google Colab](#). Finally, for impractical single variable integrals, we used [this Integral Calculator](#). Finally, for other pictures and drawings we used [Matcha](#).

### 3 Notation

#### 3.1 Pauli notation

In this thesis, we are going to use the following notation, which is very well described in [26]. For scalar products, the metric we are going to use is the *Euclidean metric*, or *Dutch metric*:

$$\delta_{\mu\nu} = \text{diag}(1, 1, 1, 1)$$

To reproduce the scalar products obtained using a Minkowskian metric, instead, we redefine the 4-vector:

$$a_\mu = (a_0, a_1, a_2, a_3)^T \quad \rightarrow \quad a_\mu = (a_1, a_2, a_3, ia_0)^T = (a_1, a_2, a_3, a_4)^T$$

with this redefinition of  $a_4 = ia_0$  as the fourth component, since we are using a simple identity matrix to raise and lower indices, there actually is no difference between upper and lower indices:

$$a^\mu = \delta^{\mu\nu} a_\nu = (a_1, a_2, a_3, a_4)^T = a_\mu$$

this has a rigorous mathematical interpretation in terms of representation of groups.

With a  $\eta_{\mu\nu}$  metric, we define the signature of the Lorentz group, which is  $\text{SO}(1, 3) \cong \text{SU}(2) \times \text{SU}(2)$  in terms of group decomposition (its algebra is *semisimple*). For every tensor in the Lorentz group we can simply keep track of how many times we tensorize the fundamental irreducible representation (hereafter, we are going to call it *irrep*) of each  $\text{SU}(2)$  group, by simply defining two decks of indices:  ${}^\mu$  and  ${}_\mu$ .

Instead, when using  $\delta_{\mu\nu}$ , the underlying group for which the Euclidean metric gives signature is  $\text{SO}(4)$ . It has the same dimension of the Lorentz group, and it represents rotations in four dimension (time included).  $\text{SO}(4)$  has a real, simple Lie algebra, with only one fundamental irrep, and hence we really only need one deck of indices to characterize every tensor transforming under this group.

When taking a scalar product using the Euclidean metric:

$$a_\mu b_\mu = a_1 b_1 + a_2 b_2 + a_3 b_3 + a_4 b_4 = a_1 b_1 + a_2 b_2 + a_3 b_3 - a_0 b_0 \quad (3.1)$$

which is equivalent to the scalar product for a mostly plus metric  $\eta_{\mu\nu}$ . For a 4-momentum, this means that  $p^2 = -m^2$ ,  $m$  being the mass of the particle, as norm changes sign.

The redefinition  $a_4 = ia_0$  is actually called *Wick rotation*. In a path integral formulation of Quantum Field Theory, the evolution operator  $\exp[-iHt]$  is not bound in Minkowskian spacetime. Instead, if we define  $\tau = it$ , it becomes  $\exp[-H\tau]$ , which is, indeed, bound for  $\tau > 0$ .

Mathematically, this procedure is formally defined by performing *analytic continuation* in the complex plane for the time component. Imposing causality for correlation functions in this extended time plane generates cuts in the plane. In this, Wick rotation is defined as:

$$a_4 = \lim_{\theta \rightarrow \frac{\pi}{2}^-} e^{i\theta} a_0$$

which corresponds to a specific choice of time component "under" one of these cuts.

Finally, it is worth mentioning that in this notation, integrals in spacetime usually come as:

$$\int \frac{d^4x}{(2\pi)^4} = \int \frac{dx_0}{2\pi} \int \frac{d^3x}{(2\pi)^3} \quad \rightarrow \quad \int \frac{dx_4}{2\pi i} \int \frac{d^3x}{(2\pi)^3} = \int \frac{d^4x}{(2\pi)^4 i}$$

which is why every propagator will be accompanied by a factor of  $1/(2\pi)^4 i$ .

So, the effect of Wick rotation is the shift in metric from Minkowski to Euclidean/Dutch, that allows for a more rigorous formulation of any QFT. However, we are not exploiting this formalism in this thesis, so we would have no reason at all to use this notation. Then, why do we employ it nonetheless? There are a few advantages:

- The absence of distinction between indices is very useful. We only need to worry about contraction of indices, and not their absolute position. For now on, we are going to write them only in the lower deck.
- This notation offers a few tricks that allow to check progress and correctness of calculations, as we shall see.
- Gamma matrices can be naturally redefined as hermitian (we shall see how in the next chapter).
- To perform harder calculations, throughout the thesis we are going to be using FORM, a useful tool for tensor calculus (see subsection G.1). FORM only works in Dutch metric  $\delta_{\mu\nu}$ .

## 3.2 Gamma matrices

In the Minkowskian, Dirac equation is:

$$(i\partial - m) \psi = 0 \quad (3.2)$$

which is the famous *Bjorken-Drell notation*. If we indicate  $\hat{\gamma}_\mu$  as the gamma matrices in Dirac basis, Dirac operator is:

$$i\partial - m = i\hat{\gamma}_0 \frac{\partial}{\partial x_0} + i\hat{\gamma}_i \frac{\partial}{\partial x_i} - m$$

now, we go to the Euclidean:  $x_0 = -ix_4$ , and we define new gamma matrices  $\gamma_\mu$ :

$$\gamma_4 = \hat{\gamma}_0 \quad \gamma_i = -i\hat{\gamma}_i \quad (3.3)$$

If we ever needed  $\gamma_0$ , we would define it as  $\gamma_0 = -i\hat{\gamma}_0$ , to have the correspondence  $\gamma_\mu = -i\hat{\gamma}_\mu$ . So, the operator becomes:

$$i\partial - m = - \left( \gamma_i \frac{\partial}{\partial x_i} + \gamma_4 \frac{\partial}{\partial x_4} + m \right) = -(\partial + m)$$

which means that in the Euclidean, Dirac equation [Equation 3.2](#) becomes:

$$(\partial + m) \psi = 0 \quad (3.4)$$

By having  $\sigma_i$  as Pauli matrices<sup>2</sup>, our new gamma matrices are:

$$\begin{aligned} \gamma_1 &= \sigma_2 \otimes \sigma_1 = \begin{pmatrix} 0 & 0 & 0 & -i \\ 0 & 0 & -i & 0 \\ 0 & i & 0 & 0 \\ i & 0 & 0 & 0 \end{pmatrix} & \gamma_2 &= \sigma_2 \otimes \sigma_2 = \begin{pmatrix} 0 & 0 & 0 & -1 \\ 0 & 0 & 1 & 0 \\ 0 & 1 & 0 & 0 \\ -1 & 0 & 0 & 0 \end{pmatrix} \\ \gamma_3 &= \sigma_2 \otimes \sigma_3 = \begin{pmatrix} 0 & 0 & -i & 0 \\ 0 & 0 & 0 & i \\ i & 0 & 0 & 0 \\ 0 & -i & 0 & 0 \end{pmatrix} & \gamma_4 &= \sigma_3 \otimes \mathbb{1}_2 = \begin{pmatrix} 1 & 0 & 0 & 0 \\ 0 & 1 & 0 & 0 \\ 0 & 0 & -1 & 0 \\ 0 & 0 & 0 & -1 \end{pmatrix} \end{aligned}$$

and we notice immediately that  $(\gamma_\mu)^\dagger = \gamma_\mu$ , as these new gamma matrices are hermitian. Clifford algebra becomes:

$$\{\gamma_\mu, \gamma_\nu\} = 2\delta_{\mu\nu}\mathbb{1}_4 \quad (3.5)$$

Finally, we can define  $\gamma_5$ :

$$\gamma_5 = -\hat{\gamma}_5 = -i\hat{\gamma}_0\hat{\gamma}_1\hat{\gamma}_2\hat{\gamma}_3 = \gamma_1\gamma_2\gamma_3\gamma_4 = \begin{pmatrix} 0 & 0 & -1 & 0 \\ 0 & 0 & 0 & -1 \\ -1 & 0 & 0 & 0 \\ 0 & -1 & 0 & 0 \end{pmatrix} = -\sigma_1 \otimes \mathbb{1}_2$$

with the following anticommutation rules:

$$\begin{aligned} \gamma_5\gamma_4 &= -(\sigma_1 \otimes \mathbb{1}_2)(\sigma_3 \otimes \mathbb{1}_2) = -(\sigma_1\sigma_3) \otimes \mathbb{1}_2 = (\sigma_3\sigma_1) \otimes \mathbb{1}_2 = (\sigma_3 \otimes \mathbb{1}_2)(\sigma_1 \otimes \mathbb{1}_2) = -\gamma_5\gamma_4 \\ \gamma_5\gamma_i &= -(\sigma_1 \otimes \mathbb{1}_2)(\sigma_2 \otimes \sigma_i) = -(\sigma_1\sigma_2) \otimes \sigma_i = (\sigma_2\sigma_1) \otimes \sigma_i = (\sigma_2 \otimes \sigma_i)(\sigma_1 \otimes \mathbb{1}_2) = -\gamma_i\gamma_5 \end{aligned}$$

meaning:

$$\{\gamma_5, \gamma_\mu\} = 0 \quad (3.6)$$

Also, with this minus sign in the definition of  $\gamma_5$ , the chirality projectors become:

$$P_L = \frac{\mathbb{1}_4 + \gamma_5}{2} \quad P_R = \frac{\mathbb{1}_4 - \gamma_5}{2} \quad (3.7)$$

which is the opposite convention to the one it is usually found in literature.

<sup>2</sup>These are:

$$\sigma_1 = \begin{pmatrix} 0 & 1 \\ 1 & 0 \end{pmatrix} \quad \sigma_2 = \begin{pmatrix} 0 & -i \\ i & 0 \end{pmatrix} \quad \sigma_3 = \begin{pmatrix} 1 & 0 \\ 0 & -1 \end{pmatrix}$$

with commutation rules:  $[\sigma_i, \sigma_j] = 2i\varepsilon_{ijk}\sigma_k$ , and  $\{\sigma_i, \sigma_j\} = 2\delta_{ij}\mathbb{1}_2$ .

### 3.3 Sum over fermion polarizations

Finally, we are using a specific normalization of the fields such that the sum over fermion polarizations becomes:

$$\left\{ \begin{array}{l} \sum_{\lambda} u_a(p, \lambda) \bar{u}_b(p, \lambda) = \left( \frac{-i\gamma + m\mathbb{1}_4}{2p_4} \right)_{ab} \\ \sum_{\lambda} v_a(p, \lambda) \bar{v}_b(p, \lambda) = \left( \frac{-i\gamma - m\mathbb{1}_4}{2p_4} \right)_{ab} \end{array} \right. \quad (3.8)$$

which also implies that we will not use the normalization  $1/2p_4$  in fermion fields, as this factor has been shifted to the spinors themselves. However, this notation retains this factor for any other field normalization (scalar, vector, tensor), as we will see.

### 3.4 Feynman rules in Pauli notation

Remember that we are currently employing Pauli notation. Below, we are listing all the Feynman rules that are going to be used from this point onward:

**Propagators:** We are going to derive them throughout the thesis. We are listing here their expressions:

$$\text{Fermion:} \quad D_{ab}(x-y) = \int \frac{d^4q}{(2\pi)^4 i} \hat{D}_{ab}(q) e^{iq(x-y)}$$

$$\hat{D}_{ab}(q) = \frac{(-iq + m\mathbf{1})_{ab}}{q^2 + m^2 - i\epsilon}$$

$$\text{Massless spin 1:} \quad D_{\mu\nu}^\xi(x-y) = \int \frac{d^4q}{(2\pi)^4 i} \hat{D}_{\mu\nu}^\xi(q) e^{iq(x-y)}$$

$$\hat{D}_{\mu\nu}^\xi(q) = \frac{1}{q^2 - i\epsilon} \left[ \delta_{\mu\nu} + \left( 1 - \frac{1}{\xi} \right) \frac{q_\mu q_\nu}{q^2} \right]$$

$$\text{Massive spin 1:} \quad D_{\mu\nu}(x-y) = \int \frac{d^4p}{(2\pi)^4 i} \hat{D}_{\mu\nu}(p) e^{ip(x-y)}$$

$$\hat{D}_{\mu\nu}(p) = \frac{1}{p^2 + m^2 - i\epsilon} \left[ \delta_{\mu\nu} + \frac{p_\mu p_\nu}{m^2} \right]$$

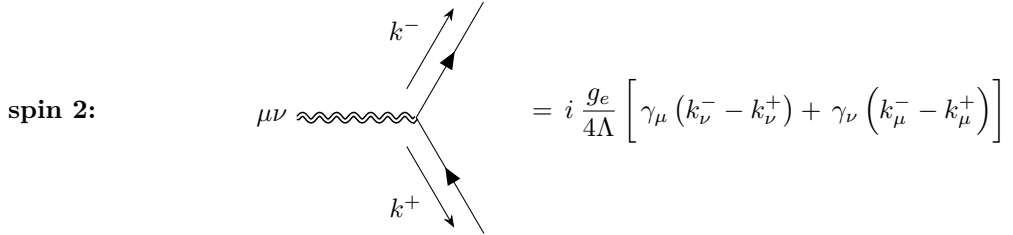
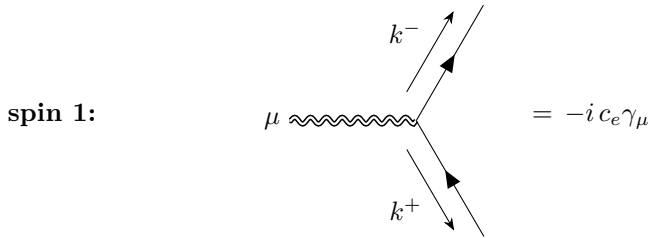
$$\text{Massive spin 2:} \quad D_{\mu\nu\rho\sigma}(x-y) = \int \frac{d^4p}{(2\pi)^4 i} \hat{D}_{\mu\nu\rho\sigma}(p) e^{ip(x-y)}$$

$$\hat{D}_{\mu\nu\rho\sigma}(p) = \frac{N_{\mu\nu\rho\sigma}(p)}{p^2 + m^2 - i\epsilon}$$

$$N_{\mu\nu\rho\sigma} = \frac{1}{2} (P_{\mu\rho} P_{\nu\sigma} + P_{\mu\sigma} P_{\nu\rho}) - \frac{1}{3} P_{\mu\nu} P_{\rho\sigma}$$

$$P_{\mu\nu} = \delta_{\mu\nu} + \frac{p_\mu p_\nu}{m^2}$$

**Feynman rules:** We are going to derive the interaction rules in [subsection 4.3](#).



$$\begin{aligned} \mu\nu \text{ wavy line} &\rightarrow \rho = -i \frac{g_e e}{2\Lambda} [\gamma_\mu \delta_{\nu\rho} + \gamma_\nu \delta_{\mu\rho}] \\ \mu\nu \text{ wavy line} &\rightarrow \rho \\ &\quad \text{loop} \\ &\quad k_1 \quad \rho \\ &\quad k_2 \quad \sigma \\ &= \frac{g_\gamma}{\Lambda} \Pi_{\mu\nu\rho\sigma}^\xi(k_1, k_2) \end{aligned}$$

where:

$$\begin{aligned} \Pi_{\mu\nu\rho\sigma}^\xi(k_1, k_2) &= \delta_{\rho\sigma} (k_{1,\mu} k_{2,\nu} + k_{1,\nu} k_{2,\mu}) - \delta_{\mu\rho} k_{1,\sigma} k_{2,\nu} - \delta_{\mu\sigma} k_{1,\nu} k_{2,\rho} \\ &\quad - \delta_{\nu\sigma} k_{1,\mu} k_{2,\rho} - \delta_{\nu\rho} k_{1,\sigma} k_{2,\mu} + k_1 \cdot k_2 (\delta_{\mu\sigma} \delta_{\nu\rho} + \delta_{\nu\sigma} \delta_{\mu\rho}) \\ &\quad + \frac{1}{\xi} [-\delta_{\mu\rho} k_{2,\sigma} k_{2,\nu} - \delta_{\mu\sigma} k_{1,\nu} k_{1,\rho} - \delta_{\nu\sigma} k_{1,\mu} k_{1,\rho} - \delta_{\nu\rho} k_{2,\sigma} k_{2,\mu}] \end{aligned}$$

In addition to those, we are using electrodynamics Feynman rule:

$$\begin{aligned} \mu \text{ wavy line} &\rightarrow k^- \\ &\quad k^+ \\ &= -i e \gamma_\mu \end{aligned}$$

**Other rules:** Additionally, we require the following factor in front of each amplitude, taking into account our choices for normalization of the fields, vertices and propagators (as we learned from subsection A.2):

- Each vertex of interaction requires a factor of  $(2\pi)^4 i$ .
- Each propagator requires a factor of  $1/[(2\pi)^4 i]$ .
- When squaring Dirac's delta for conservation of energy, another factor  $1/(2\pi)^4$  is required.
- Each field is normalized with respect to the volume of the spacetime in which we are performing the integration:  $1/\sqrt{V}$ . Of course, we expect volume dependence to be erased in the final process cross section.
- Each scalar or vector field requires additional normalization of  $1/\sqrt{2E}$ ,  $E$  being its energy (which we label with the subscript 4, as in our notation it is the fourth component). This is not required for fermions, as this factor is absorbed in  $u$  and  $v$  spinors in our normalization (see subsection 3.3).

### 3.5 From Pauli to Bjorken-Drell notation

There is a small Appendix at the end of [26], outlining the rules needed to translate every expression in Pauli notation into the more common Bjorken-Drell notation. Without giving justification here, we will only list the rules we will be needing in this thesis here, for better comprehension of the reader:

- As we have explained,  $\gamma_\mu$  must be replaced with  $-i\hat{\gamma}_\mu$ , and  $\gamma_5$  with  $-\gamma_5$ .
- To retain Clifford algebra,  $\delta_{\mu\nu}$  must be replaced with  $-\eta_{\mu\nu} = -\text{diag}(1, -1, -1, -1)$ .
- Every lower deck index must be moved up *except* for  $\partial_\mu$ .
- Every dot product must be changed in sign,  $k \cdot p \rightarrow -k \cdot p$ . This also implies that Mandelstam variables  $s, t, u$  are defined with a minus sign with respect to Bjorken-Drell notation ( $s$  is always negative).

- $\not{p}$  must be replaced by  $i\not{p}$ , while  $\not{\partial}$  must be replaced by  $-i\not{\partial}$ .
- For every lower index contraction, insert  $-\eta_{\mu\nu}$ :  $p_\mu k_\mu \rightarrow -p^\mu k^\nu \eta_{\mu\nu}$ .
- The addition of  $(2\pi)^4$  follows different rules in the two notations. In Pauli notation, one gets a factor  $(2\pi)^4$  for each vertex of interaction, a factor  $(2\pi)^{-4}$  for each propagator, and a factor  $(2\pi)^{-4}$  when squaring the delta function in conservation of momentum. In Bjorken-Drell notation, one gets a factor  $(2\pi)^{-4}$  for every loop integral, and a factor  $(2\pi)^4$  when taking the  $S$ -matrix element squared. The total tally of the factors is the same in both notations.
- In Pauli notation, one includes separately a factor  $i$  for each vertex and a factor  $1/i$  for each propagator. In Bjorken-Drell notation, these have to be included directly in the diagrams. The rule is: for every vertex add a factor  $i$ , and for every propagator add a factor of  $1/i$ .

We will justify some of these rules when studying the contractions in the  $S$ -matrix expansion, in the Appendices (see subsection A.2).

As a useful exercise, one can translate Feynman rules in subsection 3.4 in Bjorken-Drell notation:

The diagram shows four Feynman rules:

- spin 1:** A wavy line labeled  $\mu$  with arrows pointing right and left. It splits into two lines labeled  $k^-$  and  $k^+$ . To its right is the equation  $= -i c_e \gamma^\mu$ .
- spin 2:** A wavy line labeled  $\mu\nu$  with arrows pointing right and left. It splits into two lines labeled  $k^-$  and  $k^+$ . To its right is the equation  $= i \frac{g_e}{4\Lambda} [\gamma^\mu (k_-^\nu - k_+^\nu) + \gamma^\nu (k_-^\mu - k_+^\mu)]$ .
- spin 3:** A wavy line labeled  $\mu\nu$  with arrows pointing right and left. It splits into two lines labeled  $\rho$  and  $\sigma$ . To its right is the equation  $= -i \frac{g_e e}{2\Lambda} [\gamma^\mu \eta^{\nu\rho} + \gamma^\nu \eta^{\mu\rho}]$ .
- spin 4:** A wavy line labeled  $\mu\nu$  with arrows pointing right and left. It splits into two wavy lines labeled  $k_1$  and  $k_2$ . The top wavy line is labeled  $\rho$  and the bottom wavy line is labeled  $\sigma$ . To its right is the equation  $= -i \frac{g_\gamma}{\Lambda} \Pi_\xi^{\mu\nu\rho\sigma}(k_1, k_2)$ .

where:

$$\begin{aligned} \Pi_\xi^{\mu\nu\rho\sigma}(k_1, k_2) &= \eta^{\rho\sigma} (k_1^\mu k_2^\nu + k_2^\mu k_1^\nu) - \eta^{\mu\rho} k_1^\sigma k_2^\nu - \eta^{\mu\sigma} k_1^\nu k_2^\rho \\ &\quad - \eta^{\nu\sigma} k_1^\mu k_2^\rho - \eta^{\nu\rho} k_1^\sigma k_2^\mu + k_1 \cdot k_2 (\eta^{\mu\sigma} \eta^{\nu\rho} + \eta^{\nu\sigma} \eta^{\mu\rho}) \\ &\quad + \frac{1}{\xi} [-\eta^{\mu\rho} k_2^\sigma k_2^\nu - \eta^{\mu\sigma} k_1^\nu k_1^\rho - \eta^{\nu\sigma} k_1^\mu k_1^\rho - \eta^{\nu\rho} k_2^\sigma k_2^\mu] \end{aligned}$$

when  $\xi = 1$ , in the Feynman gauge, there is a perfect matching between these rules and rules found in [13]<sup>3</sup>.

<sup>3</sup>Although I am not 100% sure about  $X \rightarrow e^+ e^- \gamma$  rule, as it is never listed in the reference.

## 4 Effective coupling with Standard Model

Our resonance  $X$  to be a new particle to extend the Standard Model with. We have to write down the possible effective couplings with the Standard Model particles to try and predict the rates of decay  $\Gamma(X \rightarrow e^-e^+)$  and  $\Gamma(X \rightarrow \gamma\gamma)$ . The diagrams are shown in Figure 1:

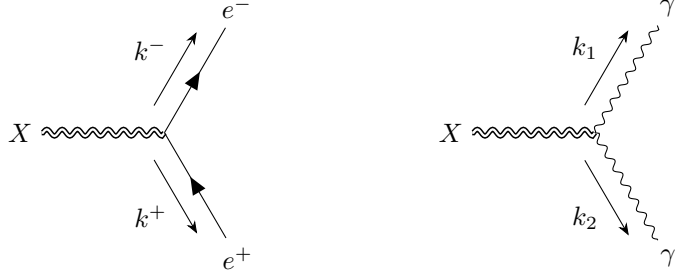


Figure 1: Diagrams corresponding to tree level decay of  $X$  resonance into electron - positron pair and two photons. By conservation of energy,  $p = k_1 + k_2$ .

We are now assuming that our  $X$  resonance is actually a massive spin 2 particle, with mass  $m_X = 17 \text{ MeV}$ . This makes sense if we consider that no other hypothesis can actually explain the experimental data:  $J^P$ 's of  $0^-, 0^+$  are excluded by the ATOMKI collaboration ([21]), while  $1^-, 1^+$  are excluded by the Russian collaboration at JINR, as per Landau Yang theorem the 2 photons channel is impossible for a massive, odd spin resonance (check out subsection F.1).

### 4.1 Representation of a spin 2 massive particle

If we classify the finite dimensional representations of the Lorentz group, we classify  $SU(2) \times SU(2)$  representations. In the proper orthochronous Lorentz group, parity is not included. So, if we classify irreducible representations as  $\mathcal{D}(j_1, j_2)$ , where  $j_1$  is spin of first  $SU(2)$ , and  $j_2$  is spin of second  $SU(2)$ , then the action of parity is studied as follows:

- Call  $J^i$  and  $K^i$  ( $i \in \{1, 2, 3\}$ ) the generators of the Lorentz rotations and boosts, respectively.
- The normalized generators for the individual  $SU(2)$  are obtained through a Wigner rotation into complex numbers. This is because Lorentz group  $SO^\dagger(1, 3)$  is non-compact, while  $SU(2) \times SU(2)$  algebra is. As a result, while Lie algebras should normally be *real* vector spaces, in this example, Lorentz algebra is compact only if complex. Then, generators are:

$$M^i = \frac{1}{2} (J^i + iK^i) \quad N^i = \frac{1}{2} (J^i - iK^i) \quad (4.1)$$

Where  $[M^i, M^j] = i\varepsilon^{ijk} M^k$  and  $[N^i, N^j] = i\varepsilon^{ijk} N^k$  satisfy algebra of rotations.

- Under parity, rotations are left unchanged, but Lorentz boost invert sign:  $\mathcal{P} : J^i \rightarrow J^i$  and  $\mathcal{P} : K^i \rightarrow -K^i$ . Hence, we get  $\mathcal{P} : M^i \rightarrow N^i$ .
- In the language of representations,  $\mathcal{P} : \mathcal{D}(j_1, j_2) \rightarrow \mathcal{D}(j_2, j_1)$ .

Given that we are not going to include chiral terms in our Lagrangian (only vector interactions would be studied, mostly with electrons and photons), parity should be a valid symmetry to be included. This simply requires us to set  $j_1 = j_2$  to obtain a finite dimensional irreducible representation of Lorentz group that also includes parity.

So, the simplest representation of a spin 2 particle that also includes parity is  $\mathcal{D}(1, 1)$ , since  $1 \otimes 1 = 0 \oplus 1 \oplus 2$ . The number of independent degrees of freedom (states) in massive case should be  $3 \times 3 = 1 + 3 + 5$ , so for  $j = 2$  we get 5 possible states.

The challenge is to now derive this consistent representation and a free Lagrangian for any spin 2 massive particle. Because we need to tensorize two vector representations  $V^\mu \sim (0 \oplus 1)$ , then the spin 2 field will be described by 2 independent indices. Take any tensor of this kind, and decompose it in the following way:

$$T^{\mu\nu} \sim V^\mu \otimes V^\nu \sim (0 \oplus 1) \otimes (0 \oplus 1) = (0 \otimes 0) \oplus (1 \otimes 0) \oplus (0 \otimes 1) \oplus (1 \otimes 1) \quad (4.2)$$

so, spin 2 representation is hidden in the spatial part of the tensor  $T^{ij}$ :

$$T^{\mu\nu} = \begin{pmatrix} T^{00} & T^{i0} \\ T^{0j} & T^{ij} \end{pmatrix}$$

and taking  $T^{ij}$ :

$$T^{ij} = \frac{1}{3}\delta^{ij}T^{kk} + \frac{1}{2}(T^{ij} - T^{ji}) + \frac{1}{2}\left(T^{ij} + T^{ji} - \frac{2}{3}\delta^{ij}T^{kk}\right) \quad (4.3)$$

so, we have a trace term which transforms under a spin 0 representation (scalar), as  $\delta^{ij}$  is SU(2) invariant symbol. Then, an antisymmetric tensor part, which because  $i, j \in \{1, 2, 3\}$ , has 3 independent components, so it transforms under a spin 1 representation (vector), and a symmetric, traceless tensor, which has  $6 - 1 = 5$  degrees of freedom, and so it must be the part that transforms under spin 2 representation.

That is to say that our spin 2 particle must be described by a 2 indices tensor field  $X_{\mu\nu}$ , and it must be a symmetric and traceless tensor in Lorentz representation.

## 4.2 Spin 2 Lagrangian

### 4.2.1 Fierz-Pauli Lagrangian

We want to create the most general free Lagrangian possible. Take the field  $X_{\mu\nu}$  and construct the simplest Lorentz invariant operators (dimension 4). Kinetic terms will be obtained by taking two derivatives, while mass terms are obtained when contracting with  $\delta_{\mu\nu}$  (which is our metric, in Pauli notation, so it yields a trace) or itself. If everything not forbidden is compulsory by *Gell-Mann's Totalitarian Principle*, this is the most general Lagrangian:

$$\mathcal{L} = A\partial_\mu X_{\nu\rho} \partial_\mu X_{\nu\rho} + B\partial_\mu X_{\nu\rho} \partial_\nu X_{\mu\rho} + C\partial_\mu X \partial_\mu X_{\nu\rho} + D\partial_\mu X \partial_\mu X + m_X^2(E X_{\nu\rho} X_{\nu\rho} + F X^2) \quad (4.4)$$

with  $X = \delta_{\tau\theta}X_{\tau\theta}$  trace of the field and  $m_X$  has the dimension of a mass to match dimension of the Lagrangian density.

Let us derive the equations of motion:

$$\begin{aligned} \mathcal{H}_{\alpha\beta} &= \partial_\sigma \frac{\partial \mathcal{L}}{\partial (\partial_\sigma X_{\alpha\beta})} - \frac{\partial \mathcal{L}}{\partial \partial_\sigma X_{\alpha\beta}} = \mathcal{H}_{\alpha\beta}^0 - \frac{\partial \mathcal{L}}{\partial \partial_\sigma X_{\alpha\beta}} = \\ &= 2A\delta_{\mu\sigma}\delta_{\alpha\nu}\delta_{\beta\rho}\partial_\sigma\partial_\mu X_{\nu\rho} + B\delta_{\mu\sigma}\delta_{\alpha\nu}\delta_{\beta\rho}\partial_\sigma\partial_\nu X_{\mu\rho} + B\delta_{\nu\sigma}\delta_{\alpha\mu}\delta_{\beta\rho}\partial_\sigma\partial_\mu X_{\nu\rho} + C\delta_{\mu\sigma}\delta_{\tau\theta}\delta_{\alpha\tau}\delta_{\beta\theta}\partial_\rho\partial_\mu X_{\mu\rho} \\ &\quad + C\delta_{\rho\sigma}\delta_{\alpha\mu}\delta_{\beta\rho}\partial_\sigma\partial_\nu X + 2D\delta_{\mu\sigma}\delta_{\tau\theta}\delta_{\alpha\tau}\delta_{\beta\theta}\partial_\sigma\partial_\mu X - 2m_X^2(E\delta_{\alpha\nu}\delta_{\beta\rho}X_{\mu\nu} + F\delta_{\tau\theta}\delta_{\alpha\tau}\delta_{\beta\theta}X) = \\ &= 2A\partial^2 X_{\alpha\beta} + 2B\partial_\alpha\partial_\mu X_{\mu\beta} + C\delta_{\alpha\beta}\partial_\mu\partial_\rho X_{\mu\rho} + C\partial_\alpha\partial_\beta X + 2D\delta_{\alpha\beta}\partial^2 X - 2m_X^2(E X_{\alpha\beta} + F\delta_{\alpha\beta}X) = \\ &= \left(2A\partial^2 + 2B\delta_{\alpha\rho}\delta_{\alpha\mu}\partial_\mu\partial_\rho + C\delta_{\alpha\beta}\delta_{\alpha\mu}\delta_{\beta\rho}\partial_\mu\partial_\rho - 2m_X^2E\right)X_{\alpha\beta} + \left(C\partial_\alpha\partial_\beta + 2D\delta_{\alpha\beta}\partial^2 - 2m_X^2F\delta_{\alpha\beta}\right)X = \\ &= \left[(2A + 2B + C)\partial^2 - 2m_X^2E\right]X_{\alpha\beta} + \left(C\partial_\alpha\partial_\beta + 2D\delta_{\alpha\beta}\partial^2 - 2m_X^2F\delta_{\alpha\beta}\right)X = 0 \end{aligned} \quad (4.5)$$

where  $\mathcal{H}_{\alpha\beta}^0$  is the expression for the equations of motion in the case  $m_X = 0$ .

We reason as follows. If  $m_X = 0$ , then we get a massless spin 2 state, which is redundantly described in the Lagrangian and hence it requires *gauge invariance* to be consistent. Because  $X_{\mu\nu}$  is symmetric, the most general gauge transformation must take the form:

$$\delta X_{\mu\nu} = \partial_\mu\xi_\nu + \partial_\nu\xi_\mu \quad (4.7)$$

with  $\xi_\mu$  arbitrary local vector. Then, applying Gell-Mann/Levy trick:

$$\delta\mathcal{L} = \mathcal{H}_{\alpha\beta}^0\delta X_{\alpha\beta} = -\partial_\alpha\mathcal{H}_{\alpha\beta}^0\xi_\beta \quad (4.8)$$

when integrating by parts and ignoring total derivative contribution. Imposing gauge invariance means  $\delta\mathcal{L} = 0$ , so  $\partial_\alpha\mathcal{H}_{\alpha\beta}^0 = 0$  as gauge invariance condition. From [Equation 4.6](#) in massless case we get:

$$\partial_\alpha\mathcal{H}_{\alpha\beta}^0 = (2A + 2B + C)\partial_\alpha\partial^2 X_{\alpha\beta} + (C + 2D)\partial_\beta X = 0 \quad (4.9)$$

which requires  $C + 2D = 0$ , and  $2A + 2B + C = 0$ . Taking directly the derivative from the definition, you actually get different individual constraints such as  $2A + B = 0$  and  $B + C = 0$ . Hence, we select (for normalization purposes):

$$2A = -B = C = -2D = -1 \quad (4.10)$$

When reintroducing  $m_X \neq 0$ , we get the general Lagrangian:

$$\mathcal{L} = -\frac{1}{2}\partial_\mu X_{\nu\rho} \partial_\mu X_{\nu\rho} + \partial_\mu X_{\nu\rho} \partial_\nu X_{\mu\rho} - \partial_\mu X \partial_\mu X_{\nu\rho} + \frac{1}{2}\partial_\mu X \partial_\mu X + m_X^2 (E X_{\nu\rho} X_{\nu\rho} + F X^2) \quad (4.11)$$

and from [Equation 4.5](#):

$$\mathcal{H}_{\alpha\beta} = -\partial^2 X_{\alpha\beta} + 2\partial_\alpha \partial_\mu X_{\mu\beta} - \delta_{\alpha\beta} \partial_\mu \partial_\rho X_{\mu\rho} - \partial_\alpha \partial_\beta X + \delta_{\alpha\beta} \partial^2 X - 2m_X^2 (E X_{\alpha\beta} + F \delta_{\alpha\beta} X) = 0 \quad (4.12)$$

Now, by construction, we impose the same gauge condition (which then become *subsidiary conditions*, similarly to the massive vector field formalism):

$$\partial_\alpha \mathcal{H}_{\alpha\beta} = \cancel{\partial_\alpha \mathcal{H}_{\alpha\beta}} + m_X^2 (E \partial_\alpha X_{\alpha\beta} + F \partial_\beta X) = 0 \quad (4.13)$$

If we go to momentum space, we get:  $X_{\mu\nu} = \tilde{X}_{\mu\nu} e^{ikx}$ , which translates to:

$$E k_\alpha \tilde{X}_{\alpha\beta} + F k_\beta \tilde{X} = 0 \quad (4.14)$$

which are a set of 4 independent equations that we can impose<sup>4</sup> on  $X_{\mu\nu}$ . Because we already knew it was symmetric, the starting number of independent degrees of freedom in  $D = 4$  is 10 for any symmetric tensor. These conditions reduce them to 6.

We still need one more condition to get down to 5. With generic  $E$  and  $F$ , this is not guaranteed to happen, and a leftover "ghost" field will account for the unphysical degree of freedom. However, if we select  $E = -F$ , as Fierz and Pauli showed ([\[24\]](#)), we can get rid of the ghost field (at least at this quadratic order in the theory). For normalization purposes, we select  $E = 1/2$ :

$$\mathcal{L} = -\frac{1}{2}\partial_\mu X_{\nu\rho} \partial_\mu X_{\nu\rho} + \partial_\mu X_{\nu\rho} \partial_\nu X_{\mu\rho} - \partial_\mu X \partial_\mu X_{\nu\rho} + \frac{1}{2}\partial_\mu X \partial_\mu X + \frac{m_X^2}{2} (X_{\nu\rho} X_{\nu\rho} - X^2) \quad (4.15)$$

and from [Equation 4.5](#):

$$\mathcal{H}_{\alpha\beta} = -\partial^2 X_{\alpha\beta} + 2\partial_\alpha \partial_\mu X_{\mu\beta} - \delta_{\alpha\beta} \partial_\mu \partial_\rho X_{\mu\rho} - \partial_\alpha \partial_\beta X + \delta_{\alpha\beta} \partial^2 X - m_X^2 (X_{\alpha\beta} - \delta_{\alpha\beta} X) = 0 \quad (4.16)$$

this special Lagrangian is called *Fierz-Pauli Lagrangian*. Subsidiary conditions become:

$$\partial_\alpha \mathcal{H}_{\alpha\beta} = \partial_\alpha X_{\alpha\beta} - \partial_\beta X = 0 \quad (4.17)$$

If we go to momentum space:

$$k_\alpha \tilde{X}_{\alpha\beta} - k_\beta \tilde{X} = 0 \quad (4.18)$$

We have another trick. Take another divergence of [Equation 4.17](#):

$$\partial_\alpha \partial_\beta \mathcal{H}_{\alpha\beta} = \partial_\alpha \partial_\beta X_{\alpha\beta} - \partial^2 X = 0 \quad (4.19)$$

and compare them with the trace of the equations of motion:

$$\begin{aligned} \mathcal{H}_{\alpha\alpha} &= -\partial^2 X + 2\partial_\alpha \partial_\mu X_{\alpha\mu} - 4\partial_\mu \partial_\rho X_{\mu\rho} - \partial^2 X + 4\partial^2 X - m_X^2 (X - 4X) = \\ &= -2 (\cancel{\partial_\alpha \partial_\beta X_{\alpha\beta}} - \partial^2 X) - 3m_X^2 X = 0 \end{aligned} \quad (4.20)$$

which allows cancellation only because  $E = -F$ . One is left with  $X = 0$ , *traceless condition* that allows us to reduce the independent components of  $X_{\mu\nu}$  from 6 to 5, as requested. Also, notice that  $\tilde{X} = 0$  in momentum space, as well. The approach we just described is at the basis of the popular *Randall-Sundrum Model* for spin 2 massive graviton ([\[13\]](#)), which is an effective model coming from expanding metric fluctuations around Minkowskian background using a special decomposition, called Kaluza-Klein decomposition. This derivation is a bit more general, and has been employed consistently to describe not only a massive graviton, but any spin 2 resonant state as well ([\[14\]](#)).

<sup>4</sup>This method gets rid of the temporal, unphysical component of a massive vector field. For a spin 2 boson, we have not one but four constraints.

Our five independent conditions become  $\partial_\alpha X_{\alpha\beta} = 0$  and  $X = 0$ , which simplify the Lagrangian:

$$\mathcal{L} = \frac{1}{2} \partial_\mu X_{\nu\rho} \partial_\mu X_{\nu\rho} + \frac{m_X^2}{2} X_{\nu\rho} X_{\nu\rho} \quad (4.21)$$

and the equations of motion:

$$\mathcal{H}_{\alpha\beta} = \left( -\partial^2 + m_X^2 \right) X_{\alpha\beta} = 0 \quad (4.22)$$

which are revisited Klein-Gordon equations for massive spin 2 fields.

The propagator is, then:

$$D_{\mu\nu\rho\sigma}(x-y) = \int \frac{d^4 p}{(2\pi)^4 i} \hat{D}_{\mu\nu\rho\sigma}^X(p) e^{ip(x-y)} \quad (4.23)$$

where we define the propagator in momentum space as:

$$\hat{D}_{\mu\nu\rho\sigma}^X(p) = \frac{N_{\mu\nu\rho\sigma}(p)}{p^2 + m_X^2} \quad (4.24)$$

as we know that the numerator of the propagator must be the sum over all physical polarizations, because of unitarity.

To get polarizations, let us now expand the  $X_{\mu\nu}$  field:

$$X_{\mu\nu}(x) = \sum_{\lambda=1}^5 \int \frac{d^3 k}{(2\pi)^3 \sqrt{2\omega_{\vec{k}}}} \left[ a_\lambda(\vec{k}) \varepsilon_{\mu\nu}(\vec{k}, \lambda) e^{-ik \cdot x} + b_\lambda^\dagger(\vec{k}) \varepsilon_{\mu\nu}^*(\vec{k}, \lambda) e^{ik \cdot x} \right] \quad (4.25)$$

where  $\omega_{\vec{k}} = \sqrt{|\vec{k}|^2 + m_X^2}$ .

It is also possible to prove a completeness relation for the spin polarizations:

$$\sum_{\lambda=1}^5 \varepsilon_{\mu\nu}(\vec{k}, \lambda) \varepsilon_{\rho\sigma}^*(\vec{k}, \lambda) = \frac{1}{2} (P_{\mu\rho} P_{\nu\sigma} + P_{\mu\sigma} P_{\nu\rho}) - \frac{1}{3} P_{\mu\nu} P_{\rho\sigma} = N_{\mu\nu\rho\sigma}(k) \quad (4.26)$$

$$\text{where } P_{\mu\nu} = \delta_{\mu\nu} + \frac{k_\mu k_\nu}{m_X^2}$$

### 4.2.2 Non-Universal Couplings Model

The most general interaction Lagrangian between a spin 2 particle and the Standard Model is not easily written. Coming from UV completing theories, a massive graviton arises in an effective landscape, quantizing metric fluctuations in General Relativity. As such, its equations of motion must be *Einstein field equations*. It is easy to show that Fierz-Pauli effective action reproduces the linearized Einstein tensor (from [Equation 4.15](#)), with the addition of a mass dependence. In fact, final EOMs in [Equation 4.22](#) can actually be written as:

$$\mathcal{H}_{\mu\nu} = 0 \quad (4.27)$$

where  $\mathcal{H}_{\mu\nu}$  is the Einstein tensor. Then, Einstein field equations are easily reproduced by taking  $\mathcal{H}_{\mu\nu} \propto T_{\mu\nu}$ ,  $T_{\mu\nu}$  being *stress-energy tensor*, which implies that:

$$\frac{\partial \mathcal{L}_{\text{matter}}}{\partial X_{\mu\nu}} \propto T_{\mu\nu} \quad (4.28)$$

where:

$$T_{\mu\nu} = \frac{\partial \mathcal{L}}{\partial (\partial_\mu \phi_i)} \partial_\nu \phi_i - \delta_{\mu\nu} \mathcal{L} \quad \Rightarrow \quad \mathcal{L}_{\text{matter}} \ni \frac{g}{\Lambda} X_{\mu\nu} T_{\mu\nu} \quad (4.29)$$

Since we get a dimension 5 effective operator, the effective constant in front is dimensional (and real), and we split it into a  $\mathcal{O}(1)$  adimensional coupling  $g$  and a momentum cutoff  $\Lambda$ , which we will set to be the same for each interaction. Clearly, an interaction of this kind is *non renormalizable*, and the theory of spin 2 particles is only effective, meaning does not behave properly at high energies and it should be replaced by some UV completion.

This is not the most general coupling with matter, as explored in [subsubsection 4.2.3](#), nor is it justified to be the correct coupling for any spin 2 resonance, even  $X17$ , which probably does not have the same origin as a massive graviton. Still, stress-energy tensor coupling is the simplest, lowest-dimensional two-indices structure which makes physical sense to couple to a spin 2 field, and it is not very far off from the most general case. So, we decided to adopt [Equation 4.29](#) as our toy model for this dissertation.

Since we are interested in couplings with electrons and photons, let us derive the stress-energy tensors for fermions and photons from the Lagrangian:

**Fermions:** The free Lagrangian is:

$$\mathcal{L} = -\bar{\psi} (\not{D} + m) \psi = -\frac{1}{2} \bar{\psi} \gamma_\mu \partial_\mu \psi + \frac{1}{2} \partial_\mu \bar{\psi} \gamma_\mu \psi - m \bar{\psi} \psi \quad (4.30)$$

Using Dirac's equation to cancel the term  $\delta_{\mu\nu} \mathcal{L}$  in the definition of  $T_{\mu\nu}$ , we get for the stress-energy tensor:

$$\begin{aligned} T_{\mu\nu} &= \frac{\partial \mathcal{L}}{\partial (\partial_\mu \psi)} \partial_\nu \psi + \partial_\nu \bar{\psi} \frac{\partial \mathcal{L}}{\partial (\partial_\mu \bar{\psi})} = \\ &= -\frac{1}{2} \bar{\psi} \gamma_\mu \partial_\nu \psi + \frac{1}{2} \partial_\nu \bar{\psi} \gamma_\mu \psi \end{aligned} \quad (4.31)$$

which has then to be symmetrized if we remember that it has to be contracted with  $X_{\mu\nu}$ , symmetric in  $\mu \leftrightarrow \nu$  exchange (both the physical polarizations and the propagators are, in fact, symmetric):

$$T_{\mu\nu} = -\frac{1}{4} \bar{\psi} \gamma_\mu \partial_\nu \psi - \frac{1}{4} \bar{\psi} \gamma_\nu \partial_\mu \psi + \frac{1}{4} \partial_\nu \bar{\psi} \gamma_\mu \psi + \frac{1}{4} \partial_\mu \bar{\psi} \gamma_\nu \psi \quad (4.32)$$

**Electrodynamics gauge interaction:** In QED, fermions interact with photons thanks to the covariant derivative, introduced to locally gauge U(1) symmetry. For electrons:

$$\partial_\mu \rightarrow D_\mu = \partial_\mu - ie A_\mu \quad (4.33)$$

This has repercussions on the Lagrangian, which becomes:

$$\mathcal{L} = -\bar{\psi} (\not{D} + m) \psi \quad (4.34)$$

and the stress-energy tensor for electrons  $T_{\mu\nu}$  (Equation 4.31), which has now a covariant derivative definition. Exploiting the exchange index symmetry of  $X_{\mu\nu}$ :

$$\begin{aligned} T_{\mu\nu} &= \frac{\partial \mathcal{L}}{\partial (D_\mu \psi)} D_\nu \psi + D_\nu \bar{\psi} \frac{\partial \mathcal{L}}{\partial (D_\mu \bar{\psi})} = -\bar{\psi} \gamma_\mu D_\nu \psi = \\ &= -\frac{1}{2} \bar{\psi} \gamma_\mu D_\nu \psi - \frac{1}{2} \bar{\psi} \gamma_\nu D_\mu \psi \end{aligned} \quad (4.35)$$

which adds naturally interaction with a photon:

$$T_{\mu\nu} \ni ie \left[ \frac{1}{2} \bar{\psi} \gamma_\mu A_\nu \psi + \frac{1}{2} \bar{\psi} \gamma_\nu A_\mu \psi \right] \quad (4.36)$$

**Photons:** We are going to write down the Lagrangian with a gauge fixing term dependent on the real parameter  $\xi$ :

$$\mathcal{L} = -\frac{1}{4} F_{\rho\sigma} F_{\rho\sigma} - \frac{1}{2\xi} (\partial_\rho A_\rho)^2 \quad (4.37)$$

Any amplitude must be independent of the gauge choice  $\xi$ , so keeping it as a parameter is a useful cross-check of our calculations. Of course, we can recover:

- T'Hooft-Feynman gauge when  $\xi = 1$ . This is the most used gauge for loop calculations.
- Lorentz gauge when  $\xi \rightarrow \infty$ , which imposes the condition  $\partial_\rho A_\rho = 0$  on the action. It corresponds to the *unitary* gauge in abelian gauge theories, and it is useful for tree level calculations as it only deals with physical degrees of freedom.

It is useful to recover the *equations of motion* in a generic  $\xi$  gauge, by setting the functional derivative of the action to zero. This gives rise to Euler-Lagrange equations for the photon field. Let us calculate them:

$$\begin{aligned} \frac{\partial \mathcal{L}}{\partial (\partial_\mu A_\beta)} &= -\frac{1}{2} (\delta_{\rho\mu} \delta_{\beta\sigma} - \delta_{\rho\beta} \delta_{\mu\sigma}) F_{\rho\sigma} - \frac{1}{\xi} \left( \frac{1}{2} \delta_{\mu\rho} \delta_{\rho\beta} \partial_\sigma A_\sigma + \frac{1}{2} \delta_{\mu\sigma} \delta_{\sigma\beta} \partial_\sigma A_\sigma \right) = \\ &= -F_{\mu\beta} - \frac{1}{\xi} \delta_{\mu\beta} \partial_\rho A_\rho \end{aligned} \quad (4.38)$$

so, EOMs are:

$$\partial_\mu \frac{\partial \mathcal{L}}{\partial (\partial_\mu A_\beta)} - \cancel{\frac{\partial \mathcal{L}}{\partial A_\beta}} = 0 \quad (4.39)$$

which means:

$$\begin{aligned} \partial_\mu (-\partial_\mu A_\nu + \partial_\nu A_\mu) - \frac{1}{\xi} \delta_{\mu\beta} \partial_\mu \partial_\sigma A_\sigma &= 0 \\ -\partial_\mu \partial_\mu A_\nu + \left(1 - \frac{1}{\xi}\right) \partial_\mu \partial_\nu A_\mu &= 0 \\ \square A_\nu - \left(1 - \frac{1}{\xi}\right) \partial_\mu \partial_\nu A_\mu &= 0 \end{aligned} \quad (4.40)$$

with  $\xi = 1$  we recover the electromagnetic wave equation  $\square A_\nu = 0$ . While, instead, the stress-energy tensor is:

$$\begin{aligned} T_{\mu\nu} &= \frac{\partial \mathcal{L}}{\partial (\partial_\mu A_\beta)} \partial_\nu A_\beta - \delta_{\mu\nu} \mathcal{L} = \\ &= -\frac{1}{2} (\delta_{\rho\mu} \delta_{\beta\sigma} - \delta_{\rho\beta} \delta_{\mu\sigma}) F_{\rho\sigma} \partial_\nu A_\beta - \frac{1}{\xi} \delta_{\mu\beta} \partial_\sigma A_\sigma \partial_\nu A_\beta - \delta_{\mu\nu} \mathcal{L} = \\ &= -F_{\mu\beta} \partial_\nu A_\beta - \frac{1}{\xi} \partial_\sigma A_\sigma \partial_\nu A_\mu - \delta_{\mu\nu} \mathcal{L} = \\ &= -F_{\mu\beta} F_{\nu\beta} - \partial_\mu A_\beta \partial_\beta A_\nu + \partial_\beta A_\mu \partial_\beta A_\nu - \frac{1}{\xi} \partial_\beta A_\beta \partial_\nu A_\mu - \delta_{\mu\nu} \mathcal{L} \end{aligned} \quad (4.41)$$

The term:

$$\partial_\beta A_\mu \partial_\beta A_\nu \rightarrow -A_\mu \square A_\nu = -\left(1 - \frac{1}{\xi}\right) A_\mu \partial_\beta \partial_\nu A_\beta \quad (4.42)$$

because of integration by parts and the equations of motion for the photons (Equation 4.40). We also apply integration by parts for the terms  $\partial_\mu A_\beta \partial_\beta A_\nu \rightarrow -A_\nu \partial_\mu \partial_\beta A_\beta$ , and  $\partial_\beta A_\beta \partial_\nu A_\mu \rightarrow -A_\mu \partial_\nu \partial_\beta A_\beta$ . The final result is:

$$T_{\mu\nu} = -F_{\mu\beta} F_{\nu\beta} + A_\nu \partial_\mu \partial_\beta A_\beta + \left(\frac{2}{\xi} - 1\right) A_\mu \partial_\nu \partial_\beta A_\beta - \delta_{\mu\nu} \mathcal{L} \quad (4.43)$$

Notice how in the Lorentz gauge  $\partial_\beta A_\beta = 0$  we recover the symmetric Belinfante stress-energy tensor:

$$T_{\mu\nu} = -F_{\mu\beta} F_{\nu\beta} + \frac{1}{4} \delta_{\mu\nu} F_{\rho\sigma} F_{\rho\sigma} \quad (4.44)$$

Coupling to the Standard Model implies coupling to the *total* stress energy tensor  $T_{\mu\nu}$  derived by the Lagrangian of the Standard Model, of which so far we have only seen one small part (interaction with electrons and photons). The simplest interaction would then require only one universal coupling constant:

$$\mathcal{L} = \frac{g}{\Lambda} X_{\mu\nu} T_{\mu\nu} \quad (4.45)$$

This is, in a way, the most natural way to write the interaction, because the stress-energy tensor  $T_{\mu\nu}$  is a conserved quantity:  $\partial_\mu T_{\mu\nu} = 0$ .

However, the requirement that the stress-energy tensor is conserved is always an assumed but arbitrary rule<sup>5</sup>. One can, just as easily, imagine a model where this is not the case:

$$\mathcal{L} = X_{\mu\nu} \sum_i \frac{g_i}{\Lambda} T_{\mu\nu}^i \quad (4.46)$$

where  $i$  is the index running through each field. If couplings are different, clearly it is no longer true that  $\partial_\mu T_{\mu\nu}^i = 0$ .

This choice has an effect. In particular, it has to do with *unitarity*. Effective field theories produce corrections in amplitudes that increase with energy. Too fast of a growth, however, may result in particles interacting with probability larger than 1, clearly violating unitarity of the  $S$ -matrix. In particular, there exists a famous bound by Froissart ([44]) that tells us that a sufficient condition for unitarity is:

$$|\mathcal{A}| < \mathcal{O}(s \log^2 s) \quad \Rightarrow \quad \sigma < \mathcal{O}(\log^2 s) \quad (4.47)$$

$\mathcal{A}$  being the total amplitude of the process, and  $\sigma$  being the total cross section. The link between amplitude and cross section is the *optical theorem*:

$$\sigma = \frac{4\pi}{k} \text{Im}(\mathcal{A}) \quad (4.48)$$

<sup>5</sup>As a matter of fact, there are many Lagrangian theories that do not assume a conserved stress energy tensor - such as?

with  $k$  being the 3-momentum of one particle in the rest frame of the other particle (then  $s \approx 2k$ ).

Then, the more (positive) terms appear in any amplitude, the more likely it is that unitarity might break when growing with energy. Specifically, in the universal coupling model for a spin 2 massive boson, the momentum dependence in the propagator always disappears due to the conservation of the stress-energy tensor:

$$\frac{p_\mu p_\nu}{m_X^2} T_{\mu\nu} = 0$$

cancelling the fastest increasing terms with momentum. Instead, in the non universal coupling model this is no longer true, and we get extra terms in amplitudes, which may contribute, in some cases, to unitarity violation.

Fortunately, this does not happen in any of the processes that we are about to discuss in this dissertation (verified by simply checking the final formulas that we obtain with all couplings equal). Indeed, processes for which the non-universality breaks unitarity usually involve our spin 2 particles as one of the external legs (which never happens in the standard QED processes we want to correct).

For the aforementioned reasons, we introduce a different coupling for each field of the Standard Model. In this thesis, we will focus only on the coupling to electrons/positrons (we will call it  $g_e/\Lambda$ ) and the coupling to photons (that we name  $g_\gamma/\Lambda$ ).

#### 4.2.3 General interaction with matter

As we mentioned, coupling to the stress-energy tensor is not the most general coupling. In [14], they analyze any spin 2 massive resonance whose free action is described by Randall-Sundrum Model.

Focusing on production of a resonance  $X$ , calling  $\lambda_1, \lambda_2$  the helicities of the initial state  $i$  (in our case, since for now we are only focusing on electrodynamics, electrons or photons), and  $m$  the projected spin along  $z$  axis for the  $J = 2$  spin resonance, in its rest frame, the amplitudes for production with fixed helicities are parameterized using the following seven coefficients:

$$\begin{aligned} A_{++}^{\gamma\gamma} &= g_0^\gamma + i\tilde{g}_0^\gamma \\ A_{--}^{\gamma\gamma} &= g_0^\gamma - i\tilde{g}_0^\gamma \\ A_{-+}^{\gamma\gamma} &= A_{+-}^{\gamma\gamma} = g_2^\gamma \\ \\ A_{++}^{ee} &= g_0^e + i\tilde{g}_0^e \\ A_{--}^{ee} &= g_0^e - i\tilde{g}_0^e \\ A_{-+}^{ee} &= g_1^e \\ A_{+-}^{ee} &= g_{-1}^e \end{aligned}$$

where  $\pm = \pm 1$  for photons, and  $\pm = \pm 1/2$  for electrons.  $g_m$  are parity even coefficients,  $\tilde{g}_m$  are parity odd coefficients, with  $m = \lambda_1 - \lambda_2$  by kinematics selection rule.

Since individual helicities are not accessible to experiments, they calculate helicity-averaged amplitudes for resonance production:

$$\begin{aligned} \mathcal{A}(\gamma\gamma \rightarrow X) &= \frac{\sqrt{6} g_0^\gamma}{\Lambda^3} \varepsilon_{\mu\nu} p_\mu p_\nu [(\varepsilon_1 \cdot k_2)(\varepsilon_2 \cdot k_1) - (\varepsilon_1 \cdot \varepsilon_2)(k_1 \cdot k_2)] \\ &+ \frac{\sqrt{6} \tilde{g}_0^\gamma}{\Lambda^3} \epsilon_{\mu\nu\alpha\beta} \varepsilon_{1,\mu} \varepsilon_{2,\mu} k_{1,\alpha} k_{2,\beta} (\varepsilon_{\mu\nu} p_\mu p_\nu) \\ &+ \frac{\sqrt{6} g_2^\gamma}{\Lambda} \varepsilon_{\mu\nu} \left[ -(\varepsilon_1 \cdot k_2) p_\mu \varepsilon_{2,\nu} + (\varepsilon_2 \cdot k_1) p_\mu \varepsilon_{1,\nu} + 2(k_1 \cdot k_2) \varepsilon_{1,\mu} \varepsilon_{2,\nu} - \frac{1}{2} (\varepsilon_1 \cdot \varepsilon_2) p_\mu p_\nu \right] \quad (4.49) \end{aligned}$$

$$\begin{aligned} \mathcal{A}(e^+ e^- \rightarrow X) &= -\sqrt{\frac{3}{2}} \frac{g_0^e}{\Lambda^2} \bar{v}_2 u_1 (\varepsilon_{\mu\nu} p_\mu p_\nu) + \sqrt{\frac{3}{2}} \frac{\tilde{g}_0^e}{\Lambda^2} \bar{v}_2 i\gamma_5 u_1 (\varepsilon_{\mu\nu} p_\mu p_\nu) \\ &+ \varepsilon_{\mu\nu} p_\nu \left[ \frac{g_1^e}{\Lambda} \bar{v}_2 \left( \frac{1+\gamma_5}{2} \right) \gamma_\mu u_1 + \frac{\tilde{g}_1^e}{\Lambda} \bar{v}_2 \left( \frac{1-\gamma_5}{2} \right) \gamma_\mu u_1 \right] \quad (4.50) \end{aligned}$$

with  $\varepsilon_{\mu\nu}$  being the resonance polarization,  $p, k_1, k_2$  being the momenta of the resonance and the initial state, respectively,  $\varepsilon_i$  are the photon polarizations and  $\bar{v}_2$  and  $u_1$  are the  $e^+$  and  $e^-$  spinors.

We will not justify this result. Finally, they outline the on shell spin 2 Lagrangian that can produce

[Equation 4.49](#) and [Equation 4.50](#):

$$\begin{aligned}\mathcal{L} = & X_{\mu\nu} \left[ -\frac{g_2^\gamma}{\Lambda} F_{\mu\alpha} F_{\nu\alpha} - \frac{\sqrt{6} g_0^\gamma}{\Lambda^3} \partial_\mu F_{\alpha\beta} \partial_\nu F_{\alpha\beta} + \frac{\sqrt{6} \tilde{g}_0^\gamma}{\Lambda^3} \partial_\mu F_{\alpha\beta} \partial_\nu \tilde{F}_{\alpha\beta} \right] \\ & + X_{\mu\nu} \left[ \frac{g_1^e}{\Lambda} \bar{\psi} \left( \frac{1+\gamma_5}{2} \right) \gamma_\mu \partial_\nu \psi + \frac{\tilde{g}_1^e}{\Lambda} \bar{\psi} \left( \frac{1-\gamma_5}{2} \right) \gamma_\mu \partial_\nu \psi - 4\sqrt{\frac{3}{2}} \frac{g_0^e}{\Lambda^2} \partial_\mu \bar{\psi} \partial_\nu \psi + 4\sqrt{\frac{3}{2}} \frac{\tilde{g}_0^e}{\Lambda^2} \partial_\mu \bar{\psi} i\gamma_5 \partial_\nu \psi \right]\end{aligned}\quad (4.51)$$

where  $\tilde{F}_{\alpha\beta} = 1/2\epsilon_{\mu\nu\alpha\beta}F_{\mu\nu}$  is the dual electromagnetic tensor. Finally, it is worth mentioning that the operator  $F_{\mu\alpha} \tilde{F}_{\nu\alpha}$  does not appear, as there is a nice identity (number 3.17 in [\[20\]](#), only in dimension 4 spacetime):

$$X_{\mu\nu} F_{\mu\alpha} \tilde{F}_{\nu\alpha} = \frac{1}{4} X_{\mu\mu} F_{\nu\alpha} \tilde{F}_{\nu\alpha}\quad (4.52)$$

which disappears as  $X_{\mu\mu} = 0$  as we know.

This is the most general interaction Lagrangian between a spin 2 resonance (whatever its origin) and electrodynamics. Notice that:

- The lowest dimension operator is 5. Higher order operators have higher powers of the scale  $\Lambda$  at the denominator. In effective theories,  $\Lambda$  is a scale that works as a breaking point for the theory, while  $g_i$  are order 1 coefficients, meaning that as long as energy is below  $\Lambda$ , higher dimension operators will be less relevant. We will neglect these operators in this thesis.
- There are parity odds and parity even operators in the Lagrangian. For a parity invariant theory, the parity of the resonance selects only certain operators<sup>6</sup>.

In particular, dealing with a  $2^+$  resonance, we have to select  $g_1^e = \tilde{g}_1^e = g_e$ ,  $g_2^\gamma = g_\gamma$ , and ignore all other parity odd operators or higher dimension operators:

$$\mathcal{L} = X_{\mu\nu} \left[ -\frac{g_\gamma}{\Lambda} F_{\mu\alpha} F_{\nu\alpha} + \frac{g_e}{\Lambda} \bar{\psi} \gamma_\mu \partial_\nu \psi \right] = \frac{g_\gamma}{\Lambda} X_{\mu\nu} T_{\mu\nu}^\gamma + \frac{g_e}{\Lambda} X_{\mu\nu} T_{\mu\nu}^e\quad (4.53)$$

which is exactly the expression [Equation 4.46](#), the Lagrangian we have chosen in the previous section as non-universal coupling model.

While, dealing with a  $2^-$  resonance, select  $g_1^e = -\tilde{g}_1^e = g_e$ ,  $\tilde{g}_0^\gamma = g_\gamma$ , and ignore all other parity even operators and higher dimensional operators:

$$\mathcal{L} = X_{\mu\nu} \left[ \frac{\sqrt{6} g_\gamma}{\Lambda^3} \partial_\mu F_{\alpha\beta} \partial_\nu \tilde{F}_{\alpha\beta} + \frac{g_e}{\Lambda} \bar{\psi} \gamma_5 \gamma_\mu \partial_\nu \psi \right]\quad (4.54)$$

which presents a highly suppressed photon channel (dimension 7 operator). This is not the model we have chosen here.

To sum it up, [Equation 4.46](#) is the most general Lagrangian only in a parity defined theory, with even parity of the resonance. Here forth, we will always treat the  $2^+$  spin model.

### 4.3 Feynman rules

We are ready to derive the Feynman rules for the vertices of interaction between our massive spin 2 boson  $X$  with fermions and photons. All we have to do is to simply write the interaction in momentum space, so that our fields are substituted by their respective polarizations and  $\partial_\mu$  gets replaced with  $-ik_\mu$ .

**Fermions:** The interaction Lagrangian becomes, using [Equation 4.31](#) and [Equation 4.46](#):

$$\mathcal{L} = \frac{g_e}{\Lambda} X_{\mu\nu} T_{\mu\nu} = \frac{g_e}{4\Lambda} X_{\mu\nu} \left[ -\bar{\psi} \gamma_\mu \partial_\nu \psi - \bar{\psi} \gamma_\nu \partial_\mu \psi + \partial_\nu \bar{\psi} \gamma_\mu \psi + \partial_\mu \bar{\psi} \gamma_\nu \psi \right]\quad (4.55)$$

where  $g_e/\Lambda$  is the effective Wilson coefficient for the dimension 5 operator describing the interaction.

When going to momentum space, labeling the momenta according to the left diagram in [Figure 1](#) and

---

<sup>6</sup>Remember that our spin 2 irreducible representation includes parity, check out [subsection 4.1](#).

using  $\partial_\mu \rightarrow -ik_\mu$ :

$$= i \frac{g_e}{4\Lambda} \left[ \gamma_{\mu} (k_{\nu}^- - k_{\nu}^+) + \gamma_{\nu} (k_{\mu}^- - k_{\mu}^+) \right] \quad (4.56)$$

To remember the rule, we have to just write down the 4-momenta in the order given by the fermion arrow. This is to be contracted with the spin polarization of the spin 2 boson ( $\varepsilon_{\mu\nu}(p, \eta)$ ) and the 2 fermions ( $u(k^-, \lambda^-), v(k^+, \lambda^+)$ ).

**Electrodynamics gauge interaction:** We left the term in [Equation 4.36](#) out. We get one more interaction with the coupling  $g_e$  when considering it:

$$\mathcal{L} = -i \frac{g_e e}{2\Lambda} X_{\mu\nu} [\bar{\psi} \gamma_\mu A_\nu \psi + \bar{\psi} \gamma_\nu A_\mu \psi] \quad (4.57)$$

When going to momentum space, calling  $\varepsilon_\mu$  the photon polarization and  $\varepsilon_{\mu\nu}$  the  $X$  polarization:

$$\mathcal{L} = -i \frac{g_e e}{2\Lambda} \varepsilon_{\mu\nu} [\bar{\psi} \gamma_\mu \varepsilon_\nu \psi + \bar{\psi} \gamma_\nu \varepsilon_\mu \psi] \quad (4.58)$$

now, when removing the polarizations, we get the Feynman rule. Substitute polarization of the photon with one Lorentz index (call it  $\rho$ ), to get:

$$= -i \frac{g_e e}{2\Lambda} [\gamma_{\mu} \delta_{\nu\rho} + \gamma_{\nu} \delta_{\mu\rho}] \quad (4.59)$$

To be contracted with the spin polarization of the spin 2 boson ( $\varepsilon_{\mu\nu}(p, \eta)$ ), the 2 fermions ( $u(p^-, s^-), v(p^+, s^+)$ ), and the photon  $\varepsilon_\rho(k, \lambda)$ .

**Photons:** Starting from the stress-energy tensor, written as in [Equation 4.43](#) and [Equation 4.46](#), we get:

$$T_{\mu\nu} = -\partial_\mu A_\beta \partial_\nu A_\beta + \partial_\beta A_\mu \partial_\nu A_\beta + \partial_\mu A_\beta \partial_\beta A_\nu - \partial_\beta A_\mu \partial_\beta A_\nu + A_\nu \partial_\mu \partial_\beta A_\beta + \left( \frac{2}{\xi} - 1 \right) A_\mu \partial_\nu \partial_\beta A_\beta \quad (4.60)$$

The  $\delta_{\mu\nu}$  term gets canceled because the polarizations for  $X_{\mu\nu}$  are traceless, so in the contraction  $\mathcal{L}X_{\mu\mu} = 0$ .

Finally, because  $X_{\mu\nu}$  is symmetric in the exchange  $\mu \leftrightarrow \nu$ , we can eliminate the antisymmetric part and symmetrize what is left of the last two terms in [Equation 4.60](#):

$$T_{\mu\nu} = -\partial_\mu A_\beta \partial_\nu A_\beta + \partial_\beta A_\mu \partial_\nu A_\beta + \partial_\mu A_\beta \partial_\beta A_\nu - \partial_\beta A_\mu \partial_\beta A_\nu + \frac{1}{\xi} (A_\nu \partial_\mu \partial_\beta A_\beta + A_\mu \partial_\nu \partial_\beta A_\beta) \quad (4.61)$$

When going to momentum space, if we substitute the polarizations of the photons as well ( $\varepsilon_1, \varepsilon_2$ ), and we label the momenta as in right diagram in [Figure 1](#), ( $k_1, k_2$ ), we get all possible assignments of derivatives and polarizations<sup>7</sup>:

$$\begin{aligned} \tilde{T}_{\mu\nu} = & k_{1,\mu} k_{2,\nu} (\varepsilon_1 \cdot \varepsilon_2) + k_{1,\nu} k_{2,\mu} (\varepsilon_1 \cdot \varepsilon_2) - (k_1 \cdot \varepsilon_2) k_{2,\nu} \varepsilon_{1,\mu} - (k_2 \cdot \varepsilon_1) k_{1,\nu} \varepsilon_{2,\mu} \\ & - k_{1,\mu} (k_2 \cdot \varepsilon_1) \varepsilon_{2,\nu} - k_{2,\mu} (k_1 \cdot \varepsilon_2) \varepsilon_{1,\nu} + (k_1 \cdot k_2) \varepsilon_{2,\mu} \varepsilon_{1,\nu} + (k_1 \cdot k_2) \varepsilon_{1,\mu} \varepsilon_{2,\nu} \\ & + \frac{1}{\xi} [-k_{1,\mu} (k_1 \cdot \varepsilon_1) \varepsilon_{2,\nu} - k_{2,\mu} (k_2 \cdot \varepsilon_2) \varepsilon_{1,\nu} - k_{1,\nu} (k_1 \cdot \varepsilon_1) \varepsilon_{2,\mu} - k_{2,\nu} (k_2 \cdot \varepsilon_2) \varepsilon_{1,\mu}] \end{aligned} \quad (4.62)$$

<sup>7</sup>Remember that each term has two derivatives, which compound to an overall minus sign in the rule when the substitution  $\partial_\mu \rightarrow -ik_\mu$  is applied.

Instead, if we remove the polarizations of the photons, we can substitute  $(\rho, \sigma)$  Lorentz indices to the two photons, leaving:

$$\begin{aligned} \Pi_{\mu\nu\rho\sigma}^\xi(k_1, k_2) &= \delta_{\rho\sigma} (k_{1,\mu} k_{2,\nu} + k_{1,\nu} k_{2,\mu}) - \delta_{\mu\rho} k_{1,\sigma} k_{2,\nu} - \delta_{\mu\sigma} k_{1,\nu} k_{2,\rho} \\ &\quad - \delta_{\nu\sigma} k_{1,\mu} k_{2,\rho} - \delta_{\nu\rho} k_{1,\sigma} k_{2,\mu} + k_1 \cdot k_2 (\delta_{\mu\sigma} \delta_{\nu\rho} + \delta_{\nu\sigma} \delta_{\mu\rho}) \\ &\quad + \frac{1}{\xi} [-\delta_{\mu\rho} k_{2,\sigma} k_{2,\nu} - \delta_{\mu\sigma} k_{1,\nu} k_{1,\rho} - \delta_{\nu\sigma} k_{1,\mu} k_{1,\rho} - \delta_{\nu\rho} k_{2,\sigma} k_{2,\mu}] \end{aligned} \quad (4.63)$$

which tells us that:

$$\Pi_{\mu\nu\rho\sigma}^\xi(k_1, k_2) = \Pi_{\mu\nu\rho\sigma}^{\text{Lor}}(k_1, k_2) + \frac{1}{\xi} \Pi_{\mu\nu\rho\sigma}^{\text{Gauge}}(k_1, k_2) \quad (4.64)$$

where  $\Pi_{\mu\nu\rho\sigma}^{\text{Lor}}(k_1, k_2) = \Pi_{\mu\nu\rho\sigma}(k_1, k_2)$  is the Feynman rule in Lorentz (unitary) gauge, selecting  $1/\xi = 0$ .

We can also easily check that the Feynman rule in Lorentz gauge satisfies Ward identities, when contracting with external momenta on the indices  $\rho, \sigma$  (where the polarizations should go):  $\varepsilon_{1,\rho} \leftrightarrow k_{1,\rho}$ , and  $\varepsilon_{2,\sigma} \leftrightarrow k_{2,\sigma}$ :

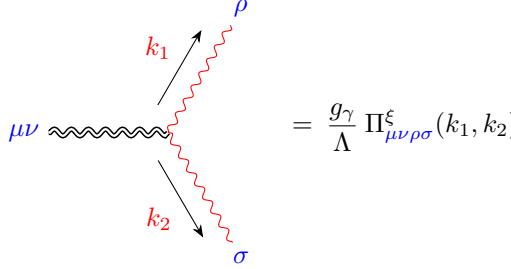
$$\begin{aligned} k_{1,\rho} \Pi_{\mu\nu\rho\sigma}(k_1, k_2) &= k_{1,\sigma} (k_{1,\mu} k_{2,\nu} + k_{1,\nu} k_{2,\mu}) - k_{1,\mu} k_{1,\sigma} k_{2,\nu} - \delta_{\mu\sigma} k_{1,\nu} k_1 \cdot k_2 \\ &\quad - \delta_{\nu\sigma} k_{1,\mu} k_1 \cdot k_2 - k_{1,\nu} k_{1,\sigma} k_{2,\mu} + k_1 \cdot k_2 (\delta_{\mu\sigma} k_{1,\nu} + \delta_{\nu\sigma} k_{1,\mu}) = 0 \end{aligned} \quad (4.65)$$

$$\begin{aligned} k_{2,\sigma} \Pi_{\mu\nu\rho\sigma}(k_1, k_2) &= k_{2,\sigma} (k_{1,\mu} k_{2,\nu} + k_{1,\nu} k_{2,\mu}) - \delta_{\mu\rho} k_{2,\nu} k_1 \cdot k_2 - k_{2,\mu} k_{1,\nu} k_{2,\rho} \\ &\quad - k_{2,\nu} k_{1,\mu} k_{2,\rho} - \delta_{\nu\rho} k_{2,\mu} k_1 \cdot k_2 + k_1 \cdot k_2 (\delta_{2,\mu} \delta_{\nu\rho} + \delta_{2,\nu} \delta_{\mu\rho}) = 0 \end{aligned} \quad (4.66)$$

$$k_{1,\rho} k_{2,\nu} \Pi_{\mu\nu\rho\sigma}(k_1, k_2) = 0 \quad (4.67)$$

Of course, in any other gauge, the gauge dependent part is not really observable because it will disappear in any amplitude, so it does not need to satisfy Ward identities, as long as the unitary Lorentz Feynman rule does.

Finally, we can infer the Feynman rule in any gauge:



$$= \frac{g_\gamma}{\Lambda} \Pi_{\mu\nu\rho\sigma}^\xi(k_1, k_2) \quad (4.68)$$

where  $g_\gamma/\Lambda$  is the effective Wilson coefficient for the dimension 5 operator describing the interaction. It is to be contracted with the spin polarization of the  $X$  ( $\varepsilon_{\mu\nu}$ ) and the 2 photons ( $\varepsilon_\rho, \varepsilon_\sigma$ ). Notice how, in both cases, because of the symmetry of the  $X_{\mu\nu}$  field, the Feynman rules must be symmetric by  $\mu \leftrightarrow \nu$  exchange. Up to differences in notation, this result is consistent to the one found in [13], when substituting  $\xi = 1$ :

$$\begin{aligned} \Pi_{\mu\nu\rho\sigma}^{\text{Feyn}}(k_1, k_2) &= \delta_{\rho\sigma} (k_{1,\mu} k_{2,\nu} + k_{1,\nu} k_{2,\mu}) - \delta_{\mu\rho} (k_{1,\sigma} k_{2,\nu} + k_{2,\sigma} k_{2,\nu}) \\ &\quad - \delta_{\mu\sigma} (k_{1,\nu} k_{2,\rho} + k_{1,\rho} k_{1,\nu}) - \delta_{\nu\sigma} (k_{1,\mu} k_{2,\rho} + k_{1,\mu} k_{1,\rho}) \\ &\quad - \delta_{\nu\rho} (k_{1,\sigma} k_{2,\mu} + k_{2,\sigma} k_{2,\mu}) + k_1 \cdot k_2 (\delta_{\mu\sigma} \delta_{\nu\rho} + \delta_{\nu\sigma} \delta_{\mu\rho}) \end{aligned} \quad (4.69)$$

From now on, we will omit the  $\xi$  symbol for the generic Feynman rule  $\Pi_{\mu\nu\rho\sigma}(k_1, k_2)$  as a short-hand notation to refer to the tensor used in this  $X\gamma\gamma$  Feynman rule. Since we always are at tree level, we could freely use Lorentz gauge for our calculations; however, using the general  $\xi$  gauge expression will help us spot mistakes in calculation.

## 4.4 Energy of EFT breaking

The idea is to evaluate corrections due to spin 2 mediation in QED processes. It is interesting that in the high energy limit, spin 2 corrections grow with energy. This is no coincidence: we elaborated an *effective theory* with

a dimension 5 operator for a massive spin 2 boson. This imposes a dimensional constant  $1/\Lambda$ , which has to be balanced in the cross section by another dimensional factor.

As energy increases, the only relevant dimensional quantity is center of mass energy (as masses can all be neglected in the ultra-relativistic limit), which appears with an extra power for every extra  $\Lambda$  power in the denominator. This is consistent in the effective landscape: eventually, as energy increases, perturbation theory breaks and the low energy model has to be substituted with a UV completing theory, as the theory is *non-renormalizable*. This does not happen with minimally coupled theories, where the dimension 4 operator for the interaction does not require extra energy factors, and in fact (running of the coupling aside) theories are self-consistent.

That is why the relative spin 2 correction always grows with energy (this is not the case with any other spin 1 or spin 0 model, where relative corrections due to extra interactions are constant in energy), and also why we are analyzing what is the energy limit for this model<sup>8</sup>.

In light of what has been said, one might think that the best course of action would be to just take experimental results at very high energy, and compare them with our predicted corrections to get upper bounds on the couplings. Unfortunately, it is not that simple:

- We need to always check that Froissart bound is satisfied to avoid unitarity violation. If this is not the case, we cannot run the theory up in energy without breaking its own consistency.
- Even if Froissart bound is satisfied, we may run the corrections up to cutoff energy  $\Lambda$ , up until where a UV completion would be needed. Usually,  $\Lambda = kM$ , where  $M$  is the mass of the heavy mode ( $M = m_X$  in our case), and  $k < 5$  in most cases. We deem  $20 - 50 \text{ MeV}$  to be an acceptable interval of values for  $\Lambda$ <sup>9</sup>.

However, just for curiosity, we may run to very high energy our theory, just to see what happens (limit would be until the production of  $Z$  in weak interaction becomes dominant, so up to  $60 \text{ GeV}$ ). It is a completely unjustified and unphysical scenario, but the graph looks nice so I am going to keep it anyway. It is utterly and completely useless, as it has no physical meaning whatsoever.

- If  $X$  is a composite particle, running up in energy may break the  $X$  into its constituents. Currently, there is not a universally accepted model about the nature of  $X$  particle: a special nuclear resonance ([15]), a QED meson ([17], [18]), a protophobic axial vector ([11], [12]), the QCD axion or any ALP ([19]) and many more...
- **(In the end, this is useless.)** Note that the energy limit we set is actually the momentum exchanged in the  $X$  propagator in all Feynman diagrams. For only  $t$ -channels corrections, in particular (only Compton scattering<sup>10</sup>) this means that  $t = 2p^2(1 - \cos \theta)$  is the limited quantity, where  $\theta$  is the scattering angle and  $p$  is the modulus of the 3-momentum of one of the two particles in the center of mass frame. For small angles, this means that  $p^2$  (so  $s$  may actually be much larger than  $t$ , allowing us to go up in energy). In particular, the relation is:

$$\sqrt{|s|} = 2E \approx \sqrt{\frac{2t}{1 - \cos \theta}} \approx \sqrt{\frac{2m_X}{1 - \cos \theta}} \quad (4.70)$$

which for  $\cos \theta = 0.96$  (usual experimental value, because small angle detectors are usually located around the beam pipe in accelerators), and  $\sqrt{t} \approx 20 - 50 \text{ MeV}$ , we get an a maximum center of mass energy of  $\sqrt{|s|} \approx 140 - 350 \text{ MeV}$ .

Everything we said can be summarized as follows, anticipating results following from next chapters:

**Bhabha scattering/Møller scattering:** they satisfy unitarity condition and do not require  $g_\gamma \neq 0$ .

- In our hypothetical scenario (since this limiting energy is not known), let us just stick with going as high as possible with energy, and see what happens. In this case, limiting maximum energy should be around  $50 \text{ GeV}$  (after that, weak interaction dominates).
- In the most likely scenario, maximum exchanged momentum is around  $20 - 50 \text{ MeV}$ .

<sup>8</sup>Instead, for spin 1 models, searching corrections to QED processes have been proposed only at the resonant energy of  $17 \text{ MeV}$  ([7]).

<sup>9</sup>When we include the JINR experiment, we cannot increase the bound, as even though it is explicitly stated that the energies of the analyzed photon pairs is  $> 250 \text{ MeV}$ , this only means that the  $X$  particle is produced boosted. However, center of mass energy of the interaction is always at  $\sqrt{|s|} = m_X$ .

<sup>10</sup>Bhabha and Møller scattering are not included, because they also have other channels diagrams correction. For us, it is impossible to control which process occurs, even at very low angles where  $t$ -channel is dominant (as we show in Figure 12). So, if other channels, with way larger momentum exchanged, can occur while employing this trick of going up in energy, momentum exchanged would be too big for the consistency of the theory, and we would probably need a different theory altogether to explain the other processes in the same event, and so we will not be using it. In the end, there is no experiment that would even allow this trick to be used, either, so it does not matter, but it is worth mentioning this because I am still learning how to do this.

**Compton scattering/Annihilation into photons:** they do not satisfy unitarity condition, and require  $g_\gamma \neq 0$ . The limit on exchanged momentum is always  $20 - 50 \text{ MeV}$ .

- Compton scattering contributes with  $t$ -channel diagram only, so at small angles (e.g.  $\cos \theta = 0.96$ ),  $\sqrt{|s|} \approx 300 \text{ MeV}$  is the limit. However, this translates to  $\omega \approx 1 \text{ TeV}$  in a reference frame where electron is at rest. This allows us to go up in energy to meet (almost) every experiment that has ever been performed on Compton scattering.
- Annihilation into two photons contributes with  $s$ -channel diagram, hence limit is always  $\sqrt{|s|} \approx 20 - 50 \text{ MeV}$ .

**Two-photon scattering:** it does not satisfy unitarity bound, and require only  $g_\gamma$ . Because of presence of all channels mediation, there is no doubt that the limit in exchanged momentum is still  $\sqrt{|s|} \approx 20 - 50 \text{ MeV}$ .

## 5 Bounds from ATOMKI and JINR

### 5.1 Decay rate for electron-positron channel

Using Feynman rule in [Equation 4.56](#), we write down the amplitude for the decay of  $X$  into electron and positron, at tree level. Since symmetrizing does not really make any difference in the final result (the antisymmetric part will just cancel), we write the amplitude of the decay directly as:

$$A = i \frac{g_e}{2\Lambda} (p_\mu^- - p_\mu^+) \gamma_\nu \varepsilon_{\mu\nu}(p, \eta) \quad (5.1)$$

$$\mathcal{A} = \bar{u}(p^-, \lambda^-) A v(p^+, \lambda^+) = \bar{u} A v \quad (5.2)$$

where  $p$  is the  $X$  momentum and  $\eta$  is its polarization, while  $p^\pm$  are the momenta of the electron and positron,  $\lambda^\pm$  are their polarizations. Hereafter, we are going to refer to polarizations as  $\varepsilon_{\mu\nu}$ ,  $u$ ,  $v$ . With our notation, the complex conjugate is obtained studying the Dirac indices:

$$\begin{aligned} \mathcal{A}^* &= (\bar{u} A v)^* = (u_a^*(\gamma_4)_{ab} A_{bc} v_c)^* = v_c^* A_{cb}^\dagger(\gamma_4^\dagger)_{ba} u_a = \\ &= v_e^*(\gamma_4)_{ed} (\gamma_4)_{dc} A_{cb}^\dagger(\gamma_4^\dagger)_{ba} u_a = \bar{v}_d (\gamma_4 A^\dagger \gamma_4)_{da} u_a = \bar{v} B u \end{aligned} \quad (5.3)$$

Dirac matrices are defined to be hermitian in the Dutch metric:

$$B = \gamma_4 A^\dagger \gamma_4 = -i \frac{g_e}{2\Lambda} \varepsilon_{\mu\nu}^*(p_\mu^- - p_\mu^+) \gamma_4 \gamma_\nu^\dagger \gamma_4 = -i \frac{g_e}{2\Lambda} \varepsilon_{\mu\nu}^*(p_\mu^- - p_\mu^+) \gamma_4 \gamma_\nu \gamma_4 \quad (5.4)$$

Evaluation of complex conjugation is not trivial in this metric, as energy component is imaginary. We dedicated an Appendix to this, (specifically [subsection F.4](#)). The phases coming out from boson polarization, momentum, and gamma matrices commutation rules all cancel, leaving:

$$B = -i \frac{g_e}{2\Lambda} \mu_p \nu_p \bar{\varepsilon}_{\mu\nu} \mu_p (p_\mu^- - p_\mu^+) (-\nu_p \gamma_\nu) = i \frac{g_e}{2\Lambda} \bar{\varepsilon}_{\mu\nu} (p_\mu^- - p_\mu^+) \gamma_\nu \quad (5.5)$$

where the momenta are now real, as the energy component can never be taken in this gauge.

Putting it all together:

$$\begin{aligned} |\mathcal{A}|^2 &= -\frac{g_e^2}{4\Lambda^2} \varepsilon_{\mu\nu} \bar{\varepsilon}_{\rho\sigma} (p_\mu^- - p_\mu^+) (p_\rho^- - p_\rho^+) [\bar{u}_a (\gamma_\nu)_{ab} v_b \bar{v}_c (\gamma_\sigma)_{cd} u_d] = \\ &= -\frac{g_e^2}{4\Lambda^2} \varepsilon_{\mu\nu} \bar{\varepsilon}_{\rho\sigma} (p_\mu^- - p_\mu^+) (p_\rho^- - p_\rho^+) \text{Tr} [\gamma_\nu (v \bar{v}) \gamma_\sigma (u \bar{u})] \end{aligned} \quad (5.6)$$

There are 5 polarizations to average over initially. When summing over the total polarizations, instead, we get:

$$\begin{aligned} |\overline{\mathcal{A}}|^2 &= \frac{1}{5} \sum_{\eta, \lambda^\pm} |\mathcal{A}|^2 = -\frac{g_e^2}{20\Lambda^2} N_{\mu\nu\rho\sigma}(p) (p_\mu^- - p_\mu^+) (p_\rho^- - p_\rho^+) \text{Tr} \left[ \gamma_\nu \left( \frac{-i\psi^+ - m_e}{2p_4^+} \right) \gamma_\sigma \left( \frac{-i\psi^- + m_e}{2p_4^-} \right) \right] = \\ &= -\frac{g_e^2}{80\Lambda^2} N_{\mu\nu\rho\sigma}(p) \frac{(p_\mu^- - p_\mu^+) (p_\rho^- - p_\rho^+)}{p_4^+ p_4^-} \left[ -4p_\nu^+ p_\sigma^- - 4p_\sigma^+ p_\nu^- + 4\delta_{\nu\sigma} (p^+ \cdot p^- - m_e^2) \right] = \\ &= \frac{g_e^2}{20\Lambda^2} N_{\mu\nu\rho\sigma}(p) \frac{(p_\mu^- - p_\mu^+) (p_\rho^- - p_\rho^+)}{p_4^+ p_4^-} \left[ p_\nu^+ p_\sigma^- + p_\sigma^+ p_\nu^- - \delta_{\nu\sigma} (p^+ \cdot p^- - m_e^2) \right] \end{aligned} \quad (5.7)$$

where  $m_e$  is the mass of the electron. Having  $2p_4$  at denominator means we will not have to have  $2p_4$  in the phase space integral denominator.

The modulus squared has been calculated with the software tool **FORM**, which makes use of Pauli notation in its calculations (which is why we employ it here). The code can be found in this [GitHub repository](#), also linked in [subsection G.1](#) (program is `spin2Decayee.frm`). Using real polarizations throughout, the result is:

$$|\overline{\mathcal{A}}|^2 = \frac{g_e^2}{5\Lambda^2} \frac{1}{p_4^+ p_4^-} \left[ -\frac{7}{6} m_e^4 - \frac{2}{3} (p^+ \cdot p^-) m_e^2 + \frac{1}{2} (p^+ \cdot p^-)^2 \right] \quad (5.8)$$

We can use kinematics now. Because it is a 2-body decay, momenta can be fixed in the rest frame of the decaying  $X$  particle. Using conservation of energy,  $k^+ + k^- = p$ , and :

$$\begin{aligned} p^+ \cdot p^- &= \frac{(p^+ + p^-)^2 + 2m_e^2}{2} = m_e^2 - \frac{m_X^2}{2} \\ p_4^+ = p_4^- &= \frac{m_X}{2} \end{aligned} \quad (5.9)$$

simplifying to:

$$|\bar{\mathcal{A}}|^2 = \frac{4g_e^2 m_X^2}{5\Lambda^2} \left[ \frac{1}{8} - \frac{1}{6} \frac{m_e^2}{m_X^2} - \frac{4}{3} \frac{m_e^4}{m_X^4} \right] = \frac{g_e^2 m_X^2}{10\Lambda^2} \left[ 1 - \frac{4}{3} \frac{m_e^2}{m_X^2} - \frac{32}{3} \frac{m_e^4}{m_X^4} \right] \quad (5.10)$$

Only phase space is left to evaluate. Using [Equation F.5](#):

$$\Gamma(X \rightarrow e^+ e^-) = \frac{1}{2m_X} \int \frac{d^3 p^+}{(2\pi)^3 2p_4^+} \frac{d^3 p^-}{(2\pi)^3 2p_4^-} (2\pi)^4 \delta^{(4)}(p - p^+ - p^-) \times 4p_4^+ p_4^- |\bar{\mathcal{A}}|^2 = \quad (5.11)$$

$$\begin{aligned} &= \frac{1}{2m_X} \frac{\sqrt{\lambda(m_X^2, m_e^2, m_e^2)}}{8\pi m_X^2} \times 4 \frac{m_X}{2} \frac{m_X}{2} |\bar{\mathcal{A}}|^2 = \\ &= \frac{\sqrt{\lambda(m_X^2, m_e^2, m_e^2)}}{16\pi m_X} |\bar{\mathcal{A}}|^2 = \frac{m_X}{16\pi} \sqrt{1 - \frac{4m_e^2}{m_X^2}} |\bar{\mathcal{A}}|^2 \end{aligned} \quad (5.12)$$

This is a general formula. Specifically, when substituting  $|\bar{\mathcal{A}}|^2$  from [Equation 5.10](#):

$$\Gamma(X \rightarrow e^+ e^-) = \frac{g_e^2}{\Lambda^2} \frac{m_X^3}{160\pi} \sqrt{1 - \frac{4m_e^2}{m_X^2}} \left[ 1 - \frac{4}{3} \frac{m_e^2}{m_X^2} - \frac{32}{3} \frac{m_e^4}{m_X^4} \right] = \quad (5.13)$$

$$= \frac{g_e^2}{\Lambda^2} \frac{m_X^3}{160\pi} \left[ 1 - \frac{4m_e^2}{m_X^2} \right]^{3/2} \left[ 1 + \frac{8}{3} \frac{m_e^2}{m_X^2} \right] \quad (5.14)$$

which corresponds to the result found in literature ([22]).

If we substitute  $m_X = 17$  MeV, and by approximating  $m_e \ll m_X$ , we get a numerical estimate for this decay rate:

$$\Gamma(X \rightarrow e^+ e^-) \approx \frac{g_e^2}{\Lambda^2} \times 10 \text{ MeV}^3 = \left( \frac{g_e}{\Lambda [\text{MeV}]} \right)^2 \times 10 \text{ MeV} \quad (5.15)$$

## 5.2 Decay rate for photon-electron-positron channel

Remember that the process  $X \rightarrow e^+ e^- \gamma$  is unlocked for free with the same  $g_e$  coupling we introduced thanks to U(1) gauge invariance. A few remarks:

- Because of the presence of the  $\alpha$  due to gauge interaction or due to electrodynamics vertex at tree level, and the suppression from 3-body phase space (even if massless), by another factor of  $\approx 8\pi$ , the resulting decay rate is highly suppressed by a factor  $10^{-3}$ . This implies that in the following chapters ([subsection 5.4](#)) we will be able to neglect its contribution to the total  $\Gamma$  estimate in the experiments.
- Moreover, this process can never enter at tree level when considering any  $2 \rightarrow 2$  scattering processes involving only Standard Model particles (like the QED processes we want to correct). By topological arguments, the lowest number of particles that can interact at tree level with a vertex  $X \rightarrow e^+ e^- \gamma$  is five.

So, this decay channel can be excluded in our estimates for the model. However, because we are very thorough and have lots of time to waste, let us evaluate this decay rate analytically at tree level.

At the same order as the direct interaction (for which we have the Feynman rule, see [Equation 4.58](#)), there are also tree level diagrams with electrodynamics vertices, which we are going to represent in [Figure 2](#):

To simplify result, we are going to assume  $m_X \gg m_e$ , so that this process is now a 3-body decay into massless states. Final result of the decay rate (not summing photon polarizations) gets easier:

$$\begin{aligned} \Gamma_\lambda(X \rightarrow e^+ e^- \gamma) &= \frac{1}{2m_X} \int \frac{d^3 p^+}{(2\pi)^3 2p_4^+} \frac{d^3 p^-}{(2\pi)^3 2p_4^-} \frac{d^3 k}{(2\pi)^3 2k_4} (2\pi)^4 \delta^{(4)}(p - k - p^+ - p^-) \times 4p_4^+ p_4^- |\bar{\mathcal{A}}|^2 = \\ &= \frac{1}{2m_X} \frac{m_X^2}{128\pi^3} \int_0^1 dx \int_{1-x}^1 dy 4p_4^+ p_4^- |\bar{\mathcal{A}}|^2 \\ &= \frac{m_X}{256\pi^3} \int_0^1 dx \int_{1-x}^1 dy 4p_4^+ p_4^- |\bar{\mathcal{A}}|^2 \end{aligned} \quad (5.16)$$

where we have used result in [subsection F.3](#) ([Equation F.7](#)). We have defined  $p_4^- = E_-$ ,  $p_4^+ = E_+$ . Then, we have introduced the adimensional variables  $x = 2E_-/m_X$  and  $y = 2E_+/m_X$ .

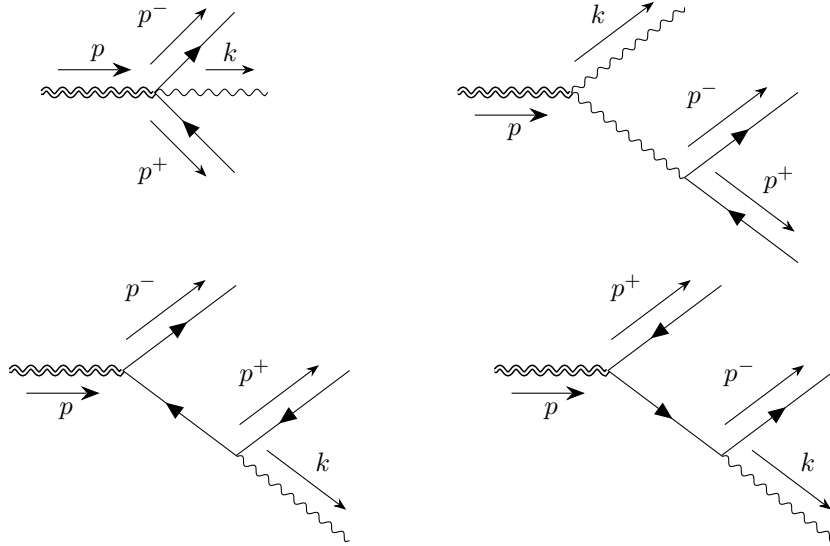


Figure 2: Diagrams corresponding to tree level decay  $X \rightarrow e^+e^-\gamma$ . On the upper left, the direct four-point interaction. On the upper right, the photon exchange diagram, with electrodynamics vertex. On the lower left, the positron exchange diagram, with electrodynamics vertex. On the lower right, the electron exchange diagram, with electrodynamics vertex.

So, our next step is to express scalar products in kinematics in terms of  $x$  and  $y$ . The easiest frame to work with is the rest frame of the  $X$ , where  $p = (\vec{0}, im_X)$ .

$$p \cdot p^- = -m_X E_- = -\frac{m_X^2}{2}x \quad p \cdot p^+ = -m_X E_+ = -\frac{m_X^2}{2}y$$

$$\begin{aligned} p^+ \cdot p^- &= \frac{(p^+ + p^-)^2 - (p^+)^2 - (p^-)^2}{2} = \frac{(p - k)^2}{2} = -\frac{m_X^2}{2} - p \cdot k = -\frac{m_X^2}{2} + m_X k_4 \\ &= -\frac{m_X^2}{2} + m_X (m_X - E_- - E_+) = \frac{m_X^2}{2} \left( 1 - \frac{2E_-}{m_X} - \frac{2E_+}{m_X} \right) \\ &= \frac{m_X^2}{2}(1 - x - y) \end{aligned}$$

As for the amplitude will not need to calculate this process, as we can use the result of the very similar process  $e^+e^- \rightarrow X\gamma$ , which we evaluate in [subsection 12.1](#), obtaining the final expression [Equation 12.25](#). There are a few adjustments we need to make:

- $e^+e^- \rightarrow X\gamma$  will be evaluated in the same massless limit for the electron and positron, so no changes there.
- First, we need to invert the 4-momentum of the photon. The process  $e^+e^-\gamma \rightarrow X$  is equivalent to the decay we are studying. In [subsection 12.1](#), momenta are called  $q_1, q_2, p_1, p_2$ . These are now translated into  $p^-, p^+, p, -k$  respectively.
- Mandelstam variables are now translated as follows, using the scalar products we have defined and conservation of energy  $k = p - p^- - p^+$ :

$$s = (q_1 + q_2)^2 = (p^- + p^+)^2 = 2p^- \cdot p^+ = m_X^2(1 - x - y)$$

$$t = (q_1 - p_1)^2 = (p^- - p)^2 = -m_X^2 - 2p^- \cdot p = -m_X^2(1 - x)$$

$$u = (q_1 - p_2)^2 = (p^- + k)^2 = (p - p^+)^2 = -m_X^2(1 - y)$$

- While in  $e^+e^- \rightarrow X\gamma$  we average over polarization of fermions (factor of 1/4), here we need to average over polarization of  $X$  (factor of 1/5), so we need to multiply that result by 4/5.

- Photon polarizations are summed trivially with:

$$\sum_{\lambda_2} \varepsilon_\rho(p_2, \lambda_2) \bar{\varepsilon}_\beta(p_2, \lambda_2) = \delta_{\rho\beta} - \frac{p_{2,\rho} p_{2,\beta}}{|p_2|^2} \quad (5.17)$$

because of *Ward identities*, we get the result of simplifying the contribution contracted with external photon momentum.

For this task, we implement a code using the **FORM** tool, which is a very useful software tool for algebraic and tensor calculus. More information on the tool can be found in [subsection G.1](#), while every code that we use throughout this thesis is linked in this [GitHub repository](#).

Namely, this conversion of amplitudes is performed by the code `from_eexg_to_Xeeg.frm`, which implements on the initial amplitude in [Equation 12.25](#) the tweaks we discussed. The output of the code is the following:

$$\begin{aligned} |\bar{\mathcal{A}}|^2 = & \frac{1}{4p_4^+ p_4^-} \frac{e^2 m_X^2}{15\Lambda^2} \left\{ g_\gamma^2 \left[ -4 - 4y - 6y^2 + 2y^3 - 4x + 16xy + 2xy^2 - 6x^2 + 2x^2y + 2x^3 \right. \right. \\ & - \frac{1+3x}{1-y} + \frac{9-15y-24x+12xy+12x^2}{1-x} + \frac{-6+12y-6y^2+12x-12xy-6x^2}{(1-x)(1-y)} \\ & \left. \left. - \frac{6+3y+12y^2+3x+12x^2}{1-x-y} + \frac{6+3x+3x^2}{(1-x-y)(1-y)} + \frac{6+3y+3y^2}{(1-x-y)(1-x)} - \frac{6}{(1-x-y)(1-x)(1-y)} \right] \right. \\ & + g_e g_\gamma \left[ 8 + 8y + 12y^2 - 4y^3 + 8x - 32xy - 4xy^2 + 12x^2 - 4x^2y - 4x^3 \right. \\ & \left. + \frac{-6+18y+24x-12xy-12x^2}{1-x} + \frac{6+6x}{1+y} + \frac{-12y+6y^2-12x+12xy+6x^2}{(1-x)(1-y)} \right] \\ & \left. + g_e^2 \left[ -4 - 4y - 6y^2 + 2y^3 - 4x + 16xy + 2xy^2 - 6x^2 + 2x^2y + 2x^3 - \frac{3+3y}{1-x} - \frac{3+3x}{1-y} + \frac{6}{(1-x)(1-y)} \right] \right\} \end{aligned} \quad (5.18)$$

which yields the rate, starting from [Equation 5.16](#):

$$\Gamma(X \rightarrow e^+ e^- \gamma) = \frac{e^2 m_X^3}{3840\pi^3 \Lambda^2} \int_0^1 dx \int_{1-x}^1 dy 4p_4^+ p_4^- \{ \dots \} \quad (5.19)$$

Notice how, because in Pauli notation  $|\bar{\mathcal{A}}|^2$  has dimension  $-2$  in energy due to the factor  $1/4p_4^+ p_4^-$  embedded in the amplitude, this expression has now the correct dimensions of a rate.

Integration in  $y$  first and in  $x$  later has been carried out using this [online Integral Calculator](#). Here is the result: Integration in  $y$  first and in  $x$  later has been carried out using this [online Integral Calculator](#).

$$\begin{aligned} \Gamma(X \rightarrow e^+ e^- \gamma) = & \frac{e^2 m_X^3}{3840\pi^3 \Lambda^2} \int_0^1 dx \frac{g_\gamma^2}{6} \left[ 72 \left( 2x^2 - 2x + 1 \right) \log x + 7x^4 - 84x^3 - 30x^2 - 96x \right] \\ & - \frac{g_e g_\gamma}{3} \left[ 7x^4 - 84x^3 + 96x^2 - 108x \right] + \frac{g_e^2}{6} \left[ 7x^4 - 84x^3 + 114x^2 - 72x \right] \\ & + 3 \int_{1-x}^1 dy \frac{x^2 + y^2}{(1-x)(1-y)} = \\ = & \frac{\alpha m_X^3}{960\pi^2 \Lambda^2} \left[ -\frac{108g_\gamma^2}{5} + \frac{208g_e g_\gamma}{15} - \frac{44g_e^2}{15} + 3g_e^2 \int_0^1 dx \int_{1-x}^1 dy \frac{x^2 + y^2}{(1-x)(1-y)} \right] = \\ = & \frac{\alpha m_X^3}{3600\pi^2 \Lambda^2} \left[ -81g_\gamma^2 + 52g_e g_\gamma - 11g_e^2 \right] + \frac{\alpha g_e^2 m_X^3}{320\pi^2 \Lambda^2} \int_0^1 dx \int_{1-x}^1 dy \frac{x^2 + y^2}{(1-x)(1-y)} \end{aligned} \quad (5.20)$$

There is an issue: the left addend is negative for every possible combination of  $g_e$  and  $g_\gamma$  (it has negative discriminant). The right addend, instead, is positively divergent. Hence, the rate is actually divergent, as the last integral is evaluated to be infinity. This is because we are in the massless limit approximation for the fermions, as the term  $1/(1-y)$  gives rise to  $\log(1-y)$ , which is divergent when evaluated between  $1-x$  and 1. However, if we considered massive fermions, the extremes of integration would shift, leaving the integral finite<sup>11</sup>.

<sup>11</sup>Still, pretty large result of the integral, so probably it would be dominant with respect to the rest of the expression, which is good news given that it is a negative quantity.

There is a physical explanation for this effect. The divergent effects arise only in  $g_e^2$  diagrams, which are the diagrams with mediation of electron and positron. However, propagators of fermions in the massless limit actually behave like  $1/p^+$  and  $1/p^-$ , which means that they are not integrable in the momentum, when evaluating phase space, as they give a logarithmic divergent result. Here, the mass term in the propagator acts as a regulator for the phase space integral.

However, since all we wanted to do is estimate the contribution of the decay, without necessarily having an analytic result, we can estimate the regulated integral using the only scales we have:  $m_X$  and  $m_e$ . The log divergence as regulator would give us something like  $\log(m_X/m_e)$  as result:

$$\Gamma(X \rightarrow e^+ e^- \gamma) \approx \frac{\alpha m_X^3}{320\pi^2} \frac{g_e^2}{\Lambda^2} \log\left(\frac{m_X}{m_e}\right) \approx \frac{\alpha}{2\pi} \log\left(\frac{m_X}{m_e}\right) \Gamma(X \rightarrow e^+ e^-) \quad (5.21)$$

which is a 1 loop estimate correction to the decay  $X \rightarrow e^+ e^-$ , and is in fact a *radiative correction* to that decay as well. So, divergence in the integral rises as an infrared divergence, arising in the massless limit and being solved by adding mass to the fermions, as regulators!

It is also worth mentioning that the vertex diagram (upper left in [Figure 2](#)), in itself is not divergent in the massless limit, as it does not represent a radiative correction. Evaluation of the single 4-vertex interaction can be found in [subsection F.5](#).

If we substitute  $m_X = 17$  MeV, we get a numerical estimate for this decay rate:

$$\Gamma(X \rightarrow e^+ e^- \gamma) \approx 4 \times 10^{-3} \Gamma(X \rightarrow e^+ e^-) \quad (5.22)$$

which is about 300 times smaller than the main decay rate  $X \rightarrow e^+ e^-$ , as expected, and so it can be neglected when evaluating the total  $\Gamma$ .

### 5.3 Decay rate for photon-photon channel

Now, using Feynman rule in [Equation 4.68](#), we write down the amplitude for the decay of X massive particle into two photons, at tree level. Contract with all the spin polarizations involved to get the amplitude:

$$\mathcal{A} = \frac{g_\gamma}{\Lambda} \varepsilon_{\mu\nu}(p, \eta) \Pi_{\mu\nu\rho\sigma}(k_1, k_2) \bar{\varepsilon}_\rho(k_1, \lambda_1) \bar{\varepsilon}_\sigma(k_2, \lambda_2) \quad (5.23)$$

Hereafter, polarizations will be referred to as  $\varepsilon_{\mu\nu}$ ,  $\varepsilon_\mu$  respectively. When taking complex conjugation, phases all cancel out according to rules in [subsection F.4](#):

$$\begin{aligned} \mathcal{A}^* &= \frac{g_\gamma}{\Lambda} \gamma_p \delta_p \varepsilon_{\gamma\delta}(p, \eta) \gamma_p \delta_p \alpha_p \beta_p \Pi_{\gamma\delta\alpha\beta}(k_1, k_2) \alpha_p \bar{\varepsilon}_\alpha(k_1, \lambda_1) \beta_p \bar{\varepsilon}_\beta(k_2, \lambda_2) = \\ &= \frac{g_\gamma}{\Lambda} \varepsilon_{\gamma\delta}(p, \eta) \Pi_{\gamma_p \delta_p \alpha_p \beta_p}(k_1, k_2) \bar{\varepsilon}_\alpha(k_1, \lambda_1) \bar{\varepsilon}_\beta(k_2, \lambda_2) \end{aligned} \quad (5.24)$$

which leads to the following squared modulus:

$$|\mathcal{A}|^2 = \frac{g_\gamma^2}{\Lambda^2} \varepsilon_{\mu\nu} \bar{\varepsilon}_{\gamma\delta} \Pi_{\mu\nu\rho\sigma}(k_1, k_2) \Pi_{\gamma\delta\alpha\beta}(k_1, k_2) \bar{\varepsilon}_{1,\rho} \bar{\varepsilon}_{2,\sigma} \varepsilon_{1,\alpha} \varepsilon_{2,\beta} \quad (5.25)$$

Where we have, once again, used the tricks in [subsection F.4](#). Absence of fermions and gamma matrices means that complex conjugate does not get a minus one overall, like in the previous chapter.

We ought to average over initial polarizations and sum over final polarizations. Since we want to keep dependence on the photon polarizations, though, we are only averaging and summing out the polarizations of X. We get:

$$|\bar{\mathcal{A}}|^2 = \frac{1}{5} \sum_\eta |\mathcal{A}|^2 = -\frac{g_\gamma^2}{5\Lambda^2} N_{\mu\nu\gamma\delta}(p) \Pi_{\mu\nu\rho\sigma}(k_1, k_2) \Pi_{\gamma\delta\alpha\beta}(k_1, k_2) \bar{\varepsilon}_{1,\rho} \bar{\varepsilon}_{2,\sigma} \varepsilon_{1,\alpha} \varepsilon_{2,\beta} \quad (5.26)$$

Using conservation of energy  $p = k_1 + k_2$ , we are able to write a FORM code that takes care of this amplitude calculation (using real photon polarizations). Code can be found in the repository linked in [subsection G.1](#) (code named `spin2Decaygg_xigauge.frm`). Result is:

$$|\bar{\mathcal{A}}|^2 = \frac{g_\gamma^2}{5\Lambda^2} S(k_1, k_2, \varepsilon_1, \varepsilon_2) \quad (5.27)$$

Where even though the code is written for a generic  $\xi$  gauge, the resulting  $S(k_1, k_2, \varepsilon_1, \varepsilon_2)$  is  $\xi$  independent, as expected.

$$\begin{aligned} S(k_1, k_2, \varepsilon_1, \varepsilon_2) = & \frac{8}{3}(k_1 \cdot k_2)(k_1 \cdot \varepsilon_2)(\varepsilon_1 \cdot k_2)(\varepsilon_1 \cdot \varepsilon_2) - \frac{4}{3m_X^2}(k_1 \cdot k_2)(k_1 \cdot e_2)^2(\varepsilon_1 \cdot k_2)^2 \\ & + \frac{8}{3m_X^2}(k_1 \cdot k_2)^2(k_1 \cdot \varepsilon_2)(\varepsilon_1 \cdot k_2)(\varepsilon_1 \cdot \varepsilon_2) + \frac{8}{3m_X^4}(k_1 \cdot k_2)^2(k_1 \cdot \varepsilon_2)^2(\varepsilon_1 \cdot k_2)^2 \\ & - \frac{4}{3}(k_1 \cdot k_2)^2(\varepsilon_1 \cdot \varepsilon_2)^2 + 2(k_1 \cdot k_2)^2 - \frac{16}{3m_X^4}(k_1 \cdot k_2)^3(k_1 \cdot \varepsilon_2)(\varepsilon_1 \cdot k_2)(\varepsilon_1 \cdot \varepsilon_2) \\ & - \frac{4}{3m_X^2}(k_1 \cdot k_2)^3(\varepsilon_1 \cdot \varepsilon_2)^2 + \frac{8}{3m_X^4}(k_1 \cdot k_2)^4(\varepsilon_1 \cdot \varepsilon_2)^2 - \frac{4}{3}(k_1 \cdot \varepsilon_2)^2(\varepsilon_1 \cdot k_2)^2 \end{aligned} \quad (5.28)$$

Now, kinematics as usual. Being a simple 2-body decay into massless particles, [Equation 5.9](#) simplifies, so that  $k_1 \cdot k_2 = -m_X^2/2$ . By plugging this result into [Equation 5.28](#):

$$S(k_1, k_2, \varepsilon_1, \varepsilon_2) = \frac{m_X^4}{2} \Rightarrow |\bar{\mathcal{A}}|^2 = \frac{g_\gamma^2}{\Lambda^2} \frac{m_X^4}{10} \quad (5.29)$$

With these kinematic constraints, the final amplitude is actually independent from the polarization of the photons emitted, (which is not what we will see when correcting for the  $e^+e^- \rightarrow \gamma\gamma$  process, see [section 10](#)). This implies that every configuration of polarizations gives the same result. There are 4 possible helicity states, therefore we multiply the result by a factor of 4 to get the unpolarized result.

Only phase space to evaluate (use [Equation F.5](#)):

$$\begin{aligned} \Gamma(X \rightarrow \gamma\gamma) = & \frac{4C}{2m_X} \int \frac{d^3 k_1}{(2\pi)^3 2E_1} \frac{d^3 k_2}{(2\pi)^3 2E_2} (2\pi)^4 \delta^{(4)}(p - k_1 - k_2) |\bar{\mathcal{A}}|^2 = \\ = & \frac{4C}{2m_X} \frac{\sqrt{\lambda(m_X^2, 0, 0)}}{8\pi m_X^2} |\bar{\mathcal{A}}|^2 = \frac{C g_\gamma^2}{\Lambda^2} \frac{m_X^3}{40\pi} \end{aligned} \quad (5.30)$$

Notice how the  $2E$  factors at denominator of phase space are taken at face value, because photon fields are normalized with  $\sqrt{2E}$ , differently than fermion fields which do not have that normalization. Also,  $\sqrt{\lambda(m_X^2, 0, 0)} = m_X^2$ ,  $E_1 = E_2 = m_X/2$ , 4 is the photon polarization factor, and  $C$  is a combinatorial factor taking identical particles into account. It is defined as:

$$C = \frac{1}{\# \text{ identical particle permutations in final state}} \quad (5.31)$$

Because final state phase space configuration of  $(k_1, \dots, k_n)$  would be indistinguishable from any other 4-momenta permutations, and therefore need to be counted once. However, phase space integration naturally includes every permutation of momenta, leading to over counting by  $n!$ . So, we need to manually remove the  $1/n!$ , using [C<sup>12</sup>](#).

In our case,  $C = 1/2! = 1/2$ . So, into [Equation 5.30](#):

$$\Gamma(X \rightarrow \gamma\gamma) = \frac{g_\gamma^2}{\Lambda^2} \frac{m_X^3}{80\pi} \quad (5.32)$$

which corresponds to the result found in literature ([\[22\]](#)).

Note that the decay amplitude also satisfies Ward identities, just because Feynman rule does (see [Equation 4.65](#)).

If we substitute  $m_X = 17$  MeV, we get an estimate of this decay rate being:

$$\Gamma(X \rightarrow \gamma\gamma) \approx \frac{g_\gamma^2}{\Lambda^2} \times 20 \text{ MeV}^3 = \left( \frac{g_\gamma}{\Lambda [\text{MeV}]} \right)^2 \times 20 \text{ MeV} \quad (5.33)$$

## 5.4 Lower bound estimation for spin 2 couplings

### 5.4.1 From ATOMKI collaboration only

The setup is the following: a proton beam (with energy below 1 MeV) hits a fixed target, inducing, by proton absorption, strong nuclear transitions in said target. The excited nucleus usually decays emitting a gamma ray. However, in some cases the photon emitted is virtual, and it excites Internal Pair Creation (or IPC) of  $e^+e^-$ .

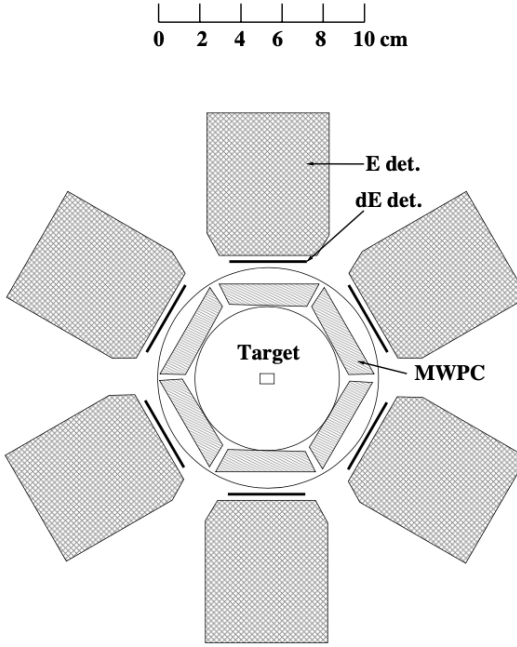


Figure 3: Geometry of the experimental apparatus in ATOMKI (courtesy of [6]). MWPC are multiwire proportional counters, while in the back there are  $\Delta E - E$  multi-detectors.

IPC is the process investigated by the ATOMKI collaboration. As targets, they used  ${}^8\text{Be}$  ([1], [4]),  ${}^4\text{He}$  ([2], [3]) and  ${}^{12}\text{C}$  ([5]). The detector geometry is set up as in Figure 3.

The MWPCs (gold-plated tungsten wires, placed at 2 mm intervals), located about 5 cm away from the target, register position of the hits of  $e^+e^-$ . Over the total distance, this segmentation gives a declared angular resolution of  $\Delta\theta_{\text{exp}} = 2^\circ$ <sup>13</sup>.

In the data analysis, the mass of the  $X$  resonance is fit using the angular correlation of the  $e^+e^-$  pairs detected. Call  $k_-$  and  $k_+$  the momenta of the electron and positron, respectively:

$$\begin{aligned}
 m_X^2 &= -(k_+ + k_-)^2 = 2m_e^2 - 2k_- \cdot k_+ = \\
 &= 2m_e^2 + 2E_-E_+ - 2|\vec{k}_-||\vec{k}_+| \cos\theta = \\
 &\approx 2E_-E_+(1 - \cos\theta) = \\
 &= 4E_-E_+ \sin^2\left(\frac{\theta}{2}\right) = \\
 &= \left(1 - y^2\right) E^2 \sin\left(\frac{\theta}{2}\right) \quad \text{where} \quad y = \frac{E_+ - E_-}{E_+ + E_-} \tag{5.34}
 \end{aligned}$$

where  $\theta$  is the relative angle of the pair,  $E_-$  and  $E_+$  are the energies,  $E = E_- + E_+$ , and  $y$  is called "asymmetry parameter".

Whenever we have a resonance, the invariant mass of decay products follows a Breit-Wigner distribution. The width of the distribution,  $\Gamma$ , is the actual decay rate of the resonance. Unfortunately, because width is smaller than the experimental resolution, ATOMKI does not measure  $\Gamma$ .

We can only exploit the geometry of the experiment to get a lower bound on  $\Gamma$ . On first glance, one could say that we could require  $X$  to have a decay length  $< 5\text{ cm}$ , to stay inside the apparatus. This would be a large overestimation, however, because the measured invariant mass depends on the relative angle between pairs (Equation 5.34). So, if  $X$  were to decay anywhere in the apparatus, the invariant mass distribution would be smeared by the exponential decay distribution of the resonance, leading to a disappearance of the  $X17$  peak itself.

<sup>12</sup>[25] makes it clear that this is in no way related to amplitudes and only regards phase space integration.

<sup>13</sup>I would argue that it should actually be:

$$\Delta\theta_{\text{exp}} = \frac{2\text{ mm}}{5\text{ cm}} \times \sqrt{\frac{2}{12}} \approx 1^\circ$$

to include the dispersion from a uniform distribution.

Hence, we need to assume that, for the mass to be always measured around  $16.9 \pm 0.2$  MeV, this exponential smearing introduced by the decay length of the particle is contained within the resolution bounds of the opening angle. This is exemplified by [Figure 4](#):

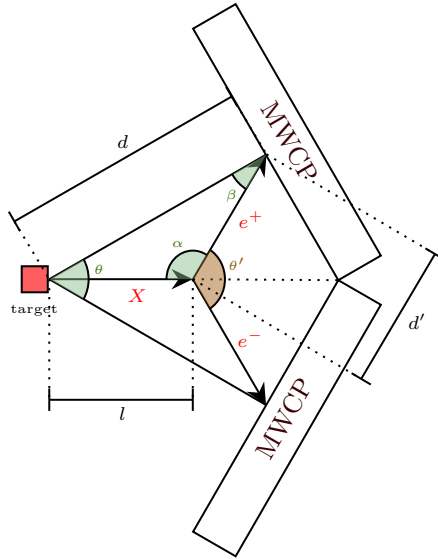


[Figure 4](#): Effect of a long decaying resonance on angle correlation. The measured angle would be  $\theta$ , but the real angle would be  $\theta'$ .

For the mass  $m_X$  to be within the accepted range, we require  $\Delta\theta = \theta' - \theta < \Delta\theta_{\text{exp}}$ . By the law of sines on the geometry, we get a constraint on the decay length  $l$ , in the lab frame:

$$\frac{\sin \beta}{l} = \frac{\sin \alpha}{d} \quad \Rightarrow \quad l = \frac{\sin \beta}{\sin \alpha} d = \frac{\sin (\Delta\theta/2)}{\sin (\theta'/2)} d \quad (5.35)$$

If we name  $l_{\text{max}}$  the maximum value of decay for  $\Delta\theta = \Delta\theta_{\text{exp}}$ , then for the different experiment we get different values for  $l_{\text{max}}$ , which then constrain  $\Gamma$ , from [Equation 5.15](#):

$$l_{\text{max}} = \frac{\sin (\Delta\theta_{\text{exp}}/2)}{\sin (\theta'/2)} d \quad \Gamma_{\text{min}} = \frac{\beta \gamma}{l_{\text{max}}} \quad \frac{g_e}{\Lambda} > \sqrt{\frac{\Gamma_{\text{min}}}{10 \text{ MeV}^3}} \quad (5.36)$$

which gives the following result ([Table 1](#)) when substituting values for all experiments at ATOMKI.

Target	$\theta [^\circ]$	$E [\text{MeV}]$	$\beta$	$\gamma$	$l_{\text{max}} [\text{cm}]$	$\Gamma_{\text{min}} [\text{MeV}^{-1}]$	$g_e/\Lambda  _{\text{min}} [\text{MeV}^{-1}]$
${}^4\text{He}$	112	21.01	0.592	1.241	0.104	$1.4 \times 10^{-10}$	$3.8 \times 10^{-6}$
		20.21	0.544	1.192		$1.2 \times 10^{-10}$	$3.6 \times 10^{-6}$
${}^8\text{Be}$	139	18.15	0.359	1.071	0.092	$8.2 \times 10^{-11}$	$3.0 \times 10^{-6}$
		17.64	0.279	1.041		$6.1 \times 10^{-11}$	$2.5 \times 10^{-6}$
${}^{12}\text{C}$	161	17.23	0.186	1.018	0.088	$4.3 \times 10^{-11}$	$2.1 \times 10^{-6}$

[Table 1](#): All values for the total energy of the pairs  $e^+e^-$  in different experimental setups, and final minimum value for the coupling  $g_e/\Lambda$  in each experiment performed by the ATOMKI collaboration. Mass of the resonance has been mediated between all ATOMKI results and assumed to be  $m_X = 16.94$  MeV.

So, to explain all results, the most conservative lower bound for the coupling constant is:

$$\frac{g_e}{\Lambda} \gtrsim 3.8 \times 10^{-6} \text{ MeV}^{-1} \quad (5.37)$$

what these bounds mean is that, were the coupling  $g_e/\Lambda$  to be smaller, then the measurement itself of the mass  $m_X$  would be smeared and shifted by at least 0.2 MeV, outside the error that ATOMKI reports.

#### 5.4.2 Adding JINR collaboration

The setup is the following: a proton or a deuteron beam (with energies of order 10 GeV) hits a fixed target (tested with carbon or copper). Energy is too high for proton absorption, so the nucleus undergoes spallation, opening the possibility for many possible final states.

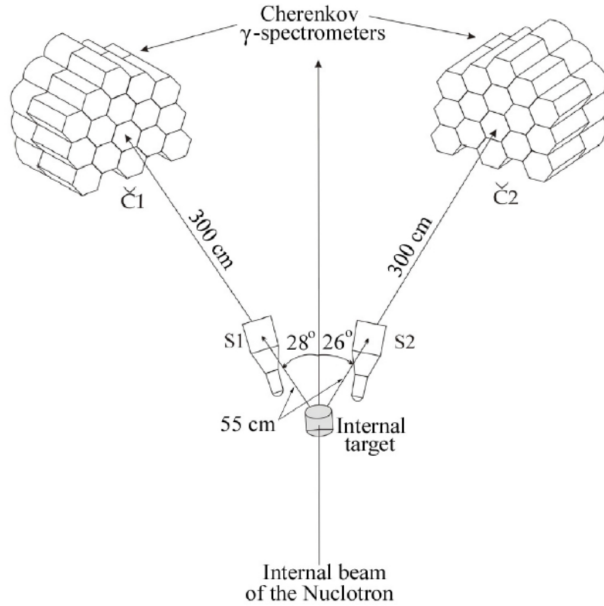


Figure 5: Geometry of the experimental apparatus in JINR (courtesy of [8]).  $S_1$  and  $S_2$  are scintillation counters, while the setup in the back consists of 32 lead glass Cherenkov spectrometers (called PHOTON-2).

The JINR collaboration has been focusing on the  $\gamma\gamma$  final state ([8]), for precision measurements. The detector geometry is set up as in Figure 5.

Experiment unfolds at a larger scale than ATOMKI, as energies are much higher. Scintillators  $S_1$  and  $S_2$  are there for triggering purposes, while position and angular measurement are relegated to the Cherenkov spectrometers, about 3.5 m distant from the target.

Again, the mass of the  $X$  resonance is fit using the angular correlation of the  $\gamma\gamma$  pairs detected. Equation 5.34 also describes the two photons setup. JINR, like ATOMKI, cannot measure  $\Gamma$ , and instead rely on a one parameter fit from angular correlation.

The only way to obtain a lower bound on  $\Gamma$  is to exploit the geometry of the experiment. Because the detectors only cover a small portion of the solid angle, the simple request that the decay products of  $X$  hit the detectors in a bee line might be even more constraining than the request that the distortion of the correlation angle due to the finite decay length be smaller than the resolution (in this case,  $\Delta\theta_{\text{exp}} = 0.9^\circ$ ). Let us calculate both constraints and compare the result.

**Collinearity constraint:** The geometrical setup is seen in Figure 5. The worst case scenario that allows for the largest decay length  $l_{\max}$  because it does not miss any detector (hence, trigger is still active) is visible in Figure 6. Let us set out a system of equations to find  $l$ :

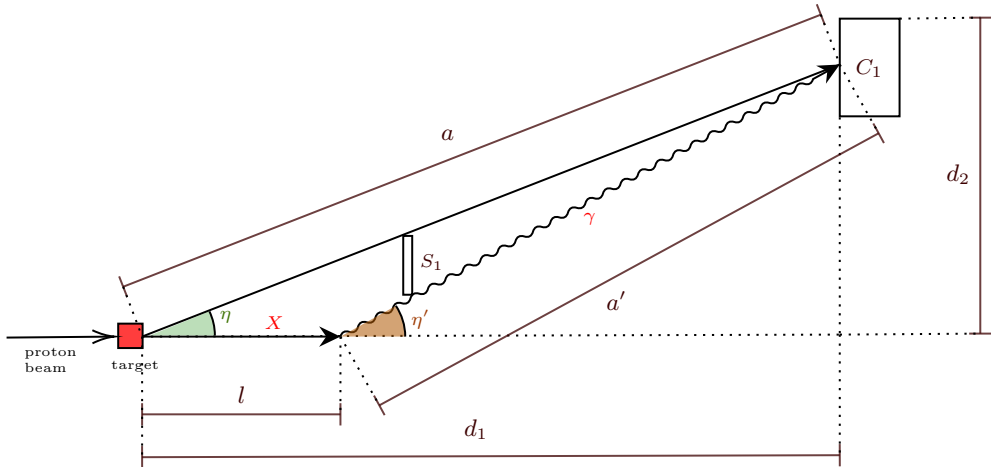


Figure 6: Aerial scheme on the left arm spectrometer. Largest decay length allowed for  $X$  that allows for detection of the produces  $\gamma$  ray is highlighted. The measured relative angle would be  $\eta$  while the true relative angle is  $\eta'$ . Decay length is called  $l$  in this image.

$$\left\{ \begin{array}{l} \frac{l}{\sin \Delta\eta} = \frac{a'}{\sin \eta} \\ a' \cos \eta' = d_1 \\ a' \sin \eta' = d_2 \end{array} \right. \quad (5.38)$$

where  $\Delta\eta = \eta' - \eta$ . Using data from the geometry of the experiment ( $\eta = 28^\circ$ ), we find the solution to the system to be  $l = l_{\max} = 24$  cm.

The trigger condition for the photon pair collection is that the total energy of the pair  $E > 250$  MeV, which implies that, from  $m_X = 16.94$  MeV<sup>14</sup>, then  $\beta = 0.998$  and  $\gamma = 14.70$ .

This implies, from Equation 5.33:

$$\Gamma_{\min} = 1.2 \times 10^{-11} \text{ MeV} \quad \Rightarrow \quad \frac{g_\gamma}{\Lambda} > \sqrt{\frac{\Gamma_{\min}}{20 \text{ MeV}^3}} = 7.7 \times 10^{-7} \text{ MeV}^{-1} \quad (5.39)$$

**Angular resolution constraint:** We can use the same exact constraint condition as in subsubsection 5.4.1, requiring  $\Delta\theta < 0.9^\circ$  which is the best angular resolution JINR achieves. From Figure 6, we surmise  $\Delta\theta = 2\Delta\eta$ , and so from Equation 5.35:

$$l_{\min} = \frac{\sin(\Delta\eta)}{\sin(\eta')} a = 2.74 \text{ cm} \quad (5.40)$$

which is actually 10 times greater than the previous result. So:

$$\Gamma_{\min} = 1.1 \times 10^{-10} \text{ MeV} \quad \Rightarrow \quad \frac{g_\gamma}{\Lambda} > \sqrt{\frac{\Gamma_{\min}}{20 \text{ MeV}^3}} = 2.3 \times 10^{-6} \text{ MeV}^{-1} \quad (5.41)$$

Now, it is crucial that in both experiments (ATOMKI and JINR), the decay length is given by the same total width of the  $X$  resonance  $\Gamma$ . When we only had  $X \rightarrow e^+e^-$ , we had one branching ratio. Now, if we switch on  $g_\gamma \neq 0$ , then we also get a contribution from  $X \rightarrow \gamma\gamma$  decay. This means that the same width that both experiments require to measure  $m_X$ , using angular correlation, gets two contributions. The request  $\Gamma > \Gamma_{\min}$  will exclude an elliptic region inside parameter space for  $g_e$  and  $g_\gamma$ . As for  $\Gamma_{\min}$ , we will take the most constraining result from both experiments, which is from ATOMKI estimate ( $\Gamma_{\min} = 1.4 \times 10^{-10}$  MeV). So:

$$\begin{aligned} \Gamma &= \Gamma(X \rightarrow e^+e^-) + \Gamma(X \rightarrow \gamma\gamma) = \\ &= \frac{g_e^2}{\Lambda^2} 9.6 \text{ MeV}^3 + \frac{g_\gamma^2}{\Lambda^2} 19.3 \text{ MeV}^3 > \Gamma_{\min} \end{aligned} \quad (5.42)$$

For the sake of argument, we will set our couplings equal to the lower bounds estimated if their contribution is dominant for the decay (with the exception of section 13 and section 14), and use it to investigate the consequences of these new couplings on QED processes.

For  $g_e$ , that is  $\Gamma(X \rightarrow e^+e^-) = \Gamma_{\min}$ , so:

$$\frac{g_e}{\Lambda} = 3.8 \times 10^{-6} \text{ MeV}^{-1} \quad (5.43)$$

and for  $g_\gamma$ ,  $\Gamma(X \rightarrow \gamma\gamma) = \Gamma_{\min}$ , so:

$$\frac{g_\gamma}{\Lambda} = 2.7 \times 10^{-6} \text{ MeV}^{-1} \quad (5.44)$$

---

<sup>14</sup>[8] does not report their value for the mass of the resonance  $X$  - although still around 17 MeV, which we then assume from the ATOMKI experiment.

## 6 Correction to Bhabha scattering

The process we are now going to study is  $e^+e^- \rightarrow e^+e^-$ , called *Bhabha scattering*. The contributing diagrams for this process are the *s-channel* and the *t-channel*, in [Figure 7](#):

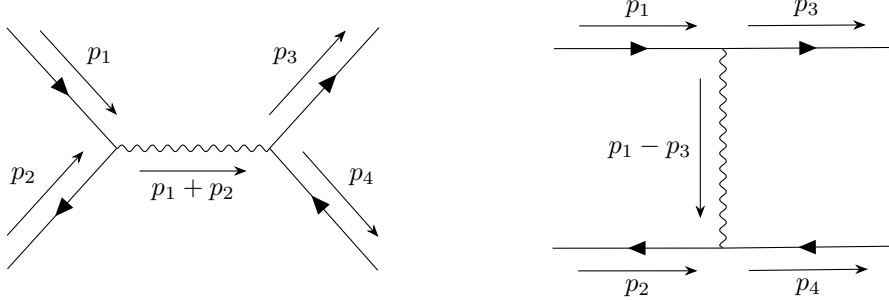


[Figure 7](#): Diagrams corresponding to tree level Bhabha scattering. On the left, the *s*-channel, hereafter denoted with  $\mathcal{A}_1$ . On the right, the *t*-channel, hereafter denoted with  $\mathcal{A}_2$ .

We add the diagram in which the  $X$  boson is mediated ([Figure 8](#)), contributing with both *s*-channel and *t*-channel:

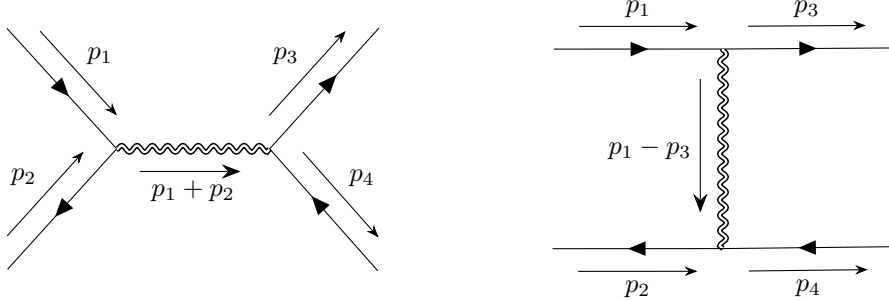


[Figure 8](#): Tree level diagrams for the mediation of massive spin 2 boson for Bhabha scattering, basically accounting for *s*-channel (left) and *t*-channel (right) contributions. We will refer to the left amplitude as  $\mathcal{A}_3$ , and to the right amplitude as  $\mathcal{A}_4$ .

The amplitudes are quite easily written following [subsection A.1](#):

$$\begin{aligned} \mathcal{A}_1 &= (-ie)^2 \hat{D}_{\mu\nu}^\xi(p_1 + p_2) [\bar{v}(p_2, \lambda_2) \gamma_\mu u(p_1, \lambda_1)] [\bar{u}(p_3, \lambda_3) \gamma_\nu v(p_4, \lambda_4)] = \\ &= -e^2 \hat{D}_{\mu\nu}^\xi(p_1 + p_2) [\bar{v}_2 \gamma_\mu u_1] [\bar{u}_3 \gamma_\nu v_4] \end{aligned} \quad (6.1)$$

$$\begin{aligned} \mathcal{A}_2 &= (-ie)^2 \hat{D}_{\mu\nu}^\xi(p_1 - p_3) [\bar{u}(p_3, \lambda_3) \gamma_\mu u(p_1, \lambda_1)] [\bar{v}(p_2, \lambda_2) \gamma_\nu v(p_4, \lambda_4)] = \\ &= -e^2 \hat{D}_{\mu\nu}^\xi(p_1 - p_3) [\bar{u}_3 \gamma_\mu u_1] [\bar{v}_2 \gamma_\nu v_4] \end{aligned} \quad (6.2)$$

where  $\hat{D}_{\mu\nu}^\xi$  is the photon propagator in the  $\xi$  gauge ([subsection A.1](#)). The usual electrodynamics Feynman rule  $-ie\gamma_\mu$  applies at each vertex,  $m_e$  is the mass of the electron,  $p_i$ ,  $i \in \{1, 2, 3, 4\}$  are the respective momenta according to [Figure 43](#) and  $\lambda_i$ ,  $i \in \{1, 2, 3, 4\}$  are the respective polarizations of fermions. Here forth, we will call  $u(p_i, \lambda_i) = u_i$ ,  $i \in \{1, 3\}$  and  $v(p_i, \lambda_i) = v_i$ ,  $i \in \{2, 4\}$ .

Instead, for  $\mathcal{A}_3$  and  $\mathcal{A}_4$  we will employ [Equation 4.56](#). Note that in the *t*-channel, both interactions see a

changed sign in one of the two momenta ( $-p$  for the  $X - e^+e^-$  interaction):

$$\begin{aligned}\mathcal{A}_3 &= \left(\frac{ig_e}{2\Lambda}\right)^2 \left[ \frac{N_{\mu\alpha\nu\beta}(p_1 + p_2)}{(p_1 + p_2)^2 + m_X^2} \right] [\bar{v}(p_2, \lambda_2) \gamma_\mu (p_{2,\alpha} - p_{1,\alpha}) u(p_1, \lambda_1)] [\bar{u}(p_3, \lambda_3) \gamma_\nu (p_{3,\beta} - p_{4,\beta}) v(p_4, \lambda_4)] = \\ &= -\frac{g_e^2}{4\Lambda^2} \left[ \frac{N_{\mu\alpha\nu\beta}(p_1 + p_2)}{(p_1 + p_2)^2 + m_X^2} \right] (p_{2,\alpha} - p_{1,\alpha}) (p_{3,\beta} - p_{4,\beta}) [\bar{v}_2 \gamma_\mu u_1] [\bar{u}_3 \gamma_\nu v_4]\end{aligned}\quad (6.3)$$

$$\begin{aligned}\mathcal{A}_4 &= \left(\frac{ig_e}{2\Lambda}\right)^2 \left[ \frac{N_{\mu\alpha\nu\beta}(p_1 - p_3)}{(p_1 - p_3)^2 + m_X^2} \right] [\bar{u}(p_3, \lambda_3) \gamma_\mu (p_{3,\alpha} + p_{1,\alpha}) u(p_1, \lambda_1)] [\bar{v}(p_2, \lambda_2) \gamma_\nu (p_{2,\beta} + p_{4,\beta}) v(p_4, \lambda_4)] = \\ &= -\frac{g_e^2}{4\Lambda^2} \left[ \frac{N_{\mu\alpha\nu\beta}(p_1 - p_3)}{(p_1 - p_3)^2 + m_X^2} \right] (p_{3,\alpha} + p_{1,\alpha}) (p_{2,\beta} + p_{4,\beta}) [\bar{u}_3 \gamma_\mu u_1] [\bar{v}_2 \gamma_\nu v_4]\end{aligned}\quad (6.4)$$

where  $N_{\mu\alpha\nu\beta}(q)$  is the numerator of spin 2 propagator, as defined in [Equation 4.26](#). A few remarks:

- First,  $\mathcal{A}_1$  and  $\mathcal{A}_3$  have the same Dirac structure. The final amplitude trace will be the same as in QED. Same goes for  $\mathcal{A}_2$  and  $\mathcal{A}_4$ . This is just because the diagrams have the same structure, the propagation is the only difference.
- In [subsection A.2](#) not only do we show why the factor  $1/2!$  in the expansion actually cancels during Wick contractions, but we also unequivocally show that  $\mathcal{A}_1$  and  $\mathcal{A}_3$  have an absolute minus sign as  $s$ -channels. Intuitively, the heuristic argument of spinor swaps with a minus sign can be made to justify it, but it is only heuristic as spinors simply commute, and it is the operators they are paired with that anticommute). This implies the total amplitude to be:

$$\mathcal{A} = -(\mathcal{A}_1 + \mathcal{A}_3) + (\mathcal{A}_2 + \mathcal{A}_4)\quad (6.5)$$

Define the usual Mandelstam variables:

$$s = (p_1 + p_2)^2 \quad t = (p_1 - p_3)^2 \quad u = (p_1 - p_4)^2$$

Then, we need to calculate the complex conjugate of these amplitudes. For  $\mathcal{A}_1$  and  $\mathcal{A}_2$ , we follow [subsection A.1](#):

$$\mathcal{A}_1^* = -e^2 \hat{D}_{\rho\sigma}^\xi(p_1 + p_2) [\bar{u}_1 \gamma_\rho v_2] [\bar{v}_4 \gamma_\sigma u_3]\quad (6.6)$$

$$\mathcal{A}_2^* = -e^2 \hat{D}_{\rho\sigma}^\xi(p_1 - p_3) [\bar{u}_1 \gamma_\rho u_3] [\bar{v}_4 \gamma_\sigma v_2]\quad (6.7)$$

Instead, for  $\mathcal{A}_3$  and  $\mathcal{A}_4$ , we use results from Appendices, namely [Equation A.5](#), [Equation F.11](#), [Equation F.14](#). Let us define the generic phase  $\alpha_p = (-1)^{\delta_{\alpha^4}}$  for simplicity. Obviously  $\alpha_p^2 = 1$ , as it is a real number. So, in order to check that all minus signs disappear, we just have to pair them up:

$$\begin{aligned}\mathcal{A}_3^* &= -\frac{g_e^2}{4\Lambda^2} \left[ \frac{N_{\rho\gamma\sigma\lambda}^*(p_1 + p_2)}{(p_1 + p_2)^2 + m_X^2} \right] (p_{2,\gamma} - p_{1,\gamma})^* (p_{3,\lambda} - p_{4,\lambda})^* [\bar{v}_2 \gamma_\rho u_1]^* [\bar{u}_3 \gamma_\sigma v_4]^* = \\ &= -\frac{g_e^2}{4\Lambda^2} \left[ \frac{\rho_p \gamma_p \sigma_p \lambda_p N_{\rho\gamma\sigma\lambda}(p_1 + p_2)}{(p_1 + p_2)^2 + m_X^2} \right] \gamma_p (p_{2,\gamma} - p_{1,\gamma}) \lambda_p (p_{3,\lambda} - p_{4,\lambda}) (-\rho_p) [\bar{u}_1 \gamma_\rho v_2] (-\sigma_p) [\bar{v}_4 \gamma_\sigma u_3] = \\ &= -\frac{g_e^2}{4\Lambda^2} \left[ \frac{N_{\rho\gamma\sigma\lambda}(p_1 + p_2)}{(p_1 + p_2)^2 + m_X^2} \right] (p_{2,\gamma} - p_{1,\gamma}) (p_{3,\lambda} - p_{4,\lambda}) [\bar{u}_1 \gamma_\rho v_2] [\bar{v}_4 \gamma_\sigma u_3]\end{aligned}\quad (6.8)$$

$$\mathcal{A}_4^* = \dots = -\frac{g_e^2}{4\Lambda^2} \left[ \frac{N_{\rho\gamma\sigma\lambda}(p_1 - p_3)}{(p_1 - p_3)^2 + m_X^2} \right] (p_{3,\gamma} + p_{1,\gamma}) (p_{2,\lambda} + p_{4,\lambda}) [\bar{u}_1 \gamma_\rho u_3] [\bar{v}_4 \gamma_\sigma v_2]\quad (6.9)$$

as expected, every phase disappears. This must be the case, as they only appear because of our choice of notation, from which amplitudes must be independent.

Now, let us exploit the Dirac structure and define:

$$\hat{S}_{\mu\nu}^\xi(p_i) = e^2 \hat{D}_{\mu\nu}^\xi(p_1 + p_2) + \frac{g_e^2}{4\Lambda^2} \left[ \frac{N_{\mu\alpha\nu\beta}(p_1 + p_2)}{(p_1 + p_2)^2 + m_X^2} \right] (p_{2,\alpha} - p_{1,\alpha}) (p_{3,\beta} - p_{4,\beta})\quad (6.10)$$

$$\hat{T}_{\mu\nu}^\xi(p_i) = e^2 \hat{D}_{\mu\nu}^\xi(p_1 - p_3) + \frac{g_e^2}{4\Lambda^2} \left[ \frac{N_{\mu\alpha\nu\beta}(p_1 - p_3)}{(p_1 - p_3)^2 + m_X^2} \right] (p_{3,\alpha} + p_{1,\alpha}) (p_{2,\beta} + p_{4,\beta})\quad (6.11)$$

with this definition it is trivial to exchange  $s$  and  $t$  channels:

$$\hat{T}_{\mu\nu}^\xi(p_1, p_2, p_3, p_4) = \hat{S}_{\mu\nu}^\xi(p_1, -p_3, -p_2, p_4)$$

so that amplitudes are easily summed:

$$\begin{aligned}\mathcal{A}_s &= \mathcal{A}_1 + \mathcal{A}_3 = \hat{S}_{\mu\nu}^\xi(p_i) [\bar{v}_2 \gamma_\mu u_1] [\bar{u}_3 \gamma_\nu v_4] \\ \mathcal{A}_t &= \mathcal{A}_2 + \mathcal{A}_3 = \hat{T}_{\mu\nu}^\xi(p_i) [\bar{u}_3 \gamma_\mu u_1] [\bar{v}_2 \gamma_\nu v_4] \\ \mathcal{A}_s^* &= \mathcal{A}_1^* + \mathcal{A}_3^* = \hat{S}_{\mu\nu}^\xi(p_i) [\bar{u}_1 \gamma_\rho v_2] [\bar{v}_4 \gamma_\sigma u_3] \\ \mathcal{A}_t^* &= \mathcal{A}_2^* + \mathcal{A}_4^* = \hat{T}_{\mu\nu}^\xi(p_i) [\bar{u}_1 \gamma_\rho u_3] [\bar{v}_4 \gamma_\sigma v_2]\end{aligned}$$

and we can write the modulus squared:

$$|\mathcal{A}|^2 = (-\mathcal{A}_s + \mathcal{A}_t)(-\mathcal{A}_s^* + \mathcal{A}_t^*) = |\mathcal{A}_s|^2 + |\mathcal{A}_t|^2 - \mathcal{A}_s \mathcal{A}_t^* - \mathcal{A}_t \mathcal{A}_s^* \quad (6.12)$$

term by term, using the calculations in Dirac space in [subsection A.2](#):

$$\begin{aligned}|\mathcal{A}_s|^2 &= \hat{S}_{\mu\nu}^\xi(p_i) \hat{S}_{\rho\sigma}^\xi(p_i) \text{Tr} [\gamma_\mu (u_1 \bar{u}_1) \gamma_\rho (v_2 \bar{v}_2)] \text{Tr} [\gamma_\nu (v_4 \bar{v}_4) \gamma_\sigma (u_3 \bar{u}_3)] \\ |\mathcal{A}_t|^2 &= \hat{T}_{\mu\nu}^\xi(p_i) \hat{T}_{\rho\sigma}^\xi(p_i) \text{Tr} [\gamma_\mu (u_1 \bar{u}_1) \gamma_\rho (u_3 \bar{u}_3)] \text{Tr} [\gamma_\nu (v_4 \bar{v}_4) \gamma_\sigma (v_2 \bar{v}_2)] \\ \mathcal{A}_s \mathcal{A}_t^* &= \hat{S}_{\mu\nu}^\xi(p_i) \hat{T}_{\rho\sigma}^\xi(p_i) \text{Tr} [\gamma_\mu (u_1 \bar{u}_1) \gamma_\rho (u_3 \bar{u}_3) \gamma_\nu (v_4 \bar{v}_4) \gamma_\sigma (v_2 \bar{v}_2)] \\ \mathcal{A}_t \mathcal{A}_s^* &= \hat{T}_{\mu\nu}^\xi(p_i) \hat{S}_{\rho\sigma}^\xi(p_i) \text{Tr} [\gamma_\mu (u_1 \bar{u}_1) \gamma_\rho (v_2 \bar{v}_2) \gamma_\nu (v_4 \bar{v}_4) \gamma_\sigma (u_3 \bar{u}_3)]\end{aligned}$$

Averaging over initial fermion polarization and summing over all of them we get the unpolarized amplitude:

$$\begin{aligned}|\bar{\mathcal{A}}|^2 &= \frac{1}{4} \sum_{\lambda_1} \sum_{\lambda_2} \sum_{\lambda_3} \sum_{\lambda_4} \left( |\mathcal{A}_s|^2 + |\mathcal{A}_t|^2 - \mathcal{A}_s \mathcal{A}_t^* - \mathcal{A}_t \mathcal{A}_s^* \right) = \frac{1}{4} \frac{1}{2p_{1,4} 2p_{2,4} 2p_{3,4} 2p_{4,4}} \times \\ &\left\{ \hat{S}_{\mu\nu}^\xi(p_i) \hat{S}_{\rho\sigma}^\xi(p_i) \text{Tr} \left[ \gamma_\mu (-i\cancel{p}_1 + m_e) \gamma_\rho (-i\cancel{p}_2 - m_e) \right] \text{Tr} \left[ \gamma_\nu (-i\cancel{p}_4 - m_e) \gamma_\sigma (-i\cancel{p}_3 + m_e) \right] \right. \\ &+ \hat{T}_{\mu\nu}^\xi(p_i) \hat{T}_{\rho\sigma}^\xi(p_i) \text{Tr} \left[ \gamma_\mu (-i\cancel{p}_1 + m_e) \gamma_\rho (-i\cancel{p}_3 + m_e) \right] \text{Tr} \left[ \gamma_\nu (-i\cancel{p}_4 - m_e) \gamma_\sigma (-i\cancel{p}_2 - m_e) \right] \\ &- \hat{S}_{\mu\nu}^\xi(p_i) \hat{T}_{\rho\sigma}^\xi(p_i) \text{Tr} \left[ \gamma_\mu (-i\cancel{p}_1 + m_e) \gamma_\rho (-i\cancel{p}_3 + m_e) \gamma_\nu (-i\cancel{p}_4 - m_e) \gamma_\sigma (-i\cancel{p}_2 - m_e) \right] \\ &\left. - \hat{T}_{\mu\nu}^\xi(p_i) \hat{S}_{\rho\sigma}^\xi(p_i) \text{Tr} \left[ \gamma_\mu (-i\cancel{p}_1 + m_e) \gamma_\rho (-i\cancel{p}_2 - m_e) \gamma_\nu (-i\cancel{p}_4 - m_e) \gamma_\sigma (-i\cancel{p}_3 + m_e) \right] \right\} \quad (6.13)\end{aligned}$$

Because we do not want to go crazy before its due time, we leave the task of computing this colossal amplitude to a computer. The FORM script used for this task is found in the repository linked in [subsection G.1](#).

The final result has thousands of addends and we do not deem it practical to report here. However, we can obtain a simplified result by directly substituting the values of the scalar products found in [subsection A.3](#), but we need to perform the integral in phase space first, locking the kinematic variables using the delta function. To carry out the calculation, we will be following closely the passages found in [subsection A.4](#). In particular, using the result in [Equation A.38](#):

$$\frac{d\sigma}{d\Omega} = \frac{E^2}{16\pi^2} |\bar{\mathcal{A}}|^2$$

where now  $\mathcal{A}$  is the amplitude where we imposed kinematics. Let us write it:

$$\begin{aligned}|\bar{\mathcal{A}}|^2 &= \frac{1}{64E^4} F(s, t, u) \\ F(s, t, u) &= F_s(s, t, u) + F_t(s, t, u) + F_{st}(s, t, u)\end{aligned}$$

where  $F(s, t, u)$  is an adimensional function of the Mandelstam variables, and it is the actual result of the FORM computation. It gets contributions from each term of the squared amplitude:  $F_s$  from  $s$ -channel squared,  $F_t$  from  $t$ -channel squared,  $F_{st}$  from interference terms.

## 6.1 Simplifying Bhabha result

The code we used is called `Bhabha_Xspin2_xigauge.frm` and it provides the result of the calculation of the traces. The result is  $\xi$  independent, because of gauge invariance, before imposing kinematics (as gauge invariance comes before kinematics). To manipulate the resulting terms, we can use [Equation A.27](#)<sup>15</sup>.

**s-channel:** It consists of 127 terms. However, for the first time we have interfering terms  $e^2 g_e^2 / \Lambda^2$ . Because coupling constant is very small, we can focus only on  $e^4$  and  $e^2 g_e^2 / \Lambda^2$  terms, and ignore  $g_e^4 / \Lambda^4$  terms. If we do it, the number of terms goes down to "only" 26 terms, before simplification:

$$F_s(s, t, u) = 8e^4 \left[ -\frac{2tu}{s^2} - \frac{u}{s} - \frac{t}{s} \right] + 16m_e^2 e^4 \left[ -\frac{u}{s^2} - \frac{t}{s^2} - \frac{3}{s} \right] + \frac{e^2 g_e^2}{\Lambda^2} \frac{1}{s + m_X^2} \times \\ \left\{ S_1(s, t, u) + \frac{m_e^2}{m_X^2} S_2(s, t, u) + m_e^2 S_3(s, t, u) + \frac{m_e^4}{m_X^2} S_4(s, t, u) + \frac{m_e^6}{m_X^2} S_5(s, t, u) \right\} \quad (6.14)$$

$$S_1(s, t, u) = \frac{4}{3} \left[ \frac{tu^2}{s} - \frac{t^2u}{s} + t^2 - u^2 \right] = \frac{4}{3s} \left[ ut(u-t) + s(t^2 - u^2) \right] = \\ = \frac{4}{3} \left( \frac{u-t}{s} \right) [ut + s(u+t)] \quad (6.15)$$

$$S_2(s, t, u) = 4 \left[ \frac{u^3}{s} + \frac{tu^2}{s} - \frac{t^2u}{s} - \frac{t^3}{s} + 2u^2 - 2t^2 + us - ts \right] = \\ = \frac{4}{s} \left[ (u-t)(u^2 + ut + t^2) + ut(u-t) - 2s(u-t)(u+t) + s^2(u-t) \right] = \\ = 4 \left( \frac{u-t}{s} \right) [(u+t)^2 + 2s(u+t) + s^2] = \\ = 4 \left( \frac{u-t}{s} \right) [(u+t+s)^2] = 64m_e^4 \left( \frac{u-t}{s} \right) \quad (6.16)$$

$$S_3(s, t, u) = \frac{16u^2}{3s} - \frac{16t^2}{3s} = \frac{16(u+t)}{3} \left( \frac{u-t}{s} \right) \quad (6.17)$$

$$S_4(s, t, u) = 32 \left[ \frac{u^2}{s} - \frac{t^2}{s} + u - t \right] = \frac{32}{s} [(u-t)(u+t) + s(u-t)] = \\ = 32 \left( \frac{u-t}{s} \right) (u+t+s) = -128m_e^2 \left( \frac{u-t}{s} \right) \quad (6.18)$$

$$S_5(s, t, u) = \frac{64u}{s} - \frac{64t}{s} = 64 \left( \frac{u-t}{s} \right) \quad (6.19)$$

---

<sup>15</sup>Whenever we are about to use  $s + t + u = -4m_e^2$ , the substituting part will be colored in blue.

Manipulation of the QED part can be found in [Equation A.43](#). In total:

$$\begin{aligned}
F_s(s, t, u) &= \frac{8e^4}{s^2} \left[ u^2 + t^2 + 8m_e^2(u+t) + 24m_e^4 \right] + \frac{e^2 g_e^2}{\Lambda^2} \frac{1}{s+m_X^2} \left( \frac{u-t}{s} \right) \times \\
&\quad \left\{ \frac{4}{3} [ut - s(u+t)] + \cancel{\frac{64 m_e^6}{m_X^2}} + \frac{16}{3} m_e^2(u+t) - \cancel{\frac{128 m_e^6}{m_X^2}} + \cancel{\frac{64 m_e^6}{m_X^2}} \right\} = \\
&= \frac{8e^4}{s^2} [\dots] + \frac{4 e^2 g_e^2}{\Lambda^2} \frac{1}{s+m_X^2} \left( \frac{u-t}{s} \right) \left[ ut - (\textcolor{blue}{u+t}) (s - 4m_e^2) \right] = \\
&= \frac{8e^4}{s^2} [\dots] + \frac{4 e^2 g_e^2}{\Lambda^2} \frac{1}{s+m_X^2} \left( \frac{u-t}{s} \right) \left[ ut + (s + 4m_e^2) (s - 4m_e^2) \right]
\end{aligned} \tag{6.20}$$

the  $m_X^2$  terms all vanish.

**t-channel:** It is immediate from the code that  $T_i(s, t, u) = S_i(t, s, u)$ , for  $i \in \{1, 2, 3, 4, 5\}$ . So, this means:

$$F_t(s, t, u) = F_s(t, s, u)$$

Manipulation is trivial, as we just need to exchange  $s$  and  $t$  to get the result. Same for the QED part (see [Equation A.43](#)):

$$\begin{aligned}
F_t(s, t, u) &= 8e^4 \left[ -\frac{2su}{t^2} - \frac{u}{t} - \frac{s}{t} \right] + 16m_e^2 e^4 \left[ -\frac{u}{t^2} - \frac{t}{t^2} - \frac{3}{t} \right] + \frac{e^2 g_e^2}{\Lambda^2} \frac{1}{t+m_X^2} \times \\
&\quad \left\{ T_1(s, t, u) + \frac{m_e^2}{m_X^2} T_2(s, t, u) + m_e^2 T_3(s, t, u) + \frac{m_e^4}{m_X^2} T_4(s, t, u) + \frac{m_e^6}{m_X^2} T_5(s, t, u) \right\} = \dots = \\
&= \frac{8e^4}{s^2} [\dots] + \frac{4 e^2 g_e^2}{\Lambda^2} \frac{1}{t+m_X^2} \left( \frac{u-s}{t} \right) \left[ us + (t + 4m_e^2) (t - 4m_e^2) \right]
\end{aligned} \tag{6.21}$$

**Interference terms:** We get 172 terms. We can focus only on  $e^4$  and  $e^2 g_e^2 / \Lambda^2$  terms, and ignore  $g_e^4 / \Lambda^4$  terms. If we do it, the number of terms goes down to "only" 69 terms, before simplification:

$$\begin{aligned}
F_{st}(s, t, u) &= 16e^4 \left[ -\frac{u}{s} - \frac{u}{t} \right] + 16m_e^2 e^4 \left[ \frac{u}{st} - \frac{3}{s} - \frac{3}{t} \right] \\
&\quad + \frac{e^2 g_e^2}{\Lambda^2} \frac{1}{s+m_X^2} \left\{ I_1(s, t, u) + \frac{m_e^2}{m_X^2} I_2(s, t, u) + m_e^2 I_3(s, t, u) + \frac{m_e^4}{m_X^2} I_4(s, t, u) \right. \\
&\quad \left. + m_e^4 I_5(s, t, u) + \frac{m_e^6}{m_X^2} I_6(s, t, u) + m_e^6 I_7(s, t, u) + \frac{m_e^8}{m_X^2} I_8(s, t, u) \right\} \\
&\quad + \frac{e^2 g_e^2}{\Lambda^2} \frac{1}{t+m_X^2} \left\{ J_1(s, t, u) + \frac{m_e^2}{m_X^2} J_2(s, t, u) + m_e^2 J_3(s, t, u) + \frac{m_e^4}{m_X^2} J_4(s, t, u) \right. \\
&\quad \left. + m_e^4 J_5(s, t, u) + \frac{m_e^6}{m_X^2} J_6(s, t, u) + m_e^6 J_7(s, t, u) + \frac{m_e^8}{m_X^2} J_8(s, t, u) \right\}
\end{aligned} \tag{6.22}$$

where we can see that from our code:  $J_i(s, t, u) = I_i(t, s, u)$  for  $i \in \{1, \dots, 8\}$  meaning:

$$F_{st}(s, t, u) = F_{st}(t, s, u)$$

and the  $s \leftrightarrow t$  exchange symmetry is preserved. So, we will only focus on the  $I_i$  function manipulation, and results for the  $J_i$  functions will follow trivially.

$$\begin{aligned}
I_1(s, t, u) &= \frac{2}{3} u^2 - \frac{2}{3} ut - \frac{2}{3} us - \frac{4}{3} \frac{u^2 s}{t} = \frac{2u}{3} \left[ u - t - s - 2 \frac{us}{t} \right] = \\
&= \frac{2u}{3} \left[ -(\textcolor{blue}{u+t+s}) + 2u \left( \frac{t-s}{t} \right) \right] = \frac{4u}{3t} \left[ 2m_e^2 t + u(t-s) \right]
\end{aligned} \tag{6.23}$$

$$\begin{aligned}
I_2(s, t, u) &= 2 \frac{u^3}{t} + 2u^2 - 2ut - 2t^2 + 8 \frac{u^2 s}{t} + 8us + 10 \frac{us^2}{t} + 6s^2 + 4 \frac{s^3}{t} = \\
&= 2 \left[ \frac{u^2}{t} (u+t) - 2t(u+t) + 4 \frac{us}{t} (\textcolor{blue}{u+t+s}) + \frac{s^2}{t} (u+3t+2s) \right] = \\
&= 2 \left[ \frac{1}{t} (u+t) (u^2 - t^2) - 16m_e^2 \frac{us}{t} + \frac{2s^2}{t} (\textcolor{blue}{u+t+s}) - \frac{s^2}{t} (u-t) \right] = \\
&= \frac{2}{t} [(u-t)(u+t)^2 - 8m_e^2 s (2u+\textcolor{blue}{s}) - s^2 (u-t)] = \\
&= \frac{2(u-t)}{t} [(u+t)^2 - s^2 - 8m_e^2 s] + 64m_e^4 \frac{s}{t} = \\
&= \frac{2(u-t)}{t} [(\textcolor{blue}{u+t+s})(u+t-s) - 8m_e^2 s] + 64m_e^4 \frac{s}{t} = \\
&= -8m_e^2 \left( \frac{u-t}{t} \right) (\textcolor{blue}{u+t+s}) + 64m_e^4 \frac{s}{t} = \\
&= 32m_e^4 \left( \frac{u-t}{t} \right) + 64m_e^4 \frac{s}{t} = \frac{32m_e^4}{t} (u-t+2s)
\end{aligned} \tag{6.24}$$

$$\begin{aligned}
I_3(s, t, u) &= -\frac{2}{3} \frac{u^2}{t} - \frac{4}{3} u - 6t + 4 \frac{su}{t} + 4\textcolor{blue}{s} + 2 \frac{s^2}{t} = \\
&= \frac{2}{t} \left( -\frac{u^2}{3} + 2su + s^2 \right) - \frac{4}{3} u - 6t - 4u - 4t - 16m_e^2 = \\
&= \frac{2}{t} \left[ (\textcolor{blue}{u+s})^2 - \frac{4}{3} u^2 \right] - \frac{16}{3} u - 10t - 16m_e^2 = \\
&= \frac{2}{t} \left( t + 4m_e^2 \right)^2 - \frac{2}{t} \left( 4u^2 + \frac{8}{3} ut + 5t^2 \right) - 16m_e^2 = \\
&= \frac{2}{t} \left( \cancel{t^2} + 8m_e^2 \cancel{t} + 16m_e^4 \right) - \frac{2}{t} \left[ 4(\textcolor{blue}{u+t})^2 + \cancel{t^2} - \frac{16}{3} ut \right] - \cancel{16m_e^2} = \\
&= \frac{8}{t} \left[ 4m_e^4 - \left( s + 4m_e^2 \right)^2 + \frac{4}{3} ut \right] = \frac{8}{t} \left[ \frac{4}{3} ut - \left( s + 2m_e^2 \right) \left( s + 6m_e^2 \right) \right]
\end{aligned} \tag{6.25}$$

$$\begin{aligned}
I_4(s, t, u) &= 32 \frac{u^2}{t} + 32u + 80 \frac{su}{t} + 48s + 48 \frac{s^2}{t} = \\
&= \frac{16}{t} \left[ 2u^2 + 2ut + 5su + 3st + 3s^2 \right] = \\
&= \frac{16}{t} [2u(\textcolor{blue}{u+t}) + 5su + 3s(\textcolor{blue}{s+t})] = \\
&= \frac{16}{t} [-2\cancel{us} - 8m_e^2 u + 5\cancel{su} - 3\cancel{us} - 12m_e^2 s] = -\frac{64m_e^2}{t} (2u + 3s)
\end{aligned} \tag{6.26}$$

$$I_5(s, t, u) = \frac{16}{t} (\textcolor{blue}{u + t + s}) = -\frac{64m_e^2}{t} \quad (6.27)$$

$$\begin{aligned} I_6(s, t, u) &= 96 + 160\frac{u}{t} + 192\frac{s}{t} = \frac{32}{t} [5(\textcolor{blue}{u + t + s}) - 2t + s] = \\ &= \frac{32}{t} (-20m_e^2 - 2t + s) \end{aligned} \quad (6.28)$$

$$I_7(s, t, u) = \frac{32}{t} \quad I_8(s, t, u) = \frac{256}{t} \quad (6.29)$$

Sum them all into [Equation 6.22](#):

$$\begin{aligned} &I_1(s, t, u) + \frac{m_e^2}{m_X^2} I_2(s, t, u) + m_e^2 I_3(s, t, u) + \frac{m_e^4}{m_X^2} I_4(s, t, u) \\ &\quad + m_e^4 I_5(s, t, u) + \frac{m_e^6}{m_X^2} I_6(s, t, u) + m_e^6 I_7(s, t, u) + \frac{m_e^8}{m_X^2} I_8(s, t, u) = \\ &= \frac{4}{3} \frac{u}{t} [u(t-s) + 2m_e^2 t] + \frac{m_e^2}{m_X^2} \left[ \frac{32m_e^4}{t} (u-t+2s) \right] + \frac{8m_e^2}{t} \left[ \frac{4}{3} ut - (s+2m_e^2)(s+6m_e^2) \right] \\ &\quad + \frac{m_e^4}{m_X^2} \left[ -\frac{64m_e^2}{t} (2u+3s) \right] - \frac{64m_e^6}{t} + \frac{m_e^6}{m_X^2} \left[ \frac{32}{t} (-20m_e^2 - 2t + s) \right] + \frac{32m_e^6}{t} + \frac{256}{t} \frac{m_e^8}{m_X^2} = \\ &= \frac{4}{t} \left\{ \frac{u}{3} [u(t-s) + 2m_e^2 t] + 2m_e^2 \left[ \frac{4}{3} ut - (s+2m_e^2)(s+6m_e^2) \right] - 8m_e^6 \right. \\ &\quad \left. + \frac{m_e^6}{m_X^2} \left[ 8(u-t+2s) - 16(2u+3s) + 8(-20m_e^2 + s - 2t) + 64m_e^2 \right] \right\} = \\ &= \frac{4}{t} \left\{ \frac{u^2(t-s)}{3} + 2m_e^2 \left[ \frac{5}{3} ut - (s+2m_e^2)(s+6m_e^2) \right] - 8m_e^6 - 8 \frac{m_e^6}{m_X^2} [-3u - 3t - 3s - 12m_e^2] \right\} = \\ &= \frac{4}{3t} \left\{ u^2(t-s) + 2m_e^2 \left[ 5ut - 3(s+2m_e^2)(s+6m_e^2) \right] - 24m_e^6 + 72 \frac{m_e^6}{m_X^2} [\cancel{\textcolor{blue}{s+t+u+4m_e^2}}] \right\} = \end{aligned}$$

Again,  $m_X^2$  terms completely vanish. When manipulating QED results as in [Equation A.43](#), and using  $J_i(s, t, u) = I_i(t, s, u)$ :

$$\begin{aligned} F_{st}(s, t, u) &= \frac{16e^4}{st} [\dots] + \frac{4}{3} \frac{e^2 g_e^2}{\Lambda^2} \frac{1}{t(s+m_X^2)} \left\{ u^2(t-s) + 2m_e^2 \left[ 5ut - 3(s+2m_e^2)(s+6m_e^2) \right] - 24m_e^6 \right\} \\ &\quad + \frac{4}{3} \frac{e^2 g_e^2}{\Lambda^2} \frac{1}{s(t+m_X^2)} \left\{ u^2(s-t) + 2m_e^2 \left[ 5us - 3(t+2m_e^2)(t+6m_e^2) \right] - 24m_e^6 \right\} \end{aligned} \quad (6.30)$$

Joining [Equation 6.20](#), [Equation 6.21](#), [Equation 6.30](#) and [Equation A.43](#) we get the final result:

$$\begin{aligned} F(s, t, u) &= 8e^4 \left\{ \frac{1}{s^2} \left[ u^2 + t^2 + 8m_e^2(u+t) + 24m_e^4 \right] + \frac{1}{t^2} \left[ u^2 + s^2 + 8m_e^2(u+s) + 24m_e^4 \right] + \frac{2}{st} \left[ u^2 + 8m_e^2u + 12m_e^4 \right] \right\} \\ &\quad + \frac{4}{3} \frac{e^2 g_e^2}{\Lambda^2} \left\{ \left( \frac{u-t}{s} \right) \frac{1}{s+m_X^2} \left[ ut + (s+4m_e^2)(s-4m_e^2) \right] + \left( \frac{u-s}{t} \right) \frac{1}{t+m_X^2} \left[ us + (t+4m_e^2)(t-4m_e^2) \right] \right. \\ &\quad \left. + \frac{1}{t(s+m_X^2)} \left[ u^2(t-s) + 10m_e^2ut - 6m_e^2(s+2m_e^2)(s+6m_e^2) - 24m_e^6 \right] \right. \\ &\quad \left. + \frac{1}{s(t+m_X^2)} \left[ u^2(s-t) + 10m_e^2us - 6m_e^2(t+2m_e^2)(t+6m_e^2) - 24m_e^6 \right] \right\} + \mathcal{O} \left( \frac{g_e^4}{\Lambda^4} \right) \end{aligned} \quad (6.31)$$

Notice how  $F(s, t, u) = F(t, s, u)$ , as this would simply swap the two diagrams, and give the same final result. From [Equation A.38](#) and [Equation A.39](#), we also get the final differential cross section:

$$\begin{aligned} \frac{d\sigma}{d\Omega} &= \frac{E^2}{16\pi^2} \frac{1}{64E^4} F(s, t, u) = \frac{F(s, t, u)}{256\pi^2|s|} = \\ &= \frac{\alpha^2}{2|s|} \left\{ \frac{1}{s^2} \left[ u^2 + t^2 + 8m_e^2(u+t) + 24m_e^4 \right] + \frac{1}{t^2} \left[ u^2 + s^2 + 8m_e^2(u+s) + 24m_e^4 \right] + \frac{2}{st} \left[ u^2 + 8m_e^2u + 12m_e^4 \right] \right\} \\ &\quad + \frac{\alpha}{\pi} \frac{g_e^2}{48\Lambda^2} \frac{1}{|s|} \left\{ \left( \frac{u-t}{s} \right) \frac{1}{s+m_X^2} \left[ ut + (s+4m_e^2)(s-4m_e^2) \right] + \left( \frac{u-s}{t} \right) \frac{1}{t+m_X^2} \left[ us + (t+4m_e^2)(t-4m_e^2) \right] \right. \\ &\quad \left. + \frac{1}{t(s+m_X^2)} \left[ u^2(t-s) + 10m_e^2ut - 6m_e^2(s+2m_e^2)(s+6m_e^2) - 24m_e^6 \right] \right. \\ &\quad \left. + \frac{1}{s(t+m_X^2)} \left[ u^2(s-t) + 10m_e^2us - 6m_e^2(t+2m_e^2)(t+6m_e^2) - 24m_e^6 \right] \right\} + \mathcal{O}\left(\frac{g_e^4}{\Lambda^4}\right) \end{aligned} \quad (6.32)$$

and when  $g_e \rightarrow 0$ , we recover the QED cross section shown in [Equation A.44](#).

This result does not take into account the diagrams due to weak interaction (mediation of the  $Z$  boson), which become dominant in the region  $\sqrt{|s|} \approx 60 - 120$  GeV. This means that our formula only works up to around 50 GeV.

It is worth taking two relevant limits:

**Non-relativistic limit:** We send  $4m_e^2/s \rightarrow -1$ , as  $E \rightarrow m_e$ . Then,  $t/s \rightarrow 0$  and  $u/s \rightarrow 0$ . In [subsection A.4](#), we justify why the  $t$ -channel is dominant in this limit, and it behaves like  $1/t^2$ .

Because the spin 2 boson is massive, however, the dominant correction behaves like  $1/t$ , and it takes terms from both  $t$ -channel and interference. The limit is easy to take, as only  $m_e^2$  and  $s$  terms have to be selected:

$$\begin{aligned} \frac{d\sigma}{d\Omega} &= \frac{8\alpha^2 m_e^4}{2|s|t^2} + \frac{\alpha}{\pi} \frac{g_e^2}{48\Lambda^2} \frac{1}{|s|} \left[ \left( -\frac{s}{t} \right) \frac{-16m_e^4}{m_X^2} - \frac{1}{t} \frac{196m_e^6}{m_X^2} \right] = \\ &= \frac{\alpha^2 m_e^2}{t^2} + \frac{\alpha}{\pi} \frac{g_e^2}{48\Lambda^2} \left[ -\frac{40}{t} \frac{m_e^4}{m_X^2} \right] = \frac{\alpha^2 m_e^2}{t^2} - \frac{5\alpha}{6\pi} \frac{g_e^2}{\Lambda^2} \frac{m_e^4}{tm_X^2} \\ &= \frac{\alpha^2 m_e^2}{t^2} \left[ 1 - \frac{5}{6\pi} \frac{g_e^2}{\alpha\Lambda^2} \frac{m_e^2}{m_X^2} t \right] \end{aligned} \quad (6.33)$$

It is a negative correction. It makes sense, as this is not a modulus squared, but a term of interference between diagrams and contributions, where because of fermion statistics we had a relative minus sign to begin with. Numerically, using [Equation 5.43](#):

$$\frac{d\sigma}{d\Omega} = \frac{d\sigma}{d\Omega} \Big|_{\text{QED}} \left[ 1 - \left( 4.3 \times 10^{-13} \text{ MeV}^{-2} \right) t \right] \quad (6.34)$$

remember that  $t = 2p^2(1 - \cos\theta)$ , and it goes to 0 as  $s \rightarrow -4m_e^2$ .

**Ultra-relativistic limit:** If we send  $m_e^2/s \rightarrow 0$ , and  $m_X^2/s \rightarrow 0$  then we can simplify mass terms in [Equation 6.32](#):

$$\begin{aligned} \frac{d\sigma}{d\Omega} &= \frac{\alpha^2}{2|s|} \left[ u^2 \left( \frac{1}{s} + \frac{1}{t} \right)^2 + \left( \frac{t}{s} \right)^2 + \left( \frac{s}{t} \right)^2 \right] \\ &\quad + \frac{\alpha}{\pi} \frac{g_e^2}{48\Lambda^2} \frac{1}{|s|} \left\{ \left( \frac{u-t}{s^2} \right) [ut + s^2] + \left( \frac{u-s}{t^2} \right) [us + t^2] + \frac{1}{ts} \overbrace{[u^2(t-s)]}^{} + \frac{1}{st} \overbrace{[u^2(s-t)]}^{} \right\} \end{aligned} \quad (6.35)$$

Substitute the Mandelstam variables in the center of mass frame:

$$s = -4E^2 \quad t \rightarrow 2E^2(1 - \cos\theta) \quad u \rightarrow 2E^2(1 + \cos\theta)$$

which for the QED part we get [Equation A.51](#), and for the spin 2 part, inside curly brackets:

$$\begin{aligned}
\{\dots\} &= \frac{4E^2 \cos \theta}{16E^4} \left[ 4E^4 (1 - \cos^2 \theta) + 16E^4 \right] + \frac{2E^2(3 + \cos \theta)}{4E^4(1 - \cos \theta)^2} \left[ -8E^4(1 + \cos \theta) + 4E^4(1 - \cos \theta)^2 \right] = \\
&= E^2 \left[ \cos \theta (5 - \cos^2 \theta) + \frac{3 + \cos \theta}{(1 - \cos \theta)^2} (-4 - 4 \cos \theta + 2 + 2 \cos^2 \theta - 4 \cos \theta) \right] = \\
&= E^2 \left[ 5 \cos \theta - \cos^3 \theta + \frac{2(3 + \cos \theta)}{(1 - \cos \theta)^2} (\cos^2 \theta - 4 \cos \theta - 1) \right] = \\
&= E^2 \left[ 5 \cos \theta - \cos^3 \theta + \frac{2(3 + \cos \theta)[(1 - \cos \theta)^2 - 2 \cos \theta - 2]}{(1 - \cos \theta)^2} \right] = \\
&= E^2 \left[ 6 + 7 \cos \theta - \cos^3 \theta - \frac{4(3 + \cos \theta)(1 + \cos \theta)}{(1 - \cos \theta)^2} \right] = \\
&= E^2 \left[ (1 + \cos \theta)(6 + \cos \theta - \cos^2 \theta) - \frac{4(3 + \cos \theta)(1 + \cos \theta)}{(1 - \cos \theta)^2} \right] = \\
&= \frac{E^2(1 + \cos \theta)}{(1 - \cos \theta)^2} \left[ (6 + \cos \theta - \cos^2 \theta)(1 - \cos \theta)^2 - 4(3 + \cos \theta) \right] = \\
&= \frac{-E^2(1 + \cos \theta)}{(1 - \cos \theta)^2} [6 + 15 \cos \theta - 3 \cos^2 \theta - 3 \cos^3 \theta + \cos^4 \theta]
\end{aligned} \tag{6.36}$$

Notice immediately that if  $\cos \theta = -1$ , correction is null automatically. A quick search online also revealed another zero for the correction, in the range  $[-1, 1]$ , for  $\cos \theta \cong -0.383$ .

Another remark is that this high energy amplitude satisfies Froissart bound (see [Equation 4.47](#)). This means that running up in energy does not violate unitarity. However, as in [subsection 4.4](#), our limit is 50 MeV, so it is very small anyway.

If we send  $\theta \rightarrow \pi/2$  we get:  $-6E^2 = 3s/2$ , which is negative. Together with [Equation A.52](#) we get the estimate of the final, ultra-relativistic cross section at high angles:

$$\begin{aligned}
\frac{d\sigma}{d\Omega} &= \frac{9\alpha^2}{4|s|} + \frac{\alpha}{\pi} \frac{g_e^2}{48\Lambda^2} \frac{3s}{2|s|} = \frac{9\alpha^2}{4|s|} \left[ 1 + \frac{1}{72\pi} \frac{g_e^2}{\Lambda^2 \alpha} s \right] = \\
&= \frac{d\sigma}{d\Omega} \Big|_{\text{QED}} \left[ 1 - \frac{1}{72\pi} \frac{g_e^2}{\Lambda^2 \alpha} |s| \right]
\end{aligned} \tag{6.37}$$

which numerically, gives:

$$\frac{d\sigma}{d\Omega} = \frac{d\sigma}{d\Omega} \Big|_{\text{QED}} \left[ 1 - \left( 8.3 \times 10^{-12} \text{ MeV}^{-2} \right) |s| \right] \tag{6.38}$$

as a conservative correction estimate (lower bound for the coupling constant). This means that it is a very large correction. If  $\sqrt{|s|} = 50$  GeV, the large angle cross section would receive a 2% decrease.

Instead, if we send  $\theta \rightarrow 0$ , and approximate  $\cos \theta \rightarrow 1$ ,  $\sin \theta \rightarrow \theta$  and  $1 - \cos \theta \rightarrow \theta^2/2$ , the dominant term is the one with  $(1 - \cos \theta)^2$  in the denominator, which leaves us with  $-128E^2/\theta^4 = -32|s|/\theta^4$ , again negative. Together with [Equation A.53](#) we get the estimate of the final, ultra-relativistic cross section at low angles:

$$\begin{aligned}
\frac{d\sigma}{d\Omega} &= \frac{16\alpha^2}{|s|} \frac{1}{\theta^4} - \frac{\alpha}{\pi} \frac{g_e^2}{48\Lambda^2} \frac{1}{|s|} \frac{32|s|}{\theta^4} = \frac{16\alpha^2}{|s|} \frac{1}{\theta^4} \left[ 1 - \frac{1}{24\pi} \frac{g_e^2}{\Lambda^2 \alpha} |s| \right] = \\
&= \frac{d\sigma}{d\Omega} \Big|_{\text{QED}} \left[ 1 - \frac{1}{24\pi} \frac{g_e^2}{\Lambda^2 \alpha} |s| \right]
\end{aligned} \tag{6.39}$$

numerically estimated to be:

$$\frac{d\sigma}{d\Omega} = \frac{d\sigma}{d\Omega} \Big|_{\text{QED}} \left[ 1 - \left( 2.5 \times 10^{-11} \text{ MeV}^{-2} \right) |s| \right] \tag{6.40}$$

as a conservative correction estimate (lower bound for the coupling constant). This means that it is an even bigger correction. If  $\sqrt{|s|} = 50 \text{ GeV}$ , the low angle cross section would receive a *6% decrease*.

## 6.2 Testing spin 2 for Bhabha

### 6.2.1 Behavior of Bhabha cross section

We report the graphs displaying the behavior of the corrected Bhabha scattering in [Figure 9](#) and [Figure 10](#). In

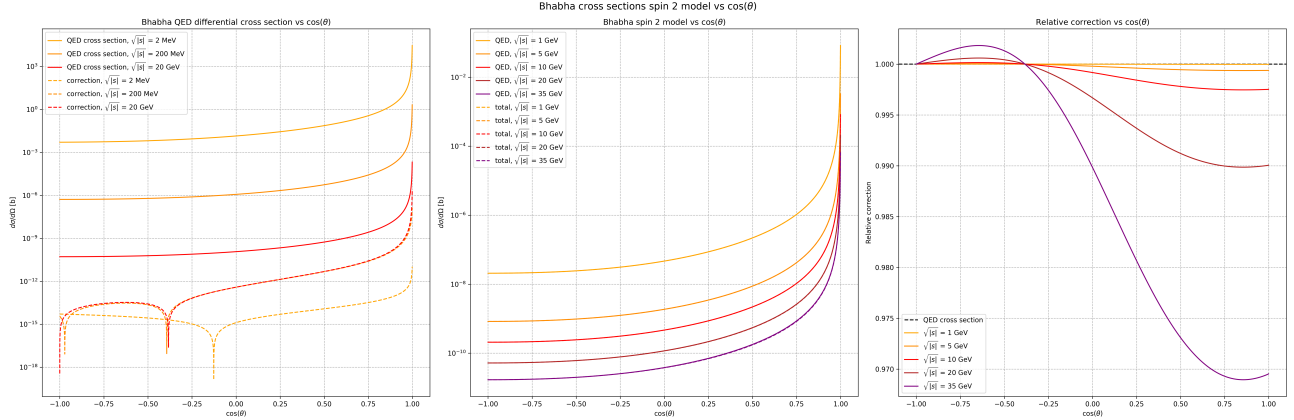


**Figure 9:** Graph of behavior of Bhabha corrections as a function of the scattering angle  $\cos \theta$ . On the left, we plot separately both the QED result and the actual absolute value of spin 2 correction (dashed line), for different values of the center of mass energy  $\sqrt{|s|}$ . In the middle, comparison between QED differential cross section and total cross section (including spin 2 correction), for different fixed  $\sqrt{|s|}$ . On the right, relative correction to the QED cross section of the total (QED + spin 2) cross section, always at different energetic values for  $\sqrt{|s|}$ .

[Figure 9](#), you can see how spin 2 corrections grow quite fast. We range from 13 orders of magnitude ratio (at a few MeV) to 2 orders of magnitude (at 20 GeV).

- Dependence from the angle stays the same for QED cross section, as in [Equation A.51](#), and it goes down with energy (left image). It diverges when  $\cos \theta \rightarrow 1$ , which is the forward scattering limit (from [Equation A.53](#), it goes like  $1/\theta^4$ ).
- Still in the left image, for the correction, we get a general larger dependence on  $\cos \theta$ , and it becomes constant at higher energy (as we have seen in [Equation 6.37](#) and [Equation 6.39](#)). There are also zeros in the correction. In the high energy limit shown (dashed red line), they are for  $\cos \theta = -1$ ,  $\cos \theta = -0.383$  (proved in [Equation 6.36](#)). In the low energy limit,  $\cos \theta = -1$  is not a zero anymore.
- In the middle graph, corrections start to become visible at  $\mathcal{O}(10 \text{ GeV})$ . On the right, about a 3% correction at large angles at 35 GeV is visible. However, small scattering angle corrections are zero, because QED cross section diverges, while spin 2 correction stays constant. The two zeros in the ultra-relativistic limit are perfectly visible.

In [Figure 10](#), we get the behavior we discussed in this section.

- In the left image, for the QED part, in the very beginning we have the non-relativistic limit, where the cross section goes like  $1/t^2$ . Then, it slows down in the ultra-relativistic limit to  $1/|s|$ .
- In the left diagram, it is shown the absolute value of the spin 2 correction (dashed lines). There are four main behaviors for the spin 2 correction that are visible on the left image. First, when  $\sqrt{|s|} = m_X$ , from [Equation 6.32](#), correction is infinite for every angle (resonant production of  $X$ ). Moreover, at each angle it is possible to find a kinematic configuration such that correction is zero (it is not a trivial calculation, and it defeats the purposes of this thesis). In the non relativistic limit, although it is hard to see, correction goes like  $1/t$  ( $\sqrt{|s|} < 2 \text{ MeV}$ ), while, in the ultra-relativistic limit, correction is, indeed, constant (also proven in this section).
- So, the graph in the middle has a correction that becomes relevant in the  $\mathcal{O}(10 \text{ GeV})$  region, as the relative correction grows like  $|s|$ . This is also shown in the graph on the right. Correction is negative, as our analytical limits also prove.

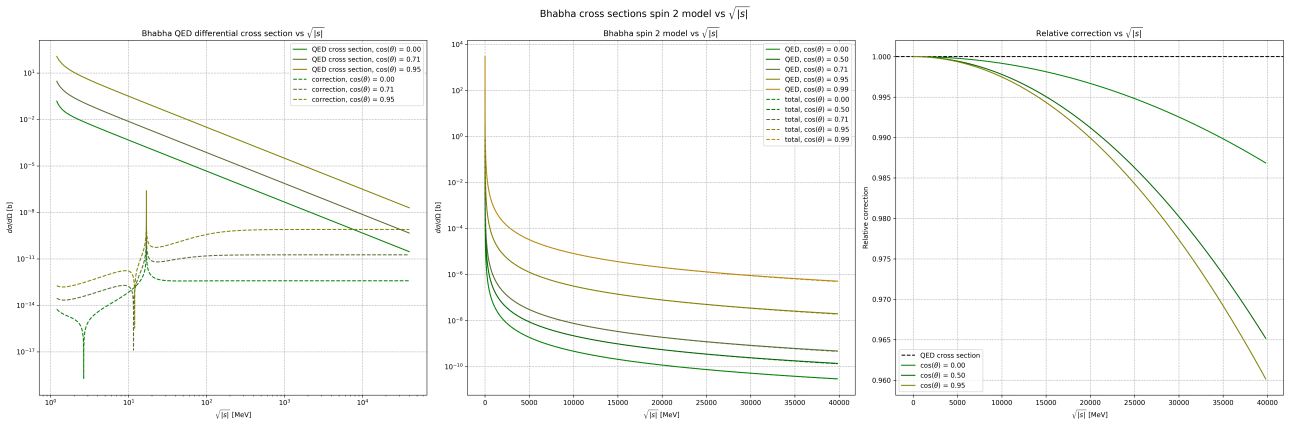


Figure 10: Graph of behavior of Bhabha corrections as a function of the center of mass energy  $\sqrt{|s|}$ . On the left, we plot separately both the QED result and the actual absolute value of the spin 2 correction (dashed line), for different values of the  $\cos \theta$ . In the middle, comparison between QED differential cross section and total cross section (including spin 2 correction), for different fixed  $\cos \theta$ . On the right, relative correction to the QED cross section of the total (QED + spin 2) cross section, always at different angular values for  $\cos \theta$ .

Finally, since Bhabha scattering has access to a  $t$ -channel, let us study the behavior of its contribution over the whole scattering cross section, especially in light of the necessity to increase center of mass energy as much as possible to increase relative correction. Where the  $t$ -channel contribution is dominant, exchanged momentum goes like Equation 4.70, and so we need to focus on forward scattering Bhabha. Behavior is shown in Figure 11.

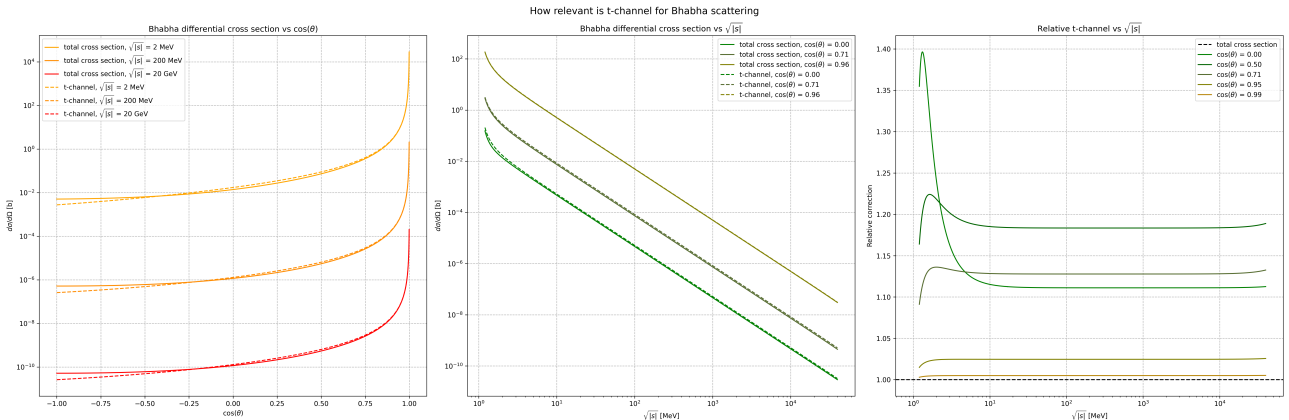


Figure 11: Graph of behavior of Bhabha  $t$ -channel contribution over the whole scattering cross section. We plot separately both the total cross section result and the  $t$ -channel only (dashed line), as function of the scattering angle  $\cos \theta$  (on the left) and center of mass energy  $\sqrt{|s|}$ . On the right, relative contribution of Bhabha  $t$ -channel as a function of the energy.

Notice that  $t$ -channel contribution is larger than the total energy contribution at positive angles and large energies. This is because the relative diagrams have a relative minus sign, and so interference terms are actually negative with respect to  $s$ -channel and  $t$ -channel contribution<sup>16</sup>. Also, these interference terms also contain  $t$ , and are hence somewhat relevant even at high energy. To see if  $t$ -channel really is dominant, we need to compare it to  $s$ -channel contribution only. This is shown in Figure 12. In figure, forward scattering has a dominant effect over cross section, which, for  $\sqrt{|s|} > 10$  MeV, depends only on the scattering angle, and not at all on the center of mass energy. This is perfect, because we can use Equation 4.70 at basically every energy we want, as long as the scattering angle is fairly small.  $\cos \theta > 0.7$  is already enough, as  $t$ -channel is 100 times larger than  $s$ -channel.

### 6.2.2 Bhabha experimental results

Large angle Bhabha scattering is important for luminosity estimates in  $B$ -factories ([49]), and it needs theoretical precision to be around 0.1%.

<sup>16</sup>Plus, the spin 2 corrections are also negative, but that is because they are interference terms with spin 2 diagrams.

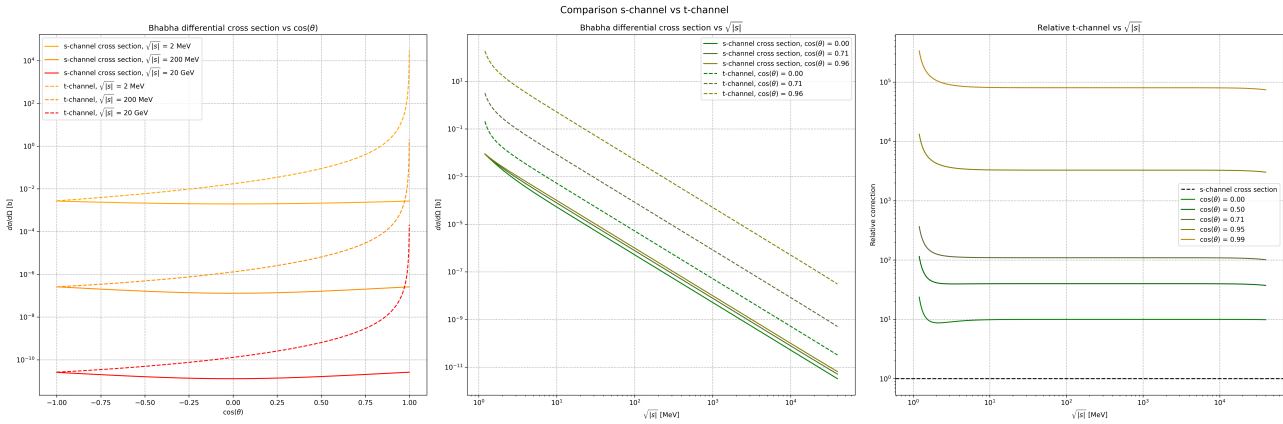


Figure 12: Graph of behavior of Bhabha  $t$ -channel and  $s$ -channel contribution. We plot separately both the  $s$ -channel (full line) and  $t$ -channel (dashed line) cross sections as function of the scattering angle  $\cos\theta$  (on the left) and center of mass energy  $\sqrt{|s|}$ . On the right, relative contribution of Bhabha  $t$ -channel over  $s$ -channel as a function of the energy.

- However, energies are not quite as high as the one reported in [47], which is performed at TRISTAN (KEK), in Japan ( $\sqrt{|s|} = 58$  GeV, well below  $Z$  resonance peak). In the paper, the precision reported for Bhabha scattering at large angles (central region,  $|\cos\theta| \leq 0.743$ ) is 0.5%, which is around four times smaller than our correction.
- Instead, small angle Bhabha scattering is a fundamental process used in lepton accelerators to measure the total luminosity. This requires an extreme precision in measurement and theoretical prediction using MonteCarlo methods ([50]). The most precise measurement we have available is for highly energetic interaction at LEP: [48] reports relative correction of the order of  $10^{-4}$  and overall accuracy better than 0.05% - 500 ppm. However, it is measured at 92 GeV center of mass energy, which is right at the  $Z$  resonance peak, therefore outside our region of interest.

Useful measurement within our range can be sought in  $B$ -factories, even though energy is a little low. Highest energy to accuracy ratio well below  $Z$  resonance can be found in a 1996 paper ([47]), where center of mass energy for Bhabha scattering is found to be  $\sqrt{|s|} = 58$  GeV at TRISTAN (KEK), in Japan. A precision of 0.7% is found in the forward region  $0.822 \leq |\cos\theta| \leq 0.968$ , which corresponds to our small angle region, well below our estimated correction due to spin 2 interaction in this energy range.

- Note that both  $B$  factories, BELLE II (at KEK, Japan) and BaBar (at PEP, Stanford, California) do not provide us with feasible data, at  $\sqrt{|s|} = 10.58$  GeV, and large angle Bhabha scattering. On the one hand, energy is lower than TRISTAN result, so why use them for our "hypothetical high energy scenario". On the other hand, because they still focus on high angle Bhabha scattering (understandable, as large angle is to be preferred because of greater coverage - there are not many other detectors in the way like at LEP), results cannot be used for the composite spin 2 model, neither.
- Finally, for the energy range allowed by effective theory (around exchanged momentum of 20 – 50 MeV), we are forced to go lower in energy. A nice result was published by the OLYMPUS Collaboration (2013–2021), ([53], [54]), at DESY (Hamburg, Germany). They carried out an experiment in which an electron (or positron) beam of  $E = 2$  GeV hit on a fixed target of hydrogen gas ( $\sqrt{|s|} = 44$  MeV, still in the ultra-relativistic limit). Their goal was to characterize  $e^\pm p$  cross section. However, they were also equipped with a forward Bhabha/Møller scattering detector (called SYMB, SYmmetric Møller/Bhabha), at  $\eta = 1.29^\circ$  to monitor background events. Inverting the relation to link angles in the lab frame ( $\eta$ ) to angles in the center of mass ( $\theta$ ):

$$\tan \eta = \frac{\sin \theta}{\gamma_{cm} (\beta_{cm}/\beta + \cos \theta)} \quad (6.41)$$

with  $\eta = 1.29^\circ$ ,  $\beta = 0.999$  and  $\gamma_{cm} = 44$ , we get  $\theta = \pi/2$ . This is not relevant in terms of EFT energy limit, as energy is so low that it does not matter to us whether the experiment selects low or high angles, but it is relevant in terms of what formula to use to compare results with (which is Equation 6.37).

OLYMPUS collaboration are able to measure Bhabha scattering, annihilation into two photons events when positron beam hits electron in hydrogen, and Møller scattering events when electron beam hits electron in hydrogen. Their experimental precision is about 1% ([54]), while our Bhabha low angle high energy prediction for spin 2 correction is about 10 ppb (by Equation 6.37). So, spin 2 corrections are very much still invisible to this detector at low energy.

## 7 Correction to Møller scattering

Let us repeat what we did in [section 6](#), but for the process:  $e^-e^- \rightarrow e^-e^-$  (called *Møller scattering*). The contributing diagrams for this process are the *t-channel* and the *u-channel*, in [Figure 13](#):

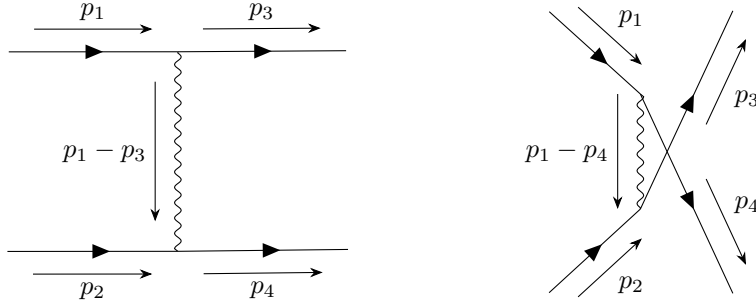


Figure 13: On the left, the *t*-channel, hereafter denoted with  $\mathcal{A}_1$ . On the right, the *u*-channel, hereafter denoted with  $\mathcal{A}_2$ .

We add the diagram in which the  $X$  boson is mediated ([Figure 8](#)), contributing with both *t*-channel and *u*-channel: Because spin 2 mediation occurs with the exact same diagrams as in QED, then the crossing

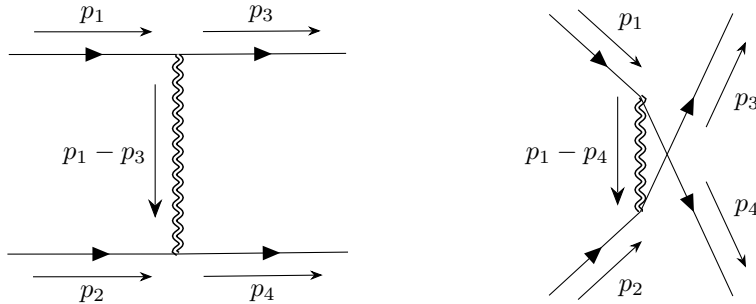


Figure 14: Tree level diagrams for the mediation of massive spin 2 boson for Bhabha scattering, basically accounting for *t*-channel (left) and *u*-channel (right) contributions. We will refer to the left amplitude as  $\mathcal{A}_3$ , and to the right amplitude as  $\mathcal{A}_4$ .

symmetry argument we have used in [subsection B.3](#) can be extended for spin 2 corrections as well. In short, using simple rigid movements it is possible to rearrange Bhabha diagrams into Møller diagrams by sending also  $(s, t, u) \rightarrow (t, u, s)$ :

$$\mathcal{A}(\text{Møller}; s, t, u) = \mathcal{A}(\text{Bhabha}; t, u, s) \quad (7.1)$$

This means that we can write amplitudes for all four diagrams starting [Equation 6.1](#) and [Equation 6.3](#) but using only electron spinors  $u$  and the changing the 4-momenta according to [Equation B.6](#):

$$\begin{aligned} \mathcal{A}_1 &= (-ie)^2 \hat{D}_{\mu\nu}^\xi(p_1 - p_3) [\bar{u}(p_4, \lambda_4) \gamma_\mu u(p_2, \lambda_2)] [\bar{u}(p_3, \lambda_3) \gamma_\nu u(p_1, \lambda_1)] = \\ &= -e^2 \hat{D}_{\mu\nu}^\xi(p_1 - p_3) [\bar{u}_4 \gamma_\mu u_2] [\bar{u}_3 \gamma_\nu u_1] \end{aligned} \quad (7.2)$$

$$\begin{aligned} \mathcal{A}_2 &= (-ie)^2 \hat{D}_{\mu\nu}^\xi(p_1 - p_4) [\bar{u}(p_4, \lambda_4) \gamma_\mu u(p_1, \lambda_1)] [\bar{u}(p_3, \lambda_3) \gamma_\nu u(p_2, \lambda_2)] = \\ &= -e^2 \hat{D}_{\mu\nu}^\xi(p_1 - p_4) [\bar{u}_4 \gamma_\mu u_1] [\bar{u}_3 \gamma_\nu u_2] \end{aligned} \quad (7.3)$$

$$\begin{aligned}\mathcal{A}_3 &= \left(\frac{ig_e}{2\Lambda}\right)^2 \left[ \frac{N_{\mu\alpha\nu\beta}(p_1 - p_3)}{(p_1 - p_3)^2 + m_X^2} \right] \left[ \bar{u}(p_4, \lambda_4) \gamma_\mu (-p_{3,\alpha} - p_{1,\alpha}) u(p_2, \lambda_2) \right] \left[ \bar{u}(p_3, \lambda_3) \gamma_\nu (p_{4,\beta} + p_{2,\beta}) u(p_1, \lambda_1) \right] = \\ &= \frac{g_e^2}{4\Lambda^2} \left[ \frac{N_{\mu\alpha\nu\beta}(p_1 - p_3)}{(p_1 - p_3)^2 + m_X^2} \right] (p_{3,\alpha} + p_{1,\alpha}) (p_{4,\beta} + p_{2,\beta}) [\bar{u}_4 \gamma_\mu u_2] [\bar{u}_3 \gamma_\nu u_1]\end{aligned}\quad (7.4)$$

$$\begin{aligned}\mathcal{A}_4 &= \left(\frac{ig_e}{2\Lambda}\right)^2 \left[ \frac{N_{\mu\alpha\nu\beta}(p_1 - p_4)}{(p_1 - p_4)^2 + m_X^2} \right] \left[ \bar{u}(p_4, \lambda_4) \gamma_\mu (p_{4,\alpha} + p_{1,\alpha}) u(p_1, \lambda_1) \right] \left[ \bar{u}(p_3, \lambda_3) \gamma_\nu (-p_{3,\beta} - p_{2,\beta}) u(p_2, \lambda_2) \right] = \\ &= \frac{g_e^2}{4\Lambda^2} \left[ \frac{N_{\mu\alpha\nu\beta}(p_1 - p_4)}{(p_1 - p_4)^2 + m_X^2} \right] (p_{1,\alpha} + p_{4,\alpha}) (p_{2,\beta} + p_{3,\beta}) [\bar{u}_4 \gamma_\mu u_1] [\bar{u}_3 \gamma_\nu u_2]\end{aligned}\quad (7.5)$$

Notice that there is a relative minus sign between  $\mathcal{A}_{1,2}$  and  $\mathcal{A}_{3,4}$ .

We also checked [Equation 7.1](#) by writing the code `Moller_Xspin2_xigauge.frm`, found in the GitHub repository linked in [subsection G.1](#). The result verifies crossing symmetry by exchange of  $(s, t, u) \rightarrow (t, u, s)$  between Bhabha and Møller.

Moreover, thanks to the particles having same mass in both processes, phase space is also exactly the same. So, by reshuffling Mandelstam variables in the amplitude, we immediately get the resulting cross section for Møller scattering, including spin 2 interference correction, from [Equation 6.32](#):

$$\begin{aligned}\frac{d\sigma}{d\Omega} &= \frac{\alpha^2}{2|s|} \left\{ \frac{1}{t^2} \left[ s^2 + u^2 + 8m_e^2(s+u) + 24m_e^4 \right] + \frac{1}{u^2} \left[ s^2 + t^2 + 8m_e^2(s+t) + 24m_e^4 \right] + \frac{2}{tu} \left[ s^2 + 8m_e^2s + 12m_e^4 \right] \right\} \\ &\quad + \frac{\alpha}{\pi} \frac{g_e^2}{48\Lambda^2} \frac{1}{|s|} \left\{ \left( \frac{s-u}{t} \right) \frac{1}{t+m_X^2} \left[ su + (t+4m_e^2)(t-4m_e^2) \right] + \left( \frac{s-t}{u} \right) \frac{1}{u+m_X^2} \left[ st + (u+4m_e^2)(u-4m_e^2) \right] \right. \\ &\quad \left. + \frac{1}{u(t+m_X^2)} \left[ s^2(u-t) + 10m_e^2su - 6m_e^2(t+2m_e^2)(t+6m_e^2) - 24m_e^6 \right] \right. \\ &\quad \left. + \frac{1}{t(u+m_X^2)} \left[ s^2(t-u) + 10m_e^2st - 6m_e^2(u+2m_e^2)(u+6m_e^2) - 24m_e^6 \right] \right\} + \mathcal{O}\left(\frac{g_e^4}{\Lambda^4}\right)\end{aligned}\quad (7.6)$$

When  $g_e \rightarrow 0$ , we recover the QED result in [Equation B.8](#).

This result does not take into account the diagrams due to weak interaction (mediation of the  $Z$  boson), which become dominant in the region  $\sqrt{|s|} \approx 60 - 120$  GeV. This means that our formula only works up to around 50 GeV.

Take the usual two relevant limits:

**Non-relativistic limit:** We send  $4m_e^2/s \rightarrow -1$ , as  $E \rightarrow m_e$ . Then,  $t/s \rightarrow 0$  and  $u/s \rightarrow 0$ . QED result for this limit is in [Equation B.9](#). The limit is easy to take, as only  $m_e^2$  and  $s$  terms have to be chosen:

$$\begin{aligned}\frac{d\sigma}{d\Omega} &= \frac{\alpha^2 m_e^2}{4p^4} \left[ \frac{1+3\cos^2\theta}{\sin^2\theta} \right]^2 + \frac{\alpha}{\pi} \frac{g_e^2}{48\Lambda^2} \frac{1}{|s|} \left[ \left( \frac{s}{t} \right) \frac{-16m_e^4}{m_X^2} + \left( \frac{s}{u} \right) \frac{-16m_e^4}{m_X^2} - \frac{1}{t} \frac{96m_e^6}{m_X^2} - \frac{1}{u} \frac{96m_e^6}{m_X^2} \right] = \\ &= \frac{\alpha^2 m_e^2}{4p^4} \left[ \frac{1+3\cos^2\theta}{\sin^2\theta} \right]^2 + \frac{\alpha}{\pi} \frac{g_e^2}{48\Lambda^2} \left[ -\frac{8m_e^4}{m_X^2} \left( \frac{1}{t} + \frac{1}{u} \right) \right] = \\ &= \frac{\alpha^2 m_e^2}{4p^4} \left[ \frac{1+3\cos^2\theta}{\sin^2\theta} \right]^2 - \frac{\alpha}{\pi} \frac{g_e^2}{6\Lambda^2} \frac{m_e^4}{m_X^2} \frac{1}{p^2 \sin^2\theta} \\ &= \frac{\alpha^2 m_e^2}{4p^4} \left[ \frac{1+3\cos^2\theta}{\sin^2\theta} \right]^2 \left[ 1 - \frac{2}{3\pi} \frac{g_e^2}{\alpha\Lambda^2} \frac{m_e^2}{m_X^2} \frac{p^2 \sin^2\theta}{1+3\cos^2\theta} \right]\end{aligned}\quad (7.7)$$

It is a negative correction. It makes sense, as this is not a modulus squared, but a term of interference between diagrams and contributions, where because of fermion statistics we had a relative minus sign to begin with. Numerically, using [Equation 5.43](#):

$$\frac{d\sigma}{d\Omega} = \frac{d\sigma}{d\Omega} \Big|_{\text{QED}} \left[ 1 - \left( 5.7 \times 10^{-12} \text{ MeV}^{-2} \right) \frac{p^2 \sin^2\theta}{1+3\cos^2\theta} \right]\quad (7.8)$$

remember that  $t = 2p^2(1 - \cos\theta)$ , and it goes to 0 as  $s \rightarrow -4m_e^2$ .

**Ultra-relativistic limit:** If we send  $m_e^2/s \rightarrow 0$ , and  $m_X^2/s \rightarrow 0$  then we can simplify mass terms in [Equation 7.6](#):

$$\frac{d\sigma}{d\Omega} = \frac{\alpha^2}{2|s|} \left[ s^2 \left( \frac{1}{t} + \frac{1}{u} \right)^2 + \left( \frac{u}{t} \right)^2 + \left( \frac{t}{u} \right)^2 \right] + \frac{\alpha}{\pi} \frac{g_e^2}{48\Lambda^2} \frac{1}{|s|} \left\{ \left( \frac{s-u}{t^2} \right) [su+t^2] + \left( \frac{s-t}{u^2} \right) [st+u^2] + \frac{1}{ut} \overbrace{[s^2(u-t)]} + \frac{1}{tu} \overbrace{[s^2(t-u)]} \right\} \quad (7.9)$$

Substitute the Mandelstam variables in the center of mass frame. For the QED part we get [Equation B.12](#), the spin 2 part, inside the curly brackets:

$$\begin{aligned} \{\dots\} &= \frac{-4E^2 - 2E^2(1+\cos\theta)}{4E^4(1-\cos\theta)^2} [-8E^4(1+\cos\theta) + 4E^4(1-\cos\theta)^2] \\ &\quad + \frac{-4E^2 - 2E^2(1-\cos\theta)}{4E^4(1+\cos\theta)^2} [-8E^4(1-\cos\theta) + 4E^4(1+\cos\theta)^2] = \\ &= 2E^2 \left[ \frac{(\cos^4\theta - 4\cos\theta - 1)(-3 - \cos\theta)}{(1 - \cos\theta)^2} + \frac{(\cos^4\theta + 4\cos\theta - 1)(-3 + \cos\theta)}{(1 + \cos\theta)^2} \right] = \\ &= 2E^2 \left[ -6 + \frac{2(1 + \cos\theta)(3 + \cos\theta)}{(1 - \cos\theta)^2} + \frac{2(1 - \cos\theta)(3 - \cos\theta)}{(1 + \cos\theta)^2} \right] \end{aligned} \quad (7.10)$$

Note that this high energy amplitude satisfies Froissart bound (see [Equation 4.47](#)), like Bhabha scattering. This means that running up in energy does not violates unitarity. However, as in [subsection 4.4](#), our limit is 50 GeV.

If we send  $\theta \rightarrow \pi/2$  we get:  $12E^2 = 3|s|$ , which is positive. Together with [Equation B.13](#) we get the estimate of the final, ultra-relativistic cross section at high angles:

$$\begin{aligned} \frac{d\sigma}{d\Omega} &= \frac{9\alpha^2}{|s|} + \frac{\alpha}{\pi} \frac{g_e^2}{48\Lambda^2} \frac{3|s|}{|s|} = \frac{9\alpha^2}{|s|} \left[ 1 + \frac{1}{144\pi} \frac{g_e^2}{\Lambda^2\alpha} |s| \right] = \\ &= \frac{d\sigma}{d\Omega} \Big|_{\text{QED}} \left[ 1 + \frac{1}{144\pi} \frac{g_e^2}{\Lambda^2\alpha} |s| \right] \end{aligned} \quad (7.11)$$

which numerically gives:

$$\frac{d\sigma}{d\Omega} = \frac{d\sigma}{d\Omega} \Big|_{\text{QED}} \left[ 1 + \left( 4.0 \times 10^{-12} \text{ MeV}^{-2} \right) |s| \right] \quad (7.12)$$

as a conservative correction estimate (lower bound for the coupling constant). This means that it is not a negligible correction. If  $\sqrt{|s|} = 50$  GeV, the large angle cross section would receive a 1% correction.

Instead, if we send  $\theta \rightarrow 0$ , and approximate  $\cos\theta \rightarrow 1$ ,  $\sin\theta \rightarrow \theta$  and  $1 - \cos\theta \rightarrow \theta^2/2$ , the dominant term is the one with  $(1 - \cos\theta)^2$  in the denominator, which leaves us with  $128E^2/\theta^4 = 32|s|/\theta^4$ , again positive. Together with [Equation B.14](#) we get the estimate of the final, ultra-relativistic cross section at low angles:

$$\begin{aligned} \frac{d\sigma}{d\Omega} &= \frac{16\alpha^2}{|s|} \frac{1}{\theta^4} + \frac{\alpha}{\pi} \frac{g_e^2}{48\Lambda^2} \frac{1}{|s|} \frac{32|s|}{\theta^4} = \frac{16\alpha^2}{|s|} \frac{1}{\theta^4} \left[ 1 + \frac{1}{24\pi} \frac{g_e^2}{\Lambda^2\alpha} |s| \right] = \\ &= \frac{d\sigma}{d\Omega} \Big|_{\text{QED}} \left[ 1 + \frac{1}{24\pi} \frac{g_e^2}{\Lambda^2\alpha} |s| \right] \end{aligned} \quad (7.13)$$

numerically estimated to be:

$$\frac{d\sigma}{d\Omega} = \frac{d\sigma}{d\Omega} \Big|_{\text{QED}} \left[ 1 + \left( 2.5 \times 10^{-11} \text{ MeV}^{-2} \right) |s| \right] \quad (7.14)$$

as a conservative correction estimate (lower bound for the coupling constant). This means that it is an even bigger correction. If  $\sqrt{|s|} = 20$  GeV, the low angle cross section would receive a 1% increase.

## 7.1 Testing spin 2 for Møller

### 7.1.1 Behavior of Møller cross section

We report the graphs displaying the behavior of the corrected Møller scattering in [Figure 15](#) and [Figure 16](#): In

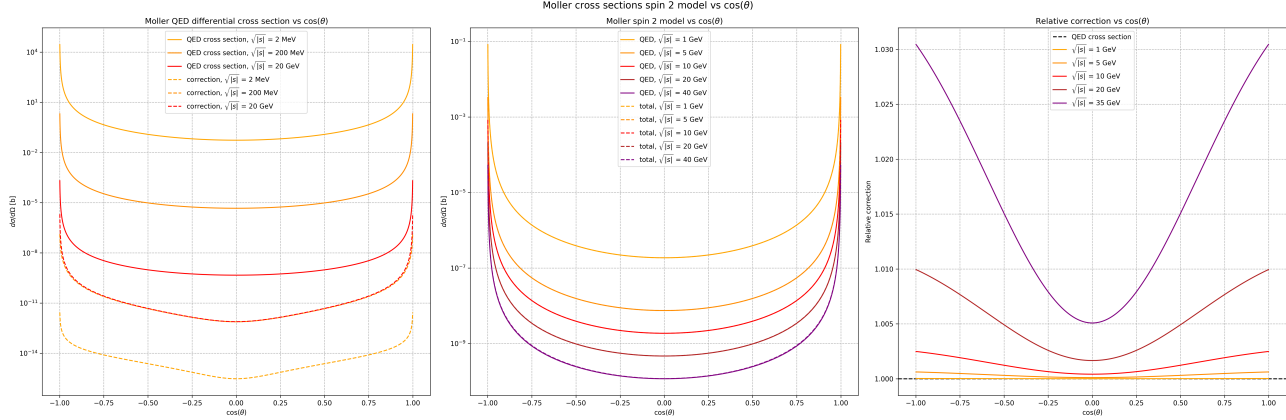


**Figure 15:** Graph of behavior of Møller corrections as a function of the scattering angle  $\cos\theta$ . On the left, we plot separately both the QED result and the actual absolute value of spin 2 correction (dashed line), for different values of the center of mass energy  $\sqrt{|s|}$ . In the middle, comparison between QED differential cross section and total cross section (including spin 2 correction), for different fixed  $\sqrt{|s|}$ . On the right, relative correction to the QED cross section of the total (QED + spin 2) cross section, always at different energetic values for  $\sqrt{|s|}$ .

[Figure 15](#), you can see how spin 2 corrections grow quite fast. We range from 13 orders of magnitude ratio (at a few MeV) to 2 orders of magnitude (at 20 GeV).

- Dependence from the angle stays the same for QED cross section, due to [Equation B.13](#), and it goes down with energy (left image). It is also symmetric in  $\cos\theta$ , and it diverges when  $\cos\theta \rightarrow 1$ , which is the forward scattering limit (from [Equation B.14](#), it goes like  $1/\theta^4$ ).
- Still in the left image, for the correction, we get a general larger dependence on  $\cos\theta$ , and it becomes constant at higher energy (as we have seen in [Equation 7.11](#)).
- In the middle graph, corrections start to become visible at  $\mathcal{O}(10 \text{ GeV})$ . On the right, it is shown how correction reaches almost 3% at small angles, and it is about 0.5% at large angles, at 35 GeV is visible.

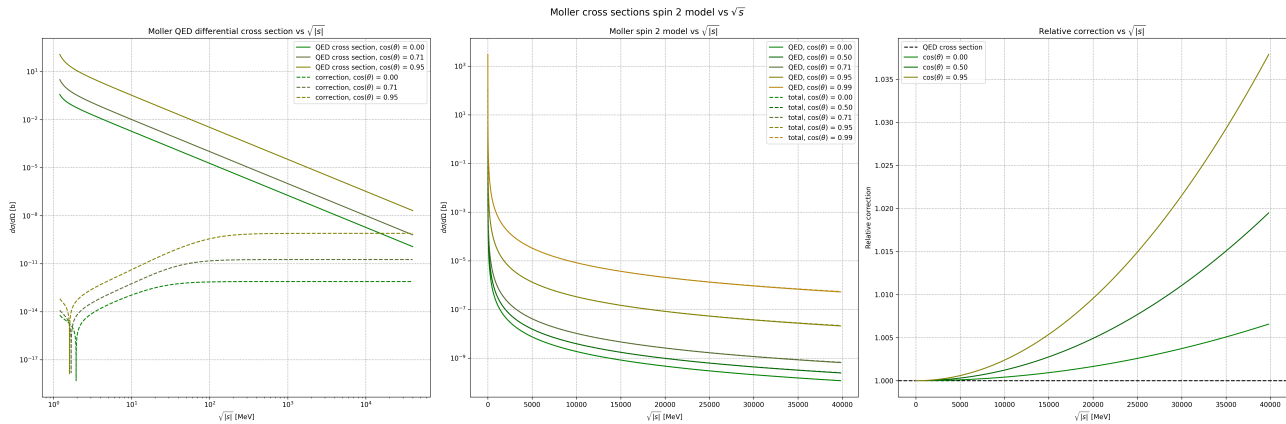


**Figure 16:** Graph of behavior of Møller corrections as a function of the center of mass energy  $\sqrt{|s|}$ . On the left, we plot separately both the QED result and the actual absolute value of spin 2 correction (dashed line), for different values of the  $\cos\theta$ . In the middle, comparison between QED differential cross section and total cross section (including spin 2 correction), for different fixed  $\cos\theta$ . On the right, relative correction to the QED cross section of the total (QED + spin 2) cross section, always at different angular values for  $\cos\theta$ .

In [Figure 16](#), we get the behavior we discussed in this section.

- In the left image, for the QED part, in the very beginning we have the non-relativistic limit, where the cross section goes like  $1/p^4 \propto t^2$ . Then, it slows down in the ultra-relativistic limit to  $1/|s|$ , like Bhabha scattering.

- In the left diagram, it is shown the absolute value of the spin 2 correction (dashed lines). There are four main behaviors for the spin 2 correction that are visible on the left image. In the non-relativistic limit, correction goes like  $1/p^2 \propto 1/t$ . There is a zero of the correction (again, complicated to find because it is located in the non-relativistic region). Notice that Møller scattering cannot produce  $X$  resonance, as in the denominator of the correction there is no  $s + m_X^2$  (only  $t$ -channel and  $u$ -channel). We calculated how in the ultra-relativistic limit  $\sqrt{|s|} \gg m_X$  we get a constant correction, as in [Equation 7.11](#) and [Equation 7.13](#), but it is also easy to see that for  $m_e \ll \sqrt{|s|} \ll m_X$ , correction grows with energy, because we have  $m_X^2$  instead of  $t$  or  $u$  in the denominator.
- So, the graph in the middle has a positive correction that becomes relevant in the  $\mathcal{O}(10\text{ GeV})$  region, as the relative correction grows like  $|s|$ . This is also shown in the graph on the right. At 40 GeV, forward scattering correction is 3.5% of the QED cross section.

### 7.1.2 Møller experimental results

Unfortunately, high energy Møller scattering is not as studied as Bhabha scattering, especially at very high energies, where our correction might start getting relevant. It is used for electroweak precision measurements ([52]), for parity violating purposes.

- However, in a 1975 experiment, they studied polarized Møller scattering at the Stanford Linac ([46]), and achieved a precision of about 4% at  $\sqrt{|s|} = 20\text{ GeV}$ . This is still 1 order of magnitude above spin 2 mediation effect, hence it is still invisible.
- As for lower energy, there is no paper at all about Møller scattering characterization with any of the characteristics we are looking for: few GeV of energy, with very low scattering angle to exploit  $t$ -channel suppressed exchanged momentum<sup>17</sup>. The best experimental result is still from OLYMPUS Collaboration (see [subsubsection 6.2.2](#), and [54]), for which their precision is 1%, and our prediction for spin 2 correction is 5 ppb (from [Equation 7.11](#)).

---

<sup>17</sup>In the future, Møller scattering will be studied in the MØLLER Experiment, which will start taking data at the end of this year, and aims to measure precisely weak angle mixing.

## 8 Digression on a spin 1 toy model

We have seen that, in an spin 2 effective theory landscape, corrections due to the presence of this  $X$  resonance that can couple to both electrons and photons are always growing with energy, because of higher dimension operators. Instead, we may not expect the same behavior on a minimally coupled spin 1 model for the  $X$  particle. If the interaction is described by a dimension 4 operator, the behaviour of the amplitude with energy will be the same as the other QED predicted amplitudes, resulting in a constant relative correction to the cross section.

It is still be worth asking whether this relative constant correction can be experimentally seen. Among all processes we studied so far, Compton and annihilation into two photons cannot be mediated by a spin 1 particle, because of Landau-Yang theorem that prohibits photon coupling (both on shell and off shell). So, Bhabha and Møller scattering are the only processes that can be corrected by a spin 1 mediator. Let us focus on Bhabha, because of its higher relevance in experimental particle physics.

### 8.1 Spin 1 coupling with fermions

We only have to get an idea of what happens, so let us just create a toy model for the vector spin 1  $X$  resonance ( $1^-$ ). Suppose a photon-like behavior (massive spin 1 vector-like mediation). The Lorentz representation a vector boson is ascribed to is  $(1, 0)$ , or  $(0, 1)$ <sup>18</sup>, which in our notation gives us a tensor with only one index. If the boson field is  $X_\mu$ , then:

$$X_\mu(x) = \sum_{\lambda=1}^3 \int \frac{d^3k}{(2\pi)^3 \sqrt{2\omega_{\vec{k}}}} \left[ a_\lambda(\vec{k}) \varepsilon_\mu(\vec{k}, \lambda) e^{-ik \cdot x} + b_\lambda^\dagger(\vec{k}) \varepsilon_\mu^*(\vec{k}, \lambda) e^{ik \cdot x} \right] \quad (8.1)$$

where  $\omega_{\vec{k}} = \sqrt{|\vec{k}|^2 + m_X^2}$ .

It is also possible to prove a completeness relation for the spin polarizations:

$$\sum_{\lambda=1}^3 \varepsilon_\mu(\vec{k}, \lambda) \varepsilon_\nu^*(\vec{k}, \lambda) = \delta_{\mu\nu} + \frac{k_\mu k_\nu}{m_X^2}$$

We can now find the propagator of the massive spin 1 boson field, by inverting the equations of motion, starting from the Proca Lagrangian:

$$(-\square + m_X^2) X_\mu = 0 \quad (8.2)$$

which are Maxwell equations for a "massive" photon. To them, the subsidiary condition:  $\partial_\mu X_\mu = 0$  needs to be added, so that the free components go from 4 to 3. The propagator is, then:

$$D_{\mu\nu}(x - y) = \int \frac{d^4p}{(2\pi)^4 i} \hat{D}_{\mu\nu}^X(p) e^{ip(x-y)} \quad (8.3)$$

where we define the propagator in momentum space as:

$$\hat{D}_{\mu\nu}^X(p) = \frac{1}{p^2 + m_X^2 - i\epsilon} \left[ \delta_{\mu\nu} + \frac{p_\mu p_\nu}{m_X^2} \right] \quad (8.4)$$

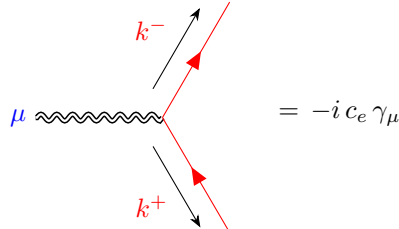
as we know that the numerator of the propagator must be the sum over all physical polarizations, because of unitarity.

The minimal coupling between vector boson and two fermions is trivial to write down, if we see  $X\mu$  coupled like in a covariant derivative. The interaction Lagrangian is:

$$\mathcal{L} = -ic_e \bar{\psi} \gamma_\mu \psi X_\mu \quad (8.5)$$

where  $X_\mu$  is our massive vector boson.

When going to momentum space:



$$= -i c_e \gamma_\mu \quad (8.6)$$

<sup>18</sup>In our Pauli notation, these are indistinguishable. In Bjorken-Drell notation, the two irreps describe covariant and contravariant vectors.

To be contracted with the spin polarization of the spin 1 boson ( $\varepsilon_\mu$ ) and the 2 fermions ( $u(k^-)$ ,  $v(k^+)$ ). This is equal to the QED coupling, in fact.

## 8.2 Spin 1 decay rate for electron-positron channel

Using Feynman rule in [Equation 8.6](#), we write down the amplitude for the decay of X massive particle into electron and positron, at tree level:

$$A = -ic_e \gamma_\mu \varepsilon_\mu \quad (8.7)$$

$$\mathcal{A} = \bar{u}(k^-) A v(k^+) = \bar{u} A v \quad (8.8)$$

from [Equation 5.3](#) we get the complex conjugate of this  $\mathcal{A}^* = \bar{v} B u$  where:

$$B = \gamma_4 A^\dagger \gamma_4 = ic_e \varepsilon_\mu^* \gamma_4 \gamma_\mu^\dagger \gamma_4 = -ic_e \bar{\varepsilon}_\mu \gamma_\mu \quad (8.9)$$

because  $\varepsilon_\mu^* = \mu_p \bar{\varepsilon}_\mu$  and  $\gamma_4 \gamma_\mu^\dagger \gamma_4 = -\mu_p \gamma_\mu$ , as we used throughout this thesis.

Putting it all together:

$$\begin{aligned} |\mathcal{A}|^2 &= -c_e^2 \varepsilon_\mu(p) \bar{\varepsilon}_\nu(p) [\bar{u}(k^-)_a (\gamma_\mu)_{ab} v(k^+)_b \bar{v}(k^+)_c (\gamma_\nu)_{cd} u(k^-)_d] = \\ &= -c_e^2 \varepsilon_\mu(p) \bar{\varepsilon}_\nu(p) \text{Tr} [\gamma_\mu (v \bar{v}) \gamma_\nu (u \bar{u})] \end{aligned} \quad (8.10)$$

with  $p = k^+ + k^-$  by energy conservation. There are 3 polarizations of the  $X$  to average over initially. When summing over the total polarizations, instead, we get:

$$\begin{aligned} |\bar{\mathcal{A}}|^2 &= \frac{1}{3} \sum_{\text{pol}} |\mathcal{A}|^2 = -\frac{c_e^2}{3} \left[ \delta_{\mu\nu} + \frac{p_\mu p_\nu}{m_X^2} \right] \text{Tr} \left[ \gamma_\mu \left( \frac{-ik^+ - m_e}{2k_4^+} \right) \gamma_\nu \left( \frac{-ik^- + m_e}{2k_4^-} \right) \right] = \\ &= -\frac{c_e^2}{12k_4^+ k_4^-} \left[ \delta_{\mu\nu} + \frac{p_\mu p_\nu}{m_X^2} \right] \left[ -4k_\mu^+ k_\nu^- - 4k_\nu^+ k_\mu^- + 4\delta_{\mu\nu} (k^+ \cdot k^- - m_e^2) \right] = \\ &= \frac{c_e^2}{3k_4^+ k_4^-} \left[ \delta_{\mu\nu} + \frac{p_\mu p_\nu}{m_X^2} \right] \left[ k_\mu^+ k_\nu^- + k_\nu^+ k_\mu^- - \delta_{\mu\nu} (k^+ \cdot k^- - m_e^2) \right] = \\ &= \frac{c_e^2}{3k_4^+ k_4^-} \left[ -2k^+ \cdot k^- + 4m_e^2 + 2 \frac{(p \cdot k^+) (p \cdot k^-)}{m_X^2} - \frac{p^2}{m_X^2} (k^+ \cdot k^- - m_e^2) \right] \end{aligned} \quad (8.11)$$

where we can impose kinematics directly, as phase space integration will fix the momenta of the decay:

$$k^+ \cdot k^- = \frac{(k^+ + k^-)^2 + 2m_e^2}{2} = m_e^2 - \frac{m_X^2}{2}$$

$$p \cdot k^- = p \cdot k^+ = -m_e^2 + k^+ \cdot k^- = -\frac{m_X^2}{2}$$

and also  $k_4^+ = k_4^- = m_X/2$ . Substituting kinematics into [Equation 8.11](#):

$$\begin{aligned} |\bar{\mathcal{A}}|^2 &= \frac{4}{3} \frac{c_e^2}{m_X^2} \left[ -2m_e^2 + m_X^2 + 4m_e^2 + \frac{2}{m_X^2} \left( -\frac{m_X^2}{2} \right) \left( -\frac{m_X^2}{2} \right) + \frac{m_X^2}{m_X^2} \left( -\frac{m_X^2}{2} \right) \right] = \\ &= \frac{4}{3} \frac{c_e^2}{m_X^2} \left[ m_X^2 + 2m_e^2 \right] = \frac{4c_e^2}{3} \left[ 1 + \frac{2m_e^2}{m_X^2} \right] \end{aligned} \quad (8.12)$$

Finally, from [Equation 5.12](#):

$$\begin{aligned} \Gamma(X \rightarrow e^+ e^-) &= \frac{m_X}{16\pi} \sqrt{1 - \frac{4m_e^2}{m_X^2}} |\bar{\mathcal{A}}|^2 = \\ &= \frac{c_e^2 m_X}{12\pi} \left[ 1 - \frac{4m_e^2}{m_X^2} \right]^{1/2} \left[ 1 + \frac{2m_e^2}{m_X^2} \right] \end{aligned} \quad (8.13)$$

If we expand in  $m_e^2/m_X^2 \ll 1$ , then we get approximately:

$$\Gamma(X \rightarrow e^+e^-) \approx \frac{c_e^2 m_X}{12\pi} \left[ 1 - \frac{2m_e^2}{m_X^2} \right] \left[ 1 + \frac{2m_e^2}{m_X^2} \right] = \frac{c_e^2 m_X}{12\pi} \left[ 1 - \frac{4m_e^4}{m_X^4} \right] \approx \frac{c_e^2 m_X}{12\pi} \quad (8.14)$$

If we substitute  $m_X = 17 \text{ MeV}$ , we get an estimate of this decay rate being:

$$\Gamma(X \rightarrow e^+e^-) \approx c_e^2 \times 0.45 \text{ MeV} \quad (8.15)$$

We now repeat the same reasoning outlined in [subsubsection 5.4.1](#) to achieve a lower bound on the coupling constant:

$$c_e > \sqrt{\frac{\Gamma_{\min}}{0.45 \text{ MeV}}} \quad (8.16)$$

which translates to the following [Table 2](#):

Target	$\theta^{[\circ]}$	$E[\text{MeV}]$	$\beta$	$\gamma$	$l_{\max}[\text{cm}]$	$\Gamma_{\min}[\text{MeV}^{-1}]$	$c_e _{\min}$
${}^4\text{He}$	112	21.01	0.592	1.241	0.104	$1.4 \times 10^{-10}$	$1.8 \times 10^{-5}$
		20.21	0.544	1.192		$1.2 \times 10^{-10}$	$1.6 \times 10^{-5}$
${}^8\text{Be}$	139	18.15	0.359	1.071	0.092	$8.2 \times 10^{-11}$	$1.3 \times 10^{-5}$
		17.64	0.279	1.041		$6.1 \times 10^{-11}$	$1.2 \times 10^{-5}$
${}^{12}\text{C}$	161	17.23	0.186	1.018	0.088	$4.3 \times 10^{-11}$	$1.0 \times 10^{-5}$

Table 2: All values for the total energy of the pairs  $e^+e^-$  in different experimental setups, and final minimum value for the coupling  $c_e$  in each experiment performed by the ATOMKI collaboration. Mass of the resonance has been mediated between all ATOMKI results and assumed to be  $m_X = 16.94 \text{ MeV}$ .

which gives, as the most constraining result:

$$c_e > 1.8 \times 10^{-5} \quad (8.17)$$

and, as usual, we will be assuming the most conservative result for our assumption:  $c_e = 1.8 \times 10^{-5}$ .

### 8.3 Spin 1 correction to Bhabha scattering

We will follow exactly the same method seen in [section 6](#). Start with the usual diagrams:

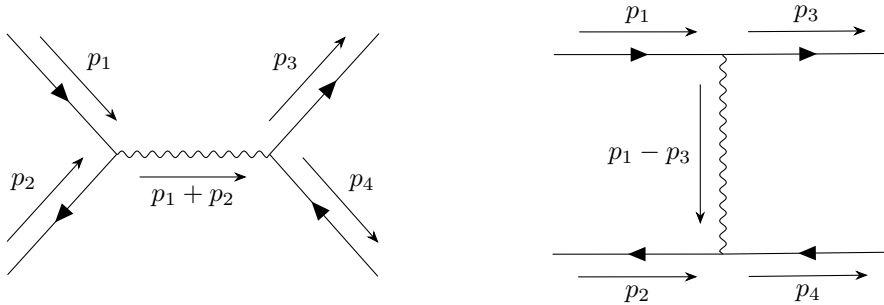


Figure 17: Diagrams corresponding to tree level Bhabha scattering. On the left, the  $s$ -channel, hereafter denoted with  $\mathcal{A}_1$ . On the right, the  $t$ -channel, hereafter denoted with  $\mathcal{A}_2$ .

We add the diagram in which the  $X$  boson is mediated ([Figure 18](#)), contributing with both  $s$ -channel and  $t$ -channel:

The QED amplitudes are always the same:

$$\mathcal{A}_1 = -e^2 \hat{D}_{\mu\nu}^\xi(p_1 + p_2) [\bar{v}_2 \gamma_\mu u_1] [\bar{u}_3 \gamma_\nu v_4] \quad (8.18)$$

$$\mathcal{A}_2 = -e^2 \hat{D}_{\mu\nu}^\xi(p_1 - p_3) [\bar{u}_3 \gamma_\mu u_1] [\bar{v}_2 \gamma_\nu v_4] \quad (8.19)$$

where  $\hat{D}_{\mu\nu}^\xi$  is the photon propagator in the  $\xi$  gauge ([subsection A.1](#)). The usual electrodynamics Feynman rule  $ie\gamma_\mu$  applies at each vertex,  $m_e$  is the mass of the electron,  $p_i$ ,  $i \in \{1, 2, 3, 4\}$  are the respective momenta

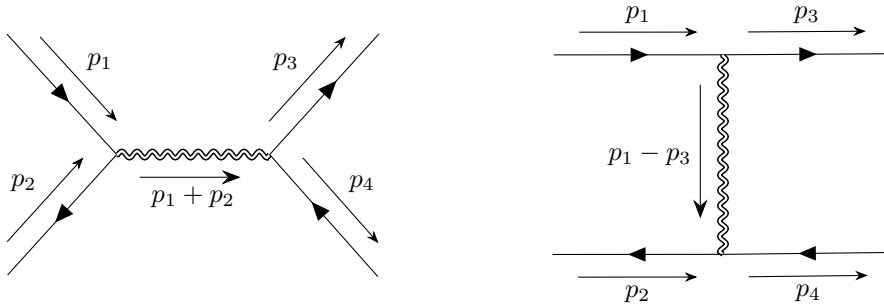


Figure 18: Tree level diagrams for the mediation of massive spin 1 boson for Bhabha scattering, basically accounting for  $s$ -channel (left) and  $t$ -channel (right) contributions. We will refer to the left amplitude as  $\mathcal{A}_3$ , and to the right amplitude as  $\mathcal{A}_4$ .

according to [Figure 43](#) and  $\lambda_i$ ,  $i \in \{1, 2, 3, 4\}$  are the respective polarizations of fermions. Here forth, we will call  $u(p_i, \lambda_i) = u_i$ ,  $i \in \{1, 3\}$  and  $v(p_i, \lambda_i) = v_i$ ,  $i \in \{2, 4\}$ .

Instead, for  $\mathcal{A}_3$  and  $\mathcal{A}_4$  we will employ [Equation 8.6](#):

$$\begin{aligned} \mathcal{A}_3 &= (-ic_e)^2 \hat{D}_{\mu\nu}^X(p_1 + p_2) \left[ \bar{v}(p_2, \lambda_2) \gamma_\mu (p_{2,\alpha} - p_{1,\alpha}) u(p_1, \lambda_1) \right] \left[ \bar{u}(p_3, \lambda_3) \gamma_\nu (p_{3,\beta} - p_{4,\beta}) v(p_4, \lambda_4) \right] = \\ &= -c_e^2 \hat{D}_{\mu\nu}^X(p_1 + p_2) (p_{2,\alpha} - p_{1,\alpha}) (p_{3,\beta} - p_{4,\beta}) [\bar{v}_2 \gamma_\mu u_1] [\bar{u}_3 \gamma_\nu v_4] \end{aligned} \quad (8.20)$$

$$\begin{aligned} \mathcal{A}_4 &= (-ic_e)^2 \hat{D}_{\mu\nu}^X(p_1 - p_3) \left[ \bar{u}(p_3, \lambda_3) \gamma_\mu (p_{3,\alpha} + p_{1,\alpha}) u(p_1, \lambda_1) \right] \left[ \bar{v}(p_2, \lambda_2) \gamma_\nu (p_{2,\beta} + p_{4,\beta}) v(p_4, \lambda_4) \right] = \\ &= -c_e^2 \hat{D}_{\mu\nu}^X(p_1 - p_3) (p_{3,\alpha} + p_{1,\alpha}) (p_{2,\beta} + p_{4,\beta}) [\bar{u}_3 \gamma_\mu u_1] [\bar{v}_2 \gamma_\nu v_4] \end{aligned} \quad (8.21)$$

where  $\hat{D}_{\mu\nu}^X(p)$  is the spin 1 massive propagator, as defined in [Equation 8.4](#). Like in [section 6](#),  $\mathcal{A}_1$  and  $\mathcal{A}_3$  have the same Dirac structure. Same goes for  $\mathcal{A}_2$  and  $\mathcal{A}_4$ . Because of fermion statistics (as thoroughly explained), total amplitude is:

$$\mathcal{A} = -(\mathcal{A}_1 + \mathcal{A}_3) + (\mathcal{A}_2 + \mathcal{A}_4)$$

Define the usual Mandelstam variables:

$$s = (p_1 + p_2)^2 \quad t = (p_1 - p_3)^2 \quad u = (p_1 - p_4)^2$$

Complex conjugate of each amplitude is now a known result that we can just copy:

$$\mathcal{A}_1^* = -e^2 \hat{D}_{\rho\sigma}^\xi(p_1 + p_2) [\bar{u}_1 \gamma_\rho v_2] [\bar{v}_4 \gamma_\sigma u_3]$$

$$\mathcal{A}_2^* = -e^2 \hat{D}_{\rho\sigma}^\xi(p_1 - p_3) [\bar{u}_1 \gamma_\rho u_3] [\bar{v}_4 \gamma_\sigma v_2]$$

$$\mathcal{A}_3^* = -c_e^2 \hat{D}_{\rho\sigma}^X(p_1 + p_2) [\bar{u}_1 \gamma_\rho v_2] [\bar{v}_4 \gamma_\sigma u_3]$$

$$\mathcal{A}_4^* = -c_e^2 \hat{D}_{\rho\sigma}^X(p_1 - p_3) [\bar{u}_1 \gamma_\rho u_3] [\bar{v}_4 \gamma_\sigma v_2]$$

Now, let us exploit the Dirac structure and define:

$$\hat{S}_{\mu\nu}^\xi(p_i) = e^2 \hat{D}_{\mu\nu}^\xi(p_1 + p_2) + c_e^2 \hat{D}_{\mu\nu}^X(p_1 + p_2) \quad (8.22)$$

$$\hat{T}_{\mu\nu}^\xi(p_i) = e^2 \hat{D}_{\mu\nu}^\xi(p_1 - p_3) + c_e^2 \hat{D}_{\mu\nu}^X(p_1 - p_3) \quad (8.23)$$

term by term, using the calculations in Dirac space in [subsection A.2](#):

$$|\mathcal{A}_s|^2 = |\mathcal{A}_1 + \mathcal{A}_3|^2 = \hat{S}_{\mu\nu}^\xi(p_i) \hat{S}_{\rho\sigma}^\xi(p_i) \text{Tr} [\gamma_\mu (u_1 \bar{u}_1) \gamma_\rho (v_2 \bar{v}_2)] \text{Tr} [\gamma_\nu (v_4 \bar{v}_4) \gamma_\sigma (u_3 \bar{u}_3)]$$

$$|\mathcal{A}_t|^2 = |\mathcal{A}_2 + \mathcal{A}_4|^2 = \hat{T}_{\mu\nu}^\xi(p_i) \hat{T}_{\rho\sigma}^\xi(p_i) \text{Tr} [\gamma_\mu (u_1 \bar{u}_1) \gamma_\rho (u_3 \bar{u}_3)] \text{Tr} [\gamma_\nu (v_4 \bar{v}_4) \gamma_\sigma (v_2 \bar{v}_2)]$$

$$\mathcal{A}_s \mathcal{A}_t^* = \hat{S}_{\mu\nu}^\xi(p_i) \hat{T}_{\rho\sigma}^\xi(p_i) \text{Tr} [\gamma_\mu (u_1 \bar{u}_1) \gamma_\rho (u_3 \bar{u}_3) \gamma_\nu (v_4 \bar{v}_4) \gamma_\sigma (v_2 \bar{v}_2)]$$

$$\mathcal{A}_t \mathcal{A}_s^* = \hat{T}_{\mu\nu}^\xi(p_i) \hat{S}_{\rho\sigma}^\xi(p_i) \text{Tr} [\gamma_\mu (u_1 \bar{u}_1) \gamma_\rho (v_2 \bar{v}_2) \gamma_\nu (v_4 \bar{v}_4) \gamma_\sigma (u_3 \bar{u}_3)]$$

Averaging over initial fermion polarization and summing over all of them we get the unpolarized amplitude:

$$\begin{aligned} |\bar{\mathcal{A}}|^2 &= \frac{1}{4} \sum_{\lambda_1} \sum_{\lambda_2} \sum_{\lambda_3} \sum_{\lambda_4} \left( |\mathcal{A}_s|^2 + |\mathcal{A}_t|^2 - \mathcal{A}_s \mathcal{A}_t^* - \mathcal{A}_t \mathcal{A}_s^* \right) = \frac{1}{4} \frac{1}{2p_{1,4} 2p_{2,4} 2p_{3,4} 2p_{4,4}} \times \\ &\left\{ \hat{S}_{\mu\nu}^\xi(p_i) \hat{S}_{\rho\sigma}^\xi(p_i) \text{Tr} \left[ \gamma_\mu (-i\cancel{p}_1 + m_e) \gamma_\rho (-i\cancel{p}_2 - m_e) \right] \text{Tr} \left[ \gamma_\nu (-i\cancel{p}_4 - m_e) \gamma_\sigma (-i\cancel{p}_3 + m_e) \right] \right. \\ &+ \hat{T}_{\mu\nu}^\xi(p_i) \hat{T}_{\rho\sigma}^\xi(p_i) \text{Tr} \left[ \gamma_\mu (-i\cancel{p}_1 + m_e) \gamma_\rho (-i\cancel{p}_3 + m_e) \right] \text{Tr} \left[ \gamma_\nu (-i\cancel{p}_4 - m_e) \gamma_\sigma (-i\cancel{p}_2 - m_e) \right] \\ &- \hat{S}_{\mu\nu}^\xi(p_i) \hat{T}_{\rho\sigma}^\xi(p_i) \text{Tr} \left[ \gamma_\mu (-i\cancel{p}_1 + m_e) \gamma_\rho (-i\cancel{p}_3 + m_e) \gamma_\nu (-i\cancel{p}_4 - m_e) \gamma_\sigma (-i\cancel{p}_2 - m_e) \right] \\ &\left. - \hat{T}_{\mu\nu}^\xi(p_i) \hat{S}_{\rho\sigma}^\xi(p_i) \text{Tr} \left[ \gamma_\mu (-i\cancel{p}_1 + m_e) \gamma_\rho (-i\cancel{p}_2 - m_e) \gamma_\nu (-i\cancel{p}_4 - m_e) \gamma_\sigma (-i\cancel{p}_3 + m_e) \right] \right\} \quad (8.24) \end{aligned}$$

A new FORM code will perform the calculation for us. The FORM script used for this task is found in the repository linked in [subsection G.1](#).

As usual, the final result has thousands of addends and we do not deem it practical to report here. Substituting the values of the scalar products found in [subsection A.3](#) simplifies the result, but we need to perform the integral in phase space first. We already did that several times, and we obtained:

$$\frac{d\sigma}{d\Omega} = \frac{E^2}{16\pi^2} |\bar{\mathcal{A}}|^2$$

where now  $\mathcal{A}$  is the amplitude where we imposed kinematics. Let us write it:

$$\begin{aligned} |\bar{\mathcal{A}}|^2 &= \frac{1}{64E^4} F(s, t, u) \\ F(s, t, u) &= F_s(s, t, u) + F_t(s, t, u) + F_{st}(s, t, u) \end{aligned}$$

where  $F(s, t, u)$  is an adimensional function of the Mandelstam variables, and it is the actual result of the FORM computation. It gets contributions from each term of the squared amplitude:  $F_s$  from  $s$ -channel squared,  $F_t$  from  $t$ -channel squared,  $F_{st}$  from interference terms.

The code we used is called `Bhabha_Xspin1_xigauge.frm` and it provides the result of the calculation of the traces. The result is  $\xi$  independent, because of gauge invariance, before imposing kinematics (as gauge invariance comes before kinematics). To manipulate the resulting terms, we can use [Equation A.27](#)<sup>19</sup>.

Even though the terms  $e^2 c_e^2$  are dominant, one can see that because of the structure of vector theories, the terms  $c_e^4$  are equivalent to the  $e^4$  terms, as the  $p_\mu p_\nu / m_X^2$  part in the propagator cancels exactly like in gauge invariance. So, we can actually write the full amplitude.

<sup>19</sup>Whenever we are about to use  $s + t + u = -4m_e^2$ , the substituting part will be colored in blue.

**s-channel:** It consists of 18 terms, before simplification:

$$\begin{aligned}
F_s(s, t, u) &= \left( \frac{8e^4}{s^2} + \frac{8c_e^4}{(s + m_X^2)^2} \right) [-2tu - us - st] + 16m_e^2 \left( \frac{e^4}{s^2} + \frac{c_e^4}{(s + m_X^2)^2} \right) [-u - t - 3s] \\
&\quad + \frac{e^2 c_e^2}{s + m_X^2} \left\{ -16 \left[ 2 \frac{ut}{s} + \textcolor{blue}{u + t} \right] - 32m_e^2 \left[ 3 + \frac{\textcolor{blue}{u + t}}{s} \right] \right\} = \\
&= \left( \frac{8e^4}{s^2} + \frac{8c_e^4}{(s + m_X^2)^2} \right) [u^2 + t^2 + 8m_e^2(u + t) + 24m_e^4] \\
&\quad + \frac{16e^2 c_e^2}{s + m_X^2} \left[ -2 \frac{ut}{s} + s + \cancel{4m_e^2} + 2 \frac{m_e^2}{s} (4m_e^2 - 2s) \right] = \\
&= \left( \frac{8e^4}{s^2} + \frac{8c_e^4}{(s + m_X^2)^2} \right) [u^2 + t^2 + 8m_e^2(u + t) + 24m_e^4] + \frac{16}{s} \frac{e^2 c_e^2}{s + m_X^2} [-2ut + s^2 + 8m_e^4]
\end{aligned} \tag{8.25}$$

Manipulation of the QED part can be found in [Equation A.43](#).

**t-channel:** It is immediate from the code that  $T_i(s, t, u) = S_i(t, s, u)$ , for  $i \in \{1, 2\}$ . So, this means:

$$F_t(s, t, u) = F_s(t, s, u)$$

Manipulation is trivial, as we just need to exchange  $s$  and  $t$  to get the result. Same for the QED part (see [Equation A.43](#)):

$$F_t(s, t, u) = \left( \frac{8e^4}{t^2} + \frac{8c_e^4}{(t + m_X^2)^2} \right) [u^2 + s^2 + 8m_e^2(u + s) + 24m_e^4] + \frac{16}{t} \frac{e^2 c_e^2}{t + m_X^2} [-2us + t^2 + 8m_e^4] \tag{8.26}$$

**Interference terms:** We get 25 terms, before simplification:

$$\begin{aligned}
F_{st}(s, t, u) &= \left( \frac{16e^4}{st} + \frac{16c_e^4}{(s + m_X^2)(t + m_X^2)} \right) \left[ -\frac{u}{s} - \frac{u}{t} + 2m_e^2 \left( \frac{u}{st} - \frac{3}{s} - \frac{3}{t} \right) \right] \\
&\quad + \frac{e^2 c_e^2}{s + m_X^2} \left\{ -16 \left[ u + \frac{us}{t} \right] - 16m_e^2 \left[ 3 - \frac{u}{t} + \frac{3s}{t} \right] \right\} \\
&\quad + \frac{e^2 c_e^2}{t + m_X^2} \left\{ -16 \left[ u + \frac{ut}{s} \right] - 16m_e^2 \left[ 3 - \frac{u}{s} + \frac{3t}{s} \right] \right\} = \\
&= \left( \frac{16e^4}{st} + \frac{16c_e^4}{(s + m_X^2)(t + m_X^2)} \right) [u^2 + 8m_e^2 u + 12m_e^4] \\
&\quad + \frac{16}{t} \frac{e^2 c_e^2}{s + m_X^2} \left\{ -u [\textcolor{blue}{t + s}] + m_e^2 [u - 3(\textcolor{blue}{t + s})] \right\} \\
&\quad + \frac{16}{s} \frac{e^2 c_e^2}{t + m_X^2} \left\{ -u [\textcolor{blue}{s + t}] + m_e^2 [u - 3(\textcolor{blue}{s + t})] \right\} = \\
&= \left( \frac{16e^4}{st} + \frac{16c_e^4}{(s + m_X^2)(t + m_X^2)} \right) [u^2 + 8m_e^2 u + 12m_e^4] \\
&\quad + 16e^2 c_e^2 \left[ \frac{1}{t(s + m_X^2)} + \frac{1}{s(t + m_X^2)} \right] (u + 6m_e^2)(u + 2m_e^2)
\end{aligned} \tag{8.27}$$

Joining [Equation 8.25](#), [Equation 8.26](#), [Equation 8.27](#) and [Equation A.43](#) we get the final result:

$$\begin{aligned} F(s, t, u) = & 8e^4 \left\{ \frac{1}{s^2} [u^2 + t^2 + 8m_e^2(u+t) + 24m_e^4] + \frac{1}{t^2} [u^2 + s^2 + 8m_e^2(u+s) + 24m_e^4] + \frac{2}{st} [u^2 + 8m_e^2u + 12m_e^4] \right\} \\ & + 16e^2c_e^2 \left\{ \frac{-2ut + s^2 + 8m_e^4}{s(s+m_X^2)} + \frac{-2us + t^2 + 8m_e^4}{t(t+m_X^2)} + \left[ \frac{1}{t(s+m_X^2)} + \frac{1}{s(t+m_X^2)} \right] (u+6m_e^2)(u+2m_e^2) \right\} \\ & + 8c_e^4 \left\{ \frac{u^2 + t^2 + 8m_e^2(u+t) + 24m_e^4}{(s+m_X^2)^2} + \frac{u^2 + s^2 + 8m_e^2(u+s) + 24m_e^4}{(t+m_X^2)^2} + \frac{2[u^2 + 8m_e^2u + 12m_e^4]}{(s+m_X^2)(t+m_X^2)} \right\} \end{aligned} \quad (8.28)$$

Notice how  $F(s, t, u) = F(t, s, u)$ , as this would simply swap the two diagrams, and give the same final result. We do not need the  $g_e^4$  terms for our estimate, but it was an interesting check to be done nonetheless. From now on, we will exclude it from calculations.

From [Equation A.38](#) and [Equation A.39](#), we get the final differential cross section:

$$\begin{aligned} \frac{d\sigma}{d\Omega} = & \frac{E^2}{16\pi^2} \frac{1}{64E^4} F(s, t, u) = \frac{F(s, t, u)}{256\pi^2|s|} = \\ = & \frac{\alpha^2}{2|s|} \left\{ \frac{1}{s^2} [u^2 + t^2 + 8m_e^2(u+t) + 24m_e^4] + \frac{1}{t^2} [u^2 + s^2 + 8m_e^2(u+s) + 24m_e^4] + \frac{2}{st} [u^2 + 8m_e^2u + 12m_e^4] \right\} \\ + & \frac{\alpha c_e^2}{\pi 4|s|} \left\{ \frac{-2ut + s^2 + 8m_e^4}{s(s+m_X^2)} + \frac{-2us + t^2 + 8m_e^4}{t(t+m_X^2)} + \left[ \frac{1}{t(s+m_X^2)} + \frac{1}{s(t+m_X^2)} \right] (u+6m_e^2)(u+2m_e^2) \right\} + \mathcal{O}\left(\frac{c_e^4}{\Lambda^4}\right) \end{aligned} \quad (8.29)$$

and when  $c_e \rightarrow 0$ , we recover the QED cross section shown in [Equation A.44](#).

This result does not take into account the diagrams due to weak interaction (mediation of the  $Z$  boson), which become dominant in the region  $\sqrt{|s|} \approx 60 - 120$  GeV. This means that our formula only works up to around 50 GeV.

Take the usual two limits:

**Non-relativistic limit:** We send  $4m_e^2/s \rightarrow -1$ , as  $E \rightarrow m_e$ . Then,  $t/s \rightarrow 0$  and  $u/s \rightarrow 0$ . In [subsection A.4](#), we justify why the  $t$ -channel is dominant in this limit, and it behaves like  $1/t^2$ .

Because the spin 1 boson is massive, however, the dominant correction behaves like  $1/t$ , and it takes terms from both  $t$ -channel and interference. The limit is easy to take, as only  $m_e^2$  and  $s$  terms have to be preserved:

$$\begin{aligned} \frac{d\sigma}{d\Omega} = & \frac{8\alpha^2 m_e^4}{2|s|t^2} + \frac{\alpha c_e^2}{\pi 4|s|} \left[ \frac{8}{t} \frac{m_e^4}{m_X^2} + \frac{12}{t} \frac{m_e^4}{m_X^2} \right] = \\ = & \frac{\alpha^2 m_e^2}{t^2} + \frac{5\alpha c_e^2 m_e^2}{4\pi t m_X^2} = \\ = & \frac{\alpha^2 m_e^2}{t^2} \left[ 1 + \frac{5}{4\pi\alpha} \frac{c_e^2 m_e^2}{m_X^2} \right] \end{aligned} \quad (8.30)$$

It is a positive, constant relative correction. Numerically, we can estimate the lower bound of the correction with [Equation 8.17](#):

$$\frac{d\sigma}{d\Omega} = \frac{d\sigma}{d\Omega} \Big|_{\text{QED}} \left[ 1 + 1.5 \times 10^{-11} \right] \quad (8.31)$$

**Ultra-relativistic limit:** If we send  $m_e^2/s \rightarrow 0$ , and  $m_X^2/s \rightarrow 0$  then we can simplify mass terms in [Equation 8.29](#):

$$\begin{aligned} \frac{d\sigma}{d\Omega} = & \frac{\alpha^2}{2|s|} \left[ u^2 \left( \frac{1}{s} + \frac{1}{t} \right)^2 + \left( \frac{t}{s} \right)^2 + \left( \frac{s}{t} \right)^2 \right] + \frac{\alpha c_e^2}{\pi 4|s|} \left\{ 2 - \frac{2ut}{s^2} - \frac{2us}{t^2} + \frac{2u^2}{st} \right\} = \\ = & \frac{\alpha^2}{2|s|} \left[ u^2 \left( \frac{1}{s} + \frac{1}{t} \right)^2 + \left( \frac{t}{s} \right)^2 + \left( \frac{s}{t} \right)^2 \right] + \frac{\alpha c_e^2}{\pi 2|s|} \left\{ 1 - u \left[ \frac{t}{s^2} + \frac{s}{t^2} - \frac{u}{st} \right] \right\} \end{aligned} \quad (8.32)$$

Substitute the Mandelstam variables in the center of mass frame:

$$s = -4E^2 \quad t \rightarrow 2E^2(1 - \cos \theta) \quad u \rightarrow 2E^2(1 + \cos \theta)$$

which for the QED part we get [Equation A.51](#), and for the spin 1 part, inside curly brackets:

$$\begin{aligned} \{\dots\} &= 1 - 2E^2(1 + \cos \theta) \left[ \frac{2E^2(1 - \cos \theta)}{16E^4} - \frac{4E^2}{4E^4(1 - \cos \theta)^2} + \frac{2E^2(1 + \cos \theta)}{8E^4(1 - \cos \theta)} \right] = \\ &= 1 - 2(1 + \cos \theta) \left[ \frac{1 - \cos \theta}{8} - \frac{1}{(1 - \cos \theta)^2} + \frac{1 + \cos \theta}{4(1 - \cos \theta)} \right] = \\ &= 1 - \frac{1 + \cos \theta}{4(1 - \cos \theta)^2} \left[ (1 - \cos \theta)^3 - 8 + 2(1 - \cos^2 \theta) \right] = \\ &= 1 + \frac{1 + \cos \theta}{4(1 - \cos \theta)^2} \left[ 5 + 3\cos \theta - \cos^2 \theta + \cos^3 \theta \right] \end{aligned} \tag{8.33}$$

In the range  $[-1, 1]$ , there are no zeros. So, correction does not vanish for any angle in the ultra-relativistic regime.

If we send  $\theta \rightarrow \pi/2$  we get:  $1 + 5/4 = 9/4$ , which is positive. Together with [Equation A.52](#) we get the estimate of the final, ultra-relativistic cross section at high angles:

$$\begin{aligned} \frac{d\sigma}{d\Omega} &= \frac{9\alpha^2}{4|s|} + \frac{9\alpha}{4\pi} \frac{c_e^2}{2|s|} = \frac{9\alpha^2}{4|s|} \left[ 1 + \frac{1}{2\pi} \frac{c_e^2}{\alpha} \right] = \\ &= \frac{d\sigma}{d\Omega} \Big|_{\text{QED}} \left[ 1 + \frac{1}{2\pi} \frac{c_e^2}{\alpha} \right] \end{aligned} \tag{8.34}$$

which numerically, using [Equation 5.43](#), gives:

$$\frac{d\sigma}{d\Omega} = \frac{d\sigma}{d\Omega} \Big|_{\text{QED}} \left[ 1 + 7.2 \times 10^{-9} \right] \tag{8.35}$$

as a conservative correction estimate (lower bound for the coupling constant). This correction is a constant in energy, and it is below the best experimental precision for Bhabha scattering by about 3 orders of magnitude ([\[47\]](#)).

Instead, if we send  $\theta \rightarrow 0$ , and approximate  $\cos \theta \rightarrow 1$ ,  $\sin \theta \rightarrow \theta$  and  $1 - \cos \theta \rightarrow \theta^2/2$ , the dominant term is the one with  $(1 - \cos \theta)^2$  in the denominator, which leaves us with  $16/\theta^4$ , again negative. Together with [Equation A.53](#) we get the estimate of the final, ultra-relativistic cross section at low angles:

$$\begin{aligned} \frac{d\sigma}{d\Omega} &= \frac{16\alpha^2}{|s|} \frac{1}{\theta^4} + \frac{\alpha}{\pi} \frac{c_e^2}{2|s|} \frac{16}{\theta^4} = \frac{16\alpha^2}{|s|} \frac{1}{\theta^4} \left[ 1 + \frac{1}{2\pi} \frac{c_e^2}{\alpha} \right] = \\ &= \frac{d\sigma}{d\Omega} \Big|_{\text{QED}} \left[ 1 + \frac{1}{2\pi} \frac{c_e^2}{\alpha} \right] \end{aligned} \tag{8.36}$$

exactly the same correction as [Equation 8.34](#):

$$\frac{d\sigma}{d\Omega} = \frac{d\sigma}{d\Omega} \Big|_{\text{QED}} \left[ 1 + 7.2 \times 10^{-9} \right] \tag{8.37}$$

as a conservative correction estimate (lower bound for the coupling constant). This correction is a constant in energy, and it is below the best experimental precision for Bhabha scattering by about 3 orders of magnitude ([\[47\]](#)).

### 8.3.1 Testing spin 1 for Bhabha

In the end, experimental precision for Bhabha scattering is not enough to see corrections due to spin 1 massive bosons mediation, for our simple toy model. There clearly is a huge practical difference between spin 1 model and spin 2 model in terms of dependence on energy of the cross section.

This is why the JINR result is so crucial: without it, spin 1 models would be the most popular to explain  $X$  resonance, but also impossible to exclude experimentally due to the indirect insignificant effect on observables. The only verification for these models would be direct production ([7]).

Instead, thanks to the two photon channels excluding spin 1 models by Landau-Yang theorem, only effective theories are left as viable models. But in these cases, indirect corrections to cross sections would increase with energy allowing experimental testing (which is what happened for our spin 2 model).

We report the graphs displaying the behavior of the corrected Bhabha scattering in [Figure 19](#) and [Figure 20](#): In [Figure 19](#), you can see how spin 1 corrections are decreasing in energy, and have the same behavior as the

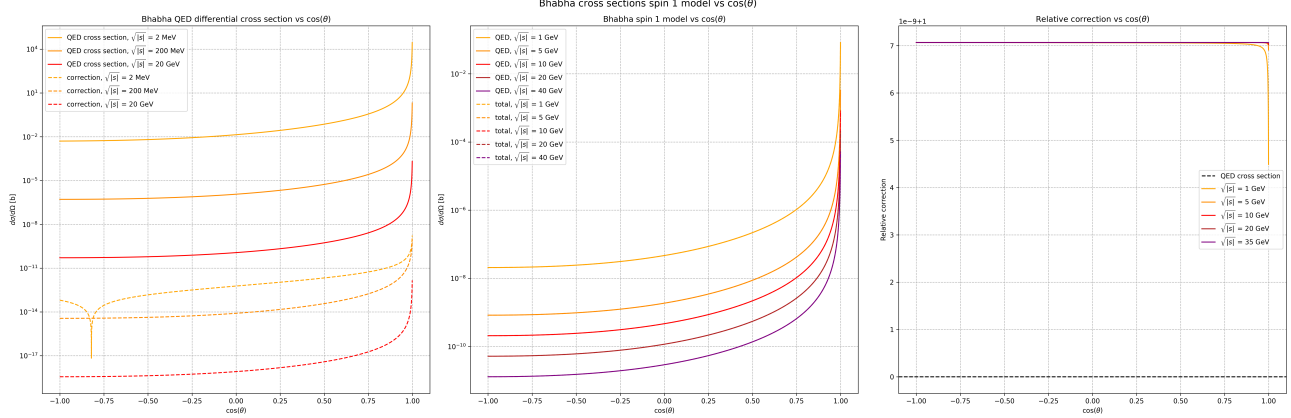


Figure 19: Graph of behavior of Bhabha corrections as a function of the scattering angle  $\cos \theta$ . On the left, we plot separately both the QED result and the actual absolute value of spin 1 correction (dashed line), for different values of the center of mass energy  $\sqrt{|s|}$ . In the middle, comparison between QED differential cross section and total cross section (including spin 1 correction), for different fixed  $\sqrt{|s|}$ . On the right, relative correction to the QED cross section of the total (QED + spin 2) cross section, always at different energetic values for  $\sqrt{|s|}$ .

QED cross section as a function of the angle.

- QED cross section has already been described in [subsection 6.2](#). In the left image, for the correction, we get the same dependence  $\cos \theta$ , and it goes down at higher energy (as we have seen in [Equation 8.34](#)). Low energy also presents one zero (not easy to find kinematically).
- In the middle graph, corrections stays invisible at  $\mathcal{O}(10 \text{ GeV})$ , and we can see why on the right: correction stays exactly constant for every value of  $\cos \theta$  and it is equal to  $7 \times 10^{-9}$ , hence it is not detectable.

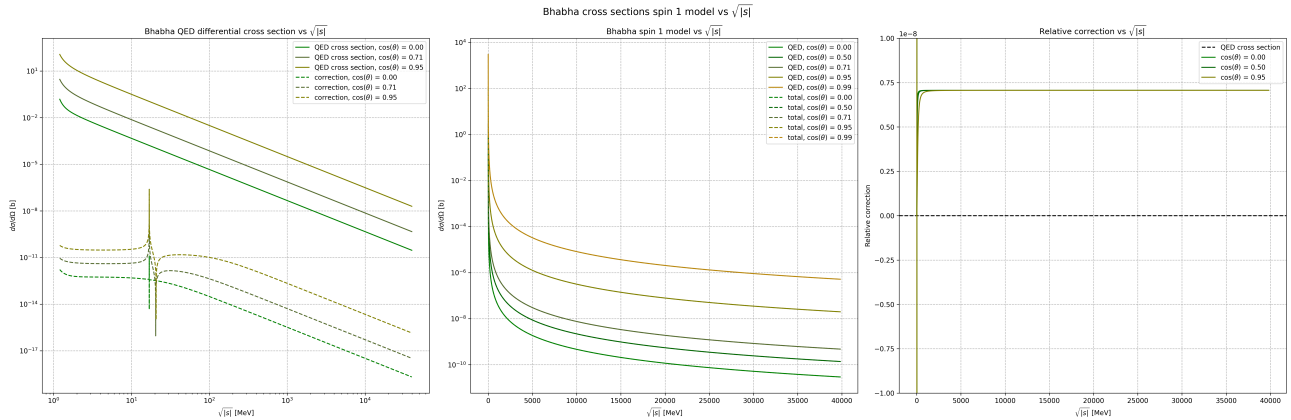


Figure 20: Graph of behavior of Bhabha corrections as a function of the center of mass energy  $\sqrt{|s|}$ . On the left, we plot separately both the QED result and the actual absolute value of the spin 1 correction (dashed line), for different values of the  $\cos \theta$ . In the middle, comparison between QED differential cross section and total cross section (including spin 1 correction), for different fixed  $\cos \theta$ . On the right, relative correction to the QED cross section of the total (QED + spin 1) cross section, always at different angular values for  $\cos \theta$ .

In [Figure 20](#), we get the behavior we discussed in this section. QED part has been thoroughly discussed already.

- In the left diagram, it is shown the absolute value of the spin 1 correction (dashed lines). There are two main behaviors for the spin 1 correction that are visible on the left image. First, when  $\sqrt{|s|} = m_X$ , from

[Equation 8.29](#), correction is infinite for every angle (resonant production of  $X$ ). Moreover, while in the ultra-relativistic limit there are no zeros, as we said, at lower energies there are zeros for certain kinematics configurations (to us, are not relevant). Then, according to [Equation 8.34](#) and [Equation 8.36](#), goes like  $1/|s|$ .

- So, relative correction is always constant and invisible at every energy and scattering angle, and numerically it is equal to  $7 \times 10^{-9}$ .

Again, this shows how spin 1 corrections hide very well at every energy and angle configuration (except at resonance, but that does not pertain our analysis).

## 9 Correction to Compton scattering

It is now time to focus on those processes for which  $g_\gamma \neq 0$ . Let us repeat what we did in [section 6](#) and [section 7](#), but for the process:  $e^- \gamma \rightarrow e^- \gamma$  (called *Compton scattering*). The tree level diagrams for it are in [Figure 21](#), and correspond to a *s*-channel and a *u*-channel.

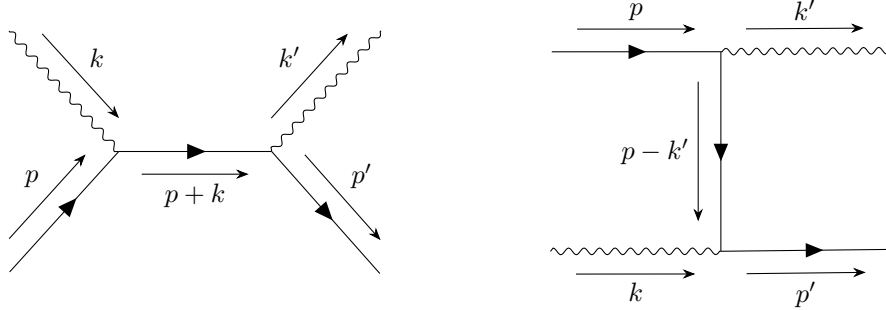


Figure 21: Diagrams corresponding to tree level Compton scattering. On the left, the *s*-channel, hereafter denoted with  $\mathcal{A}_1$ . On the right, the *u*-channel, hereafter denoted with  $\mathcal{A}_2$ .

We add the diagram in which the  $X$  boson is mediated ([Figure 22](#)), contributing with a *t*-channel:

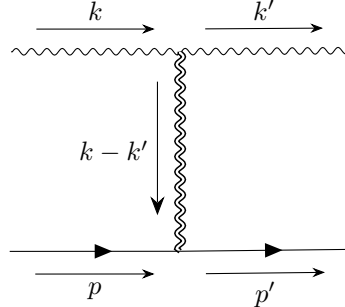


Figure 22: Tree level diagram for the mediation of massive spin 2 boson for Compton scattering, basically accounting for a *t*-channel contribution. We will refer to this amplitude as  $\mathcal{A}_3$ .

The amplitudes are quite easily written following [subsection C.2](#):

$$\mathcal{A}_1 = (-ie)^2 \bar{u}(p', s') \bar{\varepsilon}_\mu(k', \lambda') \gamma_\mu \left[ \frac{-i(\not{p} + \not{k}) + m_e}{(p+k)^2 + m_e^2} \right] \varepsilon_\nu(k, \lambda) \gamma_\nu u(p, s) = -e^2 \bar{u}' O_1 u \quad (9.1)$$

$$\mathcal{A}_2 = (-ie)^2 \bar{u}(p', s') \varepsilon_\mu(k, \lambda) \gamma_\mu \left[ \frac{-i(\not{p} - \not{k}') + m_e}{(p-k')^2 + m_e^2} \right] \bar{\varepsilon}_\nu(k', \lambda') \gamma_\nu u(p, s) = -e^2 \bar{u}' O_2 u \quad (9.2)$$

where the usual electrodynamics Feynman rule  $-ie\gamma_\mu$  applies at each vertex,  $m_e$  is the mass of the electron,  $p, p', k, k'$  are the respective momenta according to [Figure 49](#) and  $s, s', \lambda, \lambda'$  are the polarizations of fermions and photons, respectively. Here forth, we will call  $u(p, s) = u$ ,  $u(p', s') = u'$ ,  $\varepsilon_\mu(k, \lambda) = \varepsilon_\mu$ ,  $\varepsilon_\mu(k', \lambda') = \varepsilon'_\mu$ . Finally, the reason why we have  $(-ie)^2$  and not  $(-ie)^2/2!$  is outlined in [subsection C.1](#), where we carry out Wick contractions.

Instead, for  $\mathcal{A}_3$  we will employ [Equation 4.56](#) and [Equation 4.68](#). Note that this being a *t*-channel, both interactions see a changed sign in one of the two momenta ( $-p$  for the  $X - e^+ e^-$  interaction, and  $-k$  for the  $X - \gamma\gamma$  interaction):

$$\begin{aligned} \mathcal{A}_3 &= \left[ \frac{g_\gamma}{\Lambda} \right] \left[ \frac{ig_e}{2\Lambda} \right] \bar{u}(p', s') \gamma_\rho(p'_\sigma + p_\sigma) u(p, s) \left[ \frac{N_{\mu\nu\rho\sigma}(k - k')}{(k - k')^2 + m_X^2} \right] \Pi_{\mu\nu\alpha\beta}(-k, k') \varepsilon_\alpha(k, \lambda) \bar{\varepsilon}_\beta(k', \lambda') = \\ &= \frac{ig_e g_\gamma}{2\Lambda^2} \bar{u}' O_3 u \end{aligned} \quad (9.3)$$

Realizing that propagator momenta build Mandelstam variables...

$$\begin{aligned} (p+k)^2 + m_e^2 &= s + m_e^2 = -m_e^2 + \not{k}^2 + 2p \cdot k + m_e^2 = 2p \cdot k \\ (p-k')^2 + m_e^2 &= u + m_e^2 = -m_e^2 + \not{k}'^2 - 2p \cdot k' + m_e^2 = -2p \cdot k' \\ (k-k')^2 + m_X^2 &= t + m_X^2 = -2k \cdot k' + m_X^2 \end{aligned}$$

... we can write  $O_1$ ,  $O_2$ , and  $O_3$ :

$$\begin{aligned} O_1 &= \bar{\varepsilon}'_\mu \gamma_\mu \left[ \frac{-i(\not{p} + \not{k}) + m_e}{2p \cdot k} \right] \varepsilon_\nu \gamma_\nu \\ O_2 &= \varepsilon_\nu \gamma_\nu \left[ \frac{-i(\not{p} - \not{k}') + m_e}{-2p \cdot k'} \right] \bar{\varepsilon}'_\mu \gamma_\mu \\ O_3 &= \varepsilon_\alpha \left[ \gamma_\rho (p'_\sigma + p_\sigma) \frac{N_{\mu\nu\rho\sigma}(k - k')}{-2k \cdot k' + m_X^2} \Pi_{\mu\nu\alpha\beta}(-k, k') \right] \bar{\varepsilon}'_\beta \end{aligned}$$

We can calculate the complex conjugate of those amplitudes, following the procedure highlighted in [subsection F.4](#):

$$\begin{aligned} \mathcal{A}_1^* &= (ie)^2 \bar{u} \left( \gamma_4 O_1^\dagger \gamma_4 \right) u' = -e^2 \bar{u} P_1 u' \\ \mathcal{A}_2^* &= (ie)^2 \bar{u} \left( \gamma_4 O_2^\dagger \gamma_4 \right) u' = -e^2 \bar{u} P_2 u' \\ \mathcal{A}_3^* &= \frac{-ig_e g_\gamma}{2\Lambda^2} \bar{u} \left( \gamma_4 O_3^\dagger \gamma_4 \right) u' = \frac{-ig_e g_\gamma}{2\Lambda^2} \bar{u} P_3 u' \end{aligned}$$

exploiting  $\varepsilon_4 = \varepsilon'_4 = 0$  in our gauge choice:

$$\begin{aligned} P_1 &= \bar{\varepsilon}_\sigma \gamma_\sigma \left[ \frac{-i(\not{p} + \not{k}) + m_e}{2p \cdot k} \right] \varepsilon'_\rho \gamma_\rho \\ P_2 &= \bar{\varepsilon}'_\rho \gamma_\rho \left[ \frac{-i(\not{p} - \not{k}') + m_e}{-2p \cdot k'} \right] \varepsilon_\sigma \gamma_\sigma \\ P_3 &= \varepsilon_\gamma^* \left[ \gamma_4 (\gamma_\delta)^\dagger \gamma_4 (p'_\theta + p_\theta)^* \frac{N_{\zeta\tau\delta\theta}^*(k - k')}{-2k \cdot k' + m_X^2} \Pi_{\zeta\tau\gamma\lambda}^*(-k, k') \right] \bar{\varepsilon}'_\lambda^* \end{aligned}$$

To see how  $P_1$  and  $P_2$  are elaborated, just look at [subsection C.2](#).

As for  $P_3$ , we use all the tricks introduced in [subsection C.2](#). Let us define the generic phase  $\alpha_p = (-1)^{\delta_{\alpha 4}}$  for simplicity. Obviously  $\alpha_p^2 = 1$ , as it is a real number. So, in order to check that all minus signs disappear, we just have to pair them up. Let us do just that: all the minus signs disappear leaving a  $(-1)$  overall in the  $P_3$  operator:

$$\begin{aligned} P_3 &= \varepsilon_\gamma^* \left[ \gamma_4 (\gamma_\delta)^\dagger \gamma_4 (p'_\theta + p_\theta)^* \frac{N_{\zeta\tau\delta\theta}^*(k - k')}{-2k \cdot k' + m_X^2} \Pi_{\zeta\tau\gamma\lambda}^*(-k, k') \right] \bar{\varepsilon}'_\lambda^* = \\ &= -\cancel{\gamma_p \lambda_p \delta_p \theta_p} \bar{\varepsilon}_\gamma \left[ \gamma_\delta (p'_\theta + p_\theta) \cancel{\zeta_p \tau_p \delta_p \theta_p} \frac{N_{\zeta\tau\delta\theta}(k - k')}{-2k \cdot k' + m_X^2} \cancel{\zeta_p \tau_p \gamma_p \lambda_p} \Pi_{\zeta\tau\gamma\lambda}(-k, k') \right] \varepsilon'_\lambda \\ &= -\bar{\varepsilon}_\gamma \left[ \gamma_\delta (p'_\theta + p_\theta) \frac{N_{\zeta\tau\delta\theta}(k - k')}{-2k \cdot k' + m_X^2} \Pi_{\zeta\tau\gamma\lambda}(-k, k') \right] \varepsilon'_\lambda \end{aligned} \tag{9.4}$$

the minus sign is compensated by the  $i$  factor changing sign.

So, with this, we can write down the squared amplitude:

$$\begin{aligned} |\mathcal{A}|^2 &= (\mathcal{A}_1 + \mathcal{A}_2 + \mathcal{A}_3)(\mathcal{A}_1^* + \mathcal{A}_2^* + \mathcal{A}_3^*) = \\ &= \left\{ \bar{u}'_a \left[ -e^2 (O_1 + O_2) + \frac{ig_e g_\gamma}{2\Lambda^2} O_3 \right]_{ab} u_b \bar{u}_c \left[ -e^2 (P_1 + P_2) - \frac{ig_e g_\gamma}{2\Lambda^2} P_3 \right]_{cd} u'_d \right\} = \\ &= \text{Tr} \left\{ \left[ -e^2 (O_1 + O_2) + \frac{ig_e g_\gamma}{2\Lambda^2} O_3 \right] u \bar{u} \left[ -e^2 (P_1 + P_2) - \frac{ig_e g_\gamma}{2\Lambda^2} P_3 \right] u' \bar{u}' \right\} \end{aligned} \tag{9.5}$$

and then average over initial electron polarizations (there are two) and sum over all fermion polarizations using [Equation 3.8](#):

$$\begin{aligned} |\overline{\mathcal{A}}|^2 &= \frac{1}{2} \sum_{s,s'} |\mathcal{A}|^2 = \\ &= \frac{1}{2} \frac{1}{2p_4 2p'_4} \text{Tr} \left\{ \left[ -e^2 (O_1 + O_2) + \frac{ig_e g_\gamma}{2\Lambda^2} O_3 \right] (-i\not{p} + m_e) \left[ -e^2 (P_1 + P_2) - \frac{ig_e g_\gamma}{2\Lambda^2} P_3 \right] (-i\not{p}' + m_e) \right\} \end{aligned} \tag{9.6}$$

We choose to delegate the arduous task of evaluating this trace to a computer. The FORM script used for this task is found in the repository linked in [subsection G.1](#).

The final trace has hundreds of addends and we do not deem it practical to report here. However, we can obtain a simplified result by directly substituting the values of the scalar products found in [subsection C.3](#). This can be done if we perform the integral in phase space first, locking the kinematic variables using the delta function. To carry out the calculation, we will be following closely the steps found in [subsection C.4](#). In particular, using the result in [Equation C.28](#):

$$\sigma(e^- \gamma \rightarrow e^- \gamma) = \frac{1}{16\pi^2} \int \frac{d^3 k'}{k_4 k'_4} |\bar{\mathcal{A}}|^2 \delta(p_4 + k_4 - p'_4 - k'_4) \quad (9.7)$$

where we write:

$$|\bar{\mathcal{A}}|^2 = \frac{F(p, k, p', k'; \varepsilon, \varepsilon')}{8 p_4 p'_4} \quad (9.8)$$

where  $F$  is the result of the trace calculation, and an adimensional kinematics factor, function of all 4-momenta and the photon polarizations  $\varepsilon$  and  $\varepsilon'$ . Then, following up on [Equation C.31](#), we get:

$$\begin{aligned} \frac{d\sigma}{d\Omega} &= \frac{1}{16\pi^2} \int_0^\infty d\omega' \frac{\omega'}{\omega} \frac{p'_4 \omega_c}{m_e \omega} \delta(\omega' - \omega_c) \frac{F(p, k, p', k'; \varepsilon, \varepsilon')}{8 p_4 p'_4} = \\ &= \frac{1}{16\pi^2} \frac{1}{8m_e^2} \left( \frac{\omega_c}{\omega} \right)^2 F(\omega, \omega_c; k, k', \varepsilon, \varepsilon') \end{aligned} \quad (9.9)$$

meaning that  $F$  is the trace result with the substitution of the 4-momenta concerning the actual kinematics of the annihilation (found in [subsection C.3](#)), where the actual variables are the initial photon energy  $\omega$ , the final photon energy  $\omega_c$  (Compton kinematics is decided only by these two variables, as there is a 1 : 1 correspondence between  $\omega_c$  and the scattering angle  $\theta$ ), and the unconstrained scalar products  $k \cdot \varepsilon', k' \cdot \varepsilon, \varepsilon \cdot \varepsilon'$ .

This way, the FORM trace reduces to "only" 124 addends, of which the first 5 actually recover the Compton cross section without any spin 2 mediation (using the script `Compton_Xspin2_xigauge.frm` in the GitHub repository), and the last 72 are actually squared moduli of the spin 2 correction, of the order  $g_e^2 g_\gamma^2 / \Lambda^4$ . Now, because couplings are very small, squared moduli contribution are much smaller than interference terms, so we can neglect them (we calculate these term in [subsection C.5](#)). So, focusing only on interference terms, we get terms like  $e^2 g_e g_\gamma / \Lambda^2$ .

Let us keep calling  $\omega_c = \omega'$  for simplicity, and define  $\Delta\omega = \omega - \omega'$ :

$$F(\omega, \omega'; k, k', \varepsilon, \varepsilon') = 2e^4 \left[ \frac{\Delta\omega}{\omega'} - \frac{\Delta\omega}{\omega} + 4(\varepsilon \cdot \varepsilon')^2 \right] + \frac{8e^2 g_e g_\gamma}{\Lambda^2} \frac{m_e}{t + m_X^2} G(\omega, \omega'; k, k', \varepsilon, \varepsilon') \quad (9.10)$$

$$\begin{aligned} G(\omega, \omega'; k, k', \varepsilon, \varepsilon') &= (k \cdot \varepsilon') (k' \cdot \varepsilon) (\varepsilon \cdot \varepsilon') g_1(\omega, \omega') + (k \cdot \varepsilon')^2 (k' \cdot \varepsilon)^2 g_2(\omega, \omega') \\ &\quad + (k \cdot \varepsilon')^2 g_3(\omega, \omega') + (k' \cdot \varepsilon)^2 g_4(\omega, \omega') + (\varepsilon \cdot \varepsilon')^2 g_5(\omega, \omega') \end{aligned} \quad (9.11)$$

Where we analyze functions one by one:

$$\begin{aligned} g_1(\omega, \omega') &= -\omega' + \omega - \frac{8}{3} m_e + \frac{4 m_e^2 \omega'}{3 m_X^2} - \frac{4 m_e^2 \omega}{3 m_X^2} - \frac{4 m_e}{3 \omega'} \omega + \frac{4 m_e \omega}{3 \omega} + \frac{2 m_e^2 \omega'^2}{3 m_X^2 \omega} \\ &\quad - \frac{4 m_e^2 \omega'}{3 m_X^2} + \frac{2 m_e^2 \omega}{3 m_X^2} + \frac{4 m_e \omega'}{3 \omega'} - \frac{4 m_e \omega}{3 \omega'} - \frac{2 m_e^2 \omega'}{3 m_X^2} + \frac{4 m_e^2 \omega}{3 m_X^2} - \frac{2 m_e^2 \omega^2}{3 m_X^2 \omega'} = \\ &= \Delta\omega - \frac{8}{3} m_e - \frac{4 m_e^2 \Delta\omega}{3 m_X^2} + \frac{4 m_e \Delta\omega}{3 \omega} - \frac{4 m_e \Delta\omega}{3 \omega'} + \frac{2 m_e^2 \Delta\omega}{3 m_X^2 \omega} - \frac{2 m_e^2 \Delta\omega}{3 m_X^2 \omega'} = \\ &= \Delta\omega - \frac{8}{3} m_e - \frac{4 m_e^2 \Delta\omega}{3 m_X^2} + \frac{2}{3} m_e \Delta\omega \left[ 2 \left( \frac{1}{\omega} - \frac{1}{\omega'} \right) - \frac{m_e \Delta\omega}{m_X^2} \left( \frac{1}{\omega} - \frac{1}{\omega'} \right) \right] \\ &= \Delta\omega - \frac{8}{3} m_e - \frac{4 m_e^2 \Delta\omega}{3 m_X^2} + \frac{2}{3} \frac{m_e \Delta\omega^2}{\omega \omega'} \left[ \frac{m_e \Delta\omega}{m_X^2} - 2 \right] \end{aligned} \quad (9.12)$$

$$\begin{aligned}
g_2(\omega, \omega') &= \frac{2}{3} \frac{1}{\omega} - \frac{1}{3} \frac{m_e \omega'}{m_X^2 \omega} + \frac{1}{3} \frac{\omega}{m_X^2 \omega} - \frac{2}{3} \frac{1}{\omega'} + \frac{1}{3} \frac{m_e \omega'}{m_X^2 \omega'} - \frac{1}{3} \frac{\omega}{m_X^2 \omega'} = \\
&= \frac{2}{3} \left( \frac{1}{\omega} - \frac{1}{\omega'} \right) - \frac{1}{3} \frac{m_e}{m_X^2} \left( \frac{1}{\omega} - \frac{1}{\omega'} \right) = \\
&= \frac{1}{3} \frac{\Delta\omega}{\omega\omega'} \left[ \frac{m_e \Delta\omega}{m_X^2} - 2 \right]
\end{aligned} \tag{9.13}$$

$$g_3(\omega, \omega') = \frac{1}{2} \omega' - \frac{1}{2} \frac{\omega'^2}{\omega} = \frac{1}{2} \left( \omega' - \frac{\omega'^2}{\omega} \right) = \frac{1}{2} \frac{\Delta\omega \omega'}{\omega} \tag{9.14}$$

$$g_4(\omega, \omega') = \frac{1}{2} \omega - \frac{1}{2} \frac{\omega^2}{\omega'} = \frac{1}{2} \left( \omega - \frac{\omega^2}{\omega'} \right) = \frac{1}{2} \frac{\Delta\omega \omega}{\omega'} \tag{9.15}$$

$$\begin{aligned}
g_5(\omega, \omega') &= m_e \omega'^2 + 2m_e \omega \omega' + m_e \omega^2 + \frac{8}{3} m_e^2 \omega' - \frac{8}{3} m_e^2 \omega - \frac{4}{3} \frac{m_e^3 \omega'^2}{m_X^2} + \frac{8}{3} \frac{m_e^3 \omega \omega'}{m_X^2} - \frac{4}{3} \frac{m_e^3 \omega^2}{m_X^2} \\
&\quad + \frac{2}{3} \frac{m_e^2 \omega'^2}{\omega} - \frac{4}{3} \frac{m_e^2 \omega' \omega}{\omega} + \frac{2}{3} \frac{m_e^2 \omega^2}{\omega} - \frac{1}{3} \frac{m_e^3 \omega'^3}{m_X^2 \omega} + \frac{m_e^3 \omega'^2 \omega}{m_X^2 \omega} - \frac{m_e^3 \omega' \omega^2}{m_X^2 \omega} + \frac{1}{3} \frac{m_e^3 \omega^3}{m_X^2 \omega} \\
&\quad - \frac{2}{3} \frac{m_e^2 \omega'^2}{\omega'} + \frac{4}{3} \frac{m_e^2 \omega' \omega}{\omega'} - \frac{2}{3} \frac{m_e^2 \omega^2}{\omega'} + \frac{1}{3} \frac{m_e^3 \omega'^3}{m_X^2 \omega'} + \frac{m_e^3 \omega'^2 \omega}{m_X^2 \omega'} + \frac{m_e^3 \omega' \omega^2}{m_X^2 \omega'} - \frac{1}{3} \frac{m_e^3 \omega^3}{m_X^2 \omega'} = \\
&= m_e (\omega + \omega')^2 - \frac{8}{3} m_e^2 \Delta\omega - \frac{4}{3} \frac{m_e^3 \Delta\omega^2}{m_X^2} + \frac{2}{3} \frac{m_e^2 \Delta\omega^2}{\omega} - \frac{1}{3} \frac{m_e^3 \Delta\omega^3}{m_X^2 \omega} - \frac{2}{3} \frac{m_e^2 \Delta\omega^2}{\omega'} + \frac{1}{3} \frac{m_e^3 \Delta\omega^3}{m_X^2 \omega'} = \\
&= m_e (\omega + \omega')^2 - \frac{8}{3} m_e^2 \Delta\omega - \frac{4}{3} \frac{m_e^3 \Delta\omega^2}{m_X^2} + \frac{1}{3} m_e^2 \Delta\omega^2 \left[ 2 \left( \frac{1}{\omega} - \frac{1}{\omega'} \right) - \frac{m_e \Delta\omega}{m_X^2} \left( \frac{1}{\omega} - \frac{1}{\omega'} \right) \right] = \\
&= m_e (\omega + \omega')^2 - \frac{8}{3} m_e^2 \Delta\omega - \frac{4}{3} \frac{m_e^3 \Delta\omega^2}{m_X^2} + \frac{1}{3} \frac{m_e^2 \Delta\omega^3}{\omega \omega'} \left[ \frac{m_e \Delta\omega}{m_X^2} - 2 \right]
\end{aligned} \tag{9.16}$$

Notice how the result of the calculation is  $\xi$  independent, even though in the FORM code the Feynman rule has been written in a generic  $\xi$  gauge. This is expected as the amplitude is gauge invariant.

Put everything together, and we actually get a nice result:

$$\begin{aligned}
G(\omega, \omega'; k, k', \varepsilon, \varepsilon') &= (k \cdot \varepsilon') (k' \cdot \varepsilon) (\varepsilon \cdot \varepsilon') \left[ \Delta\omega - \frac{8}{3} m_e - \frac{4}{3} \frac{m_e^2 \Delta\omega}{m_X^2} \right] + \frac{\Delta\omega}{2} \left[ (k \cdot \varepsilon')^2 \frac{\omega'}{\omega} + (k' \cdot \varepsilon)^2 \frac{\omega}{\omega'} \right] \\
&\quad + (\varepsilon \cdot \varepsilon')^2 \left[ m_e (\omega + \omega')^2 - \frac{8}{3} m_e^2 \Delta\omega - \frac{4}{3} \frac{m_e^3 \Delta\omega^2}{m_X^2} \right] + \frac{1}{3} \frac{\Delta\omega}{\omega \omega'} \left[ \frac{m_e \Delta\omega}{m_X^2} - 2 \right] \times \\
&\quad \left[ (k \cdot \varepsilon') (k' \cdot \varepsilon) (\varepsilon \cdot \varepsilon') 2m_e \Delta\omega + (k \cdot \varepsilon')^2 (k' \cdot \varepsilon)^2 + (\varepsilon \cdot \varepsilon')^2 m_e^2 \Delta\omega^2 \right] = \\
&= (k \cdot \varepsilon') (k' \cdot \varepsilon) (\varepsilon \cdot \varepsilon') \Delta\omega + (\varepsilon \cdot \varepsilon')^2 m_e (\omega + \omega')^2 + \frac{\Delta\omega}{2} \left[ (k \cdot \varepsilon')^2 \frac{\omega'}{\omega} + (k' \cdot \varepsilon)^2 \frac{\omega}{\omega'} \right] \\
&\quad - \frac{4m_e}{3} \left[ \frac{m_e \Delta\omega}{m_X^2} + 2 \right] \left[ (k \cdot \varepsilon') (k' \cdot \varepsilon) (\varepsilon \cdot \varepsilon') + (\varepsilon \cdot \varepsilon')^2 m_e \Delta\omega \right] \\
&\quad + \frac{1}{3} \frac{\Delta\omega}{\omega \omega'} \left[ \frac{m_e \Delta\omega}{m_X^2} - 2 \right] \left[ (k \cdot \varepsilon') (k' \cdot \varepsilon) + (\varepsilon \cdot \varepsilon') m_e \Delta\omega \right]^2
\end{aligned} \tag{9.17}$$

How do we know that this result is correct? Well, since this is the first time someone performs this specific calculation, there is no reference we can quote. However, we can carry out a few checks to make sure we are on the right track. For example, *Ward identities*.

This result is comprised of the contribution of three diagrams, with interference terms between the QED diagrams and the spin 2 correction. Because the first two diagrams' gauge invariance is accounted for (you

can check that using the code `Compton.frm` on the GitHub repository), we know that for those Ward identities already work, because the QED part in the cross product is automatically zero. So, the real hassle is actually verifying that the spin 2 part, independently from QED cancellations, satisfies Ward identities. To that end, we created the code `Compton_onlyX_xigauge.frm`, in which we only focus on this latter diagram squared. This code isolates the spin 2 diagram and cancels common factors and constants, to help analyze terms under the surface.

In formulas, what we expect is:

$$\left\{ \begin{array}{l} F(p, k, p', k'; \mathbf{k}, \varepsilon') = \underline{F_{\text{QED}}(p, k, p', k'; \mathbf{k}, \varepsilon')} + \underline{F_{\text{interf}}(p, k, p', k'; \mathbf{k}, \varepsilon')} + F_X(p, k, p', k'; \mathbf{k}, \varepsilon') = 0 \\ F(p, k, p', k'; \varepsilon, \mathbf{k}') = \underline{F_{\text{QED}}(p, k, p', k'; \varepsilon, \mathbf{k}')} + \underline{F_{\text{interf}}(p, k, p', k'; \varepsilon, \mathbf{k}')} + F_X(p, k, p', k'; \varepsilon, \mathbf{k}') = 0 \end{array} \right. \quad (9.18)$$

A couple of remarks are needed:

- *Gauge invariance comes before kinematics*, meaning we cannot use the kinematics constraints coming from the phase space integration. These constraints are listed in the `Compton_onlyX_xigauge.frm` code and in subsection C.2. Namely,  $p \cdot \varepsilon = p \cdot \varepsilon' = 0$  are all kinematics dependent, and must therefore be commented when carrying out the Ward identities check.

The only valid constraints are  $k \cdot \varepsilon = k' \cdot \varepsilon' = 0$ , as polarizations are always to be chosen transverse to their respective momenta.

- Not only are the ignored constraints kinematics dependent, but they also are *reference frame dependent*. Photon polarizations are not 4-vectors, because under the Lorentz group they transform with a non-linear term (which is why we introduce gauge invariance in the first place), hence scalar products that involve them are not Lorentz invariant.

This is why in a annihilation-like reference frame (electron and positron center of mass frame), it is also true that  $k \cdot \varepsilon' = k' \cdot \varepsilon = 0$  (note that they are indeed in positronium decay, see section 10)<sup>20</sup>.

Fortunately, this check on the `Compton_onlyX_xigauge.frm` is successful, and the new diagram indeed satisfies Ward identities (in a generic  $\xi$  gauge) as written:

$$F_X(p, k, p', k'; \mathbf{k}, \varepsilon') = F_X(p, k, p', k'; \varepsilon, \mathbf{k}') = 0 \quad (9.19)$$

## 9.1 Polarized cross section

This is a complicated amplitude to write. To simplify it, we can take various limits in different energy regimes:

**Low energy or low scattering angle:** This regime is reached when we either impose  $\omega \ll m_e$  (energies below MeV), or we require:

$$\omega(1 - \cos \theta) \ll m_e \quad \Rightarrow \quad \frac{\theta^2}{2} \ll \frac{m_e}{\omega} \quad \Rightarrow \quad \theta \ll \sqrt{\frac{2m_e}{\omega}} \quad (9.20)$$

meaning this is the forward scattering limit, sometimes called the *Thomson limit*.

In this limit, we get  $\omega' \rightarrow \omega$ , and the Compton scattering becomes elastic for the photon, as it bounces on the electron without losing energy. Then, if in Equation 9.10 we impose  $\Delta\omega \rightarrow 0$ , we get a significant simplification.

Moreover, because  $\omega \ll m_X$  as well, then we can calculate using kinematics from subsection C.3:

$$t + m_X^2 = -2k \cdot k' + m_X^2 = 2m_e \Delta\omega + m_X^2 \approx m_X^2 \quad (9.21)$$

All in all, we get:

$$G(\omega; k, k', \varepsilon, \varepsilon') = (\varepsilon \cdot \varepsilon')^2 4m_e \omega^2 - \frac{8m_e}{3} (k \cdot \varepsilon') (k' \cdot \varepsilon) (\varepsilon \cdot \varepsilon') \quad (9.22)$$

Because  $\omega \ll m_e \ll m_X$ , then  $t \ll m_X^2$ , so the total result from the FORM code becomes:

$$F(\omega; k, k', \varepsilon, \varepsilon') = 8e^4 (\varepsilon \cdot \varepsilon')^2 + \frac{32 e^2 g_e g_\gamma}{\Lambda^2} \frac{m_e^2}{m_X^2} \left[ (\varepsilon \cdot \varepsilon')^2 \omega^2 - \frac{2}{3} (k \cdot \varepsilon') (k' \cdot \varepsilon) (\varepsilon \cdot \varepsilon') \right] \quad (9.23)$$

<sup>20</sup>All the more reason not to include these frame dependent constraints when checking Ward identities.

which gives the following differential cross section, from substituting [Equation 9.9](#) into [Equation 9.23](#):

$$\begin{aligned} \frac{d\sigma}{d\Omega} &= \frac{1}{128\pi^2 m_e^2} \left( \frac{\omega'}{\omega} \right)^2 \left\{ 8e^4 (\varepsilon \cdot \varepsilon')^2 + \frac{32e^2 g_e g_\gamma}{\Lambda^2} \frac{m_e^2}{m_X^2} \left[ (\varepsilon \cdot \varepsilon')^2 \omega^2 - \frac{2}{3} (k \cdot \varepsilon') (k' \cdot \varepsilon) (\varepsilon \cdot \varepsilon') \right] \right\} = \\ &= \frac{\alpha^2}{m_e^2} (\varepsilon \cdot \varepsilon')^2 + \frac{\alpha g_e g_\gamma}{\pi \Lambda^2} \frac{1}{m_X^2} \left[ (\varepsilon \cdot \varepsilon')^2 \omega^2 - \frac{2}{3} (k \cdot \varepsilon') (k' \cdot \varepsilon) (\varepsilon \cdot \varepsilon') \right] \end{aligned} \quad (9.24)$$

where the first term retrieves the differential cross section due to QED only (see [Equation C.31](#), setting  $\omega_c = \omega' = \omega$ ).

**High energy and high scattering angle:** We require  $\omega \gg m_e$ , and moreover  $1 - \cos\theta > 0$  to avoid  $\omega'$  to explode.

In this limit, we get  $\omega' \rightarrow m_e$ , as in the scattering the photon loses most of its energy and it transfers it to the electron, especially if we look at higher and higher angles  $\theta \rightarrow \pi/2$ .

Then, if in [Equation 9.10](#) we impose  $\Delta\omega \rightarrow \omega$  and  $\omega' \rightarrow m_e$ , we can ignore subdominant terms starting from  $m_e/\omega$  and  $m_e^2/m_X^2$ . Moreover, suppose  $\omega^2 \gg 2m_X/m_e$  as well, then we can calculate using kinematics from [subsection C.3](#):

$$t + m_X^2 = -2k \cdot k' + m_X^2 = 2m_e \Delta\omega + m_X^2 \approx 2m_e \omega \quad (9.25)$$

we can directly calculate our  $G(\omega; k, k', \varepsilon, \varepsilon')$ :

$$\begin{aligned} G(\omega, \omega'; k, k', \varepsilon, \varepsilon') &= (k \cdot \varepsilon') (k' \cdot \varepsilon) (\varepsilon \cdot \varepsilon') \omega + (\varepsilon \cdot \varepsilon')^2 m_e \omega^2 + (k' \cdot \varepsilon)^2 \frac{\omega^2}{2m_e} \\ &\quad - \frac{4m_e}{3} \left[ \frac{m_e \omega}{m_X^2} + 2 \right] \left[ (k \cdot \varepsilon') (k' \cdot \varepsilon) (\varepsilon \cdot \varepsilon') + (\varepsilon \cdot \varepsilon')^2 m_e \omega \right] \\ &\quad + \frac{1}{3m_e} \left[ \frac{m_e \omega}{m_X^2} - 2 \right] \left[ (k \cdot \varepsilon') (k' \cdot \varepsilon) + (\varepsilon \cdot \varepsilon') m_e \omega \right]^2 \end{aligned} \quad (9.26)$$

we still get different regimes, depending on the values of  $\omega/m_X$  and  $m_e \omega/m_X^2$ . For simplicity, let us only consider the case for which  $\omega \gg m_X$ . Then, the main cutoff energy value is:

$$\frac{m_e \omega}{m_X^2} = 1 \quad \Rightarrow \quad \omega = \frac{m_X^2}{m_e} \approx 600 \text{ MeV} \quad (9.27)$$

*a priori*, no  $g_i$  is negligible, because every addend goes like  $m_e \omega^2$ , if we also consider the scalar products in front of the  $g_i$ . Then, we get two different cases:

- $m_e \ll \omega \ll m_X^2/m_e$ , then:

$$\begin{aligned} G(\omega, \omega'; k, k', \varepsilon, \varepsilon') &= (k \cdot \varepsilon') (k' \cdot \varepsilon) (\varepsilon \cdot \varepsilon') \omega + (\varepsilon \cdot \varepsilon')^2 m_e \omega^2 + (k' \cdot \varepsilon)^2 \frac{\omega^2}{2m_e} \\ &\quad - \frac{8m_e}{3} \left[ (k \cdot \varepsilon') (k' \cdot \varepsilon) (\varepsilon \cdot \varepsilon') + (\varepsilon \cdot \varepsilon')^2 m_e \omega \right] \\ &\quad - \frac{2}{3m_e} \left[ (k \cdot \varepsilon') (k' \cdot \varepsilon) + (\varepsilon \cdot \varepsilon') m_e \omega \right]^2 = \\ &= (k \cdot \varepsilon') (k' \cdot \varepsilon) (\varepsilon \cdot \varepsilon') \left[ \omega - \frac{8}{3} m_e - \frac{4}{3} \omega \right] + (k' \cdot \varepsilon)^2 \frac{\omega^2}{2m_e} \\ &\quad + (\varepsilon \cdot \varepsilon')^2 \left[ m_e \omega^2 - \frac{8}{3} m_e^2 \omega - \frac{2}{3} m_e \omega^2 \right] - (k \cdot \varepsilon')^2 (k' \cdot \varepsilon)^2 \frac{2}{3m_e} = \\ &\approx -\frac{\omega}{3} (k \cdot \varepsilon') (k' \cdot \varepsilon) (\varepsilon \cdot \varepsilon') + \frac{\omega^2}{2m_e} (k' \cdot \varepsilon)^2 + \frac{m_e \omega^2}{3} (\varepsilon \cdot \varepsilon')^2 \\ &\quad - \frac{2}{3m_e} (k \cdot \varepsilon')^2 (k' \cdot \varepsilon)^2 \end{aligned} \quad (9.28)$$

- $\omega \gg m_X^2/m_e$ , then:

$$\begin{aligned}
G(\omega, \omega'; k, k', \varepsilon, \varepsilon') &= (k \cdot \varepsilon') (k' \cdot \varepsilon) (\varepsilon \cdot \varepsilon') \omega + (\varepsilon \cdot \varepsilon')^2 m_e \omega^2 + (k' \cdot \varepsilon)^2 \frac{\omega^2}{2m_e} \\
&\quad - \frac{4m_e}{3} \left( \frac{m_e \omega}{m_X^2} \right) \left[ (k \cdot \varepsilon') (k' \cdot \varepsilon) (\varepsilon \cdot \varepsilon') + (\varepsilon \cdot \varepsilon')^2 m_e \omega \right] \\
&\quad + \frac{1}{3m_e} \left( \frac{m_e \omega}{m_X^2} \right) \left[ (k \cdot \varepsilon') (k' \cdot \varepsilon) + (\varepsilon \cdot \varepsilon') m_e \omega \right]^2 = \\
&= (k \cdot \varepsilon') (k' \cdot \varepsilon) (\varepsilon \cdot \varepsilon') \left[ \omega - \frac{4}{3} m_e \left( \frac{m_e \omega}{m_X^2} \right) + \frac{2}{3} \omega \left( \frac{m_e \omega}{m_X^2} \right) \right] + (k' \cdot \varepsilon)^2 \frac{\omega^2}{2m_e} \\
&\quad + (\varepsilon \cdot \varepsilon')^2 \left[ m_e \omega^2 - \frac{4}{3} m_e^2 \omega \left( \frac{m_e \omega}{m_X^2} \right) + \frac{1}{3} m_e \omega^2 \left( \frac{m_e \omega}{m_X^2} \right) \right] + (k \cdot \varepsilon')^2 (k' \cdot \varepsilon)^2 \frac{1}{3m_e} \left( \frac{m_e \omega}{m_X^2} \right) = \\
&\approx \frac{1}{3} \left( \frac{m_e \omega}{m_X^2} \right) \left[ 2\omega (k \cdot \varepsilon') (k' \cdot \varepsilon) (\varepsilon \cdot \varepsilon') + m_e \omega^2 (\varepsilon \cdot \varepsilon')^2 + \frac{1}{3m_e} (k \cdot \varepsilon')^2 (k' \cdot \varepsilon)^2 \right]
\end{aligned} \tag{9.29}$$

and we get the following differential cross section as a result:

$$\begin{aligned}
\frac{d\sigma}{d\Omega} &= \frac{1}{128\pi^2 m_e^2} \left( \frac{\omega'}{\omega} \right)^2 \left\{ 2e^4 \left[ \frac{\Delta\omega}{\omega'} - \frac{\Delta\omega}{\omega} + 4(\varepsilon \cdot \varepsilon')^2 \right] + \frac{8e^2 g_e g_\gamma}{\Lambda^2} \frac{m_e}{t + m_X^2} G(\omega; k, k', \varepsilon, \varepsilon') \right\} = \\
&= \frac{1}{128\pi^2 \omega^2} \left\{ 2e^4 \left[ \frac{\omega}{m_e} - 1 + 4(\varepsilon \cdot \varepsilon')^2 \right] + \frac{8e^2 g_e g_\gamma}{\Lambda^2} \frac{m_e}{t + m_X^2} G(\omega; k, k', \varepsilon, \varepsilon') \right\}
\end{aligned} \tag{9.30}$$

which means, for  $m_e \ll \omega \ll m_X^2/m_e$  ( $t + m_X^2 \rightarrow m_X^2$ ):

$$\begin{aligned}
\frac{d\sigma}{d\Omega} &= \frac{\alpha^2}{4\omega^2} \left[ \frac{\omega}{m_e} - 1 + 4(\varepsilon \cdot \varepsilon')^2 \right] + \frac{\alpha}{4\pi} \frac{g_e g_\gamma}{\Lambda^2} \frac{m_e}{m_X^2 \omega^2} \left\{ -\frac{\omega}{3} (k \cdot \varepsilon') (k' \cdot \varepsilon) (\varepsilon \cdot \varepsilon') \right. \\
&\quad \left. + \frac{\omega^2}{2m_e} (k' \cdot \varepsilon)^2 + \frac{m_e \omega^2}{3} (\varepsilon \cdot \varepsilon')^2 - \frac{2}{3m_e} (k \cdot \varepsilon')^2 (k' \cdot \varepsilon)^2 \right\}
\end{aligned} \tag{9.31}$$

and for  $\omega \gg m_X^2/m_e$  ( $t + m_X^2 \rightarrow t \approx 2m_e \omega$ ):

$$\begin{aligned}
\frac{d\sigma}{d\Omega} &= \frac{\alpha^2}{4\omega^2} \left[ \frac{\omega}{m_e} - 1 + 4(\varepsilon \cdot \varepsilon')^2 \right] + \frac{\alpha}{8\pi} \frac{g_e g_\gamma}{\Lambda^2} \frac{1}{3\omega^3} \left( \frac{m_e \omega}{m_X^2} \right) \times \\
&\quad \left[ 2\omega (k \cdot \varepsilon') (k' \cdot \varepsilon) (\varepsilon \cdot \varepsilon') + m_e \omega^2 (\varepsilon \cdot \varepsilon')^2 + \frac{1}{3m_e} (k \cdot \varepsilon')^2 (k' \cdot \varepsilon)^2 \right]
\end{aligned} \tag{9.32}$$

## 9.2 Unpolarized cross section

Now that we have the polarized cross section result, we can go ahead and average over initial photon polarizations and sum over all photon polarizations. To do that, we can use the very useful results in [subsection F.7](#). Let us focus on the differential cross section from [Equation 9.9](#), using [Equation C.36](#) for the QED part:

$$\begin{aligned}
\frac{d\sigma}{d\Omega} &= \frac{1}{2} \frac{1}{128\pi^2 m_e^2} \left( \frac{\omega'}{\omega} \right)^2 \sum_{\lambda, \lambda'} F(\omega, \omega'; k, k', \varepsilon, \varepsilon') = \\
&= \frac{\alpha^2}{2m_e^2} \left( \frac{\omega'}{\omega} \right)^2 \left[ \frac{\Delta\omega}{\omega'} - \frac{\Delta\omega}{\omega} + 1 + \cos^2 \theta \right] + \frac{\alpha}{8\pi} \frac{g_e g_\gamma}{\Lambda^2 m_e} \left( \frac{\omega'}{\omega} \right)^2 \frac{1}{t + m_X^2} \sum_{\lambda, \lambda'} G(\omega, \omega'; k, k', \varepsilon, \varepsilon')
\end{aligned} \tag{9.33}$$

Since we are calculating the general result when graphing our cross section, let us start directly from [Equation 9.11](#):

$$\begin{aligned} \sum_{\lambda, \lambda'} G(\omega, \omega'; k, k', \varepsilon, \varepsilon') &= -\omega\omega' \cos\theta \left(1 - \cos^2\theta\right) g_1(\omega, \omega') + \omega^2\omega'^2 \left(1 - \cos^2\theta\right) g_2(\omega, \omega') \\ &\quad + 2\omega^2 \left(1 - \cos^2\theta\right) g_3(\omega, \omega') + 2\omega'^2 \left(1 - \cos^2\theta\right) g_4(\omega, \omega') + \left(1 + \cos^2\theta\right) g_5(\omega, \omega') \end{aligned} \quad (9.34)$$

and  $g_i(\omega, \omega')$  are the functions listed below [Equation 9.11](#).

Now, let us obtain the total result in the three different limits we studied in [subsection 9.1](#). To carry the sums out we can use the results in [Equation 9.10](#):

**$\omega \ll m_e$ :** Remember that  $\omega' \rightarrow \omega$  and  $\Delta\omega \rightarrow 0$ . Starting point is [Equation 9.22](#):

$$\begin{aligned} \sum_{\lambda, \lambda'} G(\omega, \omega'; k, k', \varepsilon, \varepsilon') &= 4m_e \left[ \omega^2 \left(1 + \cos^2\theta\right) + \frac{2}{3}\omega'\omega \cos\theta \left(1 - \cos^2\theta\right) \right] = \\ &\approx 4m_e\omega^2 \left[ 1 + \frac{2}{3}\cos\theta + \cos^2\theta - \frac{2}{3}\cos^3\theta \right] \end{aligned} \quad (9.35)$$

then, into [Equation 9.33](#), exploiting  $t \ll m_X^2$  as well:

$$\frac{d\sigma}{d\Omega} = \frac{\alpha^2}{2m_e^2} \left(1 + \cos^2\theta\right) + \frac{\alpha}{2\pi} \frac{g_e g_\gamma}{\Lambda^2} \frac{\omega^2}{m_X^2} \left[ 1 + \frac{2}{3}\cos\theta + \cos^2\theta - \frac{2}{3}\cos^3\theta \right] \quad (9.36)$$

which can be integrated in solid angle, using:

$$\int_{-1}^1 d\cos\theta \cos^2\theta = \frac{2}{3} \quad \int_{-1}^1 d\cos\theta \cos^4\theta = \frac{2}{5} \quad (9.37)$$

to obtain:

$$\begin{aligned} \sigma(e^- \gamma \rightarrow e^- \gamma) &= \frac{8\pi\alpha^2}{3m_e^2} + \frac{\alpha}{2\pi} \frac{g_e g_\gamma}{\Lambda^2} \frac{\omega^2}{m_X^2} 2\pi \left[ 2 + \frac{2}{3} \right] = \\ &= \frac{8\pi\alpha^2}{3m_e^2} + \frac{8\alpha}{3} \frac{g_e g_\gamma}{\Lambda^2} \frac{\omega^2}{m_X^2} = \\ &= \frac{8\pi\alpha^2}{3m_e^2} \left[ 1 + \frac{1}{\pi} \frac{g_e g_\gamma}{\alpha\Lambda^2} \frac{m_e^2\omega^2}{m_X^2} \right] \end{aligned} \quad (9.38)$$

Now, from [Equation 5.43](#) and [Equation 5.44](#), we have:

$$\frac{g_e g_\gamma}{\Lambda^2} = 1.0 \times 10^{-11} \text{ MeV}^{-2} \quad (9.39)$$

which means that we get a correction factor to the cross section:

$$\sigma(e^- \gamma \rightarrow e^- \gamma) = \sigma_{\text{QED}}(e^- \gamma \rightarrow e^- \gamma) \left[ 1 + \left( 1.3 \times 10^{-12} \text{ MeV}^{-2} \right) \omega^2 \right] \quad (9.40)$$

for low energy Compton scattering. While correction grows extremely fast, this behavior only holds for small photon energies.

**$m_e \ll \omega \ll m_X^2/m_e$ :** Remember that  $\omega' \rightarrow m_e$  and  $\Delta\omega \rightarrow \omega$ , as we are also sending  $\theta \rightarrow \pi/2$ . Starting point is [Equation 9.28](#):

$$\begin{aligned} \sum_{\lambda, \lambda'} G(\omega, \omega'; k, k', \varepsilon, \varepsilon') &= -\frac{\omega^2\omega'}{3} \cos\theta \left(1 - \cos^2\theta\right) - \frac{\omega^2\omega'^2}{m_e} \left(1 - \cos^2\theta\right) \\ &\quad + \frac{m_e\omega^2}{3} \left(1 + \cos^2\theta\right) - \frac{2\omega^2\omega'^2}{3m_e} \left(1 - \cos^2\theta\right)^2 = \\ &\approx \frac{m_e\omega^2}{3} \left[ \cos\theta - \cos^3\theta + 3 - 3\cos^2\theta + 1 + \cos^2\theta - 2 + 4\cos^2\theta - 2\cos^4\theta \right] = \\ &= \frac{m_e\omega^2}{3} \left[ 2 + \cos\theta + 2\cos^2\theta - \cos^3\theta - 2\cos^4\theta \right] \approx \frac{2m_e\omega^2}{3} \end{aligned} \quad (9.41)$$

remember how  $\theta \rightarrow \pi/2$ . For the differential cross section in [Equation 9.33](#), exploiting  $t \approx m_X^2$ :

$$\begin{aligned}\frac{d\sigma}{d\Omega} &= \frac{\alpha^2}{2\omega^2} \left[ \frac{\omega}{m_e} + e \cos^2 \theta \right] + \frac{\alpha}{8\pi} \frac{g_e g_\gamma}{\Lambda^2} \frac{m_e}{m_X^2 \omega^2} \frac{2m_e \omega^2}{3} = \\ &= \frac{\alpha^2}{2m_e \omega} + \frac{\alpha}{12\pi} \frac{g_e g_\gamma}{\Lambda^2} \frac{m_e^2}{m_X^2}\end{aligned}\quad (9.42)$$

We cannot integrate over  $d \cos \theta$ .

Another interesting result is that the dominant correction term is constant in energy, hence it wins over the  $1/\omega$  behavior of the QED result:

$$\begin{aligned}\frac{d\sigma}{d \cos \theta} &= \frac{\pi \alpha^2}{m_e \omega} \left[ 1 + \frac{1}{6\pi} \frac{g_e g_\gamma}{\alpha \Lambda^2} \frac{m_e^3 \omega}{m_X^2} \right] = \\ &= \frac{d\sigma}{d \cos \theta} \Big|_{\text{QED}} \left[ 1 + \left( 3.5 \times 10^{-14} \text{ MeV}^{-1} \right) \omega \right]\end{aligned}\quad (9.43)$$

and this is the correction for high (but not too high) Compton scattering energy, at large scattering angles. It is an extremely small correction that is actually smaller than the integrated non-relativistic correction. This has to do with the fact that the factor  $\omega'/\omega$ , which was order 1 in the non-relativistic case, is very suppressing in this large limit.

$\omega \gg m_X^2/m_e$ : Remember that  $\omega' \rightarrow m_e$  and  $\Delta\omega \rightarrow \omega$ , as we are also sending  $\theta \rightarrow \pi/2$ . Starting point is [Equation 9.29](#):

$$\begin{aligned}\sum_{\lambda, \lambda'} G(\omega, \omega'; k, k', \varepsilon, \varepsilon') &= \frac{1}{3} \left( \frac{m_e \omega}{m_X^2} \right) \left[ -2\omega^2 \omega \cos \theta (1 - \cos^2 \theta) + m_e \omega^2 (1 + \cos^2 \theta) + \frac{\omega^2 \omega'^2}{m_e} (1 - \cos^2 \theta)^2 \right] = \\ &\approx \frac{m_e \omega^2}{3} \left( \frac{m_e \omega}{m_X^2} \right) [2 - 2 \cos \theta + 3 \cos^2 \theta + 2 \cos^3 \theta + \cos^4 \theta] = \\ &\approx \frac{2m_e \omega^2}{3} \left( \frac{m_e \omega}{m_X^2} \right)\end{aligned}\quad (9.44)$$

where we have taken the dominant term, given by the ratio  $m_X/m_e \approx 35$ , and we canceled the cosines as  $\theta \rightarrow \pi/2$ .

Finally, substitute in [Equation 9.33](#), exploiting  $t \approx 2m_e \omega \gg m_X^2$ , we get a similar result as [Equation 9.42](#):

$$\begin{aligned}\frac{d\sigma}{d\Omega} &= \frac{\alpha^2}{2\omega^2} \left[ \frac{\omega}{m_e} + e \cos^2 \theta \right] + \frac{\alpha}{8\pi} \frac{g_e g_\gamma}{\Lambda^2} \frac{1}{2\omega^3} \frac{2m_e \omega^2}{3} \left( \frac{m_e \omega}{m_X^2} \right) = \\ &= \frac{\alpha^2}{2m_e \omega} + \frac{\alpha}{24\pi} \frac{g_e g_\gamma}{\Lambda^2} \frac{m_e^2}{m_X^2}\end{aligned}\quad (9.45)$$

Notice how this result is actually constant in energy, like the correction at intermediate energy. Again, it is not possible to integrate properly, as this result is obtained fixing high angles. However, we can estimate the result of an integral around the forward scattering cone. Ignoring angular dependencies, the dominant contribution estimate is very promising:

$$\begin{aligned}\frac{d\sigma}{d \cos \theta} &\approx \frac{\pi \alpha^2}{m_e \omega} + \frac{\alpha}{12} \frac{g_e g_\gamma}{\Lambda^2} \frac{m_e^2}{m_X^2} = \\ &= \frac{\pi \alpha^2}{m_e \omega} \left[ 1 + \frac{1}{12\pi} \frac{g_e g_\gamma}{\alpha \Lambda^2} \frac{m_e^3 \omega}{m_X^2} \right]\end{aligned}\quad (9.46)$$

with the usual coupling estimate, we get the correction:

$$\frac{d\sigma}{d \cos \theta} = \frac{d\sigma}{d \cos \theta} \Big|_{\text{QED}} \left[ 1 + \left( 1.7 \times 10^{-14} \text{ MeV}^{-1} \right) \omega \right]\quad (9.47)$$

which is a correction that *grows with energy!* This is an indefinite growth, that starts already with  $m_e \omega / m_X^2 \gg 1$ , and can increase the tree level correction of the spin 2 massive boson mediation up to any number.

This cross section does satisfy Froissart bound, being constant, meaning we could go up in energy as we would like. However, the breaking of the "composite" spin 2 state should still occur at the usual limit in energy: 20 – 50 MeV. Using the  $t$ -channel trick, this means we can go up to about 300 MeV in energy. However, we do not even need it, because of [Equation C.25](#), which already gives an upper bound on photon energy of  $\omega = 1$  TeV, more than enough to beat (almost) every experiment that has even been performed on Compton scattering.

## 9.3 Testing spin 2 for Compton scattering

### 9.3.1 Behavior of Compton cross section

We report graphs displaying the behavior of the corrected, unpolarized Compton scattering in [Figure 23](#) and [Figure 24](#): In [Figure 23](#), you can see how small the spin 2 corrections are, relative to the QED values. We range

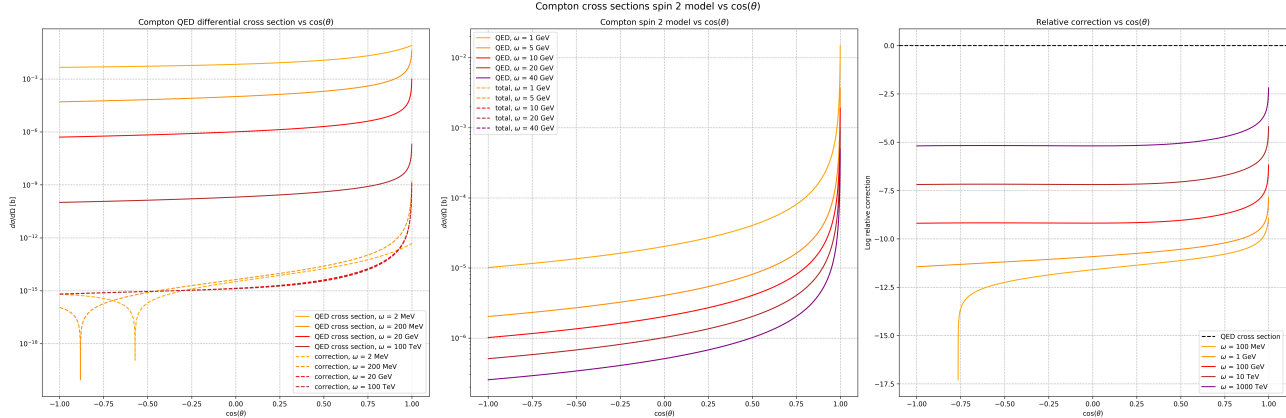


[Figure 23](#): Graph of behavior of Compton scattering corrections as a function of the scattering angle  $\cos \theta$ . On the left, we plot separately both the QED result and the actual spin 2 correction (dashed line), for different values of the photon energy  $\omega$ . In the middle, comparison between QED differential cross section and total cross section (including spin 2 correction), for different fixed  $\omega$ . On the right, relative correction to the QED cross section of the total (QED + spin 2) cross section, always at different energetic values for  $\omega$ .

from 14 orders of magnitude ratio (at a few MeV) to 5 orders of magnitude (at 100 TeV). Corrections increase in the forward scattering limit, but only because the differential cross section diverges if  $\theta \rightarrow 0$  (because in the ultra-relativistic limit,  $\omega'/\omega \rightarrow \infty$  when  $\theta \rightarrow 0$ ). Notice how the behaviors highlighted in [subsection 9.2](#) are visible in figure. In [Equation 9.38](#), we see how cross section initially grows with  $\omega^2$ , but then in [Equation 9.42](#) and in [Equation 9.45](#) corrections become constant in energy, which is what happens. The QED contribution, instead, gets smaller and smaller as  $\omega$  grows.

There are also a few angles for which corrections vanish. This has to do with some combination of cosines in the general expression that allows for such cancellations, which we did not focus on while taking the limits for  $\theta \rightarrow \pi/2$ .

In [Figure 24](#), we get the behavior we discussed in this section.

- In the left image, for the QED part, you can immediately see that at very low energies  $\omega \ll m_e$ , we get a constant cross section, while when  $\omega \gg m_e$  the cross section scales like  $1/\omega$ , as we can see in log scale.
- The three main limits for the spin 2 correction are perfectly visible on the left image: for  $\omega \ll m_e$ , the growth of the correction goes like  $\omega^2$  ([Equation 10.49](#)). In the intermediate region  $m_e \ll \omega \ll m_X^2/m_e$ , up until 600 MeV, ([Equation 9.42](#)) we get a constant behavior (it arches, actually, but there probably is no "space" to reach the ideal limit we calculated, since it is very slow), and when  $\omega \gg m_X^2/m_e$ , cross section is still constant, but as [Equation 9.45](#) shows, it gets smaller by a factor of 2 from the "middle" energy limit.
- So, the graph to the right should first go like  $\omega^2$ , then briefly, and then it should grow like  $\omega$ . Since the scale is not logarithmic, this is the dominant behavior we see on the right.

The corrected correction is perfectly invisible on top of the QED result, no matter the energy  $\omega$  or the angle  $\cos \theta$ .

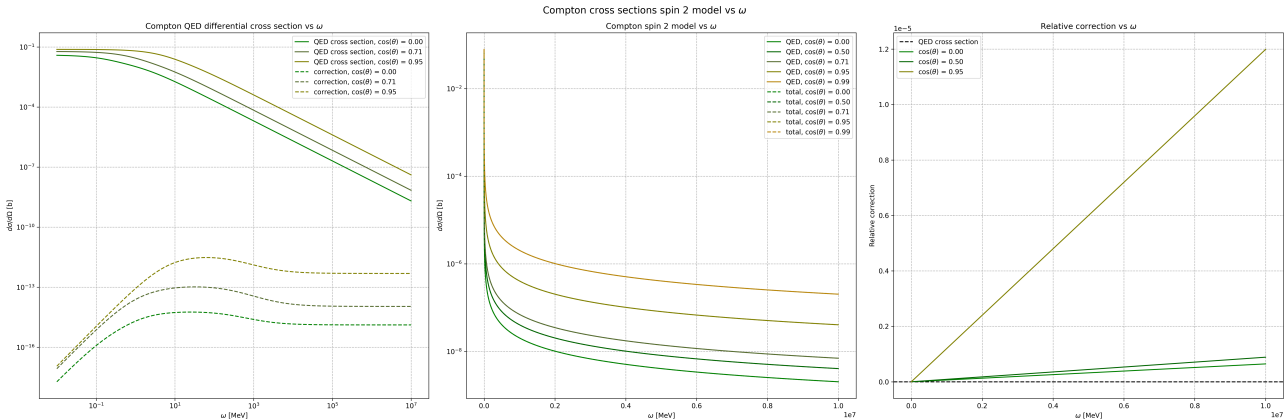


Figure 24: Graph of behavior of Compton scattering corrections as a function of the photon energy  $\omega$ . On the left, we plot separately both the QED result and the actual spin 2 correction (dashed line), for different values of the  $\cos\theta$ . In the middle, comparison between QED differential cross section and total cross section (including spin 2 correction), for different fixed  $\cos\theta$ . On the right, relative correction to the QED cross section of the total (QED + spin 2) cross section, always at different angular values for  $\cos\theta$ .

### 9.3.2 Compton experimental results

Now that we have corrected Compton scattering at tree level with this new effective interaction, we need to compare this small effect to the best theoretical predictions and experimental measurements of Compton effect.

Compton scattering is omnipresent at every energy magnitude, and it is studied for a wide range of applications, from Standard Model precision measurements ([39]) to X-ray imaging ([41]), from QCD processes at high energy ([35]) to astrophysics ([28], [37], [38]), from Dark Matter detection techniques ([43]) to plasma diagnostics ([36]).

Let us go through various hypothesis for testing our spin 2 effective model, by means of Compton scattering tree level corrections:

- Thomson scattering at very low energies (keV) can be used for plasma diagnostics, i.e. determining the structure and composition of plasma. In [36], Thomson scattering is used to probe a laser produced plasma, namely to measure electron temperature and density, plasma flow, and other characteristics. This being a relatively novel technique, large uncertainties on the observables (about 10%) are inevitable. This means that our spin 2 effect at low energies, as from Equation 9.40, would yield an infinitesimally low relative correction of  $\mathcal{O}(10^{-18})$ , probably never to be measured.
- At very low energy, we can expect Dark Matter interactions to produce electron recoils at energies below  $\mathcal{O}(100 \text{ eV})$ . Thomson scattering is the main source of background for these experiments, and it has been thoroughly studied by the DAMIC collaboration, as seen in [43]. They performed a calibration with a  $^{241}\text{Am}$   $\gamma$  source, and probed the very small recoil energy region using a CCD camera.

Systematics on the measured spectrum of the electrons come from dissipation through bound state energies from  $K$ -shell and  $L$ -shell of silicon, and finite CCD camera resolution. Even with high statistics, a few % of uncertainty on the Thomson scattering spectrum is reported as final result. Finally, simulation of said spectrum using **Geant4** code is systematically off by more than 10%.

Our estimate of the correction due to spin 2 interaction comes from low energy, unpolarized (because the photon polarization is never measured) Compton scattering from Equation 9.40. At the energies of the  $^{241}\text{Am}$  gamma emission,  $\omega = 59.6 \text{ keV}$ , the relative correction is estimated to be  $\mathcal{O}(10^{-15})$ . Clearly, this effect is totally invisible.

- A new compact X-ray laser ([41]) has been developed using inverse Compton scattering. Highly relativistic electrons (300 MeV) scatter against photons producing a stable X-ray laser, useful for X-ray imaging. In terms of the parameters of the ordinary Compton scattering, a Lorentz boost would bring photons to  $\omega \approx 300 \text{ MeV}$ , meaning that we are in the "high but not too high" energy limit for our correction to Compton scattering, in the polarized case (as the laser is linearly polarized and accounted for).

One could think that, ideally, this laser's specifics' measurements could be used to infer the spin 2 contribution effect to Compton scattering. Remember that, according to Equation 9.43, the correction due to spin 2 effects at high angles is constant in energy, and it is about  $\mathcal{O}(10^{-11})$ . Looking at the paper, only the 5% systematics error on the photon flux is enough to make this proposition totally unfeasible.

- In recent years ([28], [37], [38]), the importance of Compton and inverse Compton scattering in astrophysics (which is the same as Compton scattering, but the electron is ultra-relativistic) have been highlighted. These processes are relevant in the analysis of the radiation spectrum of isolated magnetars (magnetically pulsating neutron stars). The highly polarized and highly energetic photons (10 keV-100 keV) emitted by these astronomical objects have been detected on Earth by balloon-borne telescopes such as *X-Calibur* ([42]).

This would mean that, in terms of ordinary Compton scattering parameters, we are in the same energy range as the compact X-ray laser in the previous point: "high but not too high" energy limit, polarized case. Still, we would have the same  $\mathcal{O}(10^{-11})$  relative correction, constant in energy, at high scattering angles.

Unfortunately, [42] reports few percent systematic uncertainty on the photon flux in the atmosphere and in the photons' polarization itself, making these data extremely unreliable for high precision measurements of Compton scattering. Moreover, the initial scattering angle of the inverse Compton scattering in magnetars is not known, meaning it would be nearly impossible to recreate the kinematics conditions we explored in this thesis.

- The only hope of ever testing spin 2 models in QED is the very high energy limit. Although Compton scattering is an electrodynamics process, it is not very well measured at all at high energies. The first study at photon energy  $\omega = 5 \text{ GeV}$  was carried out only in 2019 by the PrimEx Collaboration at Jefferson Lab ([39]). The study reports by far the lowest uncertainties for the total, unpolarized, high energy Compton scattering cross section found anywhere else in literature (2.6%), which agrees very well with theoretical predictions.

Among the limits we studied, this is the very high energy, unpolarized case, as seen in [Equation 9.47](#). At  $\omega = 5 \text{ GeV}$ , the correction of the differential cross section at high angles, due to spin 2 is  $\mathcal{O}(10^{-14})$ .

- Another paper quotes large energy quasi-real Compton scattering measurement ([30]) using the L3 detector at LEP. In this process, one of the incoming beam electrons remains inside the beam pipe and it is not detected. They report measurements in the center of mass energy ranging from 25 to 170 GeV, quoting a total relative cross section error of around 10%. At  $\sqrt{|s|} = 170 \text{ GeV}$ , we are well beyond the limit of validity for our effective field theory, and this result cannot be used.

Not that it matters, but, on the theoretical side, we would need far better prediction than the ones we have available today. Compton scattering is actually one of the less known processes in QED, as the  $\mathcal{O}(\alpha^3)$  terms have been analytically calculated only in 2021 ([40]). This means that, as of today, the best theoretical prediction for the total Compton scattering cross section is actually precise at relative order  $\alpha$  (matching the experimental result in [39] perfectly). However, in [40] is also shown that one loop corrections actually become a dominant contribution of the cross section as energy increases (as  $\alpha$  grows with energy). At 1 GeV (or  $\omega = 2 \text{ TeV}$ ), radiative correction are 8.2% . This is around our maximum limit in energy. At this value in center of mass energy, correction is  $\mathcal{O}(10^{-8})$ , or about 9 orders of magnitude smaller than the best theoretical prediction (at small angles of scattering).

So, a future super-collider Compton scattering experiment has to deal with the both engineering challenges (higher energy, better precision) and theoretical obstacles (namely, the possibility of breaking perturbation theory as such high energy scales, and many loop calculations).

## 10 Correction to $e^+e^-$ annihilation into two photons

Let us repeat what we did in [section 6](#), [section 7](#) and [section 9](#), but for the process:  $e^+e^- \rightarrow \gamma\gamma$ . The contributing diagrams for this process are the *t-channel* and the *u-channel*, in [Figure 25](#):

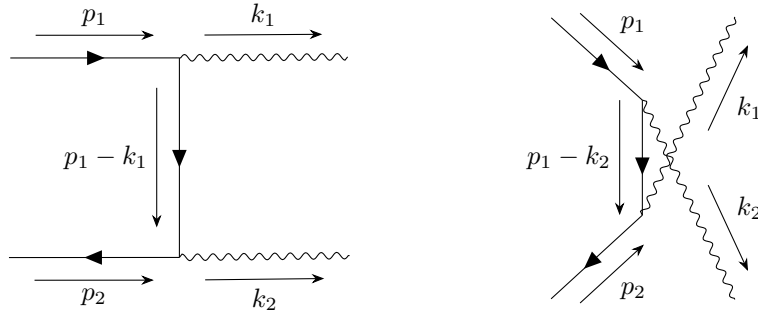


Figure 25: Diagrams corresponding to tree level electron-positron annihilation into 2 photons. On the left, the *t*-channel, hereafter denoted with  $\mathcal{A}_1$ . On the right, the *u*-channel, hereafter denoted with  $\mathcal{A}_2$ .

We add the diagram in which the  $X$  boson is mediated ([Figure 26](#)), contributing with a *s*-channel: Resulting

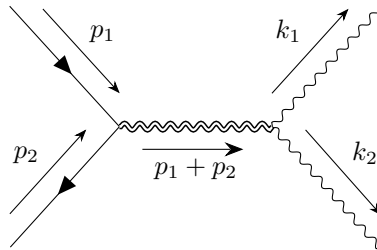


Figure 26: Tree level diagram for the mediation of massive spin 2 boson for Compton scattering, basically accounting for a *s*-channel contribution. We will refer to this amplitude as  $\mathcal{A}_3$ .

amplitudes will be linked to Compton amplitudes by *crossing symmetry*. Electron-positron annihilation diagrams are exactly equal to Compton scattering diagrams after a "90° rotation", which translates to a different time axis, resulting in the same amplitudes but with the exchange of *s* and *t* variables:

$$\mathcal{A}_1 = (-ie)^2 \bar{v}(p_2, s_2) \bar{\varepsilon}_\mu(k_2, \lambda_2) \gamma_\mu \left[ \frac{-i(\not{p}_1 - \not{k}_1) + m_e}{(p_1 - k_1)^2 + m_e^2} \right] \bar{\varepsilon}_\nu(k_1, \lambda_1) \gamma_\nu u(p_1, s_1) = -e^2 \bar{v} O_1 u \quad (10.1)$$

$$\mathcal{A}_2 = (-ie)^2 \bar{v}(p_2, s_2) \bar{\varepsilon}_\mu(k_1, \lambda_1) \gamma_\mu \left[ \frac{-i(\not{p}_1 - \not{k}_2) + m_e}{(p_1 - k_2)^2 + m_e^2} \right] \bar{\varepsilon}_\nu(k_2, \lambda_2) \gamma_\nu u(p_1, s_1) = -e^2 \bar{v} O_2 u \quad (10.2)$$

where the usual electrodynamics Feynman rule  $ie\gamma_\mu$  applies at each vertex,  $m_e$  is the mass of the electron,  $p_1, p_2, k_1, k_2$  are the respective momenta according to [Figure 51](#) and  $s_1, s_2, \lambda_1, \lambda_2$  are the polarizations of fermions and photons, respectively. Here forth, we will call  $u(p_1, s_1) = u$ ,  $v(p_2, s_2) = v$ ,  $\varepsilon_\mu(k_1, \lambda_1) = \varepsilon_{1,\mu}$ ,  $\varepsilon_\mu(k_2, \lambda_2) = \varepsilon_{2,\mu}$ . Finally, the reason why we have  $(-ie)^2$  and not  $(-ie)^2/2!$  is outlined in [subsection D.1](#), where we carry out Wick contractions.

For  $\mathcal{A}_3$  we use the same Feynman rules we derived in [subsection 4.3](#):

$$\begin{aligned} \mathcal{A}_3 &= \left[ \frac{g_\gamma}{\Lambda} \right] \left[ \frac{ig_e}{2\Lambda} \right] \bar{v}(p_2, s_2) \gamma_\rho(p_{2\sigma} - p_{1\sigma}) u(p_1, s_1) \left[ \frac{N_{\mu\nu\rho\sigma}(k_1 + k_2)}{(k_1 + k_2)^2 + m_X^2} \right] \Pi_{\mu\nu\alpha\beta}(k_1, k_2) \bar{\varepsilon}_\alpha(k_1, \lambda_1) \bar{\varepsilon}_\beta(k_2, \lambda_2) = \\ &= \frac{ig_e g_\gamma}{2\Lambda^2} \bar{v} O_3 u \end{aligned} \quad (10.3)$$

Kinematics confirms the  $s - t$  swap:

$$\begin{aligned} (p_1 - k_1)^2 + m_e^2 &= t + m_e^2 = -2p_1 \cdot k_1 \\ (p_1 - k_2)^2 + m_e^2 &= u + m_e^2 = -2p_1 \cdot k_2 \\ (k_1 + k_2)^2 + m_X^2 &= s + m_X^2 = 2k_1 \cdot k_2 + m_X^2 \end{aligned}$$

so that we can write  $O_1$ ,  $O_2$  (see [subsection D.2](#) for further detail) and  $O_3$ :

$$\begin{aligned} O_1 &= -\bar{\varepsilon}_{2,\mu}\gamma_\mu \left[ \frac{-i(p'_1 - k'_1) + m_e}{2p_1 \cdot k_1} \right] \bar{\varepsilon}_{1,\nu}\gamma_\nu \\ O_2 &= -\bar{\varepsilon}_{1,\nu}\gamma_\nu \left[ \frac{-i(p'_1 - k'_2) + m_e}{2p_1 \cdot k_2} \right] \bar{\varepsilon}_{2,\mu}\gamma_\mu \\ O_3 &= \bar{\varepsilon}_{1,\alpha} \left[ \gamma_\rho(p_{2,\sigma} - p_{1,\sigma}) \frac{N_{\mu\nu\rho\sigma}(k_1 + k_2)}{2k_1 \cdot k_2 + m_X^2} \Pi_{\mu\nu\alpha\beta}(k_1, k_2) \right] \bar{\varepsilon}_{2,\beta} \end{aligned}$$

Then, complex conjugate operators:

$$\begin{aligned} \mathcal{A}_1^* &= (ie)^2 \bar{u} \left( \gamma_4 O_1^\dagger \gamma_4 \right) v = -e^2 \bar{u} P_1 v \\ \mathcal{A}_2^* &= (ie)^2 \bar{u} \left( \gamma_4 O_2^\dagger \gamma_4 \right) v = -e^2 \bar{u} P_2 v \\ \mathcal{A}_3^* &= \frac{-ig_e g_\gamma}{2\Lambda^2} \bar{u} \left( \gamma_4 O_3^\dagger \gamma_4 \right) v = \frac{-ig_e g_\gamma}{2\Lambda^2} \bar{u} P_3 v \end{aligned}$$

exploiting  $\varepsilon_4 = \varepsilon'_4 = 0$  in our gauge choice:

$$\begin{aligned} P_1 &= \dots = -\bar{\varepsilon}_{1,\sigma}\gamma_\sigma \left[ \frac{-i(p'_1 - k'_1) + m_e}{2p_1 \cdot k_1} \right] \bar{\varepsilon}_{2,\rho}\gamma_\rho \\ P_2 &= \dots = -\bar{\varepsilon}_{2,\rho}\gamma_\rho \left[ \frac{-i(p'_1 - k'_2) + m_e}{2p_1 \cdot k_2} \right] \bar{\varepsilon}_{2,\sigma}\gamma_\sigma \\ P_3 &= \bar{\varepsilon}_{1,\gamma}^* \left[ \gamma_4 (\gamma_\delta)^\dagger \gamma_4 (p_{2,\theta} - p_{1,\theta})^* \frac{N_{\zeta\tau\delta\theta}^*(k_1 + k_2)}{2k_1 \cdot k_2 + m_X^2} \Pi_{\zeta\tau\gamma\lambda}^*(k_1, k_2) \right] \bar{\varepsilon}_{2,\lambda}^* \end{aligned}$$

We have already seen in [section 9](#), that all the minus signs emerging from the complex conjugation cancel leaving a  $(-1)$  overall, which will be compensated by the extra  $i$  factor changing sign:

$$P_3 = -\varepsilon_{1,\gamma} \left[ \gamma_\delta (p_{2,\theta} - p_{1,\theta}) \frac{N_{\zeta\tau\delta\theta}(k_1 + k_2)}{2k_1 \cdot k_2 + m_X^2} \Pi_{\zeta\tau\gamma\lambda}(k_1, k_2) \right] \varepsilon_{2,\lambda} \quad (10.4)$$

The squared amplitude becomes:

$$|\mathcal{A}|^2 = \text{Tr} \left\{ \left[ -e^2 (O_1 + O_2) + \frac{ig_e g_\gamma}{2\Lambda^2} O_3 \right] u\bar{u} \left[ -e^2 (P_1 + P_2) - \frac{ig_e g_\gamma}{2\Lambda^2} P_3 \right] v\bar{v} \right\} \quad (10.5)$$

and then average over initial polarizations (now there are four, because of both electron and positron in the initial state) and sum over all fermion polarizations:

$$\begin{aligned} |\bar{\mathcal{A}}|^2 &= \frac{1}{4} \sum_{s_1, s_2} |\mathcal{A}|^2 = \\ &= \frac{1}{4} \frac{1}{2p_{1,4} 2p_{2,4}} \text{Tr} \left\{ \left[ -e^2 (O_1 + O_2) + \frac{ig_e g_\gamma}{2\Lambda^2} O_3 \right] (-i\gamma_1 + m_e) \left[ -e^2 (P_1 + P_2) - \frac{ig_e g_\gamma}{2\Lambda^2} P_3 \right] (-i\gamma_2 - m_e) \right\} \end{aligned} \quad (10.6)$$

Where the positron now gives a  $-m_e$  in the polarization sum. The FORM script used for this task is found in the repository linked in [subsection G.1](#).

The final trace has hundreds of addends and we do not deem it practical to report here. However, we can obtain a simplified result by directly substituting the values of the scalar products found in [subsection D.3](#). This can be done if we perform the integral in phase space first, locking the kinematic variables using the delta function. To carry out the calculation, we will be following closely the steps found in [subsection D.4](#). In particular, using the result in [Equation D.21](#):

$$\sigma(e^+e^- \rightarrow \gamma\gamma) = \frac{E}{32\pi^2 p} \int \frac{d^3 k_2}{k_{1,4} k_{2,4}} |\bar{\mathcal{A}}|^2 \delta(p_{1,4} + p_{2,4} - k_{1,4} - k_{2,4}) \quad (10.7)$$

where we write:

$$|\bar{\mathcal{A}}|^2 = \frac{F(p_1, p_2, k_1, k_2; \varepsilon_1, \varepsilon_2)}{16 p_{1,4} p_{2,4}} \quad (10.8)$$

where  $F$  is the result of the trace calculation, and an adimensional kinematics factor, function of all 4-momenta and the photon polarizations  $\varepsilon_1$  and  $\varepsilon_2$ . Then, following up on [Equation D.24](#), we get:

$$\begin{aligned} \frac{d\sigma}{d\Omega} &= \frac{E}{32\pi^2 p} \int_0^\infty dk_{2,4} \frac{k_{2,4}}{k_{1,4}} \frac{1}{2} \delta(E - k_{2,4}) \frac{F(p_1, p_2, k_1, k_2; \varepsilon_1, \varepsilon_2)}{16 p_{1,4} p_{2,4}} = \\ &= \frac{E}{(32\pi)^2 p} \frac{1}{E^2} F(E, p, \theta; \varepsilon_1, \varepsilon_2) = \frac{F(E, p, \theta; \varepsilon_1, \varepsilon_2)}{(32\pi)^2 p E} \end{aligned} \quad (10.9)$$

meaning that  $F$  is now the trace result with the substitution of the 4-momenta concerning the actual kinematics of the annihilation (found in [subsection D.3](#)), where the actual variables are the energy  $E$  and momentum  $p = |\vec{p}|$  of the electron, the scattering angle  $\theta$ , and the photon polarizations which are unaffected by phase space integration.

This way, the FORM trace reduces to "only" 20 addends, of which the first 3 actually recover the annihilation cross section without any spin 2 mediation (using the script `Annihilation_Xspin2_xigauge.frm` in the GitHub repository), and the last 10 are actually squared moduli of the spin 2 correction, of the order  $g_e^2 g_\gamma^2 / \Lambda^4$ . Now, because couplings are very small, squared moduli contribution are much smaller than interference terms, so we can neglect them (we calculate these term in [subsection D.5](#)). So, focusing only on interference terms, we get terms like  $e^2 g_e g_\gamma / \Lambda^2$ .

$$F(E, p, \theta; \varepsilon_1, \varepsilon_2) = 4e^4 \left[ \frac{E}{E + p \cos \theta} + \frac{E}{E - p \cos \theta} - 2(\varepsilon_1 \cdot \varepsilon_2)^2 \right] + \frac{32e^2 g_e g_\gamma (\varepsilon_1 \cdot \varepsilon_2)^2 E^2}{\Lambda^2} G(E, p, \theta) \quad (10.10)$$

$$\begin{aligned} G(E, p, \theta) &= p^2 \cos^2 \theta - \frac{4}{3} \frac{m_e^2 E^2}{m_X^2} + \frac{2}{3} \frac{m_e^2 E^2}{m_X^2} \left[ \frac{E}{E + p \cos \theta} + \frac{E}{E - p \cos \theta} \right] \\ &\quad + \frac{4}{3} m_e^2 - \frac{2}{3} m_e^2 \left[ \frac{E}{E + p \cos \theta} + \frac{E}{E - p \cos \theta} \right] = \\ &= \frac{2}{3} m_e^2 \left[ \frac{E}{E + p \cos \theta} + \frac{E}{E - p \cos \theta} - 2 \right] \left( \frac{E^2}{m_X^2} - 1 \right) + p^2 \cos^2 \theta = \\ &= \frac{2}{3} m_e^2 \left[ \frac{2p^2 \cos^2 \theta}{E^2 - p^2 \cos^2 \theta} \right] \left( \frac{E^2}{m_X^2} - 1 \right) + p^2 \cos^2 \theta = \\ &= \frac{4}{3} \frac{m_e^2 (E^2 - m_X^2)}{m_X^2} \left[ \frac{2\beta^2 \cos^2 \theta}{1 - \beta^2 \cos^2 \theta} \right] + E^2 \beta^2 \cos^2 \theta \end{aligned} \quad (10.11)$$

where we used  $p/m_e = \beta\gamma$  and  $E/m_e = \gamma$ , with regards to the velocities of the electrons in the center of mass frame. Henceforth, we will write  $G(E, p, \theta) = m_X^2 g(E, \theta)$ , where  $g$  is the squared parenthesis in [Equation 10.11](#):

$$g(E, \theta) = \frac{8}{3} \frac{m_e^2}{m_X^2} \left[ \frac{E^2}{m_X^2} - 1 \right] \left[ \frac{\beta^2 \cos^2 \theta}{1 - \beta^2 \cos^2 \theta} \right] + \frac{E^2}{m_X^2} \beta^2 \cos^2 \theta \quad (10.12)$$

which tells us that  $g(E, \pi/2) = 0$ , while  $g(m_X, \theta) = \beta^2 \cos^2 \theta$ .

Also, it is possible to see that  $g(E, \theta) = 0$  for a specific value of energy, in the non relativistic limit  $\beta \rightarrow 0$ :

$$\begin{aligned} \frac{8m_e^2}{3} \left[ \frac{E^2}{m_X^2} - 1 \right] + E^2 &= E^2 - \frac{8m_e^2}{3} + \frac{8}{3} \cancel{\frac{m_e^2}{m_X^2}} E^2 = 0 \\ \rightarrow \quad E &\approx \sqrt{\frac{8m_e^2}{3}} = \frac{2\sqrt{2}}{3} m_e \end{aligned} \quad (10.13)$$

which numerically is around  $E = 0.83$  MeV, or  $\sqrt{|s|} = 1.67$  MeV.

Notice how the result of the calculation is  $\xi$  independent, even though in the FORM code the Feynman rule has been written in a generic  $\xi$  gauge. This is expected as the amplitude is gauge invariant.

If we continue with cross section calculations, we exploit [Equation D.24](#) to add our correction:

$$\frac{d\sigma}{d\Omega} = \frac{\alpha^2}{16pE} \left[ \frac{1 + \beta^2 \cos^2 \theta}{1 - \beta^2 \cos^2 \theta} + 1 - 2(\varepsilon_1 \cdot \varepsilon_2)^2 \right] + \frac{e^2 g_e g_\gamma}{32\pi^2 p E \Lambda^2} \frac{(\varepsilon_1 \cdot \varepsilon_2)^2}{s + m_X^2} E^2 m_X^2 g(E, \theta) \quad (10.14)$$

Since in every experimental bound, ever, polarizations of photons are ignored, so let us sum over them. The terms that are polarization independent get a factor of 4 (2 polarizations per photon), whilst the other dependence is  $(\varepsilon_1 \cdot \varepsilon_2)^2$ , which we can easily sum:

$$\begin{aligned} \sum_{\lambda_1, \lambda_2} (\varepsilon_1 \cdot \varepsilon_2)^2 &= \sum_{\lambda_1} \varepsilon_i(k_1, \lambda_1) \varepsilon_j(k_1, \lambda_1) \sum_{\lambda_2} \varepsilon_i(k_2, \lambda_2) \varepsilon_j(k_2, \lambda_2) = \\ &= (\delta_{ij} - \hat{k}_{1,i} \hat{k}_{1,j}) (\delta_{ij} - \hat{k}_{2,i} \hat{k}_{2,j}) = \\ &= 3 - |\hat{k}_1|^2 - |\hat{k}_2|^2 + (\hat{k}_1 \cdot \hat{k}_2)^2 = 3 - 1 - 1 + (-1)^2 = 2 \end{aligned} \quad (10.15)$$

where  $\hat{k}_1 \cdot \hat{k}_2 = -1$ , as photons are back-to-back. The final unpolarized differential cross section is:

$$\frac{d\sigma}{d\Omega} = \frac{\alpha^2}{4pE} \left[ \frac{1 + \beta^2 \cos^2 \theta}{1 - \beta^2 \cos^2 \theta} \right] + \frac{\alpha}{4\pi} \frac{g_e g_\gamma}{\Lambda^2} \frac{1}{\beta} \frac{m_X^2}{s + m_X^2} g(E, \theta) \quad (10.16)$$

which adds directly a correction term to [Equation D.25](#).

Finally, we are interested in the actual total cross section, so we ought to integrate in the solid angle. In [subsection D.4](#), we carry out the calculation for the original QED contribution. Here, we calculate the integral regarding the spin 2 contribution. In total:

$$\begin{aligned} \sigma(e^+e^- \rightarrow \gamma\gamma) &= \frac{\pi\alpha^2}{pE} \left[ -1 + \frac{1}{\beta} \log \left( \frac{1+\beta}{1-\beta} \right) \right] + \frac{\alpha}{4\pi} \frac{g_e g_\gamma}{\Lambda^2} \frac{1}{\beta} \frac{m_X^2}{s + m_X^2} \int_{-1}^1 d\cos\theta \int_0^{2\pi} d\phi \, g(E, \theta) = \\ &= \frac{\pi\alpha^2}{pE} \left[ -1 + \frac{1}{\beta} \log \left( \frac{1+\beta}{1-\beta} \right) \right] + \frac{\alpha}{2\beta} \frac{g_e g_\gamma}{\Lambda^2} \frac{m_X^2}{s + m_X^2} \int_{-1}^1 d\cos\theta \, g(E, \theta) \end{aligned} \quad (10.17)$$

Calling  $x = \beta \cos\theta$ , using [Equation D.26](#), another useful integral to carry out:

$$\begin{aligned} \int dx \frac{x^2}{1-x^2} &= \int dx \left[ \frac{1+x^2}{1-x^2} - \frac{1}{1-x^2} \right] = \\ &= -x + \log \left| \frac{1+x}{1-x} \right| + \frac{1}{2} \int dx \left[ \frac{1}{1+x} + \frac{1}{1-x} \right] = \\ &= -x + \log \left| \frac{1+x}{1-x} \right| - \frac{1}{2} \log \left| \frac{1+x}{1-x} \right| = -x + \frac{1}{2} \log \left| \frac{1+x}{1-x} \right| \end{aligned} \quad (10.18)$$

so that:

$$\begin{aligned} \int_{-1}^1 d\cos\theta \frac{\beta^2 \cos^2 \theta}{1 - \beta^2 \cos^2 \theta} &= \frac{1}{\beta} \int_{-\beta}^{\beta} dx \frac{x^2}{1-x^2} = \\ &= \frac{1}{\beta} \left[ -x + \frac{1}{2} \log \left| \frac{1+x}{1-x} \right| \right]_{-\beta}^{\beta} = -2 + \frac{1}{\beta} \log \left( \frac{1+\beta}{1-\beta} \right) \end{aligned} \quad (10.19)$$

and we make use of [Equation 9.37](#) to obtain:

$$\int_{-1}^1 d\cos\theta g(E, \theta) = \frac{8}{3} \frac{m_e^2}{m_X^2} \left[ \frac{E^2}{m_X^2} - 1 \right] \left[ -2 + \frac{1}{\beta} \log \left( \frac{1+\beta}{1-\beta} \right) \right] + \frac{2}{3} \frac{E^2 \beta^2}{m_X^2} \quad (10.20)$$

which yields our final cross section:

$$\begin{aligned} \sigma(e^+e^- \rightarrow \gamma\gamma) &= \frac{\pi\alpha^2}{pE} \left[ -1 + \frac{1}{\beta} \log \left( \frac{1+\beta}{1-\beta} \right) \right] + \\ &+ \frac{\alpha}{2\beta} \frac{g_e g_\gamma}{\Lambda^2} \frac{m_X^2}{s + m_X^2} \left\{ \frac{8}{3} \frac{m_e^2}{m_X^2} \left[ \frac{E^2}{m_X^2} - 1 \right] \left[ -2 + \frac{1}{\beta} \log \left( \frac{1+\beta}{1-\beta} \right) \right] + \frac{2}{3} \frac{E^2 \beta^2}{m_X^2} \right\} \end{aligned} \quad (10.21)$$

This formula will be essential in the next chapter.

Again, how do we know that this result is correct? We can carry out a few checks to make sure we are on the right track, like, *Ward identities*.

This result is comprised of the contribution of three diagrams, with interference terms between the QED diagrams and the spin 2 correction. Because the first two diagrams' gauge invariance is accounted for (you can check that using the code `Annihilation.frm` on the GitHub repository), we know that for those Ward identities already work, because the QED part in the cross product is automatically zero. So, the real hassle is actually verifying that the spin 2 part, independently from QED cancellations, satisfies Ward identities. To that end, we created the code `Annihilation_onlyX_xigauge.frm`, in which we only focus on this latter diagram squared. This code isolates the spin 2 diagram and cancels common factors and constants, to help analyze terms under the surface.

In formulas, what we expect is:

$$\left\{ \begin{array}{l} F(p_1, p_2, k_1, k_2; \mathbf{k}_1, \varepsilon_2) = \overbrace{F_{\text{QED}}(p_1, p_2, k_1, k_2; \mathbf{k}_1, \varepsilon_2)} + \overbrace{F_{\text{interf}}(p_1, p_2, k_1, k_2; \mathbf{k}_1, \varepsilon_2)} + F_X(p_1, p_2, k_1, k_2; \mathbf{k}_1, \varepsilon_2) = 0 \\ F(p_1, p_2, k_1, k_2; \varepsilon_1, \mathbf{k}_2) = \overbrace{F_{\text{QED}}(p_1, p_2, k_1, k_2; \varepsilon_1, \mathbf{k}_2)} + \overbrace{F_{\text{interf}}(p_1, p_2, k_1, k_2; \varepsilon_1, \mathbf{k}_2)} + F_X(p_1, p_2, k_1, k_2; \varepsilon_1, \mathbf{k}_2) = 0 \end{array} \right. \quad (10.22)$$

A couple of remarks are needed:

- *Gauge invariance comes before kinematics*, meaning we cannot use the kinematics constraints coming from the phase space integration. These constraints are listed in the `Annihilation_onlyX_xigauge.frm` code and in subsection D.2. Namely,  $p_1 \cdot \varepsilon_1 = p_1 \cdot \varepsilon_2 = k_1 \cdot \varepsilon_2 = k_2 \cdot \varepsilon_1 = 0$  are all kinematics dependent, and must therefore be commented when carrying out the Ward identities check.

The only valid constraints are  $k_1 \cdot \varepsilon_1 = k_2 \cdot \varepsilon_2 = 0$ , as polarizations are always to be chosen transverse to their respective momenta.

- Not only are the ignored constraints kinematics dependent, but they also are *reference frame dependent*, as we already discussed in section 9 how these scalar products are actually not Lorentz invariant.

In a Compton scattering-like reference frame (electron at rest and positron moving), it is no longer true that  $k_1 \cdot \varepsilon_2 = k_2 \cdot \varepsilon_1 = 0$  (indeed, these are not constraints in Compton scattering, see section 9)<sup>21</sup>.

Fortunately, this check on the `Annihilation_onlyX_xigauge.frm` is successful, and the new diagram indeed satisfies Ward identities (in a generic  $\xi$  gauge) as written:

$$F_X(p_1, p_2, k_1, k_2; \mathbf{k}_1, \varepsilon_2) = F_X(p_1, p_2, k_1, k_2; \varepsilon_1, \mathbf{k}_2) = 0 \quad (10.23)$$

## 10.1 Correction to positronium decay

### 10.1.1 Positronium

Another system that is very precisely measured in electrodynamics, and very well linked to the  $e^-e^+ \rightarrow \gamma\gamma$  annihilation, is *positronium*. It is a bound state of an electron and a positron. It can be described in quantum mechanics exactly like a hydrogen atom, just with a different reduced mass (for this section, we will call  $m = m_e$  not to confuse it with  $m$  magnetic quantum number).

$$\mu = \frac{m_e^2}{2m_e} = \frac{m_e}{2} \quad (10.24)$$

The Hamiltonian can be written, in the non relativistic limit, as:

$$H = \frac{|\vec{p}_1|^2}{2m_e} + \frac{|\vec{p}_2|^2}{2m_e} - \frac{\alpha}{|\vec{r}_1 - \vec{r}_2|} \quad (10.25)$$

Where in natural units,  $\alpha = e^2/4\pi$  and the vacuum dielectric constant  $\varepsilon_0 = 1$ .

This is a 2-body Hamiltonian to be easily simplified by treating separately the center of mass Hamiltonian and the Hamiltonian of the relative position  $\vec{r} = \vec{r}_1 - \vec{r}_2$  and momentum  $\vec{p} = \vec{p}_1 - \vec{p}_2$ . In the center of mass frame, we can just write:

$$H = \frac{p^2}{2\mu} - \frac{\alpha}{r} \quad (10.26)$$

where  $p = |\vec{p}|$  and  $r = |\vec{r}|$ . Details on how we derive non relativistic energy levels and wavefunctions can be found in subsection F.8. Energy levels are:

$$E_n = -\frac{\alpha^2 m_e}{4n^2} \quad (10.27)$$

<sup>21</sup>All the more reason not to include these frame dependent constraints when checking Ward identities.

from [Equation F.45](#). Of course, there are relativistic corrections to be included, and those effects are of order  $\alpha^2$  as well.

The Hilbert space of electron and positron has 2 possible spin states, being a tensorization of two spin 1/2 spaces. SU(2) tensor products rules give us:  $1/2 \otimes 1/2 = 0 \oplus 1$ . With the notation  ${}^{2s+1}l_j$  for states, and  $l = S, P, D, F, \dots$  as the hydrogen orbitals, we get the two possible ground states of positronium:

- ${}^1S_0$ , called **parapositronium**. It has parity  $P = (-1)^{l+1} = -1$  and charge conjugation (being neutral)  $C = (-1)^{l+s} = 1$ . In terms of  $J^{PC}$  quantum numbers, it is  $0^-+$ .
- ${}^3S_1$ , called **orthopositronium**. It has parity  $P = (-1)^{l+1} = -1$  and charge conjugation  $C = (-1)^{l+s} = -1$ . In terms of  $J^{PC}$  quantum numbers, it is  $0^{--}$ .

To effectively describe a positronium state starting with electron and positron states, first we tensorize  $e^+, e^-$  one particle states into a two particle state:

$$\begin{aligned} |e^-(\vec{p}_1, s_1)\rangle &= \sqrt{2E(p_1)} a_{s_1}^\dagger(p_1) |0\rangle \\ |e^+(\vec{p}_2, s_2)\rangle &= \sqrt{2E(p_2)} b_{s_2}^\dagger(p_2) |0\rangle \end{aligned}$$

$$|e^-(\vec{p}_1, s_1); e^+(\vec{p}_2, s_2)\rangle = |e^-(\vec{p}_1, s_1)\rangle \otimes |e^+(\vec{p}_2, s_2)\rangle \quad (10.28)$$

Since our treatment will be non relativistic,  $\sqrt{2E(p_1)}, \sqrt{2E(p_2)} \rightarrow \sqrt{2m_e}$ .

Then, we shall choose the center of mass frame ( $\vec{p}_1 = -\vec{p}_2$ ) and take linear combinations of momentum states, weighted with the wavefunctions we found in [subsection F.8](#), to combine them into the different bound states of positronium ([34]). Effectively, what we do is:

$$|n, l, m\rangle = \int \frac{d^3 p}{(2\pi)^3} \Psi_{nlm}(\vec{p}) |e^-(\vec{p}, s_1); e^+(\vec{p}, s_2)\rangle = \int \frac{d^3 p}{(2\pi)^3} \Psi_{nlm}(\vec{p}) |l, m\rangle |s_1, s_2\rangle \quad (10.29)$$

with  $|l, m\rangle |s_1, s_2\rangle = |l, m, s_1, s_2\rangle$ , and:

$$\Psi_{nlm}(\vec{p}) = \int d^3 x e^{i\vec{p}\cdot\vec{x}} \psi_{nlm}(\vec{x})$$

simply being the Fourier transform of the wavefunction in momentum space. This is a positronium state, but it is not in the form  ${}^{2s+1}l_j$  that has definite total angular momentum. To obtain that, we need two steps.

1. First, we need to combine spin of the fermions to get a definite spin state  $|S, S_z\rangle$ :

$$|S, S_z\rangle = \sum_{s=-\frac{1}{2}}^{\frac{1}{2}} \langle s, S_z - s | S, S_z \rangle |s, S_z - s\rangle \quad (10.30)$$

where  $\langle s, S_z - s | S, S_z \rangle$  are the Clebsch-Gordan coefficients for the basis change  $(1/2, s_1; 1/2, s_2)$  to  $(S, S_z, 1/2, 1/2)$ .

2. Then, we must combine spin and orbital angular momentum to get a definite state with defined total angular momentum  $j$ , effectively performing another basis change  $(l, l_z, S, S_z)$  to  $(j, j_z, l, S)$ . Since  $l, m$  are fixed, we only need to sum over all possible spin states  $|S, S_z\rangle$ :

$$|{}^{2s+1}l_j, j_z, n\rangle = \sum_{S_z=-S}^S \int \frac{d^3 p}{(2\pi)^3} \Psi_{nlm}(\vec{p}) \langle l, m, S, S_z | j, j_z \rangle |l, m, S, S_z\rangle \quad (10.31)$$

where  $\langle l, m, S, S_z | j, j_z \rangle$  are another set of Clebsch-Gordan coefficients needed for the basis change.

With [Equation 10.30](#) and [Equation 10.31](#), we can finally write down the two ground states of positronium:

$$|^1S_0, 0, 0\rangle = 2\sqrt{m_e} \int \frac{d^3 p}{(2\pi)^3} \Psi_{100}(\vec{p}) \frac{1}{\sqrt{2}} \left[ a_{\frac{1}{2}}^\dagger(\vec{p}) b_{-\frac{1}{2}}^\dagger(-\vec{p}) - a_{-\frac{1}{2}}^\dagger(\vec{p}) b_{\frac{1}{2}}^\dagger(-\vec{p}) \right] |0\rangle \quad (10.32)$$

$$|^3S_1, 0, 0\rangle = 2\sqrt{m_e} \int \frac{d^3 p}{(2\pi)^3} \Psi_{100}(\vec{p}) \frac{1}{\sqrt{2}} \left[ a_{\frac{1}{2}}^\dagger(\vec{p}) b_{-\frac{1}{2}}^\dagger(-\vec{p}) + a_{-\frac{1}{2}}^\dagger(\vec{p}) b_{\frac{1}{2}}^\dagger(-\vec{p}) \right] |0\rangle \quad (10.33)$$

$$|^3S_1, \pm 1, 0\rangle = 2\sqrt{m_e} \int \frac{d^3 p}{(2\pi)^3} \Psi_{100}(\vec{p}) a_{\pm\frac{1}{2}}^\dagger(\vec{p}) b_{\pm\frac{1}{2}}^\dagger(-\vec{p}) |0\rangle \quad (10.34)$$

The factor  $2\sqrt{m_e}$  is a required normalization factor for positronium state, since in non relativistic regime creation and annihilation operators in the state come with  $1/\sqrt{2m_e}$ . One can easily check that  $\langle {}^{2s+1}l_j, j_z, n | {}^{2s+1}l_j, j_z, n \rangle = 1$ .

There are four total spin states for the ground state  $n = 0, l = 0$  of positronium. Notice that for  $l = 0$ , the second step is trivial, so we are only left with the combination that gives the correct spin.

### 10.1.2 Tree level decay rate

What does positronium decay into? Well, we know that  $e^+e^- \rightarrow \gamma\gamma$  is a valid electrodynamics process, but special care is needed in positronium, because quantum numbers of bound states may be different than those of free states, and sometimes that can result in the suppression of decay channels due to mismatch of quantum numbers that should be conserved.

In the case of positronium, that special quantum number is charge conjugation, since electromagnetic interactions do conserve  $C$ . A pair of photons have intrinsic charge conjugation  $(-1)^2 = 1$ , which already means that *orthopositronium cannot decay into a pair of photons*. As so it happens,  ${}^3S_1 \rightarrow \gamma\gamma\gamma$  is the main decay channel for orthopositronium.

Instead, for parapositronium, charge conjugation is not violated in the decay into two photons. Let us now match all the quantum numbers for two photons. Results shown in [Table 3](#): Parity conservation requires  $l = 1$ .

		${}^1S_0$	$\gamma\gamma$
not conserved	$S$	0	$1 \otimes 1 = 0 \oplus 1 \oplus 2$
	$L$	0	$l$
conserved	$J$	0	$l \otimes s$
	$J_z$	0	$l_z + s_z$
	$P$	-1	$(-1)^2 \times (-1)^l$
	$C$	1	$(-1)^2$

Table 3: Selection rules for the decay of  ${}^1S_0 \rightarrow \gamma\gamma$ . The decay is possible if we select  $l = 1$  and  $s = 1$ .

Then, total angular momentum conservation requires  $s = 1$ , as singlets  $j = 0$  can only occur in SU(2) if  $l = s$ . All the quantum numbers match. Still, there are two remarks to be made:

- Photons do not really have spin, but helicity. The state  $|1, 0\rangle$  does not occur in massless bosons. So, although Clebsch-Gordan combinations still follow the same rules, some states may be missing. In particular, when taking a pair of photons, it is impossible to combine their  $s_z$  to get  $\pm 1$ , but we can only get 0, 2. So, in our case  $s = 1$ , the states  $|1, \pm 1\rangle$  do not exist, and the only possible combination is:

$$|1, 0\rangle_{\text{tot}} = \frac{1}{\sqrt{2}} [ |1, 1\rangle |1, -1\rangle - |1, -1\rangle |1, 1\rangle ] \quad (10.35)$$

so, the only possible  $s_z$  for photons is 0, meaning that also  $l_z = 0$  is required.

- Photons are bosons. A pair of photons must have completely symmetric wavefunction, which is a tensor product of an orbital part and a spin part. So, either both orbital and spin part are symmetric, or they are antisymmetric. By looking at [Equation 10.35](#), the spin state is antisymmetric, so orbital part must be antisymmetric. Sure enough,  $l = 1$ , and the orbital wavefunction is, indeed, antisymmetric.

So, we conclude that parapositronium can decay into two photons.

We now evaluate the transition amplitude from positronium to photons, in the usual center of mass frame. For simplicity of notation, we omit photon polarizations  $\lambda_1, \lambda_2$ :

$$\begin{aligned} \mathcal{A}(\vec{k}_1, \vec{k}_2) &= \left\langle \gamma(\vec{k}_1), \gamma(\vec{k}_2) \middle| {}^1S_0, 0, 0 \right\rangle = \\ &= 2\sqrt{m_e} \int \frac{d^3 p}{(2\pi)^3} \Psi_{100}(\vec{p}) \left\langle \gamma(\vec{k}_1), \gamma(\vec{k}_2) \middle| \frac{1}{\sqrt{2}} \left[ a_{\frac{1}{2}}^\dagger(\vec{p}) b_{-\frac{1}{2}}^\dagger(-\vec{p}) - a_{-\frac{1}{2}}^\dagger(\vec{p}) b_{\frac{1}{2}}^\dagger(-\vec{p}) \right] \middle| 0 \right\rangle = \\ &= 2\sqrt{m_e} \int \frac{d^3 p}{(2\pi)^3} \Psi_{100}(\vec{p}) \frac{1}{2m_e} \left\langle \gamma(\vec{k}_1), \gamma(\vec{k}_2) \middle| e^-(\vec{p}), e^+(-\vec{p}); S = 0, S_z = 0 \right\rangle = \\ &= \frac{1}{\sqrt{m_e}} \int \frac{d^3 p}{(2\pi)^3} \Psi_{100}(\vec{p}) \mathcal{A}_{ee \rightarrow \gamma\gamma}(\vec{k}_1, \vec{k}_2) = \\ &= \frac{\mathcal{A}_{ee \rightarrow \gamma\gamma}(\vec{k}_1, \vec{k}_2)}{\sqrt{m_e}} \int \frac{d^3 p}{(2\pi)^3} \Psi_{100}(\vec{p}) = \\ &= \frac{\mathcal{A}_{ee \rightarrow \gamma\gamma}(\vec{k}_1, \vec{k}_2)}{\sqrt{m_e}} \psi_{100}(\vec{0}) \end{aligned} \quad (10.36)$$

where by definition:

$$\psi_{nlm}(\vec{x}) = \int \frac{d^3 p}{(2\pi)^3} e^{-i\vec{p}\cdot\vec{x}} \Psi_{nlm}(\vec{p}) \quad \rightarrow \quad \int \frac{d^3 p}{(2\pi)^3} \Psi_{100}(\vec{p}) = \psi_{100}(\vec{x}) \quad (10.37)$$

It is very important to mention that, looking at [Equation F.47](#), the only wavefunctions that do not vanish at  $\vec{x} = 0$  have  $l = 0$ . That is because when  $l > 0$ , the centrifugal potential acts dominantly creating a potential barrier that goes like  $1/r^2$  near the origin, preventing the wavefunction to exist in 0. From now on, we will simply call  $\psi_{100} = \psi$ .

Also, we get the total amplitude of the electron positron annihilation because the spin configuration  $S = 0$ ,  $S_z = 0$  is really the only one that allows for such process to occur in the first place. That amplitude is independent of the initial momentum  $\vec{p}$ , so we can take it out of the integral.

When we take the modulus squared, because we did not average over the initial fermion polarization, we get a factor of 4 with respect to  $|\bar{\mathcal{A}}_{ee \rightarrow \gamma\gamma}|^2$  in [Equation 10.6](#), and we get another factor of  $2p_{1,4}2p_{2,4}$ , because positronium decay does not require sum over polarizations of electron and positron (which in the formula would have that factor in the denominator), since polarization is fixed here<sup>22</sup>. Because we are in non relativistic limit, this factor translates to  $4m_e^2$ :

$$|\mathcal{A}(\vec{k}_1, \vec{k}_2)|^2 = \frac{4}{m_e} 4m_e^2 |\psi(0)|^2 |\bar{\mathcal{A}}_{ee \rightarrow \gamma\gamma}(\vec{k}_1, \vec{k}_2)|^2 \quad (10.38)$$

We go to the decay rate. For a decay, we get one less normalization factor of  $1/(\sqrt{V})^2$  because we have one less particle in the initial state. At the same time, we do not get the factor  $V/v_{rel}$  like we do in the cross section. Also, there is one extra  $1/2M$  in the rate, where  $M$  is the mass of the decaying particle (here  $M = 2m_e$ , the mass of the positronium). So, defining a fixed kinematic rate (look at [Equation D.20](#) for comparison):

$$\begin{aligned} \Gamma(k_1, k_2) &= \frac{|S_{fi}|^2}{T} = \frac{1}{T} \frac{(2\pi)^8 |\bar{\mathcal{A}}(\vec{k}_1, \vec{k}_2)|^2}{V^3 2k_{1,4} 2k_{2,4}} \frac{VT}{(2\pi)^4} \delta(p_1 + p_2 - k_1 - k_2) = \\ &= 16m_e |\psi(0)|^2 \Gamma_{ee \rightarrow \gamma\gamma}(k_1, k_2) \end{aligned} \quad (10.39)$$

and integrating in phase space, we get the rate:

$$\begin{aligned} \Gamma(^1S_0 \rightarrow \gamma\gamma) &= \frac{1}{2 \cdot (2m_e)} \int \frac{V d^3 k'}{(2\pi)^3} \frac{V d^3 p'}{(2\pi)^3} \Gamma(k_1, k_2) = \\ &= \frac{16m_e}{2 \cdot (2m_e)} |\psi(0)|^2 \int \frac{V d^3 k'}{(2\pi)^3} \frac{V d^3 p'}{(2\pi)^3} \Gamma_{ee \rightarrow \gamma\gamma}(k_1, k_2) \\ &= 4 |\psi(0)|^2 \int \frac{V d^3 k'}{(2\pi)^3} \frac{V d^3 p'}{(2\pi)^3} \Gamma_{ee \rightarrow \gamma\gamma}(k_1, k_2) \end{aligned} \quad (10.40)$$

looking at [Equation D.21](#), with a  $\Gamma$  defined with one less volume  $V$  at denominator, we get:

$$\int \frac{V d^3 k'}{(2\pi)^3} \frac{V d^3 p'}{(2\pi)^3} \Gamma(k_1, k_2) = \frac{v_{rel}}{V} \times V \times \sigma(e^+e^- \rightarrow \gamma\gamma) = v_{rel} \sigma(e^+e^- \rightarrow \gamma\gamma) \quad (10.41)$$

meaning that in the end:

$$\Gamma(^1S_0 \rightarrow \gamma\gamma) = 4 |\psi(0)|^2 v_{rel} \sigma(e^+e^- \rightarrow \gamma\gamma) \quad (10.42)$$

This rate is called *Pirenne-Wheeler formula* ([\[34\]](#)). It has a really simple interpretation: the only way for a positronium state to decay is for electron and positron to occupy the same position in space. This happens with probability  $\rho = |\psi(0)|^2$ . Then, the rate for any process to occur simply becomes:

$$\Gamma = \rho v_{rel} \sigma$$

And because we have do not average over initial polarizations,  $\sigma = 4\bar{\sigma}$ , and we are done. Now, take the non relativistic cross section from [Equation D.30](#):

$$\sigma(e^+e^- \rightarrow \gamma\gamma) = \frac{\pi\alpha^2}{m_e^2\beta} = \frac{\pi\alpha^2}{m_e^2 v_{rel}}$$

<sup>22</sup>In other notations, it is more obvious that this factor should not be here, because  $1/2p_{1,4}2p_{2,4}$  appears directly in the cross section formula as normalization of the incoming fields. Clearly, in the decay of the positronium, the individual electron and positron do not really exist individually, so there is no need for such a normalization factor. The only needed normalization factor would be  $1/2E_{pos}$ , for the positronium itself, which in the rest frame becomes  $1/2M_{pos} = 1/2(2m_e)$ , and it is already present in the rate formula (by default).

then, take from [Equation F.49](#) the value for  $\psi(0)$ :

$$|\psi(0)|^2 = \frac{1}{\pi r_0^3} = \frac{\alpha^3 \mu^3}{\pi} = \frac{\alpha^3 m_e^3}{8\pi} \quad (10.43)$$

Putting [Equation 10.43](#), in [Equation 10.42](#):

$$\Gamma(^1S_0 \rightarrow \gamma\gamma) = 4 \frac{\alpha^3 m_e^3}{8\pi} v_{rel} \frac{\pi \alpha^2}{m_e^2 v_{rel}} = \frac{m_e \alpha^5}{2} \quad (10.44)$$

which gives  $\tau = 1.24 \times 10^{-10}$  s as first order term.

### 10.1.3 Correction to parapositronium decay

Radiative corrections to parapositronium decay are of relative order  $\alpha$ , one loop diagrams to this process give corrections of relative order  $\alpha^2$ . Relativistic effects to the energy, the potential and the wavefunction give the same relative order  $\alpha^2$  as corrections. In [32], [33], an actual expansion in powers of  $\alpha$ , up to next to leading log terms, is given:

$$\begin{aligned} \Gamma(^1S_0 \rightarrow \gamma\gamma) &= \frac{m_e \alpha^5}{2} [1 + \varepsilon] \\ \varepsilon &= \left( \frac{\pi^2}{4} - 5 \right) \frac{\alpha}{\pi} + \left( \frac{\alpha}{\pi} \right)^2 \left[ -2\pi^2 \log \alpha + 5.1243(33) \right] + \\ &\quad \frac{\alpha^3}{\pi} \left[ -\frac{3}{2} \log^2 \alpha + \left( \frac{533}{90} - \frac{\pi^2}{2} + 10 \log 2 \right) \log \alpha + \mathcal{O}(\alpha^3) \right] \end{aligned} \quad (10.45)$$

which is an extremely precise theoretical prediction:

$$\Gamma(^1S_0 \rightarrow \gamma\gamma) = 7989.50(2) \mu\text{s}^{-1}$$

of 2 ppm, and it agrees with experimental measurements. From the experimental side ([29]), the best result is:

$$\Gamma(^1S_0 \rightarrow \gamma\gamma) = (7990.9 \pm 1.7) \mu\text{s}^{-1}$$

which has a precision of about 200 ppm.

We also have a new correction, coming from a tree level  $s$ -channel diagram with an exchange of the  $X$  resonance particle. Whilst Pirenne-Wheeler formula stays the same, the total annihilation cross section changes to accommodate our new contribution.

From [Equation F.51](#), we get  $\beta = \alpha \ll 1$  for parapositronium, so we can expand the result in [Equation 10.21](#). Take the fundamental result from [Equation 10.21](#), and let us expand the QED cross section and only keep terms up to  $\mathcal{O}(\beta)$ , meaning that  $\gamma \approx 1 + \beta^2/2 \approx 1$ , and neglect  $m_e^2/m_X^2$ . Let us expand the logarithm part first:

$$\begin{aligned} \frac{1}{\beta} \log \left( \frac{1+\beta}{1-\beta} \right) &= \frac{1}{\beta} [\log(1+\beta) - \log(1-\beta)] = \\ &= \frac{1}{\beta} \left[ \beta - \frac{\beta^2}{2} + \frac{\beta^3}{3} + \mathcal{O}(\beta^4) - \left( -\beta - \frac{\beta^2}{2} - \frac{\beta^3}{3} + \mathcal{O}(\beta^4) \right) \right] = \\ &= \frac{1}{\beta} \left[ 2\beta + \frac{2\beta^3}{3} + \mathcal{O}(\beta^5) \right] = 2 + \frac{2\beta^2}{3} + \mathcal{O}(\beta^4) \end{aligned}$$

so, then:

$$\frac{\pi \alpha^2}{pE} \left[ -1 + \frac{1}{\beta} \log \left( \frac{1+\beta}{1-\beta} \right) \right] = \frac{\pi \alpha^2}{4\beta E^2} \left[ -1 + 2 + \mathcal{O}(\beta^2) \right] \approx \frac{\pi \alpha^2}{4m_e^2 \beta} \left[ 1 + \mathcal{O}(\beta^2) \right] \quad (10.46)$$

Whilst for the interference terms, instead, we get:

$$\begin{aligned} &\frac{\alpha}{2\beta} \frac{g_e g_\gamma}{\Lambda^2} \frac{m_X^2}{s + m_X^2} \left\{ \frac{8}{3} \frac{m_e^2}{m_X^2} \left[ \frac{E^2}{m_X^2} - 1 \right] \left[ -2 + \frac{1}{\beta} \log \left( \frac{1+\beta}{1-\beta} \right) \right] + \frac{2}{3} \frac{E^2 \beta^2}{m_X^2} \right\} = \\ &\approx \frac{\alpha}{2\beta} \frac{g_e g_\gamma}{\Lambda^2} \frac{m_X^2}{-4m_e^2 + m_X^2} \left\{ \frac{8}{3} \frac{m_e^2}{m_X^2} \left[ \frac{m_e^2}{m_X^2} - 1 \right] \left[ \frac{2\beta^2}{3} + \mathcal{O}(\beta^4) \right] + \frac{2}{3} \frac{m_e^2 \beta^2}{m_X^2} \right\} = \\ &\approx \frac{\alpha}{2\beta} \frac{g_e g_\gamma}{\Lambda^2} \left[ \left( -\frac{8}{3} + 1 \right) \frac{2}{3} \frac{m_e^2 \beta}{m_X^2} \right] = -\frac{5\alpha\beta}{9} \frac{g_e g_\gamma}{\Lambda^2} \frac{m_e^2}{m_X^2} \end{aligned} \quad (10.47)$$

notice that in the non relativistic limit, *the correction to the cross section is negative*. Don't panic, it is okay since these is the effect of interference.

When substituting  $\beta = \alpha$ , we get the final cross section for the positronium decay:

$$\begin{aligned}\sigma(e^+e^- \rightarrow \gamma\gamma) &\approx \frac{\pi\alpha^2}{4m_e^2\beta} \left[ 1 + \mathcal{O}(\beta^2) \right] - \frac{5\alpha\beta}{9} \frac{g_e g_\gamma}{\Lambda^2} \frac{m_e^2}{m_X^2} = \\ &= \frac{\pi\alpha^2}{4m_e^2\beta} \left[ 1 + \mathcal{O}(\beta^2) - \frac{20}{9\pi} \frac{\beta^2}{\alpha} \frac{g_e g_\gamma}{\Lambda^2} \frac{m_e^4}{m_X^2} \right] = \\ &= \frac{\pi\alpha}{4m_e^2} \left[ 1 + \mathcal{O}(\beta^2) - \frac{20\alpha}{9\pi} \frac{g_e g_\gamma}{\Lambda^2} \frac{m_e^4}{m_X^2} \right] = \end{aligned}\quad (10.48)$$

$$= \frac{\pi\alpha}{4m_e^2} \left[ 1 - \left( 1.2 \times 10^{-6} \text{ MeV}^2 \right) \times \frac{g_e g_\gamma}{\Lambda^2} \right] \quad (10.49)$$

Now, from [Equation 5.43](#) and [Equation 5.44](#), we have:

$$\frac{g_e g_\gamma}{\Lambda^2} = 1.0 \times 10^{-11} \text{ MeV}^{-2} \quad (10.50)$$

which means that we get a correction factor to the cross section:

$$\sigma(e^+e^- \rightarrow \gamma\gamma) = \sigma_{\text{QED}}(e^+e^- \rightarrow \gamma\gamma) \left[ 1 + \mathcal{O}(10^{-17}) \right] \quad (10.51)$$

which is about 11 orders of magnitude smaller than the best precision in theoretical calculations, and about 13 orders of magnitude smaller than the best experimental precision.

We report the graphs displaying the behavior of the corrected annihilation into two photons in [Figure 27](#): In

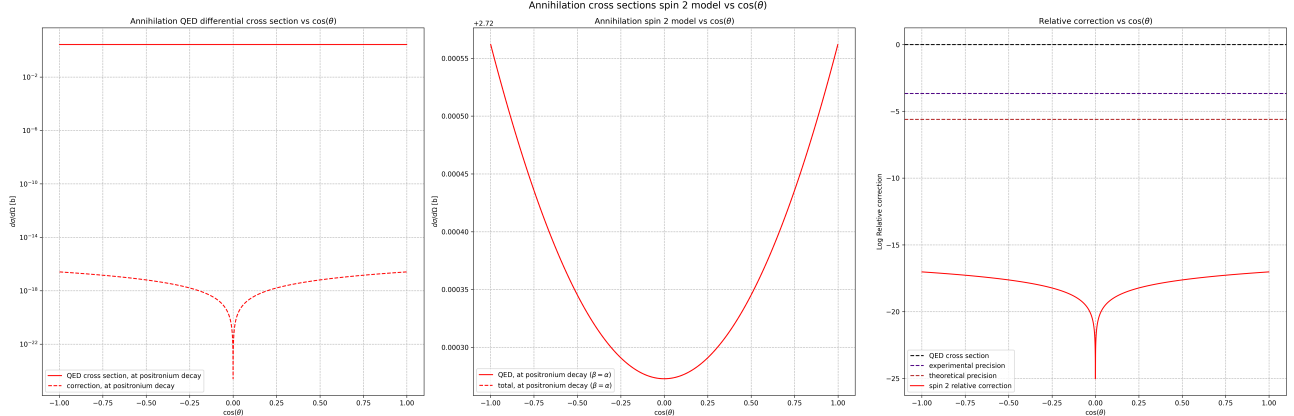


**Figure 27:** Graph of behavior of annihilation corrections as a function of the scattering angle  $\cos\theta$ . On the left, we plot separately both the QED result and the actual spin 2 correction (dashed line), for different values of the center of mass energy  $\sqrt{|s|}$ . In the middle, comparison between QED differential cross section and total cross section (including spin 2 correction), for different fixed  $\sqrt{|s|}$ . On the right, relative correction to the QED cross section of the total (QED + spin 2) cross section, always at different energetic values for  $\sqrt{|s|}$ .

[Figure 27](#), you can see how small spin 2 correction is. As we said, there are 17 orders of magnitude of difference. It is interesting to notice how the correction actually vanishes for  $\cos\theta = 0$ , which we have already noticed.

Hence, a spin 2 mediation with the coupling characteristics inferred by ATOMKI for  $e^+e^-$  channel and JINR for  $\gamma\gamma$  channel, would be well below experimental constraint on the parapositronium decay.

## 10.2 Simplifying annihilation result

Let us study the annihilation into two photons differential cross section. From [Equation 10.16](#) and [Equation 10.12](#):

$$\frac{d\sigma}{d\Omega} = \frac{\alpha^2}{4pE} \left[ \frac{1 + \beta^2 \cos^2 \theta}{1 - \beta^2 \cos^2 \theta} \right] + \frac{\alpha}{4\pi} \frac{g_e g_\gamma}{\Lambda^2} \frac{1}{\beta} \frac{m_X^2}{s + m_X^2} g(E, \theta)$$

$$g(E, \theta) = \frac{8}{3} \frac{m_e^2}{m_X^2} \left[ \frac{E^2}{m_X^2} - 1 \right] \left[ \frac{\beta^2 \cos^2 \theta}{1 - \beta^2 \cos^2 \theta} \right] + \frac{E^2}{m_X^2} \beta^2 \cos^2 \theta$$

We can take the two relevant limits.

**Non-relativistic limit:** We send  $4m_e^2/s \rightarrow -1$ , as  $E \rightarrow m_e$  and  $p \rightarrow 0$ . Then,  $\beta \rightarrow 0$  and  $\gamma \rightarrow 1$ , and  $m_e^2 \ll m_X^2$ . QED limits can be found in [subsection D.4](#). Then:

$$g(E, \theta) = \frac{8}{3} \frac{m_e^2}{m_X^2} \left[ \frac{m_e^2}{m_X^2} - 1 \right] \left[ \frac{\beta^2 \cos^2 \theta}{1 - \beta^2 \cos^2 \theta} \right] + \frac{m_e^2}{m_X^2} \beta^2 \cos^2 \theta =$$

$$= \frac{m_e^2}{m_X^2} \beta^2 \cos^2 \theta \left( -\frac{8}{3} + 1 \right) = -\frac{5}{3} \frac{m_e^2}{m_X^2} \beta^2 \cos^2 \theta \quad (10.52)$$

$$\frac{d\sigma}{d\Omega} = \frac{\alpha^2}{4m_e^2 \beta} + \frac{\alpha}{4\pi} \frac{g_e g_\gamma}{\Lambda^2} \frac{1}{\beta} \frac{m_X^2}{s + m_X^2} \left[ -\frac{5}{3} \frac{m_e^2}{m_X^2} \beta^2 \cos^2 \theta \right] =$$

$$\approx \frac{\alpha^2}{4m_e^2 \beta} - \frac{5\alpha}{12\pi} \frac{g_e g_\gamma}{\Lambda^2} \frac{m_e^2}{m_X^2} \beta \cos^2 \theta =$$

$$= \frac{\alpha^2}{4m_e^2 \beta} \left[ 1 - \frac{5}{3\pi} \frac{g_e g_\gamma}{\alpha \Lambda^2} \frac{m_e^4}{m_X^2} \beta^2 \cos^2 \theta \right] \quad (10.53)$$

It is a negative correction, as since this is the result of interference both signs would have been acceptable. This is the case in non-relativistic limit. Numerically, using [Equation 5.43](#) and [Equation 5.44](#):

$$\frac{d\sigma}{d\Omega} = \frac{d\sigma}{d\Omega} \Big|_{\text{QED}} \left[ 1 - \left( 1.8 \times 10^{-13} \text{ MeV}^{-2} \right) \beta^2 \cos^2 \theta \right] \quad (10.54)$$

which is an extremely small correction, just like in Compton effect, as  $p \rightarrow 0$ .

**Ultra-relativistic limit:** If we send  $m_e^2/s \rightarrow 0$ , and  $m_X^2/s \rightarrow 0$ , with  $s \rightarrow -4E^2$  and  $\beta \rightarrow 1$ . Then it is immediate to see that  $g(E, \theta)$  has a dominant  $E^2/m_X^2$  term, without the suppression of  $m_e^2/m_X^2$ :

$$\frac{d\sigma}{d\Omega} = \frac{\alpha^2}{|s|} \left[ \frac{1 + \cos^2 \theta}{1 - \cos^2 \theta} \right] + \frac{\alpha}{4\pi} \frac{g_e g_\gamma}{\Lambda^2} \frac{1}{\beta} \frac{m_X^2}{s + m_X^2} \left( \frac{E^2}{m_X^2} \beta^2 \cos^2 \theta \right)$$

$$= \frac{\alpha^2}{|s|} \left[ \frac{1 + \cos^2 \theta}{1 - \cos^2 \theta} \right] - \frac{\alpha}{16\pi} \frac{g_e g_\gamma}{\Lambda^2} \cos^2 \theta \quad (10.55)$$

This cross section satisfies Froissart bound, because it has an absolute constant correction in energy (a relative growth  $\propto |s|$ ). Everything is consistent, but unfortunately due to the nature we expect of the  $X$  resonance, the limit in energy is given by the value for which there is experimental verification: 20 – 50 MeV, as we thoroughly explained in [subsection 4.4](#).

It is also worth mentioning that if we send  $\theta \rightarrow \pi/2$ , correction is automatically zero (even the bits we neglected get to 0), while if we send  $\theta \rightarrow 0$ , QED result diverges, making relative correction due to spin 2 null again.

So:

$$\frac{d\sigma}{d\Omega} = \frac{\alpha^2}{|s|} \left[ \frac{1 + \cos^2 \theta}{1 - \cos^2 \theta} \right] \left[ 1 - \frac{|s|}{16\pi} \frac{g_e g_\gamma}{\alpha \Lambda^2} \frac{\cos^2 \theta (1 - \cos^2 \theta)}{1 + \cos^2 \theta} \right] =$$

$$= \frac{d\sigma}{d\Omega} \Big|_{\text{QED}} \left[ 1 - \frac{|s|}{16\pi} \frac{g_e g_\gamma}{\alpha \Lambda^2} \frac{\cos^2 \theta (1 - \cos^2 \theta)}{1 + \cos^2 \theta} \right] \quad (10.56)$$

which numerically, gives:

$$\frac{d\sigma}{d\Omega} = \frac{d\sigma}{d\Omega} \Big|_{\text{QED}} \left[ 1 - \left( 2.8 \times 10^{-11} \text{ MeV}^{-2} \right) |s| \frac{\cos^2 \theta (1 - \cos^2 \theta)}{1 + \cos^2 \theta} \right] \quad (10.57)$$

as a conservative correction estimate (lower bound for the coupling constant). To be a relevant correction, for  $\sqrt{|s|} = 20 \text{ GeV}$ , the large angle cross section would receive a *1.1% correction* (which would break EFT), before considering angles. The angular function, instead, has a maximum of 0.17, at  $\cos \theta \approx \pm 0.64$ , meaning the maximum correction at that energy is around 0.2%. At our actual energy limit, instead, correction would be  $\mathcal{O}(10^{-9})$ , which is totally invisible.

It is also worth mentioning that, if you look at squared moduli contributions, term like  $g_e^2 g_\gamma^2 / \Lambda^4$  (see subsection D.5), since their relative correction grows like  $s^3$  (they go like  $s^2$ , violating Froissart bound), their contribution starts at a lower value but grows much faster, overtaking interference terms contribution around  $\mathcal{O}(\text{GeV})$ . This is another hint on the fact that we should not go that high in energy.

Instead, if we send  $\theta \rightarrow 0$ , and approximate  $\cos \theta \rightarrow 1$ , and  $1 - \cos \theta \rightarrow \theta^2/2$ , we get the estimate of the final, ultra-relativistic cross section at low angles:

$$\begin{aligned} \frac{d\sigma}{d\Omega} &= \frac{2\alpha^2}{|s|} \frac{1}{\theta^2} - \frac{\alpha}{16\pi} \frac{g_e g_\gamma}{\Lambda^2} = \\ &= \frac{d\sigma}{d\Omega} \Big|_{\text{QED}} \left[ 1 - \frac{|s|}{32\pi} \frac{g_e g_\gamma}{\alpha \Lambda^2} \theta^2 \right] \end{aligned} \quad (10.58)$$

numerically estimated to be:

$$\frac{d\sigma}{d\Omega} = \frac{d\sigma}{d\Omega} \Big|_{\text{QED}} \left[ 1 - \left( 1.4 \times 10^{-11} \text{ MeV}^{-2} \right) |s| \theta^2 \right] \quad (10.59)$$

as  $\theta \rightarrow 0$ , relative spin 2 correction vanishes (it stays constant, while QED contribution diverges).

## 10.3 Testing spin 2 for annihilation

### 10.3.1 Behavior of annihilation cross section

We report the graphs displaying the behavior of the corrected annihilation into two photons in Figure 28 and Figure 29: In Figure 28, you can see how spin 2 corrections grow quite fast. We range from 8 orders of magnitude

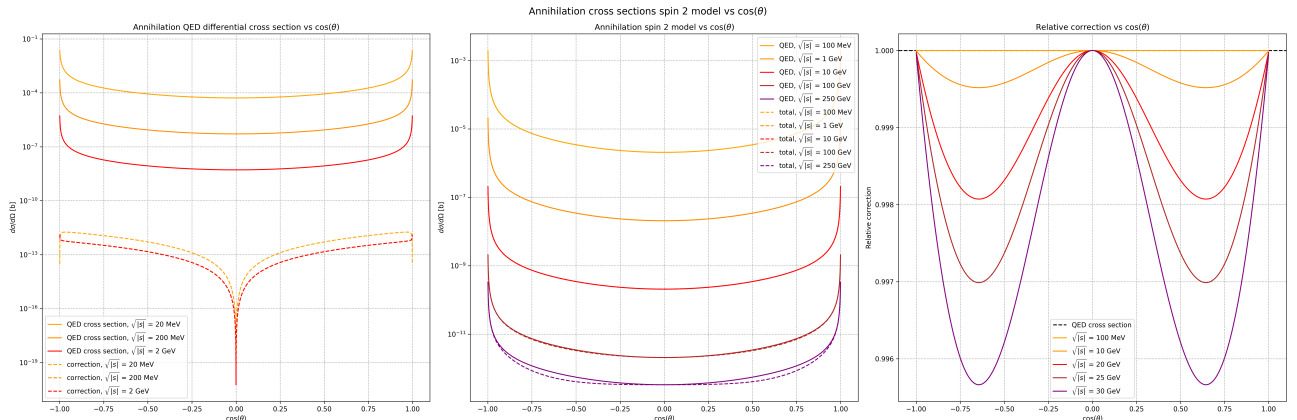


Figure 28: Graph of behavior of annihilation corrections as a function of the scattering angle  $\cos \theta$ . On the left, we plot separately both the QED result and the actual spin 2 correction (dashed line), for different values of the center of mass energy  $\sqrt{|s|}$ . In the middle, comparison between QED differential cross section and total cross section (including spin 2 correction), for different fixed  $\sqrt{|s|}$ . On the right, relative correction to the QED cross section of the total (QED + spin 2) cross section, always at different energetic values for  $\sqrt{|s|}$ .

ratio (at a few MeV) to 5 orders of magnitude (at 2 GeV).

- Dependence from the angle stays the same for QED cross section, due to Equation D.25, and it goes down with energy. It is also symmetric in  $\cos \theta$ , and it diverges when  $\cos \theta \rightarrow \pm 1$ , which is the forward scattering limit (from Equation D.28, it goes like  $1/\theta^2$ ).

- For the correction, instead, the dependence shows a vanishing behavior for  $\cos\theta = 0$ , as we have talked about. At  $\mathcal{O}(\text{GeV})$ , it produces a constant correction in the angle (see [Equation 10.55](#)).
- In the middle graph, corrections start to become visible at  $\mathcal{O}(100 \text{ GeV})$ . On the right, a more than 0.4% correction at large angles at 30 GeV is visible (as [Equation 10.56](#) confirms). However, small scattering angle corrections are zero, because QED cross section diverges, while spin 2 correction stays constant (see [Equation 10.58](#)).
- On the right, we can see that relative correction is null for  $\cos\theta = \pm 1$ , because QED cross section diverges, while correction does not, and at  $\cos\theta = 0$ , as spin 2 correction vanishes altogether. The maximum value for the correction (negative) is for  $\cos\theta = \pm 0.64$ , and the angular factor is around 0.17. This yields the 0.2% correction at  $\sqrt{|s|} = 20 \text{ GeV}$  we mentioned earlier.

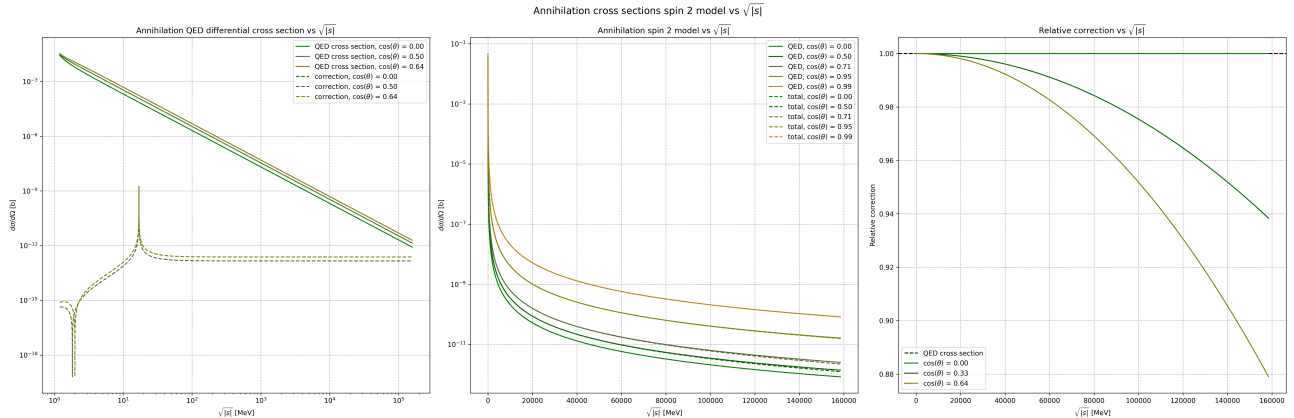


Figure 29: Graph of behavior of annihilation corrections as a function of the center of mass energy  $\sqrt{|s|}$ . On the left, we plot separately both the QED result and the actual spin 2 correction (dashed line), for different values of the  $\cos\theta$ . In the middle, comparison between QED differential cross section and total cross section (including spin 2 correction), for different fixed  $\cos\theta$ . On the right, relative correction to the QED cross section of the total (QED + spin 2) cross section, always at different angular values for  $\cos\theta$ .

In [Figure 29](#), we get the behavior we discussed in this section.

- In the left image, for the QED part, you can immediately see that at very low energies  $\sqrt{|s|} \ll m_e$ , we get a constant cross section, while when  $\sqrt{|s|} \gg m_e$  the cross section scales like  $1/|s|$ , as we can see in log scale.
- There are three main features for the spin 2 correction that are visible on the left image. First, when  $\sqrt{|s|} = 4m_e/\sqrt{3} \approx 1.67 \text{ MeV}$ , correction vanishes<sup>23</sup> (see [Equation 10.13](#)). Then, when  $\sqrt{|s|} = m_X$  from [Equation 10.16](#), correction is infinite for every angle. After the resonance, instead, correction stays constant in energy (see [Equation 10.55](#)). Finally, you can see that the line representing  $\cos\theta = 0$  is absent. That's because  $g(E, 0) = 0$ , and in log scale means a horizontal line at  $-\infty$ , which is not shown in graph.
- So, the graph in the middle has a correction that becomes relevant in the  $\mathcal{O}(100 \text{ GeV})$  region, as the relative correction grows like  $|s|$ . At  $\mathcal{O}(100 \text{ GeV})$ , spin 2 correction is at most about 5% of the QED contribution at tree level.

One could ask why for Compton scattering we get so corrections that are so small, and for annihilation we get corrections that are so large, when their amplitudes are actually linked thanks to crossing symmetry. The reality is that Compton corrections would be huge if the unit was  $\sqrt{|s|}$  instead of  $\omega$ . If  $\sqrt{|s|} = 100 \text{ GeV}$ , then the  $\omega$  that gives that center of mass is  $10^7 \text{ GeV}$ , for which Compton correction is dominant. Unfortunately, with the electron at rest, the scale at which experiments are usually performed is  $\omega \approx \mathcal{O}(\text{GeV})$ .

### 10.3.2 Annihilation experimental results

Actual, useful experimental results are:

- The limit in energy is still not much above the GeV, because of unitarity violation of the cross section. Suppose we could exceed the energy limit, just to see what happens. Then, we could use Belle II result

<sup>23</sup>Value is not exact and it is a bit dependent on  $\cos\theta$ . We neglected that dependence when we assumed  $\beta \rightarrow 0$ .

([56]), from KEK  $B$ -meson factory in Japan. They claim a precision of 0.6%, for large angle annihilation into two photons, at a center of mass energy of 10.58 GeV. Our prediction at that energy, by [Equation 10.56](#), is 50 ppb, which is way lower than experimental precision. However, we are in a range of energies for which squared modulus is actually dominant (it depends on  $g_e^2 g_\gamma^2 / \Lambda^4$ , but grows like  $s^3$ ). Looking at [Equation D.44](#), where we also calculate that contribution, relative correction is 0.04%, only 1 order of magnitude off the experimental result.

- In a physical scenario for  $X$ , one needs to go to lower energies, too high in energy (as 20 – 50 MeV is the limit), is still the OLYMPUS Collaboration, at  $\sqrt{|s|} = 44$  MeV, for which a 1% precision is reported ([54]).

However, there is a problem: the scattering angle that the OLYMPUS Collaboration measures is  $\theta = 90^\circ$ , for which our spin 2 interference terms vanish ([Equation 10.56](#)). This implies that, once again, we need to rely on squared modulus corrections: using [Equation D.44](#), our prediction for the spin 2 correction is actually  $\mathcal{O}(10^{-17})$ , so 15 orders of magnitude smaller than what we can see, unfortunately. So, it is even worse than Compton scattering, in the end.

## 11 Correction to two-photon scattering

We are missing a  $g_\gamma$  only constraint. The easiest process involving only photons is the photon-photon elastic scattering (sometimes referred to as Light-by-Light scattering, but we call it two-photon scattering), which is a one-loop (fourth order in perturbation theory) process.

Let us repeat what we did in [section 6](#), [section 7](#), [section 9](#) and [section 10](#), but for the process:  $\gamma\gamma \rightarrow \gamma\gamma$ . The contributing diagrams for this process are the *s-channel*, *t-channel* and *u-channel*, contributing at one loop in [Figure 30](#). We left the photon polarizations not contracted, and because of that we needed to select Lorentz

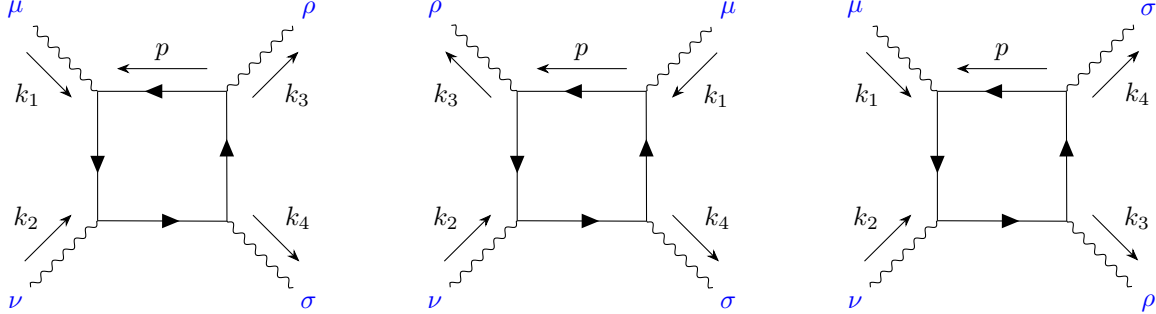


Figure 30: Three diagrams for loop contribution in QED for two-photon scattering. On the left, *s*-channel (hereafter called  $M_{\mu\nu\rho\sigma}^s$ ), in the middle *t*-channel (hereafter called  $M_{\mu\nu\rho\sigma}^t$ ) and on the right *u*-channel (hereafter called  $M_{\mu\nu\rho\sigma}^u$ ). The diagrams with inverted fermion arrows are not drawn, and are already taken in [subsection E.1](#).

indices for the photon legs.

We now add the diagrams for which the  $X$  boson is mediated, contributing *at tree level*, for which there is a *s-channel*, *t-channel* and *u-channel*, because  $X \rightarrow \gamma\gamma$  is a tree level coupling. Contributions are shown in [Figure 31](#): Here, we will be contracting with photon polarizations right away, so there is no need to write

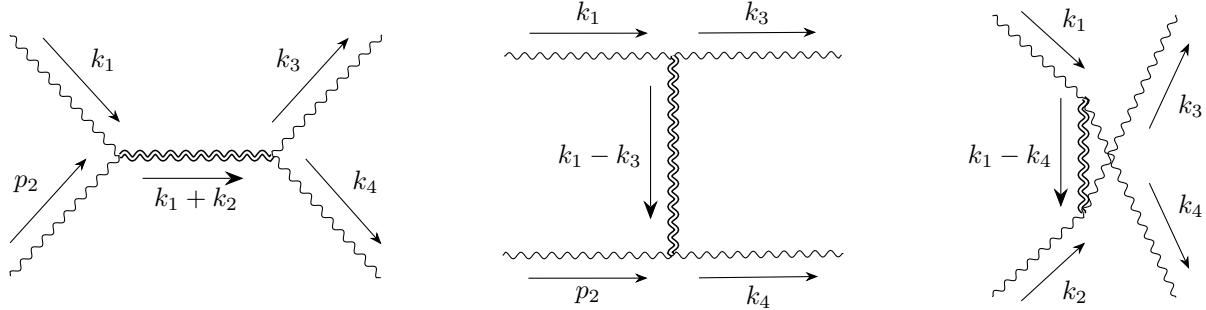


Figure 31: Tree level diagram for the mediation of massive spin 2 boson for two-photon scattering, accounting for a *s*-channel (on the left), *t*-channel (in the middle) and *u*-channel (on the right) contribution. These amplitudes will be referred respectively as  $\mathcal{M}^s$ ,  $\mathcal{M}^t$  and  $\mathcal{M}^u$ .

indices in the diagrams.

Let us write QED amplitudes before photon polarization contractions:

$$M_{\mu\nu\rho\sigma}^{\text{QED},s} = -2(-ie)^4 \int \frac{d^4 p}{(2\pi)^4 i} \frac{I_{\mu\rho\sigma\nu}(p, p+k_3, p+k_1+k_2, p+k_1)}{[p^2 + m_e^2] [(p+k_3)^2 + m_e^2] [(p+k_1+k_2)^2 + m_e^2] [(p+k_1)^2 + m_e^2]} \quad (11.1)$$

$$M_{\mu\nu\rho\sigma}^{\text{QED},t} = -2(-ie)^4 \int \frac{d^4 p}{(2\pi)^4 i} \frac{I_{\rho\mu\sigma\nu}(p, p-k_1, p-k_3+k_2, p-k_3)}{[p^2 + m_e^2] [(p-k_1)^2 + m_e^2] [(p-k_3+k_2)^2 + m_e^2] [(p-k_3)^2 + m_e^2]} \quad (11.2)$$

$$M_{\mu\nu\rho\sigma}^{\text{QED},u} = -2(-ie)^4 \int \frac{d^4 p}{(2\pi)^4 i} \frac{I_{\mu\sigma\rho\nu}(p, p+k_4, p+k_1+k_2, p+k_1)}{[p^2 + m_e^2] [(p+k_4)^2 + m_e^2] [(p+k_1+k_2)^2 + m_e^2] [(p+k_1)^2 + m_e^2]} \quad (11.3)$$

where:

$$I_{\mu\nu\rho\sigma}(k_1, k_2, k_3, k_4) = \text{Tr} \left[ \gamma_\mu (-ik_1 + m_e) \gamma_\nu (-ik_2 + m_e) \gamma_\rho (-ik_3 + m_e) \gamma_\sigma (-ik_4 + m_e) \right] \quad (11.4)$$

is the loop function in the most generic form. Now, these amplitudes are treated in the Appendices (see [Appendix E](#)), and we will not be repeating calculations for those amplitudes here.

So, let us focus on the spin 2 correcting tree level amplitudes, using the Feynman rule derived in [subsection 4.3](#):

$$\mathcal{M}^s = \left[ \frac{g_\gamma}{\Lambda} \right]^2 \Pi_{\alpha\beta\mu\nu}(-k_1, -k_2) \left[ \frac{N_{\alpha\beta\gamma\delta}(k_1 + k_2)}{(k_1 + k_2)^2 + m_X^2} \right] \Pi_{\gamma\delta\rho\sigma}(k_3, k_4) \varepsilon_\mu(k_1, \lambda_1) \varepsilon_\nu(k_2, \lambda_2) \bar{\varepsilon}_\rho(k_3, \lambda_3) \bar{\varepsilon}_\sigma(k_4, \lambda_4) \quad (11.5)$$

$$\mathcal{M}^t = \left[ \frac{g_\gamma}{\Lambda} \right]^2 \Pi_{\alpha\beta\mu\rho}(-k_1, k_3) \left[ \frac{N_{\alpha\beta\gamma\delta}(k_1 - k_3)}{(k_1 - k_3)^2 + m_X^2} \right] \Pi_{\gamma\delta\nu\sigma}(-k_2, k_4) \varepsilon_\mu(k_1, \lambda_1) \varepsilon_\nu(k_2, \lambda_2) \bar{\varepsilon}_\rho(k_3, \lambda_3) \bar{\varepsilon}_\sigma(k_4, \lambda_4) \quad (11.6)$$

$$\mathcal{M}^u = \left[ \frac{g_\gamma}{\Lambda} \right]^2 \Pi_{\alpha\beta\mu\sigma}(-k_1, k_4) \left[ \frac{N_{\alpha\beta\gamma\delta}(k_1 - k_4)}{(k_1 - k_4)^2 + m_X^2} \right] \Pi_{\gamma\delta\nu\rho}(-k_2, k_3) \varepsilon_\mu(k_1, \lambda_1) \varepsilon_\nu(k_2, \lambda_2) \bar{\varepsilon}_\rho(k_3, \lambda_3) \bar{\varepsilon}_\sigma(k_4, \lambda_4) \quad (11.7)$$

where  $\lambda_i$  with  $i \in \{1, 2, 3, 4\}$  are photon polarizations. Here forth, we will call  $\varepsilon_i^{\lambda_i}$  these polarizations. Each amplitude  $\mathcal{M} = \mathcal{M}_{\lambda_1\lambda_2\lambda_3\lambda_4}$  is dependent on the polarization of photons.

In [\[27\]](#) and [\[67\]](#), QED results of amplitudes are given with specific choices of polarizations (in circular polarization basis), in the center of mass frame. We will have to do the same in this case to match helicities between QED result and corrections. So, we will select  $\lambda_i = \pm 1 = \pm$ , where the sign represent the helicity of the photon.

In [subsection E.3](#), we calculate polarizations in this basis, in the center of mass frame. Results are reported in the following:

$$\begin{aligned} \varepsilon_1^+ &= \frac{1}{\sqrt{2}} (0, 1, i, 0)^T & \varepsilon_1^- &= \frac{1}{\sqrt{2}} (0, 1, -i, 0)^T \\ \varepsilon_2^+ &= \frac{1}{\sqrt{2}} (0, -1, i, 0)^T & \varepsilon_2^- &= \frac{1}{\sqrt{2}} (0, -1, -i, 0)^T \\ \varepsilon_3^+ &= \frac{1}{\sqrt{2}} (-\sin \theta, \cos \theta, i, 0)^T & \varepsilon_3^- &= \frac{1}{\sqrt{2}} (-\sin \theta, \cos \theta, -i, 0)^T \\ \varepsilon_4^+ &= \frac{1}{\sqrt{2}} (\sin \theta, -\cos \theta, i, 0)^T & \varepsilon_4^- &= \frac{1}{\sqrt{2}} (\sin \theta, -\cos \theta, -i, 0)^T \end{aligned}$$

where  $\theta$  is the scattering angle between  $k_1$  and  $k_3$ . All possible scalar products can be found in [subsection E.3](#).

Amplitudes in QED are usually reported dependent on Mandelstam variables  $s, t, u$ , and with a specific choice of helicities, which implies that we ought to do the same, selecting helicities for photons to calculate every contribution to add to QED at amplitude level. We proved in [subsection E.2](#) that there are 5 independent possibilities for the choice of helicities:  $\mathcal{M}_{++++}, \mathcal{M}_{++--}, \mathcal{M}_{+-+-}, \mathcal{M}_{+-+}, \mathcal{M}_{++-}$ , where we define:

$$\mathcal{M}_{\lambda_1\lambda_2\lambda_3\lambda_4} = \mathcal{M}_{\lambda_1\lambda_2\lambda_3\lambda_4}^s + \mathcal{M}_{\lambda_1\lambda_2\lambda_3\lambda_4}^t + \mathcal{M}_{\lambda_1\lambda_2\lambda_3\lambda_4}^u$$

the total spin 2 contribution for each channel. These are summed according to [Equation E.25](#):

$$\begin{aligned} |\overline{M}_{fi}|^2 &= \frac{1}{4} \sum_{\lambda_1} \sum_{\lambda_2} \sum_{\lambda_3} \sum_{\lambda_4} |M_{\lambda_1\lambda_2\lambda_3\lambda_4}(s, t, u)|^2 = \\ &= \frac{1}{4} \left[ 2|M_{++++}|^2 + 2|M_{++--}|^2 + 2|M_{+-+-}|^2 + 2|M_{+-+}|^2 + 8|M_{++-}|^2 \right] \end{aligned} \quad (11.8)$$

which sum up the 16 total possibilities for helicities. We are referring to:

$$M_{\lambda_1\lambda_2\lambda_3\lambda_4} = M_{\lambda_1\lambda_2\lambda_3\lambda_4}^{\text{QED}} + \mathcal{M}_{\lambda_1\lambda_2\lambda_3\lambda_4}$$

where the QED contributions reported in [subsection E.2](#) are called  $M^{\text{QED}}$  in this chapter (while in the Appendices they are just  $M$ ).

We have the QED result, and we need the spin 2 correction result. To carry out calculations, since we are now accustomed to letting a computer do all the hard work, we implemented a `FORM` code, linked in the GitHub repository in [subsection G.1](#), called `Twophoton_onlyX_xigauge.frm`. The code returns  $\mathcal{M}_{\lambda_1\lambda_2\lambda_3\lambda_4}$  for all possible independent choices of photon polarizations (read the instructions of the code to know how to substitute polarizations). All the scalar products in [subsection E.3](#) have been implemented in the code. Two remarks are needed here:

- The Feynman rule  $X \rightarrow \gamma\gamma$  has been implemented in the  $\xi$  gauge. However, you can check easily (removing all polarizations from the returned local variable in the code) that the result is always  $\xi$  independent.
- Again, we have no check for our calculations, because we did not find any corroborating result in literature. However, there are some checks that we can carry out to at least convince ourselves that result might just be correct. One check is the kinematics structure arising from the choice of polarizations, that matches the structure of QED results given in subsection E.2, and the other check consists of *Ward identities*. Because of gauge invariance:

$$k_{1,\mu} M_{\mu\nu\rho\sigma} = k_{2,\nu} M_{\mu\nu\rho\sigma} = k_{3,\rho} M_{\mu\nu\rho\sigma} = k_{4,\sigma} M_{\mu\nu\rho\sigma} = 0 \quad (11.9)$$

However, thanks to Equation E.13, we know that Ward identities are satisfied in QED amplitudes only:

$$k_{1,\mu} M_{\mu\nu\rho\sigma}^{\text{QED}} = k_{2,\nu} M_{\mu\nu\rho\sigma}^{\text{QED}} = k_{3,\rho} M_{\mu\nu\rho\sigma}^{\text{QED}} = k_{4,\sigma} M_{\mu\nu\rho\sigma}^{\text{QED}} = 0 \quad (11.10)$$

which means that, individually, our spin 2 amplitudes at tree level must satisfy Ward identities, as well:

$$k_{1,\mu} \mathcal{M}_{\mu\nu\rho\sigma} = k_{2,\nu} \mathcal{M}_{\mu\nu\rho\sigma} = k_{3,\rho} \mathcal{M}_{\mu\nu\rho\sigma} = k_{4,\sigma} \mathcal{M}_{\mu\nu\rho\sigma} = 0 \quad (11.11)$$

where we call  $\mathcal{M}_{\mu\nu\rho\sigma}$  the sum of the diagrams in Figure 31 before contracting with photon polarizations.

Our code `Twophoton_onlyX_xigauge.frm` easily verifies them: by substituting  $k_{1,\mu}$  (or any other momentum, for that matter) in place of  $\varepsilon_{1,\mu}$ , we get 0, as expected<sup>24</sup>.

Finally, we need to stress that without kinematics scalar products imposed, our code returns hundreds of terms. This leaves no choice but to integrate in phase space first, to fix kinematics, and simplify the result. This means that we use Equation E.39:

$$\frac{d\sigma}{d\Omega} = \frac{|\bar{M}_{fi}|^2}{256\pi^2\omega^2} \quad (11.12)$$

And now, code outputs simplify significantly.

## 11.1 Simplifying two-photon result

Notice that, when applying barred to the polarizations in our  $\varepsilon_i$ , polarizations swap, as the  $i$  factor changes sign:  $\bar{\varepsilon}_i^\pm = \varepsilon_i^\mp$ . Because, however, our code does not register complex polarizations, we have to implement the "bar" manually, selecting opposing helicities to begin with. Let us see the results, to understand what we mean<sup>25</sup>.

**$\mathcal{M}_{++++}$ :** To obtain this amplitude, substitute in the code the polarizations  $\varepsilon_1^+, \varepsilon_2^+, \varepsilon_3^-, \varepsilon_4^-$ , because exiting photons are barred and helicities are swapped. Here is the result:

$$\begin{aligned} \mathcal{M}_{++++}(s, t, u) = & \frac{g_\gamma^2}{6\Lambda^2} \left[ \frac{A_t(s, t, u)}{m_X^4(t + m_X^2)} + \frac{A_u(s, t, u)}{m_X^4(u + m_X^2)} + \frac{B_t(s, t, u)}{m_X^2(t + m_X^2)} \right. \\ & \left. + \frac{B_u(s, t, u)}{m_X^2(u + m_X^2)} + \frac{C_t(s, t, u)}{t + m_X^2} + \frac{C_u(s, t, u)}{u + m_X^2} + \frac{3D_s(s, t, u)}{s + m_X^2} \right] \end{aligned} \quad (11.13)$$

$$\begin{aligned} A_t(s, t, u) = & -\frac{t^3 u^3}{s^2} - \frac{2t^4 u^2}{s^2} - \frac{t^5 u}{s^2} + t^3 u + t^4 = \\ = & -t^3 \left[ \frac{u}{s^2} (u^2 + 2ut + t^2) - (u + t) \right] = t^3 (1 - \textcolor{blue}{u} + \textcolor{blue}{t}) \left[ \frac{u}{s^2} (\textcolor{blue}{u} + \textcolor{blue}{t}) \right] = st^3 \left[ \frac{-\textcolor{blue}{u} - s}{s} \right] = t^4 \end{aligned} \quad (11.14)$$

<sup>24</sup>Ward identities have priority over kinematics, so to check them you need to comment every kinematic-dependent scalar product, and only leave  $k_i^2 = 0$  and  $k_i \cdot \varepsilon_i = 0$ . In the code, such scalar products are highlighted, to make it easier for the user.

<sup>25</sup>For manipulating Mandelstam variables, we will be using  $s + t + u = 0$  consistently. Each usage will be highlighted by blue color in the equations.

$$\begin{aligned}
B_t(s, t, u) &= -\frac{t^2 u^3}{s^2} - \frac{4t^3 u^2}{s^2} - \frac{5t^4 u}{s^2} - \frac{2t^5}{s^2} + t^2 u + t^3 = \\
&= -t^2 \left[ \frac{1}{s^2} (u^3 + 4u^2 t + 5u t^2 + 2t^3) - (u + t) \right] = t^2 (1 - \textcolor{blue}{u + t}) \left[ \frac{u^2 + 3u t + 2t^2}{s^2} \right] = \\
&= st^2 \left[ \frac{(u + 2t)(\textcolor{blue}{u + t})}{s^2} - 1 \right] = st^2 \left[ -\frac{\textcolor{blue}{u + 2t + s}}{s} \right] = -t^3
\end{aligned} \tag{11.15}$$

$$\begin{aligned}
C_t(s, t, u) &= -\frac{6tu^3}{s^2} - \frac{20t^2 u^2}{s^2} - \frac{22t^3 u}{s^2} - \frac{8t^4}{s^2} + 3t^2 = \\
&= -\frac{t}{s^2} (6u^3 + 20tu^2 + 22u^2 t + 8t^3) + 3t^2 = -\frac{2t}{s^2} (\textcolor{blue}{u + t})^2 (3u + 4t) + 3t^2 = \\
&= -6ut - 8t^2 + 3t^2 = -t(6\textcolor{blue}{u} + 5t) = t(t + 5s)
\end{aligned} \tag{11.16}$$

$$D_s(s, t, u) = u^2 + t^2 \tag{11.17}$$

and  $A_u(s, t, u) = A_t(s, u, t)$ ,  $B_u(s, t, u) = B_t(s, u, t)$ ,  $C_u(s, t, u) = C_t(s, u, t)$ . Result is:

$$\mathcal{M}_{++++}(s, t, u) = \frac{g_\gamma^2}{6\Lambda^2} \frac{1}{m_X^4} \left[ \frac{t^4 - m_X^2 t^3 + m_X^4 t(t + 5s)}{t + m_X^2} + \frac{u^4 - m_X^2 u^3 + m_X^4 u(u + 5s)}{u + m_X^2} + \frac{3m_X^4 (u^2 + t^2)}{s + m_X^2} \right] \tag{11.18}$$

Notice that  $\mathcal{M}_{++++}(s, t, u) = \mathcal{M}_{++++}(s, u, t)$ , because of crossing symmetry argument [Equation E.28](#).

**$\mathcal{M}_{+++-}$ :** To obtain this amplitude, substitute in the code the polarizations  $\varepsilon_1^+, \varepsilon_2^+, \varepsilon_3^-, \varepsilon_4^+$ . Here is the result:

$$\mathcal{M}_{+++-}(s, t, u) = -\frac{g_\gamma^2}{6\Lambda^2} \frac{1}{m_X^4 (t + m_X^2)} \left[ \left( \frac{t}{m_X^2} + 1 \right) E_t(s, t, u) \right] \tag{11.19}$$

$$\begin{aligned}
E_t(s, t, u) &= \frac{tu^4}{s^2} + \frac{3t^2 u^3}{s^2} + \frac{3t^3 u^2}{s^2} + \frac{ut^4}{s^2} + \frac{2tu^3}{s} + \frac{4t^2 u^2}{s} + \frac{2t^3 u}{s} + tu^2 + t^2 u = \\
&= \frac{tu}{s^2} (\textcolor{blue}{u + t})^3 + \frac{2tu}{s} (\textcolor{blue}{u + t})^2 + ut(\textcolor{blue}{u + t}) = -uts + 2uts - uts = 0
\end{aligned} \tag{11.20}$$

Result is:

$$\mathcal{M}_{+++-}(s, t, u) = 0 \tag{11.21}$$

So, while the QED loop result in [Equation E.40](#) is negligible because always subdominant with respect to the others, the spin 2 correction result is identically 0 at tree level.

**$\mathcal{M}_{++--}$ :** To obtain this amplitude, substitute in the code the polarizations  $\varepsilon_1^+, \varepsilon_2^+, \varepsilon_3^+, \varepsilon_4^+$ . Here is the result:

$$\mathcal{M}_{++--}(s, t, u) = \frac{g_\gamma^2}{2\Lambda^2} \left[ \frac{F_t(s, t, u)}{t + m_X^2} + \frac{F_u(s, t, u)}{u + m_X^2} \right] \tag{11.22}$$

$$\begin{aligned}
F_t(s, t, u) &= \frac{u^4}{s^2} + \frac{4tu^3}{s^2} + \frac{6t^2 u^2}{s^2} + \frac{4t^3 u}{s^2} + \frac{t^4}{s} + u^2 = \\
&= \frac{1}{s^2} (\textcolor{blue}{u + t})^4 + u^2 = s^2 + u^2
\end{aligned} \tag{11.23}$$

And  $F_u(s, t, u) = F_t(s, u, t)$ . Result is:

$$\mathcal{M}_{++--}(s, t, u) = \frac{g_\gamma^2}{2\Lambda^2} \left[ \frac{u^2 + s^2}{t + m_X^2} + \frac{s^2 + t^2}{u + m_X^2} + \frac{t^2 + u^2}{s + m_X^2} \right] \tag{11.24}$$

which is perfectly symmetric under any Mandelstam variable exchange. This is the same structure that is found in the QED result for  $M_{+-+}^{\text{QED}}$ , in [Equation E.40](#).

$\mathcal{M}_{+-+}$ : To obtain this amplitude, substitute in the code the polarizations  $\varepsilon_1^+, \varepsilon_2^-, \varepsilon_3^-, \varepsilon_4^+$ . Code result is:

$$\begin{aligned}\mathcal{M}_{+-+}(s, t, u) &= \frac{g_\gamma^2}{6\Lambda^2} \left[ \frac{A_t(s, t, u)}{m_X^4(t + m_X^2)} + \frac{A_s(s, t, u)}{m_X^4(s + m_X^2)} + \frac{B_t(s, t, u)}{m_X^2(t + m_X^2)} \right. \\ &\quad \left. + \frac{B_s(s, t, u)}{m_X^2(s + m_X^2)} + \frac{C_t(s, t, u)}{t + m_X^2} + \frac{C_s(s, t, u)}{s + m_X^2} + \frac{3D_u(s, t, u)}{u + m_X^2} \right] = \dots \\ &= \frac{g_\gamma^2}{6\Lambda^2} \frac{1}{m_X^4} \left[ \frac{t^4 - m_X^2 t^3 + m_X^4 t(t + 5u)}{t + m_X^2} + \frac{s^4 - m_X^2 s^3 + m_X^4 s(s + 5u)}{s + m_X^2} + \frac{3m_X^4 (s^2 + t^2)}{u + m_X^2} \right]\end{aligned}\tag{11.25}$$

which verifies the crossing symmetry argument in [Equation E.27](#), as  $\mathcal{M}_{+-+}(s, t, u) = \mathcal{M}_{++++}(u, t, s)$ .

$\mathcal{M}_{+-+}$ : To obtain this amplitude, substitute in the code the polarizations  $\varepsilon_1^+, \varepsilon_2^-, \varepsilon_3^+, \varepsilon_4^-$ . Code result is:

$$\begin{aligned}\mathcal{M}_{+-+}(s, t, u) &= \frac{g_\gamma^2}{6\Lambda^2} \left[ \frac{A_s(s, t, u)}{m_X^4(s + m_X^2)} + \frac{A_u(s, t, u)}{m_X^4(u + m_X^2)} + \frac{B_s(s, t, u)}{m_X^2(s + m_X^2)} \right. \\ &\quad \left. + \frac{B_u(s, t, u)}{m_X^2(u + m_X^2)} + \frac{C_s(s, t, u)}{s + m_X^2} + \frac{C_u(s, t, u)}{u + m_X^2} + \frac{3D_t(s, t, u)}{t + m_X^2} \right] = \dots \\ &= \frac{g_\gamma^2}{6\Lambda^2} \frac{1}{m_X^4} \left[ \frac{s^4 - m_X^2 s^3 + m_X^4 s(s + 5t)}{s + m_X^2} + \frac{u^4 - m_X^2 u^3 + m_X^4 u(u + 5t)}{u + m_X^2} + \frac{3m_X^4 (u^2 + s^2)}{t + m_X^2} \right]\end{aligned}\tag{11.26}$$

which verifies the crossing symmetry argument in [Equation E.26](#), as  $\mathcal{M}_{+-+}(s, t, u) = \mathcal{M}_{++++}(t, s, u)$ .

To compare results with QED, we need to take matching limits:

**Non-relativistic limit:** If we send  $\omega/m_e \rightarrow 0$ , so  $|s|, t, u \ll m_e^2 \ll m_X^2$ , then amplitudes are approximated like this:

$$\begin{aligned}\mathcal{M}_{++++}(s, t, u) &= \frac{g_\gamma^2}{6\Lambda^2} \frac{1}{m_X^2} [t^2 + 5st + u^2 + 5su + 3u^2 + 3t^2] = \frac{g_\gamma^2}{6\Lambda^2} \frac{1}{m_X^2} [4(t^2 + u^2) - 5s^2] \\ \mathcal{M}_{+-+}(s, t, u) &= \dots = \frac{g_\gamma^2}{6\Lambda^2} \frac{1}{m_X^2} [4(s^2 + t^2) - 5u^2] \\ \mathcal{M}_{+-+}(s, t, u) &= \dots = \frac{g_\gamma^2}{6\Lambda^2} \frac{1}{m_X^2} [4(u^2 + s^2) - 5t^2] \\ \mathcal{M}_{+-+}(s, t, u) &= \frac{g_\gamma^2}{\Lambda^2} \left[ \frac{s^2 + t^2 + u^2}{m_X^2} \right]\end{aligned}$$

while  $\mathcal{M}_{++-}(s, t, u) = 0$ . Now, add the results from QED, to get the squared amplitude. Because these amplitudes are all real, from [Equation 11.8](#) and setting  $M_{++-} = 0$  from QED and spin 2 correction:

$$\begin{aligned}|\overline{M}_{fi}|^2 &= \frac{1}{4} \sum_{\lambda_1} \sum_{\lambda_2} \sum_{\lambda_3} \sum_{\lambda_4} |M_{\lambda_1 \lambda_2 \lambda_3 \lambda_4}(s, t, u)|^2 = \\ &= \frac{1}{2} \left[ |M_{++++}^{\text{QED}}|^2 + |M_{++-}^{\text{QED}}|^2 + |M_{+-+}^{\text{QED}}|^2 + |M_{+-+}^{\text{QED}}|^2 + \right. \\ &\quad \left. + |\cancel{\mathcal{M}}_{++++}|^2 + |\cancel{\mathcal{M}}_{++-}|^2 + |\cancel{\mathcal{M}}_{+-+}|^2 + |\cancel{\mathcal{M}}_{+-+}|^2 \right] \\ &\quad + M_{++++}^{\text{QED}} \mathcal{M}_{++++} + M_{++-}^{\text{QED}} \mathcal{M}_{++-} + M_{+-+}^{\text{QED}} \mathcal{M}_{+-+} + M_{+-+}^{\text{QED}} \mathcal{M}_{+-+} \tag{11.27}\end{aligned}$$

because  $g_\gamma$  is small, we will neglect squared moduli of  $\mathcal{M}$  amplitudes, and only select interference terms as corrections. QED part will yield [Equation E.42](#), while the rest will be manipulated using cyclic Mandelstam variables properties in [Equation E.32](#) and [Equation E.33](#)<sup>26</sup>:

$$\begin{aligned}
|\overline{M}_{fi}|^2 &= \frac{256}{4} \frac{139 \alpha^4 \omega^8}{90^2 m_e^8} (3 + \cos^2 \theta)^2 + \frac{g_\gamma^2}{15 \Lambda^2} \frac{\alpha^2}{m_e^4 m_X^2} (s^2 + t^2 + u^2)^2 \\
&\quad + \frac{11 g_\gamma^2}{270 \Lambda^2} \frac{\alpha^2}{m_e^4 m_X^2} \left[ s^2 (4t^2 + 4u^2 - 5s^2) + t^2 (4s^2 + 4u^2 - 5t^2) + u^2 (4s^2 + 4t^2 - 5u^2) \right] = \\
&= \frac{256}{4} \frac{139 \alpha^4 \omega^8}{90^2 m_e^8} (3 + \cos^2 \theta)^2 + \frac{g_\gamma^2}{15 \Lambda^2} \frac{\alpha^2}{m_e^4 m_X^2} (s^2 + t^2 + u^2)^2 \\
&\quad + \frac{11 g_\gamma^2}{270 \Lambda^2} \frac{\alpha^2}{m_e^4 m_X^2} \left[ 8(s^2 t^2 + t^2 u^2 + u^2 s^2) - 5(s^4 + t^4 + u^4) \right] = \\
&= \frac{256}{4} \frac{139 \alpha^4 \omega^8}{90^2 m_e^8} (3 + \cos^2 \theta)^2 + \frac{g_\gamma^2}{15 \Lambda^2} \frac{\alpha^2}{m_e^4 m_X^2} (s^2 + t^2 + u^2)^2 \\
&\quad + \frac{11 g_\gamma^2}{270 \Lambda^2} \frac{\alpha^2}{m_e^4 m_X^2} \left[ 4(s^2 + t^2 + u^2)^2 - 9(s^4 + t^4 + u^4) \right] = \\
&= \frac{256}{4} \frac{139 \alpha^4 \omega^8}{90^2 m_e^8} (3 + \cos^2 \theta)^2 + \frac{g_\gamma^2}{15 \Lambda^2} \frac{\alpha^2}{m_e^4 m_X^2} \left[ \frac{13}{9} (s^2 + t^2 + u^2)^2 - \frac{11}{2} (s^4 + t^4 + u^4) \right] \\
&= \frac{256}{4} \frac{139 \alpha^4 \omega^8}{90^2 m_e^8} (3 + \cos^2 \theta)^2 + \frac{32 g_\gamma^2}{15 \Lambda^2} \frac{\alpha^2 \omega^8}{m_e^4 m_X^2} (3 + \cos^2 \theta)^2 \left[ \frac{26}{9} - \frac{11}{2} \right] = \\
&= \frac{256}{4} \frac{139 \alpha^4 \omega^8}{90^2 m_e^8} (3 + \cos^2 \theta)^2 - \frac{752 g_\gamma^2}{135 \Lambda^2} \frac{\alpha^2 \omega^8}{m_e^4 m_X^2} (3 + \cos^2 \theta)^2 = \\
&= \frac{256}{4} \frac{139 \alpha^4 \omega^8}{90^2 m_e^8} (3 + \cos^2 \theta)^2 \left[ 1 - \frac{705}{139} \frac{g_\gamma^2}{\alpha^2 \Lambda^2} \frac{m_e^4}{m_X^2} \right]
\end{aligned} \tag{11.28}$$

which, finally, yields the cross section (using [Equation 11.12](#)):

$$\begin{aligned}
\frac{d\sigma}{d\Omega} &= \frac{139 \alpha^4 \omega^6}{(180\pi)^2 m_e^8} (3 + \cos^2 \theta)^2 \left[ 1 - \frac{705}{139} \frac{g_\gamma^2}{\alpha^2 \Lambda^2} \frac{m_e^4}{m_X^2} \right] = \\
&= \left. \frac{d\sigma}{d\Omega} \right|_{\text{QED}} \left[ 1 - \frac{705}{139} \frac{g_\gamma^2}{\alpha^2 \Lambda^2} \frac{m_e^4}{m_X^2} \right]
\end{aligned} \tag{11.29}$$

Numerically, using the value in [Equation 5.44](#):

$$\frac{d\sigma}{d\Omega} = \left. \frac{d\sigma}{d\Omega} \right|_{\text{QED}} \left[ 1 - 1.5 \times 10^{-10} \right] \tag{11.30}$$

which is a constant, negative correction in energy, and very much not detectable by all accounts in the non-relativistic limit.

**Forward scattering limit:** While, for QED, the ultra-relativistic limit required only  $|s| \gg 4m_e^2$ , for these amplitudes that requirement is not enough to be in the ultra-relativistic limit, as here we need  $|s| \gg m_X^2$ . We can only set  $\theta = 0$ , and so we get  $t = 0$ , and  $u = -s = |s|$ . Then, the only independent variable in

<sup>26</sup>We will highlight in blue the expressions we will substitute.

our amplitudes will be  $x = \sqrt{|s|} = 2\omega$ . So:

$$\begin{aligned}\mathcal{M}_{++++}(x) &= \frac{g_\gamma^2}{6\Lambda^2} \frac{x^4}{m_X^4} \left[ \frac{x^4 - m_X^2 x^2 - 4m_X^4}{x^2 + m_X^2} + \frac{3m_X^4}{-x^2 + m_X^2} \right] = \\ &= \frac{g_\gamma^2}{6\Lambda^2} \frac{-x^4}{m_X^4 (m_X^4 - x^4)} [x^6 - 2m_X^2 x^4 - 6m_X^4 x^2 + m_X^6]\end{aligned}\quad (11.31)$$

$$\begin{aligned}\mathcal{M}_{+-+-}(x) &= \frac{g_\gamma^2}{6\Lambda^2} \frac{x^4}{m_X^4} \left[ \frac{x^4 + m_X^2 x^2 - 4m_X^4}{-x^2 + m_X^2} + \frac{3m_X^4}{x^2 + m_X^2} \right] \\ &= \frac{g_\gamma^2}{6\Lambda^2} \frac{x^4}{m_X^4 (m_X^4 - x^4)} [x^6 + 2m_X^2 x^4 - 6m_X^4 x^2 - m_X^6]\end{aligned}\quad (11.32)$$

$$\begin{aligned}\mathcal{M}_{+--+}(x) &= \frac{g_\gamma^2}{6\Lambda^2} \frac{x^4}{m_X^4} \left[ \frac{x^4 + m_X^2 x^2 + m_X^4}{-x^2 + m_X^2} + \frac{x^4 - m_X^2 x^2 + m_X^4}{x^2 + m_X^2} + 6m_X^2 \right] = \\ &= \frac{g_\gamma^2}{3\Lambda^2} \frac{x^4}{m_X^2} \left[ \frac{4m_X^4 - x^4}{m_X^4 - x^4} \right]\end{aligned}\quad (11.33)$$

$$\begin{aligned}\mathcal{M}_{+---}(x) &= -\frac{g_\gamma^2}{2\Lambda^2} \left[ \frac{2x^4}{m_X^2} + \frac{x^4}{m_X^2 + x^2} + \frac{x^4}{m_X^2 - x^2} \right] = \\ &= \frac{g_\gamma^2}{2\Lambda^2} \frac{x^4}{m_X^2} \left[ 2 + \frac{m_X^2}{m_X^2 + x^2} + \frac{m_X^2}{m_X^2 - x^2} \right] = \frac{g_\gamma^2}{\Lambda^2} \frac{x^4}{m_X^2} \left[ \frac{2m_X^4 - x^4}{m_X^4 - x^4} \right]\end{aligned}\quad (11.34)$$

while  $\mathcal{M}_{+++-}(x) = 0$ .  $\mathcal{M}_{+--+}$  and  $\mathcal{M}_{+---}$  are subdominant, as they will grow as  $x^4$  and not as  $x^8$  in the ultra-relativistic limit. Remember that  $x = \sqrt{|s|} > 0$ . There are a few notable values for  $x$ :

- Every amplitude diverges at resonance, for  $x = \sqrt{|s|} = m_X$ . Because the resonance is very narrow, we do not expect any experiment to see this easily (only a few exceptions, like [7] in the future).
- $\mathcal{M}_{++++} = 0$  for  $\sqrt{|s|} = 6.75$  MeV and  $\sqrt{|s|} = 32.1$  MeV.
- $\mathcal{M}_{+-+-} = 0$  only for  $\sqrt{|s|} = 22.4$  MeV.
- $\mathcal{M}_{+--+} = 0$  only for  $\sqrt{|s|} = \sqrt{2}m_X = 24.0$  MeV.
- $\mathcal{M}_{+---} = 0$  only for  $\sqrt{|s|} = \sqrt[4]{2}m_X = 20.1$  MeV.

Now, because  $M_{+--+}^{\text{QED}} = M_{+---}^{\text{QED}} = 0$  in this limit, we will calculate the total  $M_{fi}$  amplitude as:

$$\begin{aligned}|\overline{M}_{fi}|^2 &= \frac{1}{4} \sum_{\lambda_1} \sum_{\lambda_2} \sum_{\lambda_3} \sum_{\lambda_4} |M_{\lambda_1 \lambda_2 \lambda_3 \lambda_4}(s, t, u)|^2 = \\ &= \frac{1}{2} \left[ |M_{++++}^{\text{QED}}|^2 + |M_{+-+-}^{\text{QED}}|^2 + |\mathcal{M}_{+--+}|^2 + |\mathcal{M}_{+--+}|^2 + |\mathcal{M}_{+---}|^2 + |\mathcal{M}_{+---}|^2 \right] \\ &\quad + M_{++++}^{\text{QED}} \mathcal{M}_{++++} + M_{+-+-}^{\text{QED}} \mathcal{M}_{+-+-}\end{aligned}\quad (11.35)$$

where we decided to keep moduli squared to compare helicity-fixed spin 2 correction terms, and because at high energies, squared moduli will be dominant (even if not physical). For the QED part, we employ

Equation E.48.

$$\begin{aligned}
|\overline{M}_{fi}|^2 &= 256\alpha^4 \log^4 \left( \frac{x}{2m_e} \right) + \frac{1}{2} \frac{g_\gamma^4}{9\Lambda^4} \frac{x^8}{m_X^4} \left[ \frac{4m_X^4 - x^4}{m_X^4 - x^4} \right]^2 + \frac{1}{2} \frac{g_\gamma^4}{\Lambda^4} \frac{x^8}{m_X^4} \left[ \frac{2m_X^4 - x^4}{m_X^4 - x^4} \right]^2 \\
&\quad + \frac{1}{2} \frac{g_\gamma^4}{36\Lambda^4} \frac{x^8}{m_X^8} \left[ \frac{x^6 - 2m_X^2x^4 - 6m_X^4x^2 + m_X^6}{m_X^4 - x^4} \right]^2 + \frac{1}{2} \frac{g_\gamma^4}{36\Lambda^4} \frac{x^8}{m_X^8} \left[ \frac{x^6 + 2m_X^2x^4 - 6m_X^4x^2 - m_X^6}{m_X^4 - x^4} \right]^2 \\
&\quad + \frac{8}{3} \frac{\alpha^2 g_\gamma^2}{\Lambda^2} \log^2 \left( \frac{x}{2m_e} \right) \frac{x^4}{m_X^4} \left[ \frac{x^8 - 2m_X^2x^4 - 6m_X^4x^2 + m_X^6}{m_X^4 - x^4} \right] \\
&\quad - \frac{8}{3} \frac{\alpha^2 g_\gamma^2}{\Lambda^2} \log^2 \left( \frac{x}{2m_e} \right) \frac{x^4}{m_X^4} \left[ \frac{x^8 + 2m_X^2x^4 - 6m_X^4x^2 - m_X^6}{m_X^4 - x^4} \right] = \\
&= 256\alpha^4 \log^4 \left( \frac{x}{2m_e} \right) + \frac{16}{3} \frac{\alpha^2 g_\gamma^2}{\Lambda^2} \log^2 \left( \frac{x}{2m_e} \right) \frac{x^4}{m_X^2} \left[ \frac{m_X^4 - 2x^4}{m_X^4 - x^4} \right] \\
&\quad + \frac{g_\gamma^4}{18\Lambda^4} \frac{x^8}{m_X^4} \left[ \frac{10x^8 - 44m_X^4x^4 + 52m_X^8}{(m_X^4 - x^4)^2} \right] + \frac{g_\gamma^4}{72\Lambda^4} \frac{x^8}{m_X^8} \left[ \frac{2x^{12} - 16m_X^4x^8 + 64m_X^8x^4 + 2m_X^{12}}{(m_X^4 - x^4)^2} \right]
\end{aligned} \tag{11.36}$$

This is the most general result, without any approximation, of forward scattering amplitude.

Notice how, for  $x = m_X/\sqrt{2} = 14.2$  MeV, the "interfering" correction term disappears. Also, the same term has a cancellation of highest power in energy, leaving dependence on  $x^4$ , instead of  $x^6$ .

Cross section uses Equation 11.12, with  $\omega^2 = x^2/4$ :

$$\begin{aligned}
\frac{d\sigma}{d\Omega} &= \frac{4\alpha^4}{\pi^2 x^2} \log^4 \left( \frac{x}{2m_e} \right) + \frac{1}{12\pi^2} \frac{\alpha^2 g_\gamma^2}{\Lambda^2} \frac{x^2}{m_X^2} \left[ \frac{m_X^4 - 2x^4}{m_X^4 - x^4} \right] \log^2 \left( \frac{x}{2m_e} \right) \\
&\quad + \frac{g_\gamma^4}{1152\pi^2\Lambda^4} \frac{x^6}{m_X^4} \left[ \frac{10x^8 - 44m_X^4x^4 + 52m_X^8}{(m_X^4 - x^4)^2} \right] + \frac{g_\gamma^4}{4608\pi^2\Lambda^4} \frac{x^6}{m_X^8} \left[ \frac{2x^{12} - 16m_X^4x^8 + 64m_X^8x^4 + 2m_X^{12}}{(m_X^4 - x^4)^2} \right]
\end{aligned} \tag{11.37}$$

It is evident how this cross section does not satisfy Froissart bound, as dependence on  $x^{12}$  is growing too fast<sup>27</sup>. Of course, bound on our energy in the EFT is still 50 MeV. Now, we have to ask what are the dominating terms at different energies.

Now, we are free to take the limit for  $x \gg m_X$ , so that we can neglect subleading terms for each amplitude contribution:

$$\begin{aligned}
\frac{d\sigma}{d\Omega} &= \frac{4\alpha^4}{\pi^2 x^2} \log^4 \left( \frac{x}{2m_e} \right) + \frac{1}{6\pi^2} \frac{\alpha^2 g_\gamma^2}{\Lambda^2} \frac{x^2}{m_X^2} \log^2 \left( \frac{x}{2m_e} \right) + \frac{5}{576\pi^2} \frac{g_\gamma^4}{\Lambda^4} \frac{x^6}{m_X^4} + \frac{1}{2304\pi^2} \frac{g_\gamma^4}{\Lambda^4} \frac{x^{10}}{m_X^8} = \\
&= \frac{d\sigma}{d\Omega} \Big|_{\text{QED}} + \frac{1}{6\pi^2} \frac{\alpha^2 g_\gamma^2}{\Lambda^2} \log^2 \left( \frac{x}{2m_e} \right) \frac{x^2}{m_X^2} + \frac{5}{576\pi^2} \frac{g_\gamma^4}{\Lambda^4} \frac{x^6}{m_X^4} \left[ 1 + \frac{1}{20} \frac{x^4}{m_X^4} \right]
\end{aligned} \tag{11.38}$$

where the first term is the QED result, the second term is the result of "interfering"  $M^{\text{QED}} \mathcal{M}$  terms, the third term is the result of subdominant amplitudes squared  $|\mathcal{M}_{+-+}|^2$  and  $|\mathcal{M}_{++-}|^2$ , and the last term is the square of fastest growing amplitudes:  $|\mathcal{M}_{++++}|^2$  and  $|\mathcal{M}_{+-+-}|^2$ .

Because of  $g_\gamma/\alpha\Lambda$  suppression, fast growing amplitudes will not be dominant right away:

- Ratio of dominant squared moduli terms and interfering terms is:

$$\frac{1}{384} \frac{g_\gamma^2}{\alpha^2 \Lambda^2} \frac{x^8}{m_X^6} \log^{-2} \left( \frac{x}{2m_e} \right) \approx (1.5 \times 10^{-17} \text{ MeV}^{-8}) x^8 \log^{-2} \left( \frac{x}{2m_e} \right)$$

so that it becomes comparable with 1 when  $x \approx 200$  MeV.

<sup>27</sup>Relative growth is much larger whenever we include interactions with photons. The higher the number of vertices  $X \rightarrow \gamma\gamma$ , the higher the power of energy the amplitude depends upon.

- In  $x < 200 \text{ MeV}$  (our region of interest), interfering  $M^{\text{QED}} \mathcal{M}$  terms are the dominant corrections:

$$\frac{d\sigma}{d\Omega} = \left. \frac{d\sigma}{d\Omega} \right|_{\text{QED}} \left[ 1 + \frac{1}{24} \frac{g_\gamma^2}{\alpha^2 \Lambda^2} \frac{x^4}{m_X^2} \log^{-2} \left( \frac{x}{2m_e} \right) \right] \quad (11.39)$$

which is a positive correction. When substituting numerical estimates [Equation 5.44](#):

$$\frac{d\sigma}{d\Omega} = \left. \frac{d\sigma}{d\Omega} \right|_{\text{QED}} \left[ 1 + \left( 2.0 \times 10^{-11} \text{ MeV}^{-4} \right) x^4 \log^{-2} \left( \frac{x}{2m_e} \right) \right] \quad (11.40)$$

which, at our limit energy  $x = 200 \text{ MeV}$ , leaves us with a positive correction of the order of 0.1%, which is already pretty reasonable (but non realistic). At  $x = 50 \text{ MeV}$ , correction is about 8 ppm, which is the maximum we can realistically aspire for).

- Instead, for  $x > 200 \text{ MeV}$ , squared moduli from  $|\mathcal{M}_{++++}|^2$  and  $|\mathcal{M}_{+-+-}|^2$  are dominant corrections:

$$\frac{d\sigma}{d\Omega} = \left. \frac{d\sigma}{d\Omega} \right|_{\text{QED}} \left[ 1 + \frac{1}{9216} \frac{g_\gamma^4}{\alpha^4 \Lambda^4} \frac{x^{12}}{m_X^8} \log^{-4} \left( \frac{x}{2m_e} \right) \right] \quad (11.41)$$

clearly, correction is positive as moduli squared are always positive. Substituting numerical estimates [Equation 5.44](#):

$$\frac{d\sigma}{d\Omega} = \left. \frac{d\sigma}{d\Omega} \right|_{\text{QED}} \left[ 1 + \left( 3.0 \times 10^{-28} \text{ MeV}^{-12} \right) x^{12} \log^{-4} \left( \frac{x}{2m_e} \right) \right] \quad (11.42)$$

which at our lower bound starts from 0.1% (where the other case interrupts), and at  $x = 1 \text{ GeV}$  it is at the order of  $10^5$  times larger than QED result.

- Unfortunately, the other squared moduli,  $|\mathcal{M}_{+-+}|^2$  and  $|\mathcal{M}_{++--}|^2$ , will never be dominant. Ratio with interfering terms is:

$$\frac{5}{96} \frac{g_\gamma^2}{\alpha^2 \Lambda^2} \frac{x^4}{m_X^2} \log^{-2} \left( \frac{x}{2m_e} \right) \approx \left( 2.5 \times 10^{-11} \text{ MeV}^{-4} \right) x^4 \log^{-2} \left( \frac{x}{2m_e} \right)$$

which would be comparable with 1 when  $x \approx 1 \text{ GeV}$ , which is much lower than the other terms. The effect of subdominance loses  $x^4$  as power in energy.

Discussion beyond  $x \approx 200 \text{ MeV}$  is useless speculation, as we are already well beyond physical range for our theory.

## 11.2 Testing spin 2 for two-photon

### 11.2.1 Behavior of two-photon cross section

We report the graphs displaying the behavior of the corrected two-photon scattering. For the first part, we will be analyzing the low energy regime, for  $\sqrt{|s|} \ll 2m_e$ . Results in [Figure 32](#) Notice how the energies we use are much smaller than usual, and we peak at 0.1 MeV. Because of the factor  $(3 + \cos^2 \theta)^2$ , cross section does not vary much with angle (factor of 9 at  $\theta = \pi/2$ , and factor of 16 at  $\theta = 0, \pi$ , meaning a less than factor of 2 of oscillation).

We have already proven in [Equation 11.29](#) that the corrections to the cross section is constant, and angle independent, and numerically about  $1.5 \times 10^{-10}$  in relative terms to QED Euler-Heisenberg cross section.

In [Figure 33](#), there is not much to see. Again, you can see the factor of two of difference between the two  $\cos \theta$  cases, and relative correction is constant in this regime and it is worth  $1.5 \times 10^{-10}$  in relative terms. Also, the dependence of the cross section on the energy, still from [Equation 11.29](#), is  $\sigma \propto \omega^6 \propto \sqrt{|s|}^6$ .

It is much more interesting to go up in energy and look at the forward scattering "relativistic" limit. Results in [Figure 34](#). Let us unpack the left image in [Figure 34](#):

- Energy range shown is  $2 \text{ MeV} < x = \sqrt{|s|} < 250 \text{ MeV}$ . So, we are in the range dominated by "interfering" amplitudes  $M_{++++}^{\text{QED}} \mathcal{M}_{++++}$  and  $M_{+-+-}^{\text{QED}} \mathcal{M}_{+-+-}$ .
- Blue continuous line is the QED cross section. We started after the change in behavior (not predicted by our two limits formulas), and we can see that it has a maximum because of the  $\log^4$  term, around  $x = \sqrt{|s|} = 5 \text{ MeV}$ , and then decreases like  $x^{-2}$ .

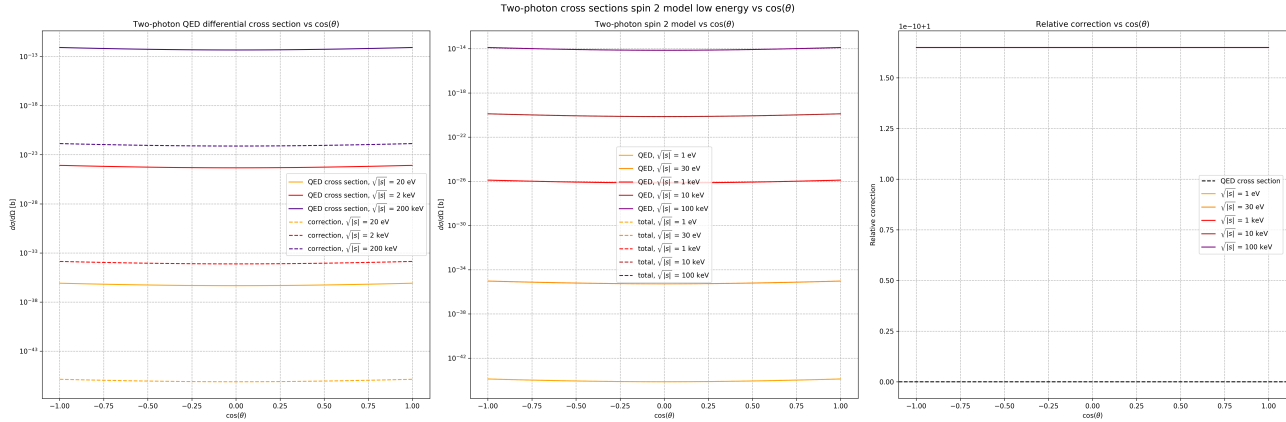


Figure 32: Graph of behavior of two-photon corrections as a function of the scattering angle  $\cos \theta$ . On the left, we plot separately both the QED result and the actual spin 2 correction (dashed line), for different values of the center of mass energy  $\sqrt{|s|}$ . In the middle, comparison between QED differential cross section and total cross section (including spin 2 correction), for different fixed  $\sqrt{|s|}$ . On the right, relative correction to the QED cross section of the total (QED + spin 2) cross section, always at different energetic values for  $\sqrt{|s|}$ .

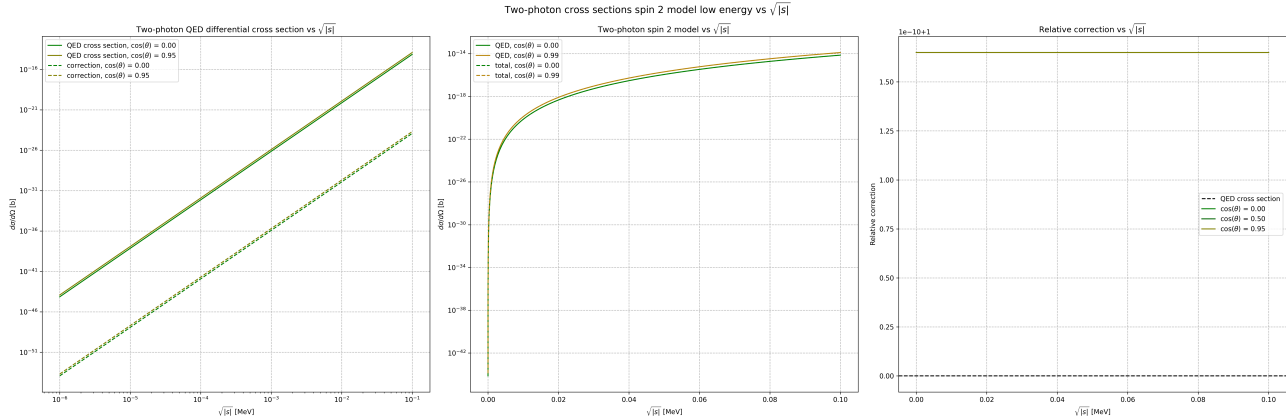


Figure 33: Graph of behavior of annihilation corrections as a function of the center of mass energy  $\sqrt{|s|}$ . On the left, we plot separately both the QED result and the actual spin 2 correction (dashed line), for different values of the  $\cos \theta$ . In the middle, comparison between QED differential cross section and total cross section (including spin 2 correction), for different fixed  $\cos \theta$ . On the right, relative correction to the QED cross section of the total (QED + spin 2) cross section, always at different angular values for  $\cos \theta$ .

- Magenta dashed line is the dominant contribution  $+++$  in helicity, which at this energy range is  $M_{++++}^{\text{QED}} \mathcal{M}_{++++}$ . It has two zeros (in Equation 11.31) for  $x = 6.75$  MeV and  $x = 32.1$  MeV, as well as the divergence for  $x = m_X$ . Amplitude grows like  $x^6$ , so cross section grows like  $x^4$ .
- Indigo dashed line is the dominant contribution  $+--$  in helicity, which at this energy range is  $M_{+-+-}^{\text{QED}} \mathcal{M}_{+-+-}$ . It has a zero (in Equation 11.32) for  $x = 22.4$  MeV, as well as the divergence for  $x = m_X$ . Amplitude grows like  $x^6$ , so cross section grows like  $x^4$ .
- Orange dashed line is the subdominant contribution  $--+$  in helicity, which has no QED part hence only  $|\mathcal{M}_{--+}|^2$  is shown. It has a zero (in Equation 11.33) for  $x = \sqrt{2}m_X = 24.0$  MeV, as well as the divergence for  $x = m_X$ . It is suppressed by  $g_\gamma^2/\alpha^2\Lambda^2 \approx 10^{-7}$ , but it grows faster being squared modulus. Amplitude grows like  $x^8$ , so cross section grows like  $x^6$ .
- Green dashed line is the subdominant contribution  $++-$  in helicity, which has no QED part hence only  $|\mathcal{M}_{++-}|^2$  is shown. From Equation 11.34, it has a factor 3 extra with respect to the orange contribution. It has a zero for  $x = \sqrt[4]{2}m_X = 20.1$  MeV, as well as the divergence for  $x = m_X$ . It is suppressed by  $g_\gamma^2/\alpha^2\Lambda^2 \approx 10^{-7}$ , but it grows faster being squared modulus. Amplitude grows like  $x^8$ , so cross section grows like  $x^6$ .
- Red continuous contribution is the total correction contribution, visible in Equation 11.37. The dominant correction is the  $\alpha^2 g_\gamma^2/\Lambda^2 \log^2$  part, which vanishes for  $x = m_X/\sqrt{2} = 14.2$  MeV. It also has a divergence in  $x = m_X$ . Most importantly, the two dominant contributions, when added together, cancel  $x^4$

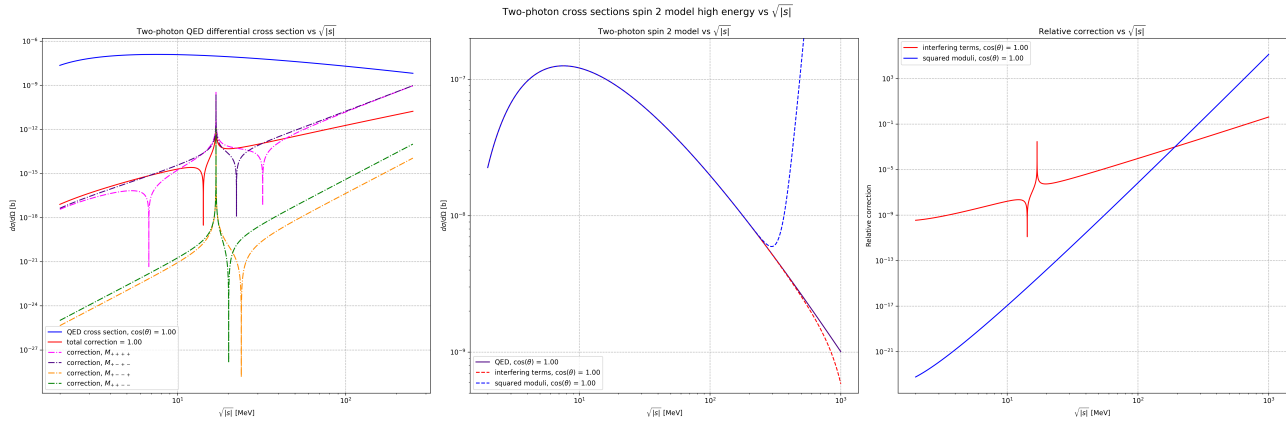


Figure 34: Graph of behavior of annihilation corrections as a function of the center of mass energy  $\sqrt{|s|}$ . On the left, we plot separately both the QED result and the modulus of spin 2 corrections (dashed line) for all helicity-fixed amplitudes contributions, in the forward scattering limit. In the middle, comparison between QED differential cross section and total cross section (including interfering spin 2 correction and squared moduli spin 2 correction), in forward scattering. On the right, relative correction to the QED cross section of the total (QED vs spin 2 interfering and QED vs spin 2 squared moduli) cross section, in the forward scattering.

dependence, leaving a total correction that grows like  $x^2$  (visible in Equation 11.37).

In the middle and right graph of Figure 34 simply shows the correction, which is negative, to the cross section, and the relative absolute correction. Energy range has been extended to 1 GeV, to show the takeover of moduli squared terms with respect to interfering terms:

- For interfering terms  $M_{++++}^{QED} \mathcal{M}_{++++}$  and  $M_{+-+-}^{QED} \mathcal{M}_{+-+-}$  (red dashed line in graphs), correction is zero at  $x = m_X/\sqrt[4]{2}$ , diverging at  $x = m_X$ , and growing relatively like  $x^4$ . Correction is negative.
- For squared moduli terms  $|\mathcal{M}_{++++}|^2$  and  $|\mathcal{M}_{+-+-}|^2$  (blue dashed line in graphs). It grows like  $x^{12}$  with respect to the QED cross section, but it starts lower because of suppression of  $g_\gamma^2/\alpha^2 \Lambda^2$ , and of the extra factor 1000 in Equation 11.37. Intersection between the two contributions occurs around  $x = 200$  MeV, as discussed. Correction is positive.

Of course, this analysis is purely speculative, as it pertains to no physics whatsoever, as GeV ranges in energy are not realistic for our EFT.

### 11.2.2 Two-photon experiments

Before 2016, there was no direct observation of light-by-light scattering ([70]), because of its very low cross section. Unfortunately, even if correction is larger than other processes, even at low energy, because of QED loop suppression, the same suppression does not help us now, with experiments.

- In 2016, ATLAS discovered the process using  $\sqrt{|s|} = 5.02$  TeV Pb-Pb collisions, and followed it up in 2019 with the most accurate measurement ([73]) of  $78 \pm 13(\text{stat.}) \pm 7(\text{syst.}) \pm 3(\text{lumi.})$  nb. This result was obtained looking at invariant mass events  $\sqrt{|s|} > 6$  GeV. In 2018, CMS confirmed ATLAS discovery ([72]), although measurement is slightly less accurate and energy is slightly lower.

These are the only two measurements of elastic light-by-light scattering ever performed. ATLAS discovery is way beyond our range of EFT, and even at threshold energy of 6 GeV spin 2 correction would conservatively be  $1.1 \times 10^{14}$  times larger than actual QED cross section (and only in the forward scattering region). This experiment is not useful to us.

- As for lower range experiments, the best experimental upper bound for cross section comes from the PVLAS experiment ([69]). In their experiment, magnetic birefringence of vacuum is studied through a 1064 nm = 1.16 eV laser inserted in a strong magnetic field. They set a limit on cross section of four photons interactions:

$$\sigma_{\gamma\gamma}^{\text{PVLAS}} < 4.6 \times 10^{-58} \text{ cm}^2$$

while the Standard Model prediction is:

$$\sigma_{\gamma\gamma}^{\text{QED}} = 1.8 \times 10^{-65} \text{ cm}^2$$

Although center of mass energy for this interaction is not trivially calculated, it is also not relevant, as for  $\sqrt{|s|} \ll 2m_e$  (which is of course realized in this experiment) spin 2 correction is always constant and equal to  $1.5 \times 10^{-10}$  in the most conservative bound for coupling constant.

- Finally, there has been a proposal ([71]) to observe light-by-light scattering at the MeV region (where the QED cross section is largest), in which case the spin 2 correction is of the order of  $10^{-10}$  to  $10^{-7}$ , which would be a very nice constraint on the coupling constant. However, the experiment is still in its design phase, and it is unlikely to see the light of day anytime soon.

## 12 Other relevant phenomena

### 12.1 Scattering process $e^+e^- \rightarrow X\gamma$

We have to calculate this process to evaluate properly the decay rate  $X \rightarrow e^+e^-\gamma$ , and make sure it is negligible with respect to the dominant  $X \rightarrow e^+e^-$  (see subsection 5.2).

At tree level, there is no QED diagram contributing (seeing as this is not a process that is corrected by the presence of  $X$ , as  $X$  is actually produced on shell here), along with the direct interaction, there are several other diagrams contributing, in Figure 35: Now, let us employ our beloved Feynman rules to write down all four

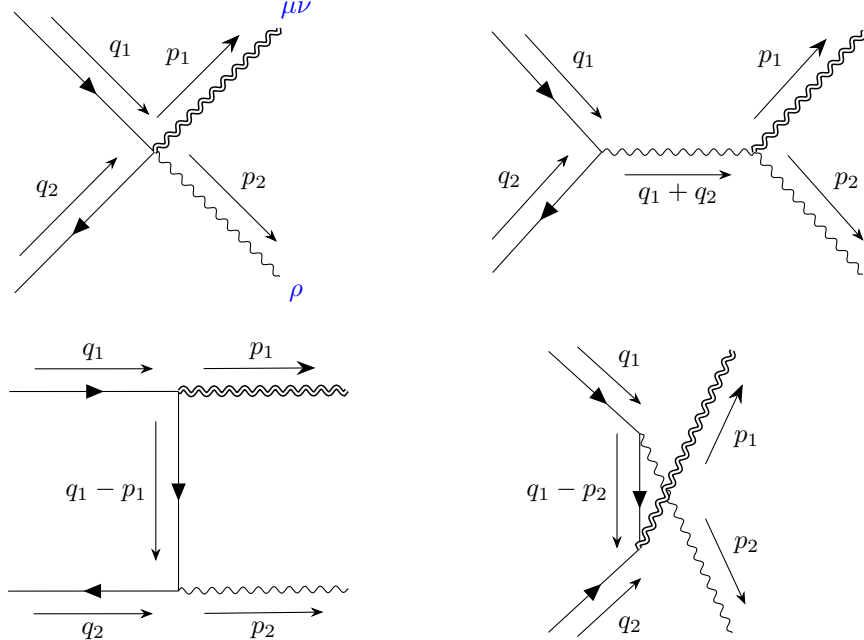


Figure 35: Diagrams corresponding to tree level scattering  $e^+e^- \rightarrow X\gamma$ . On the upper left, the direct four-point interaction hereafter denoted with  $\mathcal{A}_1$ . On the upper right, the  $s$ -channel with photon exchange, hereafter denoted with  $\mathcal{A}_2$ . On the lower left, the  $t$ -channel with fermion exchange, hereafter denoted with  $\mathcal{A}_3$ . On the lower right, the  $u$ -channel with fermion exchange, hereafter denoted with  $\mathcal{A}_4$ .

amplitudes. The symmetric structure of  $X \rightarrow e^+e^-$  and  $X \rightarrow e^+e^-\gamma$  interaction has been reduced to single addend terms because it is easier to write, and since  $\varepsilon_{\mu\nu}$  is symmetric anyway, no difference ensues:

$$A_1 = \left[ \frac{-i g_e e}{\Lambda} \right] \varepsilon_{\mu\nu}(p_1, \eta_1) \varepsilon_\rho(p_2, \lambda_2) [\gamma_\mu \delta_{\nu\rho}] \quad (12.1)$$

$$A_2 = \left[ \frac{g_\gamma(-ie)}{\Lambda} \right] \varepsilon_{\mu\nu}(p_1, \eta_1) \varepsilon_\rho(p_2, \lambda_2) [\Pi_{\mu\nu\rho\sigma}^{\xi_1}(-p_2, q_1 + q_2) \hat{D}_{\sigma\alpha}^{\xi_2}(q_1 + q_2) \gamma_\alpha] \quad (12.2)$$

$$A_3 = \left[ \frac{(ig_e)(-ie)}{2\Lambda} \right] \varepsilon_{\mu\nu}(p_1, \eta_1) \varepsilon_\rho(p_2, \lambda_2) [\gamma_\rho \hat{D}(q_1 - p_1) \gamma_\mu (q_2 - p_2 - q_1)_\nu] \quad (12.3)$$

$$A_4 = \left[ \frac{(ig_e)(-ie)}{2\Lambda} \right] \varepsilon_{\mu\nu}(p_1, \eta_1) \varepsilon_\rho(p_2, \lambda_2) [\gamma_\mu (q_2 + p_2 - q_1)_\nu \hat{D}(q_1 - p_2) \gamma_\rho] \quad (12.4)$$

where  $p_1, \eta_1$  are 4-momentum and polarization of  $X$  (here forth called  $\varepsilon_{\mu\nu}$ ),  $p_2, \lambda_2$  are 4-momentum and polarization of the photon (here forth called  $\varepsilon_\rho$ ). The usual electrodynamics rule  $-ie\gamma_\mu$  applies.  $\Pi_{\mu\nu\rho\sigma}^{\xi_1}$  is the tensor describing  $X \rightarrow \gamma\gamma$  Feynman rule, in the  $\xi_1$  gauge.

Finally,  $\hat{D}_{\sigma\alpha}^{\xi_2}$  and  $\hat{D}$  are photon propagator (in  $\xi_2$  gauge) and fermion propagator, respectively. There is no apparent reason to have two different gauge parameters  $\xi_1$ , and  $\xi_2$ , but we will see that it does not matter at all in the final expression.

Also, we will be employing another simplification: electron and positron will be assumed to be massless ( $m_e \ll m_X$ ), to simplify the final result, so the propagator is:

$$\hat{D}_{ab}(k) = \frac{(-ik)}{k^2} \quad (12.5)$$

It also means that  $X$  is the only massive particle in the process, leading to the following Mandelstam identity:  $s + t + u = -m_X^2$ , that we are going to use throughout.

We then define:

$$\mathcal{A}_i = \bar{v}(q_2, s_2) A_i u(q_1, s_1) = \bar{v} A_i u \quad i \in \{1, 2, 3, 4\} \quad (12.6)$$

where  $q_1, s_1$  and  $q_2, s_2$  are 4-momenta and polarizations of electron and positron, respectively (here forth called simply  $u, v$ ).

Now, it is time to find the complex conjugates, using the usual rules for complex conjugation in [subsection F.4](#):

$$\mathcal{A}_i^* = \bar{u} \left( \gamma_4 A_i^\dagger \gamma_4 \right) v = \bar{u} B_i v \quad (12.7)$$

where the Dirac propagator is untouched:

$$\begin{aligned} \gamma_4 \hat{D}^\dagger(k) \gamma_4 &= \gamma_4 \left[ \frac{(-i)^* k_\eta^* \gamma_\eta^\dagger}{k^2} \right] \gamma_4 = \\ &= \cancel{\eta_p} \frac{i k_\eta}{k^2} \gamma_4 \gamma_\eta^\dagger \gamma_4 = -\cancel{\eta_p^2} \frac{i k_\eta}{k^2} \gamma_\eta = \frac{-ik}{k^2} = \hat{D}(k) \end{aligned}$$

and where the operators  $B_i$  are found to be:

$$\begin{aligned} B_1 &= \gamma_4 A_1^\dagger \gamma_4 = \left[ \frac{i g_e e}{\Lambda} \right] \varepsilon_{\zeta\tau}^* \varepsilon_\beta^* \left[ \gamma_4 \gamma_\zeta^\dagger \gamma_4 \delta_{\tau\beta} \right] = \\ &= -\cancel{\zeta_p \tau_p \beta_p \zeta_p} \left[ \frac{i g_e e}{\Lambda} \right] \bar{\varepsilon}_{\zeta\tau} \bar{\varepsilon}_\beta \left[ \gamma_\zeta \delta_{\tau\beta} \right] = \left[ \frac{-i g_e e}{\Lambda} \right] \bar{\varepsilon}_{\zeta\tau} \bar{\varepsilon}_\beta \left[ \gamma_\zeta \delta_{\tau\beta} \right] \end{aligned} \quad (12.8)$$

$$\begin{aligned} B_2 &= \gamma_4 A_2^\dagger \gamma_4 = \left[ \frac{i g_\gamma e}{\Lambda} \right] \varepsilon_{\zeta\tau}^* \varepsilon_\beta^* \left[ \Pi_{\zeta\tau\beta\gamma}^{\xi_1*}(-p_2, q_1 + q_2) \hat{D}_{\gamma\theta}^{\xi_2*}(q_1 + q_2) \gamma_4 \gamma_\theta^\dagger \gamma_4 \right] = \\ &= -\cancel{\zeta_p \tau_p \beta_p \zeta_p \tau_p \beta_p \gamma_p \theta_p \theta_p} \left[ \frac{i g_\gamma e}{\Lambda} \right] \bar{\varepsilon}_{\zeta\tau} \bar{\varepsilon}_\beta \left[ \Pi_{\zeta\tau\beta\gamma}^{\xi_1} \hat{D}_{\gamma\theta}^{\xi_2}(q_1 + q_2) \gamma_\theta \right] = \\ &= \left[ \frac{-i g_\gamma e}{\Lambda} \right] \bar{\varepsilon}_{\zeta\tau} \bar{\varepsilon}_\beta \left[ \Pi_{\zeta\tau\beta\gamma}^{\xi_1} \hat{D}_{\gamma\theta}^{\xi_2}(q_1 + q_2) \gamma_\theta \right] \end{aligned} \quad (12.9)$$

$$\begin{aligned} B_3 &= \gamma_4 A_3^\dagger \gamma_4 = \left[ \frac{g_e e}{2\Lambda} \right] \varepsilon_{\zeta\tau}^* \varepsilon_\beta^* \left[ (q_2 - p_2 - q_1)_\tau^* \gamma_4 \gamma_\zeta^\dagger \cancel{\gamma_4 \gamma_4} \hat{D}^\dagger(q_1 - p_1) \cancel{\gamma_4 \gamma_4} \gamma_\beta^\dagger \gamma_4 \right] = \\ &= (-1)^2 \cancel{\zeta_p \tau_p \beta_p \tau_p \zeta_p} \left[ \frac{g_e e}{2\Lambda} \right] \bar{\varepsilon}_{\zeta\tau} \bar{\varepsilon}_\beta \left[ (q_2 - p_2 - q_1)_\tau \gamma_\zeta \hat{D}(q_1 - p_1) \gamma_\beta \right] = \\ &= \left[ \frac{g_e e}{2\Lambda} \right] \bar{\varepsilon}_{\zeta\tau} \bar{\varepsilon}_\beta \left[ (q_2 - p_2 - q_1)_\tau \gamma_\zeta \hat{D}(q_1 - p_1) \gamma_\beta \right] \end{aligned} \quad (12.10)$$

$$\begin{aligned} B_4 &= \gamma_4 A_4^\dagger \gamma_4 = \left[ \frac{g_e e}{2\Lambda} \right] \varepsilon_{\zeta\tau}^* \varepsilon_\beta^* \left[ (q_2 + p_2 - q_1)_\tau^* \gamma_4 \gamma_\beta^\dagger \cancel{\gamma_4 \gamma_4} \hat{D}^\dagger(q_1 - p_2) \cancel{\gamma_4 \gamma_4} \gamma_\zeta^\dagger \gamma_4 \right] = \\ &= (-1)^2 \cancel{\zeta_p \tau_p \beta_p \tau_p \beta_p \zeta_p} \left[ \frac{g_e e}{2\Lambda} \right] \bar{\varepsilon}_{\zeta\tau} \bar{\varepsilon}_\beta \left[ (q_2 + p_2 - q_1)_\tau \gamma_\beta \hat{D}(q_1 - p_2) \gamma_\zeta \right] = \\ &= \left[ \frac{g_e e}{2\Lambda} \right] \bar{\varepsilon}_{\zeta\tau} \bar{\varepsilon}_\beta \left[ (q_2 + p_2 - q_1)_\tau \gamma_\beta \hat{D}(q_1 - p_2) \gamma_\zeta \right] \end{aligned} \quad (12.11)$$

This Dirac structure has been explored many times (check out [section 10](#)), and modulus squared has always the same structure:

$$\begin{aligned} |\mathcal{A}|^2 &= \bar{v} [A_1 + A_2 + A_3 + A_4] u \bar{u} [B_1 + B_2 + B_3 + B_4] v = \\ &= \text{Tr} \{ [A_1 + A_2 + A_3 + A_4] (u \bar{u}) [B_1 + B_2 + B_3 + B_4] (v \bar{v}) \} \end{aligned} \quad (12.12)$$

and then average over initial polarizations (now there are four, because of both electron and positron in the initial state) and sum over all fermion polarizations:

$$\begin{aligned} |\bar{\mathcal{A}}|^2 &= \frac{1}{4} \sum_{s_1, s_2} |\mathcal{A}|^2 = \\ &= \frac{1}{4} \frac{1}{2q_{1,4} 2q_{2,4}} \text{Tr} \left\{ [A_1 + A_2 + A_3 + A_4] (-i\gamma_1) [B_1 + B_2 + B_3 + B_4] (-i\gamma_2) \right\} \end{aligned} \quad (12.13)$$

And finally, we want to get the unpolarized result, which requires summing over  $X$  polarizations and photon polarizations as well. Notice that the sum over photon polarizations is:

$$\sum_{\lambda_2} \varepsilon_\rho(p_2, \lambda_2) \bar{\varepsilon}_\beta(p_2, \lambda_2) = \delta_{\rho\beta} - \frac{p_{2,\rho} p_{2,\beta}}{|\vec{p}_2|^2} \quad (12.14)$$

which would correspond to the numerator of the photon propagator in unitary gauge (Lorentz gauge,  $1/\xi_2 \rightarrow 0$ ). However, the  $p_{2,\rho} p_{2,\beta}/|\vec{p}_2|^2$  part immediately simplifies onto the amplitude, because of *Ward identities*, so that the final expression for the amplitude is:

$$\begin{aligned} |\bar{\mathcal{A}}|^2 &= \frac{e^2}{4\Lambda^2} \frac{N_{\mu\nu\xi\tau}(p_1) \delta_{\rho\beta}}{2q_{1,4} 2q_{2,4}} \times \\ &\text{Tr} \left\{ \left[ -ig_e \gamma_\mu \delta_{\nu\rho} - ig_\gamma \Pi_{\mu\nu\rho\sigma}^{\xi_1}(-p_2, q_1 + q_2) \hat{D}_{\sigma\alpha}^{\xi_2}(q_1 + q_2) \gamma_\alpha + \right. \right. \\ &\quad \left. \left. + \frac{g_e}{2} \gamma_\rho \hat{D}(q_1 - p_1) \gamma_\mu (q_2 - p_2 - q_1)_\nu + \frac{g_e}{2} \gamma_\mu (q_2 + p_2 - q_1)_\nu \hat{D}(q_1 - p_2) \gamma_\rho \right] (-i\gamma_1) \right. \\ &\quad \left. \left[ -ig_e \gamma_\zeta \delta_{\tau\beta} - ig_\gamma \Pi_{\zeta\tau\beta\gamma}^{\xi_1}(-p_2, q_1 + q_2) \hat{D}_{\gamma\theta}^{\xi_2}(q_1 + q_2) \gamma_\theta + \right. \right. \\ &\quad \left. \left. + \frac{g_e}{2} \gamma_\zeta \hat{D}(q_1 - p_1) \gamma_\beta (q_2 - p_2 - q_1)_\tau + \frac{g_e}{2} \gamma_\beta (q_2 + p_2 - q_1)_\tau \hat{D}(q_1 - p_2) \gamma_\zeta \right] (-i\gamma_2) \right\} \end{aligned} \quad (12.15)$$

### 12.1.1 Differential cross section of $e^+e^- \rightarrow X\gamma$

Now, let us derive  $S$ -matrix elements according to the rules of Pauli notation:

$$S_{fi} = \frac{[(2\pi)^4 i]^2}{[(2\pi)^4 i]} \frac{\bar{\mathcal{A}}}{V^2 \sqrt{2p_{1,4} p_{2,4}}} \delta(q_1 + q_2 - p_1 - p_2) \quad (12.16)$$

which requires  $1/\sqrt{2p_{1,4}}$  at denominator because  $X$  is an integer spin state, and rule in [subsection 3.4](#) states that bosons and scalar need that factor. Taking squared modulus, we can calculate the usual rate of the process per kinematic configuration:

$$\Gamma(p_1, p_2) = \frac{|S_{fi}|^2}{T} = \frac{1}{T} \frac{(2\pi)^8 |\bar{\mathcal{A}}|^2}{V^4 4p_{1,4} p_{2,4}} \frac{VT}{(2\pi)^4} \delta(q_1 + q_2 - p_1 - p_2) \quad (12.17)$$

the total rate of the process is obtained by integrating in phase space all valid configurations. To get the cross section, we need the usual formula:

$$\sigma(e^+e^- \rightarrow X\gamma) = \frac{\Gamma(e^+e^- \rightarrow X\gamma) V}{v_{rel}} \quad (12.18)$$

where the "relative velocity" of electron and positron, in the massless limit, is  $2p/e \rightarrow 2^{28}$ .

---

<sup>28</sup>Kinematics of the initial state is the same as two-photon scattering.

This leads us to the final cross section:

$$\begin{aligned}
\sigma(e^+e^- \rightarrow X\gamma) &= \frac{V}{v_{rel}} \int \frac{V d^3 p_1}{(2\pi)^3} \frac{V d^3 p_2}{(2\pi)^3} \Gamma(p_1, p_2) = \\
&= \frac{V}{v_{rel}} \int \frac{V d^3 p_1}{(2\pi)^3} \frac{V d^3 p_2}{(2\pi)^3} \left[ \frac{1}{T} \frac{(2\pi)^8 |\bar{\mathcal{A}}|^2}{V^4} \frac{VT}{(2\pi)^4} \delta(q_1 + q_2 - p_1 - p_2) \right] = \\
&= \frac{1}{(2\pi)^2 v_{rel}} \int \frac{d^3 p_1 d^3 p_2}{4p_{1,4} p_{2,4}} |\bar{\mathcal{A}}|^2 \delta(q_1 + q_2 - p_1 - p_2) = \\
&= \frac{1}{8\pi^2} \int \frac{d^3 p_2}{2p_{2,4}} \int d^4 p_1 |\bar{\mathcal{A}}|^2 \delta(q_1 + q_2 - p_1 - p_2) \delta(p_1^2 + m_X^2) \theta(p_{1,4}) = \\
&= \frac{1}{16\pi^2} \int \frac{d^3 p_2}{p_{2,4}} |\bar{\mathcal{A}}|^2 \delta((q_1 + q_2 - p_2)^2 + m_X^2) = \\
&= \frac{1}{16\pi^2} \int \frac{d^3 p_2}{p_{2,4}} |\bar{\mathcal{A}}|^2 \delta((q_1 + q_2)^2 - 2(q_1 + q_2) \cdot p_2 + m_X^2) = \\
&= \frac{1}{16\pi^2} \int \frac{d^3 p_2}{p_{2,4}} |\bar{\mathcal{A}}|^2 \delta(s + 2\sqrt{|s|} p_{2,4} + m_X^2) = \\
&= \frac{1}{32\pi^2 \sqrt{|s|}} \int \frac{d^3 p_2}{p_{2,4}} |\bar{\mathcal{A}}|^2 \delta\left[p_{2,4} - \frac{|s| - m_X^2}{2\sqrt{|s|}}\right] = \\
&= \frac{1}{32\pi^2 \sqrt{|s|}} \int_0^\infty dp_{2,4} p_{2,4} \delta\left[p_{2,4} - \frac{|s| - m_X^2}{2\sqrt{|s|}}\right] \int d\Omega |\bar{\mathcal{A}}|^2 = \\
&= \frac{\bar{p}_{2,4}}{32\pi^2 \sqrt{|s|}} \int d\Omega |\bar{\mathcal{A}}|^2
\end{aligned} \tag{12.19}$$

where we used a famous integral, also found in [subsection F.2](#).  $\bar{p}_{2,4}$  is the energy (would be the momentum but the photon is massless) of the photon in the final state, fixed by kinematics. We used the fact that in the center of mass frame,  $q_1 + q_2 = (0, i\sqrt{|s|})$ . This leaves us with the final differential cross section:

$$\frac{d\sigma}{d\Omega} = \frac{\bar{p}_{2,4} |\bar{\mathcal{A}}|^2}{32\pi^2 \sqrt{|s|}} \tag{12.20}$$

we substituted the kinematics into  $\mathcal{A}$ . Notice that, differently from Bjorken-Drell notation,  $|\bar{\mathcal{A}}|^2$  is not dimensionless, because of the extra factors  $1/4q_{1,4} q_{2,4}$  coming from fermion polarization sum.

### 12.1.2 Amplitude result

To achieve the result, of course we are going to use our beloved FORM tool to calculate this squared amplitude in [Equation 12.15](#). The code to be looking for is `ee_into_Xg.frm`, which is found in the usual GitHub repository linked [here](#).

Now, the code itself works as all the other codes we have written so far. Novelties are the dependence of the amplitude of two different gauge parameters  $\xi_1$  and  $\xi_2$ , the former the Feynman rule  $X \rightarrow \gamma\gamma$ , and the latter in the photon propagator, which is just to show that the result is gauge invariant.

Another check that can be done is of *Ward identities*, which can be done substituting  $\delta_{\rho\beta} \rightarrow p_{2,\rho} p_{2,\beta}$  in [Equation 12.15](#). Of course, substituting photon momenta to the squared amplitude yields zero automatically, which also justifies why we used  $\delta_{\rho\beta}$  as expression for the sum over photon polarizations.

It is worth mentioning that this result is also well-known in literature, as both [13] and [9] report it, although the process calculated is actually  $qq \rightarrow Xg$ , as the strong interaction counterpart of what we are doing here. The difference between  $qq \rightarrow Xg$  and  $e^+e^- \rightarrow X\gamma$  is a color factor of  $4/9$ , as:

- The factor  $1/9$  comes when averaging over all initial states, which for quarks means polarizations *and* color, leaving  $1/3^2$  in the denominator.
- The factor of  $4$  comes from a trace in color space for the gluon, as amplitude would get a factor:  $\text{Tr}[T^a T^b] \delta_{ab} = \delta_{ab} \delta_{ab}/2 = 4$ , as the adjoint irrep of  $SU(3)_c$  has dimension  $8$ .

To compare our result with literature, we suggest operating the following kinematics substitutions:

- To get  $g_\gamma^2$  section, multiply squared amplitude by  $12m_X^4 s$ , and substitute  $s = -t - u - m_X^2$ .

- To get  $g_\gamma g_e$  section, multiply squared amplitude by  $12m_X^4$ , and substitute  $t = -s - u - m_X^2$ .
- To get  $g_e^2$  section, multiply squared amplitude by  $12m_X^4 tu$ , and substitute  $s = -t - u - m_X^2$ .

Here is the result we obtain:

$$\begin{aligned} |\bar{\mathcal{A}}|^2 &= \frac{1}{2q_{1,4} 2q_{2,4}} \frac{-e^2}{12\Lambda^2 m_X^4 stu} \times \\ &\left\{ 2g_\gamma^2 tu \left[ m_X^4 (7t^2 + 12tu + 7u^2) + 2m_X^2 (t^3 + 7t^2u + 7tu^2 + u^3) + (t+u)^2 (t^2 + u^2) \right] \right. \\ &+ 4g_e g_\gamma stu \left[ -9m_X^6 - 4m_X^4 (s+3u) - 2m_X^2 (s^2 + 7us + 6u^2) - s (s^2 + 2su + u^2) \right] \\ &- g_e^2 s \left[ 6m_X^{10} + 6m_X^8 (t+u) + 3m_X^6 (t^2 + u^2) + 12m_X^4 tu(t+u) + 2m_X^2 tu (t^2 + 12tu + u^2) + 2tu (u^3 + u^2t + ut^2 + t^3) \right] \left. \right\} \end{aligned} \quad (12.21)$$

which is the same as reported in the Appendices of [13], if you consider that in our notation there is an extra  $1/2q_{1,4} 2q_{2,4}$ , that  $s, t, u$  are defined with a minus sign with respect to Bjorken-Drell notation, and that in [13] the process is  $qq \rightarrow Xg$ , so there is an extra color factor of  $4/9$  and the constant  $e$  is replaced by  $g_s$ , coupling of strong interaction.

There is also a manipulation we can do to present this result in a more useful way. If we define  $f_1(s, t, u)$ ,  $f_2(s, t, u)$ ,  $f_3(s, t, u)$  such that what is inside curly brackets in Equation 12.21 can be written as:

$$2g_\gamma^2 tu f_1(s, t, u) + 4g_e g_\gamma stu f_2(s, t, u) - g_e^2 s f_3(s, t, u)$$

then we can write this as:

$$\begin{aligned} &2g_\gamma^2 tuf_1 + 4g_e g_\gamma stu f_2 - g_e^2 s f_3 = \\ &= 2g_\gamma^2 tuf_1 + 4g_e g_\gamma stu f_2 - (g_\gamma - g_e)^2 s f_3 + g_\gamma^2 s f_3 - 2g_e g_\gamma s f_3 = \\ &= g_\gamma^2 [2tuf_1 + sf_3] + 2g_e g_\gamma s [2tuf_2 - f_3] - (g_\gamma - g_e)^2 s f_3 = \\ &= g_\gamma^2 [2tuf_1 + sf_3] + 2g_\gamma (g_e - g_\gamma) s [2tuf_2 - f_3] + 2g_\gamma^2 s [2tuf_2 - f_3] - (g_\gamma - g_e)^2 s f_3 = \\ &= g_\gamma^2 [2tuf_1 + 4stu f_2 - sf_3] + g_\gamma (g_e - g_\gamma) [4stu f_2 - 2sf_3] - (g_e - g_\gamma)^2 s f_3 = \\ &:= 3g_\gamma^2 m_X^4 f_4(s, t, u) - 6m_X^4 sg_\gamma (g_e - g_\gamma) f_5(s, t, u) - (g_e - g_\gamma)^2 s f_3(s, t, u) \end{aligned} \quad (12.22)$$

where we defined:

$$f_4(s, t, u) = \frac{2tuf_1(s, t, u) + 4stu f_2(s, t, u) - sf_3(s, t, u)}{3m_X^4}$$

$$f_5(s, t, u) = \frac{2f_3(s, t, u) - 4tuf_2(s, t, u)}{6m_X^4}$$

the expression for these is found using the code `manip_eexg.frm`, again in the GitHub repository. It just checks that the newly defined functions are:

$$f_4(s, t, u) = \left[ 2m_X^4 + 2m_X^2 (t+u) + t^2 + u^2 \right] \left[ m_X^4 + m_X^2 (t+u) + 4tu \right] \quad (12.23)$$

$$f_5(s, t, u) = m_X^6 + m_X^2 s (s+2u) + 2su(u+s) \quad (12.24)$$

using the usual Mandelstam identity  $s+t+u = -m_X^2$ . Because we are already substituting kinematics, we can use the fact that  $s = -4q_{1,4} q_{2,4}$  and we can write the final expression for the squared modulus:

$$\begin{aligned} |\bar{\mathcal{A}}|^2 &= \frac{e^2}{12\Lambda^2 m_X^4 s^2 tu} \left\{ 3g_\gamma^2 m_X^4 \left[ 2m_X^4 + 2m_X^2 (t+u) + t^2 + u^2 \right] \left[ m_X^4 + m_X^2 (t+u) + 4tu \right] \right. \\ &- 6g_\gamma (g_e - g_\gamma) s \left[ m_X^6 + m_X^2 s (s+2u) + 2su(u+s) \right] \\ &- (g_e - g_\gamma)^2 s \left[ 6m_X^{10} + 6m_X^8 (t+u) + 3m_X^6 (t^2 + u^2) + 12m_X^4 tu(t+u) \right. \\ &\left. \left. + 2m_X^2 tu (t^2 + 12tu + u^2) + 2tu (u^3 + u^2t + ut^2 + t^3) \right] \right\} \end{aligned} \quad (12.25)$$

which is, with the same tweaks we already described, perfectly equivalent to [13]<sup>29</sup> and [9] results.

<sup>29</sup>There is a typo in the result presented on page 50. The first line has  $m_X^4 + 2m_X^2 (t+u) + 4tu$ , with an extra factor of 2.

This result is important because it is pedagogic: it combines every Feynman rule we introduced and it shows why in the non universal coupling model unitarity is more easily violated: you can see that if we set  $g_e = g_\gamma$ , then a solid chunk of [Equation 12.25](#) disappears. Namely,  $s^3$  dependence only appears when the two coupling constants are different. However, it is interesting to see that Froissart bound is always satisfied, having our cross section be:

$$\frac{d\sigma}{d\Omega} = \frac{\bar{p}_{2,4} |\bar{\mathcal{A}}|^2}{32\pi^2 \sqrt{|s|}} \quad (12.26)$$

which means the factor in front of  $\mathcal{A}$  is constant at high energy. So,  $\sigma \propto |\bar{\mathcal{A}}|^2 \propto 1/s^{30}$ .

As for us, we need this result to compute the decay rate  $X \rightarrow e^+ e^- \gamma$ , which is needed to confirm that this decay channel is highly suppressed and can be neglected when studying  $X$  decay rate (see [subsection 5.2](#)).

## 12.2 $g - 2$ of the electron

One of most precise measurement in physics is the  $g - 2$  of the electron. The relevant quantity usually reported in experiments is  $a_e$ , which is:

$$a_e = \frac{g_e - 2}{2} \quad (12.27)$$

The most precise direct measurement of  $a_e$  is from a 2008 experiment ([59]):

$$a_e(\text{exp}) = 0.001\,159\,652\,180\,73(28) \quad (12.28)$$

Recent experiments involving precision study of Bloch oscillations of  $^{133}\text{Cs}$  (in 2018, [60]) and  $^{87}\text{Rb}$  (in 2020, [58]) have instead measured  $\alpha$ , with a never before seen precision. With those new measurements, it was possible to predict the value of  $a_e$  using QED and Standard Model. However, the two resulting theoretical predictions are incompatible between each other and with the experimental value:

$$\Delta a_e(^{87}\text{Rb}) = (4.8 \pm 3.0) \times 10^{-13} \quad (12.29)$$

$$\Delta a_e(^{122}\text{Cs}) = (-8.8 \pm 3.6) \times 10^{-13} \quad (12.30)$$

Where  $\Delta a_e$  are the differences between the 2008 best direct experimental value, and the two different theoretical predictions. These are discrepancies respectively of  $1.6\sigma$  and  $2.4\sigma$ .

While, theoretically, QED diagrams have been calculated up to 4 loops, a possible contribution due to a massive spin 2 boson in an effective landscape has already been computed, at one loop, in [61] (their goal was to explain the anomaly in the  $g - 2$  for the muon, but the formula still works for electrons). The intervening diagrams are all vertex corrections<sup>31</sup>.

The reported contribution is, in our notation:

$$\delta a_e = \frac{m_e^2}{48\pi^2} \left( \frac{\Lambda_c}{m_X} \right)^4 \frac{g_e}{\Lambda} \left( \frac{g_e}{\Lambda} - \frac{2g_\gamma}{\Lambda} \right) \quad (12.31)$$

where  $\delta a_e$  is the absolute difference between Standard Model prediction and spin 2 model correction.

Notice that there is a bare dependence on a cutoff  $\Lambda_c$ , because of the hard cutoff regularization procedure that left power law divergences in  $\Lambda_c^4/m_X^4$ . Because this is an effective theory, this cutoff is actually physical, as for higher energy scales perturbation theory breaks and UV corrections cannot be neglected. So far, throughout the thesis, we used interchangeably  $\Lambda$  and  $\Lambda_c$ , setting this value of cutoff to 20 – 50 MeV. [61] does the same, and they explore different ratios for  $\Lambda_c/m_X$ , between 2 and 5 (even though they work at the TeV scale).

One realizes that in the case  $g_e = 2g_\gamma$ ,  $\delta a_e = 0$ . However, this is a "one dimensional" constraint, highly sensitive to higher order corrections. We are not to trust regions not excluded by this constraint as viable regions for our model.

Notice that the correction is relevant even when  $g_\gamma = 0$ . In this case:

$$\delta a_e = \frac{m_e^2}{48\pi^2} \left( \frac{\Lambda_c}{m_X} \right)^4 \left( \frac{g_e}{\Lambda} \right)^2 \quad (12.32)$$

which will be very useful in [section 13](#). The value of  $\Lambda$  will decide the feasibility of the one parameter model for  $g_e$ .

Now, how can we constrain our spin 2 model in light of these experimental results? There are two possible approaches:

<sup>30</sup>In [13], because amplitude squared is defined without the  $1/s$  at the denominator due to fermion polarization sum, the amplitude behavior in the non universal scheme is constant, while in the universal scheme it goes like  $1/s$ . In our case, however, in the non universal scheme the amplitude goes like  $1/s$ , and in the universal scheme like  $1/s^2$ .

<sup>31</sup>Technically,  $\alpha$  would be corrected by  $X$  mediation as well, but that is just a higher order correction than  $g - 2$ .

- On the one hand, we could require that this new arising physics from a spin 2 massive boson could explain the anomalies in the results found in [60], [58]. This would mean imposing that our correction allows for experimental results to be inside  $1\sigma$  of the theoretical Standard Model + spin 2 prediction (see [Figure 40](#) and [Figure 41](#)), requiring both an upper and lower bound:

$$\Delta a_e - \sigma < \delta a_e < \Delta a_e + \sigma \quad (12.33)$$

where  $\Delta a_e$  is the discrepancy between theory and experiment,  $\delta a_e$  is the correction of the spin 2 model, and  $\sigma$  is the reported uncertainty.

- On the other hand, we could assume that all measurements that were performed are in a region of precision so high that tiny inconsistencies may be caused by the smallest of effects. So, conservatively speaking, we could take the midpoint between the Cesium and Rubidium measurements and require, as conservatively as possible, that our spin 2 correction (not touching  $\alpha$ , only  $\Delta a_e$ ) does not allow us to exit this very small region of values. Once that occurs, we then require our spin 2 correction to be invisible. This would mean:

$$|\delta a_e| < \frac{\Delta a_e^{(87\text{Rb})} - \Delta a_e^{(122\text{Cs})}}{2} = 6.8 \times 10^{-13} \quad (12.34)$$

as in [Figure 42](#). This would appear as a simple upper bound on the model.

**Cutoff choice for  $\Lambda_c$**  : we want to commit for a specific  $\Lambda_c$ , because it is the first time it actually makes a difference. One could argue that  $\Lambda_c = \Lambda$ , as this would be the scale of the effective theory. But this is not the correct picture, as the two values have a different physical meaning:

- $\Lambda$  comes from the Wilson coefficient. If the UV theory requires mediation of a certain particle, whose interaction becomes local in the EFT, then  $\Lambda$  is expression of that specific mass mediation, meaning that it has to do with the masses of the heavy modes in the theory<sup>32</sup>.
- $\Lambda_c$  is the cutoff of the theory. In loop integrals, integration may go up only to where we are confident our theory holds up. One would say that this limit is the energy value  $\Lambda_c$  at which heavy states appear in the theory, which should restore renormalizability.

The problem lies in what we consider our heavy mode to be. If you extend the theory with an elementary particle (like in the case of [61], where they use the actual graviton to explain muon  $g - 2$  anomaly), the heavy mode is the spin 2 particle itself, and you can identify  $\Lambda = \Lambda_c$ , as they both hint to the same theory as being "more fundamental".

Our  $X$  resonance, however, is believed to be a *composite* spin 2 state, meaning it should be some sort of excitation produced by strong nuclear processes. As such, the approach we should follow is then similar to chiral perturbation theory, where the real heavy mediator disappears locally into the  $X$  state, the lightest of many resonances, which then couples with electrodynamics.

So, we should imagine that there must be a scale  $f_X$ , sort of like the pion decay constant, that controls every process in this EFT. This scale is clearly  $f_X \approx m_X$ . So, like in  $\chi$ PT, the limit cutoff should be  $\Lambda_c \approx k f_X \approx k m_X$ . As in  $\chi$ PT, if we choose  $k = 4\pi$ , we get  $\Lambda_c \approx 200 \text{ MeV}$ , which is the actual scale at which EFT breaks. The role of  $\Lambda_c$  is then the same role of  $\Lambda_{\text{QCD}}$ , appearing naturally when running the coupling (dimensional transmutation).

Then,  $\Lambda$  and  $\Lambda_c$  really do have different meanings, because  $\Lambda_c$  depends on the renormalization flow characteristics, while  $\Lambda$  depends on the UV mediation. We will fix, for our spin 2 effective theory,  $\Lambda_c \approx 4\pi m_X$ . This will be treated as the highest possible value for the cutoff.

Finally, to have another reference, we will also choose  $k = 2$ , so  $\Lambda_c = 2m_X \approx 34 \text{ MeV}$  to be the most conservative cutoff value possible, and compare our constraints in both cases, in [section 13](#) and [section 14](#).

## 12.3 Perturbativity constraint

Starting from  $g - 2$  correction, the same paper ([61]) elaborates further, imposing an extra constraint on perturbativity looking at estimates on loop contributions. The idea is that the  $n$ -th loop correction contribution to  $g - 2$ , with a spin 2 particle mediation, must be smaller than the  $(n - 1)$ -th loop correction, for the methods of perturbation theory to work. We shall now argue that this imposes a constraint on the coupling itself.

Start with the definition of  $a_e$ , which is the magnetic moment of the electron. If we take vertex correction amplitude, it should be:

$$\mathcal{M} \propto e\gamma_\mu F_1(q^2) + \frac{ie\sigma_{\mu\nu}q_\nu}{2m_e} F_2(q^2) \quad (12.35)$$

<sup>32</sup>Think of Fermi's constant  $G_F \propto m_W^{-2}$ .

where  $a_e = F_2(0)$  as by magnetic form factor with no exchanged momentum  $q$ .

Then, by *spurion* arguments, we can argue that  $\mathcal{M} \propto m_e$ . This is true for any vector correction diagram in a vector-like theory, like QED extended with our spin 2 correction. The operators describing vertex correction (in Figure 36) have an even number of gamma matrices, forcing the fermion field structure to be  $\bar{\psi}_L \psi_R$ , to get Lorentz invariance. This implies that the axial U(1) in QED, already broken by mass terms, would also be broken by these vertex operators, as  $\bar{\psi}_L \psi_R \sim (-1, 1)$  according to  $U(1)_L \times U(1)_R$ .

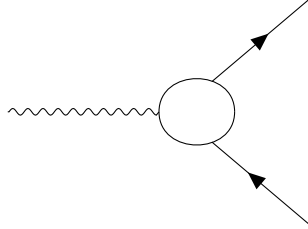


Figure 36: Generic three point vertex function in QED.  $g - 2$  corrections come from these diagrams.

However, if our extension of QED has the same symmetries of QED itself, then the spurions of the extension would be the same as QED. Spin 2 vertex corrections operators would then have to be proportional to a linear mass term  $m_e$ , whose spurious transformation properties would be  $(1, -1)$ , compensating vertex operator and restoring axial U(1).

In the end,  $\mathcal{M} \propto m_e$ , hence  $a_e = F_2(0) \propto m_e^2$ , and so will our correction  $\delta a_e$ .

In our estimate, other relevant dimensional quantities are the couplings  $g/\Lambda$ , which are easy to count in each diagram,  $m_X$  and  $\Lambda_c$ . Dependence of estimates on  $m_X$  can be deduced by the structure of the spin 2 propagator:

$$\hat{D}_{\mu\nu\rho\sigma}^X(p) = \frac{N_{\mu\nu\rho\sigma}(p)}{p^2 + m_X^2}$$

In each loop where spin 2 correction enter, there should be at least one internal propagator over whose momentum we integrate in one of the loop integrals. Integrals will arrive only up to  $\Lambda_c$ , which is assumed to be much larger than  $m_X$ . As a result, dependence on  $m_X$  should be chosen depending on the highest powers of the momentum that enter in the integral.

If we look at the denominator, then we select  $p^2$  to be dominant. Instead, in the numerator we get  $N_{\mu\nu\rho\sigma}$ , which contains products of projectors  $P_{\mu\nu} = \delta_{\mu\nu} + p_\mu p_\nu / m_X^2$ . The term  $p_\mu p_\nu / m_X^2$  dominates, leaving then:

$$\hat{D}_{\mu\nu\rho\sigma}^X(p) \propto \frac{p^2}{m_X^4}$$

which allows to infer that every extra internal spin 2 propagator will leave a  $1/m_X^4$  power in the estimate.

Finally, only  $\Lambda_c$  is left to estimate. However, dimensional analysis immediately gives us the correct power dependence of  $\Lambda_c$ , as  $\Delta a_e$  must be adimensional. Remembering the geometrical factor  $1/16\pi^2$  in each loop, we are good to go.

So, we are left with our estimates. Take examples of one loop and two loop contributions involving the addition of  $X e^+ e^-$  interactions only (as in Figure 37): Following the sketched rules, there are the estimates for

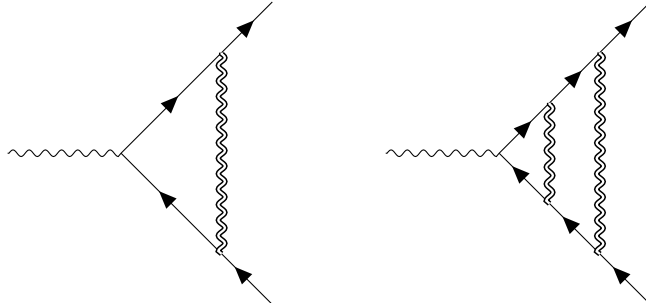


Figure 37: Loop diagrams with spin 2 mediation contributing to  $g - 2$ . On the left, a one loop example. On the right, a two loop example. Notice that the difference between the two diagrams is the  $g_e/\Lambda$  addition as extra loop.

the contributions of the two diagrams:

$$\Delta a_e^{(1)} \approx \frac{g_e^2}{16\pi^2} \frac{m_e^2}{\Lambda^2} \frac{\Lambda_c^4}{m_X^4} \quad \Delta a_e^{(2)} \approx \left( \frac{g_e^2}{16\pi^2} \right)^2 \frac{m_e^2}{\Lambda^4} \frac{\Lambda_c^{10}}{m_X^8} \quad (12.36)$$

so, requiring:

$$\Delta a_e^{(2)} < \Delta a_e^{(1)} \quad \Rightarrow \quad \frac{g_e^2}{16\pi^2 \Lambda^2} \frac{\Lambda_c^6}{m_X^4} < 1$$

means that the upper limit for the coupling is:

$$\frac{g_e}{\Lambda} < \frac{4\pi m_X^2}{\Lambda_c^3} = \frac{4\pi}{k^3 m_X} \quad (12.37)$$

where  $k = \Lambda_c/m_X$ , which is a number between 2 and  $4\pi$ , defined in [subsection 12.2](#).

Similar examples can be found for the other coupling, as in [Figure 38](#): where the estimates now are:

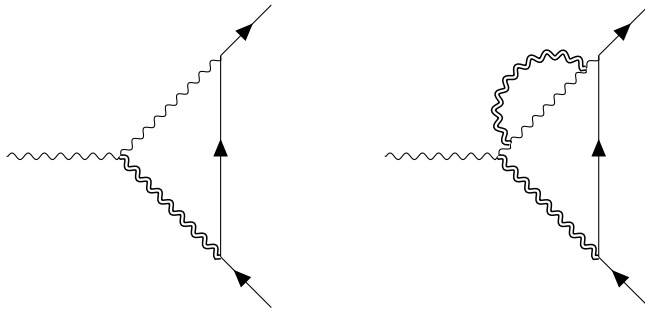


Figure 38: Loop diagrams with spin 2 mediation contributing to  $g - 2$ . On the left, a one loop example. On the right, a two loop example. Notice that the difference between the two diagrams is the  $g_\gamma/\Lambda$  addition as extra loop.

$$\Delta a_e^{(1)} \approx \frac{g_e g_\gamma}{16\pi^2} \frac{m_e^2}{\Lambda^2} \frac{\Lambda_c^4}{m_X^4} \quad \Delta a_e^{(2)} \approx \frac{g_e g_\gamma^3}{(16\pi)^2} \frac{m_e^2}{\Lambda^4} \frac{\Lambda_c^{10}}{m_X^8} \quad (12.38)$$

which ends in the same result as [Equation 12.37](#):

$$\frac{g_\gamma}{\Lambda} < \frac{4\pi m_X^2}{\Lambda_c^3} = \frac{4\pi}{k^3 m_X} \quad (12.39)$$

Numerical values for the two extremes are:

$$k = 4\pi : \quad \frac{g_e}{\Lambda}, \frac{g_\gamma}{\Lambda} < 3.7 \times 10^{-4} \text{ MeV}^{-1} \quad (12.40)$$

$$k = 2 : \quad \frac{g_e}{\Lambda}, \frac{g_\gamma}{\Lambda} < 9.3 \times 10^{-2} \text{ MeV}^{-1} \quad (12.41)$$

## 12.4 Unitarity constraint

From the unitarity of the  $S$  matrix, there is a very important bound to be imposed. Defining for a 2-2 scattering, in the center of mass of the process, whose matrix element is  $\mathcal{M}_{fi}$ :

$$a_0(\sqrt{|s|}) = \frac{1}{32\pi} \sqrt{\frac{4|\vec{p}_i||\vec{p}_f|}{2^{\delta_i+\delta_f}|s|}} \int_{-1}^1 d\cos\theta \mathcal{M}_{fi} \quad (12.42)$$

where  $\delta_i, \delta_f$  are equal to 1 for identical particles and to 0 for different particles in the initial and final state,  $|\vec{p}_i|, |\vec{p}_f|$  are moduli of 3-momenta of particles in the initial and final state<sup>33</sup>, and  $\theta$  is the scattering angle (the only to be kinematically relevant in a 2-2 scattering). The constraint is, then:

$$\text{Re} [a_0(\sqrt{|s|})] \leq \frac{1}{2} \quad (12.43)$$

called *partial wave unitarity constraint*. In [subsubsection 12.4.1](#), we will explore where this bound comes from.

<sup>33</sup>3-momentum modulus for each particle in initial (or final) state is the same in the center of mass frame.

If we look at [62], their goal is to try and constrain  $g_e/\Lambda$  and  $g_\gamma/\Lambda$  individually, using 2-2 scattering processes such as  $e^+e^- \rightarrow e^+e^-$  (Bhabha scattering, for  $g_e$ ) and  $\gamma\gamma \rightarrow \gamma\gamma$  (two-photon scattering, for  $g_\gamma$ ). For every scattering they evaluate, they fix the chiralities. For Bhabha scattering, we will not reiterate the calculations, and only present what they find (which agrees to our results on Bhabha scattering at least in terms of dimensions of  $m_X$ , couplings and overall symmetry properties). In regards to photon scattering, instead, we will repeat calculations using our own helicity dependent amplitudes which we have evaluated in section 11, since chirality and helicity are in 1:1 correspondence in massless particles<sup>34</sup>.

Finally, if Equation 12.43 is true for every value of  $|s|$  accepted in our EFT, and because corrections grow with energy, then the bound will be at its most constraining when  $\sqrt{|s|} = 2\Lambda_c$  at the cutoff<sup>35</sup>. So, we will then evaluate results at the cutoff energy, making this constraint cutoff dependent, like the perturbativity constraint.

### 12.4.1 Derivation

This derivation is taken from [74]. Start from taking the non trivial part of the  $S$ -matrix  $S = \mathbb{1} + iT$ . Now, a multiparticle state  $a$ , with momentum set  $\{p\}$  and a state  $b$  with momentum set  $\{k\}$ . The  $T$ -matrix element relative to the transition  $a \rightarrow b$  is then proportional to the amplitude of the process  $\mathcal{M}_{ba}$ . Define:

$$T_{ba} = \langle \{k, b\} | iT | \{p, a\} \rangle = i\mathcal{M}_{ba}(2\pi)^4 \delta(\{k\} - \{p\}) \quad (12.44)$$

Now, let us impose unitarity:

$$\mathbb{1} = S^\dagger S = \mathbb{1} - i(T^\dagger - T) + T^\dagger T \quad (12.45)$$

looking at the matrix element, we need to impose:

$$\langle \{k, b\} | T^\dagger T | \{p, a\} \rangle = -i \langle \{k, b\} | T - T^\dagger | \{p, a\} \rangle$$

The right side can be expanded simply as matrix elements:

$$-i \langle \{k, b\} | T - T^\dagger | \{p, a\} \rangle = -(2\pi)^4 i \left[ \mathcal{M}_{ba} - (\mathcal{M})_{ba}^\dagger \right] \delta(\{k\} - \{p\}) \quad (12.46)$$

As for the left side, we have to insert a complete set of states<sup>36</sup>:

$$\begin{aligned} \langle \{k, b\} | T^\dagger T | \{p, a\} \rangle &= \sum_n \sum_{c_n} d\Pi_n \langle \{k, b\} | T^\dagger | \{q_n, c_n\} \rangle \langle \{q_n, c_n\} | T | \{p, a\} \rangle = \\ &= \sum_n \sum_{c_n} d\Pi_n (2\pi)^8 (\mathcal{M})_{bc_n}^\dagger \mathcal{M}_{c_n a} \delta(\{q_n\} - \{p\}) \delta(\{k\} - \{q_n\}) = \\ &= \sum_n \sum_{c_n} d\Pi_n (2\pi)^8 \mathcal{M}_{c_n a} \mathcal{M}_{c_n b}^* \delta(\{q_n\} - \{p\}) \delta(\{k\} - \{p\}) \end{aligned}$$

We will now calculate the contribution  $n = 2$ , which translates into a simple 2-body phase space integration. Remember the factor  $1/2\delta_c$ , where  $\delta_c = 0, 1$  depending on the identity of the particles in the intermediate state, as we did in the two-photon scattering calculations:

$$\begin{aligned} \langle \{k, b\} | T^\dagger T | \{p, a\} \rangle &= (2\pi)^4 \delta(\{k\} - \{p\}) \left[ \sum_c \frac{1}{2\delta_c} \int d\Pi_2 \mathcal{M}_{ca} \mathcal{M}_{cb}^* (2\pi)^4 \delta(\{q_n\} - \{p\}) + \right. \\ &\quad \left. + \sum_{n>2} \sum_{c_n} d\Pi_n \mathcal{M}_{c_n a} \mathcal{M}_{c_n b}^* (2\pi)^4 \delta(\{q_n\} - \{p\}) \right] \end{aligned}$$

Before angular integration, 2-body phase space integrals are reduced to Equation F.2, where  $M = \sqrt{|s|}$  is now the center of mass energy, and there is an extra factor  $\int d\Omega/4\pi$ . Instead, the second addend contribution to the left hand side, which is interpreted as the mediation of  $n$ -multiparticle state as intermediate state between  $a$  and  $b$ , is clearly a positive contribution, leaving the following inequality:

$$\langle \{k, b\} | T^\dagger T | \{p, a\} \rangle \geq (2\pi)^4 \delta(\{k\} - \{p\}) \sum_c \frac{2^{-\delta_c} |\vec{q}_c|}{16\pi^2 \sqrt{|s|}} \int d\Omega_c \mathcal{M}_{ca} \mathcal{M}_{cb}^* \quad (12.47)$$

<sup>34</sup>Also, we do not agree with their results, as they claim  $1/m_X^2$  and  $1/m_X^4$  dependence vanish in the integration, while we claim it is true only for some helicity-fixed amplitudes and not for all of them.

<sup>35</sup>As the theory is integrable in loop momenta up to  $\Lambda_c$  for individual momenta.

<sup>36</sup>Like when proving optical theorem, completeness of the Hilbert space where our QFT is defined is no trivial property that we assume to be true here.

where  $|\vec{q}_c|$  is well defined in the center of mass of 2-2 scattering. Combining [Equation 12.46](#) and [Equation 12.47](#), leaves us with:

$$-i \left[ \mathcal{M}_{ba} - (\mathcal{M})_{ba}^\dagger \right] \geq \sum_c \frac{2^{-\delta_c} |\vec{q}_c|}{16\pi^2 \sqrt{|s|}} \int d\Omega_c \mathcal{M}_{ca} \mathcal{M}_{cb}^* \quad (12.48)$$

Now, let us fix the unit vectors that define the  $a \rightarrow c \rightarrow b$  scattering process:

$$\hat{p}_a = (1, 0, 0) \quad \hat{k}_b = (z_b, \sin \theta_b, 0) \quad \hat{q}_c = (z_c, \sin \theta_c \cos \phi_c, \sin \theta_c \sin \phi_c)$$

where  $z_b = \cos \theta_b$  and  $z_c = \cos \theta_c$ . Notice how, while the scattering plane for  $a \rightarrow b$  process is well defined and hence we do not need  $\phi_b$ , since the intermediate state can be generated with any possible orientation, we need a new relative set of spherical coordinates to describe it. This set of coordinates we also integrate upon, as  $d\Omega_c = dz_c d\phi_c$ .

In the following, matrix elements will be expanded into partial waves, according to:

$$\left\{ \begin{array}{l} \mathcal{M}_{ba} = 16\pi \sum_{J=0}^{\infty} (2J+1) P_J(z_b) \hat{a}_{ba}^J(|s|) \\ \mathcal{M}_{ca} = 16\pi \sum_{J=0}^{\infty} (2J+1) P_J(z_c) \hat{a}_{ca}^J(|s|) \\ \mathcal{M}_{cb} = 16\pi \sum_{J=0}^{\infty} (2J+1) P_J(\hat{k}_b \cdot \hat{q}_c) \hat{a}_{cb}^J(|s|) \end{array} \right. \quad (12.49)$$

where  $P_J(z)$  are *Legendre polynomials*, and they satisfy:

$$\int_{-1}^1 P_J(z) P_{J'}(z) = \frac{2\delta_{JJ'}}{2J+1} \quad P_0(z) = 1 \quad (12.50)$$

which into [Equation 12.48](#):

$$\begin{aligned} & -16\pi i \sum_J (2J+1) P_J(z_b) \left[ \hat{a}_{ba}^J - \hat{a}_{ba}^{\dagger J} \right] \geq \\ & \geq \sum_c \frac{2^{-\delta_c} |\vec{q}_c| (16\pi)^2}{16\pi^2 \sqrt{|s|}} \sum_{J'J''} (2J'+1)(2J''+1) \int dz_c d\phi_c P_{J'}(z_c) P_{J''}(\hat{k}_b \cdot \hat{q}_c) \hat{a}_{ca}^{J'} \hat{a}_{cb}^{*J''} \end{aligned}$$

Now, apply to both sides:  $\int_{-1}^1 dz_b P_J(z_b)$ . The left side will leave its sum over  $J$  using [Equation 12.50](#), while the right side will get another integral:

$$-2i \frac{2J+1}{2J+1} \left[ \hat{a}_{ba}^J - \hat{a}_{ba}^{\dagger J} \right] \geq \sum_c \frac{2^{-\delta_c} |\vec{q}_c|}{\pi \sqrt{|s|}} \sum_{J'J''} (2J'+1)(2J''+1) \int dz_b dz_c d\phi_c P_J(z_b) P_{J'}(z_c) P_{J''}(\hat{k}_b \cdot \hat{q}_c) \hat{a}_{ca}^{J'} \hat{a}_{cb}^{*J''} \quad (12.51)$$

Then, use the following expansion in spherical harmonics:

$$P_J(\hat{k}_b \cdot \hat{q}_c) = \frac{4\pi}{2J+1} \sum_{m=-J}^J Y_{Jm}(\theta_b, \phi_b) Y_{Jm}^*(\theta_c, \phi_c) \quad (12.52)$$

Notice that this is the only place where in the integral we get dependence on  $\phi_b$  and  $\phi_c$ . However, remember that:

$$Y_{Jm}(\theta, \phi) \propto e^{im\phi} P_J^m(\cos \theta) \quad Y_{J0} = \sqrt{\frac{2J+1}{4\pi}} P_J(\cos \theta) \quad (12.53)$$

where  $P_J^m(z)$  are *associated Legendre polynomials*, and are such that  $P_J^0(z) = P_J(z)$ . In our case  $\phi_b = 0$ , as we selected the scattering plane at the beginning. So, only the integral in  $\phi_c$  is left:

$$\int_0^{2\pi} d\phi_c e^{-im\phi_c} = 2\pi \delta_{m0}$$

which then forces  $m = 0$  in [Equation 12.52](#), for which we have a neat expression thanks to [Equation 12.53](#):

$$\begin{aligned} P_J(\hat{k}_b \cdot \hat{q}_c) &= \frac{4\pi}{2J+1} Y_{J0}(\theta_b, \phi_b) Y_{J0}^*(\theta_c, \phi_c) = \\ &= \frac{4\pi}{2J+1} \sqrt{\frac{2J+1}{4\pi}} \sqrt{\frac{2J+1}{4\pi}} P_J(z_b) P_J(z_c) = P_J(z_b) P_J(z_c) \end{aligned} \quad (12.54)$$

substitute [Equation 12.54](#) into [Equation 12.51](#):

$$\begin{aligned} -2i \left[ \hat{a}_{ba}^J - \hat{a}_{ba}^{\dagger J} \right] &\geq \sum_c \frac{2^{-\delta_c} |\vec{q}_c| 2\kappa}{\kappa \sqrt{|s|}} \sum_{J' J''} (2J'+1)(2J''+1) \int dz_b dz_c P_J(z_b) P_{J'}(z_c) P_{J''}(z_b) P_{J''}(z_c) \hat{a}_{ca}^{J'} \hat{a}_{cb}^{*J''} \\ &\geq \sum_c \frac{2^{-\delta_c} |2\vec{q}_c|}{\sqrt{|s|}} \sum_{J' J''} (2J'+1)(2J''+1) \frac{2\delta_{JJ'}}{2J'+1} \frac{2\delta_{JJ''}}{2J''+1} \hat{a}_{ca}^{J'} \hat{a}_{cb}^{*J''} \\ &\geq \sum_c \frac{2^{-\delta_c} |8\vec{q}_c|}{\sqrt{|s|}} \hat{a}_{ca}^J \hat{a}_{cb}^{*J} \end{aligned}$$

which gives us the final expression:

$$-\frac{i}{2} \left[ \hat{a}_{ba}^J - \hat{a}_{ba}^{\dagger J} \right] \geq \sum_c \frac{2^{-\delta_c} |2\vec{q}_c|}{\sqrt{|s|}} \hat{a}_{ca}^J \hat{a}_{cb}^{*J} \quad (12.55)$$

Now, just normalize our operators to simplify the result:

$$\hat{a}_{ba}^J = \sqrt{\frac{2^{\delta_a + \delta_b} |s|}{4|\vec{p}_a||\vec{p}_b|}} a_{ba}^J \quad (12.56)$$

so that [Equation 12.55](#) becomes:

$$-\frac{i}{2} \sqrt{\frac{2^{\delta_a + \delta_b} |s|}{4|\vec{p}_a||\vec{p}_b|}} \left[ a_{ba}^J - a_{ba}^{\dagger J} \right] \geq \sum_c \frac{2^{-\delta_c} |2\vec{q}_c|}{\sqrt{|s|}} \sqrt{\frac{2^{\delta_a + \delta_c} |s|}{4|\vec{p}_a||\vec{p}_c|}} \sqrt{\frac{2^{\delta_c + \delta_b} |s|}{4|\vec{p}_c||\vec{p}_b|}} a_{ca}^J a_{cb}^{*J}$$

which simplifies into:

$$-\frac{i}{2} \left[ a_{ba}^J - a_{ba}^{\dagger J} \right] \geq a_{ca}^J a_{cb}^{*J} = a_{bc}^{\dagger J} a_{ca}^J = \left( a^{\dagger} a \right)_{ba}^J \quad (12.57)$$

Notice that we could have repeated the same exact reasoning using  $TT^\dagger$  instead of  $T^\dagger T$ . Because of unitarity of  $S$ , as  $S^\dagger S = SS^\dagger = 1$ , this implies normality of  $T$ , as  $T^\dagger T = TT^\dagger$ , which in turn implies that  $a^J$  is normal.

A very important generalization of *spectral theorem* proves that normal matrices  $a^J$  and  $a^{\dagger J}$  can be diagonalized with the same unitary matrix, so that [Equation 12.57](#) is translated into an identity of eigenvalues  $a_i^J$ :

$$\text{Im}(a_i^J) \geq |a_i^J|^2 = \text{Re}(a_i^J)^2 + \text{Im}(a_i^J)^2 \quad (12.58)$$

calling  $\text{Re}(a_i^J) = x$  and  $\text{Im}(a_i^J) = y$ , we obtain the inequality:

$$x^2 + y^2 - y \leq 0 \quad \rightarrow \quad x^2 + \left( y - \frac{1}{2} \right)^2 \leq \frac{1}{4} \quad (12.59)$$

which describes points inside a circumference of radius  $1/2$ , centered around  $(0, 1/2)$ , in the complex plane where  $a_i^J$  is defined. This immediately tells us that:

$$|x| \leq \frac{1}{2} \quad \left| \text{Re}[a_i^J(\sqrt{|s|})] \right| \leq \frac{1}{2} \quad (12.60)$$

which is the *unitarity constraint* we were trying to prove in the first place.

Now, let us go back the chain of definition to find out what is the expression of the partial wave  $a_{ba}^J$ . First, we invert [Equation 12.49](#):

$$\begin{aligned} \int_{-1}^1 d\cos\theta P_J(\cos\theta) \mathcal{M}_{ba} &= 16\pi \sum_{J'} (2J'+1) \int_{-1}^1 d\cos\theta P_J(\cos\theta) P_{J'}(\cos\theta) \hat{a}_{ba}^{J'} = \\ &= 16\pi \sum_{J'} (2J'+1) \frac{2\delta_{JJ'}}{2J'+1} \hat{a}_{ba}^{J'} = 32\pi \hat{a}_{ba}^J \end{aligned}$$

which gives us the final expression:

$$a_{ba}^J = \sqrt{\frac{4|\vec{p}_a||\vec{p}_b|}{2^{\delta_a + \delta_b}|s|}} \hat{a}_{ba}^J = \frac{1}{32\pi} \sqrt{\frac{4|\vec{p}_a||\vec{p}_b|}{2^{\delta_a + \delta_b}|s|}} \int_{-1}^1 d\cos\theta P_J(\cos\theta) \mathcal{M}_{ba} \quad (12.61)$$

We are only interested in the  $S$ -wave only, so  $J = 0$ , and  $P_0(z) = 1$ . Calling  $a = i$  and  $b = f$  as initial and final states:

$$a_0(\sqrt{|s|}) = \frac{1}{32\pi} \sqrt{\frac{4|\vec{p}_i||\vec{p}_f|}{2^{\delta_i+\delta_f}|s|}} \int_{-1}^1 d\cos\theta \mathcal{M}_{fi} \quad \text{Re}[a_0(\sqrt{|s|})] \leq \frac{1}{2} \quad (12.62)$$

which was the constraint we were looking for in [Equation 12.43](#).

There is a catch: the constraint is non perturbative. We never used perturbation theory expansion, so the bound should be valid for the infinitely summed result. However, we are only stopping at tree level for the evaluation of  $\mathcal{M}$ . The interpretation of the bound, then, is that we have to require  $\text{Re}[a_0(\text{tree})] \leq 1/2$  because we do not want to stray away too much from that circumference in which  $a_0$  is well-defined. If contributions at higher orders in perturbation theory are smaller, if  $a_0(\text{tree})$  itself is much bigger than  $1/2$ , then there is no way to have the non perturbative  $a_0$  inside the final circle.

### 12.4.2 Application to lepton scattering

Let us now report results from [62] in regards of Bhabha scattering, and substituting  $\sqrt{|s|} = 2\Lambda_c = 2k m_X$ :

$$\begin{aligned} a_0(e_R^- e_L^+ \rightarrow e_R^- e_L^+) &= a_0(e_L^- e_R^+ \rightarrow e_L^- e_R^+) \approx \frac{1}{16\pi^2} \frac{g_e^2}{4\Lambda^2} |s| \left[ \frac{14}{3} - 4 \log \left( \frac{|s| + m_X^2}{m_X^2} \right) \right] \\ &\approx \frac{k^2 m_X^2}{16\pi^2} \frac{g_e^2}{\Lambda^2} \left[ \frac{14}{3} - 4 \log(1 + 4k^2) \right] \approx \frac{k^2 m_X^2}{16\pi^2} \frac{g_e^2}{\Lambda^2} \left[ \frac{14}{3} - 8 \log(2k) \right] \end{aligned} \quad (12.63)$$

$$\begin{aligned} a_0(e_R^- e_R^+ \rightarrow e_R^- e_R^+) &= a_0(e_L^- e_L^+ \rightarrow e_L^- e_L^+) \approx \frac{1}{16\pi^2} \frac{g_e^2}{4\Lambda^2} |s| \left[ 3 - 4 \log \left( \frac{|s| + m_X^2}{m_X^2} \right) \right] \\ &\approx \frac{k^2 m_X^2}{16\pi^2} \frac{g_e^2}{\Lambda^2} \left[ 3 - 4 \log(1 + 4k^2) \right] \approx \frac{k^2 m_X^2}{16\pi^2} \frac{g_e^2}{\Lambda^2} [3 - 8 \log(2k)] \end{aligned} \quad (12.64)$$

$$a_0(e_R^- e_L^+ \rightarrow e_L^- e_R^+) = a_0(e_L^- e_R^+ \rightarrow e_R^- e_L^+) \approx \frac{1}{16\pi} \frac{g_e^2}{24\Lambda^2} |s| = \frac{k^2 m_X^2}{96\pi} \frac{g_e^2}{\Lambda^2} \quad (12.65)$$

Since in our search for Bhabha scattering experiments, we only found studies in which helicities were not considered (hence summed upon), in the unpolarized case we ought to take the most constraining result of them all, which comes from [Equation 12.64](#). Using unitarity constraint:

$$\text{Re}[a_0(e_R^- e_R^+ \rightarrow e_R^- e_R^+)] \leq \frac{1}{2} \quad \Rightarrow \quad \frac{g_e}{\Lambda} \leq \sqrt{\frac{8\pi}{k^2 m_X^2 |3 - 8 \log(2k)|}} \quad (12.66)$$

which numerically, in the limiting cases  $k = 2$  and  $k = 4\pi$ :

$$k = 4\pi : \quad \frac{g_e}{\Lambda} < 4.9 \times 10^{-3} \text{ MeV}^{-1} \quad (12.67)$$

$$k = 2 : \quad \frac{g_e}{\Lambda} < 5.2 \times 10^{-2} \text{ MeV}^{-1} \quad (12.68)$$

### 12.4.3 Application to photon scattering

In [section 11](#), we calculated fixed-helicity amplitudes for the  $X$  mediated photon-photon scattering, fixing helicities. Using kinematics for massless particles:  $|s| = 4|\vec{p}_i||\vec{p}_f|$ , while photons in initial and final states are indistinguishable ( $\delta_i = \delta_f = 1$ ), so [Equation 12.62](#) becomes:

$$a_0(\sqrt{|s|}) = \frac{1}{64\pi} \int_{-1}^1 d\cos\theta \mathcal{M}_{fi} \quad (12.69)$$

Our  $\mathcal{M}_{\lambda_1\lambda_2\lambda_3\lambda_4}$  are functions of  $s, t, u$  for now. Substitute:  $t = -s/2(1 - \cos\theta)$  and

$$t = -\frac{s}{2}(1 - \cos\theta) \quad u = -\frac{s}{2}(1 + \cos\theta) \quad (12.70)$$

which is performed using the code `unitar_gggg.frm`, found in the usual GIT repository<sup>37</sup>. Results of the substitution have been fed as inputs for [this Integral Calculator](#), which has then integrated in  $dx = d \cos \theta$ .

Because we evaluating at  $|s| = 4\Lambda_c^2 \gg m_X^2$ , in this approximation we can look at the dominant term in  $s/m_X^2$  only, after the integration. Critically, what [62] claims about terms in  $s/m_X^2$  and  $s^2/m_X^4$  vanishing is only true for  $\mathcal{M}_{++++}$ , and not for the other cases. In the end, calling  $a_0(\lambda_1\lambda_2\lambda_3\lambda_4)$  the partial wave obtained from  $\mathcal{M}_{\lambda_1\lambda_2\lambda_3\lambda_4}$ , these are the results we find:

$$a_0^{++++} \approx \frac{5m_X^2}{96\pi} \frac{g_\gamma^2}{\Lambda^2} \log\left(\frac{|s| + m_X^2}{m_X^2}\right) \approx \frac{5m_X^2}{48\pi} \frac{g_\gamma^2}{\Lambda^2} \log(2k) \quad (12.71)$$

$$a_0^{++--} \approx \frac{1}{16\pi} \frac{g_\gamma^2}{\Lambda^2} |s| \log\left(\frac{|s| + m_X^2}{m_X^2}\right) \approx \frac{k^2 m_X^2}{2\pi} \frac{g_\gamma^2}{\Lambda^2} \log(2k) \quad (12.72)$$

$$a_0^{+-+-} = a_0^{+-+-} \approx \frac{7}{4608\pi} \frac{g_\gamma^2}{\Lambda^2} \frac{|s|^3}{m_X^4} \approx \frac{7k^6 m_X^2}{96\pi} \frac{g_\gamma^2}{\Lambda^2} \quad (12.73)$$

Again, we expect to use experimental results of unpolarized scattering, meaning that we ought to take the most constraining of the list, considering the value of  $k$ . It is interesting that [Equation 12.73](#) is the most constraining when  $k = 4\pi$ , while [Equation 12.72](#) wins when  $k = 2$ :

$$\text{Re}[a_0^{+-+-}] \leq \frac{1}{2} \quad \Rightarrow \quad \frac{g_\gamma}{\Lambda} \leq \sqrt{\frac{96\pi}{7k^6 m_X^2}} \quad (12.74)$$

$$\text{Re}[a_0^{++--}] \leq \frac{1}{2} \quad \Rightarrow \quad \frac{g_\gamma}{\Lambda} \leq \sqrt{\frac{2\pi}{k^2 m_X^2 \log(2k)}} \quad (12.75)$$

and numerically:

$$k = 4\pi : \quad \frac{g_\gamma}{\Lambda} < 2.0 \times 10^{-4} \text{ MeV}^{-1} \quad (12.76)$$

$$k = 2 : \quad \frac{g_\gamma}{\Lambda} < 4.4 \times 10^{-2} \text{ MeV}^{-1} \quad (12.77)$$

## 12.5 Constraints we did not consider

There are several experiments that tried to reveal directly the presence of a new particle  $X$  at around MeV, without any success, and were used to put bounds on the coupling constants we defined in this thesis. However, for our dissertation, we did not consider their bounds, usually because of the energy of the experiment that far exceeded the center of mass limit for our EFT. Let us name a few examples:

**KLOE:** At this experiment held at INFN center in Frascati, the idea is to use the  $e^+e^-$  collider DAΦNE to produce and watch rare  $\phi$  meson decays, at  $\sqrt{|s|} = 1.02 \text{ GeV}$  ([75]).

With the same technology, the KLOE detector has been used to search for hidden vector bosons ([76]), so far without success. The process analyzed is  $e^+e^- \rightarrow X\gamma$ , and then study  $X \rightarrow e^+e^-$ . These are processes that, in the spin 2 hypothesis, are possible and have been calculated by us, so we could repeat the estimates they do based on their results and adapt bounds on a spin 2 model.

This would not work, however, because the center of mass energy for the experiment is always  $\sqrt{|s|} = 1.02 \text{ GeV}$ , meaning that too much energy is poured into our hidden  $X$  particle for production<sup>38</sup>.

**NA64:** This is an experiment held at CERN, in Switzerland. The goal of the experiment is to detect hidden sector and new particles, mainly dark photons and axions, using a beam of 100 GeV electrons against a fixed target. It has been a benchmark in DM research for the past few years.

In 2018, they released a study ([77]) concerning the direct production of our resonance  $X$ , as a hidden boson mediator. In 2022, another study ([79]) was published, concerning data analysis for spin 2 massive boson mediator.

<sup>37</sup>The variable  $\cos \theta$  is called  $x$  in the code.

<sup>38</sup>This is not like  $e^+e^- \rightarrow X$ , in which no matter the center of mass energy,  $X$  is produced at its own mass. Here, another photon is also produced, so the energy in the center of mass is, indeed, too high.

The idea of the experiment is to produce the hidden mediator using bremsstrahlung process inside an electromagnetic calorimeter (e-m), with  $e^- + Z \rightarrow e^+ + Z + X$ , and then  $X \rightarrow e^+ e^-$  is studied by another ECAL, further away from the beam. Since the  $X$  is expected to decay inside ECAL, the energy measured in the two calorimeters would be:

- Inside the first e-m calorimeter, the total energy detected, caused by the shower, would not be the total energy of the process of 100 GeV, as  $X$  is expected to escape the e-m calorimeter.
- Inside the ECAL calorimeter, the decay  $X \rightarrow e^+ e^-$  is expected to occur. The invariant mass of the electron and positron should be equal to the mass of the  $X$  hidden particle, while the sum of the individual energies of  $e^+ e^-$ , by conservation, must be exactly equal to the missing energy of the signal in e-m.

And you see where the problem lies. Again, the center of mass energy for the process is too high, because  $X$  is not produced alone, but as a result of a bremsstrahlung process<sup>39</sup>. This means that the  $X$  is expected to be produced extremely boosted (simulations like the one in [78] show that the majority of total missing energy events would be with a deficit of about 10 GeV).

Since [79] is operating on the assumption that the hidden particle is a portal, a mediator, then they assume it to be "elementary", hence center of mass energy can grow indefinitely and  $X$  would still exist (although their theory would still have a limit, as any spin 2 theory is an EFT because it requires dimension 5 operators), so their analysis is still valid. To us, however,  $X$  is merely a low energy composite state whose phenomenology could be described by a spin 2 EFT that has a cutoff  $\Lambda_c < 1$  GeV, hence we cannot use those results to set a bound in the theory.

---

<sup>39</sup>The bremsstrahlung process cross section, by the way, is proportional to the  $e^+ e^- \rightarrow X\gamma$  cross section we already calculated in subsection 12.1. This is expected as the diagrams are very similar, they are just rotated and the  $\gamma$  is reabsorbed by the nucleus igniting the bremsstrahlung.

## 13 Constraints on one coupling spin 2 model

Hence forth (in this chapter and the next one), we will refer to our couplings as  $g_e/\Lambda = 1/\Lambda_e$  and  $g_\gamma/\Lambda = 1/\Lambda_\gamma$ <sup>40</sup>. In this chapter only, we will set  $1/\Lambda_\gamma = 0$ . In the analysis we performed so far, we have assumed  $1/\Lambda_e = 3.8 \times 10^{-6} \text{ MeV}^{-1}$ , instead of having this numerical value as lower bound for the coupling constant. This was because we wanted to take the most conservative estimate for the spin 2 effective couplings, and to study their effect (to be intended as a lower bound effect) on QED processes at tree level (Bhabha and Møller scattering).

It is now time to let this coupling vary and identify its allowed range of values, using the best constraints from experimental data.

We explained in subsection 4.4 that this implies that exchanged momentum must be small (not exceeding  $20 - 50 \text{ MeV}$ ) in practice, but we might want to indulge in high energy limits (even if not physical or consistent) just to see what happens.

Let us take the most constraining experimental result for each process:

**$X \rightarrow e^+e^-$  decay:** This can be seen by ATOMKI collaboration ([1], [2], [3], [4], [5]). Result for the prediction is found in Equation 5.14. Direct lower bound for individual coupling constant, considering all nuclear transitions and geometry of the experiment:  $1/\Lambda_e > 3.8 \times 10^{-6} \text{ MeV}^{-1}$ .

**Bhabha scattering:** The most constraining experimental results are always ultra-relativistic and at low angles. Let us invert Equation 6.37 and Equation 6.39:

$$\frac{1}{\Lambda_e} < \left( \frac{C_B \alpha \delta\sigma}{\sqrt{|s|}} \right)^{1/2} \quad (13.1)$$

Where  $C_B = 24\pi$  in the small angle case, and  $C_B = 72\pi$  in the large angle case.

In the high energy limit (not physically accessible, but we are curious about it anyway), the best experimental result below  $Z$  resonance peak is found in a paper from TRISTAN (KEK) collaboration (1996, [47]), with  $\sqrt{|s|} = 58 \text{ GeV}$  and  $\delta\sigma = 0.007$  being the relative uncertainty on the QED cross section measured. Direct upper bound for  $1/\Lambda_e$  is found to be  $1/\Lambda_e < 1.1 \times 10^{-6} \text{ MeV}^{-1}$ .

Instead, for lower energies, we can use OLYMPUS result ([53], [54]) with  $\sqrt{|s|} = 44 \text{ MeV}$  and  $\delta\sigma = 0.01$  being the relative uncertainty on the QED cross section measured. Direct upper bound for  $1/\Lambda_e$  is found to be  $1/\Lambda_e < 2.9 \times 10^{-3} \text{ MeV}^{-1}$ .

**Møller scattering:** The most constraining experimental results are always ultra-relativistic and at low angles.

Let us invert Equation 7.13 and Equation 7.11:

$$\frac{1}{\Lambda_e} < \left( \frac{C_M \alpha \delta\sigma}{\sqrt{|s|}} \right)^{1/2} \quad (13.2)$$

Where  $C_M = 24\pi$  in the small angle case, and  $C_M = 144\pi$  in the large angle case.

In the high energy limit, best experimental result below  $Z$  resonance peak is found in a paper from Stanford LINAC experiment (1975, [46]), with  $\sqrt{|s|} \approx 20 \text{ GeV}$  and  $\delta\sigma = 0.04$  being the relative uncertainty on the QED cross section measured. Direct upper bound for  $1/\Lambda_e$  is found to be  $1/\Lambda_e < 7.4 \times 10^{-6} \text{ MeV}^{-1}$ .

For lower energies, we can use OLYMPUS result ([53], [54]), which is the same we used in section 13, with  $\sqrt{|s|} = 44 \text{ MeV}$  and  $\delta\sigma = 0.01$  being the relative uncertainty on the QED cross section measured. Direct upper bound for  $1/\Lambda_e$  is found to be  $1/\Lambda_e < 4.1 \times 10^{-3} \text{ MeV}^{-1}$ .

**$g - 2$  of electron:** Inverting constraint from Equation 12.32 on this very precise result yields:

$$\frac{1}{\Lambda_e} < \frac{4\pi}{m_e} \left( \frac{m_X}{\Lambda_c} \right)^2 \sqrt{3\delta a_e} = \frac{4\pi}{m_e k^2} \sqrt{3\delta a_e} \quad (13.3)$$

where  $\Lambda_c$  is the cutoff of our model, and  $k = \Lambda_c/m_X$ . We said in subsection 12.2 that there are two ways to approach this.

If we require model to explain the discrepancies in [60] and [58], we have to impose according to Equation 12.33:

$$\begin{aligned} 1.8 \times 10^{-13} < \delta a_e < 7.8 \times 10^{-13} &\quad \text{for } {}^{87}\text{Rb} \\ -12.4 \times 10^{-13} < \delta a_e < -5.2 \times 10^{-13} &\quad \text{for } {}^{122}\text{Cs} \end{aligned}$$

<sup>40</sup>This is not done lightheartedly, because a coupling between three fields of this kind must also carry a "coupling" dimension, in terms of powers of  $\hbar$ . In this sense,  $1/\Lambda_i$  carries both a dimension of mass and a dimension of coupling.

where  $\delta a_e$  is the correction of the spin 2 model. Notice that there is no value for  $\delta a_e$  that can explain both discrepancies measured, as the experimental values are not compatible with one another.

Also, there is no value for  $1/\Lambda_e$  that could explain the result with the Cesium, which is negative (while correction regarding only electron channel is positive).

Instead, if we require our correction to simply be invisible in the span of these very precise results (like in [Equation 12.34](#)),  $|\delta a_e| < \sigma_{\text{best}} = 6.8 \times 10^{-13}$  is our request.

It is clear that  $\Lambda_c$  is the discriminating parameter that decides the feasibility of the model:

- In the case  $k = 4\pi$ :

$$\begin{aligned} 1.1 \times 10^{-7} \text{ MeV}^{-1} &< \frac{1}{\Lambda_e} < 2.4 \times 10^{-7} \text{ MeV}^{-1} && \text{for } {}^{87}\text{Rb} \\ \frac{1}{\Lambda_e} &< 2.2 \times 10^{-7} \text{ MeV}^{-1} && \text{for "invisibility"} \end{aligned}$$

- In the case  $k = 2$ :

$$\begin{aligned} 4.5 \times 10^{-6} \text{ MeV}^{-1} &< \frac{1}{\Lambda_e} < 9.4 \times 10^{-6} \text{ MeV}^{-1} && \text{for } {}^{87}\text{Rb} \\ \frac{1}{\Lambda_e} &< 8.8 \times 10^{-6} \text{ MeV}^{-1} && \text{for "invisibility"} \end{aligned}$$

Putting these constraints together:

- **"Elementary" spin 2 model:** In this case, we take the most constraining results at high energies. This gives us a contradiction, as:

$$3.8 \times 10^{-6} \text{ MeV}^{-1} < \frac{g_e}{\Lambda} < 1.1 \times 10^{-6} \text{ MeV}^{-1} \quad (13.4)$$

Note that, actually, none of the bounds required to explain each of the ATOMKI experimental solves this inconsistent inequality (see [Table 1](#)). The model is excluded a priori, always.

- **Feasible spin 2 model:** In this case, the most constraining result at low energy may not give rise to contradiction, depending on  $\Lambda_c$ . The results we need are the bound from decay in ATOMKI and the  $g - 2$  of the electron. The actual valid range of values for  $1/\Lambda_c$  is:

$$\begin{cases} \text{to adjust } {}^{87}\text{Rb:} & \Lambda_c < 53 \text{ MeV} \\ \text{to be invisible} & \Lambda_c < 51 \text{ MeV} \end{cases} \quad (13.5)$$

This model is excluded only for certain values of  $\Lambda_c$ .

## 14 Constraints on two couplings spin 2 model

In the analysis we performed so far, we have assumed  $1/\Lambda_e = 3.8 \times 10^{-6} \text{ MeV}^{-1}$  and  $1/\Lambda_\gamma = 2.7 \times 10^{-6} \text{ MeV}^{-1}$ , instead of having these numerical values as lower bounds for the coupling constants. This was because we wanted to take the most conservative estimate for the spin 2 effective couplings, and to study their effect (to be intended as a lower bound effect) on QED processes at tree level (Compton, Bhabha, Møller scattering and annihilation into two photons - with positronium decay).

It is now time to let these couplings vary and identify their allowed region in parameter space, using the best constraints from experimental data. We are excluding positronium decay from this analysis, because its correction is too small. Since in this model we are assuming  $1/\Lambda_\gamma \neq 0$ , we need to take JINR result as valid.

Let us take the most constraining experimental result for each process:

**X decay:** This can be seen by ATOMKI collaboration ([1], [2], [3], [4], [5]), and by JINR collaboration ([8]).

The constraint for the coupling is actually an ellipse, described in [Equation 5.42](#), which translates roughly to:

$$\frac{1}{\Lambda_e^2} + \frac{2}{\Lambda_\gamma^2} > \frac{160\pi}{m_X^3} \Gamma_{\min} = 1.4 \times 10^{-11} \text{ MeV}^{-2} \quad (14.1)$$

**Bhabha scattering:** The most constraining experimental results are always ultra-relativistic and at low angles. Let us invert [Equation 6.37](#) and [Equation 6.39](#):

$$\frac{1}{\Lambda_e} < \left( \frac{C_B \alpha \delta\sigma}{\sqrt{|s|}} \right)^{1/2} \quad (14.2)$$

Where  $C_B = 24\pi$  in the small angle case,  $C_B = 72\pi$  in the large angle case and  $\delta\sigma$  is the relative difference in differential cross section.

In the high energy limit (to which we are interested in even though it is not physical), the best experimental result below  $Z$  resonance peak is found in a paper from TRISTAN (KEK) collaboration (1996, [47]), with  $\sqrt{|s|} = 58 \text{ GeV}$  and  $\delta\sigma = 0.007$  being the relative uncertainty on the QED cross section measured. Direct upper bound for  $1/\Lambda_e$  is found to be  $1/\Lambda_e < 1.1 \times 10^{-6} \text{ MeV}^{-1}$ .

Instead, for lower energies, we can use OLYMPUS result ([53], [54]) with  $\sqrt{|s|} = 44 \text{ MeV}$  and  $\delta\sigma = 0.01$  being the relative uncertainty on the QED cross section measured. Direct upper bound for  $1/\Lambda_e$  is found to be  $1/\Lambda_e < 2.9 \times 10^{-3} \text{ MeV}^{-1}$ .

**Møller scattering:** The most constraining experimental results are always ultra-relativistic and at low angles.

Let us invert [Equation 7.13](#) and [Equation 7.11](#):

$$\frac{1}{\Lambda_e} < \left( \frac{C_M \alpha \delta\sigma}{\sqrt{|s|}} \right)^{1/2} \quad (14.3)$$

Where  $C_M = 24\pi$  in the small angle case,  $C_M = 144\pi$  in the large angle case and  $\delta\sigma$  is the relative difference in differential cross section.

In the high energy limit, best experimental result below  $Z$  resonance peak is found in a paper from Stanford LINAC experiment (1975, [46]), with  $\sqrt{|s|} \approx 20 \text{ GeV}$  and  $\delta\sigma = 0.04$  being the relative uncertainty on the QED cross section measured. Direct upper bound for  $1/\Lambda_e$  is found to be  $1/\Lambda_e < 1.1 \times 10^{-6} \text{ MeV}^{-1}$ .

For lower energies, we can use OLYMPUS result ([53], [54]), which is the same we used in [section 13](#), with  $\sqrt{|s|} = 44 \text{ MeV}$  and  $\delta\sigma = 0.01$  being the relative uncertainty on the QED cross section measured. Direct upper bound for  $1/\Lambda_e$  is found to be  $1/\Lambda_e < 1.7 \times 10^{-3} \text{ MeV}^{-1}$ , which is not constraining at all.

**Compton scattering:** The most constraining experimental result is ultra-relativistic, but at large angles.

This process has to be considered only in this  $1/\Lambda_\gamma \neq 0$  layout. Let us invert [Equation 9.46](#):

$$\frac{1}{\Lambda_e} \frac{1}{\Lambda_\gamma} < \frac{12\pi\alpha}{m_X^2 m_e^3} \frac{\delta\sigma}{\omega} \quad (14.4)$$

where  $\omega$  is the photon energy in the electron rest frame, and  $\delta\sigma$  is the relative variation of the differential cross section.

There is only one high energy result that can be used (composite of elementary does not matter, as  $\omega = 5 \text{ GeV}$ , so  $\sqrt{|s|} = 70 \text{ MeV}$ ), which is the result by the PrimEx Collaboration, at Jefferson Lab ([39]). The precision obtained is  $\delta\sigma = 0.026$ . We get an upper bound on the product of coupling constants in the model:  $1/\Lambda_e \Lambda_\gamma < 3.1 \times 10^{-3} \text{ MeV}^{-2}$ .

**Annihilation into two photons:** The most constraining experimental results are always ultra-relativistic, but at large angles. This process has to be considered only in this  $1/\Lambda_\gamma \neq 0$  layout. Let us invert [Equation 10.56](#):

$$\frac{1}{\Lambda_e} \frac{1}{\Lambda_\gamma} < \frac{16\pi\alpha}{K} \frac{\delta\sigma}{|s|} \quad (14.5)$$

with  $K = 0.18$  being the maximum of the angular part in the formula. However, given that in high energy limit the squared modulus dominates, and in the low energy range our chosen experiment (OLYMPUS, [53], [54]) has  $\theta = \pi/2$ , for which interference terms cancel, we ought to use, actually, the squared modulus bounds (looking at [Equation D.44](#)):

$$\frac{1}{\Lambda_e} \frac{1}{\Lambda_\gamma} < \left( 2304\pi^2\alpha^2 \frac{m_X^4}{m_e^2} \frac{\delta\sigma}{|s|^3} \right)^{1/2} \quad (14.6)$$

In the high energy limit (which cannot be too high because of unitarity violation) the best experimental result is found in a paper from BELLE II Collaboration at KEK ([56]), with  $\sqrt{|s|} = 10.58$  GeV and  $\delta\sigma = 0.006$  is the reported relative uncertainty on the QED cross section measured. We get an upper bound on the product of coupling constants in the model:  $1/\Lambda_e\Lambda_\gamma < 4.8 \times 10^{-11}$  MeV $^{-2}$ .

For lower energies, we can use OLYMPUS result ([53], [54]), which also studies digamma production, with  $\sqrt{|s|} = 44$  MeV and  $\delta\sigma = 0.01$  being the relative uncertainty on the QED cross section measured. Another upper bound on the product of coupling constants in the model:  $1/\Lambda_e\Lambda_\gamma < 7.3 \times 10^{-4}$  MeV $^{-2}$ .

**Two-photon scattering:** For the ATLAS (non-physical result for the model) experiment ([73]), let us invert [Equation 11.41](#):

$$\frac{1}{\Lambda_\gamma} < \left( 9216\alpha^4 m_X^8 \frac{\delta\sigma}{s^6} \log^4 \left( \frac{\sqrt{|s|}}{2m_e} \right) \right)^{1/4} \quad (14.7)$$

with  $\delta\sigma \approx 30\%$  as result [73], we expect an upper bound on the single coupling constant in the model:  $1/\Lambda_\gamma < 6.1 \times 10^{-10}$  MeV $^{-1}$  (which is non realistic, but I am going to keep it anyway).

For lower energies, we can use PVLAS upper bound ([69]), which states that they could have been able to detect spin 2 corrections at low energy only if  $\delta\sigma = 2.6 \times 10^7$ <sup>41</sup>. Inverting [Equation 11.29](#):

$$\frac{1}{\Lambda_\gamma} < \left( \frac{139}{705} \frac{\alpha^2 m_X^2}{m_e^4} \delta\sigma \right)^{1/2} \quad (14.8)$$

which leaves us with an upper bound on photon coupling constant:  $1/\Lambda_\gamma < 1.1 \times 10^3$  MeV $^{-1}$ , which is our final result on the model.

**$g - 2$  of electron:** Inverting constraint on [Equation 12.31](#):

$$\frac{1}{\Lambda_e} \left( \frac{1}{\Lambda_e} - \frac{2}{\Lambda_\gamma} \right) = \frac{48\pi^2}{m_e^2} \left( \frac{m_X}{\Lambda_c} \right)^4 \delta a_e \quad (14.9)$$

where  $\Lambda_c$  is the cutoff energy for the model (we will select  $\Lambda_c = 2m_X$  and  $\Lambda_c = 4\pi m_X$  as the two extremes), and  $\delta a_e$  is the correction due to spin 2 mediation. is the absolute uncertainty on  $a_e = (g - 2)/2$ . This becomes a parabolic constraint on couplings.

The approaches followed here are the same outlined in [section 13](#):

$$\begin{aligned} 1.8 \times 10^{-13} &< \delta a_e < 7.8 \times 10^{-13} & \text{for } {}^{87}\text{Rb ([58])} \\ -12.4 \times 10^{-13} &< \delta a_e < -5.2 \times 10^{-13} & \text{for } {}^{122}\text{Cs ([60])} \\ |\delta a_e| &< \sigma_{\text{best}} = 6.8 \times 10^{-13} & \text{to avoid detection ([58])} \end{aligned}$$

**Perturbativity:** Inverting constraint for our model to be perturbative, from [Equation 12.37](#) and [Equation 12.39](#):

$$\frac{1}{\Lambda_e} < \frac{4\pi m_X^2}{\Lambda_c^3} = \frac{4\pi}{k^3 m_X} \quad \frac{1}{\Lambda_\gamma} < \frac{4\pi m_X^2}{\Lambda_c^3} = \frac{4\pi}{k^3 m_X} \quad (14.10)$$

where  $k = \Lambda_c/m_X$ . So, this constraint is also  $\Lambda_c$  dependent.

<sup>41</sup>Meaning they could not even measure the QED process. But there is nothing stopping our cross section to be so dominant at lower energy (where EFT holds), that spin 2 contribution could be millions of times larger than QED.

**Unitarity:** Another similar constraint, which requires scattering amplitudes to be manifestly unitary, which  $S$ -matrix theory requires. Using lepton and photon scattering contributions (see [subsubsection 12.4.2](#) and [subsubsection 12.4.3](#)), we obtain constraints on the individual couplings as well (see [Equation 12.66](#), [Equation 12.74](#) and [Equation 12.75](#)):

$$\frac{1}{\Lambda_e} \leq \sqrt{\frac{8\pi}{k^2 m_X^2 |3 - 8 \log(2k)|}} \quad (14.11)$$

$$\text{if } k = 4\pi \quad \frac{1}{\Lambda_\gamma} \leq \sqrt{\frac{96\pi}{7k^6 m_X^2}} \quad (14.12)$$

$$\text{if } k = 2 \quad \frac{1}{\Lambda_\gamma} \leq \sqrt{\frac{2\pi}{k^2 m_X^2 \log(2k)}} \quad (14.13)$$

with  $k = \Lambda_c/m_X$  is the cutoff parameter. This is another constraint that depends on the cutoff  $\Lambda_c$ .

Putting everything together, for the two couplings spin 2 model, in the nonphysical, non consistent, EFT breaking high energy limit (that we take just for mere curiosity), the exclusion plot is shown in [Figure 39](#)<sup>42</sup>. We

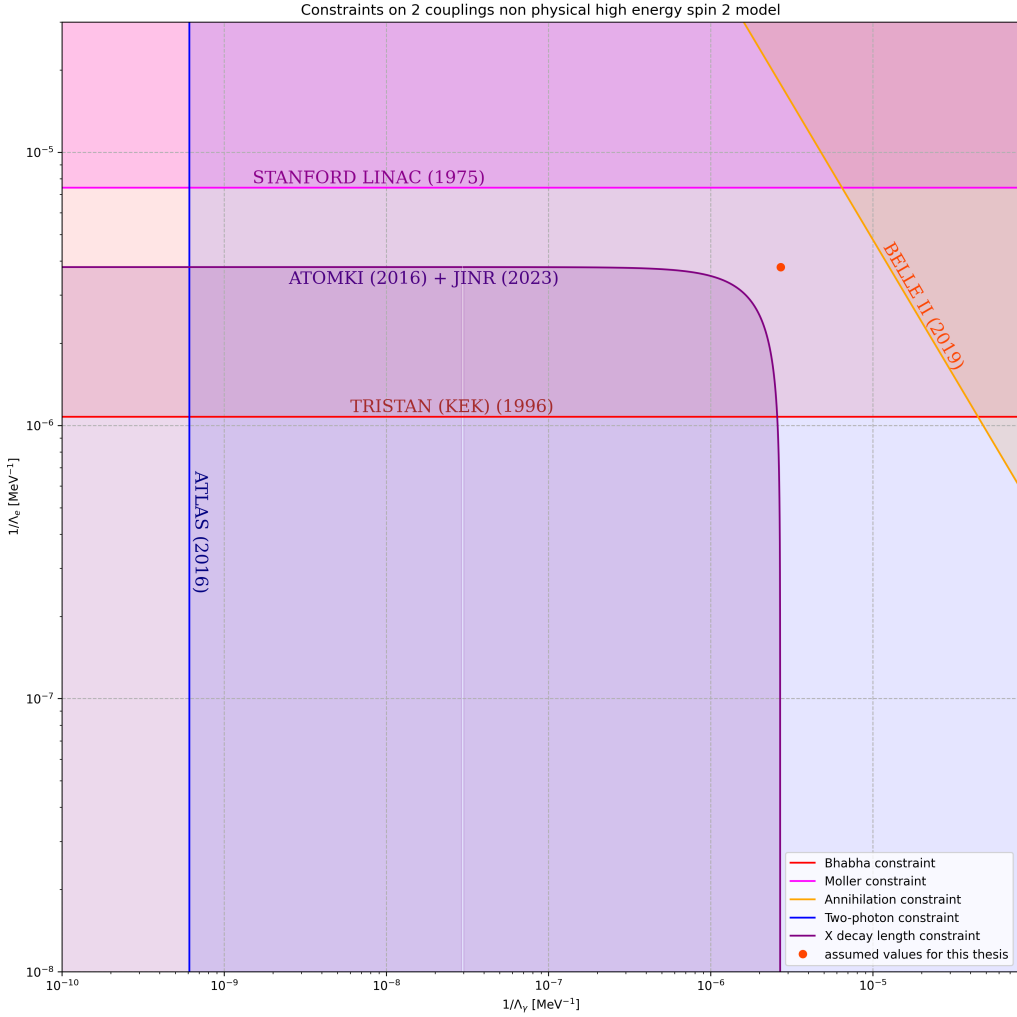


Figure 39: Region of parameter space allowed by experimental constraints, in the EFT breaking high energy limit. Regions excluded by each constraint are shaded with different colors. Bhabha ([47]), Møller ([46]) are upper bounds for  $1/\Lambda_e$ .  $X$  decay is a lower bound on both couplings ([1] - [5], [8]). Compton scattering is not shown as its constraint is not useful here. Annihilation into two photons ([56]) is an upper bound for  $1/\Lambda_e \Lambda_\gamma$ . Two-photon scattering ([73]) constraint is an upper bound for  $1/\Lambda_\gamma$ .

did not include every possible constraint, because this version of the model is excluded either way. This case is non physical, anyway.

<sup>42</sup>It is worth mentioning that the results of the one parameter model are found here on the  $y$  axis of each graph, setting  $1/\Lambda_\gamma = 0$ .

For the model to be feasible, we should be able to find a region in this parameter space that satisfies every constraint (i.e. a region that has no color in [Figure 39](#)). This is not the case here, as Bhabha (red line), two-photon scattering (blue line) and coupling lower bounds (purple ellipse) are clashing against one another.

Let us now report physical exclusion plots for realistic and physical settings for our spin 2 model. In Figure 40, we report constraints with the request that spin 2 correction explains discrepancy in the  $^{87}\text{Rb}$  oscillations experiments ([58]), selecting  $\Lambda_c = 4\pi m_X$ , on the left, or  $\Lambda_c = 2m_X$ , on the right. Remember that

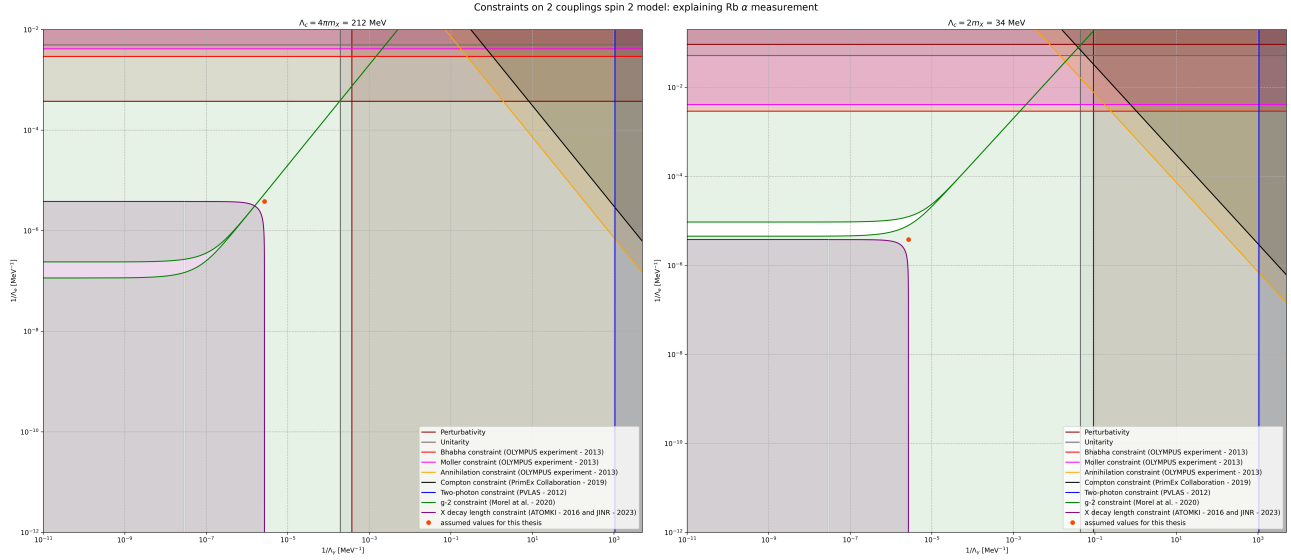


Figure 40: Regions of parameter space allowed by experimental constraints, within EFT energy exchanged limit. Regions excluded by each constraint are shaded with different colors. Bhabha and Møller are upper bounds for  $1/\Lambda_e$ , while annihilation is upper bound for  $1/\Lambda_e \Lambda_\gamma$  ([53], [54]). Compton scattering is upper bound for  $1/\Lambda_e \Lambda_\gamma$  ([39]). Two-photon scattering is upper bound for  $1/\Lambda_\gamma$  ([69]).  $X$  decay is an elliptical lower bound on both couplings ([1] - [5], [8]). One loop correction for  $g - 2$  of electron is shown with in two different settings: explaining  $g - 2$  discrepancy for the  $^{87}\text{Rb}$  oscillations experiments ([58]), with  $\Lambda_c = 4\pi m_X$  (left) and  $\Lambda_c = 2m_X$  (right): result is a parabolic upper and lower bound. Finally, perturbativity and unitarity constraints are shown as vertical and horizontal lines, constraining  $1/\Lambda_e$  and  $1/\Lambda_\gamma$  ([61], [62]).

we are looking for white region in parameter space, which are regions not yet excluded by any constraint so far. Feasibility of the model is not guaranteed for every value of  $\Lambda_c$ . We have already mentioned that for  $\Lambda_c > 53$  MeV the model is completely excluded (as an example, look to the left of Figure 40). There is a very narrow, diagonal strip running from the  $g - 2$  constraint, which represents the case in which correction vanishes at one-loop, as  $1/\Lambda_e = 2/\Lambda_\gamma$ , identifying a 1D manifold solution in a 2D parameter space. This strip is not stable under higher order corrections, hence we ought to ignore it.

However, the white strip on the right figure of Figure 40 is a valid region of parameter space. If  $\Lambda_c = 2m_X$ , we get that the region of parameters is:

$$4.5 \times 10^{-6} \text{ MeV}^{-1} < \frac{1}{\Lambda_e} < 9.4 \times 10^{-6} \text{ MeV}^{-1}$$

$$\frac{1}{\Lambda_\gamma} < 2.7 \times 10^{-6} \text{ MeV}^{-1}$$

The two branching ratios for the decays of  $X$  would be:

$$\text{BR}(X \rightarrow e^+ e^-) = \frac{\Lambda_e^{-2}}{\Lambda_e^{-2} + 2\Lambda_\gamma^{-2}} \quad \text{BR}(X \rightarrow \gamma\gamma) = \frac{2\Lambda_\gamma^{-2}}{\Lambda_e^{-2} + 2\Lambda_\gamma^{-2}} \quad (14.14)$$

this would result in a relatively high branching ratio for  $e^+ e^-$  channel seen by the ATOMKI collaboration (about 60%-85%) and a relatively lower branching ratio for the  $\gamma\gamma$  channel measured by JINR (about 15%-40%).

Now, we report physical exclusion plots for the explanation of the  $g - 2$  discrepancy in Cesium. In [Figure 41](#), we report constraints with the request that spin 2 correction explains discrepancy in the  $^{122}\text{Cs}$  oscillations experiments ([60]), selecting  $\Lambda_c = 4\pi m_X$ , on the left, or  $\Lambda_c = 2m_X$ , on the right.

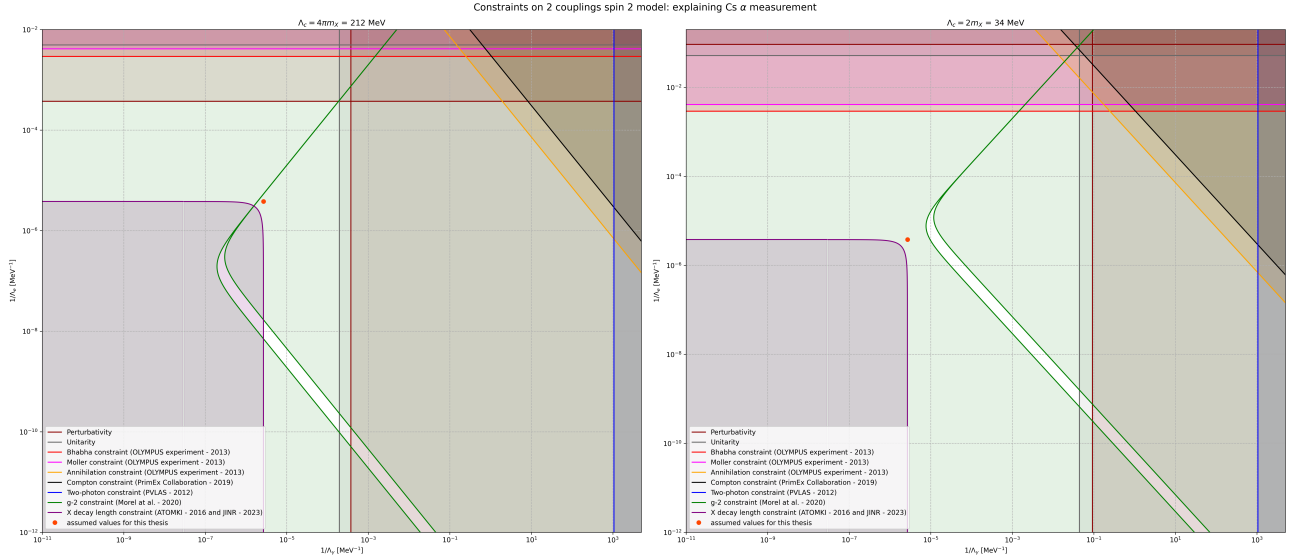


[Figure 41](#): Regions of parameter space allowed by experimental constraints, within EFT energy exchanged limit. Regions excluded by each constraint are shaded with different colors. Bhabha and Møller are upper bounds for  $1/\Lambda_e$ , while annihilation is upper bound for  $1/\Lambda_e \Lambda_\gamma$  ([53], [54]). Compton scattering is upper bound for  $1/\Lambda_e \Lambda_\gamma$  ([39]). Two-photon scattering is upper bound for  $1/\Lambda_\gamma$  ([69]).  $X$  decay is an elliptical lower bound on both couplings ([1] - [5], [8]). One loop correction for  $g - 2$  of electron is shown with in two different settings: explaining  $g - 2$  discrepancy for the  $^{122}\text{Cs}$  oscillations experiments ([60]), with  $\Lambda_c = 4\pi m_X$  (left) and  $\Lambda_c = 2m_X$  (right): result is a parabolic upper and lower bound. Finally, perturbativity and unitarity constraints are shown as vertical and horizontal lines, constraining  $1/\Lambda_e$  and  $1/\Lambda_\gamma$  ([61], [62]).

Immediately notice that explaining Cesium result and Rubidium result together appears to be impossible, as measurements clash with one another.

Differently for the Rubidium case, in [Figure 41](#) there is a white, available strip for our parameters to stay in. It necessarily requires  $1/\Lambda_\gamma \neq 0$ .

For  $k = 4\pi$  (left image), the region is:

$$\begin{aligned} 2.7 \times 10^{-6} \text{ MeV}^{-1} &< \frac{1}{\Lambda_\gamma} < 4.9 \times 10^{-3} \text{ MeV}^{-1} \\ \left(5.9 \times 10^{-15} \text{ MeV}^{-1}\right) \Lambda_\gamma &< \frac{1}{\Lambda_e} < \left(1.4 \times 10^{-14} \text{ MeV}^{-1}\right) \Lambda_\gamma \end{aligned} \quad (14.15)$$

which implies a branching ratio which is extremely small in the  $e^+e^-$  channel, as at most:  $1/\Lambda_\gamma = 2.7 \times 10^{-6} \text{ MeV}^{-1}$  and  $1/\Lambda_e = 5.3 \times 10^{-9} \text{ MeV}^{-1}$ , which implies an electron channel branching ratio of  $2 \times 10^{-6}$ . Then, to explain ATOMKI signal, one would need an extremely high production cross section (from the nuclear transition) to compensate for the suppressed branching ratio, but then might require stronger bounds on  $1/\Lambda_e$  and maybe invalidate the whole model.

For  $k = 2$  (left image), the region is:

$$\begin{aligned} 10^{-5} \text{ MeV}^{-1} &< \frac{1}{\Lambda_\gamma} < 5.2 \times 10^{-2} \text{ MeV}^{-1} \\ \left(9.4 \times 10^{-12} \text{ MeV}^{-1}\right) \Lambda_\gamma &< \frac{1}{\Lambda_e} < \left(2.2 \times 10^{-11} \text{ MeV}^{-1}\right) \Lambda_\gamma \end{aligned} \quad (14.16)$$

which, for branching ratio purposes, it is much better than before. The highest value of  $1/\Lambda_e = 1.7 \times 10^{-5} \text{ MeV}^{-1}$ , when  $1/\Lambda_\gamma = 10^{-5} \text{ MeV}^{-1}$ , producing a branching ratio of 60%.

Finally, in [Figure 42](#), we show results for a model in which the presence of spin 2 corrections are always not detected, in any experiment (so, the "invisible" case for  $g - 2$  constraint).

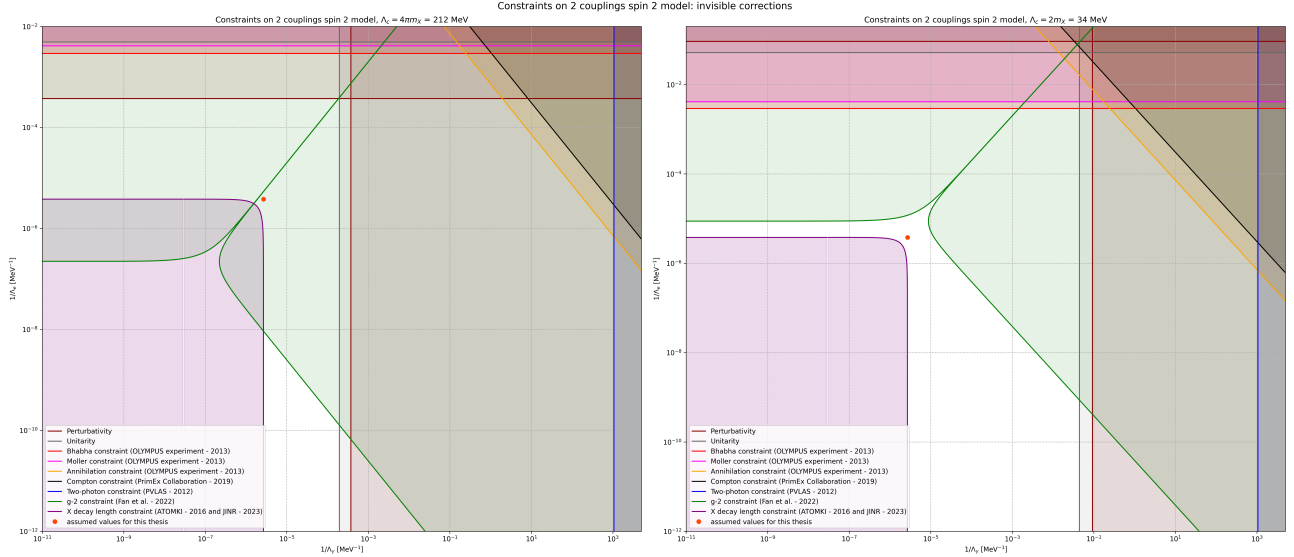


[Figure 42](#): Regions of parameter space allowed by experimental constraints, within EFT energy exchanged limit. Regions excluded by each constraint are shaded with different colors. Bhabha and Møller are upper bounds for  $1/\Lambda_e$ , while annihilation is upper bound for  $1/\Lambda_e \Lambda_\gamma$  ([53], [54]). Compton scattering is upper bound for  $1/\Lambda_e \Lambda_\gamma$  ([39]). Two-photon scattering is upper bound for  $1/\Lambda_\gamma$  ([69]).  $X$  decay is an elliptical lower bound on both couplings ([1] - [5], [8]). One loop correction for  $g - 2$  of electron is shown with in two different settings: explaining  $g - 2$  discrepancy in a very conservative way, requiring correction to be smaller than some combination of both experiments results ([60], [58]), with  $\Lambda_c = 4\pi m_X$  (left) and  $\Lambda_c = 2m_X$  (right): result is a parabolic upper bound. Finally, perturbativity and unitarity constraints are shown as vertical and horizontal lines, constraining  $1/\Lambda_e$  and  $1/\Lambda_\gamma$  ([61], [62]).

This ([Figure 42](#)) is the graph obtained in the hypothesis that the  $g - 2$  discrepancies are just systematic effects, and one would expect a future reconciliation between the two values. As for now, a conservative estimate would be  $|\delta a_e| < 6.8 \times 10^{-13}$ , which is the half-sum of the two values (assuming approximately the same uncertainty for both measures). So,  $g - 2$  has only an upper bound constraint. Valid, white regions are now trapezoids, bounded in  $1/\Lambda_\gamma$  between JINR decay rates and unitarity constraints, and blocked from above by  $g - 2$  constraint.

Again, in the case  $k = 4\pi$ , we have the same branching ratio issue as for Cesium discrepancy graph ([Figure 41](#)):

$$\begin{aligned} 2.7 \times 10^{-6} \text{ MeV}^{-1} &< \frac{1}{\Lambda_\gamma} < 4.9 \times 10^{-3} \text{ MeV}^{-1} \\ \frac{1}{\Lambda_e} &< \left( 7.8 \times 10^{-15} \text{ MeV}^{-1} \right) \Lambda_\gamma \end{aligned} \quad (14.17)$$

At most:  $1/\Lambda_\gamma = 2.7 \times 10^{-6} \text{ MeV}^{-1}$  and  $1/\Lambda_e = 2.9 \times 10^{-9} \text{ MeV}^{-1}$ , which implies an electron channel branching ratio of  $6 \times 10^{-7}$ , which is even worse than before.

Instead, for  $k < 3$  ( $\Lambda_c < 51 \text{ MeV}$ ), we have a much higher opening, and the trapezoid tips over the elliptical (purple) constraint, allowing for  $1/\Lambda_e$  and  $1/\Lambda_\gamma$  a much wider range of values (both could dominate the interaction at will), as visible in the right image of [Figure 42](#).

## 15 Conclusions

After the recent experimental confirmation of the anomalous resonance peak of  $X17$  by the JINR Collaboration, we have questioned the axial vector hypothesis which cannot decay into two photons. As a result, we have elaborated an effective field model for a massive spin 2 resonance at lower energy, which only deals with two free couplings with electrons and photons.

After having reviewed standard QED processes in light of a new spin  $2^+$  state, we have identified a parameter space region for our couplings that is not excluded by experimental data, or by consistency constraints of our theory.

The model we elaborated is not predictive, because there is no quark coupling. Hence, it cannot describe the production of the resonance through rare nuclear transitions. However, a generalized version of this model, with quark couplings and both  $\pm$  spin 2 parities is currently being investigated. On one hand, the objective is to better constrain our free parameters when considering productions mechanisms, and on the other hand we seek to create a predictive model which would, at least in principle, foretell which nuclear transitions allow for anomalous  $X17$  production, so that experimental confirmation would be possible.

Moreover, a new experiment is underway ([7]) to independently search for the  $X17$  anomaly, at PADME (Frascati, Rome), in the  $e^+e^-$  production channel (with Bhabha scattering background). We hope it will help shed more light on the nature of the resonance.

Whether  $X17$  really is the long sought sign of New Physics beyond the Standard Model, or just an experimental fluke, is actively being debated among particle physicists. New exciting scenarios and theories emerge in an attempt to reveal its nature, as the "particle drought" of the past decades might have finally come to an end.

# Appendices

## A Bhabha scattering at tree level

We derive here the well-known amplitudes and cross section for the electrodynamics process  $e^+e^- \rightarrow e^+e^-$ , at tree level. The eventual correction due to the tree level diagram of the  $X$  resonance acts at this order in perturbation theory. However, in this Appendix, we will not consider it. For the additional contribution of the spin 2 resonance, see [section 6](#).

### A.1 Bhabha amplitude

Let us see the contributing diagrams for this process, the *s-channel* and the *t-channel*:

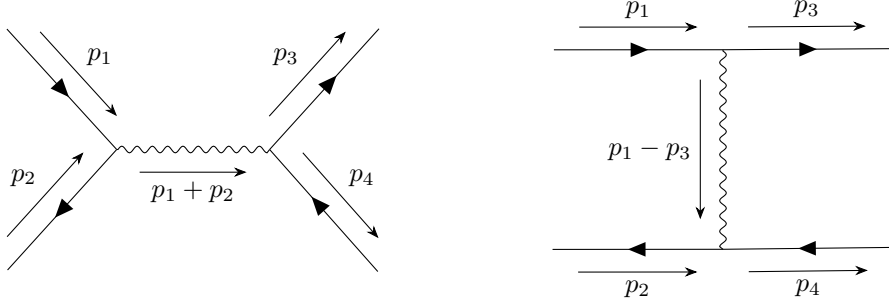


Figure 43: Diagrams corresponding to tree level Bhabha scattering. On the left, the *s*-channel, hereafter denoted with  $\mathcal{A}_1$ . On the right, the *t*-channel, hereafter denoted with  $\mathcal{A}_2$ .

Before writing the amplitudes, we need to write down the photon propagator. By inverting the equation of motion of photons in a generic  $\xi$  gauge ([Equation 4.40](#)), we define the propagator as:

$$D_{\mu\nu}^\xi(x-y) = \int \frac{d^4q}{(2\pi)^4 i} \hat{D}_{\mu\nu}^\xi(q) e^{iq(x-y)} \quad (\text{A.1})$$

where we define the propagator in momentum space as:

$$\hat{D}_{\mu\nu}^\xi(q) = \frac{1}{q^2 - i\epsilon} \left[ \delta_{\mu\nu} + \left(1 - \frac{1}{\xi}\right) \frac{q_\mu q_\nu}{q^2} \right] \quad (\text{A.2})$$

as a check, we can verify that every amplitude with a photon propagator must, in fact, be gauge independent (hence  $\xi$  independent). Instead, the unitary part of the propagator in [Equation A.2](#) satisfies Ward identities (if  $1/\xi \rightarrow 0$ , then  $q_\mu \hat{D}_{\mu\nu}(q) = 0$ ). This makes sense as the gauge fixing part of the propagator is not really physical, and will never be observed, hence it is not constrained by Ward identities. This is exactly what happens with the  $X \rightarrow \gamma\gamma$  Feynman rule in [Equation 4.65](#) as well.

The amplitudes are easily written:

$$\begin{aligned} \mathcal{A}_1 &= (-ie)^2 \hat{D}_{\mu\nu}^\xi(p_1 + p_2) [\bar{v}(p_2, \lambda_2) \gamma_\mu u(p_1, \lambda_1)] [\bar{u}(p_3, \lambda_3) \gamma_\nu v(p_4, \lambda_4)] = \\ &= -e^2 \hat{D}_{\mu\nu}^\xi(p_1 + p_2) [\bar{v}_2 \gamma_\mu u_1] [\bar{u}_3 \gamma_\nu v_4] \end{aligned} \quad (\text{A.3})$$

$$\begin{aligned} \mathcal{A}_2 &= (-ie)^2 \hat{D}_{\mu\nu}^\xi(p_1 - p_3) [\bar{u}(p_3, \lambda_3) \gamma_\mu u(p_1, \lambda_1)] [\bar{v}(p_2, \lambda_2) \gamma_\nu v(p_4, \lambda_4)] = \\ &= -e^2 \hat{D}_{\mu\nu}^\xi(p_1 - p_3) [\bar{u}_3 \gamma_\mu u_1] [\bar{v}_2 \gamma_\nu v_4] \end{aligned} \quad (\text{A.4})$$

where the usual electrodynamics Feynman rule  $-ie\gamma_\mu$  applies at each vertex,  $m_e$  is the mass of the electron,  $p_i, i \in \{1, 2, 3, 4\}$  are the respective momenta according to [Figure 43](#) and  $\lambda_i, i \in \{1, 2, 3, 4\}$  are the respective polarizations of fermions. Here forth, we will call  $u(p_i, \lambda_i) = u_i, i \in \{1, 3\}$  and  $v(p_i, \lambda_i) = v_i, i \in \{2, 4\}$ .

The next step is the complex conjugation of  $\mathcal{A}_1$  and  $\mathcal{A}_2$ . First, we need to swap the spinors:

$$\begin{aligned} (\bar{\chi} \gamma_\mu \psi)^* &= [\chi_a^* (\gamma_4)_{ab} (\gamma_m u)_{bc} \psi_c]^* = \chi_a (\gamma_4^*)_{ab} (\gamma_\mu^*)_{bc} \psi_c^* = \\ &= \psi_c^* (\gamma_\mu^\dagger)_{cb} (\gamma_4^\dagger)_{ba} \chi_a = \psi_c^* (\gamma_\mu)_{cb} (\gamma_4)_{ba} \chi_a = \\ &= -\mu_p \psi_c^* (\gamma_4)_{cb} (\gamma_\mu)_{ba} \chi_a = -\mu_p (\bar{\psi} \gamma_\mu \chi) \end{aligned} \quad (\text{A.5})$$

where we used  $\gamma_\mu \gamma_4 = -(-1)^{\delta_{\mu 4}} \gamma_4 \gamma_\mu = -\mu_p \gamma_4 \gamma_\mu$ , as we defined phases in [section 9](#).

Then, we conjugate the propagator:

$$\left[ \hat{D}_{\mu\nu}^\xi(q) \right]^* = \frac{1}{q^2 - i\epsilon} \left[ \delta_{\mu\nu} + \mu_p \nu_p \left( 1 - \frac{1}{\xi} \right) \frac{q_\mu q_\nu}{q^2} \right] \quad (\text{A.6})$$

as  $q_\mu^* = \mu_p q_\mu$ , as time component is imaginary.

Finally, putting all together, and changing the indices from  $\mu, \nu$  to  $\rho, \sigma$ :

$$\begin{aligned} \mathcal{A}_1^* &= -e^2 (-\rho_p)(-\sigma_p) \left[ \hat{D}_{\rho\sigma}^\xi(p_1 + p_2) \right]^* [\bar{u}_1 \gamma_\rho v_2] [\bar{v}_4 \gamma_\sigma u_3] = \\ &= -e^2 \frac{1}{q^2} \left[ \delta_{\rho\sigma} \rho_p \sigma_p + \rho_p^2 \sigma_p^2 \left( 1 - \frac{1}{\xi} \right) \frac{q_\rho q_\sigma}{q^2} \right] [\bar{u}_1 \gamma_\rho v_2] [\bar{v}_4 \gamma_\sigma u_3] = \\ &= -e^2 \frac{1}{q^2} \left[ \delta_{\rho\sigma} + \left( 1 - \frac{1}{\xi} \right) \frac{q_\rho q_\sigma}{q^2} \right] [\bar{u}_1 \gamma_\rho v_2] [\bar{v}_4 \gamma_\sigma u_3] = \\ &= -e^2 \hat{D}_{\rho\sigma}^\xi(p_1 + p_2) [\bar{u}_1 \gamma_\rho v_2] [\bar{v}_4 \gamma_\sigma u_3] \end{aligned} \quad (\text{A.7})$$

$$\mathcal{A}_2^* = -e^2 \hat{D}_{\rho\sigma}^\xi(p_1 - p_3) [\bar{u}_1 \gamma_\rho u_3] [\bar{v}_4 \gamma_\sigma v_2] \quad (\text{A.8})$$

Does this mean we can finally sum? No, because there is a relative sign that we are missing. Notice, in fact, that between  $\mathcal{A}_1$  and  $\mathcal{A}_2$  there is only one exchange of fermions  $v_2 \leftrightarrow u_3$ , meaning that a minus sign must come out due to Dirac statistics (not for the spinors, but for the creation and annihilation operators that the spinors are paired up to, which are not present in the Feynman amplitude).

However, this heuristic reasoning does not tell us what is the absolute sign of the two diagrams (which does not matter in this QED calculation when taking the modulus squared, but it might matter when adding the spin 2 correction).

## A.2 Bhabha amplitude from Wick contractions

To find out the correct absolute sign of the two diagrams, let us take a step back and look at the  $S$ -matrix element. Define an initial and final state  $|i\rangle = |e^+ e^-\rangle = |f\rangle$ . Then, the first order at which we find a non trivial contribution (other than forward scattering) is the second order, which is our tree level. The exponential of the  $T$ -ordered product gets expanded into normal ordered interaction terms:

$$\begin{aligned} S_{fi} &= \langle f | S | i \rangle = \langle e^+ e^- | S | e^+ e^- \rangle = \\ &= \frac{(-ie)^2}{2!} \int d^4x d^4y \langle e^+ e^- | :(\bar{\psi} \gamma_\nu A_\nu \psi)_y : :(\bar{\psi} \gamma_\mu A_\mu \psi)_x : | e^+ e^- \rangle = \\ &= \frac{(-ie)^2}{2!} \int d^4x d^4y D_{\mu\nu}^\xi(x-y) \langle e^+ e^- | :(\bar{\psi} \gamma_\nu \psi)_y : :(\bar{\psi} \gamma_\mu \psi)_x : | e^+ e^- \rangle \end{aligned} \quad (\text{A.9})$$

where we contracted the two photon fields into a propagator because in the final and initial state there is no photon. Also, as Grassmann variables, the combination  $\bar{\psi} \gamma_\mu \psi$  has parity +1, meaning that it commutes with other  $\bar{\psi} \gamma_\nu \psi$  combinations. This implies that whatever non zero contraction we get in [Equation A.9](#), there is an equal contraction obtained by exchanging  $x$  and  $y$  interaction points. So, we can cancel the  $1/2!$  and are left with 2 possible contractions:

$$\begin{aligned} S_{fi} &= (-ie)^2 \int d^4x d^4y D_{\mu\nu}^\xi(x-y) \langle \overbrace{e^+}^{\square} \overbrace{e^-}^{\square} | :(\psi^\dagger \gamma_4 \gamma_\nu \psi)_y : :(\psi^\dagger \gamma_4 \gamma_\mu \psi)_x : | e^+ e^- \rangle \\ &\quad + (-ie)^2 \int d^4x d^4y D_{\mu\nu}^\xi(x-y) \langle \overbrace{e^+}^{\square} \overbrace{e^-}^{\square} | :(\psi^\dagger \gamma_4 \gamma_\nu \psi)_y : :(\psi^\dagger \gamma_4 \gamma_\mu \psi)_x : | e^+ e^- \rangle \end{aligned} \quad (\text{A.10})$$

where  $\psi$  can annihilate an electron and create a positron, while  $\psi^\dagger$  can create an electron and annihilate a positron. The two contractions in [Equation A.10](#) correspond respectively to the  $s$ -channel (we annihilate everything in  $x$  and create it back in  $y$ ) and the  $t$ -channel (one at a time, we propagate electron in  $x$  and positron in  $y$ ) diagrams in [subsection A.1](#).

To perform the contraction, we need to substitute the fermion field normal mode expansion:

$$\left\{ \begin{array}{l} \psi(z) = \sum_{\sigma} \int \frac{d^3 k}{\sqrt{(2\pi)^3} \sqrt{2k_4}} [u(k, \sigma) a_{\sigma}(k) e^{-ikz} + v(k, \sigma) b_{\sigma}^{\dagger}(k) e^{ikz}] \\ \psi^{\dagger}(z) = \sum_{\sigma} \int \frac{d^3 k}{\sqrt{(2\pi)^3} \sqrt{2k_4}} [u^{\dagger}(k, \sigma) a_{\sigma}^{\dagger}(k) e^{ikz} + v^{\dagger}(k, \sigma) b_{\sigma}(k) e^{-ikz}] \end{array} \right. \quad (\text{A.11})$$

where the normalization is relativistic and in the continuous limit we substituted  $\sqrt{V} \rightarrow \sqrt{(2\pi)^3}$ . We assign the following spin and momenta names:

$$\begin{aligned} \psi(x) &\rightarrow (k_1, \sigma_1) & \psi^{\dagger}(x) &\rightarrow (k_2, \sigma_2) \\ \psi(y) &\rightarrow (k_4, \sigma_4) & \psi^{\dagger}(y) &\rightarrow (k_3, \sigma_3) \end{aligned}$$

Also:

$$\left\{ \begin{array}{l} |i\rangle = |e^+e^-\rangle = |e^+(p_2, \lambda_2); e^-(p_1, \lambda_1)\rangle = \sqrt{2p_{2,4}} \sqrt{2p_{1,4}} b_{\lambda_2}^{\dagger}(p_2) a_{\lambda_1}^{\dagger}(p_1) |0\rangle \\ \langle f| = \langle e^+e^-| = \langle e^+(p_4, \lambda_4); e^-(p_3, \lambda_3)| = \sqrt{2p_{3,4}} \sqrt{2p_{4,4}} \langle 0| a_{\lambda_3}(p_3) b_{\lambda_4}(p_4) \end{array} \right. \quad (\text{A.12})$$

where the order of these operator has to be coherent. Our convention is positron-electron in creation order, then electron-positron in annihilation order.

We can now substitute the expansions [Equation A.11](#), and [Equation A.12](#) into [Equation A.10](#), to get:

$$\begin{aligned} S_{fi} = (ie)^2 \int d^4 x d^4 y D_{\mu\nu}^{\xi}(x-y) \prod_{i=1}^4 \left( \sum_{\sigma_i} \int \frac{d^3 k_i}{\sqrt{(2\pi)^3} \sqrt{2k_{i,4}}} \right) \times \left( \prod_{i=1}^4 \sqrt{2p_{i,4}} \right) \\ \left[ \bar{v}(k_2, \sigma_2) e^{-ik_2 x} \gamma_{\mu} u(k_1, \sigma_1) e^{-ik_1 x} \bar{u}(k_3, \sigma_3) e^{ik_3 y} \gamma_{\nu} v(k_4, \sigma_4) e^{ik_4 y} \right. \\ \left. \langle 0| a_{\lambda_3}(p_3) b_{\lambda_4}(p_4) b_{\sigma_4}^{\dagger}(k_4) a_{\sigma_3}^{\dagger}(k_3) b_{\sigma_2}(k_2) a_{\sigma_1}(k_1) b_{\lambda_2}^{\dagger}(p_2) a_{\lambda_1}^{\dagger}(p_1) |0\rangle + \right. \\ \left. \bar{u}(k_2, \sigma_2) e^{ik_2 x} \gamma_{\mu} u(k_1, \sigma_1) e^{-ik_1 x} \bar{v}(k_3, \sigma_3) e^{-ik_3 y} \gamma_{\nu} v(k_4, \sigma_4) e^{ik_4 y} \right. \\ \left. \langle 0| a_{\lambda_3}(p_3) b_{\lambda_4}(p_4) b_{\sigma_4}^{\dagger}(k_4) b_{\sigma_3}(k_3) a_{\sigma_2}^{\dagger}(k_2) a_{\sigma_1}(k_1) b_{\lambda_2}^{\dagger}(p_2) a_{\lambda_1}^{\dagger}(p_1) |0\rangle \right] = \quad (\text{A.13}) \end{aligned}$$

$$= S_{fi}^{(1)} + S_{fi}^{(2)} \quad (\text{A.14})$$

Study individually *s*-channel and *t*-channel. Normal ordering requires every creation operator to be placed to the left of every annihilation operator. In order to do that, use anticommutation rules:

$$\{a_{\lambda}(p), a_{\sigma}^{\dagger}(k)\} = \{b_{\lambda}(p), b_{\sigma}^{\dagger}(k)\} = \delta_{\lambda\sigma} \delta(\vec{p} - \vec{k}) \quad (\text{A.15})$$

while every other combination of operators vanishes.

**s-channel:** It is the first added in [Equation A.14](#). Using [Equation A.15](#):

$$\begin{aligned} \langle 0| a_{\lambda_3}(p_3) b_{\lambda_4}(p_4) b_{\sigma_4}^{\dagger}(k_4) a_{\sigma_3}^{\dagger}(k_3) b_{\sigma_2}(k_2) a_{\sigma_1}(k_1) b_{\lambda_2}^{\dagger}(p_2) a_{\lambda_1}^{\dagger}(p_1) |0\rangle = \\ = \langle 0| a_{\lambda_3}(p_3) b_{\sigma_4}^{\dagger}(k_4) b_{\lambda_4}(p_4) a_{\sigma_3}^{\dagger}(k_3) b_{\sigma_2}(k_2) b_{\lambda_2}^{\dagger}(p_2) a_{\sigma_1}(k_1) a_{\lambda_1}^{\dagger}(p_1) |0\rangle \\ - \delta_{\lambda_4\sigma_4} \delta(\vec{p}_4 - \vec{k}_4) \langle 0| a_{\lambda_3}(p_3) a_{\sigma_3}^{\dagger}(k_3) b_{\sigma_2}(k_2) b_{\lambda_2}^{\dagger}(p_2) a_{\sigma_1}(k_1) a_{\lambda_1}^{\dagger}(p_1) |0\rangle \end{aligned}$$

the first added is null when normal ordered, as normal ordering operators are of course null when interpolated between vacuum states:

$$\langle 0| a_{\lambda_3}(p_3) b_{\sigma_4}^{\dagger}(k_4) \dots = - \langle 0| b_{\sigma_4}^{\dagger}(k_4) a_{\lambda_3}(p_3) \dots = 0$$

whilst the second added can be treated by executing three non trivial anticommutations, leaving just a normal ordered product of operators, which, again, vanishes:

$$\begin{aligned} \langle 0| a_{\lambda_3}(p_3) b_{\lambda_4}(p_4) b_{\sigma_4}^{\dagger}(k_4) a_{\sigma_3}^{\dagger}(k_3) b_{\sigma_2}(k_2) a_{\sigma_1}(k_1) b_{\lambda_2}^{\dagger}(p_2) a_{\lambda_1}^{\dagger}(p_1) |0\rangle = \\ - [\delta_{\lambda_4\sigma_4} \delta(\vec{p}_4 - \vec{k}_4)] [\delta_{\lambda_3\sigma_3} \delta(\vec{p}_3 - \vec{k}_3)] [\delta_{\lambda_2\sigma_2} \delta(\vec{p}_2 - \vec{k}_2)] [\delta_{\lambda_1\sigma_1} \delta(\vec{p}_1 - \vec{k}_1)] \langle 0|0\rangle^1 \quad (\text{A.16}) \end{aligned}$$

This result cancels every sum over polarization and every integral over momenta, but *it leaves an absolute minus sign*, which is why the  $s$ -channel is always reported having a minus sign in Bhabha scattering. All we have to do is substitute  $\sigma_i \rightarrow \lambda_i$ ,  $k_i \rightarrow p_i$  for  $i \in \{1, 2, 3, 4\}$ , into first addend of [Equation A.14](#):

$$\begin{aligned}
S_{fi}^{(1)} &= \frac{(-i)(-ie)^2}{\left[\sqrt{(2\pi)^3}\right]^4} \int d^4x d^4y D_{\mu\nu}^\xi(x-y) [\bar{v}(p_2, \lambda_2) \gamma_\mu u(p_1, \lambda_1)] \times \\
&\quad \times [\bar{u}(p_3, \lambda_3) \gamma_\nu v(p_4, \lambda_4)] e^{-i(p_1+p_2)x} e^{i(p_3+p_4)y} = \\
&= \frac{(-i)(-ie)^2}{(2\pi)^6} [\bar{v}_2 \gamma_\mu u_1] [\bar{u}_3 \gamma_\nu v_4] \int d^4x d^4y e^{-i(p_1+p_2)x} e^{i(p_3+p_4)y} \int \frac{d^4q}{(2\pi)^4 i} \hat{D}_{\mu\nu}^\xi(q) e^{iq(x-y)} = \\
&= \frac{(-i)(-ie)^2}{(2\pi)^6} [\bar{v}_2 \gamma_\mu u_1] [\bar{u}_3 \gamma_\nu v_4] \int \frac{d^4q}{(2\pi)^4 i} \hat{D}_{\mu\nu}^\xi(q) \int d^4x e^{-i(p_1+p_2-q)x} \int d^4y e^{i(p_3+p_4-q)y} = \\
&= \frac{(-i)(-ie)^2}{(2\pi)^6} [\bar{v}_2 \gamma_\mu u_1] [\bar{u}_3 \gamma_\nu v_4] \int \frac{d^4q}{(2\pi)^4 i} \hat{D}_{\mu\nu}^\xi(q) [(2\pi)^4 i]^2 \delta(p_1 + p_2 - q) \delta(p_3 + p_4 - q) = \\
&= \frac{(-i)(-ie)^2}{(2\pi)^6} \hat{D}_{\mu\nu}^\xi(p_1 + p_2) [\bar{v}_2 \gamma_\mu u_1] [\bar{u}_3 \gamma_\nu v_4] \frac{[(2\pi)^4 i]^2}{(2\pi)^4 i} \delta(p_1 + p_2 - p_3 - p_4) = \\
&= -\frac{(2\pi)^4 i \mathcal{A}_1}{(2\pi)^6} \delta(p_1 + p_2 - p_3 - p_4)
\end{aligned} \tag{A.17}$$

If we go back to "finite" volume, we have to substitute back  $\sqrt{(2\pi)^3} \rightarrow \sqrt{V}$ , which in turn gives us:

$$S_{fi}^{(1)} = -\frac{(2\pi)^4 i \mathcal{A}_1}{V^2} \delta(p_1 + p_2 - p_3 - p_4) \tag{A.18}$$

Notice how this result is exactly what we get from the seemingly arbitrary rules in [subsection C.2](#), which for Compton scattering leads us to [Equation C.23](#), and for annihilation into two photons leads us to [Equation D.18](#). The only thing that comprehensive set of rules did not give us is the *absolute minus sign* due to fermion statistics. Now, we retrieved it.

**$t$ -channel:** It is the second added in [Equation A.14](#). Using [Equation A.15](#):

$$\begin{aligned}
\langle 0 | a_{\lambda_3}(p_3) b_{\lambda_4}(p_4) b_{\sigma_4}^\dagger(k_4) \color{red}{b_{\sigma_3}(k_3)} \color{red}{a_{\sigma_2}^\dagger(k_2)} a_{\sigma_1}(k_1) b_{\lambda_2}^\dagger(p_2) a_{\lambda_1}^\dagger(p_1) | 0 \rangle = \\
= -\langle 0 | a_{\lambda_3}(p_3) b_{\lambda_4}(p_4) b_{\sigma_4}^\dagger(k_4) a_{\sigma_2}^\dagger(k_2) b_{\sigma_3}(k_3) a_{\sigma_1}(k_1) b_{\lambda_2}^\dagger(p_2) a_{\lambda_1}^\dagger(p_1) | 0 \rangle
\end{aligned}$$

notice how this expression is exactly the same expression we have for the  $s$ -channel, with the only differences that we have an overall minus sign, and that we exchanged  $(k_2, \sigma_2) \leftrightarrow (k_3, \sigma_3)$ . Then, it follows from rewriting [Equation A.16](#) with consideration to what has changed:

$$\begin{aligned}
\langle 0 | a_{\lambda_3}(p_3) b_{\lambda_4}(p_4) b_{\sigma_4}^\dagger(k_4) a_{\sigma_3}^\dagger(k_3) b_{\sigma_2}(k_2) a_{\sigma_1}(k_1) b_{\lambda_2}^\dagger(p_2) a_{\lambda_1}^\dagger(p_1) | 0 \rangle = \\
= \left[ \delta_{\lambda_4 \sigma_4} \delta(\vec{p}_4 - \vec{k}_4) \right] \left[ \delta_{\lambda_3 \sigma_2} \delta(\vec{p}_3 - \vec{k}_2) \right] \left[ \delta_{\lambda_2 \sigma_3} \delta(\vec{p}_2 - \vec{k}_3) \right] \left[ \delta_{\lambda_1 \sigma_1} \delta(\vec{p}_1 - \vec{k}_1) \right] \langle 0 | 0 \rangle^1
\end{aligned} \tag{A.19}$$

Procedure is the same, but the minus sign has now disappeared:

$$\begin{aligned}
S_{fi}^{(2)} &= \frac{(-ie)^2}{\left[\sqrt{(2\pi)^3}\right]^4} \int d^4x d^4y D_{\mu\nu}^\xi(x-y) [\bar{u}(p_3, \lambda_3) \gamma_\mu u(p_1, \lambda_1)] \times \\
&\quad \times [\bar{v}(p_2, \lambda_2) \gamma_\nu v(p_4, \lambda_4)] e^{-i(p_1-p_3)x} e^{i(p_2-p_4)y} = \dots = \\
&= \frac{(-ie)^2}{(2\pi)^6} \hat{D}_{\mu\nu}^\xi(p_1 - p_3) [\bar{u}_3 \gamma_\mu u_1] [\bar{v}_2 \gamma_\nu v_4] \frac{[(2\pi)^4 i]^2}{(2\pi)^4 i} \delta(p_1 + p_2 - p_3 - p_4) = \\
&= \frac{(2\pi)^4 i \mathcal{A}_2}{(2\pi)^6} \delta(p_1 + p_2 - p_3 - p_4)
\end{aligned} \tag{A.20}$$

with the usual substitution  $\sqrt{(2\pi)^3} \rightarrow \sqrt{V}$ :

$$S_{fi}^{(2)} = \frac{(2\pi)^4 i \mathcal{A}_2}{V^2} \delta(p_1 + p_2 - p_3 - p_4) \tag{A.21}$$

Finally, joining into a single amplitude  $\mathcal{A}_1$  and  $\mathcal{A}_2$ :

$$S_{fi} = S_{fi}^{(1)} + S_{fi}^{(2)} = \frac{(2\pi)^4 i}{V^2} (-\mathcal{A}_1 + \mathcal{A}_2) \delta(p_1 + p_2 - p_3 - p_4) \quad (\text{A.22})$$

where it's convenient to have defined  $\mathcal{A} = -\mathcal{A}_1 + \mathcal{A}_2$ .

Now, we can proceed with the modulus squared, using final results from [subsection A.1](#):

$$|\mathcal{A}|^2 = (-\mathcal{A}_1 + \mathcal{A}_2)(-\mathcal{A}_1^* + \mathcal{A}_2^*) = |\mathcal{A}_1|^2 + |\mathcal{A}_2|^2 - \mathcal{A}_1 \mathcal{A}_2^* - \mathcal{A}_2 \mathcal{A}_1^* \quad (\text{A.23})$$

term by term, highlighting Dirac indices  $a \rightarrow h$ :

$$\begin{aligned} |\mathcal{A}_1|^2 &= e^4 \hat{D}_{\mu\nu}^\xi(p_1 + p_2) \hat{D}_{\rho\sigma}^\xi(p_1 + p_2) \left[ \bar{v}_{2,a} (\gamma_\mu)_{ab} u_{1,b} \right] \left[ \bar{u}_{1,c} (\gamma_\rho)_{cd} v_{2,d} \right] \left[ \bar{u}_{3,e} (\gamma_\nu)_{ef} v_{4,f} \right] \left[ \bar{v}_{4,g} (\gamma_\sigma)_{gh} u_{3,h} \right] = \\ &= e^4 \hat{D}_{\mu\nu}^\xi(p_1 + p_2) \hat{D}_{\rho\sigma}^\xi(p_1 + p_2) \left[ (\gamma_\mu)_{ab} (u_1 \bar{u}_1)_{bc} (\gamma_\rho)_{cd} (v_2 \bar{v}_2)_{da} \right] \left[ (\gamma_\nu)_{ef} (v_4 \bar{v}_4)_{fg} (\gamma_\sigma)_{gh} (u_3 \bar{u}_3)_{he} \right] = \\ &= e^4 \hat{D}_{\mu\nu}^\xi(p_1 + p_2) \hat{D}_{\rho\sigma}^\xi(p_1 + p_2) \text{Tr} [\gamma_\mu (u_1 \bar{u}_1) \gamma_\rho (v_2 \bar{v}_2)] \text{Tr} [\gamma_\nu (v_4 \bar{v}_4) \gamma_\sigma (u_3 \bar{u}_3)] \end{aligned}$$

$$|\mathcal{A}_2|^2 = \dots = e^4 \hat{D}_{\mu\nu}^\xi(p_1 - p_3) \hat{D}_{\rho\sigma}^\xi(p_1 - p_3) \text{Tr} [\gamma_\mu (u_1 \bar{u}_1) \gamma_\rho (u_3 \bar{u}_3)] \text{Tr} [\gamma_\nu (v_4 \bar{v}_4) \gamma_\sigma (v_2 \bar{v}_2)]$$

$$\mathcal{A}_1 \mathcal{A}_2^* = \dots = e^4 \hat{D}_{\mu\nu}^\xi(p_1 + p_2) \hat{D}_{\rho\sigma}^\xi(p_1 - p_3) \text{Tr} [\gamma_\mu (u_1 \bar{u}_1) \gamma_\rho (u_3 \bar{u}_3) \gamma_\nu (v_4 \bar{v}_4) \gamma_\sigma (v_2 \bar{v}_2)]$$

$$\mathcal{A}_2 \mathcal{A}_1^* = \dots = e^4 \hat{D}_{\mu\nu}^\xi(p_1 - p_3) \hat{D}_{\rho\sigma}^\xi(p_1 + p_2) \text{Tr} [\gamma_\mu (u_1 \bar{u}_1) \gamma_\rho (v_2 \bar{v}_2) \gamma_\nu (v_4 \bar{v}_4) \gamma_\sigma (u_3 \bar{u}_3)]$$

Averaging over initial fermion polarization and summing over all of them we get the unpolarized amplitude:

$$\begin{aligned} |\bar{\mathcal{A}}|^2 &= \frac{1}{4} \sum_{\lambda_1} \sum_{\lambda_2} \sum_{\lambda_3} \sum_{\lambda_4} \left( |\mathcal{A}_1|^2 + |\mathcal{A}_2|^2 - \mathcal{A}_1 \mathcal{A}_2^* - \mathcal{A}_2 \mathcal{A}_1^* \right) = \frac{1}{4} \frac{e^4}{2p_{1,4}2p_{2,4}2p_{3,4}2p_{4,4}} \times \\ &\left\{ \hat{D}_{\mu\nu}^\xi(p_1 + p_2) \hat{D}_{\rho\sigma}^\xi(p_1 + p_2) \text{Tr} \left[ \gamma_\mu \left( -i\cancel{p}_1 + m_e \right) \gamma_\rho \left( -i\cancel{p}_2 - m_e \right) \right] \text{Tr} \left[ \gamma_\nu \left( -i\cancel{p}_4 - m_e \right) \gamma_\sigma \left( -i\cancel{p}_3 + m_e \right) \right] \right. \\ &+ \hat{D}_{\mu\nu}^\xi(p_1 - p_3) \hat{D}_{\rho\sigma}^\xi(p_1 - p_3) \text{Tr} \left[ \gamma_\mu \left( -i\cancel{p}_1 + m_e \right) \gamma_\rho \left( -i\cancel{p}_3 + m_e \right) \right] \text{Tr} \left[ \gamma_\nu \left( -i\cancel{p}_4 - m_e \right) \gamma_\sigma \left( -i\cancel{p}_2 - m_e \right) \right] \\ &- \hat{D}_{\mu\nu}^\xi(p_1 - p_3) \hat{D}_{\rho\sigma}^\xi(p_1 + p_2) \text{Tr} \left[ \gamma_\mu \left( -i\cancel{p}_1 + m_e \right) \gamma_\rho \left( -i\cancel{p}_3 + m_e \right) \gamma_\nu \left( -i\cancel{p}_4 - m_e \right) \gamma_\sigma \left( -i\cancel{p}_2 - m_e \right) \right] \\ &- \left. \hat{D}_{\mu\nu}^\xi(p_1 + p_2) \hat{D}_{\rho\sigma}^\xi(p_1 - p_3) \text{Tr} \left[ \gamma_\mu \left( -i\cancel{p}_1 + m_e \right) \gamma_\rho \left( -i\cancel{p}_2 - m_e \right) \gamma_\nu \left( -i\cancel{p}_4 - m_e \right) \gamma_\sigma \left( -i\cancel{p}_3 + m_e \right) \right] \right\} \quad (\text{A.24}) \end{aligned}$$

and finally, the unpolarized  $S$ -matrix element squared becomes from [Equation A.22](#):

$$|S_{fi}|^2 = |\langle e^+ e^- | S | e^+ e^- \rangle|^2 = \frac{(2\pi)^8 |\bar{\mathcal{A}}|^2}{V^4} |\delta(p_1 + p_2 - p_3 - p_4)|^2 \quad (\text{A.25})$$

For this kind of calculation, we should rely on a FORM code. The code we used is called `Bhabha.frm` and it provides the result of the traces calculations. The result is  $\xi$  independent, because of gauge invariance, before imposing kinematics (as gauge invariance comes before kinematics). However, the result is quite complicated to write down, so it is convenient to introduce some kinematic constraints to simplify the result...

### A.3 Bhabha kinematics

Kinematics of Bhabha scattering will be evaluated in the center of mass reference frame. By simply imposing energy conservation, we can write down the four 4-momenta:

$$p_1 = (\vec{p}, iE) \quad p_2 = (-\vec{p}, iE) \quad p_3 = (\vec{p}', iE) \quad p_4 = (-\vec{p}', iE)$$

with  $|\vec{p}| = |\vec{p}'| = p$ . As in the annihilation case ([subsection D.3](#)), the only parameter not fixed in this frame is the scattering angle  $\theta$  (once we fix the value of  $\phi$  for the choice of scattering plane).

Kinematics is outlined in [Figure 44](#):

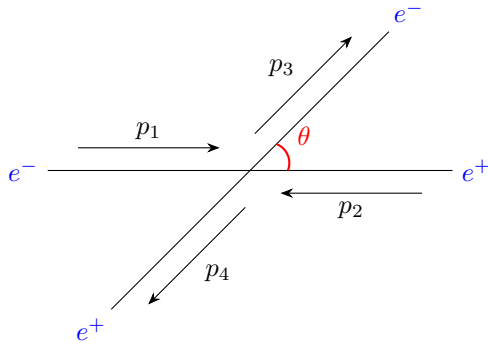


Figure 44: Kinematics of Bhabha scattering, in the center of mass system.

However, for Bhabha scattering, it is actually more convenient to always use the Mandelstam variables, which are Lorentz invariant:

$$\begin{cases} s = (p_1 + p_2)^2 = (p_3 + p_4)^2 = -m_e^2 + p_1^2 + 2p_1 \cdot p_2 = -4E^2 \\ t = (p_1 - p_3)^2 = (p_2 - p_4)^2 = -2m_e^2 - 2p_1 \cdot p_3 = 2p^2(1 - \cos\theta) \\ u = (p_1 - p_4)^2 = (p_2 - p_3)^2 = -2m_e^2 - 2p_1 \cdot p_4 = 2p^2(1 + \cos\theta) \end{cases} \quad (\text{A.26})$$

so that by energy conservation:

$$s + t + u = -4m_e^2 + p_1 \cdot \cancel{(p_1 + p_2 - p_3 - p_4)} = -4m_e^2 \quad (\text{A.27})$$

Then, all the scalar products are constrained:

$$\begin{aligned} p_1 \cdot p_2 &= \frac{(p_1 + p_2)^2}{2} + m_e^2 = \frac{s}{2} + m_e^2 \\ p_3 \cdot p_4 &= \frac{(p_3 + p_4)^2}{2} + m_e^2 = \frac{s}{2} + m_e^2 \\ p_1 \cdot p_3 &= -\frac{(p_1 - p_3)^2}{2} - m_e^2 = -\frac{t}{2} - m_e^2 \\ p_2 \cdot p_4 &= -\frac{(p_2 - p_4)^2}{2} - m_e^2 = -\frac{t}{2} - m_e^2 \\ p_1 \cdot p_4 &= -\frac{(p_1 - p_4)^2}{2} - m_e^2 = -\frac{u}{2} - m_e^2 \\ p_2 \cdot p_3 &= -\frac{(p_2 - p_3)^2}{2} - m_e^2 = -\frac{u}{2} - m_e^2 \end{aligned}$$

and we can also calculate:

$$\begin{aligned} v_{rel} &= \frac{1}{p_{1,4} p_{2,4}} \sqrt{(p_1 \cdot p_2)^2 - p_1^2 p_2^2} = \frac{1}{E^2} \sqrt{(-p^2 - E^2)^2 - m_e^4} = \\ &= \frac{1}{E^2} \sqrt{(m_e^2 - 2E^2)^2 - m_e^4} = \frac{2E^2}{E^2} \sqrt{1 - \frac{m_e^2}{E^2}} = \frac{2p}{E} \end{aligned} \quad (\text{A.28})$$

which is exactly the same as [Equation D.19](#), as the initial state is equivalent.

#### A.4 Bhabha cross section

We can intuitively see what is the modulus squared of a Dirac's delta, by applying Fourier transform:

$$\delta(E) = \int \frac{dt}{2\pi} e^{iEt} = \lim_{T \rightarrow \infty} \int_{-\frac{T}{2}}^{\frac{T}{2}} \frac{dt}{2\pi} e^{iEt} = \lim_{T \rightarrow \infty} \frac{1}{2\pi} \frac{\sin(ET/2)}{E/2} \quad (\text{A.29})$$

$$|\delta(E)|^2 = \lim_{T \rightarrow \infty} \frac{1}{(2\pi)^2} \left( \frac{\sin(ET/2)}{E/2} \right)^2 \approx \frac{2\pi T}{(2\pi)^2} \delta(E) = \frac{T}{2\pi} \delta(E) \quad (\text{A.30})$$

so, it makes sense that:

$$|\delta(p_i - p_f)|^2 \approx \frac{VT}{(2\pi)^4} \delta(p_i - p_f) \quad (\text{A.31})$$

Now, we can relate the S-matrix element squared to a *rate* of the process, obtained by fixing the specific kinematic configuration in the final state:

$$\Gamma(p_3, p_4) = \frac{|S_{fi}|^2}{T} = \frac{1}{T} \frac{(2\pi)^8 |\bar{\mathcal{A}}|^2}{V^4} \frac{VT}{(2\pi)^4} \delta(p_1 + p_2 - p_3 - p_4) \quad (\text{A.32})$$

which is just a probability density over time component of our spacetime. To get the total rate of the process, we got to integrate over phase space as well, remembering that the density of momentum states in a finite box quantization is:

$$d^3n = \frac{V}{(2\pi)^3} d^3p_f \quad (\text{A.33})$$

Finally, the cross section will simply be the rate divided by the flux of incoming positrons (per units of time and surface), which by fixing the number of positrons to 1:

$$\sigma(e^+e^- \rightarrow e^+e^-) = \frac{\Gamma(e^+e^- \rightarrow e^+e^-)}{\# \text{ positrons}/ST} = \frac{\Gamma(e^+e^- \rightarrow e^+e^-) V}{v_{rel}} \quad (\text{A.34})$$

which is where our relative velocity comes from. Altogether, our final cross section is:

$$\begin{aligned} \sigma(e^+e^- \rightarrow e^+e^-) &= \frac{V}{v_{rel}} \int \frac{V d^3p_3}{(2\pi)^3} \frac{V d^3p_4}{(2\pi)^3} \Gamma(p_3, p_4) = \\ &= \frac{V}{v_{rel}} \int \frac{V d^3p_3}{(2\pi)^3} \frac{V d^3p_4}{(2\pi)^3} \left[ \frac{1}{T} \frac{(2\pi)^8 |\bar{\mathcal{A}}|^2}{V^4} \frac{VT}{(2\pi)^4} \delta(p_1 + p_2 - p_3 - p_4) \right] = \\ &= \frac{1}{(2\pi)^2 v_{rel}} \int d^3p_3 d^3p_4 |\bar{\mathcal{A}}|^2 \delta(p_1 + p_2 - p_3 - p_4) = \\ &= \frac{E}{8\pi^2 p} \int d^3p_4 |\bar{\mathcal{A}}|^2 \delta(p_{1,4} + p_{2,4} - p_{3,4} - p_{4,4}) \end{aligned} \quad (\text{A.35})$$

with  $v_{rel}$  substituted with [Equation A.28](#), and integrated  $p_3$  out, leaving only the conservation of energy to deal with.

$$\frac{d\sigma}{d\Omega} = \frac{E}{8\pi^2 p} \int_0^\infty d|\vec{p}_4| |\vec{p}_4|^2 |\bar{\mathcal{A}}|^2 \delta(p_{1,4} + p_{2,4} - p_{3,4} - p_{4,4}) \quad (\text{A.36})$$

Notice that  $d|\vec{p}_4|^2 = d(p_{4,4}^2 - m_e^2) = dp_{4,4}^2$ , so we can change variable:

$$d|\vec{p}_4| |\vec{p}_4|^2 = dp_{4,4} p_{4,4} |\vec{p}_4|$$

As for the Dirac's delta:

$$\begin{aligned} \delta(p_{1,4} + p_{2,4} - p_{3,4} - p_{4,4}) &= \delta\left(2E - \sqrt{|\vec{p}_1 + \vec{p}_2 - \vec{p}_4|^2 + m_e^2} - p_{4,4}\right) = \\ &= \delta\left(2E - \sqrt{|\vec{p}_4|^2 + m_e^2} - p_{4,4}\right) = \\ &= \delta(2E - 2p_{4,4}) = \frac{1}{2} \delta(E - p_{4,4}) \end{aligned} \quad (\text{A.37})$$

so:

$$\begin{aligned} \frac{d\sigma}{d\Omega} &= \frac{E}{8\pi^2 p} \int_0^\infty dp_{4,4} p_{4,4} |\vec{p}_4| |\bar{\mathcal{A}}|^2 \frac{1}{2} \delta(E - p_{4,4}) = \\ &= \frac{E^2 p}{16\pi^2 p} |\bar{\mathcal{A}}|^2 = \frac{E^2}{16\pi^2} |\bar{\mathcal{A}}|^2 \end{aligned} \quad (\text{A.38})$$

where if  $p_{4,4} = E$ , then  $|\vec{p}_4| = p$ . Now,  $\mathcal{A}$  can be calculated imposing the kinematics constraints due to the conservation of energy and momentum imposition. Result can now be written down. The code used is `Bhabha.frm` in the GitHub repository. How this code works is explained in [subsection G.1](#). From [Equation A.24](#), we can write the amplitude as:

$$|\bar{\mathcal{A}}|^2 = \frac{1}{64E^4} F(s, t, u) \quad (\text{A.39})$$

$$F(s, t, u) = F_s(s, t, u) + F_t(s, t, u) + F_{st}(s, t, u) \quad (\text{A.40})$$

where  $F(s, t, u)$  is an adimensional function of the Mandelstam variables, and it is the actual result of the FORM computation. It gets contributions from each term of the squared amplitude:  $F_s$  from  $s$ -channel squared,  $F_t$  from  $t$ -channel squared,  $F_{st}$  from interference terms. To manipulate these terms, we can use Equation A.27<sup>43</sup>:

$$\begin{aligned}
F_s(s, t, u) &= 8e^4 \left[ -\frac{2tu}{s^2} - \frac{u}{s} - \frac{t}{s} \right] + 16m_e^2 e^4 \left[ -\frac{u}{s^2} - \frac{t}{s^2} - \frac{3}{s} \right] = \\
&= 8e^4 \left[ -\frac{2tu + \textcolor{blue}{s}(u+t)}{s^2} \right] + 16m_e^2 e^4 \left[ -\frac{u+t+3s}{s^2} \right] = \\
&= 8e^4 \left[ -\frac{2tu - (t+u+4m_e^2)(u+t)}{s^2} \right] + 16m_e^2 e^4 \left[ -\frac{u+t+3s}{s^2} \right] = \\
&= 8e^4 \left[ -\frac{2tu - (u+t)^2}{s^2} \right] + 32m_e^2 e^4 \frac{u+t}{s^2} + 16m_e^2 \left[ -\frac{u+t+3s}{s^2} \right] = \\
&= 8e^4 \left[ \frac{u^2 + t^2}{s^2} \right] + 16m_e^2 e^4 \left[ \frac{u+t-3\textcolor{blue}{s}}{s^2} \right] = \\
&= 8e^4 \left[ \frac{u^2 + t^2}{s^2} \right] + 16m_e^2 e^4 \left[ \frac{u+t+3(u+t+4m_e^2)}{s^2} \right] = \\
&= 8e^4 \left[ \frac{u^2 + t^2}{s^2} \right] + 16m_e^2 e^4 \left[ \frac{4(u+t) + 12m_e^2}{s^2} \right] = \\
&= \frac{8e^4}{s^2} \left[ u^2 + t^2 + 8m_e^2(u+t) + 24m_e^4 \right] \tag{A.41}
\end{aligned}$$

$$\begin{aligned}
F_t(s, t, u) &= 8e^4 \left[ -\frac{2su}{t^2} - \frac{u}{t} - \frac{s}{t} \right] + 16m_e^2 e^4 \left[ -\frac{u}{t^2} - \frac{s}{t^2} - \frac{3}{t} \right] = \\
&= \dots = \frac{8e^4}{t^2} \left[ u^2 + s^2 + 8m_e^2(u+s) + 24m_e^4 \right] \tag{A.42}
\end{aligned}$$

$$\begin{aligned}
F_{st}(s, t, u) &= 16e^4 \left[ -\frac{u}{s} - \frac{u}{t} \right] + 16m_e^2 e^4 \left[ \frac{u}{st} - \frac{3}{s} - \frac{3}{t} \right] = \\
&= 16e^4 \left[ -\frac{u(\textcolor{blue}{s}+\textcolor{blue}{t})}{st} + m_e^2 \left( \frac{u-3t-3s}{st} \right) \right] = \\
&= \frac{16e^4}{st} \left[ u^2 + 4m_e^2 u + m_e^2 u - 3m_e^2 (\textcolor{blue}{s}+\textcolor{blue}{t}) \right] = \\
&= \frac{16e^4}{st} \left[ u^2 + 8m_e^2 u + 12m_e^4 \right] \tag{A.43}
\end{aligned}$$

notice how  $F_t(s, t, u) = F_s(t, s, u)$ , by simple exchange of  $s$  and  $t$ , as this would just swap the two diagrams in Figure 43, giving the same cross section.

If we substitute these results into Equation A.39, and into Equation A.39, we obtain the final Bhabha scattering unpolarized differential cross section, using  $s = -4E^2$  and  $\alpha = e^2/4\pi$ :

$$\begin{aligned}
\frac{d\sigma}{d\Omega} &= \frac{E^2}{16\pi^2} \frac{e^4}{64E^4} \left\{ \frac{8}{s^2} [\dots] + \frac{8}{t^2} [\dots] + \frac{16}{st} [\dots] \right\} = \frac{e^4}{16\pi^2 8E^2} \left\{ \frac{1}{s^2} [\dots] + \frac{1}{t^2} [\dots] + \frac{2}{st} [\dots] \right\} = \\
&= \frac{\alpha^2}{2|s|} \left\{ \frac{1}{s^2} \left[ u^2 + t^2 + 8m_e^2(u+t) + 24m_e^4 \right] + \frac{1}{t^2} \left[ u^2 + s^2 + 8m_e^2(u+s) + 24m_e^4 \right] + \frac{2}{st} \left[ u^2 + 8m_e^2 u + 12m_e^4 \right] \right\} \tag{A.44}
\end{aligned}$$

This result is symmetric under  $s \leftrightarrow t$  exchange (as it should be), and it is consistent to what is found in literature (from Bardin and Passarino, [45]), but we need to remember that the linear term in  $s, t, u$  is given

<sup>43</sup>Whenever we are about to use  $s+t+u = -4m_e^2$ , the substituting part will be colored in blue.

with opposite sign. This is because in [subsection A.3](#), thanks to our notation, we defined Mandelstam variables with a negative sign overall with respect to the standard, mostly minus metric.

Like the annihilation cross section, there are two relevant limits to consider, as shown in [45]:

- **Non-relativistic limit:** We send  $4m_e^2/s \rightarrow -1$ , as  $E \rightarrow m_e$ . Then,  $t/s \rightarrow 0$  and  $u/s \rightarrow 0$ . Clearly, the  $t$ -channel is dominant in this limit, as  $1/t^2$  at denominator wins in [Equation A.44](#). This is also very intuitive, as  $s$ -channel requires annihilation and creation of  $e^+e^-$  pair, whilst the  $t$ -channel is a simple elastic scattering, dominating the "classical" limit:

$$\frac{d\sigma}{d\Omega} = \frac{\alpha^2}{2|s|} \left[ \frac{s^2 + 8m_e^2 s + 24m_e^2}{t^2} \right] = \frac{8\alpha^2 m_e^4}{2|s| t^2} \quad (\text{A.45})$$

substituting  $s = -4m_e^2$  and  $t = 2p^2(1 - \cos\theta) = 4p^2 \sin^2(\theta/2)$ :

$$\frac{d\sigma}{d\Omega} = \frac{\alpha^2 m_e^2}{t^2} = \frac{\alpha^2 m_e^2}{16p^4 \sin^4(\theta/2)} \quad (\text{A.46})$$

coherent with what is found in [45]. Finally, let us explore the limit  $\theta \rightarrow \pi/2$  to simplify expression:

$$\frac{d\sigma}{d\Omega} = \frac{\alpha^2 m_e^2}{4p^4} = \frac{\alpha^2}{4m_e^2 \beta^4} \quad (\text{A.47})$$

- **Ultra-relativistic limit:** If we send  $m_e^2/s \rightarrow 0$ , then we get from [Equation A.44](#):

$$\frac{d\sigma}{d\Omega} = \frac{\alpha^2}{2|s|} \left[ \frac{u^2 + t^2}{s^2} + \frac{u^2 + s^2}{t^2} + \frac{2u^2}{st} \right] = \frac{\alpha^2}{2|s|} \left[ u^2 \left( \frac{1}{s} + \frac{1}{t} \right)^2 + \left( \frac{t}{s} \right)^2 + \left( \frac{s}{t} \right)^2 \right] \quad (\text{A.48})$$

which is the very well-known tree level formula. None of the Mandelstam variables goes to 0, as by [Equation A.26](#):

$$s = -4E^2 \quad t \rightarrow 2E^2(1 - \cos\theta) \quad u \rightarrow 2E^2(1 + \cos\theta) \quad (\text{A.49})$$

which into [Equation A.48](#) gives:

$$\begin{aligned} \frac{d\sigma}{d\Omega} &= \frac{\alpha^2}{2|s|} \left[ \frac{4E^4 [(1 + \cos\theta)^2 + (1 - \cos\theta)^2]}{16E^4} + \frac{4E^4 [(1 + \cos\theta)^2 + 4]}{4E^4(1 - \cos\theta)^2} - \frac{8E^4(1 + \cos\theta)^2}{8E^4(1 - \cos\theta)} \right] = \\ &= \frac{\alpha^2}{2|s|} \left[ \frac{(1 + \cos\theta)^2}{4} + \frac{(1 - \cos\theta)^2}{4} + \frac{(1 + \cos\theta)^2 + 4}{(1 - \cos\theta)^2} - \frac{(1 + \cos\theta)^2}{1 - \cos\theta} \right] = \\ &= \frac{\alpha^2}{2|s|} \left[ \cos^4(\theta/2) + \sin^4(\theta/2) + \frac{\cos^4(\theta/2) + 1}{\sin^4(\theta/2)} - \frac{2\cos^4(\theta/2)}{\sin^2(\theta/2)} \right] \end{aligned} \quad (\text{A.50})$$

again, reported in [45]. It can also be simplified:

$$\begin{aligned} \frac{d\sigma}{d\Omega} &= \frac{\alpha^2}{2|s|} \frac{(1 + \cos\theta)^2(1 - \cos\theta)^2 + (1 - \cos\theta)^4 + 4(1 + \cos\theta)^2 + 16 + 4(1 + \cos\theta)^2(1 - \cos\theta)}{4(1 - \cos\theta)^2} = \\ &= \frac{\alpha^2}{2|s|} \frac{1}{4(1 - \cos\theta)^2} \left[ 18 + 12\cos^2\theta + 2\cos^4\theta \right] \end{aligned}$$

which is just a square:

$$\frac{d\sigma}{d\Omega} = \frac{\alpha^2}{4|s|} \left[ \frac{3 + \cos^2\theta}{1 - \cos\theta} \right]^2 \quad (\text{A.51})$$

Note that when integrated in solid angle, [Equation A.51](#) gives an infinite cross section. This is perfectly fine, as massless mediators, responsible for  $1/r$  interactions, give infinite cross sections because the interaction does not scale fast enough (this happens in classical physics, too). In reality, one would always measure a finite quantity over a finite distance. The real observable is always the differential cross section.

In the limit  $\theta \rightarrow \pi/2$ :

$$\frac{d\sigma}{d\Omega} = \frac{\alpha^2}{4|s|} \left[ \frac{3 + \cos^2\theta}{1 - \cos\theta} \right]^2 \rightarrow \frac{9\alpha^2}{4|s|} \quad (\text{A.52})$$

While in the limit  $\theta \rightarrow 0$ , where we approximate  $\cos\theta \rightarrow 1$ ,  $\sin\theta \rightarrow \theta$  and  $1 - \cos\theta \rightarrow \theta^2/2$ :

$$\frac{d\sigma}{d\Omega} = \frac{\alpha^2}{4|s|} \left[ \frac{3 + \cos^2\theta}{1 - \cos\theta} \right]^2 \rightarrow \frac{16\alpha^2}{|s|} \frac{1}{\theta^4} \quad (\text{A.53})$$

## B Møller scattering at tree level

We derive here the well-known amplitudes and cross section for the electrodynamics process  $e^-e^- \rightarrow e^-e^-$ , at tree level, using crossing symmetry arguments starting from Bhabha scattering. The eventual correction due to the tree level diagram of the  $X$  resonance acts at this order in perturbation theory. However, in this Appendix, we will not consider it. For the additional contribution of the spin 2 resonance, see [section 7](#).

### B.1 Møller amplitude

Let us see the contributing diagrams for this process, the *t-channel* and the *u-channel*:

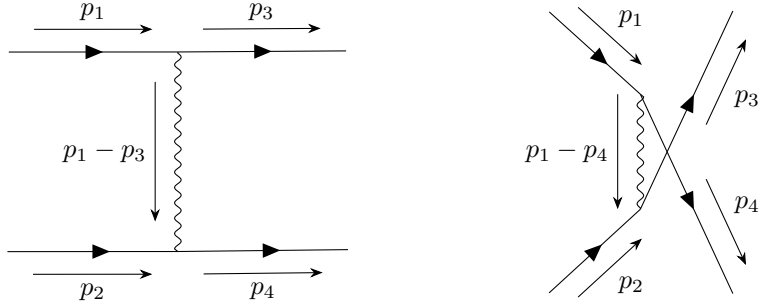


Figure 45: Diagrams corresponding to tree level Møller scattering. On the left, the *t-channel*, hereafter denoted with  $\mathcal{A}_1$ . On the right, the *u-channel*, hereafter denoted with  $\mathcal{A}_2$ .

The amplitudes are easily written:

$$\begin{aligned} \mathcal{A}_1 &= (-ie)^2 \hat{D}_{\mu\nu}^\xi(p_1 - p_3) [\bar{u}(p_4, \lambda_4) \gamma_\mu u(p_2, \lambda_2)] [\bar{u}(p_3, \lambda_3) \gamma_\nu u(p_1, \lambda_1)] = \\ &= -e^2 \hat{D}_{\mu\nu}^\xi(p_1 - p_3) [\bar{u}_4 \gamma_\mu u_2] [\bar{u}_3 \gamma_\nu u_1] \end{aligned} \quad (\text{B.1})$$

$$\begin{aligned} \mathcal{A}_2 &= (-ie)^2 \hat{D}_{\mu\nu}^\xi(p_1 - p_4) [\bar{u}(p_4, \lambda_4) \gamma_\mu u(p_1, \lambda_1)] [\bar{u}(p_3, \lambda_3) \gamma_\nu u(p_2, \lambda_2)] = \\ &= -e^2 \hat{D}_{\mu\nu}^\xi(p_1 - p_4) [\bar{u}_4 \gamma_\mu u_1] [\bar{u}_3 \gamma_\nu u_2] \end{aligned} \quad (\text{B.2})$$

where the usual electrodynamics Feynman rule  $-ie\gamma_\mu$  applies at each vertex,  $m_e$  is the mass of the electron,  $p_i$ ,  $i \in \{1, 2, 3, 4\}$  are the respective momenta according to [Figure 43](#) and  $\lambda_i$ ,  $i \in \{1, 2, 3, 4\}$  are the respective polarizations of fermions. Here forth, we will call  $u(p_i, \lambda_i) = u_i$ ,  $i \in \{1, 2, 3, 4\}$ .

### B.2 Møller Wick contractions

Again, we have the problem of the combinatorics of the two diagrams. Look at the  $S$ -matrix element. Define an initial and final state  $|i\rangle = |e^-e^-\rangle = |f\rangle$ . Then, the first order at which we find a non trivial contribution (other than forward scattering) is the second order, which is our tree level. The exponential of the  $T$ -ordered product gets expanded into normal ordered interaction terms:

$$\begin{aligned} S_{fi} &= \langle f | S | i \rangle = \langle e^-e^- | S | e^-e^- \rangle = \\ &= \frac{(-ie)^2}{2!} \int d^4x d^4y \langle e^-e^- | :(\bar{\psi}\gamma_\nu A_\nu\psi)_y : :(\bar{\psi}\gamma_\mu A_\mu\psi)_x : | e^-e^- \rangle = \\ &= \frac{(-ie)^2}{2!} \int d^4x d^4y D_{\mu\nu}^\xi(x-y) \langle e^-e^- | :(\bar{\psi}\gamma_\nu\psi)_y : :(\bar{\psi}\gamma_\mu\psi)_x : | e^-e^- \rangle \end{aligned} \quad (\text{B.3})$$

where we contracted the two photon fields into a propagator because in the final and initial state there is no photon. Whatever non zero contraction we get in [Equation B.3](#), there is an equal contraction obtained by exchanging  $x$  and  $y$  interaction points. So, we can cancel the  $1/2!$  and are left with 2 possible contractions:

$$\begin{aligned} S_{fi} &= (-ie)^2 \int d^4x d^4y D_{\mu\nu}^\xi(x-y) \langle e^-e^- | :(\psi^\dagger\gamma_4\gamma_\nu\psi)_y : :(\psi^\dagger\gamma_4\gamma_\mu\psi)_x : | e^-e^- \rangle \\ &\quad + (-ie)^2 \int d^4x d^4y D_{\mu\nu}^\xi(x-y) \langle e^-e^- | :(\psi^\dagger\gamma_4\gamma_\nu\psi)_y : :(\psi^\dagger\gamma_4\gamma_\mu\psi)_x : | e^-e^- \rangle \end{aligned} \quad (\text{B.4})$$

where  $\psi$  can annihilate an electron, while  $\psi^\dagger$  can create an electron. Notice how the first and second rows are equivalent to each other, the only difference being that we exchange the two photons in the initial state. Same goes for third and fourth row. Thanks to this symmetry, we can eliminate the  $1/2!$  in the expansion, and be left with only two independent contributions.

The two contractions in [Equation B.4](#) correspond respectively to the  $t$ -channel (one at a time, we propagate electron in  $x$  and positron in  $y$ ) and the  $u$ -channel (exactly like  $t$ -channel, but exchanging final state electrons) diagrams in [subsection B.1](#).

Here, multiplicity of states is more relevant than ever, and there are four total permutations of the initial and final states. However, it is the assignment of the fields to interaction points that seals the diagrams, and there really are only two of them.

### B.3 Crossing symmetry argument

We now argue that there is literally nothing to calculate for Møller scattering, as we already have every ingredient to derive its cross section. The heart of it is: Møller cross section can be derived from Bhabha's using *crossing symmetry*!

We also had crossing symmetry for Compton scattering and electron-positron annihilation into two photons. However, because we had a different frame of reference, and different kinematics (yielding different phase space integral result), the two cross sections had actually different expressions, so we decided to pursue independent calculations nonetheless.

However, as masochist as one might be, they would be fools not to use crossing symmetry here, as there is no better application than the Møller-Bhabha connection. However, seeing how the diagrams are linked together, as obvious as it might appear, still requires little imagination. To see it, first sketch the Bhabha diagrams: [Figure 46](#) has no specific mediator, as the argument is interaction independent for vector theories.

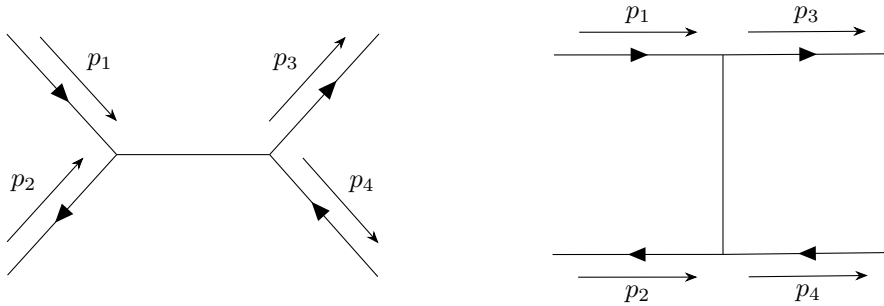


Figure 46: Sketching Bhabha diagrams. Full picture is shown in [Figure 43](#).

Now, Bhabha is  $e^+e^- \rightarrow e^+e^-$ . To get to Møller, which is  $e^-e^- \rightarrow e^-e^-$ , all we have to do is move the positron in the initial state to an electron in the final state, and move the positron in the final state to an electron in the initial state (because, if  $CPT$  is a good symmetry of QFT, performing  $T$  requires performing  $CP$  as well: to move a particle backwards in time, it has to be converted into its antiparticle). This will affect the anti fermion legs only ( $p_2$  and  $p_4$ ).

Acting on the geometry of the diagrams, this is a rigid movement "rotation" of the external legs, which has to preserve interaction vertices and the relation between momentum arrows and fermion arrow. Drawing the diagrams gives: Now, we are almost there, as the diagram to the left and the diagram to the right in [Figure 47](#)

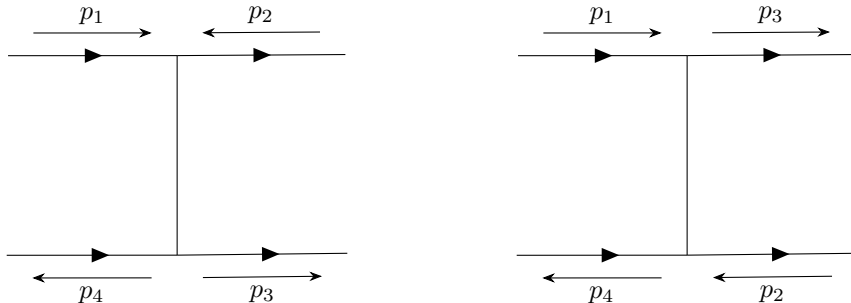


Figure 47: Result of the rigid leg movement. Diagrams are not compatible with the same process, as external final momenta have to be exchanged.

have different external momenta, and still not pertain to the same process. Not to worry, take the diagram to

the right and exchange the final fermions: And these in [Figure 48](#) are now the  $t$ -channel and  $u$ -channel for the

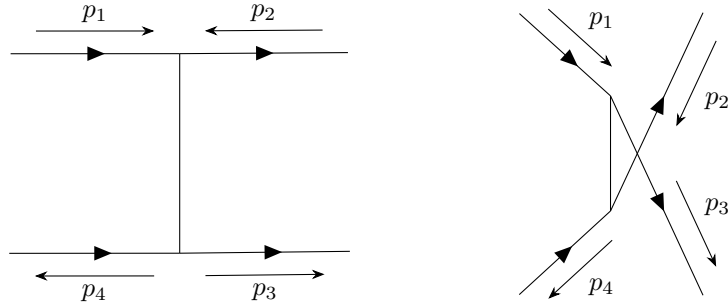


Figure 48: Now, a Møller scattering process. Diagrams shown are  $t$ -channel (left) and  $u$ -channel (right).

Møller scattering. The only thing left to do is to rename momenta and define new Mandelstam variables:

$$p'_1 = p_1 \quad p'_2 = -p_4 \quad p'_3 = -p_2 \quad p'_4 = p_3 \quad (\text{B.5})$$

which means that:

$$p_1 = p'_1 \quad p_2 = -p'_3 \quad p_3 = p'_4 \quad p_4 = -p'_2 \quad (\text{B.6})$$

and

$$\begin{aligned} s' &= (p'_1 + p'_2)^2 = (p_1 - p_4)^2 = u \\ t' &= (p'_1 - p'_3)^2 = (p_1 + p_2)^2 = s \\ u' &= (p'_1 - p'_4)^2 = (p_1 - p_3)^2 = t \end{aligned}$$

which is just a reshuffle. Between the two sets of diagrams, all we did was rigid movement of the diagram, which in vector theories has no effect whatsoever in the amplitude. So, we can effectively write the amplitudes of Bhabha scattering and made it a Møller scattering just by shuffling Mandelstam variables:

$$\mathcal{A}(\text{Bhabha}; s, t, u) = \mathcal{A}(\text{Møller}; s', t', u') = \mathcal{A}(\text{Møller}; u, s, t)$$

which means:

$$\mathcal{A}(\text{Møller}; s, t, u) = \mathcal{A}(\text{Bhabha}; t, u, s) \quad (\text{B.7})$$

which is a nice correspondence we found.

Of course, we also checked this correspondence by writing a FORM code for Møller scattering. The code is `Moller.frm`, found in the GitHub repository linked in [subsection G.1](#). Comparison of the amplitude of Bhabha and Møller in QED yields the exact exchange  $(s, t, u) \rightarrow (t, u, s)$ .

However, it is not over. Because the process only involved particles with identical mass ( $e^-$  and  $e^+$ ), the integral over phase space also yields the same exact result for the cross section (without reshuffling variables, it is just plainly the same). And [Equation B.7](#) is actually interaction independent, as long as diagrams stay the same. So, just by taking [Equation A.44](#), we immediately derive the cross section for Møller scattering:

$$\frac{d\sigma}{d\Omega} = \frac{\alpha^2}{2|s|} \left\{ \frac{1}{t^2} \left[ s^2 + u^2 + 8m_e^2(s+u) + 24m_e^4 \right] + \frac{1}{u^2} \left[ s^2 + t^2 + 8m_e^2(s+t) + 24m_e^4 \right] + \frac{2}{tu} \left[ s^2 + 8m_e^2s + 12m_e^4 \right] \right\} \quad (\text{B.8})$$

which is our final QED result.

Let us look at the usual limits:

- **Non-relativistic limit:** We send  $4m_e^2/s \rightarrow -1$ , as  $E \rightarrow m_e$ . Then,  $t/s \rightarrow 0$  and  $u/s \rightarrow 0$ . All channels

have to be considered:

$$\begin{aligned}
\frac{d\sigma}{d\Omega} &= \frac{\alpha^2}{2|s|} \left[ \frac{s^2 + 8m_e^2 s + 24m_e^2}{t^2} + \frac{s^2 + 8m_e^2 s + 24m_e^2}{u^2} + \frac{2(s^2 + 8m_e^2 s + 12m_e^4)}{tu} \right] = \\
&= \frac{\alpha^2}{8m_e^2} 8m_e^4 \left[ \frac{1}{t^2} + \frac{1}{u^2} + \frac{1}{ut} \right] = \\
&= \frac{\alpha^2 m_e^2}{4p^4} \left[ \frac{1}{(1 - \cos \theta)^2} + \frac{1}{(1 + \cos \theta)^2} - \frac{1}{1 - \cos^2 \theta} \right] = \\
&= \frac{\alpha^2 m_e^2}{4p^4} \left[ \frac{(1 + \cos \theta)^2 + (1 - \cos \theta)^2 - (1 - \cos^2 \theta)}{(1 - \cos^2 \theta)^2} \right] = \\
&= \frac{\alpha^2 m_e^2}{4p^4} \left[ \frac{1 + 3\cos^2 \theta}{\sin^2 \theta} \right]^2
\end{aligned} \tag{B.9}$$

Let us explore the limit  $\theta \rightarrow \pi/2$  to simplify expression:

$$\frac{d\sigma}{d\Omega} = \frac{\alpha^2 m_e^2}{4p^4} = \frac{\alpha^2}{4m_e^2 \beta^4} \tag{B.10}$$

- **Ultra-relativistic limit:** If we send  $m_e^2/s \rightarrow 0$ , then we get from [Equation B.8](#):

$$\frac{d\sigma}{d\Omega} = \frac{\alpha^2}{2|s|} \left[ \frac{s^2 + u^2}{t^2} + \frac{s^2 + t^2}{u^2} + \frac{2s^2}{tu} \right] = \frac{\alpha^2}{2|s|} \left[ s^2 \left( \frac{1}{t} + \frac{1}{u} \right)^2 + \left( \frac{u}{t} \right)^2 + \left( \frac{t}{u} \right)^2 \right] \tag{B.11}$$

which is the very well-known tree level formula. None of the Mandelstam variables goes to 0, as by [Equation A.49](#). Into [Equation B.11](#):

$$\begin{aligned}
\frac{d\sigma}{d\Omega} &= \frac{\alpha^2}{2|s|} \left[ \frac{16E^4 + 4E^4(1 + \cos \theta)^2}{4E^4(1 - \cos \theta)^2} + \frac{16E^4 - 4E^4(1 + \cos \theta)^2}{4E^4(1 + \cos \theta)^2} + \frac{32E^4}{4E^4(1 - \cos^2 \theta)} \right] = \\
&= \frac{\alpha^2}{2|s|} \left[ \frac{4(1 + \cos \theta)^2 + (1 + \cos \theta)^4 + 4(1 - \cos \theta)^2 + (1 - \cos \theta)^4 + 8(1 - \cos^2 \theta)}{(1 - \cos^2 \theta)^2} \right] = \\
&= \frac{\alpha^2}{2|s|} \left[ \frac{2\cos^4 \theta + 12\cos^2 \theta + 18}{(1 - \cos^2 \theta)^2} \right] = \\
&= \frac{\alpha^2}{|s|} \left[ \frac{3 + \cos^2 \theta}{\sin^2 \theta} \right]^2
\end{aligned} \tag{B.12}$$

Again, total cross section is infinite. This happens often in QED processes, as electromagnetic interaction scales like  $1/r$ , and it characterizes the scatterer as having "infinite size". Therefore, the actual observable is always the differential cross section.

In the limit  $\theta \rightarrow \pi/2$ :

$$\frac{d\sigma}{d\Omega} = \frac{\alpha^2}{|s|} \left[ \frac{3 + \cos^2 \theta}{\sin^2 \theta} \right]^2 \rightarrow \frac{9\alpha^2}{|s|} \tag{B.13}$$

While in the limit  $\theta \rightarrow 0$ , where we approximate  $\cos \theta \rightarrow 1$ ,  $\sin \theta \rightarrow \theta$ :

$$\frac{d\sigma}{d\Omega} = \frac{\alpha^2}{|s|} \left[ \frac{3 + \cos^2 \theta}{\sin^2 \theta} \right]^2 \rightarrow \frac{16\alpha^2}{|s|} \frac{1}{\theta^4} \tag{B.14}$$

It is worth mentioning that the final state is made of indistinguishable particles, hence only when integrating the total cross section, we need an extra, independent factor of  $1/2$  from [Equation 5.31](#) (see [25], chap. 4).

## C Compton scattering at tree level

We derive here the well-known amplitudes and cross section for the Compton scattering, at tree level. The eventual correction due to the tree level diagram of the  $X$  resonance acts at this order in perturbation theory. However, in this Appendix, we will not consider it. For the additional correction due to a massive spin 2 boson, see [section 9](#).

Before writing the amplitudes, we need to write down the fermion propagator. By inverting Dirac's equation for fermions, we define the propagator as:

$$D_{ab}(x - y) = \int \frac{d^4 q}{(2\pi)^4 i} \hat{D}_{ab}(q) e^{iq(x-y)} \quad (\text{C.1})$$

where we define the propagator in momentum space as:

$$\hat{D}_{ab}(q) = \frac{(-iq + m\mathbb{1})_{ab}}{q^2 + m^2 - i\epsilon} \quad (\text{C.2})$$

where  $a, b$  are Dirac indices and  $m$  is the mass of the fermion in question.  $m = m_e$  in our case.

### C.1 Compton Wick contractions

It is better to start by carrying out the necessary Wick contractions that define Compton scattering. With the exception of the trivial forward scattering, the first order in the  $T$ -ordered product expansion that interpolates the initial and final state  $|i\rangle = |f\rangle = |e^-\gamma\rangle$  is second order. The exponential of the  $T$ -ordered product gets expanded into normal ordered interaction terms:

$$\begin{aligned} S_{fi} &= \langle f | S | i \rangle = \langle e^- \gamma | S | e^- \gamma \rangle = \\ &= \frac{(-ie)^2}{2!} \int d^4x d^4y \langle e^- \gamma | :(\bar{\psi} \gamma_\nu A_\nu \psi)_y : :(\bar{\psi} \gamma_\mu A_\mu \psi)_x : | e^- \gamma \rangle \end{aligned} \quad (\text{C.3})$$

Now, we need to write down every possible contraction:

$$\begin{aligned} S_{fi} &= \frac{(-ie)^2}{2!} \int d^4x d^4y \langle e^- \gamma | :(\bar{\psi}^\dagger \gamma_4 \gamma_\nu A_\nu \psi)_y : :(\bar{\psi}^\dagger \gamma_4 \gamma_\mu A_\mu \psi)_x : | e^- \gamma \rangle \\ &\quad + \frac{(-ie)^2}{2!} \int d^4x d^4y \langle e^- \gamma | :(\bar{\psi}^\dagger \gamma_4 \gamma_\nu A_\nu \psi)_y : :(\bar{\psi}^\dagger \gamma_4 \gamma_\mu A_\mu \psi)_x : | e^- \gamma \rangle \\ &\quad + \frac{(-ie)^2}{2!} \int d^4x d^4y \langle e^- \gamma | :(\bar{\psi}^\dagger \gamma_4 \gamma_\nu A_\nu \psi)_y : :(\bar{\psi}^\dagger \gamma_4 \gamma_\mu A_\mu \psi)_x : | e^- \gamma \rangle \\ &\quad + \frac{(-ie)^2}{2!} \int d^4x d^4y \langle e^- \gamma | :(\bar{\psi}^\dagger \gamma_4 \gamma_\nu A_\nu \psi)_y : :(\bar{\psi}^\dagger \gamma_4 \gamma_\mu A_\mu \psi)_x : | e^- \gamma \rangle \end{aligned} \quad (\text{C.4})$$

Notice how, really, the first row is equivalent to the fourth, and second row are equivalent to the third, the only difference begin that we inverted  $x$  and  $y$  interaction points. Thanks to this symmetry, we can eliminate the  $1/2!$  in the expansion, and be left with only two contributions, which will be the two tree level diagrams for Compton scattering:

$$\begin{aligned} S_{fi} &= (-ie)^2 \int d^4x d^4y \langle e^- \gamma | :(\bar{\psi}^\dagger \gamma_4 \gamma_\nu A_\nu \psi)_y D_{ab}(x-y) (\gamma_4 \gamma_\mu A_\mu \psi)_x : | e^- \gamma \rangle \\ &\quad + (-ie)^2 \int d^4x d^4y \langle e^- \gamma | :(\bar{\psi}^\dagger \gamma_4 \gamma_\nu A_\nu \psi)_y D_{ab}(x-y) (\gamma_4 \gamma_\mu A_\mu \psi)_x : | e^- \gamma \rangle \end{aligned} \quad (\text{C.5})$$

We always get an internal fermion propagator from  $x$  to  $y$ . The first row corresponds to a  $s$ -channel diagram, as electron and photon are annihilated in  $x$  and created in  $y$  together. Instead, the second row is a  $u$  channel diagram, as we exchanged the two photon contractions, leaving us with a vertex in  $x$  where an electron is annihilated and a photon is created, and a vertex in  $y$  where an electron is created and a photon is annihilated.

Now that we know what the two contributions actually are, and what factor goes in front, we can use QED Feynman rules to write down the actual amplitudes of the two diagrams, which we will be doing in the next paragraph.

## C.2 Compton amplitude

Let us see the contributing diagrams for this process, the *s-channel* and the *u-channel*:

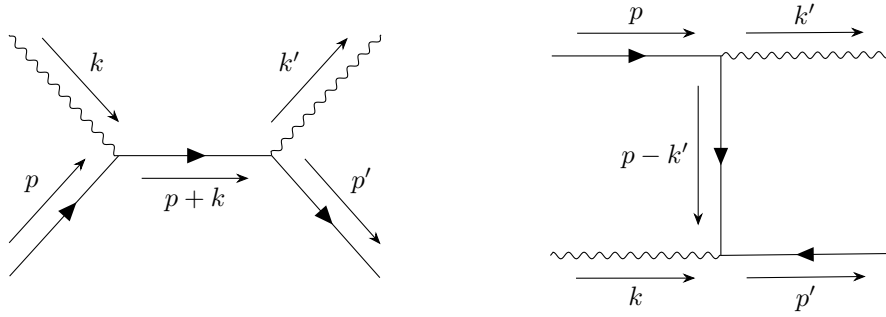


Figure 49: Diagrams corresponding to tree level Compton scattering. On the left, the *s*-channel, hereafter denoted with  $\mathcal{A}_1$ . On the right, the *u*-channel, hereafter denoted with  $\mathcal{A}_2$ .

The amplitudes are easily written:

$$\mathcal{A}_1 = (-ie)^2 \bar{u}(p', s') \bar{\varepsilon}_\mu(k', \lambda') \gamma_\mu \left[ \frac{-i(\not{p} + \not{k}) + m_e}{(p+k)^2 + m_e^2} \right] \varepsilon_\nu(k, \lambda) \gamma_\nu u(p, s) = -e^2 \bar{u}' O_1 u \quad (\text{C.6})$$

$$\mathcal{A}_2 = (-ie)^2 \bar{u}(p', s') \varepsilon_\mu(k, \lambda) \gamma_\mu \left[ \frac{-i(\not{p} - \not{k}') + m_e}{(p-k')^2 + m_e^2} \right] \bar{\varepsilon}_\nu(k', \lambda') \gamma_\nu u(p, s) = -e^2 \bar{u}' O_2 u \quad (\text{C.7})$$

where the usual electrodynamics Feynman rule  $-ie\gamma_\mu$  applies at each vertex,  $m_e$  is the mass of the electron,  $p, p', k, k'$  are the respective momenta according to Figure 49 and  $s, s', \lambda, \lambda'$  are the polarizations of fermions and photons, respectively. Here forth, we will call  $u(p, s) = u$ ,  $u(p', s') = u'$ ,  $\varepsilon_\mu(k, \lambda) = \varepsilon_\mu$ ,  $\varepsilon_\mu(k', \lambda') = \varepsilon'_\mu$ .

With the help of kinematics, we realize that:

$$(p+k)^2 + m_e^2 = s + m_e^2 = -m_e^2 + \not{k}^2 + 2p \cdot k + m_e^2 = 2p \cdot k \quad (\text{C.8})$$

$$(p-k')^2 + m_e^2 = u + m_e^2 = -m_e^2 + \not{k}'^2 - 2p \cdot k' + m_e^2 = -2p \cdot k' \quad (\text{C.9})$$

so that we can write  $O_1, O_2$ :

$$O_1 = \bar{\varepsilon}'_\mu \gamma_\mu \left[ \frac{-i(\not{p} + \not{k}) + m_e}{2p \cdot k} \right] \varepsilon_\nu \gamma_\nu \quad (\text{C.10})$$

$$O_2 = \varepsilon_\nu \gamma_\nu \left[ \frac{-i(\not{p} - \not{k}') + m_e}{-2p \cdot k'} \right] \bar{\varepsilon}'_\mu \gamma_\mu \quad (\text{C.11})$$

Additionally, we require the following factor in front of each amplitude, taking into account our choices for normalization of the fields, vertices and propagators:

- Each vertex of interaction requires a factor of  $(2\pi)^4 i$ .
- Each propagator requires a factor of  $1/[(2\pi)^4 i]$ .
- Each field is normalized with respect to the volume of the spacetime in which we are performing the integration:  $1/\sqrt{V}$ . Of course, we expect volume dependence to be erased in the final process cross section.
- Each photon field requires additional normalization of  $1/\sqrt{2E}$ ,  $E$  being its energy (which we label with the subscript  $_4$ , as in our notation it is the fourth component).

So, overall:

$$\frac{[(2\pi)^4 i]^2}{(2\pi)^4 i} \left( \frac{1}{\sqrt{V}} \right)^4 \frac{1}{\sqrt{2k_4 2k'_4}} = \frac{(2\pi)^4 i}{V^2 \sqrt{2k_4 2k'_4}} \quad (\text{C.12})$$

Notice how this result is exactly what we get from the Wick contractions in subsection A.2, which for Bhabha scattering leads us to Equation A.25. This comprehensive set of rules does not give the absolute minus sign due to fermion statistics. For that, we need Wick contractions, unfortunately.

The next step consists of calculating the complex conjugates of  $\mathcal{A}_1$  and  $\mathcal{A}_2$ . We will be employing [Equation 5.3](#). Remembering that the spinors get swapped:

$$\mathcal{A}_1^* = -e^2 \bar{u} \left( \gamma_4 O_1^\dagger \gamma_4 \right) u' = -e^2 \bar{u} P_1 u' \quad (\text{C.13})$$

$$\mathcal{A}_2^* = -e^2 \bar{u} \left( \gamma_4 O_2^\dagger \gamma_4 \right) u' = -e^2 \bar{u} P_2 u' \quad (\text{C.14})$$

Before calculating  $P_1$  and  $P_2$ , we can easily realize that with this clever rewriting, we get a trace in Dirac space. Let us highlight Dirac indices to see it:

$$\begin{aligned} |\mathcal{A}|^2 &= (\mathcal{A}_1 + \mathcal{A}_2)(\mathcal{A}_1^* + \mathcal{A}_2^*) = \\ &= \left[ -e^2 \bar{u}'_a (O_1 + O_2)_{ab} u_b (-e^2) \bar{u}_c (P_1 + P_2)_{cd} u'_d \right] = \\ &= e^4 \left[ \bar{u}'_a (O_1 + O_2)_{ab} u_b \bar{u}_c (P_1 + P_2)_{cd} u'_d \right] = \\ &= e^4 \left[ (O_1 + O_2)_{ab} (u \bar{u})_{bc} (P_1 + P_2)_{cd} (u' \bar{u}')_{da} \right] = \\ &= e^4 \text{Tr} \left[ (O_1 + O_2) u \bar{u} (P_1 + P_2) u' \bar{u}' \right] \end{aligned} \quad (\text{C.15})$$

Now, let us calculate  $P_1$  and  $P_2$ . We need a couple of identities:

- The gamma matrices, as we defined them in [section 3](#), are hermitian ( $\gamma_\mu^\dagger = \gamma_\mu$ ). Moreover, we can write down a compact expression for commutation of gamma matrices with  $\gamma_4$ :

$$\gamma_\mu \gamma_4 = -(-1)^{\delta_{\mu 4}} \gamma_4 \gamma_\mu \quad (\text{C.16})$$

That is because if  $\mu \neq 4$ , they anticommute, so we get a minus sign. When, instead,  $\mu = 4$ , we get a trivial commutation, with a plus sign.

- With the definitions we gave of a 4-vector components,  $q_\mu^* = (-1)^{\delta_{\mu 4}} q_\mu$ , as the energy component is imaginary.
- When writing down the photon polarization, even the spatial components might be imaginary (i.e. circular polarization). A barred polarization for outward photons ( $\bar{\varepsilon}$ ) simply takes the complex conjugate with respect to the spatial components only. Since the imaginary time component is not touched:  $\varepsilon_\mu^* = (-1)^{\delta_{\mu 4}} \bar{\varepsilon}_\mu$

All in all, this allows us to write:

$$\begin{aligned} \not{q}^* \gamma_4 &= q_\mu^* \gamma_\mu \gamma_4 = -[(-1)^{\delta_{\mu 4}}]^2 q_\mu \gamma_4 \gamma_\mu = -\gamma_4 \not{q} \\ \not{\varepsilon}^* \gamma_4 &= \varepsilon_\mu^* \gamma_\mu \gamma_4 = -[(-1)^{\delta_{\mu 4}}]^2 \bar{\varepsilon}_\mu \gamma_4 \gamma_\mu = -\gamma_4 \not{\varepsilon} \\ \not{\bar{\varepsilon}}^* \gamma_4 &= \bar{\varepsilon}_\mu^* \gamma_\mu \gamma_4 = -[(-1)^{\delta_{\mu 4}}]^2 \varepsilon_\mu \gamma_4 \gamma_\mu = -\gamma_4 \not{\bar{\varepsilon}} \end{aligned} \quad (\text{C.17})$$

So, we can finally write our operators, using the identities we just proved:

$$\begin{aligned} P_1 &= \gamma_4 \left[ \bar{\varepsilon}'_\rho \gamma_\rho \left( \frac{-i(\not{p} + \not{k}) + m_e}{2p \cdot k} \right) \varepsilon_\sigma \gamma_\sigma \right]^\dagger \gamma_4 = \gamma_4 \gamma_\sigma \varepsilon_\sigma^* \left[ \frac{i(\not{p}^* + \not{k}^*) + m_e}{2p \cdot k} \right] \gamma_\rho \bar{\varepsilon}'_\rho^* \gamma_4 = \\ &= \gamma_4 \not{\varepsilon}^* \color{red}{\gamma_4 \gamma_4} \left[ \frac{i(\not{p}^* + \not{k}^*) + m_e}{2p \cdot k} \right] \color{red}{\gamma_4 \gamma_4} \not{\bar{\varepsilon}}'^* \gamma_4 = \not{\bar{\varepsilon}} \left[ \frac{-i(\not{p} + \not{k}) + m_e}{2p \cdot k} \right] \not{\varepsilon}' = \\ &= \bar{\varepsilon}_\sigma \gamma_\sigma \left[ \frac{-i(\not{p} + \not{k}) + m_e}{2p \cdot k} \right] \varepsilon'_\rho \gamma_\rho \end{aligned} \quad (\text{C.18})$$

$$P_2 = \dots = \bar{\varepsilon}'_\rho \gamma_\rho \left[ \frac{-i(\not{p} - \not{k}') + m_e}{-2p \cdot k'} \right] \varepsilon_\sigma \gamma_\sigma \quad (\text{C.19})$$

We want a polarized amplitude for the photons, therefore we will not use the completeness relation for photons. However, we still must average over initial polarizations of the electron (there are two) and sum over fermion polarizations using [Equation 3.8](#). Taking from [Equation C.15](#):

$$\begin{aligned} |\overline{\mathcal{A}}|^2 &= \frac{1}{2} \sum_{s,s'} |\mathcal{A}|^2 = \frac{1}{2} \sum_{s,s'} e^4 \text{Tr} \left[ (O_1 + O_2) u \bar{u} (P_1 + P_2) u' \bar{u}' \right] = \\ &= \frac{1}{2} \frac{e^4}{2p_4 2p'_4} \text{Tr} \left[ (O_1 + O_2) \left( -i\not{p} + m_e \right) (P_1 + P_2) \left( -i\not{p}' + m_e \right) \right] \end{aligned} \quad (\text{C.20})$$

Calculations from here on out are quite involved. Useful simplifications can be exploited:

- From our choice of the Feynman gauge,  $\partial_\mu A_\mu = 0$ , requiring then  $k \cdot \varepsilon = k' \cdot \varepsilon' = 0$ .
- From the normalization of the polarizations,  $\varepsilon \cdot \varepsilon = \varepsilon' \cdot \varepsilon' = 1$  as well.
- Finally, from fixing  $\varepsilon_4 = \varepsilon'_4 = 0$  from the choice of gauge (nonphysical time component), we realize that for an electron initially at rest:  $p \cdot \varepsilon = p \cdot \varepsilon' = 0$ .

Still, better to delegate the arduous task of evaluating this trace to a computer. The FORM code found in subsection G.1 (on the GitHub repository) - named `Compton.frm` - yields this final amplitude:

$$|\bar{\mathcal{A}}|^2 = \frac{2e^4}{8p_4 p'_4} \left[ \frac{k \cdot k'}{p \cdot k'} - \frac{k \cdot k'}{p \cdot k} + 4(\varepsilon \cdot \varepsilon')^2 \right] \quad (\text{C.21})$$

Note that FORM always treats photon polarizations as real, so we had to fix  $\bar{\varepsilon} = \varepsilon$  (i.e. linear polarizations).

Joining the factor Equation C.12 with Equation C.21, and the  $\delta$  that imposes the conservation of momentum, we just computed the non-trivial part of the  $S$ -matrix for this process:

$$\langle e^- \gamma | S | e^- \gamma \rangle = S_{fi} = \frac{(2\pi)^4 i \bar{\mathcal{A}}}{V^2 \sqrt{2k_4 2k'_4}} \delta(p + k - p' - k') \quad (\text{C.22})$$

When taking the modulus squared:

$$|S_{fi}|^2 = \frac{(2\pi)^8 |\bar{\mathcal{A}}|^2}{V^4 2k_4 2k'_4} |\delta(p + k - p' - k')|^2 \quad (\text{C.23})$$

### C.3 Compton kinematics

To continue with the evaluation of the cross section, we need to assess scalar products of kinematic variables. This being a 2-body scattering, in the center of mass frame momenta are all fixed. However, we will choose the reference frame in which the photon hits on a static electron, so  $p = (\vec{0}, im)$ , and  $k = (\vec{k}, i\omega)$ , with  $\omega = |\vec{k}|$ .

Kinematics is outlined in Figure 50:

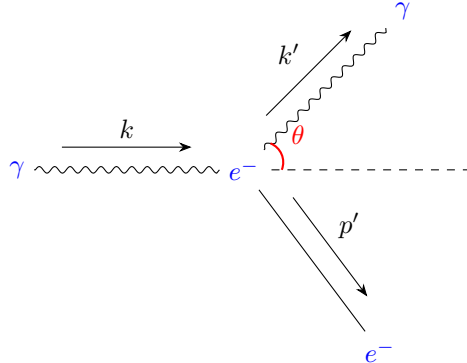


Figure 50: Kinematics of Compton scattering, in the center of mass system.

Call  $\theta$  the angle between incident and scattered photon, then we apply conservation of 4-momentum:

$$\begin{aligned} p' &= p + k - k' && \text{squaring it} \\ m_e^2 &= m_e^2 + 2p \cdot (k - k') - 2k \cdot k' && \Rightarrow -m_e(\omega - \omega') = -\omega\omega'(1 - \cos\theta) \end{aligned}$$

We get the famous *Compton's formula*:

$$\omega' = \omega_c = \frac{m_e\omega}{m_e + \omega(1 - \cos\theta)} \quad (\text{C.24})$$

Also:

$$\begin{aligned} p \cdot k &= -m_e\omega \\ p \cdot k' &= -m_e\omega' \\ k \cdot k' &= -m_e(\omega - \omega') \\ v_{rel} &= \frac{1}{p_4 k_4} \sqrt{(k \cdot p)^2 - k^2 p^2} = \frac{m_e\omega}{m_e\omega} = 1 \end{aligned}$$

where  $v_{rel}$  is the relative velocity between photon and electron (clearly equal to the speed of light), and it will appear in the cross section result.

One final result: the relation between center of mass energy  $s$  and initial photon energy  $\omega$ :

$$s = (p + k)^2 = p^2 + k'^2 + 2p \cdot k = -m_e^2 - 2m_e\omega \quad \Rightarrow \quad \omega = -\frac{s + m_e^2}{2m_e} \quad (\text{C.25})$$

which is going to be useful in [subsection 9.2](#), when graphing the result due to spin 2 correction.

## C.4 Compton cross section

The procedure for the cross section is the same we followed in [subsection A.4](#). Using [Equation A.31](#) and [Equation A.25](#), we can calculate the rate of the process in a specific final state phase space configuration:

$$\Gamma(p', k') = \frac{|S_{fi}|^2}{T} = \frac{1}{T} \frac{(2\pi)^8 |\bar{\mathcal{A}}|^2}{V^4 2k_4 2k'_4} \frac{VT}{(2\pi)^4} \delta(p + k - p' - k') \quad (\text{C.26})$$

which is just a probability density over time component of our spacetime. To get the total rate of the process, we got to integrate over phase space as well. The cross section will simply be the rate divided by the flux of incoming photons (per units of time and surface), which by fixing the number of photons to 1:

$$\sigma(e^- \gamma \rightarrow e^- \gamma) = \frac{\Gamma(e^- \gamma \rightarrow e^- \gamma)}{\# \text{ photons}/ST} = \frac{\Gamma(e^- \gamma \rightarrow e^- \gamma) V}{v_{rel}} \quad (\text{C.27})$$

Using [Equation A.33](#), this leads to:

$$\begin{aligned} \sigma(e^- \gamma \rightarrow e^- \gamma) &= \frac{V}{v_{rel}} \int \frac{V d^3 k'}{(2\pi)^3} \frac{V d^3 p'}{(2\pi)^3} \Gamma(p', k') = \\ &= \frac{V}{v_{rel}} \int \frac{V d^3 k'}{(2\pi)^3} \frac{V d^3 p'}{(2\pi)^3} \left[ \frac{1}{T} \frac{(2\pi)^8}{V^4 2k_4 2k'_4} \frac{VT}{(2\pi)^4} |\bar{\mathcal{A}}|^2 \delta(p + k - p' - k') \right] = \\ &= \frac{1}{4(2\pi)^2 v_{rel}} \int \frac{d^3 k' d^3 p'}{k_4 k'_4} |\bar{\mathcal{A}}|^2 \delta(p + k - p' - k') = \\ &= \frac{1}{16\pi^2} \int \frac{d^3 k'}{k_4 k'_4} |\bar{\mathcal{A}}|^2 \delta(p_4 + k_4 - p'_4 - k'_4) \end{aligned} \quad (\text{C.28})$$

remember that  $v_{rel} = 1$  in units of  $c$ . We have also integrated  $p'$  out, leaving only conservation of energy.

Focusing on the differential cross section, and imposing  $|\vec{k}'| = k'_4$ :

$$\frac{d\sigma}{d\Omega} = \frac{1}{16\pi^2} \int_0^\infty \frac{dk'_4 (k'_4)^2}{k_4 k'_4} \frac{2e^4}{8 p_4 p'_4} \left[ \frac{k \cdot k'}{p \cdot k'} - \frac{k \cdot k'}{p \cdot k} + 4(\epsilon \cdot \epsilon')^2 \right] \delta(p_4 + k_4 - p'_4 - k'_4) \quad (\text{C.29})$$

Let us treat the delta with kinematics, and notice that  $\omega' = \omega_c$  nullifies the argument by conservation of energy:

$$\begin{aligned}
\delta(p_4 + k_4 - p'_4 - k'_4) &= \delta \left( m + \omega - \sqrt{|\vec{p} + \vec{k} - \vec{k}'|^2 + m_e^2} - \omega' \right) = \\
&= \delta \left( m_e + \omega - \sqrt{\omega^2 + (\omega')^2 - 2\omega\omega' \cos\theta + m_e^2} - \omega' \right) = \\
&= \delta(\omega' - \omega_c) \left| \frac{d}{d\omega'} \left[ m_e + \omega - \sqrt{\omega^2 + (\omega')^2 - 2\omega\omega' \cos\theta + m_e^2} - \omega' \right] \right|_{\omega_c}^{-1} = \\
&= \delta(\omega' - \omega_c) \left| \left[ \frac{\omega' - \omega \cos\theta}{\sqrt{\omega^2 + (\omega')^2 - 2\omega\omega' \cos\theta + m_e^2}} + 1 \right] \right|_{\omega_c}^{-1} = \\
&= \delta(\omega' - \omega_c) \left| \left[ \frac{\omega' - \omega \cos\theta}{p'_4} + 1 \right] \right|_{\omega_c}^{-1} = \\
&= \delta(\omega' - \omega_c) \left| \frac{\omega_c - \omega \cos\theta + p'_4}{p'_4} \right|^{-1} = \\
&= \delta(\omega' - \omega_c) \left| \frac{m_e + \omega(1 - \cos\theta)}{p'_4} \right|^{-1} = \\
&= \delta(\omega' - \omega_c) \left| \frac{m_e \omega}{p'_4 \omega_c} \right|^{-1} = \frac{p'_4 \omega_c}{m_e \omega} \delta(\omega' - \omega_c)
\end{aligned} \tag{C.30}$$

So, substituting in [Equation C.29](#), and setting  $k'_4 = \omega'$ ,  $p_4 = m_e$ , we solve a trivial integral and substitute all our scalar products to get the final answer:

$$\begin{aligned}
\frac{d\sigma}{d\Omega} &= \frac{1}{16\pi^2} \int_0^\infty d\omega' \frac{\omega'}{\omega} \frac{p'_4 \omega_c}{m_e \omega} \delta(\omega' - \omega_c) \frac{2e^4}{8p_4 p'_4} \left[ \frac{k \cdot k'}{p \cdot k'} - \frac{k \cdot k'}{p \cdot k} + 4(\varepsilon \cdot \varepsilon')^2 \right] = \\
&= \frac{e^4}{16\pi^2} \frac{1}{4m_e^2} \left( \frac{\omega_c}{\omega} \right)^2 \left[ \frac{k \cdot k'}{p \cdot k'} - \frac{k \cdot k'}{p \cdot k} + 4(\varepsilon \cdot \varepsilon')^2 \right] = \\
&= \frac{\alpha^2}{4m_e^2} \left( \frac{\omega_c}{\omega} \right)^2 \left[ \frac{\omega - \omega_c}{\omega_c} - \frac{\omega - \omega_c}{\omega} + 4(\varepsilon \cdot \varepsilon')^2 \right] = \\
&= \frac{\alpha^2}{4m_e^2} \left( \frac{\omega_c}{\omega} \right)^2 \left[ \frac{\omega}{\omega_c} + \frac{\omega_c}{\omega} - 2 + 4(\varepsilon \cdot \varepsilon')^2 \right]
\end{aligned} \tag{C.31}$$

where  $\alpha = e^2/4\pi$  is the *fine structure constant*. We have obtained the full tree-level polarized cross section for Compton scattering, also called *Klein-Nishina formula*, as reported in Peskin-Schroeder ([\[25\]](#)).

We can also ignore the polarizations of the photons and sum over them as well, to get the unpolarized cross section. In Feynman gauge, with our notation, and setting  $\varepsilon_4 = 0$  (and real polarizations) the sum over photon polarizations is:

$$\sum_\lambda \varepsilon_i(k, \lambda) \varepsilon_j(k, \lambda) = \delta_{ij} - \frac{k_i k_j}{|\vec{k}|^2} \tag{C.32}$$

If we take [Equation C.31](#) and average and sum only over initial polarization  $\varepsilon$ , we get:

$$\frac{1}{2} \varepsilon'_i \varepsilon'_j \sum_\lambda \varepsilon_i(k, \lambda) \varepsilon_j(k, \lambda) = \frac{1}{2} \varepsilon'_i \varepsilon'_j \left( \delta_{ij} - \hat{k}_i \hat{k}_j \right) = \frac{1}{2} - \frac{1}{2} (\varepsilon' \cdot \hat{k})^2 \tag{C.33}$$

into [Equation C.31](#):

$$\frac{d\sigma}{d\Omega} = \frac{\alpha^2}{4m_e^2} \left( \frac{\omega_c}{\omega} \right)^2 \left[ \frac{\omega}{\omega_c} + \frac{\omega_c}{\omega} - 2(\varepsilon' \cdot \hat{k})^2 \right] \tag{C.34}$$

So, cross section is enhanced if  $\varepsilon' \cdot \hat{k} = 0$ . Remembering that  $\varepsilon' \cdot \hat{k}' = 0$  as well, we get that Compton scattering is more likely if outward photon is polarized in the orthogonal direction with respect to the scattering plane  $(\vec{k}, \vec{k}')$ .

Finally, we can also sum with respect to the final photon polarization:

$$\hat{k}_i \hat{k}_j \sum_{\lambda'} \varepsilon_i(k', \lambda') \varepsilon_j(k', \lambda') = \hat{k}_i \hat{k}_j (\delta_{ij} - \hat{k}'_i \hat{k}'_j) = 1 - \cos^2 \theta \quad (\text{C.35})$$

returning also a factor of 2 in the part independent on photon polarizations, as we did not average over final polarization:

$$\frac{d\sigma}{d\Omega} = \frac{\alpha^2}{2m_e^2} \left( \frac{\omega_c}{\omega} \right)^2 \left[ \frac{\omega}{\omega_c} + \frac{\omega_c}{\omega} - 1 + \cos^2 \theta \right] \quad (\text{C.36})$$

which is also reported in [25].

Notice that in the non relativistic limit,  $\omega_c = \omega$ , and it becomes independent of the scattering angle:

$$\frac{d\sigma}{d\Omega} = \frac{\alpha^2}{2m^2} (1 + \cos^2 \theta) \quad (\text{C.37})$$

This means that we can integrate in the solid angle:

$$\begin{aligned} \sigma(e^- \gamma \rightarrow e^- \gamma) &= \frac{\alpha^2}{2m_e^2} \left[ 4\pi + 2\pi \int_{-1}^1 d\cos \theta \cos^2 \theta \right] = \\ &= \frac{\alpha^2}{2m_e^2} \left[ 4\pi + \frac{2}{3} 2\pi \right] \\ &= \frac{8\pi}{3} \frac{\alpha^2}{m_e^2} \end{aligned} \quad (\text{C.38})$$

We just recovered the cross section for Thomson scattering, at low energy, by identifying the "classical electron radius" as  $r = \alpha/m_e$  (also coherent with [25]).

## C.5 Compton squared modulus spin 2 correction

Since we have nothing better to do, let us eliminate the constraint  $g_e^2 = 0$  to only focus on interference terms and evaluate the resulting squared moduli of the spin 2 correction. To see the interference terms  $e^2 g_e g_\gamma / \Lambda^2$ , have a look at [section 9](#).

The evaluation of moduli squared terms ( $g_e^2 g_\gamma^2 / \Lambda^4$ ) still occurs using the FORM code `Compton_Xspin2_xigauge.frm`, linked in the usual repository. There are 72 total terms, reduced to 26 terms once defining  $\Delta\omega = \omega - \omega'$ :

$$H(\omega, \omega'; k, k', \varepsilon, \varepsilon') = \frac{8g_e^2 g_\gamma^2}{\Lambda^4} \frac{m_e^3}{(t + m_X^2)^2} J(\omega, \omega'; k, k', \varepsilon, \varepsilon') \quad (\text{C.39})$$

$$\begin{aligned} J(\omega, \omega'; k, k', \varepsilon, \varepsilon') &= (k \cdot \varepsilon') (k' \cdot \varepsilon) (\varepsilon \cdot \varepsilon') j_1(\omega, \omega') + (k \cdot \varepsilon')^2 (k' \cdot \varepsilon)^2 j_2(\omega, \omega') \\ &\quad + (k \cdot \varepsilon')^2 j_3(\omega, \omega') + (k' \cdot \varepsilon)^2 j_4(\omega, \omega') + (\varepsilon \cdot \varepsilon')^2 j_5(\omega, \omega') \end{aligned} \quad (\text{C.40})$$

$$\begin{aligned} j_1(\omega, \omega') &= -\frac{16}{3} m_e \omega \omega' + \omega \omega' \Delta\omega - \frac{8}{9} m_e \Delta\omega^2 + \frac{4}{9} \frac{m_e^2}{m_X^2} \Delta\omega [\Delta\omega^2 - 6\omega \omega'] \\ &\quad + \frac{32}{9} m_e^2 \Delta\omega + \frac{4}{9} \frac{m_e^3}{m_X^4} \Delta\omega^4 + \frac{32}{9} \frac{m_e^3}{m_X^2} \Delta\omega^2 + \frac{8}{9} \frac{m_e^4}{m_X^4} \Delta\omega^3 \end{aligned}$$

$$j_2(\omega, \omega') = \frac{16}{9} m_e - \frac{4}{9} \Delta\omega + \frac{2}{9} \frac{m_e}{m_X^2} \Delta\omega^2 + \frac{2}{9} \frac{m_e^2}{m_X^4} \Delta\omega^3 + \frac{16}{9} \frac{m_e^2}{m_X^2} \Delta\omega + \frac{4}{9} \frac{m_e^3}{m_X^4} \Delta\omega^2$$

$$j_3(\omega, \omega') = \frac{1}{2} \omega'^2 \Delta\omega \quad j_4(\omega, \omega') = \frac{1}{2} \omega^2 \Delta\omega$$

$$\begin{aligned} j_5(\omega, \omega') &= m_e \omega \omega' (\omega + \omega')^2 - \frac{4}{9} m_e^2 \Delta\omega^3 - \frac{16}{9} m_e^2 \omega \omega' \Delta\omega + \frac{8}{9} \frac{m_e^3}{m_X^2} \Delta\omega^4 - \frac{2}{3} \frac{m_e^3}{m_X^2} \Delta\omega^2 (\omega + \omega')^2 \\ &\quad + \frac{16}{9} m_e^3 \Delta\omega^2 + \frac{2}{9} \frac{m_e^3}{m_X^4} \Delta\omega^5 + \frac{16}{9} \frac{m_e^4}{m_X^2} \Delta\omega^3 + \frac{4}{9} \frac{m_e^5}{m_X^4} \Delta\omega^4 \end{aligned}$$

Notice how:

- The result of the calculation is  $\xi$  independent, even though in the FORM code the Feynman rule has been written in a generic  $\xi$  gauge. This is expected as the amplitude is gauge invariant.
- Now that there is no cross interference term between the standard QED diagrams and our spin 2  $X$  interaction addition, we can check *Ward identities* independently for the squared modulus part

We can basically isolate our spin 2 contribution and study its gauge invariance singularly. To that end, we created the code `Compton_onlyX_xigauge.frm`, in which we only focus on this latter diagram squared. This code isolates the spin 2 diagram and cancels common factors and constants, to help analyze terms under the surface.

In formulas, what we expect is:

$$\left\{ \begin{array}{l} F(p, k, p', k'; \mathbf{k}, \varepsilon') = \underline{F_{\text{QED}}(p, k, p', k'; \mathbf{k}, \varepsilon')} + \underline{F_{\text{interf}}(p, k, p', k'; \mathbf{k}, \varepsilon')} + F_X(p, k, p', k'; \mathbf{k}, \varepsilon') = 0 \\ F(p, k, p', k'; \varepsilon, \mathbf{k}') = \underline{F_{\text{QED}}(p, k, p', k'; \varepsilon, \mathbf{k}')} + \underline{F_{\text{interf}}(p, k, p', k'; \varepsilon, \mathbf{k}')} + F_X(p, k, p', k'; \varepsilon, \mathbf{k}') = 0 \end{array} \right. \quad (\text{C.41})$$

The usual remarks are needed:

- *Gauge invariance comes before kinematics*, meaning we cannot use the kinematics constraints coming from the phase space integration. These constraints are listed in the `Compton_onlyX_xigauge.frm` code and in subsection C.2. Namely,  $p \cdot \varepsilon = p \cdot \varepsilon' = 0$  are all kinematics dependent, and must therefore be commented when carrying out the Ward identities check.

The only valid constraints are  $k \cdot \varepsilon = k' \cdot \varepsilon' = 0$ , as polarizations are always to be chosen transverse to their respective momenta.

- Not only are the ignored constraints kinematics dependent, but they also are *reference frame dependent*. Photon polarizations are not 4-vectors, because under the Lorentz group they transform with a non-linear term (which is why we introduce gauge invariance in the first place), hence scalar products that involve them are not Lorentz invariant.

This is why in a annihilation-like reference frame (electron and positron center of mass frame), it is also true that  $k \cdot \varepsilon' = k' \cdot \varepsilon = 0$  (note that they are indeed in positronium decay, see section 10)<sup>44</sup>.

Fortunately, this check on the `Compton_onlyX_xigauge.frm` is successful, and the new diagram indeed satisfies Ward identities (in a generic  $\xi$  gauge) as written:

$$F_X(p, k, p', k'; \mathbf{k}, \varepsilon') = F_X(p, k, p', k'; \varepsilon, \mathbf{k}') = 0 \quad (\text{C.42})$$

### C.5.1 Polarized cross section squared modulus

This is a complicated amplitude to write. To simplify it, we can take various limits in different energy regimes:

**Low energy or low scattering angle:** This regime is reached when we either impose  $\omega \ll m_e$  (energies below MeV), or we require:

$$\omega(1 - \cos \theta) \ll m_e \quad \Rightarrow \quad \frac{\theta^2}{2} \ll \frac{m_e}{\omega} \quad \Rightarrow \quad \theta \ll \sqrt{\frac{2m_e}{\omega}}$$

meaning this is the forward scattering limit, sometimes called the *Thomson limit*.

In this limit, we get  $\omega' \rightarrow \omega$ , and the Compton scattering becomes elastic for the photon, as it bounces on the electron without losing energy. Then, if in Equation 9.10 we impose  $\Delta\omega \rightarrow 0$ , we get a significant simplification.

Moreover, because  $\omega \ll m_X$  as well, then we can calculate using kinematics from subsection C.3:

$$t + m_X^2 = -2k \cdot k' + m_X^2 = 2m_e \Delta\omega + m_X^2 \approx m_X^2$$

All in all, we get:

$$\begin{aligned} J(\omega; k, k', \varepsilon, \varepsilon') &= (k \cdot \varepsilon')(k' \cdot \varepsilon)(\varepsilon \cdot \varepsilon') \left[ -\frac{16}{3}m_e\omega^2 \right] + (k \cdot \varepsilon')^2(k' \cdot \varepsilon)^2 \left[ \frac{16}{9}m_e \right] + (\varepsilon \cdot \varepsilon')^2 \left[ 4m_e\omega^4 \right] = \\ &= 4m_e \left[ (\varepsilon \cdot \varepsilon')^2 \omega^4 + \frac{4}{3}(k \cdot \varepsilon')(k' \cdot \varepsilon)(\varepsilon \cdot \varepsilon')\omega^2 + \frac{4}{9}(k \cdot \varepsilon')^2(k' \cdot \varepsilon)^2 \right] = \\ &= 4m_e \left[ (\varepsilon \cdot \varepsilon')\omega^2 + \frac{2}{3}(k \cdot \varepsilon')(k' \cdot \varepsilon) \right]^2 \end{aligned} \quad (\text{C.43})$$

<sup>44</sup>All the more reason not to include these frame dependent constraints when checking Ward identities.

Because  $\omega \ll m_e \ll m_X$ , then  $t \ll m_X^2$ , so the total result from the FORM code becomes:

$$H(\omega; k, k', \varepsilon, \varepsilon') = 8e^4 (\varepsilon \cdot \varepsilon')^2 + \frac{32 g_e^2 g_\gamma^2}{\Lambda^4} \frac{m_e^4}{m_X^4} \left[ (\varepsilon \cdot \varepsilon') \omega^2 + \frac{2}{3} (k \cdot \varepsilon') (k' \cdot \varepsilon) \right]^2 \quad (\text{C.44})$$

which gives the following contribution to the differential cross section, from substituting [Equation 9.9](#) into [Equation 9.23](#):

$$\begin{aligned} \frac{d\sigma}{d\Omega} \Big|_{\text{extra}} &= \frac{1}{128\pi^2 m_e^2} \left( \frac{\omega}{\omega'} \right)^2 \left\{ \frac{32 g_e^2 g_\gamma^2}{\Lambda^4} \frac{m_e^4}{m_X^4} \left[ (\varepsilon \cdot \varepsilon') \omega^2 + \frac{2}{3} (k \cdot \varepsilon') (k' \cdot \varepsilon) \right]^2 \right\} = \\ &= \frac{g_e^2 g_\gamma^2}{4\pi^2 \Lambda^4} \frac{m_e^2}{m_X^4} \left[ (\varepsilon \cdot \varepsilon') \omega^2 + \frac{2}{3} (k \cdot \varepsilon') (k' \cdot \varepsilon) \right]^2 \end{aligned} \quad (\text{C.45})$$

**High energy and high scattering angle:** We require  $\omega \gg m_e$ , and moreover  $1 - \cos\theta > 0$  to avoid  $\omega'$  to explode.

In this limit, we get  $\omega' \rightarrow m_e$ , as in the scattering the photon loses most of its energy and it transfers it to the electron, especially if we look at higher and higher angles  $\theta \rightarrow \pi/2$ .

Then, if in [Equation C.39](#) we impose  $\Delta\omega \rightarrow \omega$  and  $\omega' \rightarrow m_e$ , we can ignore subdominant terms starting from  $m_e/\omega$  and  $m_e^2/m_X^2$ . Moreover, suppose  $\omega^2 \gg 2m_X/m_e$  as well, then we can calculate using kinematics from [subsection C.3](#):

$$t + m_X^2 = -2k \cdot k' + m_X^2 = 2m_e \Delta\omega + m_X^2 \approx 2m_e \omega$$

$$\begin{aligned} j_1(\omega) &= \frac{1}{9} m_e \omega^2 - \frac{16}{9} m_e^2 \omega + \frac{4}{9} \frac{m_e^2}{m_X^2} \omega \left[ \omega^2 - 6m_e \omega \right] + \frac{4}{9} \frac{m_e^3}{m_X^4} \omega^4 + \frac{32}{9} \frac{m_e^3}{m_X^2} \omega^2 + \frac{8}{9} \frac{m_e^4}{m_X^4} \omega^3 = \\ &= \omega^3 \left[ \frac{1}{9} \frac{m_e}{\omega} - \frac{16}{9} \frac{m_e^2}{\omega^2} + \frac{4}{9} \frac{m_e^2}{m_X^2} \left( 1 - \frac{6m_e}{\omega} + \frac{m_e \omega}{m_X^2} + \frac{8m_e}{\omega} + \frac{2m_e^2}{m_X^2} \right) \right] \\ &\approx \omega^3 \left[ \frac{1}{9} \frac{m_e}{\omega} + \frac{4}{9} \frac{m_e^2}{m_X^2} \left( 1 + \frac{m_e \omega}{m_X^2} \right) \right] = \frac{\omega^3 m_e}{9} \left[ 1 + \frac{4m_e \omega}{m_X^2} + \frac{4m_e^2 \omega^2}{m_X^4} \right] = \\ &= \frac{m_e \omega^2}{9} \left( 1 + \frac{2m_e \omega}{m_X^2} \right)^2 \\ j_2(\omega) &= \frac{16}{9} m_e - \frac{4}{9} \omega + \frac{2}{9} \frac{m_e}{m_X^2} \omega^2 + \frac{2}{9} \frac{m_e^2}{m_X^4} \omega^3 + \frac{16}{9} \frac{m_e^2}{m_X^2} \omega + \frac{4}{9} \frac{m_e^3}{m_X^4} \omega^2 = \\ &= -\frac{4}{9} \omega \left[ 1 - \frac{4m_e}{\omega} \right] + \frac{2}{9} \frac{m_e}{m_X^2} \omega^2 \left[ 1 + \frac{8m_e}{\omega} + \frac{m_e \omega}{m_X^2} \left( 1 + \frac{2m_e}{\omega} \right) \right] = \\ &\approx -\frac{4}{9} \omega + \frac{2}{9} \frac{m_e}{m_X^2} \omega^2 \left[ 1 + \frac{m_e \omega}{m_X^2} \right] = \\ &= \frac{2}{9} \omega \left[ -2 + \frac{m_e \omega}{m_X^2} + \left( \frac{m_e \omega}{m_X^2} \right)^2 \right] \end{aligned} \quad (\text{C.46})$$

$$j_3(\omega) = \frac{1}{2} m_e^2 \omega \qquad \qquad \qquad j_4(\omega) = \frac{1}{2} \omega^3 \quad (\text{C.47})$$

$$\begin{aligned} j_5(\omega) &= \frac{5}{9} m_e^2 \omega^3 + \frac{2}{9} \frac{m_e^3}{m_X^2} \omega^4 + \frac{2}{9} \frac{m_e^3}{m_X^3} \omega^5 + \frac{16}{9} \frac{m_e^4}{m_X^2} \omega^3 + \frac{4}{9} \frac{m_e^5}{m_X^4} \omega^4 = \\ &= \frac{5}{9} m_e^2 \omega^3 + \frac{2}{9} \frac{m_e^3}{m_X^2} \omega^4 \left[ 1 + \frac{\omega}{m_X} + \frac{8m_e}{\omega} + \frac{2m_e^2}{\omega^2} \right] = \\ &\approx \frac{1}{9} m_e^2 \omega^3 \left[ 5 + \frac{2m_e \omega}{m_X^2} \left( 1 + \frac{\omega}{m_X} \right) \right] \end{aligned} \quad (\text{C.48})$$

we still get different regimes, depending on the values of  $\omega/m_X$  and  $m_e\omega/m_X^2$ . For simplicity, let us only consider the case for which  $\omega \gg m_X$ . Then, the main cutoff energy value is:

$$\frac{m_e\omega}{m_X^2} = 1 \quad \Rightarrow \quad \omega = \frac{m_X^2}{m_e} \approx 600 \text{ MeV}$$

*a priori*, no  $g_i$  is negligible, because every addend goes like  $m_e^2\omega^3$ , if we also consider the scalar products in front of the  $g_i$ . Then, we get two different cases:

- $m_e \ll \omega \ll m_X^2/m_e$ , then:

$$\begin{aligned} J(\omega; k, k', \varepsilon, \varepsilon') &= (k \cdot \varepsilon') (k' \cdot \varepsilon) (\varepsilon \cdot \varepsilon') \frac{m_e\omega^2}{9} - (k \cdot \varepsilon')^2 (k' \cdot \varepsilon)^2 \frac{4}{9}\omega \\ &\quad + (k \cdot \varepsilon')^2 \frac{1}{2}m_e^2\omega + (k' \cdot \varepsilon)^2 \frac{1}{2}\omega^3 + (\varepsilon \cdot \varepsilon')^2 \frac{5}{9}m_e^2\omega^3 \end{aligned} \quad (\text{C.49})$$

- $\omega \gg m_X^2/m_e$ , then:

$$\begin{aligned} J(\omega; k, k', \varepsilon, \varepsilon') &= (k \cdot \varepsilon') (k' \cdot \varepsilon) (\varepsilon \cdot \varepsilon') \frac{4}{9}m_e\omega^2 \left( \frac{m_e\omega}{m_X^2} \right)^2 + (k \cdot \varepsilon')^2 (k' \cdot \varepsilon)^2 \frac{2}{9}\omega \left( \frac{m_e\omega}{m_X^2} \right)^2 \\ &\quad + (k \cdot \varepsilon')^2 \frac{1}{2}m_e^2\omega + (k' \cdot \varepsilon)^2 \frac{1}{2}\omega^3 + (\varepsilon \cdot \varepsilon')^2 \frac{2}{9}m_e^2\omega^3 \frac{m_X}{m_e} \left( \frac{m_e\omega}{m_X^2} \right)^2 \end{aligned} \quad (\text{C.50})$$

and we get the following differential cross section as a result:

$$\begin{aligned} \frac{d\sigma}{d\Omega} &= \frac{1}{128\pi^2 m_e^2} \left( \frac{\omega'}{\omega} \right)^2 \left\{ 2e^4 \left[ \frac{\Delta\omega}{\omega'} - \frac{\Delta\omega}{\omega} + 4(\varepsilon \cdot \varepsilon')^2 \right] + \frac{8g_e^2 g_\gamma^2}{\Lambda^4} \frac{m_e^3}{(t + m_X^2)^2} G(\omega; k, k', \varepsilon, \varepsilon') \right\} = \\ &= \frac{1}{128\pi^2 \omega^2} \left\{ 2e^4 \left[ \frac{\omega}{m_e} - 1 + 4(\varepsilon \cdot \varepsilon')^2 \right] + \frac{2g_e^2 g_\gamma^2}{\Lambda^4} \frac{m_e^3}{(t + m_X^2)^2} G(\omega; k, k', \varepsilon, \varepsilon') \right\} \end{aligned} \quad (\text{C.51})$$

which means, for  $m_e \ll \omega \ll m_X^2/m_e$ :

$$\begin{aligned} \frac{d\sigma}{d\Omega} \Big|_{\text{extra}} &= \frac{1}{64\pi^2} \frac{g_e^2 g_\gamma^2}{\Lambda^4} \frac{m_e^3}{\omega^2 m_X^4} \left[ (k \cdot \varepsilon') (k' \cdot \varepsilon) (\varepsilon \cdot \varepsilon') \frac{m_e\omega^2}{9} - (k \cdot \varepsilon')^2 (k' \cdot \varepsilon)^2 \frac{4}{9}\omega \right. \\ &\quad \left. + (k \cdot \varepsilon')^2 \frac{1}{2}m_e^2\omega + (k' \cdot \varepsilon)^2 \frac{1}{2}\omega^3 + (\varepsilon \cdot \varepsilon')^2 \frac{5}{9}m_e^2\omega^3 \right] \end{aligned} \quad (\text{C.52})$$

and for  $\omega \gg m_X^2/m_e$ :

$$\begin{aligned} \frac{d\sigma}{d\Omega} \Big|_{\text{extra}} &= \frac{1}{64\pi^2} \frac{g_e^2 g_\gamma^2}{\Lambda^4} \frac{m_e}{\omega^4} \left[ (k \cdot \varepsilon') (k' \cdot \varepsilon) (\varepsilon \cdot \varepsilon') \frac{4}{9}m_e\omega^2 \left( \frac{m_e\omega}{m_X^2} \right)^2 + (k \cdot \varepsilon')^2 (k' \cdot \varepsilon)^2 \frac{2}{9}\omega \left( \frac{m_e\omega}{m_X^2} \right)^2 \right. \\ &\quad \left. + \frac{(k \cdot \varepsilon')^2 m_e^2\omega}{2} + \frac{(k' \cdot \varepsilon)^2 \omega^3}{2} + (\varepsilon \cdot \varepsilon')^2 \frac{2}{9}m_e^2\omega^3 \frac{m_X}{m_e} \left( \frac{m_e\omega}{m_X^2} \right)^2 \right] \end{aligned} \quad (\text{C.53})$$

### C.5.2 Unpolarized cross section squared modulus

Now that we have the polarized extra cross section result, we can go ahead and average over initial photon polarizations and sum over all photon polarizations. To do that, we can use the very useful results in [subsection F.7](#). Let us focus on the differential cross section from [Equation 9.9](#):

$$\frac{d\sigma}{d\Omega} \Big|_{\text{extra}} = \frac{1}{2} \frac{1}{128\pi^2 m_e^2} \left( \frac{\omega'}{\omega} \right)^2 \sum_{\lambda, \lambda'} H(\omega, \omega'; k, k', \varepsilon, \varepsilon') = \frac{g_e^2 g_\gamma^2}{32\pi^2 \Lambda^4} \left( \frac{\omega'}{\omega} \right)^2 \frac{m_e}{(t + m_X^2)^2} \sum_{\lambda, \lambda'} J(\omega, \omega'; k, k', \varepsilon, \varepsilon') \quad (\text{C.54})$$

Since we are calculating the general result when graphing our cross section, let us start directly from [Equation C.39](#):

$$\begin{aligned} \sum_{\lambda, \lambda'} H(\omega, \omega'; k, k', \varepsilon, \varepsilon') &= -\omega\omega' \cos\theta (1 - \cos^2\theta) j_1(\omega, \omega') + \omega^2\omega'^2 (1 - \cos^2\theta) j_2(\omega, \omega') \\ &\quad + 2\omega^2 (1 - \cos^2\theta) j_3(\omega, \omega') + 2\omega'^2 (1 - \cos^2\theta) j_4(\omega, \omega') + (1 + \cos^2\theta) j_5(\omega, \omega') \end{aligned} \quad (\text{C.55})$$

and  $j_i(\omega, \omega')$  are the functions listed below [Equation C.39](#).

Now, let us obtain the total result in the three different limits we studied in [subsubsection C.5.1](#). To carry the sums out we can use the results in [Equation C.39](#):

$\omega \ll m_e$ : Remember that  $\omega' \rightarrow \omega$  and  $\Delta\omega \rightarrow 0$ . Starting point is [Equation C.43](#):

$$\begin{aligned} \sum_{\lambda, \lambda'} J(\omega, \omega'; k, k', \varepsilon, \varepsilon') &= 4m_e \left[ \omega^4 \left( 1 + \cos^2 \theta \right) - \frac{4}{3} \omega^3 \omega' \cos \theta \left( 1 - \cos^2 \theta \right) + \frac{4}{9} \omega'^2 \omega^2 \left( 1 - \cos^2 \theta \right)^2 \right] = \\ &\approx 4m_e \omega^4 \left[ 1 + \cos^2 \theta - \frac{4}{3} \cos \theta \left( 1 - \cos^2 \theta \right) + \frac{4}{9} \left( 1 - \cos^2 \theta \right)^2 \right] = \\ &= 4m_e \omega^4 \left[ \frac{13}{9} - \frac{4}{3} \cos \theta + \frac{1}{9} \cos^2 \theta + \frac{4}{3} \cos^3 \theta + \frac{4}{9} \cos^4 \theta \right] \end{aligned} \quad (\text{C.56})$$

then, into [Equation C.54](#), exploiting  $t \ll m_X^2$  as well:

$$\frac{d\sigma}{d\Omega} \Big|_{\text{extra}} = \frac{g_e^2 g_\gamma^2}{8\pi^2 \Lambda^4} \frac{m_e^2 \omega^4}{m_X^4} \left[ \frac{13}{9} - \frac{4}{3} \cos \theta + \frac{1}{9} \cos^2 \theta + \frac{4}{3} \cos^3 \theta + \frac{4}{9} \cos^4 \theta \right] \quad (\text{C.57})$$

which can be integrated in solid angle, using:

$$\int_{-1}^1 d\cos \theta \cos^2 \theta = \frac{2}{3} \quad \int_{-1}^1 d\cos \theta \cos^4 \theta = \frac{2}{5}$$

to obtain:

$$\begin{aligned} \sigma(e^- \gamma \rightarrow e^- \gamma) \Big|_{\text{extra}} &= \frac{g_e^2 g_\gamma^2}{8\pi^2 \Lambda^4} \frac{m_e^2 \omega^4}{m_X^4} 2\pi \left[ \frac{26}{9} + \frac{1}{9} \times \frac{2}{3} + \frac{4}{9} \times \frac{2}{5} \right] = \\ &= \frac{424}{135} \frac{g_e^2 g_\gamma^2}{4\pi \Lambda^4} \frac{m_e^2 \omega^4}{m_X^4} = \\ &\approx \frac{g_e^2 g_\gamma^2}{4\Lambda^4} \frac{m_e^2 \omega^4}{m_X^4} \end{aligned} \quad (\text{C.58})$$

where we remark the peculiar result:  $424/135 = 3.14 \approx \pi$ .

Now, from [Equation 5.43](#) and [Equation 5.44](#), we have:

$$\frac{g_e^2 g_\gamma^2}{\Lambda^4} = 1.1 \times 10^{-22} \text{ MeV}^{-4} \quad (\text{C.59})$$

which means that we get a microscopically small correction to the Compton cross section, in addition to the already very small correction due to interference terms.

$m_e \ll \omega \ll m_X^2/m_e$ : Remember that  $\omega' \rightarrow m_e$  and  $\Delta\omega \rightarrow 0$ , as we are also sending  $\theta \rightarrow \pi/2$ . Starting point is [Equation C.49](#):

$$\begin{aligned} \sum_{\lambda, \lambda'} J(\omega, \omega'; k, k', \varepsilon, \varepsilon') &= -\frac{m_e \omega^2}{9} \omega \omega' \cos \theta \left( 1 - \cos^2 \theta \right) - \frac{4\omega}{9} \omega^2 \omega'^2 \left( 1 - \cos^2 \theta \right)^2 \\ &\quad + 2\omega^2 \left( 1 - \cos^2 \theta \right) \frac{m_e^2 \omega}{2} + 2\omega'^2 \left( 1 - \cos^2 \theta \right) \frac{\omega^3}{2} + \frac{5m_e^2 \omega^3}{9} \left( 1 + \cos^2 \theta \right) = \\ &\approx m_e^2 \omega^3 \left[ \frac{1}{9} \cos \theta \left( 1 - \cos^2 \theta \right) - \frac{4}{9} \left( 1 - \cos^2 \theta \right)^2 + 2 \left( 1 - \cos^2 \theta \right) + \frac{5}{9} \left( 1 + \cos^2 \theta \right) \right] = \\ &= m_e^2 \omega^3 \left[ \frac{19}{9} - \frac{1}{9} \cos \theta - \frac{5}{9} \cos^2 \theta + \frac{1}{9} \cos^3 \theta - \frac{4}{9} \cos^4 \theta \right] = \\ &\approx \frac{19}{9} m_e^2 \omega^3 \end{aligned} \quad (\text{C.60})$$

remember how  $\theta \rightarrow \pi/2$ . For the differential cross section in [Equation C.54](#), exploiting  $t \approx 2m_e\omega \ll m_X^2$ :

$$\begin{aligned} \frac{d\sigma}{d\Omega} \Big|_{\text{extra}} &= \frac{g_e^2 g_\gamma^2}{32\pi^2 \Lambda^4} \frac{m_e}{m_X^4} \left(\frac{\omega'}{\omega}\right)^2 \frac{19}{9} m_e^2 \omega^3 = \\ &= \frac{19}{288\pi^2} \frac{g_e^2 g_\gamma^2}{\Lambda^4} \frac{m_e^5 \omega}{m_X^4} \end{aligned} \quad (\text{C.61})$$

This also means that we cannot integrate over  $d\cos\theta$ . However, we are really only interested in the order of magnitude estimate for Compton scattering correction. Clearly, the dominant term is still the  $19/9$ , so much so that if we decided to integrate the difference would not be very relevant, as long as  $\theta$  remains sufficiently big (in this limit we must avoid forward scattering).

$\omega \gg m_X^2/m_e$ : Remember that  $\omega' \rightarrow m_e$  and  $\Delta\omega \rightarrow \omega$ , as we are also sending  $\theta \rightarrow \pi/2$ . Starting point is [Equation C.50](#):

$$\begin{aligned} \sum_{\lambda, \lambda'} J(\omega, \omega'; k, k', \varepsilon, \varepsilon') &= -\frac{4m_e\omega^2}{9} \left(\frac{m_e\omega}{m_X^2}\right)^2 \omega\omega' \cos\theta (1 - \cos^2\theta) + \frac{2\omega}{9} \omega^2 \omega'^2 \left(\frac{m_e\omega}{m_X^2}\right)^2 (1 - \cos^2\theta)^2 \\ &\quad + (1 - \cos^2\theta) [m_e^2\omega^3 + \omega'^2\omega^3] + \frac{2m_e^2\omega^3}{9} \left(\frac{m_e\omega}{m_X^2}\right)^2 \frac{m_X}{m_e} (1 + \cos^2\theta) = \\ &\approx m_e^2\omega^3 \left(\frac{m_e\omega}{m_X^2}\right)^2 \left[ -\frac{4}{9} \cos\theta (1 - \cos^2\theta) + \frac{2}{9} (1 - \cos^2\theta)^2 + \right. \\ &\quad \left. + 2 \left(\frac{m_X^2}{m_e\omega}\right)^2 + \frac{2}{9} \frac{m_X}{m_e} (1 + \cos^2\theta) \right] = \\ &\approx \frac{2}{9} m_e^2\omega^3 \left(\frac{m_e\omega}{m_X^2}\right)^2 \frac{m_X}{m_e} \end{aligned} \quad (\text{C.62})$$

where we have taken the dominant term, given by the ratio  $m_X/m_e \approx 35$ , and we canceled the cosines as  $\theta \rightarrow \pi/2$ .

Finally, substitute in [Equation C.54](#), exploiting  $t \approx 2m_e\omega \gg m_X^2$ , we get a similar result as [Equation C.61](#):

$$\begin{aligned} \frac{d\sigma}{d\Omega} \Big|_{\text{extra}} &= \frac{g_e^2 g_\gamma^2}{32\pi^2 \Lambda^4} \frac{m_e}{4m_e^2 \omega^2} \left(\frac{\omega'}{\omega}\right)^2 \frac{2}{9} m_e^2 \omega^3 \left(\frac{m_e\omega}{m_X^2}\right)^2 \frac{m_X}{m_e} = \\ &= \frac{1}{576\pi^2} \frac{g_e^2 g_\gamma^2}{\Lambda^4} \frac{m_e^3}{\omega} \left(\frac{m_e\omega}{m_X^2}\right)^2 \frac{m_X}{m_e} \end{aligned} \quad (\text{C.63})$$

Again, it is not possible to integrate properly, as this result is obtained fixing high angles. However, we can estimate the result of an integral around the forward scattering cone. Ignoring angular dependencies, the dominant contribution estimate is very promising:

$$\frac{d\sigma}{d\Omega} \Big|_{\text{extra}} \approx \frac{1}{288\pi} \frac{g_e^2 g_\gamma^2}{\Lambda^4} \frac{m_e^3}{\omega} \left(\frac{m_e\omega}{m_X^2}\right)^2 \frac{m_X}{m_e} \quad (\text{C.64})$$

This is an indefinite growth, that starts already with  $m_e\omega/m_X^2 \gg 1$ , and can increase the tree level correction of the spin 2 massive boson mediation up to any number.

However, unfortunately, this contribution for the cross section does not satisfy Froissart bound. We already discussed bounds in energy in [subsection 4.4](#).

## D $e^+e^- \rightarrow \gamma\gamma$ at tree level

We derive here the well-known amplitudes and cross section for the electrodynamics process  $e^+e^- \rightarrow \gamma\gamma$ , at tree level. This will be useful for the positronium decay we will work with, in [section 10](#).

### D.1 Annihilation Wick contractions

It is better to start by carrying out the necessary Wick contractions that define annihilation of electron and positron into two photons. For this process, initial and final state  $|i\rangle = |e^+e^-\rangle$ ,  $|f\rangle = |\gamma\gamma\rangle$  are different, so there is no forward scattering contribution. The exponential of the  $T$ -ordered product gets expanded into normal ordered interaction terms, which at second order give:

$$S_{fi} = \langle f | S | i \rangle = \langle \gamma\gamma | S | e^+e^- \rangle = \\ = \frac{(-ie)^2}{2!} \int d^4x d^4y \langle \gamma\gamma | :(\bar{\psi}\gamma_\nu A_\nu\psi)_y : :(\bar{\psi}\gamma_\mu A_\mu\psi)_x : | e^+e^- \rangle \quad (\text{D.1})$$

Write down every possible contraction:

$$S_{fi} = \frac{(-ie)^2}{2!} \int d^4x d^4y \langle \gamma\gamma | :(\bar{\psi}^\dagger \gamma_4 \gamma_\nu A_\nu \psi)_y : :(\bar{\psi}^\dagger \gamma_4 \gamma_\mu A_\mu \psi)_x : | e^+e^- \rangle \\ + \frac{(-ie)^2}{2!} \int d^4x d^4y \langle \gamma\gamma | :(\bar{\psi}^\dagger \gamma_4 \gamma_\nu A_\nu \psi)_y : :(\bar{\psi}^\dagger \gamma_4 \gamma_\mu A_\mu \psi)_x : | e^+e^- \rangle \\ + \frac{(-ie)^2}{2!} \int d^4x d^4y \langle \gamma\gamma | :(\bar{\psi}^\dagger \gamma_4 \gamma_\nu A_\nu \psi)_y : :(\bar{\psi}^\dagger \gamma_4 \gamma_\mu A_\mu \psi)_x : | e^+e^- \rangle \\ + \frac{(-ie)^2}{2!} \int d^4x d^4y \langle \gamma\gamma | :(\bar{\psi}^\dagger \gamma_4 \gamma_\nu A_\nu \psi)_y : :(\bar{\psi}^\dagger \gamma_4 \gamma_\mu A_\mu \psi)_x : | e^+e^- \rangle \quad (\text{D.2})$$

Notice how, really, the first row is equivalent to the fourth, and second row are equivalent to the third, the only difference being that we inverted  $x$  and  $y$  interaction points. Thanks to this symmetry, we can eliminate the  $1/2!$  in the expansion, and be left with only two contributions, which will be the two tree level diagrams for annihilation of electron and positron:

$$S_{fi} = (-ie)^2 \int d^4x d^4y \langle \gamma\gamma | :(\bar{\psi}^\dagger \gamma_4 \gamma_\nu A_\nu)_y D_{ab}(x-y) (\gamma_4 \gamma_\mu A_\mu \psi)_x : | e^+e^- \rangle \\ + (-ie)^2 \int d^4x d^4y \langle \gamma\gamma | :(\bar{\psi}^\dagger \gamma_4 \gamma_\mu A_\mu)_x D_{ab}(x-y) (\gamma_4 \gamma_\nu A_\nu \psi)_y : | e^+e^- \rangle \quad (\text{D.3})$$

Two useful remarks:

- The symmetry of  $x$  and  $y$  assignments to the fields is translated into the multiplicity of the final state, counting the possible permutations of the two photons (just because of the specific configuration we have here).
- Compton scattering and annihilation of  $e^+e^-$  are linked by crossing symmetry, so it makes sense that the combinatorial factor in front of each Wick contribution is the same.

This is also what happens in the case of Bhabha scattering and Møller scattering, as we have explored ([subsection B.2](#)).

In [Equation D.3](#) we get a  $t$ -channel and  $u$ -channel diagrams, as in each interaction point a fermion is destroyed and a photon is created (and the two diagrams simply invert the interaction points).

Now that we know what the two contributions actually are, and what factor goes in front, we can use QED Feynman rules to write down the actual amplitudes of the two diagrams, which we will be doing in the next paragraph.

### D.2 Annihilation amplitude

Let us see the contributing diagrams for this process, the *t-channel* and the *u-channel*:

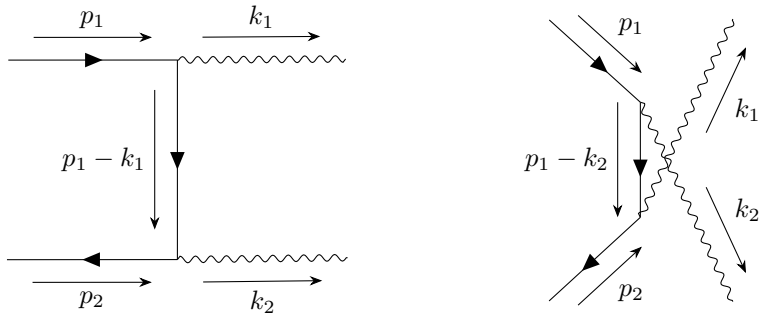


Figure 51: Diagrams corresponding to tree level electron-positron annihilation into 2 photons. On the left, the  $t$ -channel, hereafter denoted with  $\mathcal{A}_1$ . On the right, the  $u$ -channel, hereafter denoted with  $\mathcal{A}_2$ .

Not only is the procedure identical to [Appendix C](#), but the resulting amplitudes will be linked to Compton amplitudes by *crossing symmetry*. In other words, electron-positron annihilation diagrams are exactly equal to Compton scattering diagrams after a "90° rotation", which translates to a different time axis. This results in an exchange of the Mandelstam variable  $s$  to the variable  $t$ , in a change of sign in the positron polarization sums, and in a change  $\varepsilon \rightarrow \bar{\varepsilon}$  for one of the photons:

$$\mathcal{A}_1 = (-ie)^2 \bar{v}(p_2, s_2) \bar{\varepsilon}_\mu(k_2, \lambda_2) \gamma_\mu \left[ \frac{-i(\not{p}_1 - \not{k}_1) + m_e}{(p_1 - k_1)^2 + m_e^2} \right] \bar{\varepsilon}_\nu(k_1, \lambda_1) \gamma_\nu u(p_1, s_1) = -e^2 \bar{v} O_1 u \quad (\text{D.4})$$

$$\mathcal{A}_2 = (-ie)^2 \bar{v}(p_2, s_2) \bar{\varepsilon}_\mu(k_1, \lambda_1) \gamma_\mu \left[ \frac{-i(\not{p}_1 - \not{k}_2) + m_e}{(p_1 - k_2)^2 + m_e^2} \right] \bar{\varepsilon}_\nu(k_2, \lambda_2) \gamma_\nu u(p_1, s_1) = -e^2 \bar{v} O_2 u \quad (\text{D.5})$$

where the usual electrodynamics Feynman rule  $-ie\gamma_\mu$  applies at each vertex,  $m_e$  is the mass of the electron,  $p_1, p_2, k_1, k_2$  are the respective momenta according to [Figure 51](#) and  $s_1, s_2, \lambda_1, \lambda_2$  are the polarizations of fermions and photons, respectively. Here forth, we will call  $u(p_1, s_1) = u$ ,  $v(p_2, s_2) = v$ ,  $\varepsilon_\mu(k_1, \lambda_1) = \varepsilon_{1,\mu}$ ,  $\varepsilon_\mu(k_2, \lambda_2) = \varepsilon_{2,\mu}$ .

Kinematics confirms the  $s - t$  swap:

$$(p_1 - k_1)^2 + m_e^2 = t + m_e^2 = -2p_1 \cdot k_1 \quad (\text{D.6})$$

$$(p_1 - k_2)^2 + m_e^2 = u + m_e^2 = -2p_1 \cdot k_2 \quad (\text{D.7})$$

so that we can write  $O_1, O_2$ :

$$O_1 = -\bar{\varepsilon}_{2,\mu} \gamma_\mu \left[ \frac{-i(\not{p}_1 - \not{k}_1) + m_e}{2p_1 \cdot k_1} \right] \bar{\varepsilon}_{1,\nu} \gamma_\nu \quad (\text{D.8})$$

$$O_2 = -\bar{\varepsilon}_{1,\nu} \gamma_\nu \left[ \frac{-i(\not{p}_1 - \not{k}_2) + m_e}{2p_1 \cdot k_2} \right] \bar{\varepsilon}_{2,\mu} \gamma_\mu \quad (\text{D.9})$$

With the same factor in front of the amplitude:

$$\frac{(2\pi)^4 i}{V^2 \sqrt{2k_{1,4} 2k_{2,4}}} \quad (\text{D.10})$$

The evaluation of  $\mathcal{A}_1^*$  and  $\mathcal{A}_2^*$  proceeds like outlined in [subsection C.2](#), as we just substitute  $u' \rightarrow v$ , and easily get the same trace as in [Equation C.15](#):

$$\mathcal{A}_1^* = -e^2 \bar{u} P_1 v \quad (\text{D.11})$$

$$\mathcal{A}_2^* = -e^2 \bar{u} P_2 v \quad (\text{D.12})$$

$$|\mathcal{A}|^2 = e^4 \text{Tr} [(O_1 + O_2) u \bar{u} (P_1 + P_2) v \bar{v}] \quad (\text{D.13})$$

Now, let us calculate  $P_1$  and  $P_2$ , with the same identities as in [Equation C.17](#):

$$P_1 = \dots = -\bar{\varepsilon}_{1,\sigma} \gamma_\sigma \left[ \frac{-i(\not{p}_1 - \not{k}_1) + m_e}{2p_1 \cdot k_1} \right] \bar{\varepsilon}_{2,\rho} \gamma_\rho \quad (\text{D.14})$$

$$P_2 = \dots = -\bar{\varepsilon}_{2,\rho} \gamma_\rho \left[ \frac{-i(\not{p}_1 - \not{k}_2) + m_e}{2p_1 \cdot k_2} \right] \bar{\varepsilon}_{1,\sigma} \gamma_\sigma \quad (\text{D.15})$$

We want a polarized amplitude for the photons, so we must only average over initial polarizations of  $e^+$  and  $e^-$  and sum over them:

$$\begin{aligned} |\bar{\mathcal{A}}|^2 &= \frac{1}{4} \sum_{s_1, s_2} e^4 \text{Tr} [(O_1 + O_2) u\bar{u} (P_1 + P_2) v\bar{v}] = \\ &= \frac{1}{4} \frac{e^4}{2p_{1,4} 2p_{2,4}} \text{Tr} \left[ (O_1 + O_2) (-i\cancel{p}_1 + m_e) (P_1 + P_2) (-i\cancel{p}_2 - m_e) \right] \end{aligned} \quad (\text{D.16})$$

Note that now we get a minus sign for the positron. Exploiting the usual simplifications:  $k_1 \cdot \varepsilon_1 = k_2 \cdot \varepsilon_2 = p_1 \cdot \varepsilon_1 = p_1 \cdot \varepsilon_2 = 0$ , and  $\varepsilon_1 \cdot \varepsilon_1 = \varepsilon_1 \cdot \varepsilon_2 = 1$ , but also  $k_1 \cdot \varepsilon_2 = k_2 \cdot \varepsilon_1 = 0$  because the photons are back to back, and in the  $\varepsilon_4 = 0$  gauge only the spatial part decides the scalar product, so if  $k_1$  is perpendicular to  $\varepsilon_1$ , so is  $k_2$ .

Using the FORM code found in [subsection G.1](#) (on the GitHub repository) named `Annihilation.frm`, we get the final amplitude:

$$|\bar{\mathcal{A}}|^2 = \frac{2e^4}{16p_{1,4} p_{2,4}} \left[ \frac{k_1 \cdot k_2}{p_1 \cdot k_2} + \frac{k_1 \cdot k_2}{p_1 \cdot k_2} - 4(\varepsilon_1 \cdot \varepsilon_2)^2 \right] \quad (\text{D.17})$$

Again, FORM treats photon polarizations as real, so we can only have linear polarizations. Overall, we get a very similar structure to [Equation C.21](#). Finally, the modulus squared of the non-trivial part of the  $S$ -matrix:

$$|S_{fi}|^2 = \frac{(2\pi)^8 |\bar{\mathcal{A}}|^2}{V^4 2k_{1,4} 2k_{2,4}} |\delta(p_1 + p_2 - k_1 - k_2)|^2 \quad (\text{D.18})$$

### D.3 Annihilation kinematics

Kinematics of the annihilation process needs to be evaluated exclusively in the center of mass of the two fermions, where it is back-to-back. If we do that, we can set the 4-momenta:

$$p_1 = (\vec{p}, iE) \quad p_2 = (-\vec{p}, iE) \quad k_1 = (\vec{k}, i\omega) \quad k_2 = (-\vec{k}, i\omega)$$

with  $E = \omega = |\vec{k}|$  by energy conservation. Call  $\theta$  the scattering angle between the  $e^+e^-$  pair and the two photons in the center of mass, and  $p = |\vec{p}|$ .  $\theta$  and  $\phi$  are the only two parameters not fixed. However, because QED is parity invariant, every QED process should be intrinsically independent on the polar angle  $\phi$ , as each scattering plane selected by a specific  $\phi$  value is equally likely. So, in reality, the only free parameter in the final state is  $\theta$ .

Kinematics is outlined in [Figure 52](#):

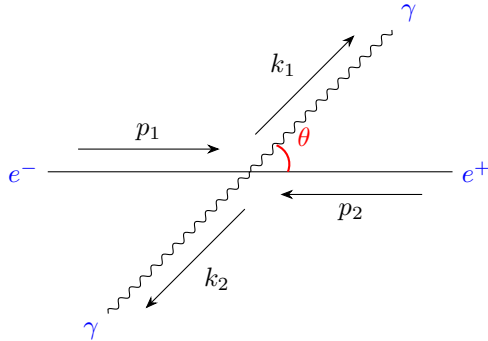


Figure 52: Kinematics of annihilation into two photons, in the center of mass system.

Calculate the scalar products:

$$\begin{aligned} p_1 \cdot k_1 &= -\vec{p} \cdot \vec{k} - E^2 = -E(E + p \cos \theta) \\ p_1 \cdot k_2 &= \vec{p} \cdot \vec{k} - E^2 = -E(E - p \cos \theta) \\ k_1 \cdot k_2 &= -|\vec{k}|^2 - \omega^2 = -2E^2 \\ s &= (p_1 + p_2)^2 = -4E^2 \end{aligned}$$

and it is also useful to have:

$$\begin{aligned} v_{rel} &= \frac{1}{p_{1,4} p_{2,4}} \sqrt{(p_1 \cdot p_2)^2 - p_1^2 p_2^2} = \frac{1}{E^2} \sqrt{(-p^2 - E^2)^2 - m_e^4} = \\ &= \frac{1}{E^2} \sqrt{(m_e^2 - 2E^2)^2 - m_e^4} = \frac{2E^2}{E^2} \sqrt{1 - \frac{m_e^2}{E^2}} = \frac{2p}{E} \end{aligned} \quad (\text{D.19})$$

where  $v_{rel}$  is the "classical" relative velocity between electron and positron (clearly does not satisfy relativistic sum of velocities), and it will appear in the cross section result.

## D.4 Annihilation cross section

Using [Equation A.31](#) and [Equation D.18](#), we can calculate the rate of the process in a specific final state phase space configuration:

$$\Gamma(k_1, k_2) = \frac{|S_{fi}|^2}{T} = \frac{1}{T} \frac{(2\pi)^8 |\bar{\mathcal{A}}|^2}{V^4 2k_{1,4} 2k_{2,4}} \frac{VT}{(2\pi)^4} \delta(p_1 + p_2 - k_1 - k_2) \quad (\text{D.20})$$

This leads to our final cross section, obtained using [Equation A.34](#):

$$\begin{aligned} \sigma(e^+e^- \rightarrow \gamma\gamma) &= \frac{V}{v_{rel}} \int \frac{V d^3 k_2}{(2\pi)^3} \frac{V d^3 k_1}{(2\pi)^3} \Gamma(k_1, k_2) = \\ &= \frac{V}{v_{rel}} \int \frac{V d^3 k_2}{(2\pi)^3} \frac{V d^3 k_1}{(2\pi)^3} \left[ \frac{1}{T} \frac{(2\pi)^8 |\bar{\mathcal{A}}|^2}{V^4 2k_{1,4} 2k_{2,4}} \frac{VT}{(2\pi)^4} \delta(p_1 + p_2 - k_1 - k_2) \right] = \\ &= \frac{1}{4(2\pi)^2 v_{rel}} \int \frac{d^3 k_2 d^3 k_1}{k_{1,4} k_{2,4}} |\bar{\mathcal{A}}|^2 \delta(p_1 + p_2 - k_1 - k_2) = \\ &= \frac{E}{32\pi^2 p} \int \frac{d^3 k_2}{k_{1,4} k_{2,4}} |\bar{\mathcal{A}}|^2 \delta(p_{1,4} + p_{2,4} - k_{1,4} - k_{2,4}) \end{aligned} \quad (\text{D.21})$$

We have substituted  $v_{rel} = 2p/E$  from [subsection D.3](#), and integrated  $k_1$  out, leaving only the conservation of energy to deal with. If we set  $|\vec{k}_2| = k_{2,4}$ , then by taking only the differential cross section:

$$\frac{d\sigma}{d\Omega} = \frac{E}{32\pi^2 p} \int_0^\infty \frac{dk_{2,4}}{k_{1,4} k_{2,4}} \frac{(k_{2,4})^2}{16 p_{1,4} p_{2,4}} \left[ \frac{k_1 \cdot k_2}{p_1 \cdot k_1} + \frac{k_1 \cdot k_2}{p_1 \cdot k_2} - 4(\varepsilon_1 \cdot \varepsilon_2)^2 \right] \delta(p_{1,4} + p_{2,4} - k_{1,4} - k_{2,4}) \quad (\text{D.22})$$

The treatment of the Dirac's delta is much easier now. Fixing  $E^2 = p^2 + m^2$ :

$$\begin{aligned} \delta(p_{1,4} + p_{2,4} - k_{1,4} - k_{2,4}) &= \delta\left(2E - \sqrt{|\vec{p}_1 + \vec{p}_2 - \vec{k}_2|^2} - k_{2,4}\right) = \\ &= \delta\left(2E - |\vec{k}_2| - k_{2,4}\right) = \\ &= \delta(2E - 2k_{2,4}) = \frac{1}{2} \delta(E - k_{2,4}) \end{aligned} \quad (\text{D.23})$$

which immediately solves the phase space integral. By also substituting the scalar products into the squared amplitude:

$$\begin{aligned} \frac{d\sigma}{d\Omega} &= \frac{E}{32\pi^2 p} \int_0^\infty dk_{2,4} \frac{k_{2,4}}{k_{1,4}} \frac{1}{2} \delta(E - k_{2,4}) \frac{2e^4}{16 p_{1,4} p_{2,4}} \left[ \frac{k_1 \cdot k_2}{p_1 \cdot k_1} + \frac{k_1 \cdot k_2}{p_1 \cdot k_2} - 4(\varepsilon_1 \cdot \varepsilon_2)^2 \right] = \\ &= \frac{e^4}{16\pi^2} \frac{E}{32pE^2} \left[ \frac{k_1 \cdot k_2}{p_1 \cdot k_1} + \frac{k_1 \cdot k_2}{p_1 \cdot k_2} - 4(\varepsilon_1 \cdot \varepsilon_2)^2 \right] = \\ &= \frac{\alpha^2}{32pE} \left[ \frac{2E}{E + p \cos \theta} + \frac{2E}{E - p \cos \theta} - 4(\varepsilon_1 \cdot \varepsilon_2)^2 \right] = \\ &= \frac{\alpha^2}{16pE} \left[ \frac{2E^2}{E^2 - p^2 \cos^2 \theta} \cancel{+1} \cancel{-1} - 2(\varepsilon_1 \cdot \varepsilon_2)^2 \right] = \\ &= \frac{\alpha^2}{16pE} \left[ \frac{E^2 + p^2 \cos^2 \theta}{E^2 - p^2 \cos^2 \theta} + 1 - 2(\varepsilon_1 \cdot \varepsilon_2)^2 \right] = \\ &= \frac{\alpha^2}{16pE} \left[ \frac{1 + \beta^2 \cos^2 \theta}{1 - \beta^2 \cos^2 \theta} + 1 - 2(\varepsilon_1 \cdot \varepsilon_2)^2 \right] \end{aligned} \quad (\text{D.24})$$

This is the final polarized differential cross section for the process  $e^-e^+ \rightarrow \gamma\gamma$ .

Like we did in [subsection C.4](#), we can directly sum over final photon polarizations to get the final unpolarized

cross section:

$$\begin{aligned}
\frac{d\sigma}{d\Omega} &= \sum_{\lambda_1, \lambda_2} \frac{\alpha^2}{16pE} \left[ \frac{1 + \beta^2 \cos^2 \theta}{1 - \beta^2 \cos^2 \theta} + 1 - 2(\varepsilon_1 \cdot \varepsilon_2)^2 \right] = \\
&= \frac{4\alpha^2}{16pE} \left[ \frac{1 + \beta^2 \cos^2 \theta}{1 - \beta^2 \cos^2 \theta} + 1 \right] - \frac{2\alpha^2}{16pE} \sum_{\lambda_1} \varepsilon_i(k_1, \lambda_1) \varepsilon_j(k_1, \lambda_1) \sum_{\lambda_2} \varepsilon_i(k_2, \lambda_2) \varepsilon_j(k_2, \lambda_2) = \\
&= \frac{\alpha^2}{4pE} \left[ \frac{1 + \beta^2 \cos^2 \theta}{1 - \beta^2 \cos^2 \theta} + 1 \right] - \frac{\alpha^2}{8pE} (\delta_{ij} - \hat{k}_{1,i}\hat{k}_{1,j}) (\delta_{ij} - \hat{k}_{2,i}\hat{k}_{2,j}) = \\
&= \frac{\alpha^2}{4pE} \left[ \frac{1 + \beta^2 \cos^2 \theta}{1 - \beta^2 \cos^2 \theta} + 1 - \frac{3}{2} + \frac{|\hat{k}_1|^2}{2} + \frac{|\hat{k}_2|^2}{2} - \frac{1}{2} (\hat{k}_1 \cdot \hat{k}_2)^2 \right] = \\
&= \frac{\alpha^2}{4pE} \left[ \frac{1 + \beta^2 \cos^2 \theta}{1 - \beta^2 \cos^2 \theta} + 1 - \frac{3}{2} + \frac{1}{2} + \frac{1}{2} - \frac{1}{2} \right] = \\
&= \frac{\alpha^2}{4pE} \left[ \frac{1 + \beta^2 \cos^2 \theta}{1 - \beta^2 \cos^2 \theta} \right]
\end{aligned} \tag{D.25}$$

where we used the fact that there really are 3 components and that since the process is back-to-back in the center of mass,  $\hat{k}_1 \cdot \hat{k}_2 = -1$ .

We can also integrate in the solid angle. A useful indefinite integral we can calculate is:

$$\begin{aligned}
\int dx \frac{1+x^2}{1-x^2} &= \int dx \left[ \frac{-1+x^2}{1-x^2} + \frac{2}{1-x^2} \right] = \\
&= -x + 2 \int dx \frac{2}{(1-x)(1+x)} = \\
&= -x + 2 \int dx \left[ \frac{1}{2(1-x)} + \frac{1}{2(1+x)} \right] = \\
&= -x + \int dx \left[ \frac{1}{x+1} - \frac{1}{x-1} \right] = \\
&= -x + \log|x+1| - \log|x-1| = \\
&= -x + \log \left| \frac{1+x}{1-x} \right|
\end{aligned} \tag{D.26}$$

Which helps here as:

$$\begin{aligned}
\sigma(e^+e^- \rightarrow \gamma\gamma) &= \frac{\alpha^2}{4pE} \int_{-1}^1 d\cos\theta \int_0^{2\pi} d\phi \frac{1 + \beta^2 \cos^2 \theta}{1 - \beta^2 \cos^2 \theta} = \\
&= \frac{\pi\alpha^2}{2pE} \int_{-1}^1 d\cos\theta \frac{1 + \beta^2 \cos^2 \theta}{1 - \beta^2 \cos^2 \theta}
\end{aligned}$$

by defining  $x = \beta \cos \theta$ , then we can exploit [Equation D.26](#):

$$\begin{aligned}
\sigma(e^+e^- \rightarrow \gamma\gamma) &= \frac{\pi\alpha^2}{2pE} \frac{1}{\beta} \int_{-\beta}^{\beta} dx \frac{1+x^2}{1-x^2} = \\
&= \frac{\pi\alpha^2}{2pE} \frac{1}{\beta} \left[ -x + \log \left| \frac{1+x}{1-x} \right| \right]_{-\beta}^{\beta} = \\
&= \frac{\pi\alpha^2}{2pE} \frac{1}{\beta} \left[ -2\beta + \log \left( \frac{1+\beta}{1-\beta} \right) - \log \left( \frac{1-\beta}{1+\beta} \right) \right] = \\
&= \frac{\pi\alpha^2}{pE} \left[ -1 + \frac{1}{\beta} \log \left( \frac{1+\beta}{1-\beta} \right) \right]
\end{aligned} \tag{D.27}$$

There are two interesting limits to this cross section:

- **Ultra-relativistic limit:**

If we take  $E \gg m_e$ , and  $\beta \rightarrow 1$  (so  $p \rightarrow E$ ), then remembering that  $s = -4E^2$ , we get:

$$\frac{d\sigma}{d\Omega} = \frac{\alpha^2}{|s|} \frac{1 + \cos^2 \theta}{1 - \cos^2 \theta} \Rightarrow \frac{d\sigma}{d\cos \theta} = \frac{2\pi\alpha^2}{|s|} \frac{1 + \cos^2 \theta}{1 - \cos^2 \theta} \quad (\text{D.28})$$

which is in the form popular for high energy collisions. Note that in reality, the total cross section in the perfect ultra relativistic limit would diverge, as seen in [Equation D.27](#) when  $\beta \rightarrow 1$ .

- **Non relativistic limit:**

If, instead, we take  $E \rightarrow m_e$  and  $\beta \rightarrow 0$ , then we recover classical momentum  $p = m_e v$ , meaning that:

$$\frac{d\sigma}{d\Omega} = \frac{\alpha^2}{4m_e^2 v} = \frac{\alpha^2}{4m_e^2 \beta} \quad (\text{D.29})$$

and it can be integrated in the solid angle:

$$\sigma(e^+e^- \rightarrow \gamma\gamma) = \frac{\pi\alpha^2}{m_e^2 \beta} \quad (\text{D.30})$$

which is the result reported by Landau<sup>45</sup> ([\[27\]](#)).

The same result can be derived from [Equation D.27](#) by expanding  $\beta \rightarrow 0$ , since:

$$-1 + \frac{1}{\beta} \log \left( \frac{1+\beta}{1-\beta} \right) \approx -1 + \frac{1}{\beta} \log (1+2\beta) \approx -1 + 2 = 1 \quad (\text{D.31})$$

## D.5 Annihilation squared modulus spin 2 correction

Since we have nothing better to do, let us eliminate the constraint  $g_e^2 = 0$  to only focus on interference terms and evaluate the resulting squared moduli of the spin 2 correction. To see the interference terms  $e^2 g_e g_\gamma / \Lambda^2$ , have a look at [section 10](#).

The evaluation of moduli squared terms ( $g_e^2 g_\gamma^2 / \Lambda^4$ ) still occurs using the FORM code `Annihilation_Xspin2_xigauge.frm`, linked in the usual repository. There are 10 total terms left:

$$H(E, p, \theta; \varepsilon_1, \varepsilon_2) = \frac{32g_e^2 g_\gamma^2}{\Lambda^4} \frac{(\varepsilon_1 \cdot \varepsilon_2)^2 E^4}{(s + m_X^2)^2} J(E, p, \theta) \quad (\text{D.32})$$

$$\begin{aligned} J(E, p, \theta) &= -p^4 \cos^4 \theta + E^2 p^2 \cos^2 \theta + \frac{16}{9} \frac{m_e^2 E^6}{m_X^4} + \frac{8}{3} \frac{m_e^2 E^2 p^2}{m_X^2} \cos^2 \theta - \frac{32}{9} \frac{m_e^2 E^4}{m_X^2} \\ &\quad - \frac{8}{3} m_e^2 p^2 \cos^2 \theta + \frac{16}{9} m_e^2 E^2 - \frac{16}{9} \frac{m_e^4 E^4}{m_X^4} + \frac{32}{9} \frac{m_e^4 E^2}{m_X^2} - \frac{16}{9} m_e^4 = \\ &= \frac{16}{9} m_e^2 \left( E^2 - m_e^2 \right) + \frac{16}{9} \frac{m_e^2}{m_X^4} E^4 \left( E^2 - m_e^2 \right) + p^2 \cos^2 \theta \left( E^2 - \frac{8}{3} m_e^2 \right) \\ &\quad - p^4 \cos^4 \theta + \frac{8}{3} \frac{m_e^2}{m_X^2} E^2 \left[ p^2 \cos^2 \theta - \frac{4}{3} \left( E^2 - m_e^2 \right) \right] = \\ &= p^2 m_e^2 \left[ \frac{16}{9} + \cos^2 \theta \left( \gamma^2 - \frac{8}{3} \right) - \beta^2 \gamma^2 \cos^4 \theta + \frac{8}{3} \frac{E^2}{m_X^2} \left( \cos^2 \theta - \frac{4}{3} \right) + \frac{16}{9} \frac{E^4}{m_X^4} \right] \quad (\text{D.33}) \end{aligned}$$

where we used  $p/m_e = \beta\gamma$  and  $E/m_e = \gamma$ , with regards to the velocities of the electrons in the center of mass frame. Henceforth, we will write  $J(E, p, \theta) = p^2 m_e^2 j(E, \theta)$ , where  $j$  is the squared parenthesis in [Equation D.33](#):

$$\begin{aligned} j(E, \theta) &= \frac{16}{9} + \cos^2 \theta \left( \gamma^2 - \frac{8}{3} \right) - \beta^2 \gamma^2 \cos^4 \theta + \frac{8}{3} \frac{E^2}{m_X^2} \left( \cos^2 \theta - \frac{4}{3} \right) + \frac{16}{9} \frac{E^4}{m_X^4} \\ &= \frac{16}{9} \left[ \frac{E^2}{m_X^2} - 1 \right]^2 + \cos^2 \theta \left[ \gamma^2 \left( 1 - \beta^2 \cos^2 \theta \right) + \frac{8}{3} \left( \frac{E^2}{m_X^2} - 1 \right) \right] \quad (\text{D.34}) \end{aligned}$$

<sup>45</sup>Landau-Lifshitz, *Volume 4, Quantum Electrodynamics*, chapter X (page 372). The units used are such that  $\alpha = e^2$ , without the factor  $4\pi$ , reabsorbed in the normalization of the photon field.

which tells us that  $j(m_X, \pi/2) \neq 0$ .

Notice how:

- Again, there is no cross interference term now, as we are ignoring the interference terms. The spin 2 contribution modulus squared can therefore be evaluated individually (summing cross sections, not amplitudes).
- The result of the calculation is  $\xi$  independent, even though in the FORM code the Feynman rule has been written in a generic  $\xi$  gauge. This is expected as the amplitude is gauge invariant.

If we continue with cross section calculations, we exploit [Equation D.24](#) to add our correction:

$$\frac{d\sigma}{d\Omega} \Big|_{\text{extra}} = \frac{g_e^2 g_\gamma^2}{32\pi^2 p E \Lambda^4} \frac{(\varepsilon_1 \cdot \varepsilon_2)^2}{(s + m_X^2)^2} E^4 p^2 m_e^2 j(E, \theta) \quad (\text{D.35})$$

Since our actual goal is to calculate corrections to positronium decay rate, and in literature there is not distinction between different photon polarizations, we can sum over them. The terms that are polarization independent get a factor of 4 (2 polarizations per photon), whilst the other dependence is  $(\varepsilon_1 \cdot \varepsilon_2)^2$ , which we can easily sum. The sum has been carried out in [Equation 10.15](#):

$$\sum_{\lambda_1, \lambda_2} (\varepsilon_1 \cdot \varepsilon_2)^2 = \dots = 2$$

where  $\hat{k}_1 \cdot \hat{k}_2 = -1$ , as photons are back-to-back. The final unpolarized differential cross section is:

$$\frac{d\sigma}{d\Omega} \Big|_{\text{extra}} = \frac{g_e^2 g_\gamma^2}{16\pi^2 \Lambda^4} \frac{E^3 p m_e^2}{(s + m_X^2)^2} j(E, \theta) \quad (\text{D.36})$$

which adds directly a correction term to [Equation D.25](#).

Finally, we are interested in the actual total cross section, so we ought to integrate in the solid angle. In [subsection D.4](#), we carry out the calculation for the original QED contribution. Here, we calculate the integral regarding the spin 2 contribution. In total:

$$\begin{aligned} \sigma(e^+e^- \rightarrow \gamma\gamma) \Big|_{\text{extra}} &= \frac{g_e^2 g_\gamma^2}{16\pi^2 \Lambda^4} \frac{E^3 p m_e^2}{(s + m_X^2)^2} \int_{-1}^1 d\cos\theta \int_0^{2\pi} d\phi j(E, \theta) = \\ &= \frac{g_e^2 g_\gamma^2}{8\pi \Lambda^4} \frac{E^3 p m_e^2}{(s + m_X^2)^2} \int_{-1}^1 d\cos\theta j(E, \theta) \end{aligned} \quad (\text{D.37})$$

where we make use of [Equation 9.37](#) to obtain:

$$\int_{-1}^1 d\cos\theta j(E, \theta) = \frac{32}{9} + \frac{2}{3} \left( \gamma^2 - \frac{8}{3} \right) - \frac{2}{5} \beta^2 \gamma^2 - \frac{16}{3} \frac{E^2}{m_X^2} + \frac{32}{9} \frac{E^4}{m_X^4} \quad (\text{D.38})$$

which yields our final cross section addition:

$$\sigma(e^+e^- \rightarrow \gamma\gamma) \Big|_{\text{extra}} = \frac{g_e^2 g_\gamma^2}{8\pi \Lambda^4} \frac{E^3 p m_e^2}{(s + m_X^2)^2} \left[ \frac{32}{9} + \frac{2}{3} \left( \gamma^2 - \frac{8}{3} \right) - \frac{2}{5} \beta^2 \gamma^2 - \frac{16}{3} \frac{E^2}{m_X^2} + \frac{32}{9} \frac{E^4}{m_X^4} \right] \quad (\text{D.39})$$

Again, given that this is the first time someone performs this specific calculation, there is no reference we can quote for the result. However, we can still check *Ward identities*, like we did at the end of [section 9](#).

This result is comprised of the contribution of three diagrams, without interference terms between the QED diagrams and the spin 2 correction. Because the first two diagrams' gauge invariance is accounted for (you can check that using the code `Annihilation.frm` on the GitHub repository), we isolate the spin 2 contribution and study its gauge invariance singularly. To that end, we wrote the code `Annihilation_onlyX_xigauge.frm`, in which we only focus on this latter diagram squared. This code isolates the spin 2 diagram and cancels common factors and constants.

In formulas, what we expect is:

$$\left\{ \begin{array}{l} F(p_1, p_2, k_1, k_2; \mathbf{k}_1, \varepsilon_2) = \overline{F_{\text{QED}}(p_1, p_2, k_1, k_2; \mathbf{k}_1, \varepsilon_2)} + \overline{F_{\text{interf}}(p_1, p_2, k_1, k_2; \mathbf{k}_1, \varepsilon_2)} + F_X(p_1, p_2, k_1, k_2; \mathbf{k}_1, \varepsilon_2) = 0 \\ F(p_1, p_2, k_1, k_2; \varepsilon_1, \mathbf{k}_2) = \overline{F_{\text{QED}}(p_1, p_2, k_1, k_2; \varepsilon_1, \mathbf{k}_2)} + \overline{F_{\text{interf}}(p_1, p_2, k_1, k_2; \varepsilon_1, \mathbf{k}_2)} + F_X(p_1, p_2, k_1, k_2; \varepsilon_1, \mathbf{k}_2) = 0 \end{array} \right. \quad (\text{D.40})$$

A couple of remarks are needed:

- *Gauge invariance comes before kinematics*, meaning we cannot use the kinematics constraints coming from the phase space integration. These constraints are listed in the `Annihilation_onlyX_xigauge.frm` code and in subsection D.2. Namely,  $p_1 \cdot \varepsilon_1 = p_1 \cdot \varepsilon_2 = k_1 \cdot \varepsilon_2 = k_2 \cdot \varepsilon_1 = 0$  are all kinematics dependent, and must therefore be commented when carrying out the Ward identities check.

The only valid constraints are  $k_1 \cdot \varepsilon_1 = k_2 \cdot \varepsilon_2 = 0$ , as polarizations are always to be chosen transverse to their respective momenta.

- Not only are the ignored constraints kinematics dependent, but they also are *reference frame dependent*, as we already discussed in section 9 how these scalar products are actually not Lorentz invariant.  
In a Compton scattering-like reference frame (electron at rest and positron moving), it is no longer true that  $k_1 \cdot \varepsilon_2 = k_2 \cdot \varepsilon_1 = 0$  (indeed, these are not constraints in Compton scattering, see section 9)<sup>46</sup>.

Fortunately, this check on the `Annihilation_onlyX_xigauge.frm` is successful, and the new diagram indeed satisfies Ward identities (in a generic  $\xi$  gauge) as written:

$$F_X(p_1, p_2, k_1, k_2; k_1, \varepsilon_2) = F_X(p_1, p_2, k_1, k_2; \varepsilon_1, k_2) = 0 \quad (\text{D.41})$$

We can take the two relevant limits.

**Non-relativistic limit:** We send  $4m_e^2/s \rightarrow -1$ , as  $E \rightarrow m_e$  and  $p \rightarrow 0$ . Then,  $\beta \rightarrow 0$  and  $\gamma \rightarrow 1$ . Then:

$$\begin{aligned} j(E, \theta) &= \frac{16}{9} \left[ \frac{m_e^2}{m_X^2} - 1 \right]^2 + \cos^2 \theta \left[ 1 + \frac{8}{3} \left( \frac{m_e^2}{m_X^2} - 1 \right) \right] = \\ &= \frac{16}{9} \left[ \frac{m_e^2}{m_X^2} - 1 \right]^2 + \cos^2 \theta \left[ -\frac{5}{3} + \frac{8}{3} \frac{m_e^2}{m_X^2} \right] \end{aligned} \quad (\text{D.42})$$

$$\begin{aligned} \left. \frac{d\sigma}{d\Omega} \right|_{\text{extra}} &= \frac{g_e^2 g_\gamma^2}{16\pi^2 \Lambda^4} \frac{m_e^6 \beta}{m_X^4} \left\{ \frac{16}{9} \left[ \frac{m_e^2}{m_X^2} - 1 \right]^2 + \cos^2 \theta \left[ -\frac{5}{3} + \frac{8}{3} \frac{m_e^2}{m_X^2} \right] \right\} = \\ &\approx \frac{g_e^2 g_\gamma^2}{16\pi^2 \Lambda^4} \frac{m_e^6 \beta}{m_X^4} \left( \frac{16}{9} - \frac{5}{3} \cos^2 \theta \right) \end{aligned} \quad (\text{D.43})$$

It is always a positive correction. It makes sense, as this is a modulus squared. Numerically, it is an extremely small correction, just like in Compton effect, as  $p \rightarrow 0$ , in addition to the already small correction due to interference terms. This result is still  $\theta$  dependent, so to get total cross section integration is still needed.

**Ultra-relativistic limit:** If we send  $m_e^2/s \rightarrow 0$ , and  $m_X^2/s \rightarrow 0$ , with  $s \rightarrow -4E^2$ . Then it is immediate to see that  $j(E, \theta)$  has a dominant  $E^4$  term:

$$\left. \frac{d\sigma}{d\Omega} \right|_{\text{extra}} = \frac{g_e^2 g_\gamma^2}{16\pi^2 \Lambda^4} \frac{E^4 m_e^2}{s^2} \frac{16}{9} \frac{E^4}{m_X^4} = \frac{1}{2304\pi^2} \frac{g_e^2 g_\gamma^2}{\Lambda^4} \frac{m_e^2 s^2}{m_X^4} \quad (\text{D.44})$$

Unfortunately, this cross section does not satisfy Froissart bound, meaning we could not go up in energy even if we wanted to. The limit in energy is given by the value for which there is experimental verification: 20 – 50 MeV.

This result is  $\theta$  independent, meaning that it will not disappear for specific values of  $\theta$ . To obtain the total cross section correction, just multiply  $4\pi$  to Equation D.44

<sup>46</sup>All the more reason not to include these frame dependent constraints when checking Ward identities.

## E Two-photon elastic scattering at one loop

We analyze the amplitudes and cross section for the photon-photon scattering process shedding some light into how these loop diagrams are evaluated in practice. The correction due to spin 2 mediation, instead, acts at tree level, making this process very constraining for our new physics. However, in this Appendix, we will not consider it. For the additional correction due to massive spin 2 boson, see [section 11](#).

### E.1 Two-photon Wick contractions

It is better to start by carrying out the necessary Wick contractions that define this photons scattering. With the exception of the trivial forward scattering, the first order in the  $T$ -ordered product expansion that interpolates the initial and final state  $|i\rangle = |f\rangle = |e^-\gamma\rangle$  is fourth order. The exponential of the  $T$ -ordered product gets expanded into normal ordered interaction terms:

$$S_{fi} = \langle f | S | i \rangle = \langle \gamma\gamma | S | \gamma\gamma \rangle = \\ = \frac{(-ie)^4}{4!} \int d^4x d^4y d^4z d^4w \langle \gamma\gamma | :(\bar{\psi}\gamma_\sigma A_\sigma\psi)_w : : (\bar{\psi}\gamma_\rho A_\rho\psi)_z : : (\bar{\psi}\gamma_\nu A_\nu\psi)_y : : (\bar{\psi}\gamma_\mu A_\mu\psi)_x : | \gamma\gamma \rangle \quad (\text{E.1})$$

Now, we need to write down every possible contraction:

$$S_{fi} = \frac{(-ie)^4}{4!} \int d^4x d^4y d^4z d^4w \times \\ \times \langle \gamma\gamma | :(\psi^\dagger \gamma_4 \gamma_\mu A_\mu \psi)_x : : (\psi^\dagger \gamma_4 \gamma_\nu A_\nu \psi)_y : : (\psi^\dagger \gamma_4 \gamma_\rho A_\rho \psi)_z : : (\psi^\dagger \gamma_4 \gamma_\sigma A_\sigma \psi)_w : | \gamma\gamma \rangle + \dots \quad (\text{E.2})$$

There are in total 576 possible contractions. However, a factor of 24 comes out from simply assigning fields to asymptotic initial and final states (four photon fields to assign to four photons, equal  $4! = 24$  identical diagrams). This will cancel the  $4!$  in the denominator of the Dyson expansion.

The 24 independent diagrams are all decided by the choice of fermion contractions. Of these 24, 18 of these contractions are disconnected, meaning we get loops involving 1, 2 or 3 vertices, but not four. These diagrams are disconnected, non interacting contributions to the scattering, and can be eliminated when studying proper vertices functions.

This leaves us with only 6 independent diagrams: 3 possible paths that propagators can take between the 4 vertices ( $x \rightarrow y \rightarrow z \rightarrow w \rightarrow x$  is *s*-channel,  $x \rightarrow z \rightarrow y \rightarrow w \rightarrow x$  is *t*-channel, and  $x \rightarrow y \rightarrow w \rightarrow z \rightarrow x$  is *u*-channel<sup>47</sup>), and 2 directions of travel for each path, corresponding to a loop of electron or a loop of positron. *CP* symmetry of QED guarantees that electron and positron loops will give us the same contribution, so the proper factor in front of each diagram is actually  $2(ie)^4$ .

This will give us, finally, the correct list of connected contractions for photon-photon elastic scattering:

$$S_{fi} = 2(-ie)^4 \int d^4x d^4y d^4z d^4w \times \\ \times \langle \gamma\gamma | :(\psi^\dagger \gamma_4 \gamma_\mu A_\mu \psi)_x : : (\psi^\dagger \gamma_4 \gamma_\nu A_\nu \psi)_y : : (\psi^\dagger \gamma_4 \gamma_\rho A_\rho \psi)_z : : (\psi^\dagger \gamma_4 \gamma_\sigma A_\sigma \psi)_w : | \gamma\gamma \rangle \\ + \langle \gamma\gamma | :(\psi^\dagger \gamma_4 \gamma_\mu A_\mu \psi)_x : : (\psi^\dagger \gamma_4 \gamma_\nu A_\nu \psi)_y : : (\psi^\dagger \gamma_4 \gamma_\rho A_\rho \psi)_z : : (\psi^\dagger \gamma_4 \gamma_\sigma A_\sigma \psi)_w : | \gamma\gamma \rangle \\ + \langle \gamma\gamma | :(\psi^\dagger \gamma_4 \gamma_\mu A_\mu \psi)_x : : (\psi^\dagger \gamma_4 \gamma_\nu A_\nu \psi)_y : : (\psi^\dagger \gamma_4 \gamma_\rho A_\rho \psi)_z : : (\psi^\dagger \gamma_4 \gamma_\sigma A_\sigma \psi)_w : | \gamma\gamma \rangle \quad (\text{E.3})$$

which are, in order, *s*-channel, *t*-channel and *u*-channel. Dirac structure comes out automatically from the loop. Remember that the contractions are:

$$\overline{\psi_b(x)\psi_a^\dagger(y)} = D_{ab}(x-y) \quad \overline{\psi_a^\dagger(x)\psi_b(y)} = -D_{ab}(x-y) \quad (\text{E.4})$$

because of the antisymmetric structure of fermions. Then, in every loop contraction there must be, topologically, an odd number of reversed order contractions, meaning that a  $-1$  overall must arise in every fermion loop (which

<sup>47</sup>All other paths are equivalent to these three under rotation.

is where this Feynman rule comes from). Also, the loop structure is manifested through a trace in Dirac space:

$$\begin{aligned}
S_{fi} = & 2(-ie)^4 (-1) \int d^4x d^4y d^4z d^4w \langle \gamma\gamma | A_\mu(x) A_\nu(y) A_\rho(z) A_\sigma(w) | \gamma\gamma \rangle \times \\
& \times [(\gamma_\mu)_{ab} D_{bc}(x-y)(\gamma_\nu)_{cd} D_{de}(y-z)(\gamma_\rho)_{ef} D_{fg}(z-w)(\gamma_\sigma)_{gh} D_{ha}(w-x) \\
& + (\gamma_\mu)_{ab} D_{bc}(x-z)(\gamma_\rho)_{cd} D_{de}(z-y)(\gamma_\nu)_{ef} D_{fg}(y-w)(\gamma_\sigma)_{gh} D_{ha}(w-x) \\
& + (\gamma_\mu)_{ab} D_{bc}(x-y)(\gamma_\nu)_{cd} D_{de}(y-w)(\gamma_\sigma)_{ef} D_{fg}(w-z)(\gamma_\rho)_{gh} D_{ha}(z-x) ] \\
= & -2e^4 \int d^4x d^4y d^4z d^4w \langle \gamma\gamma | A_\mu(x) A_\nu(y) A_\rho(z) A_\sigma(w) | \gamma\gamma \rangle \times \\
& \times \left\{ \text{Tr} [\gamma_\mu D(x-y) \gamma_\nu D(y-z) \gamma_\rho D(z-w) \gamma_\sigma D(w-x)] \right. \\
& + \text{Tr} [\gamma_\mu D(x-z) \gamma_\rho D(z-y) \gamma_\nu D(z-w) \gamma_\sigma D(w-x)] \\
& \left. + \text{Tr} [\gamma_\mu D(x-y) \gamma_\nu D(y-w) \gamma_\sigma D(w-z) \gamma_\rho D(z-x)] \right\} \quad (\text{E.5})
\end{aligned}$$

which basically already gives us the total amplitude written down, in position space. For momentum space result, check out subsection E.2.

## E.2 Two-photon amplitude

Let us see the contributing diagrams for this process: all three channels at one loop. Let us write amplitudes

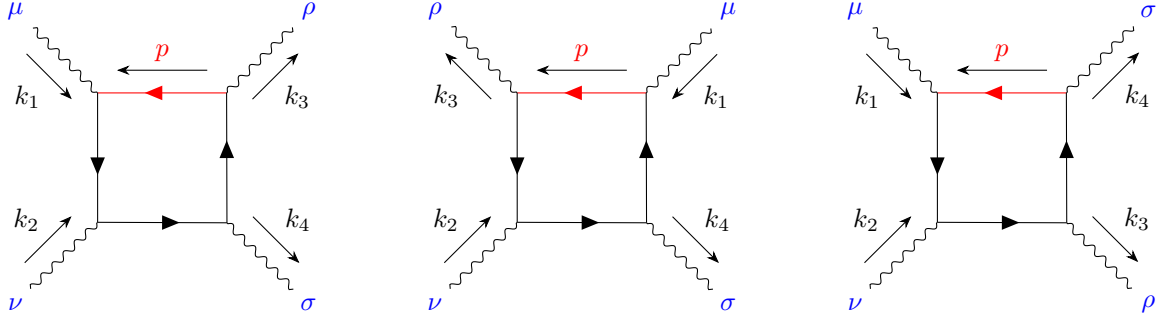


Figure 53: Three diagrams for loop contribution in QED for two-photon scattering. On the left,  $s$ -channel (hereafter called  $M_{\mu\nu\rho\sigma}^s$ ), in the middle  $t$ -channel (hereafter called  $M_{\mu\nu\rho\sigma}^t$ ) and on the right  $u$ -channel (hereafter called  $M_{\mu\nu\rho\sigma}^u$ ). The diagrams with inverted fermion arrows are not drawn, and are already taken care of (see subsection E.1).

before photon polarization contractions:

$$M_{\mu\nu\rho\sigma}^s = -2(-ie)^4 \int \frac{d^4p}{(2\pi)^4 i} \frac{I_{\mu\rho\sigma\nu}(p, p+k_3, p+k_1+k_2, p+k_1)}{[p^2 + m_e^2] [(p+k_3)^2 + m_e^2] [(p+k_1+k_2)^2 + m_e^2] [(p+k_1)^2 + m_e^2]} \quad (\text{E.6})$$

$$M_{\mu\nu\rho\sigma}^t = -2(-ie)^4 \int \frac{d^4p}{(2\pi)^4 i} \frac{I_{\rho\mu\sigma\nu}(p, p-k_1, p-k_3+k_2, p-k_3)}{[p^2 + m_e^2] [(p-k_1)^2 + m_e^2] [(p-k_3+k_2)^2 + m_e^2] [(p-k_3)^2 + m_e^2]} \quad (\text{E.7})$$

$$M_{\mu\nu\rho\sigma}^u = -2(-ie)^4 \int \frac{d^4p}{(2\pi)^4 i} \frac{I_{\mu\sigma\rho\nu}(p, p+k_4, p+k_1+k_2, p+k_1)}{[p^2 + m_e^2] [(p+k_4)^2 + m_e^2] [(p+k_1+k_2)^2 + m_e^2] [(p+k_1)^2 + m_e^2]} \quad (\text{E.8})$$

where:

$$I_{\mu\nu\rho\sigma}(k_1, k_2, k_3, k_4) = \text{Tr} \left[ \gamma_\mu (-ik_1 + m_e) \gamma_\nu (-ik_2 + m_e) \gamma_\rho (-ik_3 + m_e) \gamma_\sigma (-ik_4 + m_e) \right] \quad (\text{E.9})$$

is the loop function in the most generic form.

In front of these amplitudes, the usual  $S$ -matrix factor (whose rules are found in subsection C.2) is:

$$\frac{[(2\pi)^4 i]^4}{[(2\pi)^4 i]^3} \left( \frac{1}{\sqrt{V}} \right)^4 \frac{1}{\sqrt{2k_{1,4} 2k_{2,4} 2k_{3,4} 2k_{4,4}}} = \frac{(2\pi)^4 i}{4V^2 \sqrt{k_{1,4} k_{2,4} k_{3,4} k_{4,4}}} \quad (\text{E.10})$$

Because there are 4 photons fields to be normalized, and there is one less factor  $1/(2\pi)^4 i$  in the denominator as it is needed for loop integration.

Simple power counting tells us that these diagrams should actually diverge like  $\sim \log(p)$ , as degree of divergence  $D = 0$ . However, this is not the case, because diverging contributions all cancel out when summing all diagrams. To see how, we define:

$$M_{\mu\nu\rho\sigma} = M_{\mu\nu\rho\sigma}^s + M_{\mu\nu\rho\sigma}^t + M_{\mu\nu\rho\sigma}^u$$

as the total amplitude, and we expand it with respect to any external momentum  $k_i$ :

$$M_{\mu\nu\rho\sigma} = M_{\mu\nu\rho\sigma}(k_i = 0) + \left. \frac{dM}{dk_{i,\mu}} \right|_{k_i=0} k_{i,\mu} + \dots \quad (\text{E.11})$$

because any derivative lowers degree of divergence by 1, then the divergence of the diagram is actually contained in  $M_{\mu\nu\rho\sigma}(k_i = 0)$ , as first order expansion has  $D = -1$ , making it convergent.

Then, to evaluate  $M_{\mu\nu\rho\sigma}(k_i = 0)$  we can use the code linked in the GitHub repository `Twophoton.frm`. The code is capable of evaluating the loop functions  $I_{\mu\nu\rho\sigma}$  for any combination of external momentum (without integrating, however). In the current setting, the code returns the tensor reduced integrand for the loop amplitude:

$$\delta_{\mu\nu} \delta_{\rho\sigma} M_{\mu\nu\rho\sigma}(0, 0, 0, 0) = 0 \quad (\text{E.12})$$

This verifies that the amplitude is, indeed, finite. Having a finite amplitude, however, does not mean that one can avoid having to renormalize (Landau warns us in [27]). It is especially tricky, indeed, summing infinite individual amplitudes to get a finite result, and renormalization is key to carrying this out (as also highlighted by [68])<sup>48</sup>.

Also, it is worth mentioning that the same code `Twophoton.frm` verifies Ward identities:

$$k_{1,\mu} M_{\mu\nu\rho\sigma} = k_{2,\nu} M_{\mu\nu\rho\sigma} = k_{3,\rho} M_{\mu\nu\rho\sigma} = k_{4,\sigma} M_{\mu\nu\rho\sigma} = 0 \quad (\text{E.13})$$

If external momentum are set to be general, `Twophoton.frm` returns an output of hundreds of terms, to be integrated in  $p$ . The actual result demands arduous calculations, and faster and easier ways to evaluate these boxes have been devised in the 1960s ([66], [67]), and we will briefly explain it in the following...

**Double dispersion relation method:** We all remember *Cutkovsky rule*, whenever the mediated propagator becomes on shell, we can operate the substitution:

$$\frac{1}{p^2 + m^2 - i\epsilon} \rightarrow -(2\pi i) \delta(p^2 + m^2) \quad (\text{E.14})$$

where  $m$  is the mass of the mediator, and  $p$  its 4-momentum. It is the result of a principal value integral, and it produces a non trivial imaginary part in the amplitude.

Now, take our box diagrams in Figure 53. The amplitudes will only depend on Mandelstam variables  $s, t, u$ . Because photons are massless, in this scattering we get  $s + t + u = 0$ . Therefore, only  $s$  and  $t$  are independent variables, and  $u = -s - t$ .

We can then write the amplitudes (we will focus for instance on  $M^s$ , omitting indices for simplicity) as follows:

$$M^s(s, t) = \int d^4 p \frac{iB(p, s, t)}{[p^2 + m_e^2] [(p + k_3)^2 + m_e^2] [(p + k_1 + k_2)^2 + m_e^2] [(p + k_1)^2 + m_e^2]} \quad (\text{E.15})$$

Now, if  $s, t$  are small, the two photons cannot produce the loop particles on shell ( $e^+e^-$  pair), and this would mean that, Feynman prescription aside,  $M^s$  is real.

<sup>48</sup>I am insisting because someone in 2011 tried to argue that two-photon scattering did not need renormalization (and obtained nonsensical results for the cross section), and got ostracized by the scientific community.

However, by optical theorem, if  $|s| \geq 4m_e^2$ , while  $t = \bar{t}$  stays fixed, then  $M^s$  would acquire a relevant imaginary part. In Landau's notation ([27]), we write:

$$M^s(s, \bar{t}) = \frac{1}{\pi} \int_{-\infty}^{-4m_e^2} ds' \frac{A_{1s}(s', \bar{t})}{s' - s - i\epsilon} \quad (\text{E.16})$$

where  $A_{1s}$  is calculated with Cutkovsky rule, replacing poles with Dirac deltas, and setting  $p_4 \geq 0$ :

$$2i A_{1s}(s, \bar{t}) = (2\pi i)^2 \int d^4 p iB(p, s, \bar{t}) \theta(p_4) \frac{\delta[p^2 + m_e^2] \delta[(p + k_1 + k_2)^2 + m_e^2]}{[(p + k_3)^2 + m_e^2] [(p + k_1)^2 + m_e^2]} \quad (\text{E.17})$$

which is like cutting the loop of the  $s$ -channel vertically to produce on shell  $e^+e^-$  (left diagram in Figure 54).

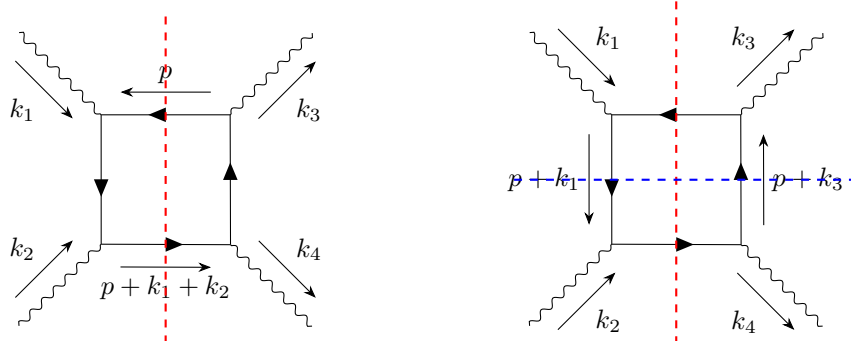


Figure 54: On the left, vertically cut  $s$ -channel diagram using Cutkovsky rule. On the right, vertically and horizontally cut  $s$ -channel diagram using Cutkovsky rule.

Now, we repeat the same reasoning for  $A_{1s}$ , this time fixing  $s = \bar{s}$ , and letting  $t$  change. Then,  $A_{1s}(\bar{s}, t)$  has similar analytic properties to  $M^s$ , except in variable  $t$ . So, we let  $t$  grow. The condition for on shell  $e^+e^-$  should be  $t \geq 4m_e^2$ , however there are also the delta functions in the numerator that restrict kinematics. In particular, the second delta in Equation E.17 depends on  $k_1 + k_2$ , hence on  $s$ , and therefore we do not really know the threshold  $t_c(s)$  after which on shell production occurs.

Keeping it as a parameter:

$$A_{1s}(\bar{s}, t) = \frac{1}{\pi} \int_{t_c(\bar{s})}^{\infty} dt' \frac{A_2(\bar{s}, t')}{t' - t + i\epsilon} \quad (\text{E.18})$$

where  $A_2$  is calculated with Cutkovsky rule, replacing last two poles with Dirac deltas:

$$(2i)^2 A_2(\bar{s}, t) = (2\pi i)^4 \int d^4 p iB(p, \bar{s}, \bar{t}) \theta(p_4) \delta[p^2 + m_e^2] \delta[(p + k_3)^2 + m_e^2] \delta[(p + k_1 + k_2)^2 + m_e^2] \delta[(p + k_1)^2 + m_e^2] \quad (\text{E.19})$$

which looks like a second cut in the diagram, as in the right picture in Figure 54.

Altogether, the total amplitude is reduced to calculating two definite integrals:

$$M^s(s, t) = \frac{1}{\pi^2} \int_{-\infty}^{-4m_e^2} ds' \int_{t_c(\bar{s})}^{\infty} dt' \frac{A_2(s', t')}{(s' - s - i\epsilon)(t' - t + i\epsilon)} \quad (\text{E.20})$$

This is the result of the *double dispersion relation method*. We will not go into much detail about the calculation itself (found in [66], [67]). We really only need the results.

Now, to write down amplitudes need to add polarizations of the photons:

$$\begin{aligned} M_{fi} &= M_{\mu\nu\rho\sigma}(s, t, u) \varepsilon_\mu(k_1, \lambda_1) \varepsilon_\nu(k_2, \lambda_2) \bar{\varepsilon}_\rho(k_3, \lambda_3) \bar{\varepsilon}_\sigma(k_4, \lambda_4) = \\ &= M_{\lambda_1\lambda_2\lambda_3\lambda_4}(s, t, u) \end{aligned} \quad (\text{E.21})$$

As basis of polarization, we choose circular polarization, meaning we are in the basis of helicity:  $\lambda_i = \pm 1 = \pm$ . There are  $2^4 = 16$  possible choices of polarizations for the four photons, leaving 16 different amplitudes. However, these are not all independent, because of symmetry arguments:

- Parity invariance leads to invariance under helicity inversion:

$$M_{\lambda_1 \lambda_2 \lambda_3 \lambda_4}(s, t, u) = M_{-\lambda_1 - \lambda_2 - \lambda_3 - \lambda_4}(s, t, u) \quad (\text{E.22})$$

- Time inversion symmetry leads to invariance under swapping initial and final states:

$$M_{\lambda_1 \lambda_2 \lambda_3 \lambda_4}(s, t, u) = M_{\lambda_3 \lambda_4 \lambda_1 \lambda_2}(s, t, u) \quad (\text{E.23})$$

- If we exchange  $1 \leftrightarrow 2$  and  $3 \leftrightarrow 4$ , we are only swapping initial photons and final photons.  $s, t, u$  variables stay invariant under this transformation, and because photons are bosons there is no minus sign emerging from the exchange:

$$M_{\lambda_1 \lambda_2 \lambda_3 \lambda_4}(s, t, u) = M_{\lambda_2 \lambda_1 \lambda_4 \lambda_3}(s, t, u) \quad (\text{E.24})$$

This leads to the following chain of identities:

$$\begin{aligned} M_{++++} &= M_{----} & M_{+---} &= M_{--++} & M_{+-+-} &= M_{-+-+} & M_{+-+-} &= M_{-++-} \\ M_{+++-} &= M_{++-+} = M_{+-++} = M_{-+++} = M_{---+} = M_{--+-} = M_{-+--} = M_{+-+-} \end{aligned}$$

as independent polarizations, we choose  $M_{++++}, M_{----}, M_{+---}, M_{-+-+}, M_{+-+-}, M_{-++-}$ .

This means that when we are averaging over initial polarizations and summing over final polarizations the squared amplitude, what we are doing is:

$$\begin{aligned} |\overline{M}_{fi}|^2 &= \frac{1}{4} \sum_{\lambda_1} \sum_{\lambda_2} \sum_{\lambda_3} \sum_{\lambda_4} |M_{\lambda_1 \lambda_2 \lambda_3 \lambda_4}(s, t, u)|^2 = \\ &= \frac{1}{4} \left[ 2|M_{++++}|^2 + 2|M_{----}|^2 + 2|M_{+---}|^2 + 2|M_{-+-+}|^2 + 8|M_{+-+-}|^2 \right] \end{aligned} \quad (\text{E.25})$$

which sum up the 16 total possibilities.

Finally, we can reduce the number of independent amplitudes to 3 by using crossing symmetry arguments (to see how they are carried out, look at [subsection B.3](#)):

- **$s \leftrightarrow t$  exchange:** It can happen by sending  $k_2 \leftrightarrow -k_3$  (look at kinematics). When this happens,  $\lambda_2 \rightarrow -\lambda_3$  as well, as if polarization stays the same, helicity is inverted when momenta change signs:

$$M_{\lambda_1 \lambda_2 \lambda_3 \lambda_4}(s, t, u) = M_{\lambda_1 - \lambda_3 - \lambda_2 \lambda_4}(t, s, u) \quad (\text{E.26})$$

- **$s \leftrightarrow u$  exchange:** It can happen by sending  $k_2 \leftrightarrow -k_4$  (look at kinematics). When this happens,  $\lambda_2 \rightarrow -\lambda_4$ :

$$M_{\lambda_1 \lambda_2 \lambda_3 \lambda_4}(s, t, u) = M_{\lambda_1 - \lambda_4 \lambda_3 - \lambda_2}(u, t, s) \quad (\text{E.27})$$

- **$t \leftrightarrow u$  exchange:** It can happen by sending  $k_3 \leftrightarrow k_4$  (look at kinematics). When this happens,  $\lambda_3 \rightarrow \lambda_4$ :

$$M_{\lambda_1 \lambda_2 \lambda_3 \lambda_4}(s, t, u) = M_{\lambda_1 \lambda_2 \lambda_4 \lambda_3}(s, u, t) \quad (\text{E.28})$$

This can be used to derive:

$$M_{-+-+}(s, t, u) = M_{++++}(t, s, u) \quad M_{+-+-}(s, t, u) = M_{----}(u, t, s)$$

while the last one is useless as it only tells us  $M_{++++}(s, t, u) = M_{----}(s, u, t)$ .

### E.3 Two-photon kinematics

Kinematics of the two-photon scattering process needs to be evaluated exclusively in the center of mass of the two photons (which exists, as opposed to the single photon center of mass that does not exist), where process is back-to-back. If we do that, we can set the 4-momenta:

$$k_1 = (\vec{k}, i\omega) \quad k_2 = (-\vec{k}, i\omega) \quad k_3 = (\vec{k}', i\omega) \quad k_4 = (-\vec{k}', i\omega)$$

with  $\omega = |\vec{k}| = |\vec{k}'|$  by energy conservation. Call  $\theta$  the scattering angle between photons in final and initial states, and the two photons in the center of mass.  $\theta$  and  $\phi$  are the only two parameters not fixed. However, because QED is parity invariant, every QED process should be intrinsically independent on the polar angle  $\phi$ , as each scattering plane selected by a specific  $\phi$  value is equally likely. So, in reality, the only free parameter in the final state is  $\theta$  (if we fix energy  $\omega$ ).

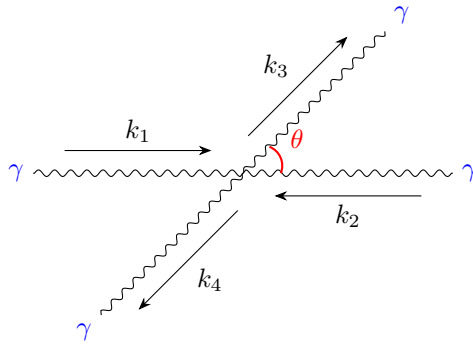


Figure 55: Kinematics of two-photon scattering, in the center of mass system.

Kinematics is outlined in Figure 55: Define the Mandelstam variables:

$$\begin{aligned}s &= (k_1 + k_2)^2 = -4\omega^2 \\t &= (k_1 - k_3)^2 = 2\omega^2(1 - \cos\theta) \\u &= (k_1 - k_4)^2 = 2\omega^2(1 + \cos\theta)\end{aligned}$$

Calculate the scalar products:

$$\begin{aligned}k_1 \cdot k_2 &= k_3 \cdot k_4 = -2\omega^2 = \frac{s}{2} \\k_1 \cdot k_3 &= k_2 \cdot k_4 = -\omega^2(1 - \cos\theta) = -\frac{t}{2} \\k_1 \cdot k_4 &= k_2 \cdot k_3 = -\omega^2(1 + \cos\theta) = -\frac{u}{2}\end{aligned}$$

and it is also useful to have:

$$v_{rel} = \frac{1}{k_{1,4} k_{2,4}} \sqrt{(k_1 \cdot k_2)^2 - k_1^2 k_2^2} = \frac{\sqrt{4\omega^4}}{\omega^2} = 2 \quad (\text{E.29})$$

where  $v_{rel}$  is the "classical" relative velocity between electron and positron (clearly does not satisfy relativistic sum of velocities), and it will appear in the cross section result.

Because the choice of photon polarization is explicit for the amplitudes to make sense, we also need to derive constraints on scalar products with said polarizations. Our basis will be circular polarizations. Selecting  $k_1$  axis to be the positive  $x$  axis:

$$\begin{aligned}\varepsilon_1^+ &= \frac{1}{\sqrt{2}} (0, 1, i, 0)^T & \varepsilon_1^- &= \frac{1}{\sqrt{2}} (0, 1, -i, 0)^T \\ \varepsilon_2^+ &= \frac{1}{\sqrt{2}} (0, -1, i, 0)^T & \varepsilon_2^- &= \frac{1}{\sqrt{2}} (0, -1, -i, 0)^T\end{aligned}$$

To get the others, take  $\varepsilon_1$  and rotate it. A rotation by  $\theta$  will yield  $\varepsilon_3$ , while a rotation of  $\pi + \theta$  will yield  $\varepsilon_4$ .

We said that action of Lorentz transformations on polarizations is not linear, hence these are not really vectors. However, this non linearity is manifest in boosts, while polarizations are perfectly covariant under rotations<sup>49</sup>:

$$\begin{aligned}\varepsilon_3^+ &= \frac{1}{\sqrt{2}} (-\sin\theta, \cos\theta, i, 0)^T & \varepsilon_3^- &= \frac{1}{\sqrt{2}} (-\sin\theta, \cos\theta, -i, 0)^T \\ \varepsilon_4^+ &= \frac{1}{\sqrt{2}} (\sin\theta, -\cos\theta, i, 0)^T & \varepsilon_4^- &= \frac{1}{\sqrt{2}} (\sin\theta, -\cos\theta, -i, 0)^T\end{aligned}$$

<sup>49</sup>Rotation matrix embedded in 4D spacetime is:

$$R(\theta) = \begin{pmatrix} \cos\theta & -\sin\theta & 0 & 0 \\ \sin\theta & \cos\theta & 0 & 0 \\ 0 & 0 & 1 & 0 \\ 0 & 0 & 0 & 1 \end{pmatrix} \quad R(\pi + \theta) = \begin{pmatrix} -\cos\theta & \sin\theta & 0 & 0 \\ -\sin\theta & -\cos\theta & 0 & 0 \\ 0 & 0 & 1 & 0 \\ 0 & 0 & 0 & 1 \end{pmatrix}$$

Acting with these on  $k_1$  generates  $k_3$  and  $k_4$ , and on  $\varepsilon_1$  generates  $\varepsilon_3$  and  $\varepsilon_4$ .

Notice that we are in the axial gauge for which  $\varepsilon_{i,4} = 0$ , no matter what.

To calculate the scalar products, define the useful quantities:

$$q = \sqrt{\frac{tu}{-2s}} = \sqrt{\frac{\omega^2(1 - \cos^2\theta)}{2}} = \frac{\omega \sin \theta}{\sqrt{2}} \quad l = \frac{1 - \cos \theta}{2} = \frac{t}{s} \quad r = \frac{1 + \cos \theta}{2} = \frac{u}{s} \quad (\text{E.30})$$

then, we can fix all scalar products:

$$\begin{aligned} k_i \cdot \varepsilon_i^\pm &= 0 \\ k_2 \cdot \varepsilon_1^\pm &= k_1 \cdot \varepsilon_2^\pm = k_3 \cdot \varepsilon_4^\pm = k_4 \cdot \varepsilon_3^\pm = 0 \\ k_1 \cdot \varepsilon_3^\pm &= k_2 \cdot \varepsilon_4^\pm = k_3 \cdot \varepsilon_2^\pm = k_4 \cdot \varepsilon_1^\pm = -q \\ k_1 \cdot \varepsilon_4^\pm &= k_2 \cdot \varepsilon_3^\pm = k_3 \cdot \varepsilon_1^\pm = k_4 \cdot \varepsilon_2^\pm = q \end{aligned}$$

and:

$$\begin{aligned} \varepsilon_i^\pm \cdot \varepsilon_i^\pm &= 1 & \varepsilon_i^\pm \cdot \varepsilon_i^\mp &= 0 \\ \varepsilon_1^\pm \cdot \varepsilon_2^\pm &= \varepsilon_3^\pm \cdot \varepsilon_4^\pm = 0 \\ \varepsilon_1^\pm \cdot \varepsilon_2^\mp &= \varepsilon_3^\pm \cdot \varepsilon_4^\mp = -1 \\ \varepsilon_1^\pm \cdot \varepsilon_3^\mp &= \varepsilon_2^\pm \cdot \varepsilon_4^\mp = -\varepsilon_1^\pm \cdot \varepsilon_4^\pm = -\varepsilon_2^\pm \cdot \varepsilon_3^\pm = l \\ \varepsilon_1^\pm \cdot \varepsilon_4^\mp &= \varepsilon_2^\pm \cdot \varepsilon_3^\mp = -\varepsilon_1^\pm \cdot \varepsilon_3^\pm = -\varepsilon_2^\pm \cdot \varepsilon_4^\pm = r \end{aligned}$$

Notice that if we decided to define all polarizations with a negative sign with respect to this choice (like in [62]), only scalar products with 4-momenta would change sign, and all the rest of kinematics would be the same. However, a quick check of any result we ever find using this kinematics shows that this change of sign leaves amplitudes invariant, as only even powers of these scalar products ever appear (**it means we did the same as the Chinese**).

Finally, some cyclic properties of Mandelstam variables (other than  $s + t + u = 0$ ):

$$\begin{aligned} st + tu + us &= -8\omega^4(1 - \cos \theta) + 4\omega^4(1 - \cos^2 \theta) - 8\omega^4(1 + \cos \theta) = \\ &= -12\omega^4 - 4\omega^4 \cos^2 \theta = -4\omega^4(3 + \cos^2 \theta) \end{aligned} \quad (\text{E.31})$$

$$s^2 + t^2 + u^2 = \cancel{(s+t+u)^2} - 2(st + tu + us) = 8\omega^4(3 + \cos^2 \theta) \quad (\text{E.32})$$

$$\begin{aligned} s^4 + t^4 + u^4 &= 256\omega^8 + 16\omega^8(1 - \cos \theta)^4 + 16\omega^8(1 + \cos \theta)^4 = \\ &= 16\omega^8[16 + 2 + 12\cos^2 \theta + 2\cos^4 \theta] = 32\omega^8(3 + \cos^2 \theta)^2 \end{aligned} \quad (\text{E.33})$$

They will be useful when studying limits of our spin 2 corrections values.

## E.4 Two-photon cross section

We need to start with the  $S$ -matrix element. Now, remember all the rules we had in subsection C.2 to write them down. Using Equation E.10, we get:

$$|S_{fi}|^2 = \frac{(2\pi)^8 |\overline{M}_{fi}|^2}{16V^4 k_{1,4} k_{2,4} k_{3,4} k_{4,4}} |\delta(k_1 + k_2 - k_3 - k_4)|^2 \quad (\text{E.34})$$

so, the rate of the process in a specific final state phase space configuration:

$$\Gamma(k_3, k_4) = \frac{|S_{fi}|^2}{T} = \frac{1}{T} \frac{(2\pi)^8 |\overline{A}|^2}{16V^4 k_{1,4} k_{2,4} k_{3,4} k_{4,4}} \frac{VT}{(2\pi)^4} \delta(k_1 + k_2 - k_3 - k_4) \quad (\text{E.35})$$

Notice that  $k_{1,4}$  and  $k_{2,4}$  appear but they are fixed.

Using [Equation A.34](#), we get the final cross section:

$$\begin{aligned}\sigma(\gamma\gamma \rightarrow \gamma\gamma) &= \frac{V}{v_{rel}} \int \frac{V d^3 k_3}{(2\pi)^3} \frac{V d^3 k_4}{(2\pi)^3} \Gamma(k_3, k_4) = \\ &= \frac{V}{v_{rel}} \int \frac{V d^3 k_3}{(2\pi)^3} \frac{V d^3 k_4}{(2\pi)^3} \left[ \frac{1}{T} \frac{(2\pi)^8 |\bar{M}_{fi}|^2}{16 V^4 k_{1,4} k_{2,4} k_{3,4} k_{4,4}} \frac{VT}{(2\pi)^4} \delta(k_1 + k_2 - k_3 - k_4) \right] = \\ &= \frac{1}{32(2\pi)^2} \int \frac{d^3 k_3 d^3 k_4}{k_{1,4} k_{2,4} k_{3,4} k_{4,4}} |\bar{M}_{fi}|^2 \delta(k_1 + k_2 - k_3 - k_4) = \\ &= \frac{1}{32(2\pi)^2} \int \frac{d^3 k_4}{k_{1,4} k_{2,4} k_{3,4} k_{4,4}} |\bar{M}_{fi}|^2 \delta(k_{1,4} + k_{2,4} - k_{3,4} - k_{4,4})\end{aligned}\quad (\text{E.36})$$

with  $v_{rel} = 2$  from [Equation E.29](#), and having integrated  $k_3$  out, leaving only conservation of energy. Integration variable will be the modulus of  $|\vec{k}_4| = k_{4,4}$ .

$$\frac{d\sigma}{d\Omega} = \frac{1}{128\pi^2} \int_0^\infty \frac{dk_{4,4} (k_{4,4})^2}{k_{1,4} k_{2,4} k_{3,4} k_{4,4}} |\bar{M}_{fi}|^2 \delta(k_{1,4} + k_{2,4} - k_{3,4} - k_{4,4}) \quad (\text{E.37})$$

The treatment of the Dirac's delta is trivial:

$$\begin{aligned}\delta(k_{1,4} + k_{2,4} - k_{3,4} - k_{4,4}) &= \delta\left(2\omega - \sqrt{|\vec{k}_1 + \vec{k}_2 - \vec{k}_4|^2} - k_{4,4}\right) = \\ &= \delta\left(2\omega - |\vec{k}_4| - k_{4,4}\right) = \\ &= \delta(2\omega - 2k_{4,4}) = \frac{1}{2} \delta(\omega - k_{4,4})\end{aligned}\quad (\text{E.38})$$

which immediately solves the phase space integral, by fixing every energy to be  $k_{1,4} = k_{2,4} = k_{3,4} = k_{4,4} = \omega$ . By also substituting the scalar products into the squared amplitude, we get the result:

$$\frac{d\sigma}{d\Omega} = \frac{1}{128\pi^2} \int_0^\infty \frac{dk_{4,4} k_{4,4}}{\omega^3} \frac{1}{2} \delta(\omega - k_{4,4}) = \frac{|\bar{M}_{fi}|^2}{256\pi^2 \omega^2} \quad (\text{E.39})$$

Now that phase space integration has imposed kinematics constraints on  $M_{fi}$ , we can substitute results for QED amplitudes. The actual result of the amplitudes reported in [\[27\]](#), [\[67\]](#) leave bare integrals to be evaluated non trivially. However, the behavior is highly non trivial only when  $|s| \approx 4m_e^2$ , which is actually not that interesting in our search for spin 2 bosons.

So, we will instead report the low energy and high energy limits of these amplitudes:

**Low energy limit:** We take  $|s| \ll 4m_e^2$ . In this limit, amplitudes are reported by [\[27\]<sup>50</sup>](#) and [\[68\]<sup>51</sup>](#):

$$M_{++++}(s, t, u) = \frac{11\alpha^2 s^2}{45 m_e^4} \quad M_{+-+-}(s, t, u) = \frac{11\alpha^2 t^2}{45 m_e^4} \quad M_{+-+-}(s, t, u) = \frac{11\alpha^2 u^2}{45 m_e^4} \quad (\text{E.40})$$

$$M_{+--+}(s, t, u) = -\frac{\alpha^2 (s^2 + t^2 + u^2)}{15 m_e^4} \quad M_{+++-}(s, t, u) = \frac{\alpha^2 stu}{15 m_e^6} \quad (\text{E.41})$$

Notice that amplitudes all satisfy the symmetry properties we found. Finally,  $M_{+++-}(s, t, u) \approx 0$ , because it is next order in kinematics with respect to all the other amplitudes.

<sup>50</sup>In this reference,  $4\pi$  factor is always absorbed in photon propagator. So, every  $e^2$  can be replaced with  $\alpha$ .

<sup>51</sup>This reference does not use barred polarizations in the final states, so amplitudes are swapped. There is no difference in the cross section result, however.

In this case, using [Equation E.40](#), and the kinematics results [Equation E.32](#) and [Equation E.33](#):

$$\begin{aligned}
|\overline{M}_{fi}|^2 &= \frac{1}{4} \left[ 2|M_{++++}|^2 + 2|M_{++--}|^2 + 2|M_{+-+-}|^2 + 2|M_{+-+-}|^2 + \cancel{8|M_{+++-}|^2} \right] = \\
&= \frac{1}{2} \left\{ \left( \frac{11\alpha^2 s^2}{45 m_e^4} \right)^2 + \left( \frac{11\alpha^2 t^2}{45 m_e^4} \right)^2 + \left( \frac{11\alpha^2 u^2}{45 m_e^4} \right)^2 + \left[ \frac{\alpha^2 (s^2 + t^2 + u^2)}{15 m_e^4} \right]^2 \right\} = \\
&= \frac{1}{2} \left( \frac{\alpha^2}{45 m_e^4} \right)^2 \left[ 121 (s^4 + t^4 + u^4) + 9 (s^2 + t^2 + u^2)^2 \right] = \\
&= \frac{1}{2} \left( \frac{\alpha^2}{45 m_e^4} \right)^2 \left[ 121 (32\omega^8) + 9 (64\omega^8) \right] (3 + \cos^2 \theta)^2 = \\
&= \frac{1}{2} \frac{64 \alpha^4 \omega^8}{45^2 m_e^8} (3 + \cos^2 \theta)^2 \left( \frac{121}{2} + 9 \right) = \\
&= \frac{256}{4} \frac{139 \alpha^4 \omega^8}{90^2 m_e^8} (3 + \cos^2 \theta)^2 \tag{E.42}
\end{aligned}$$

which in turn, into [Equation E.39](#) yields the famous *Euler-Heisenberg differential cross section* ([64], [65]):

$$\frac{d\sigma}{d\Omega} = \frac{|\overline{M}_{fi}|^2}{256\pi^2\omega^2} = \frac{139 \alpha^4 \omega^6}{(180\pi)^2 m_e^8} (3 + \cos^2 \theta)^2 \tag{E.43}$$

When integrating, remember to include the fact that the final state is made up of two identical particles. From [Equation 5.31](#), the factor to multiply is  $C = 1/2! = 1/2$ . This results in integration over a single hemisphere, and not in the total solid angle (choose to integrate  $d\cos \theta$  between 0 and 1):

$$\begin{aligned}
\sigma(\gamma\gamma \rightarrow \gamma\gamma) &= \frac{1}{2} \frac{139 \alpha^4 \omega^6}{(180\pi)^2 m_e^8} \int_0^{2\pi} d\phi \int_{-1}^1 d\cos \theta (9 + 6\cos^2 \theta + \cos^4 \theta) = \\
&= \frac{139 \alpha^4 \omega^6}{(180\pi)^2 m_e^8} \int_0^{2\pi} d\phi \int_0^1 d\cos \theta (9 + 6\cos^2 \theta + \cos^4 \theta) = \\
&= \frac{139 \alpha^4 \omega^6}{(180\pi)^2 m_e^8} 2\pi \left[ 9 + \frac{6\cos^3 \theta}{3} \Big|_0^1 + \frac{\cos^5 \theta}{5} \Big|_0^1 \right] = \\
&= \frac{278 \alpha^4 \omega^6}{180^2 \pi m_e^8} \left[ 9 + 2 + \frac{1}{5} \right] = \\
&= \frac{278 \alpha^4 \omega^6}{180^2 \pi m_e^8} \left( \frac{56}{5} \right) = \\
&= \frac{973}{10125\pi} \frac{\alpha^4 \omega^6}{m_e^8} \tag{E.44}
\end{aligned}$$

The same result could have actually been calculated using a low energy effective Lagrangian ([64], [65]), for  $|s| \ll 4m_e^2$ :

$$\mathcal{L}_{EH} = \frac{2\alpha^2}{45 m_e^4} \left[ (\mathbf{E}^2 - \mathbf{B}^2)^2 + 7(\mathbf{E} \cdot \mathbf{B})^2 \right] \tag{E.45}$$

where  $\mathbf{E}$  and  $\mathbf{B}$  are the electric and magnetic fields associated with the photon electromagnetic tensor, as  $F_{\mu\nu}F_{\mu\nu} \propto \mathbf{E}^2 - \mathbf{B}^2$ , while with the parity breaking dual tensor<sup>52</sup>  $F_{\mu\nu}\tilde{F}_{\mu\nu} \propto \mathbf{E} \cdot \mathbf{B}$ .

<sup>52</sup>We defined:

$\tilde{F}_{\mu\nu} = \epsilon_{\mu\nu\rho\sigma} F_{\rho\sigma}$  (E.46)

**Ultra-relativistic forward scattering:** Take  $|s| \gg 4m_e^2$ , and take directly  $\theta = 0$  (hence  $t = 0$ , and  $s = -u$ , so only center of mass energy is free parameter). Only [27] reports results for this case:

$$M_{++++}(s) = -16\alpha^2 \log^2 \left( \frac{\sqrt{|s|}}{2m_e} \right) \quad M_{+-+-}(s) = -16\alpha^2 \log^2 \left( \frac{\sqrt{|s|}}{2m_e} \right) \quad (\text{E.47})$$

while:

$$M_{+--+}(s) = 0 \quad M_{++--}(s) = 0 \quad M_{+++-}(s) = 0$$

Again, they satisfy symmetry arguments.

Now, instead, we use [Equation E.47](#):

$$\begin{aligned} |\overline{M}_{fi}|^2 &= \frac{1}{4} \left[ 2|M_{++++}|^2 + 2|M_{+-+-}|^2 + 2|M_{+--+}|^2 + 2|M_{++--}|^2 + 8|M_{+++-}|^2 \right] = \\ &= \frac{1}{2} \left[ 256\alpha^4 \log^4 \left( \frac{\sqrt{|s|}}{2m_e} \right) + 256\alpha^4 \log^4 \left( \frac{\sqrt{|s|}}{2m_e} \right) \right] = \\ &= 256\alpha^4 \log^4 \left( \frac{\omega}{m_e} \right) \end{aligned} \quad (\text{E.48})$$

which in turn, into [Equation E.39](#):

$$\frac{d\sigma}{d\Omega} = \frac{\alpha^4}{\pi^2 \omega^2} \log^4 \left( \frac{\omega}{m_e} \right) \quad (\text{E.49})$$

This is only valid for  $|s| \gg 4m_e^2$ , and with  $\theta = 0$  fixed.

This concludes our review of QED result of one loop two-photon scattering. The special case  $|s| = 4m_e^2$  is not considered here, because it is not really relevant for our high energy search. Cross section behaviour changes drastically as amplitude has a relevant imaginary part as soon as that energy threshold is crossed, as pair  $e^+e^-$  is now created on shell.

Because we will not be discussing this scenario, we will most often talk about the two limits separately, or at most interpolate between the two with a smooth (and non physical) curve.

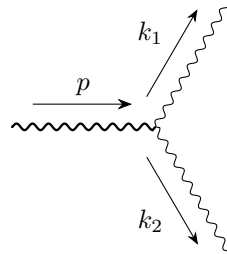
## F More calculations

### F.1 Landau-Yang theorem

**Theorem (Landau-Yang):** *It is impossible for any massive, odd spin state to decay into two massless bosons.*

We only need to prove the theorem for spin 1 massive particles into two photons. The traditional proof for this theorem consists of canceling out possible amplitudes structures for any interaction involving the boson decaying into two photons. Any example operator allowing for this decay would require the massive vector field, the two photons, and a necessary spacetime derivative to achieve dimension four and Lorentz invariance.

The derivative would then be translated into some of the involved momenta when writing the amplitude, and finally contracted with any of the vector polarizations. Simple symmetry arguments show that any of the nine possible combinations would vanish. In fact, take the decay:



Call the on shell polarizations of the photons  $\varepsilon_1$  and  $\varepsilon_2$ , and the polarization of the vector boson  $\varepsilon_V$ . Now, because of gauge invariance  $k_i \cdot \varepsilon_i = 0$ , with  $i \in \{1, 2\}$ . Moreover, because of subsidiary condition for vector bosons,  $p \cdot \varepsilon_V = 0$ .

Then, we exploit the hypothesis that starting state is massive, hence there exists a rest frame. In such frame,  $\vec{k}_1 = -\vec{k}_2$ . Now, fix the following gauge for the photons:  $\varepsilon_{1,4} = \varepsilon_{2,4} = 0$ . This implies that:

$$k_1 \cdot \varepsilon_2 = \vec{k}_1 \cdot \vec{\varepsilon}_2 = -\vec{k}_2 \cdot \vec{\varepsilon}_2 = -k_2 \cdot \varepsilon_2 = 0$$

Analogously,  $k_1 \cdot \varepsilon_1 = 0$ . By energy conservation,  $p = k_1 + k_2$ , meaning  $p \cdot \varepsilon_1 = p \cdot \varepsilon_2 = 0$ , as well.

The only non zero contraction is therefore  $k_i \cdot \varepsilon_V$ . However, because the final state is made of two identical particles, it must be symmetric under  $1 \leftrightarrow 2$  exchange. However:

$$k_1 \cdot \varepsilon_V = (p - k_2) \cdot \varepsilon_V = -k_2 \cdot \varepsilon_2$$

which is antisymmetric under the same exchange. Any symmetric  $1 \leftrightarrow 2$  exchange would then vanish, proving the theorem.

Another proof relies on possible quantum states of two identical photons. As we already mentioned studying the positron, if photons do not have the  $|1, 0\rangle$  state available, then:

$$|1, 0\rangle_{\text{tot}} = \frac{1}{\sqrt{2}} [|1\rangle_a | -1\rangle_b - | -1\rangle_a |1\rangle_b] \quad (\text{F.1})$$

(also check out [Equation 10.35](#)) is the only possible state allowed by angular momentum conservation, where on the LHS we get the vector boson state  $|J, M\rangle$ , and on the RHS the tensor product of the two photons  $|m_a\rangle |m_b\rangle$ . This is the only allowed combination and it is antisymmetric in spin under  $1 \leftrightarrow 2$  exchange.

If we assume the two-body decay to be isotropic, the photons are emitted as spherical waves. As such, the total orbital angular momentum is expected to be even, hence symmetric under  $1 \leftrightarrow 2$  exchange.

The total final state wavefunction, obtaining combining spin and orbital part, is then antisymmetric. But this fundamentally contradicts the bosonic nature of the photons, which would require a final symmetric state. Hence, we conclude that this decay is impossible.

## F.2 Generic 2-body phase space

A useful formula we used throughout that we derive here. We are going to evaluate, for a generic body of mass  $M$  (4-momentum  $p$ ) decaying into two particles of mass  $m_1$  (4-momentum  $k$ ) and  $m_2$  (4-momentum  $q$ ) respectively:

$$\begin{aligned} & \int \frac{d^3 q}{(2\pi)^3 2q_4} \frac{d^3 k}{(2\pi)^3 2k_4} (2\pi)^4 \delta^{(4)}(p - q - k) = \\ &= \frac{1}{(2\pi)^2} \int \frac{d^3 q d^4 k}{2q_4} \delta(k^2 + m_2^2) \theta(k_4) \delta^{(4)}(p - q - k) = \\ &= \frac{1}{(2\pi)^2} \int \frac{d^3 q}{2q_4} \delta \left[ (p - q)^2 + m_2^2 \right] \theta(p_4 - q_4) = \end{aligned}$$

In the rest frame of the decaying particle  $p \cdot q = -Mq_4$ . So:

$$\begin{aligned} &= \frac{1}{(2\pi)^2} \int \frac{d^3 q}{2q_4} \delta \left[ -M^2 - m_1^2 - 2Mq_4 + m_2^2 \right] \theta(M - q_4) = \\ &= \frac{1}{(2\pi)^2} \frac{1}{2M} \int \frac{d^3 q}{2q_4} \delta \left[ q_4 - \frac{M^2 + m_1^2 - m_2^2}{2M} \right] \theta(M - q_4) = \\ &= \frac{1}{(2\pi)^2} \frac{1}{2M} \int_0^\infty \frac{d|\vec{q}| |\vec{q}|^2}{2q_4} \delta(q_4 - \bar{q}_4) \int d\Omega = \end{aligned}$$

Call  $Q = |\vec{q}|$ . Because  $|\vec{q}|^2 = Q^2 = q_4^2 - m_1^2$ , then  $Q dQ = q_4 dq_4$ . If the decay is also isotropic, we integrate out the angular part, because decay amplitude cannot depend on angular coordinates. So:

$$\begin{aligned} &= \frac{4\pi}{(2\pi)^2 2M} \frac{1}{2} \int_0^\infty dq_4 Q \delta(q_4 - \bar{q}_4) = \\ &= \frac{1}{4\pi M} \bar{Q} \end{aligned} \tag{F.2}$$

where  $\bar{Q}$  is actually fixed, as:

$$\begin{aligned} \bar{Q}^2 &= \bar{q}_4^2 - m_1^2 = \frac{(M^2 + m_1^2 - m_2^2)^2 - 4m_1^2 M^2}{4M^2} = \\ &= \frac{M^4 + m_1^4 + m_2^4 - 2M^2 m_1^2 - 2M^2 m_2^2 - 2m_1^2 m_2^2}{4M^2} = \\ &= \frac{\lambda(M^2, m_1^2, m_2^2)}{4M^2} \end{aligned} \tag{F.3}$$

where  $\lambda$  is called *triangle function*, and it is defined as:

$$\lambda(a, b, c) = a^2 + b^2 + c^2 - 2ab - 2ac - 2bc \tag{F.4}$$

Hence, the final phase space result is:

$$\int \frac{d^3 q}{(2\pi)^3 2q_4} \frac{d^3 k}{(2\pi)^3 2k_4} (2\pi)^4 \delta^{(4)}(p - q - k) = \frac{\sqrt{\lambda(M^2, m_1^2, m_2^2)}}{8\pi M^2} \tag{F.5}$$

### F.3 Massless 3-body phase space

A useful formula we used throughout that we derive here. We are going to evaluate, for a generic body of mass (or center of mass energy)  $M$  (4-momentum  $p$ ) decaying into three massless particles of momenta  $k_1, k_2, k_3$ :

$$\begin{aligned} & \int \frac{d^3 k_1}{(2\pi)^3 2k_{1,4}} \frac{d^3 k_2}{(2\pi)^3 2k_{2,4}} \frac{d^3 k_3}{(2\pi)^3 2k_{3,4}} (2\pi)^4 \delta^{(4)}(p - k_1 - k_2 - k_3) = \\ &= \frac{1}{(2\pi)^5} \int \frac{d^3 k_1}{2k_{1,4}} \frac{d^3 k_2}{2k_{2,4}} d^4 k_3 \theta(k_{3,4}) \delta(k_3^2) \delta^{(4)}(p - k_1 - k_2 - k_3) = \\ &= \frac{1}{(2\pi)^5} \int \frac{d^3 k_1}{2k_{1,4}} \frac{d^3 k_2}{2k_{2,4}} \theta(M - k_{1,4} - k_{2,4}) \delta[(p - k_1 - k_2)^2] \end{aligned} \quad (\text{F.6})$$

call  $k_{1,4} = |\vec{k}_1| = E_1$ , and  $k_{2,4} = |\vec{k}_2| = E_2$ . If the decay is unpolarized, then there is no privileged direction for the decay (isotropic). So, the first decay product can be emitted in any direction, with equal probability:  $d^3 k_1 = d|\vec{k}_1||\vec{k}_1|^2 d\Omega_1 \rightarrow 4\pi dE_1 E_1^2$ .

Then, we call this decay direction  $z$ . Angles for the second decay product will be referred to as relative angles  $\theta_{12}, \phi_{12}$ . A decay of an elementary particle is planar for angular momentum conservation. The plane is characterized by the relative polar angle between the first two bodies  $\phi_{12}$ . By isotropic argument, each plane is equally likely, so  $\phi_{12} \rightarrow 2\pi$  can be integrated. The azimuthal angle, however, is correlated to momentum conservation, and is fixed. So:  $d^3 k_2 = d|\vec{k}_2||\vec{k}_2|^2 d\cos\theta_{12} d\phi_{12} \rightarrow 2\pi dE_2 E_2^2 d\cos\theta_{12}$ .

Moreover, in the rest frame of decaying particle (or center of mass frame),  $p = (\vec{0}, iM)$ . So:

$$\begin{aligned} (p - k_1 - k_2)^2 &= p^2 - 2p \cdot (k_1 + k_2) + 2k_1 \cdot k_2 = \\ &= -M^2 + 2M(E_1 + E_2) - 2E_1 E_2 (1 - \cos\theta_{12}) = \\ &= 2E_1 E_2 \cos\theta_{12} - [M^2 - 2M(E_1 + E_2) + 2E_1 E_2] \end{aligned}$$

Putting all together:

$$\begin{aligned} &= \frac{1}{4\pi^3} \int_0^\infty \frac{dE_1 E_1^2}{2E_1} \int_0^\infty \frac{dE_2 E_2^2}{2E_2} \int_{-1}^1 d\cos\theta_{12} \theta(M - E_1 - E_2) \delta \left\{ 2E_1 E_2 \cos\theta_{12} - [M^2 - 2M(E_1 + E_2) + 2E_1 E_2] \right\} = \\ &= \frac{1}{16\pi^3} \int_0^\infty dE_1 E_1 \int_0^\infty dE_2 E_2 \int_{-1}^1 d\cos\theta_{12} \theta(M - E_1 - E_2) \delta \left\{ 2E_1 E_2 \cos\theta_{12} - [M^2 - 2M(E_1 + E_2) + 2E_1 E_2] \right\} = \end{aligned}$$

define  $x = 2E_1/M$  and  $y = 2E_2/M$ . Change variables to the integral:

$$\begin{aligned} &= \frac{M^4}{256\pi^3} \int_0^\infty dx x \int_0^\infty dy y \int_{-1}^1 d\cos\theta_{12} \theta(2 - x - y) \delta \left\{ \frac{M^2 xy}{2} \cos\theta_{12} - M^2 \left[ 1 - (x + y) + \frac{xy}{2} \right] \right\} = \\ &= \frac{M^2}{128\pi^3} \int_0^\infty dx \int_0^\infty dy \int_{-1}^1 d\cos\theta_{12} \theta(2 - x - y) \delta \left[ \cos\theta_{12} - \frac{2(1 - x - y) + xy}{xy} \right] \end{aligned}$$

Integral on  $\cos\theta_{12}$  is trivial, as we just substitute that expression in  $x$  and  $y$ . Just got to be careful with the extremes of integration:

- For  $\cos\theta_{12} \geq -1$ , then  $2(1 - x - y) + 2xy = 2(1 - x)(1 - y) \geq 0$ . So, either  $x \geq 1$  and  $y \geq 1$ , which would vanish because of  $\theta(2 - x - y)$ , or  $x \leq 1$  and  $y \leq 1$ , which is the only non vanishing case.
- For  $\cos\theta_{12} \leq 1$ , then  $2(1 - x - y) \leq 0$ , which implies  $y \geq 1 - x$ .

So, in the end, *it doesn't even matter*:

$$\int \frac{d^3 k_1}{(2\pi)^3 2k_{1,4}} \frac{d^3 k_2}{(2\pi)^3 2k_{2,4}} \frac{d^3 k_3}{(2\pi)^3 2k_{3,4}} (2\pi)^4 \delta^{(4)}(p - k_1 - k_2 - k_3) = \frac{M^2}{128\pi^3} \int_0^1 dx \int_{1-x}^1 dy \quad (\text{F.7})$$

with

$$\cos\theta_{12} = \frac{2(1 - x - y) + xy}{xy} \quad (\text{F.8})$$

## F.4 Complex conjugates in Pauli notation

According to our definition of 4-momentum, the time component is imaginary, meaning that when we take the complex conjugate,  $p_\mu^* = (-1)^{\delta_{\mu 4}} p_\mu$  for any  $p_\mu$ . We can check that every time component minus sign that comes out of the complex conjugate will eventually disappear. This makes sense, as the presence of these phases in the momentum is only due to our choice of notation, hence the final result must not be affected by them<sup>53</sup>.

Let us define the generic phase  $\alpha_p = (-1)^{\delta_{\alpha 4}}$  for simplicity. Obviously  $\alpha_p^2 = 1$ , as it is a real number. So, in order to check that all minus signs disappear, we just have to pair them up. Let us see where they pop up:

- In the polarizations, as we extensively explain in subsection C.2, taking the barred and taking the complex conjugate lead to an extra minus sign in the time component:

$$\varepsilon_\gamma^* = \gamma_p \bar{\varepsilon}_\gamma \quad \bar{\varepsilon}'_\lambda^* = \lambda_p \varepsilon'_\lambda \quad \varepsilon_{\mu\nu}^* = \mu_p \nu_p \bar{\varepsilon}_{\mu\nu} \quad (\text{F.9})$$

- From Equation C.16:

$$\gamma_4 (\gamma_\delta)^\dagger \gamma_4 = -\delta_p \gamma_\delta \quad (\text{F.10})$$

- Also from the exposed momentum:

$$(p'_\theta + p_\theta)^* = \theta_p (p'_\theta + p_\theta) \quad (\text{F.11})$$

- A useful trick is:

$$\delta_{\mu\nu} \mu_p \nu_p = \delta_{\mu\nu} (-1)^{\delta_{\mu 4}} (-1)^{\delta_{\nu 4}} = \delta_{\mu\nu} \left[ (-1)^{\delta_{\mu 4}} \right]^2 = \delta_{\mu\nu} \quad (\text{F.12})$$

because trivially  $(\mu_p)^2 = 1$

- In  $N_{\zeta\tau\delta\theta}^*(k - k')$  momenta are everywhere. If we define  $q = k - k'$ :

$$N_{\zeta\tau\delta\theta}^*(q) = \left[ \frac{1}{2} \left( P_{\zeta\delta}^* P_{\tau\theta}^* + P_{\zeta\theta}^* P_{\tau\delta}^* \right) - \frac{1}{3} P_{\zeta\tau}^* P_{\delta\theta}^* \right] (q)$$

Take, for example,  $P_{\zeta\delta}^* P_{\tau\theta}^*$ . If we use our trick Equation F.12:

$$\begin{aligned} P_{\zeta\delta}^* P_{\tau\theta}^* &= \left( \delta_{\zeta\delta} + \frac{q_\zeta^* q_\delta^*}{m_X^2} \right) \left( \delta_{\tau\theta} + \frac{q_\tau^* q_\theta^*}{m_X^2} \right) = \\ &= \left( \delta_{\zeta\delta} + \zeta_p \delta_p \frac{q_\zeta q_\delta}{m_X^2} \right) \left( \delta_{\tau\theta} + \tau_p \theta_p \frac{q_\tau q_\theta}{m_X^2} \right) = \\ &= \zeta_p \delta_p \tau_p \theta_p \left( \delta_{\zeta\delta} + \frac{q_\zeta q_\delta}{m_X^2} \right) \left( \delta_{\tau\theta} + \frac{q_\tau q_\theta}{m_X^2} \right) = \zeta_p \delta_p \tau_p \theta_p P_{\zeta\delta} P_{\tau\theta} \end{aligned} \quad (\text{F.13})$$

which then simply tells us:

$$N_{\zeta\tau\delta\theta}^*(q) = \zeta_p \tau_p \delta_p \theta_p N_{\zeta\tau\delta\theta}(q) \quad (\text{F.14})$$

- The same trick Equation F.12 can be used for the Feynman rule for the photon coupling to  $X$  resonance:

$$\begin{aligned} \Pi_{\zeta\tau\gamma\lambda}^*(k_1, k_2) &= \delta_{\gamma\lambda} \zeta_p \tau_p (k_{1,\zeta} k_{2,\tau} + k_{1,\tau} k_{2,\zeta}) - \delta_{\zeta\gamma} \lambda_p \tau_p k_{1,\lambda} k_{2,\tau} - \delta_{\zeta\lambda} \tau_p \gamma_p k_{1,\tau} k_{2,\gamma} \\ &\quad - \delta_{\tau\lambda} \zeta_p \gamma_p k_{1,\zeta} k_{2,\gamma} - \delta_{\tau\gamma} \lambda_p \zeta_p k_{1,\lambda} k_{2,\zeta} + k_1 \cdot k_2 (\delta_{\zeta\lambda} \delta_{\tau\gamma} + \delta_{\tau\lambda} \delta_{\zeta\gamma}) \\ &\quad + \frac{1}{\xi} [ -\delta_{\zeta\gamma} \lambda_p \tau_p k_{2,\lambda} k_{2,\tau} - \delta_{\zeta\lambda} \tau_p \gamma_p k_{1,\tau} k_{1,\gamma} - \delta_{\tau\lambda} \zeta_p \gamma_p k_{1,\zeta} k_{1,\gamma} - \delta_{\tau\gamma} \lambda_p \zeta_p k_{2,\lambda} k_{2,\zeta} ] = \\ &= \zeta_p \tau_p \gamma_p \lambda_p \left\{ \delta_{\gamma\lambda} (k_{1,\zeta} k_{2,\tau} + k_{1,\tau} k_{2,\zeta}) - \delta_{\zeta\gamma} k_{1,\lambda} k_{2,\tau} - \delta_{\zeta\lambda} k_{1,\tau} k_{2,\gamma} \right. \\ &\quad \left. - \delta_{\tau\lambda} k_{1,\zeta} k_{2,\gamma} - \delta_{\tau\gamma} k_{1,\lambda} k_{2,\zeta} + k_1 \cdot k_2 (\delta_{\zeta\lambda} \delta_{\tau\gamma} + \delta_{\tau\lambda} \delta_{\zeta\gamma}) \right. \\ &\quad \left. + \frac{1}{\xi} [ -\delta_{\zeta\gamma} k_{2,\lambda} k_{2,\tau} - \delta_{\zeta\lambda} k_{1,\tau} k_{1,\gamma} - \delta_{\tau\lambda} k_{1,\zeta} k_{1,\gamma} - \delta_{\tau\gamma} k_{2,\lambda} k_{2,\zeta} ] \right\} = \\ &= \zeta_p \tau_p \gamma_p \lambda_p \Pi_{\zeta\tau\gamma\lambda}(k_1, k_2) \end{aligned} \quad (\text{F.15})$$

If you take any combination together, all the minus signs disappear.

<sup>53</sup>which is also why we have chosen this notation in the first place.

## F.5 Evaluation of decay rate using only 4-vertex interaction

In subsection 5.2 we said that the 4-vertex interaction is not a radiative correction, and were us to consider only that interaction, decay  $X \rightarrow e^+e^-\gamma$  would be finite (but not gauge invariant, of course, and wrong). Let us now singularly evaluate the following diagram contribution to the decay rate  $X \rightarrow e^+e^-\gamma$ :

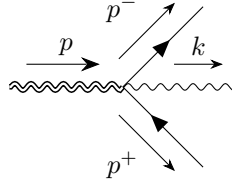


Figure 56: Diagram corresponding to the four vertex interaction in the tree level decay  $X \rightarrow e^+e^-\gamma$ .

Using Feynman rule in Equation 4.59, we write down the amplitude for the decay of  $X$  into electron, positron and photon, at tree level. Since symmetrizing does not really make any difference in the final result, we write the amplitude of the decay directly as:

$$A = -i \frac{g_e e}{\Lambda} \gamma_\mu \varepsilon_\nu(k, \lambda) \varepsilon_{\mu\nu}(p, \eta) \quad (\text{F.16})$$

$$\mathcal{A} = \bar{u}(p^-, s^-) A v(p^+, s^+) = \bar{u} A v \quad (\text{F.17})$$

where  $p$  is the  $X$  momentum and  $\eta$  is its polarization,  $p^\pm$  are the momenta of the electron and positron,  $s^\pm$  are their polarizations, and  $k$  is the momentum of the photon and  $\lambda$  its polarization. Hereafter, we are going to refer to polarizations as  $\varepsilon_{\mu\nu}, \varepsilon_\nu, u, v$ . With our notation, the complex conjugate is obtained using Equation 5.3:

$$\mathcal{A}^* = \bar{v} B u \quad B = \gamma_4 A^\dagger \gamma_4$$

Evaluation of complex conjugation done using the Appendix subsection F.4. The phases coming out from boson polarization, momentum, and gamma matrices commutation rules all cancel, leaving:

$$B = i \frac{g_e e}{\Lambda} \mu_p \nu_p \bar{\varepsilon}_{\mu\nu} \nu_p \bar{\varepsilon}_\nu (-\mu_p \gamma_\mu) = -i \frac{g_e e}{\Lambda} \bar{\varepsilon}_{\mu\nu} \bar{\varepsilon}_\nu \gamma_\mu \quad (\text{F.18})$$

Putting it all together:

$$|\mathcal{A}|^2 = -\frac{g_e^2 e^2}{\Lambda^2} \varepsilon_{\mu\nu} \bar{\varepsilon}_{\rho\sigma} \varepsilon_\nu \bar{\varepsilon}_\sigma \text{Tr} [\gamma_\mu (v \bar{v}) \gamma_\rho (u \bar{u})] \quad (\text{F.19})$$

Sum over  $X$  and fermions polarizations only (averaging over initial 5 polarizations of  $X$ ) (we will sum over photon polarizations later):

$$\begin{aligned} |\overline{\mathcal{A}}|^2 &= \frac{1}{5} \sum_{\eta, s^\pm} |\mathcal{A}|^2 = -\frac{g_e^2 e^2}{5\Lambda^2} N_{\mu\nu\rho\sigma}(p) \varepsilon_\nu \bar{\varepsilon}_\sigma \text{Tr} \left[ \gamma_\mu \left( \frac{-i\cancel{p}^+ - m_e}{2p_4^+} \right) \gamma_\rho \left( \frac{-i\cancel{p}^- + m_e}{2p_4^-} \right) \right] = \\ &= -\frac{g_e^2 e^2}{20\Lambda^2} \frac{1}{p_4^+ p_4^-} N_{\mu\nu\rho\sigma}(p) \varepsilon_\nu \bar{\varepsilon}_\sigma \text{Tr} \left[ \gamma_\mu (-i\cancel{p}^+ - m_e) \gamma_\rho (-i\cancel{p}^- + m_e) \right] \end{aligned} \quad (\text{F.20})$$

where  $m_e$  is the mass of the electron. Having  $2p_4$  at denominator means we will not have to have  $2p_4$  in the phase space integral denominator. Note that, instead, photon phase space integration will require a  $1/2k_4$ .

The modulus squared has been calculated with the software tool FORM, which makes use of the Dutch metric in its calculations (which is why we employ it here). The code can be found in the repository linked in subsection G.1 (program is `spin2Decayeeegamma_4vertex.frm`). Using real polarizations throughout, the result is:

$$|\overline{\mathcal{A}}|^2 = -\frac{g_e^2 e^2}{20\Lambda^2} \frac{1}{p_4^+ p_4^-} \left[ -\frac{4(p \cdot p^+)(p \cdot p^-)}{m_X^2} + \frac{8}{3} p^+ \cdot p^- - \frac{20}{3} m_e^2 - \frac{4}{3} (p^+ \cdot \varepsilon)(p^- \cdot \varepsilon) \right] \quad (\text{F.21})$$

In addition to  $k \cdot \varepsilon = 0$ , we used the axial gauge for which  $\varepsilon_4 = 0$ . This implies that  $p \cdot \varepsilon = 0$ , which is a very important simplification in the rest frame of the decaying  $X$ .

Equation F.21 is actually more complicated than it looks, because kinematics is much less stringent. To simplify result, we are going to assume  $m_X \gg m_e$ , so that this process is now a 3-body decay into massless

states. Final result of the decay rate (not summing photon polarizations) gets easier:

$$\begin{aligned}
\Gamma_\lambda(X \rightarrow e^+ e^- \gamma) &= \frac{1}{2m_X} \int \frac{d^3 p^+}{(2\pi)^3 2p_4^+} \frac{d^3 p^-}{(2\pi)^3 2p_4^-} \frac{d^3 k}{(2\pi)^3 2k_4} (2\pi)^4 \delta^{(4)}(p - k - p^+ - p^-) \times 4p_4^+ p_4^- |\bar{\mathcal{A}}|^2 = \\
&= \frac{1}{2m_X} \frac{m_X^2}{128\pi^3} \int_0^1 dx \int_{1-x}^1 dy 4p_4^+ p_4^- |\bar{\mathcal{A}}|^2 = \\
&= \frac{m_X}{64\pi^3} \int_0^1 dx \int_{1-x}^1 dy \left\{ \frac{g_e^2 e^2}{20\Lambda^2} \left[ \frac{4(p \cdot p^+)(p \cdot p^-)}{m_X^2} - \frac{8}{3} p^+ \cdot p^- + \cancel{\frac{20}{3} m_e^2} + \frac{4}{3} (p^+ \cdot \varepsilon)(p^- \cdot \varepsilon) \right] \right\}
\end{aligned} \tag{F.22}$$

where we have used result in [subsection F.3](#) ([Equation F.7](#)). We have defined  $p_4^- = E_-$ ,  $p_4^+ = E_+$ . Then, we have introduced the adimensional variables  $x = 2E_-/m_X$  and  $y = 2E_+/m_X$ .

So, our next step is to express scalar products in kinematics in [Equation F.21](#) in terms of  $x$  and  $y$ . The easiest frame to work with is the rest frame of the  $X$ , where  $p = (\vec{0}, im_X)$ .

$$p \cdot p^- = -m_X E_- = -\frac{m_X^2}{2} x \quad p \cdot p^+ = -m_X E_+ = -\frac{m_X^2}{2} y$$

$$\begin{aligned}
p^+ \cdot p^- &= \frac{(p^+ + p^-)^2 - (p^+)^2 - (p^-)^2}{2} = \frac{(p - k)^2}{2} = -\frac{m_X^2}{2} - p \cdot k = -\frac{m_X^2}{2} + m_X k_4 \\
&= -\frac{m_X^2}{2} + m_X (m_X - E_- - E_+) = \frac{m_X^2}{2} \left( 1 - \frac{2E_-}{m_X} - \frac{2E_+}{m_X} \right) \\
&= \frac{m_X^2}{2} (1 - x - y)
\end{aligned}$$

$$\hat{k} = \frac{\vec{k}}{|\vec{k}|} = \frac{\vec{p}_+ - \vec{p}_- - \vec{p}_+}{k_4} = -\frac{\vec{p}_- + \vec{p}_+}{m_X - E_- - E_+} = -\frac{2(\vec{p}_- + \vec{p}_+)}{m_X(2 - x - y)}$$

Now, sum over photon polarizations. Because the result is not gauge invariant, we cannot use the trick employed in [subsection 5.2](#), so we have to calculate the full sum over polarizations. Terms that do not contain  $\varepsilon$  get a factor of two. Instead, for the term that contains it, we:

$$\sum_\lambda (p^+ \cdot \varepsilon)(p^- \cdot \varepsilon) = p_i^+ p_j^- (\delta_{ij} - \hat{k}_i \hat{k}_j) = \vec{p}_+ \cdot \vec{p}_- - (\vec{p}_- \cdot \hat{k}) (\vec{p}_+ \cdot \hat{k})$$

Let us calculate it, using the expression for  $\cos \theta_{12}$  in [Equation F.8](#):

$$\begin{aligned}
\vec{p}_+ \cdot \vec{p}_- &= |\vec{p}_+| |\vec{p}_-| \cos \theta_{12} = E_- E_+ \cos \theta_{12} = \frac{m_X^2}{4} xy \cos \theta_{12} = \\
&= \frac{m_X^2}{4} [2(1 - x - y) + xy]
\end{aligned}$$

$$\begin{aligned}
\vec{p}_- \cdot \hat{k} &= -\frac{2(|\vec{p}_-|^2 + \vec{p}_+ \cdot \vec{p}_-)}{m_X(2 - x - y)} = \frac{-2E_-^2 - 2m_X^2/4 [2(1 - x - y) + xy]}{m_X(2 - x - y)} = \\
&= -\frac{m_X}{2} \left[ \frac{x^2 + 2(1 - x - y) + xy}{2 - x - y} \right] = -\frac{m_X}{2} \left[ \frac{(x+y)(x+y-2) + 2 - y(x+y)}{2 - x - y} \right] = \\
&= \frac{m_X}{2} \left[ x + y + \frac{y(x+y)-2}{2 - x - y} \right]
\end{aligned}$$

$$\vec{p}_+ \cdot \hat{k} = \dots = \frac{m_X}{2} \left[ x + y + \frac{x(x+y)-2}{2 - x - y} \right]$$

Joining results together:

$$\begin{aligned}
\sum_{\lambda} (p^+ \cdot \varepsilon)(p^- \cdot \varepsilon) &= \frac{m_X^2}{4} \left[ x + y + \frac{y(x+y)-2}{2-x-y} \right] \left[ x + y + \frac{x(x+y)-2}{2-x-y} \right] = \\
&= \frac{m_X^2}{4} \left\{ (x+y)^2 + \frac{x+y}{2-x-y} [x(x+y)-2+y(x+y)-2] + \frac{[x(x+y)-2][y(x+y)-2]}{(2-x-y)^2} \right\} = \\
&= \frac{m_X^2}{4} \left[ (x+y)^2 + \frac{(x+y)(x+y-2)(x+y+2)}{2-x-y} + \frac{xy(x+y)^2 - 2x(x+y) - 2y(x+y) + 4}{(2-x-y)^2} \right] = \\
&= \frac{m_X^2}{4} \left[ (x+y)^2 - (x+y)(x+y+2) + \frac{(xy-2)(x+y)^2 + 4}{(2-x-y)^2} \right] = \\
&= \frac{m_X^2}{4} \left[ -2(x+y) + \frac{(xy-2)(x+y)^2 + 4}{(2-x-y)^2} \right]
\end{aligned} \tag{F.23}$$

And we can add results to [Equation F.22](#), to get:

$$\begin{aligned}
\Gamma(X \rightarrow e^+ e^- \gamma) &= \sum_{\lambda} \Gamma_{\lambda}(X \rightarrow e^+ e^- \gamma) = \\
&= \frac{m_X g_e^2 e^2}{64\pi^3 20\Lambda^2} \int_0^1 dx \int_{1-x}^1 dy \left[ \sum_{\lambda} \frac{4(p \cdot p^+)(p \cdot p^-)}{m_X^2} - \frac{8}{3} \sum_{\lambda} p^+ \cdot p^- + \frac{4}{3} \sum_{\lambda} (p^+ \cdot \varepsilon)(p^- \cdot \varepsilon) \right] = \\
&= \frac{g_e^2 e^2 m_X}{1280\pi^3 \Lambda^2} \int_0^1 dx \int_{1-x}^1 dy \left\{ 2m_X^2 xy - \frac{16}{3} \frac{m_X^2}{2} (1-x-y) + \frac{4}{3} \frac{m_X^2}{4} \left[ -2(x+y) + \frac{(xy-2)(x+y)^2 + 4}{(2-x-y)^2} \right] \right\} = \\
&= \frac{g_e^2 e^2 m_X^3}{3840\pi^3 \Lambda^2} \int_0^1 dx \int_{1-x}^1 dy \left[ 6xy - 8(1-x-y) + \frac{(xy-2)(x+y)^2 + 4}{(2-x-y)^2} \right]
\end{aligned} \tag{F.24}$$

Integration has been performed with this [Integral Calculator](#). Focusing on integrals only:

$$\begin{aligned}
&\int_0^1 dx \int_{1-x}^1 dy \left[ 6xy - 8(1-x-y) + \frac{(xy-2)(x+y)^2 + 4}{(2-x-y)^2} \right] = \\
&= \int_0^1 dx \left[ -4(x-2)(x-1) \log |2-x-y| + \frac{4(x-1)^2}{x+y-2} + (12x-10)y + (7x+8)\frac{y^2}{2} \right]_{1-x}^1 = \\
&= \int_0^1 dx \left[ -4(x-2)(x-1) \log |1-x| + 4(x-1)^2 \frac{x}{x-1} + (12x-10)x + (7x+8) \left( x - \frac{x^2}{2} \right) \right] = \\
&= \int_0^1 dx \left[ -4(x-2)(x-1) \log |1-x| - \frac{7x^3}{2} + 19x^2 - 6x \right] = \frac{281}{72}
\end{aligned} \tag{F.25}$$

which does not diverge thanks to the factors  $(x-1)^n$  that cancel logarithmic divergences in the expression ([it took me two days to get this simplification](#)). Substituting [Equation F.25](#) into [Equation F.24](#), we get the final result:

$$\Gamma(X \rightarrow e^+ e^- \gamma) = \frac{281e^2}{276480\pi^3} \frac{g_e^2 m_X^3}{\Lambda^2} = \frac{281}{69120\pi^2} \frac{\alpha g_e^2 m_X^3}{\Lambda^2} = \left( \frac{\alpha}{2\pi} \right) \frac{281}{864\pi} \Gamma(X \rightarrow e^+ e^-) \tag{F.26}$$

which is convergent and not log divergent when  $m_e \rightarrow 0$ , as expected.

## F.6 On helicity flip

In theories where the interaction between fermions is mediated by Dirac bilinears, one could ask whether chirality is conserved by the interaction. This is the case for vector theories, where an odd number of gamma matrices appears. For example, let us look at  $\bar{\psi}\gamma_\mu\psi$  terms. Select a specific chirality, using projectors from [Equation 3.7](#), as  $\psi_L = P_L\psi$  and  $\psi_R = P_R\psi$ , hermiticity of gamma matrices and [Equation 3.6](#):

$$\begin{aligned}\bar{\psi}_L\gamma_\mu\psi_R &= \bar{\psi}_L^\dagger\gamma_4\gamma_\mu\psi_L = (P_L\psi)^\dagger\gamma_4\gamma_\mu P_R\psi = \\ &= \bar{\psi}^\dagger\left(\frac{\mathbb{1}_4 + \gamma_5}{2}\right)^\dagger\gamma_4\gamma_\mu P_R\psi = \bar{\psi}^\dagger\left(\frac{\mathbb{1}_4 + \gamma_5}{2}\right)\gamma_4\gamma_\mu P_R\psi \\ &= \bar{\psi}^\dagger\gamma_4\left(\frac{\mathbb{1}_4 - \gamma_5}{2}\right)\gamma_\mu P_R\psi = \bar{\psi}^\dagger\gamma_4\gamma_\mu\left(\frac{\mathbb{1}_4 - \gamma_5}{2}\right)P_R\psi = \\ &= \bar{\psi}\gamma_\mu P_L P_R\psi\end{aligned}$$

where because of orthogonality:

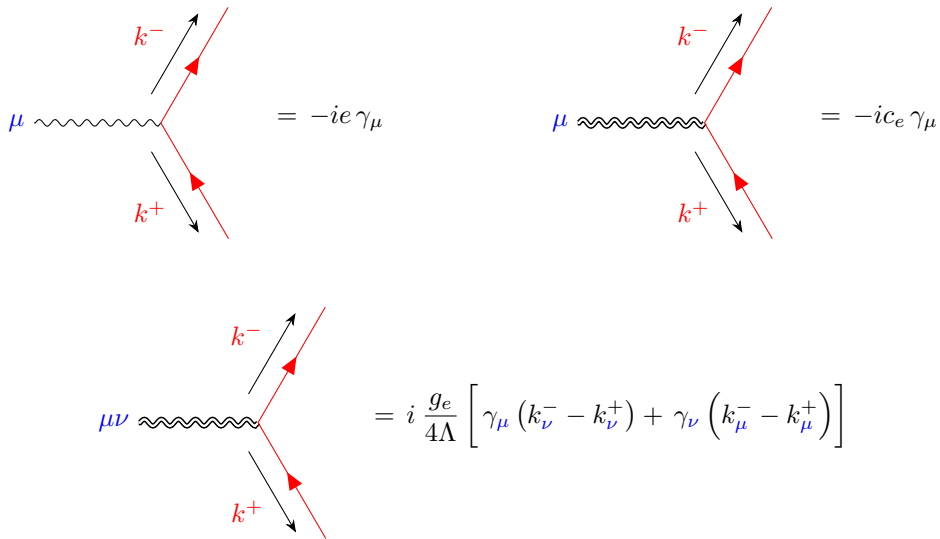
$$P_L P_R = \left(\frac{\mathbb{1}_4 + \gamma_5}{2}\right)\left(\frac{\mathbb{1}_4 - \gamma_5}{2}\right) = \frac{\mathbb{1}_4 - \gamma_5\gamma_5}{4} = 0$$

so, in the end:

$$\bar{\psi}_L\gamma_\mu\psi_R = \bar{\psi}_R\gamma_\mu\psi_L = 0 \quad \bar{\psi}_L\gamma_\mu\psi_L \neq 0 \quad \bar{\psi}_R\gamma_\mu\psi_R \neq 0 \quad (\text{F.27})$$

So, odd gamma interactions do not allow for chirality flips between fermions. In any scattering process where the same fermion is present in the initial and final state, its chirality is conserved. In the same way, fermions and anti fermions can only interact if they have the same chirality. In short, *there cannot be chirality flips caused by interaction terms described by a Dirac bilinear with an odd number of gamma matrices*.

This is the case for QED, and both our spin 1 and spin 2 toy models:



In every instance, a single gamma matrix enters in the Feynman rule, and so in every interaction that builds these vertices there must be a structure like  $\bar{\psi}\gamma_\mu\psi$  (indeed, this is the case. Look at [Equation 8.5](#) and [Equation 4.55](#)).

In the massless limit (or in the ultra-relativistic limit), chirality and helicity have a 1 : 1 correspondence. They are not the same, as it is often misinterpreted:

- *Helicity* is a property of kinematics and spin. It is a constant of motion, but it is not Lorentz invariant (boosting can flip helicity in massive particles).  
A particle with negative helicity has antiparallel spin projection and momentum (call its spinor  $u_-$  or  $v_-$ ) and a particle with positive helicity has parallel spin projection and momentum (call its spinor  $u_+$  or  $v_+$ ).
- *Chirality* is a property of the field itself. It is Lorentz invariant, but it is not necessarily a constant of motion. Eigenstates of  $P_L$  are left chirality fields, and eigenstates of  $P_R$  are right chirality fields.
- In the massless limit ( $\gamma \rightarrow \infty$ ), helicity becomes Lorentz invariant (boosting can no longer flip helicity) and chirality becomes a constant of motion. The two are now correspondent.

- For massless particles, left chirality implies negative helicity and right chirality implies positive helicity. In its field expansion:

$$u_- \in \psi_L \quad u_+ \in \psi_R$$

- For massless antiparticles, left chirality implies right helicity and right chirality implies left helicity. In its field expansion:

$$v_+ \in \psi_L \quad v_- \in \psi_R$$

So, like chirality can never flip in our toy models, so does helicity: in any scattering process where the same fermion is present in the initial and final state, its helicity is conserved. In formulas, from [Equation F.27](#):

$$\begin{aligned} \bar{\psi}_L \gamma_\mu \psi_R &= 0 & \Rightarrow & \bar{u}_- \gamma_\mu u_+ = \bar{v}_+ \gamma_\mu v_- = 0 \\ \bar{\psi}_R \gamma_\mu \psi_L &= 0 & \Rightarrow & \bar{u}_+ \gamma_\mu u_- = \bar{v}_- \gamma_\mu v_+ = 0 \end{aligned}$$

In the same way, fermions and anti fermions can only interact if they have opposite helicity. In formulas:

$$\begin{aligned} \bar{\psi}_L \gamma_\mu \psi_R &= 0 & \Rightarrow & \bar{u}_- \gamma_\mu v_- = \bar{v}_+ \gamma_\mu u_+ = 0 \\ \bar{\psi}_R \gamma_\mu \psi_L &= 0 & \Rightarrow & \bar{u}_+ \gamma_\mu v_+ = \bar{v}_- \gamma_\mu u_- = 0 \end{aligned}$$

In a nutshell: *in the ultra-relativistic regime, there cannot be helicity flips caused by interaction terms described by QED or our toy models.* In other words, *in any amplitude we wrote in this thesis, the contribution given by fermion helicity flipping terms is proportional to the mass of the fermions.*

## F.7 Useful photon polarization sums in Compton scattering

We report here the results of useful photon polarization sums, obtained by fixing  $\varepsilon_4 = \varepsilon'_4 = 0$  for every photon polarization (nonphysical time component). Remember the polarization rule from [Equation C.32](#):

$$\sum_{\lambda} \varepsilon_i(k, \lambda) \varepsilon_j(k, \lambda) = \delta_{ij} - \frac{k_i k_j}{|\vec{k}|^2} = \delta_{ij} - \hat{k}_i \hat{k}_j \quad (\text{F.28})$$

$$\sum_{\lambda'} \varepsilon_i(k', \lambda') \varepsilon_j(k', \lambda') = \delta_{ij} - \frac{k'_i k'_j}{|\vec{k}'|^2} = \delta_{ij} - \hat{k}'_i \hat{k}'_j \quad (\text{F.29})$$

Use the fact that  $|\hat{k}|^2 = |\hat{k}'|^2 = 1$ <sup>54</sup>, and  $\hat{k} \cdot \hat{k}' = \cos \theta$ , where  $\theta$  is scattering angle in Compton effect.

Let us use this to calculate the contributions for each needed term in [subsection 9.2](#):

$$\sum_{\lambda, \lambda'} (k' \cdot \varepsilon)^2 = 2 \sum_{\lambda} (k' \cdot \varepsilon)^2 = 2 k'_i k'_j (\delta_{ij} - \hat{k}'_i \hat{k}'_j) = 2 \omega'^2 (1 - \cos^2 \theta) \quad (\text{F.30})$$

$$\sum_{\lambda, \lambda'} (k \cdot \varepsilon')^2 = 2 \sum_{\lambda'} (k \cdot \varepsilon')^2 = 2 k_i k_j (\delta_{ij} - \hat{k}_i \hat{k}_j) = 2 \omega^2 (1 - \cos^2 \theta) \quad (\text{F.31})$$

$$\begin{aligned} \sum_{\lambda, \lambda'} (\varepsilon \cdot \varepsilon')^2 &= (\delta_{ij} - \hat{k}_i \hat{k}_j) (\delta_{ij} - \hat{k}'_i \hat{k}'_j) = \\ &= 3 - |\hat{k}|^2 - |\hat{k}'|^2 + (\hat{k} \cdot \hat{k}')^2 = 1 + \cos^2 \theta \end{aligned} \quad (\text{F.32})$$

$$\begin{aligned} \sum_{\lambda, \lambda'} (k' \cdot \varepsilon) (k \cdot \varepsilon') (\varepsilon \cdot \varepsilon') &= \sum_{\lambda, \lambda'} k_i \varepsilon'_i k'_j \varepsilon_j \varepsilon_k \varepsilon'_k = k_i k'_j (\delta_{jk} - \hat{k}_j \hat{k}_k) (\delta_{ik} - \hat{k}'_i \hat{k}'_k) = \\ &= k_i k'_j \left[ \delta_{ij} - \hat{k}_i \hat{k}_j - \hat{k}'_i \hat{k}'_j + \hat{k}'_i \hat{k}_j (\hat{k} \cdot \hat{k}') \right] = \\ &= (k \cdot k') - |\vec{k}| (\hat{k} \cdot \hat{k}') - |\vec{k}'| (k \cdot \hat{k}') + (k \cdot \hat{k}') (\hat{k} \cdot \hat{k}') = \\ &= \omega \omega' \cos \theta - \omega \omega' \cos \theta - \omega \omega' \cos \theta + \omega \omega' \cos^3 \theta = \\ &= -\omega \omega' \cos \theta (1 - \cos^2 \theta) \end{aligned} \quad (\text{F.33})$$

$$\begin{aligned} \sum_{\lambda, \lambda'} (k' \cdot \varepsilon)^2 (k \cdot \varepsilon')^2 &= \sum_{\lambda, \lambda'} k_i \varepsilon'_i k_j \varepsilon'_j k'_k \varepsilon_k k'_l \varepsilon_l = k_i k_j k'_k k'_l (\delta_{ij} - \hat{k}'_i \hat{k}'_j) (\delta_{kl} - \hat{k}_k \hat{k}_l) = \\ &= k_i k_j k'_k k'_l \left[ \delta_{ij} \delta_{kl} - \delta_{kl} \hat{k}'_i \hat{k}'_j - \delta_{ij} \hat{k}_k \hat{k}_l + \hat{k}'_i \hat{k}'_j \hat{k}_k \hat{k}_l \right] = \\ &= |\vec{k}|^2 |\vec{k}'|^2 - |\vec{k}'|^2 (k \cdot \hat{k}')^2 - |\vec{k}|^2 (\hat{k} \cdot \hat{k}')^2 + (k \cdot \hat{k}')^2 (\hat{k} \cdot \hat{k}')^2 = \\ &= \omega^2 \omega'^2 - \omega^2 \omega'^2 \cos^2 \theta - \omega^2 \omega'^2 \cos^2 \theta + \omega^2 \omega'^2 \cos^4 \theta = \\ &= \omega^2 \omega'^2 (1 - \cos^2 \theta)^2 \end{aligned} \quad (\text{F.34})$$

---

<sup>54</sup>remember that we are dealing with the spatial part only, so  $|\vec{k}| = \omega$ ,  $|\vec{k}'| = \omega'$ . We will be using spatial indices only, labeled with  $i, j, k, l$ .

## F.8 Positronium in quantum mechanics

The goal of this Appendix is to justify the formulas we used for the wavefunction of the system and the relative electron and positron velocities, in the non relativistic limit, used in [subsection 10.1](#). Start with a generic Hamiltonian with a spherically symmetric potential for a particle of mass  $M$ :

$$H = \frac{p^2}{2M} + V(r) \quad (\text{F.35})$$

Where in natural units,  $p^2 = -\nabla^2$ . In spherical coordinates, the Laplacian operator becomes:

$$\begin{aligned} \nabla^2 &= \frac{\partial^2}{\partial r^2} + \frac{2}{r} \frac{\partial}{\partial r} + \frac{1}{r^2} \left[ \frac{\partial^2}{\partial \theta^2} + \frac{\cos \theta}{\sin \theta} \frac{\partial}{\partial \theta} + \frac{1}{\sin^2 \theta} \frac{\partial^2}{\partial \phi^2} \right] = \\ &= \frac{\partial^2}{\partial r^2} + \frac{2}{r} \frac{\partial}{\partial r} - \frac{L^2}{r^2} \end{aligned} \quad (\text{F.36})$$

and  $L^2 = |\vec{L}|^2$  is the squared modulus of the angular momentum operator.

This means that if we want to write down the most general eigenfunction for the Schrödinger equation in spherical coordinates  $\psi(r, \theta, \phi)$ , then the equation becomes:

$$\left[ -\frac{1}{2M} \left( \frac{\partial^2}{\partial r^2} + \frac{2}{r} \frac{\partial}{\partial r} \right) + \frac{L^2}{2Mr^2} + V(r) \right] \psi(r, \theta, \phi) = E \psi(r, \theta, \phi) \quad (\text{F.37})$$

Since spherical harmonics  $Y_l^m(\theta, \phi)$  are the eigenfunctions of the angular momentum operator...

$$\begin{cases} L^2 Y_l^m(\theta, \phi) = l(l+1) Y_l^m(\theta, \phi) \\ L_z Y_l^m(\theta, \phi) = m Y_l^m(\theta, \phi) \end{cases}$$

... then we can again separate the Hamiltonian into angular and radial part by defining our solution to be:

$$\psi(r, \theta, \phi) = \frac{u(r)}{r} Y_l^m(\theta, \phi) \quad (\text{F.38})$$

This cancels dependence on  $\theta, \phi$  of the problem. Also, if we evaluate:

$$\begin{aligned} \left( \frac{\partial^2}{\partial r^2} + \frac{2}{r} \frac{\partial}{\partial r} \right) \frac{u(r)}{r} &= \frac{1}{r} \frac{\partial^2}{\partial r^2} u(r) + 2 \frac{\partial}{\partial r} \left( \frac{1}{r} \right) \frac{\partial}{\partial r} u(r) + \frac{\partial^2}{\partial^2 r} \left( \frac{1}{r} \right) u(r) + \frac{2}{r} \frac{\partial}{\partial r} u(r) + \frac{2}{r} \frac{\partial}{\partial r} \left( \frac{1}{r} \right) u(r) = \\ &= \frac{1}{r} \frac{\partial^2}{\partial r^2} u(r) - \frac{2}{r^2} \frac{\partial}{\partial r} u(r) + \frac{2}{r^3} u(r) + \frac{2}{r^2} \frac{\partial}{\partial r} u(r) - \frac{2}{r^3} u(r) = \\ &= \frac{1}{r} \frac{\partial^2}{\partial r^2} u(r) \end{aligned}$$

Hence, we only have an equation for  $u(r)$ :

$$\left[ -\frac{1}{2M} \frac{\partial^2}{\partial r^2} + \frac{l(l+1)}{2Mr^2} + V(r) \right] u(r) = E u(r) \quad (\text{F.39})$$

where the angular momentum part has been translated into the apparent centrifugal potential.

Now, take the Hamiltonian in [Equation 10.26](#):

$$H = \frac{p^2}{2\mu} - \frac{\alpha}{r}$$

where the mass is the reduced mass of the electron positron system  $\mu = m_e/2$ , and the potential is the Coulomb potential. In spherical coordinates, the equation becomes:

$$\left[ -\frac{1}{2\mu} \frac{\partial^2}{\partial r^2} + \frac{l(l+1)}{2\mu r^2} - \frac{\alpha}{r} - E \right] u(r) = 0 \quad (\text{F.40})$$

define the adimensional variable  $\rho = r\sqrt{2\mu|E|}$ :

$$\left[ \frac{\partial^2}{\partial\rho^2} - \frac{l(l+1)}{\rho^2} - \frac{\lambda}{r} - 1 \right] u(r) = 0 \quad (\text{F.41})$$

where  $\lambda = \alpha\sqrt{2\mu/|E|}$ .

To solve the equation, formulate an ansatz:  $u(\rho) = f(\rho)e^{-\rho}$ , because of the second order differential equation. Substituting into [Equation F.41](#), we get an equation for  $f$ :

$$\begin{aligned} u' &= f'e^{-\rho} - fe^{-\rho} \\ u'' &= f''e^{-\rho} - 2f'e^{-\rho} + fe^{-\rho} \\ f''(\rho) - 2f'(\rho) + \left( \frac{\lambda}{\rho} - \frac{l(l+1)}{\rho^2} \right) f(\rho) &= 0 \end{aligned} \quad (\text{F.42})$$

To find a solution for  $f$ , consider.

- for larger  $\rho$ , we can neglect the centrifugal term and  $f''$ , so that the equation becomes:

$$2f' = \frac{\lambda}{\rho} f \quad \Rightarrow \quad f \propto \rho^{\frac{\lambda}{2}}$$

- for smaller  $\rho$ , a well known behavior of Schrödinger wavefunctions on a centrifugal potential wall (here dominating for  $\rho \rightarrow 0$ ) is  $u \propto \rho^{l+1}$ .
- then, we formulate a solution that is a power series that recovers the aforementioned behavior for  $\rho \rightarrow 0$  and  $\rho \rightarrow \infty$ :

$$u(\rho) = e^{-\rho} f(\rho) = e^{-\rho} \sum_{k=0}^{\infty} c_k \rho^{l+k+1} \quad (\text{F.43})$$

into [Equation F.42](#), we get a recursive equation:

$$\begin{aligned} &\cancel{[c_0 l(l+1) - e_0 l(l+1)]} \rho^{l-1} + \\ &+ \sum_{k=0}^{\infty} [c_{k+1}(l+k+1)(l+k+2) - 2c_k(l+k+1) + c_k\lambda - l(l+1)c_{k+1}] \rho^{l+k} = 0 \end{aligned}$$

which means  $c_0$  is not fixed by the equation (normalization constant), and:

$$c_{k+1} = \frac{2(l+k+1) - \lambda}{(l+k+1)(l+k+2) - l(l-1)} c_k \quad k \geq 0 \quad (\text{F.44})$$

Notice that the series cannot really go  $\forall k \in \mathbb{N}$ , because that would mean that at large  $k$ ,  $c_{k+1}/c_k = 2/k$ . This ratio of coefficient unequivocally identifies  $f(\rho) \propto e^{2\rho}$ , as:

$$e^{2\rho} = \sum_{k=0}^{\infty} c_k \rho^k = \sum_{k=0}^{\infty} \frac{2^k}{k!} \rho^k \quad \rightarrow \quad \frac{c_{k+1}}{c_k} = \frac{2^{k+1}}{2^k} \frac{k!}{(k+1)!} = \frac{2}{k+1} \approx \frac{2}{k}$$

but this would mean  $u(\rho) \propto e^{-\rho} e^{2\rho} = e^\rho$  contradicting our initial ansatz  $u(\rho) \propto e^{-\rho}$ .

So, there must exist some  $k_0$  such that  $c_{k_0+1} = 0$ , and every coefficient after that would cancel. If we impose so on [Equation F.44](#):

$$n := l + k_0 + 1 = \frac{\lambda}{2} = \alpha \sqrt{\frac{2\mu}{|E|}}$$

because  $E < 0$  (positronium being a bound system), we finally obtain Bohr energy levels:

$$E_n = -\frac{\alpha^2 \mu}{2n^2} = -\frac{\alpha^2 m_e}{4n^2} \quad (\text{F.45})$$

As for the wave functions, we realize that [Equation F.44](#) defines the coefficients for polynomials called *associated Laguerre polynomials*  $L_{n-l-1}^{2l+1}(2\rho)$ . Notice that:

$$\rho = r\sqrt{2\mu|E_n|} = r\sqrt{\frac{\alpha^2 \mu^2}{n^2}} = \frac{r\alpha\mu}{n} = \frac{1}{n} \frac{r}{r_0}$$

Where  $r_0 = 1/\alpha\mu$  is the *Bohr radius* for positronium. So, our final wavefunction becomes:

$$u_{nl}\left(\frac{r}{nr_0}\right) = c_0 \left(\frac{r}{nr_0}\right)^{l+1} \mathcal{L}_{n-l-1}^{2l+1}\left(\frac{2r}{nr_0}\right) \exp\left[-\frac{r}{nr_0}\right] \quad (\text{F.46})$$

$$\psi_{nlm}\left(\frac{r}{nr_0}, \theta, \phi\right) = c_0 \left(\frac{r}{nr_0}\right)^l \mathcal{L}_{n-l-1}^{2l+1}\left(\frac{2r}{nr_0}\right) \exp\left[-\frac{r}{nr_0}\right] Y_l^m(\theta, \phi) \quad (\text{F.47})$$

where  $c_0 = c_0(n, l)$  is the normalization constant to be determined. In [34], we find:

$$c_0(n, l) = \sqrt{\frac{1}{2n} \left(\frac{2}{nr_0}\right)^3 \frac{(n-l-1)!}{(n+l)!}} \quad (\text{F.48})$$

In particular, we are interested in  $\psi_{100}$ , the ground state wavefunction:

$$\psi_0 = \psi_{100} = \sqrt{\frac{4}{r_0^3}} e^{-\frac{r}{r_0}} Y_0^0(\theta, \phi) = \frac{1}{\sqrt{\pi r_0^3}} e^{-\frac{r}{r_0}} \quad (\text{F.49})$$

which is the wavefunction reported by Landau-Lifschitz ([27]).

Finally, we can take relative velocity in the ground state using energy eigenvalues (Equation F.45). By *virial theorem*, in hydrogen-like systems:

$$\begin{aligned} \text{potential energy} &= -2 \times \text{kinetic energy} \\ \text{kinetic energy} &= -\text{total energy} = \frac{1}{2}\mu^2 v_{rel}^2 \end{aligned} \quad (\text{F.50})$$

for the ground state, this means:

$$|E_1| = \frac{1}{2}\mu^2 v_{rel}^2 \quad \rightarrow \quad v_{rel} = \sqrt{\frac{2|E_1|}{\mu}} = \sqrt{\frac{2\alpha^2\mu}{\mu}} = \alpha \quad (\text{F.51})$$

in units of  $c$ , this simply implies that  $\beta = 1/137$  in positronium ground state (or in hydrogen atom).

## G Tools for calculations and graphs

### G.1 FORM codes

FORM is a symbolic manipulation program used to simplify complex algebraic expression. It has been developed at Nikhef, the Dutch institute for subatomic physics, and widely popular within the theoretical particle physicists. For this thesis, we will employ FORM for calculations of amplitudes involving spin 2 mediation.

To get started and learn how to use it, you can refer to this [online manual](#).

All the codes used for calculations in this thesis use this FORM tool. Here is a [GitHub repository](#) where you can find listed all the codes that were employed for hard calculations.

- `README.md`: instructions for execution of codes in FORM.
- `spin2Decayee.frm`: this code calculates the amplitude for the decay process  $X \rightarrow e^+e^-$ , where  $X$  is a spin 2 massive boson with mass  $m_X$ , and the Feynman rule is found in [Equation 4.56](#).
- `spin2Decayeegamma_4vertex.frm`: this code calculates the amplitude for the decay process  $X \rightarrow e^+e^-\gamma$  only using the 4-vertex interaction (incomplete), where  $X$  is a spin 2 massive boson with mass  $m_X$ , and the Feynman rule is found in [Equation 4.59](#).
- `spin2Decaygg_xigauge.frm`: this code calculates the amplitude for the decay process  $X \rightarrow \gamma\gamma$ , where  $X$  is a spin 2 massive boson with mass  $m_X$ , and the Feynman rule is calculated in [Equation 4.68](#), in a generic  $\xi$  gauge.
- `Bhabha.frm`: this code calculates the traces for the Bhabha scattering, only using QED diagrams. To better comprehend the result, we suggest studying every squared term individually ( $s$ -channel,  $t$ -channel and interference). The output of the code is used in [subsection A.4](#).
- `Moller.frm`: this code calculates the traces for the Møller scattering, only using QED diagrams. To better comprehend the result, we suggest studying every squared term individually ( $t$ -channel,  $u$ -channel and interference). This code is only used to check crossing symmetry in [subsection B.3](#).
- `Compton.frm`: this code calculates the trace for the Compton scattering, only using QED diagrams. The output of the code is used in [subsection C.2](#).
- `Annihilation.frm`: this code calculates the trace for the  $e^+e^-$  annihilation into two photons, only using QED diagrams. The output is used in [subsection D.2](#).
- `Twophoton.frm`: this code calculates the QED loop trace for the two-photon scattering process. It does not perform the integration in loop momentum, and it is used only to verify that QED amplitude is gauge invariant and finite. Result is found in [subsection E.2](#).
- `Bhabha_Xspin2_xigauge.frm`: this code calculates the modulus squared of the total tree level amplitude for the Bhabha scattering, corrected by spin 2 massive boson mediation (all four diagrams included). Calculations were carried out in  $\xi$  gauge. The gauge only enters the QED part.

It is highly suggested to impose  $g_e^4 = 0$  in the code, to get rid of the computation heavy part, and speed the code up to just a couple of seconds. Also, it is suggested to study  $s$ -channel,  $t$ -channel and interference separately. The output of the code is found in [Equation 6.20](#), [Equation 6.21](#) and [Equation 6.30](#).

- `Moller_Xspin2_xigauge.frm`: this code calculates the modulus squared of the total tree level amplitude for the Møller scattering, corrected by spin 2 massive boson mediation (all four diagrams included). Calculations were carried out in  $\xi$  gauge. The gauge only enters the QED part.

It is highly suggested to impose  $g_e^4 = 0$  in the code, to get rid of the computation heavy part, and speed the code up to just a couple of seconds. Also, it is suggested to study  $s$ -channel,  $t$ -channel and interference separately. The code is only used to check crossing symmetry in [section 7](#).

- `Bhabha_Xspin1_xigauge.frm`: this code calculates the modulus squared of the total tree level amplitude for the Bhabha scattering, corrected by spin 1 massive boson mediation (all four diagrams included). Calculations were carried out in  $\xi$  gauge.

It is suggested to study  $s$ -channel,  $t$ -channel and interference separately. The gauge only enters the QED part. The output of the code is found in [Equation 8.25](#), [Equation 8.26](#) and [Equation 8.27](#).

- `Compton_onlyX_xigauge.frm`: this code calculates a simplified version of the modulus squared of the spin 2 massive boson mediated process in Compton scattering only. Since there are no interference terms between QED diagrams and the spin 2 diagram, the latter can be analyzed singularly. Calculations were carried out in  $\xi$  gauge. To speed up the software, it is recommended to substitute  $1/\xi = 0$  (Lorentz gauge). This code is used in [section 9](#) for Ward identities check.
- `Annihilation_onlyX_xigauge.frm`: this code calculates a simplified version of the modulus squared of the spin 2 massive boson mediated process in  $e^+e^-$  annihilation only. Since there are no interference terms between QED diagrams and the spin 2 diagram, the latter can be analyzed singularly. Calculations were carried out in  $\xi$  gauge. To speed up the software, it is recommended to substitute  $1/\xi = 0$  (Lorentz gauge). This code is used in [section 10](#) for Ward identities check.
- `Twophoton_onlyX_xigauge.frm`: this code calculates the total tree level amplitudes (not squared) for two-photon scattering, without mediation of QED, for every independent choice of photon polarizations (remember that final state is barred, so polarizations switch), and results are polarization dependent. Calculations were carried out in  $\xi$  gauge, and result is immediate. The outputs of the code are found in [subsection 11.1](#).
- `Compton_Xspin2_xigauge.frm`: this code calculates the modulus squared of the total tree level amplitude for the Compton scattering, corrected by spin 2 massive boson mediation (all three diagrams included). Calculations were carried out in  $\xi$  gauge. To speed up the software, it is recommended to substitute  $1/\xi = 0$  (Lorentz gauge). The output of the code is found in [Equation 9.10](#).
- `Annihilation_Xspin2_xigauge.frm`: this code calculates the modulus squared of the total tree level amplitude for the annihilation into two photons, corrected by spin 2 massive boson mediation (all three diagrams included). Calculations were carried out in  $\xi$  gauge. To speed up the software, it is recommended to substitute  $1/\xi = 0$  (Lorentz gauge). The output of the code is found in [Equation 10.11](#).
- `ee_into_Xg.frm`: this code calculates squared amplitude of the process  $e^+e^- \rightarrow X\gamma$ ,  $X$  being spin 2 particle, in the massless fermion limit. Result of the code is gauge independent (2 gauge parameters are there:  $\xi_1$  and  $\xi_2$ ), and it also satisfies Ward identities. It is suggested to substitute Mandelstam variables alternatively to quickly compare result with literature, and to multiply amplitude by  $12m_X^4stu$ . Output of the code is found in [subsubsection 12.1.2](#).
- `manip_eeXg.frm`: this code manipulates result from `ee_into_Xg.frm` code, and simply presents it in a nicer way.  $f_1, f_2, f_3$  are functions used in the initial result, and  $f_3, f_4, f_5$  are used in the final result. Output of the code is used in [Equation 12.23](#) and [Equation 12.24](#).
- `from_eeXg_to_Xeeg.frm`: this code takes the amplitude resulting from the scattering process  $e^+e^- \rightarrow X\gamma$  and translates it into the amplitude for decay of  $X \rightarrow e^+e^-\gamma$ , converting  $s, t, u$  into  $m_X, x, y$  variables and changing sign to photon momentum. Output of this code can be found in [Equation 5.18](#).
- `unitar_gggg.frm`: this code simply substitutes  $t, u$  Mandelstam variables in terms of  $s$  and  $\cos\theta = x$  as scattering angle, to be able to perform integration in  $x$  and obtain partial wave component for unitarity constraint. Output of the code is found in [subsubsection 12.4.3](#).

## G.2 Google Colab for graphs

Every graph has been drawn using `matplotlib` extension for Python 3.

Graphs can be found in the following [Google Colab](#).

## References

- [1] A.J. Krasznahorkay et al. (2016), “Observation of Anomalous Internal Pair Creation in  ${}^8\text{Be}$ : A Possible Signature of a Light, Neutral Boson”, *Phys. Rev. Lett.* **116**, 042501 (2016). [arXiv:1504.01527](#).
- [2] A.J. Krasznahorkay et al. (2019), “New evidence supporting the existence of the hypothetic X17 particle”. [arXiv:1910.10459](#).
- [3] A.J. Krasznahorkay et al. (2021), “A new anomaly observed in  ${}^4\text{He}$  supports the existence of the hypothetical X17 particle”. [arXiv:2104.10075](#).
- [4] A.J. Krasznahorkay et al. (2022), “Observation of the X17 anomaly in the  ${}^7\text{Li}(p, e^+e^-){}^8\text{Be}$  direct proton-capture reaction”. [arXiv:2205.07744](#).
- [5] A.J. Krasznahorkay et al. (2022), “New anomaly observed in  ${}^{12}\text{C}$  supports the existence and the vector character of the hypothetical X17 boson”. [arXiv:2209.10795](#).
- [6] J. Gulyś et al. (2015), “A pair spectrometer for measuring multipolarities of energetic nuclear transitions”. [arXiv:1504.00489](#).
- [7] L. Darmè et al. (2022), “Resonant search for the X17 boson at PADME”. [arXiv:2209.09261](#).
- [8] Kh.U. Abraamyan et al. (2023), “Observation of structures at  $\sim 17$  and  $\sim 38 \text{ MeV}/c^2$  in the  $\gamma\gamma$  invariant mass spectra in pC, dC, and dCu collisions at  $p_{lab}$  of a few  $\text{GeV}/c$  per nucleon”. [arXiv:2311.18632](#).
- [9] P. Artoisenet et al. (2014) ”A framework for Higgs characterisation”. [arXiv:1306.6464](#).
- [10] B. Döbrich, J. Jaeckel, F. Kahlhoefer, A. Ringwald, K. Schmidt-Hoberg (2015), “ALPtraum: ALP production in proton beam dump experiments”, *JHEP* **1602** (2016) 018. [arXiv:1512.03069](#).
- [11] J. L. Feng et al. (2016), “Protophobic Fifth Force Interpretation of the Observed Anomaly in  ${}^8\text{Be}$  Nuclear Transitions”, *Phys. Rev. Lett.* **117**, 071803 (2016). [arXiv:1604.07411](#).
- [12] J. L. Feng et al. (2017), “Particle physics models for the 17 MeV anomaly in beryllium nuclear decays”, *Phys. Rev. D* **95**, 035017.
- [13] R. Costa (2016), *Theory and Phenomenology of a Massive Spin-2 Particle*. Master’s Degree Thesis, Università di Bologna. Available [here](#) (Accessed: February 5<sup>th</sup>, 2024).
- [14] G. Panico, L. Vecchi, A. Wulzer (2016), “Resonant Diphoton Phenomenology Simplified”. [arXiv:1603.04248](#).
- [15] X. Zhang, G. A. Miller (2017), “Can nuclear physics explain the anomaly observed in the internal pair production in the Beryllium-8 nucleus?”. [arXiv:1703.04588](#).
- [16] L. Delle Rose, S. Khalil, S. Moretti (2017) “Explanation of the Beryllium Anomaly in a U(1)-Extended 2-Higgs Doublet Model”. [arXiv:1708.08806](#).
- [17] C. Y. Wong (2020), “Open string QED meson description of the X17 particle and dark matter”, *JHEP08(2020)165*. [arXiv:2001.04864](#).
- [18] C. Y. Wong (2022), “QED Meson Description of the X17 and Other Anomalous Particles”, “*Shedding light on X17: community report*”, *EPJC83(2023)230*, pp. 36-40. [arXiv:2201.09764](#).
- [19] Daniele S. M. Alves (2021), “Signals of the QCD axion with mass of  $17 \text{ MeV}/c^2$ : Nuclear transitions and light meson decays”, *Phys. Rev. D* **103**, 055018 (2021). [arXiv:2009.05578](#).
- [20] M. Chala, A. Diaz-Carmona, G. Guedes (2021), “A Greens basis for the bosonic SMEFT to dimension 8”. [arXiv:2112.12724](#).
- [21] D. Barducci, C. Toni (2022), “An updated view on the ATOMKI nuclear anomalies”. [arXiv:2212.06453](#).
- [22] D. d'Enterria, M. A. Tamlihat, L. Schoeffel, H.S. Shao, Y. Tayalati (2023), “Collider constraints on massive gravitons coupling to photons”. [arXiv:2306.15558](#).
- [23] H. X. Chen (2023), “QCD sum rule studies on the possible double-peak structure of the X17 particle”. [arXiv:2312.02763](#).

- [24] M. Fierz, W. E. Pauli (1939) “On relativistic wave equations for particles of arbitrary spin in an electromagnetic field”. *Proc. R. Soc. Lond. A.* **173** (953): 211-232. Available here.
- [25] M. E. Peskin, D. V. Schroeder (1994), *An Introduction to Quantum Field Theory*, CRC Press, Boca Raton. ISBN 13: 978-0-201-50397-5.
- [26] M. Veltman (1994), *Diagrammatica: The Path to Feynman Diagrams*, Cambridge University Press, 1st edition, Cambridge. ISBN 13: 978-0521456920
- [27] L. Landau, E. M. Lifschitz (1971), *Quantum Electrodynamics*, Volume 4 Course in Theoretical Physics, 2nd edition, USSR Academy of Sciences, Moscow. ISBN-10: 0750633719.
- [28] S. Weinberg (2019), *Lectures on Astrophysics*, 1st edition, Cambridge University Press, Cambridge. ISBN 10: 1108415075.
- [29] A. Al-Ramadhan, D. Gidley (1994), “New precision measurement of the decay rate of the singlet positronium”, *Phys. Rev. Lett.* **72**(11):1632-1635.
- [30] M. Acciarri, O. Adriani, M. Aguilar-Benitez, S. Ahlen, J. Alcaraz, et al.(1998), “Measurement of Radiative Bhabha and Quasi-Real Compton Scattering”, *Phys. Lett. B*, **1998**, *439*, pp.183-196.
- [31] A. Czarnecki, S. Karshenboim (1999), “Decay of positronium”. arXiv:hep-ph/9911410.
- [32] S. Karshenboim (2003), “Precision study of positronium: testing bound state QED theory”. arXiv:hep-ph/0310099.
- [33] A. Rubbia (2004), “Positronium as a probe for new physics beyond the Standard Model”. arXiv:hep-ph/0402151.
- [34] A. Sem, Z. K. Silagadze (2018), “Two photon decay of P-wave positronium: a tutorial”. arXiv:1812.00152.
- [35] X. Ji (1997), “Deeply-virtual Compton scattering”. *Phys. Rev. D* **55**:7114-7125, 1997. arXiv:hep-ph/9609381.
- [36] D. H. Froula et al. (2006), “Thomson scattering techniques in laser produced plasmas”. *Rev. Sci. Instrum.* **77**, 10E522 (2006).
- [37] V. Sulemainov, K. Werner (2007), “Importance of Compton scattering for radiation spectra of isolated neutron stars with weak magnetic fields”. arXiv:astro-ph/0702407.
- [38] Z. Wadiasingh et al. (2018), “Resonant Inverse Compton Scattering Spectra from Highly-magnetized Neutron Stars”. arXiv:1712.09643.
- [39] PrimEx collaboration (2019), “High precision measurement of Compton scattering in the 5 GeV region”. *Phys. Lett. B* **797**, 134884 (2019). arXiv:1903.05529.
- [40] R. Lee, M. Schwartz, X. Zhang (2021), “Compton scattering total cross section at Next to Leading Order”. PhysRevLett.**126.211801**/arXiv:2102.06718.
- [41] V. Musat, A. Latina, G. D'Auria (2022), “A High-Energy and High-Intensity Inverse Compton Scattering Source Based on CompactLight Technology”. *Photonics* **2022**, *9*(5).
- [42] Q. Abar et al. (2022), “Performance of the X-Calibur Hard X-Ray Polarimetry Mission during its 2018/19 Long-Duration Balloon Flight”. arXiv:2204.09761.
- [43] DAMIC-M Collaboration (2022), “Precision measurement of Compton scattering in silicon with a skipper CCD for dark matter detection”. *Phys. Rev. D* **106**, 092001. arXiv:2207.00809.
- [44] R. J. Eden, P. V. Landshoff, D. I. Olive, J. C. Polkinghorne (1966), “The analytic S-matrix”, 1st edition, Cambridge University Press, Cambridge. ISBN 10: 0521048699.
- [45] D. Bardin, G. Passarino (1999), *Standard Model in the Making - Precision Study of the Electroweak Interaction*, 1st edition, Clarendon Press, Oxford. ISBN 10: 019850280X.
- [46] P. S. Cooper et al. (1975), “Polarized Electron-Electron Scattering at GeV Energies”. *Phys. Rev. Lett.* **34**, 1589.
- [47] T. Arima, K. Abe et al. (1996), “Precise measurement of Bhabha scattering at a center-of-mass energy of 57.77 GeV”. *Phys. Rev. D* **55** (1997) 19-39.

- [48] G. Montagna et al. (1999), “Light-Pair Corrections to Small-Angle Bhabha Scattering in a Realistic Set-up at LEP”. [arXiv:hep-ph/9905235](https://arxiv.org/abs/hep-ph/9905235).
- [49] C.M. Carloni Calame et al. (2000), “Large-angle Bhabha scattering and luminosity at flavour factories”. *Nucl. Phys. B* 584:459-479, 2000. [arXiv:hep-ph/0003268](https://arxiv.org/abs/hep-ph/0003268).
- [50] S. Jadach (2003), “Theoretical error of luminosity cross section at LEP”. [arXiv:hep-ph/0306083](https://arxiv.org/abs/hep-ph/0306083).
- [51] F. Ambrosino (2006), “Measurement of the DAΦNE luminosity with the KLOE detector”. *Eur.Phys.J.C* 47:589-596, 2006. [arXiv:hep-ex/0604048](https://arxiv.org/abs/hep-ex/0604048).
- [52] A. Aleksejevs et al. (2011), “High precision calculations of electroweak radiative corrections for polarized Møller scattering at one loop and beyond”. *Nuovo Cimento C*, 2012. [arXiv:1110.6637](https://arxiv.org/abs/1110.6637).
- [53] OLYMPUS Collaboration (2013), “The OLYMPUS experiment”. *Nuclear Inst. and Methods in Physics Research, A* (2014). [arXiv:1312.1730](https://arxiv.org/abs/1312.1730).
- [54] OLYMPUS Collaboration (2021), “Measurement of the Charge-Averaged Elastic Lepton-Proton Scattering Cross Section by the OLYMPUS Experiment”. *Phys. Rev. Lett.* 126, 162501 (2021). [arXiv:2008.05349](https://arxiv.org/abs/2008.05349).
- [55] M. Ablikim et al. (2017), “Measurement of integrated luminosity and center-of-mass energy of data taken by BESIII at  $\sqrt{s} = 2.125$  GeV”. *Chinese Physics C, CPC(HEP & NP)*, 2009, 33(X). [arXiv:1705.09722](https://arxiv.org/abs/1705.09722).
- [56] Belle II Collaboration (2019), “Measurement of the integrated luminosity of the Phase 2 data of the Belle II experiment”. *Chinese Phys. C* 44, 021001 (2020). [arXiv:1910.05365](https://arxiv.org/abs/1910.05365).
- [57] DELPHI collaboration (2019), “Determination of the  $e + e \rightarrow \gamma\gamma(\gamma)$  cross-section at LEP 2”. *Eur.Phys.J.C* 37:405-419, 2004. [arXiv:hep-ex/0409058](https://arxiv.org/abs/hep-ex/0409058).
- [58] L. Morel et al. (2020), “Determination of the fine-structure constant with an accuracy of 81 parts per trillion”. *Nature* 588, 6165 (2020). [Available here](#).
- [59] D. Hanneke, S. Fogwell, G. Gabrielse (2008), “New Measurement of the Electron Magnetic Moment and the Fine Structure Constant”. *Phys. Rev. Lett.* 100, 120801. [Available here](#).
- [60] Parker et al. (2018), “Measurement of the Fine Structure Constant as a Test of the Standard Model”. *Science* 13 Apr 2018: Vol. 360, Issue 6385, pp. 191-195. [arXiv:1812.04130](https://arxiv.org/abs/1812.04130).
- [61] D. Huang, C-Q Geng, J. Wu (2022), “Muon  $g - 2$  Anomaly from a Massive Spin-2 Particle”. [arXiv:2207.13421](https://arxiv.org/abs/2207.13421).
- [62] D. Huang, C-Q Geng, J. Wu (2022), “Unitarity Bounds on the Massive Spin-2 Particle Explanation of Muon  $g_2$  Anomaly”. [arXiv:2208.01097](https://arxiv.org/abs/2208.01097).
- [63] X. Fan et al. (2022), “Measurement of the Electron Magnetic Moment”. *Phys. Rev. Lett.* 130, 071801 (2023). [arXiv:2209.13084](https://arxiv.org/abs/2209.13084).
- [64] W. Heisenberg, H. Euler (1936), “Consequences of Dirac Theory of the Positron”. *Z.Phys.* 98 (1936) 714-732. [arXiv:physics/0605038](https://arxiv.org/abs/physics/0605038).
- [65] R. Karplus, M. Neuman (1951), “The Scattering of Light by Light”. *Phys. Rev.* 83, 776. [Available here](#).
- [66] B. de Tassis (1964), “Dispersive Approach to Photon-Photon Scattering”. *Nuovo Cim.* 32 (1964) 3, 757-768. [available here](#).
- [67] B. de Tassis (1965), “The scattering of photons by photons”. *Nuovo Cim.* 35 (1965) 4, 1182-1193. [available here](#).
- [68] Y. Liang, A. Czarnecki (2011), “Photonphoton scattering: a tutorial”. [arXiv:1111.6126](https://arxiv.org/abs/1111.6126).
- [69] PVLAS Collaboration (2012), “Measuring the magnetic birefringence of vacuum: the PVLAS experiment”. [arXiv:1201.2309](https://arxiv.org/abs/1201.2309).
- [70] D. D'Enterria, G. G. Silveira (2013), “Observing light-by-light scattering at the Large Hadron Collider”. [arXiv:1305.7142](https://arxiv.org/abs/1305.7142).
- [71] K. Homma, K. Matsuura, K. Nakajima (2016), “Testing helicity-dependent  $\gamma\gamma \rightarrow \gamma\gamma$  scattering in the region of MeV”. *Progress of Theoretical and Experimental Physics*, Volume 2016, Issue 1, January 2016, 013C01, [Available here](#).

- [72] The CMS Collaboration (2018), “Evidence for light-by-light scattering and searches for axion-like particles in ultraperipheral PbPb collisions at  $\sqrt{s_{NN}} = 5.02 \text{ TeV}$ ”. *Phys. Lett. B* **797** (2019) 134826. [arXiv:1810.04602](#).
- [73] The ATLAS Collaboration (2019), “Observation of light-by-light scattering in ultraperipheral Pb+Pb collisions with the ATLAS detector”. *Phys. Rev. Lett.* **123** (2019) 052001. [arXiv:1904.03536](#).
- [74] M. D. Goodsell, F. Staub (2018), “Unitarity constraints on general scalar couplings with SARAH”. [arXiv:1805.07306](#).
- [75] P. Franzini, M. Moulson (2006), “The Physics of DAΦNE and KLOE”. *Ann.Rev.Nucl.Part.Sci.* **56**:207-251,2006. [arXiv:hep-ex/0606033](#).
- [76] The KLOE Collaboration (2015), “Limit on the production of a low-mass vector boson in  $e^+e^- \rightarrow U\gamma$ ,  $U \rightarrow e^+e^-$  with the KLOE experiment”. [arXiv:1509.00740](#).
- [77] The NA64 Collaboration (2018), “Search for a Hypothetical 16.7 MeV Gauge Boson and Dark Photons in the NA64 Experiment at CERN”. *Phys. Rev. Lett.* **120**, 231802 (2018). [arXiv:1803.07748](#).
- [78] S.N. Gnenenko (2016), “Missing energy signature from invisible decays of dark photons at the CERN SPS”. *Phys. Rev. D* **94**, 095025 (2016). [arXiv:1604.08432](#).
- [79] I. V. Voronchikhin, D. V. Kirpichnikov (2022), “Probing hidden spin-2 mediator of dark matter with NA64<sub>e</sub>, LDMX, NA64 <sub>$\mu$</sub>  and  $M^3$ .” [arXiv:2210.00751](#).